Linking Rheological and Processing Behavior to Molecular Structure in Sparsely-Branched Polyethylenes Using Constitutive Relationships

Christopher D. McGrady

Dissertation submitted to the Faculty of
Virginia Polytechnic Institute and State University
in partial fulfillment of the requirements for the degree of

DOCTOR OF PHILOSOPHY
IN
CHEMICAL ENGINEERING

Advisory Committee:

Dr. Donald G. Baird, Chairman
Dr. Richey M. Davis
Dr. Robert B. Moore
Dr. John Y. Walz

May 22nd, 2009
Blacksburg, VA

Keywords: polyethylene, rheology, film-casting, Pom-pom model, encapsulation

Linking Rheological and Processing Behavior to Molecular Structure in Sparsely-Branched Polyethylenes Using Constitutive Relationships

Christopher D. McGrady

Abstract

This dissertation works towards the larger objective of identifying and assessing the key features of molecular structure that lead to desired polymer processing performance with an ultimate goal of being able to tailor-make specific macromolecules that yield the desired processing response. A series of eight well-characterized, high-density polyethylene (HDPE) resins, with varying degrees of sparse long chain branching (LCB) content, is used to study the effect of both LCB content and distribution on the rheological and commercial processing response using the Pom-pom constitutive relationship. A flow instability known as ductile failure in extensional flow required the development a novel technique known as encapsulation in order to carry out shear-free rheological characterization.

Ductile failure prevents the rheological measurement of transient stress growth at higher strains for certain strain-hardening materials. This reduces the accuracy of nonlinear parameters for constitutive equations fit from transient stress growth data, as well as their effectiveness in modeling extensionally driven processes such as film casting. An experimental technique to overcome ductile failure called encapsulation in which the material that undergoes ductile failure is surrounded by a resin that readily deforms homogeneously at higher strains is introduced. A simple parallel model is shown to calculate the viscosity of the core material.

The effect of sparse long chain branching, LCB, on the film-casting process is analyzed at various drawdown ratios. A full rheological characterization in both shear and shear-free flows is also presented. At low drawdown ratios, the low-density polyethylenes, LDPE, exhibited the least degree of

necking at distances less than the HDPE frostline. The sparsely-branched HDPE resins films had similar final film-widths that were larger than those of the linear HDPE. As the drawdown ratio was increased, film width profiles separated based on branching level. Small amounts of LCB were found to reduce the amount of necking at intermediate drawdown ratios. At higher drawdown ratios, the sparsely-branched HDPE resins of lower LCB had content film-widths that mimicked that of the linear HDPE, while the sparsely-branched HDPE resins of higher LCB content retained a larger film width. Molecular structural analysis via the Pom-pom constitutive model suggested that branching that was distributed across a larger range of backbone lengths serve to improve resistance to necking. As the drawdown ratio increased, the length of the backbones dominating the response decreased, so that the linear chains were controlling the necking behavior of the sparsely-branched resins of lower LCB content while remaining in branched regime for higher LCB content HDPEs. Other processing variables such as shear viscosity magnitude, extrudate swell, and non-isothermal processing conditions were eliminated as contributing factors to the differences in the film width profile.

The effect of sparse long chain branching, LCB, on the shear step-strain relaxation modulus is analyzed using a series of eight well-characterized, high-density polyethylene (HDPE) resins. The motivation for this work is in assessing the ability of step-strain flows to provide specific information about a material's branching architecture. Fundamental to this goal is proving the validity of relaxation moduli data at times shorter than the onset of time-strain separability. Strains of 1% to 1250% are imposed on materials with LCB content ranging from zero to 3.33 LCB per 10,000 carbon atoms. All materials are observed to obey time-strain separation beyond some characteristic time, τ_k. The presence of LCB is observed to increase the value of τ_k relative to the linear resin. Furthermore, the amount of LCB content is seen to correlate positively with increasing τ_k. The behavior of the relaxation modulus at times shorter than τ_k is investigated by an analysis of the enhancement seen in the linear relaxation modulus, $G^0(t)$, as a function of strain and LCB content. This enhancement is seen to 1)

increase with increasing strain in all resins, 2) be significantly larger in the sparsely-branched HDPE resins relative to the linear HDPE resin, and 3) increase in magnitude with increasing LCB content. The shape and smoothness of the damping function is investigated to rule out the presence of wall-slip and material rupture during testing. The finite rise time to impose the desired strain is carefully monitored and compared to the Rouse relaxation time of the linear HDPE resins studied. Sparse LCB is found to increase the magnitude of the relaxation modulus at short times relative to the linear resin. It is shown that these differences are due to variations in the material architecture, specifically LCB content, and not because of mechanical anomalies.

Original Contributions

The following list illustrates the significant original contributions of this research:

1) The development of a novel technique called encapsulation that was able to overcome ductile failure in extensional flows in HDPE systems. This technique allowed for the measurement of transient extensional data at Hencky strains greater than the onset of ductile failure.

2) Molecular structural analysis via the Pom-pom constitutive model suggested that branching that was distributed on the longest backbones in the sparsely-branched HDPE resins. As LCB content was increased, this distribution was observed to increase across a larger range of backbone lengths.

3) Branching distribution was found to be key component in increasing a materials resistance to necking in the film-casting process, especially at higher drawdown ratios. Molecular structural analysis suggested that branching that was distributed across a larger range of backbone lengths serve to improve resistance to necking. As the drawdown ratio increased, the length of the backbones dominating the response decreased, so that the linear chains were controlling the necking behavior of the sparsely-branched resins of lower LCB content while remaining in branched regime for higher LCB content HDPEs.

4) Sparse LCB is found to increase the magnitude of the relaxation modulus at short times relative to the linear resin. It is shown that these differences are due to variations in the material architecture, specifically LCB content, and not because of mechanical anomalies.

Format of Dissertation

This dissertation is written in journal format. Chapters 4, 5, and 6 are self-contained papers that separately describe the experiments, results, and conclusions relative to each chapter. With the exception of the literature review and experimental methods chapters, the figures and tables are inserted after the reference section of each chapter.

Table of Contents

List of Figures

Chapter 1

Chapter 2

List of Tables

Chapter 2

Chapter 3

Chapter 4

Chapter 5

Chapter 5

1.0 - Introduction and Overview of Research Objectives

Recent developments using metallocene catalysts allow for the production of long-chain branched (LCB) polyolefin resins that have relatively narrow molecular weight distribution, MWD, (~2.0). These constrained geometry catalysts allow for the controlled addition of LCB. A long-chain branch is defined as a branch arm whose molecular weight is greater than the molecular weight for entanglement. This controlled polymerization is of commercial importance in that it allows for customizable metallocene-catalyze polyethylene (MCPE) reins based on the customer's processing needs. It allows for control of physical properties such as the melting point, clarity, toughness, and elasticity. For example, Doerpinghaus and Baird[1] show that sparsely-branched MCPE resins can be used to alter the melt fracture behavior of commercial PE, finding that as little as 0.79 LCB per 10^4 carbons is needed to alleviate slip-stick flow.

This ability to obtain desired processing performance through controlled branching has sparked an interest in understanding the melt rheology of these MCPE resins. The melt rheology of a resin can give insight as to the variation in behavior seen in the processability of a material by investigating simple shear and shear-free flows that are present in industrial processes in more complex flow combinations. The rheological response of MCPE resins have been well characterized in the literature[2-11]. A majority of these works investigate the behavior in simple shear and transient extensional flow.

In shear flows, the dependence of viscosity, both in the limit of the complex viscosity as a function of molecular weight and the zero-shear viscosity, on molecular weight, molecular weight distribution, and LCB content are investigated. Doerpingahaus and Baird[3] show the ability to isolate the effect of LCB from MW and MWD in shear viscosity measurements through the use of shift factor. The authors observe a definitive zero-shear viscosity enhancement relative to linear resins for sparsely-branched (<1 LCB per 10^4 carbons) MCPE that increases with LCB content. The authors also observe that in the highly branched linear-low density PE (LLDPE), a zero-shear viscosity reduction is seen. This is consistent with the work of Janzen and Colby[12] who predict that for constant MW and MWD, the zero-

shear viscosity enhancement as a function of LCB increases until proceeding through a maximum. Doerpingahaus and Baird[3] also show that increases in LCB lead to the onset of shear thinning behavior at significantly lower shear rates and angular frequencies (e.g. three orders of magnitude lower at the same molecular weight).

Extensional flows can serve to detect small differentiation in LCB content that is not observable either in shear flows[5] or by standard analytical techniques[13]. It is well documented[4, 5, 8, 10, 11, 14, 15] that the presence of LCB causes a rise in the extensional viscosity above the linear viscoelastic response, otherwise known as "strain-hardening." Bin Wadud and Baird[5], Doerpinghaus and Baird[4], Wood-Adams and Dealy[8], and Seay[14] all show distinguishable strain-hardening levels in sparsely-branched MCPE resins, confirming experimentally the sensitivity and characterization potential of the flow.

The question becomes what structural and topological features allow the MCPE resins to exhibit such unique rheological and processing behaviors? Structurally, we know that the branching is well-controlled through constrained geometry catalysts. But what kind of specific branching architectures compose MCPE resins? It has been proposed through numerical simulations of the reaction kinetics that metallocene-catalyzed PE's are a combination of stars, combs, and randomly branched architectures embedded in a matrix of linear chains[16]. While this finding has neither been completely confirmed nor invalidated, it is still not enough to compose a detailed molecular picture that directly relates specific branching architecture to the desired processing response. For example, even knowing that a MCPE resin is a blend of star, comb, and random branching with linear chains, specific structural information would be needed about the exact geometry, such as arm length, backbone spacing, and number of branch arms. Each of these factors is shown through rheological testing to affect the material response in shear and shear-free flows that are common in processing (for example[10, 17]). Furthermore, traditional analytical techniques such as the measurement of the radius of gyration are not adequate to identify the *specific* branching architecture or distribution.

Recent advances in constitutive modeling give rise to a new class of constitutive equation that may be able to directly relate rheological properties to the molecular structure of the melt. The original McLeish-Larson[18] Pom-pom model is based on the Doi-Edwards[19] tube theory and the ideas of relaxation through reptation. The model is formulated by assuming an ideal "pom-pom" model architecture. After deformation, these ideal branched molecules have a retarded backbone stretch relaxation that is due to the branch points on either end of the backbone acting as pinning points that will not allow the stretch to relax until after the branch arms have relaxed at which time the stretch relaxes rapidly and the backbone relaxes through reptation. The accrued stress resulting from the retarded relaxation of stretch allows the constitutive model to calculate strain-hardening behavior characteristic to branched polymers.

It has been shown by Inkson *et al.*[15] that the differential form of Pom-pom model[18] can be adapted to model the melt rheology of low-density PE resins via a multi-mode approach. This approach addresses large molecules with multiple branch points by modeling them as a series of theoretical pom-pom molecules with a different number of arms, assigning orientation relaxation time modes from the linear spectra. In the simplest terms, this model assumes that the free branch ends relax first. The associated branch points with these free ends take a diffusive step and the attached backbone relaxes in a star-arm fashion on a much longer timescales than the outer arms. This continues until the innermost branch points relax. The relaxation time of a segment is determined by its path distance to the nearest free end. It has been shown by Doerpinghaus and Baird[4] that this approach can be extended to sparsely-branched MCPE resins as well.

While modeling successes of the pom-pom model is seen to yield good agreement with experimental data (e.g. Inkson *et al.*[15] in LDPEs and Doerpinghaus and Baird[4] in sparsely-branched MCPEs) , it is still quantitatively unclear if a specific branching architecture can be determined from the parameter spectrum. If the parameters determined from this approach are quantitatively related to the

branching structure, this could allow for a direct determination of specific molecular topology from melt rheology. This in turn could lead to the synthetic customization of branching structures that obtain the exact desired processing performance, as is illustrated in Fig. 1.1.

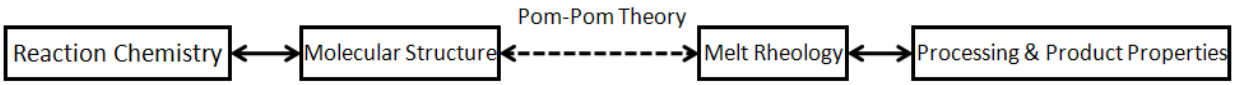

Figure 1.1 Potential of the Pom-pom model in that it allows for the understanding of molecular structure based on the melt rheology.

Our work is focused on using a combination of melt rheology and constitutive modeling to probe the possibility of such a quantitative relationship. The first objective involves developing a robust set of pom-pom model parameters for a series of sparsely-branched metallocene-catalyzed high-density polyethylene (mHDPE) resins. These materials are ideal for this study in that they have been well-characterized in previous works[8, 9, 20] and are available in sufficient quantities for both rheological and processing experiments.

A new methodology for the determination of the multimode pom-pom parameters is needed. This is due to an elastic instability that occurs in uniaxial elongation flow that can lead to multiple "best fit" sets of pom-pom parameters. Our new methodology introduces shear step-strain and a novel experimental technique called encapsulated extensional rheology in an attempt to overcome this failure.

The second objective is to determine whether the pom-pom parameters determined from rheological measurements on a model system are consistent with those of a known chemical structure. This research serves to determine if a quantitatively accurate connection can be made between the model parameters and the molecular structure. For this a set of anionically-polymerized polystyrene molecules with highly controlled model branching architectures is used.

Clearly stated, the research objectives of this work are:

1) **To characterize the rheological and the processing behavior of a series of well-defined MCPE HDPE resins, and then link this observed behavior to specific molecular structure using contemporary constitutive relationships. Central to achieving this goal are:**
    a. **Making a full rheological characterization of the HDPE resins in both simple shear and shear-free flows**
    b. **Developing a successful experimental strategy for overcoming ductile failure in extensional flow**
    c. **Developing a methodology that yields a unique set of model parameters**
    d. **Linking the structural information determined from simple flows and model parameters to behavior seen in more complex industrial polymer processing flows.**
2) **The use of well controlled model PS systems to determine if the constitutive model parameters determined from rheological measurements on a model system are consistent with those of a known chemical structure.**

1.1 – References

1. Doerpinghaus, P. J.; Baird, D. G., Comparison of the melt fracture behavior of metallocene and conventional polyethylenes. *Rheologica Acta* **2003,** 42, (6), 544-556.

2. Doerpinghaus, P. J. Flow Behavior of Sparsely Branched Metallocene-Catalyzed Polyethylenes. Virginia Tech, Blacksburg, 2002.

3. Doerpinghaus, P. J.; Baird, D. G., Separating the effects of sparse long-chain branching on rheology from those due to molecular weight in polyethylenes. *J. Rheol.* **2003,** 47, (3), 717-736.

4. Doerpinghaus, P. J.; Baird, D. G., Assessing the Branching Architecture of Sparsely Branched Metallocene-Catalyzed Polyethylenes Using the Pompom Constitutive Model. *Macromolecules* **2002,** 35, (27), 10087-10095.

5. Bin Wadud, S. E.; Baird, D. G., Shear and extensional rheology of sparsely branched metallocene-catalyzed polyethylenes. *J. Rheol.* **2000,** 44, (5), 1151-1167.

6. Dealy, J. M.; Wood-Adams, P. M., Rheological behavior of metallocene polyethylenes. *Abstracts of Papers, 223rd ACS National Meeting, Orlando, FL, United States, April 7-11, 2002* **2002**, IEC-221.

7. Wood-Adams, P. M., The effect of long chain branches on the shear flow behavior of polyethylene. *J. Rheol.* **2001,** 45, (1), 203-210.

8. Wood-Adams, P. M.; Dealy, J. M., Using Rheological Data To Determine the Branching Level in Metallocene Polyethylenes. *Macromolecules* **2000,** 33, (20), 7481-7488.

9. Wood-Adams, P. M.; Dealy, J. M.; deGroot, A. W.; Redwine, O. D., Effect of Molecular Structure on the Linear Viscoelastic Behavior of Polyethylene. *Macromolecules* **2000,** 33, (20), 7489-7499.

10. Lohse, D. J.; Milner, S. T.; Fetters, L. J.; Xenidou, M.; Hadjichristidis, N.; Mendelson, R. A.; Garcia-Franco, C. A.; Lyon, M. K., Well-Defined, Model Long Chain Branched Polyethylene. 2. Melt Rheological Behavior. *Macromolecules* **2002,** 35, (8), 3066-3075.

11. Barroso, V. C.; Maia, J. M., Influence of long-chain branching on the rheological behavior of polyethylene in shear and extensional flow. *Polymer Engineering and Science* **2005,** 45, (7), 984-997.

12. Janzen, J.; Colby, R. H., Rheological detection of long-chain branching in high-density polyethylenes. *Polymeric Materials Science and Engineering* **2000,** 82, 128-129.

13. Muenstedt, H.; Gabriel, C.; Auhl, D., Long-chain branching and elongational properties of polyethylene and polypropylene melts. *Polymer Preprints (American Chemical Society, Division of Polymer Chemistry)* **2003,** 44, (2), 27-28.

14. Seay, C. W. The Role of Molecular Architecture on Rheological Properties and its Effect on Film-Casting Performance. Virginia Tech, Blacksburg, VA, 2008.

15. Inkson, N. J.; McLeish, T. C. B.; Harlen, O. G.; Groves, D. J., Predicting low density polyethylene melt rheology in elongational and shear flows with "pom-pom" constitutive equations. *J. Rheol.* **1999,** 43, (4), 873-896.

16. Soares, J. P.; Hamielec, A. E., *Metallocene-Catalyzed Polymers: Materials, Properties, Processing & Markets*. Plastics Design Library: New York, 1998.

17. Nielsen, J. K.; Rasmussen, H. K.; Denberg, M.; Almdal, K.; Hassager, O., Nonlinear Branch-Point Dynamics of Multiarm Polystyrene. *Macromolecules* **2006,** 39, (25), 8844-8853.

18. McLeish, T. C. B.; Larson, R. G., Molecular constitutive equations for a class of branched polymers: The pom-pom polymer. *J. Rheol.* **1998,** 42, (1), 81-110.

19. Doi, M.; Edwards, S. F., *The Theory of Polymer Dynamics*. Oxford University Press: 1988.

20. Das, C.; Inkson, N. J.; Read, D. J.; Kelmanson, M. A.; McLeish, T. C. B., Computational linear rheology of general branch-on-branch polymers. *J. Rheol.* **2006,** 50, (2), 207-234.

2.0 – Literature Review

Preface

In this chapter, previous research that is relevant to the linking the rheological behavior of both metallocene-catalyzed polyethylenes and model polymer systems to their underlying macromolecular branching structure is reviewed. In section 2.1 is reviewed the role of branching architecture and MWD on the rheology of metallocene-catalyzed polyethylenes in both shear and shear-free flows. In section 2.2 is reviewed the observed rheological properties of model architecture systems. Finally, in section 2.3 is reviewed the ability of the pom-pom class of constitutive equations to model the rheological behavior branched polyethylenes.

2.1 – Role of Branching Architecture and MWD on Rheology

Presented in this section is a review that highlights the general trends seen rheologically for certain types of molecular features with emphasis on branching architecture and molecular weight distribution. A review of the shear and shear-free rheological response of sparsely-branched metallocene-catalyzed polyethylenes (mPEs) is emphasized as this class of materials is of interest in this research. A review of the rheological response of model polymer systems is given later in section 2.2.

In section 2.1.1 is introduced specific branching architectures, examples of specific molecular topologies are given, and several methods for determining long-chain branching (LCB) content are reviewed. In section 2.1.2 is reviewed the behavior of branched materials in shear flow in three subsections: in 2.1.2.1 is reviewed the relevant shear flow definitions and material functions, in 2.1.2.2 is reviewed the general effects of branching in relevant shear flows with emphasis on mPEs, and in 2.1.2.3 is reviewed the effect of molecular architecture in a special type of shear flow known as step-strain. In section 2.1.3 is reviewed the behavior of branched materials in elongational (extensional) flows in three subsections: in 2.1.3.1 is reviewed the relevant elongational flow definitions and material functions, in 2.1.3.2 is reviewed the general effects of molecular architecture on relevant elongational flows with emphasis on mPEs, and in 2.1.3.3 reviewed a common phenomenon called ductile failure seen in uniaxial elongational flow that results in the rupture of polymeric melts.

2.1.1 – Specific Molecular Architectures and Branching Structures

The sheer number of catalysts and polymerization techniques currently employed allow for the production of a wide variety of molecular architectures for materials with chemically identical repeat units. The addition of both long-chain and short-chain branching is the source of such structural differences. Long-chain branching (LCB) is defined as a branch arm with a molecular weight large than the molecular weight for entanglement, M_e. Short-chain branching (SCB) is defined as a branch arm

with a molecular weight less than M_e [1, 2]. Sparsely-branched resins are defined as having LCB content less than 1 LCB per 10^4 C. LCB and SCB polymers behave differently rheologically, and these differences will become the focal point of later sections.

The specific structure of a LCB polymer depends on the polymerization technique used to synthesis the material. In Fig. 2.1.1 is shown an example of different polymeric structures that arise from the same monomer repeat unit, specifically the major classes of polyethylene currently used in industrial applications. LDPEs are catalyzed in a high pressure process using traditional heterogeneous Ziegler-Natta catalysts[3]. Structurally the LDPE is hyper-branched, resembling a tree-like conformation. SCB and LCB are native features to LDPEs. LDPEs have enhanced melt elasticity and shear thinning. Typical molecular weight distributions for LDPE are on the order of 4-10 [4]. LLDPEs are α-olefin copolymers produced using either a solution process or a gas phase process using Ziegler-Natta heterogeneous catalysts[4]. LLDPEs only have SCB. LLDPEs are characterized by the appearance of complex comonomer distributions. The general linear structure of LLDPEs lead to a relatively weak melt elasticity[5]. HDPEs are purely linear structures devoid of branches that are catalyzed using coordination catalysts [2]. Metallocene catalyzed LLDPEs and HDPEs (mLLDPEs and mHDPEs) are able to produced either linear or LCB resin[4, 6-8]. Long-chain branching occurs because the polymerization system is able to incorporate vinyl terminated chains as commoners[6].

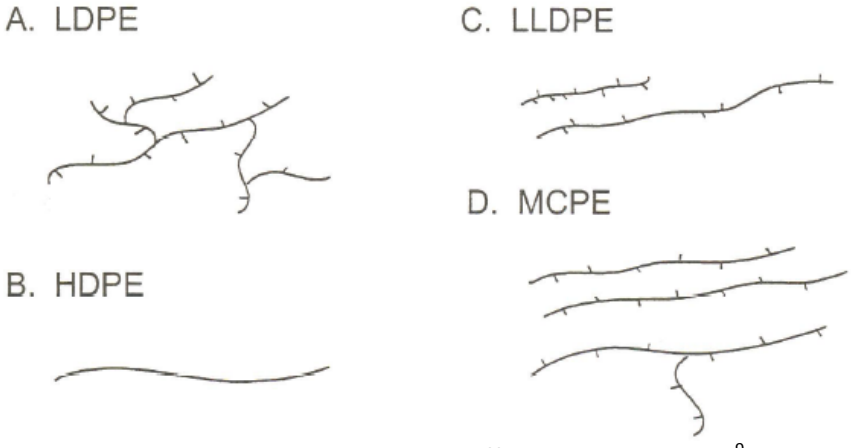

Figure 2.1.1 Some common PE structures that illustrates differences in topology[9].

The LCB polymers of interest to this study are the mLLDPEs and mHDPEs. Numerical studies by Soares and Hamilec[10-12] predict that a distribution of molecules containing linear, star, and higher branched structures exist in sparsely long-chain branched mPEs. Therefore a discussion on the specific molecular architectures that are believed to comprise mPE systems are introduced. In Fig. 2.1.2 is shown several types of common branching architecture. A pom-pom polymer is characterized by *q* number of arms attached at either end of a linear backbone. An H-polymer is simply a pom-pom with *q* equal to two. A star polymer is a polymer where all the branch points are located at a single branch point. A comb polymer is characterized as a branched polymer where all branch points emanate from the backbone, so that there exisits no branch-on-branch branching. A random branched polymer can have branching attach at any point either on the backbone or on other branches

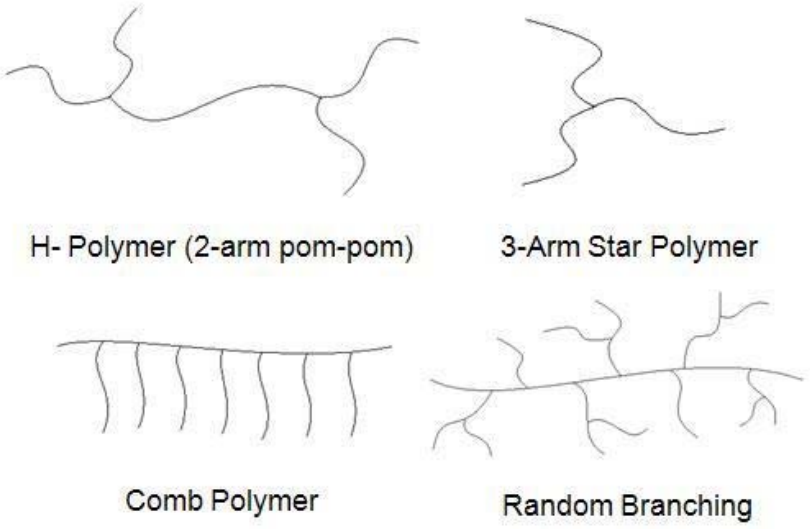

Figure 2.1.2 Common branching architectures.

Two non-rheological techniques used to characterized LCB content are commonly found in the literature. The mean square radius of gyration $\langle s^2 \rangle$ of a branched material can be used to estimate the average number of long-chain branch points per chain using the classical relationship of Zimm and Stockmayer[13, 14]

$$g = \frac{[\eta]_{branched}}{[\eta]_{linear}} = \frac{\langle s^2 \rangle_{branched}}{\langle s^2 \rangle_{linear}} \approx \left[\left(1 + \frac{m}{7}\right)^{0.5} + \frac{4m}{9\pi}\right]^{-0.5} \qquad (2.1\text{-}1)$$

where *m* is the average number of branches per molecule, $[\eta]$ is the intrinsic viscosity, and *g* is the ratio of the mean square radius of gyration of the branched resin to its linear counterpart. Barth and Mays[15] showed that *k* can have a value between 0.5 and 1.5. The mean square radius of gyration is defined as the mass-weighted average distance of monomers from the center of mass, and can be measured using multi-angle laser-light scattering (MALLS). In Eq. 2.1-1 it is assumed a random distribution of trifunctional branches occur across the entire molecular weight distribution. A trifunctional branched system has only a single branch arm extending from each branch point [13]. This technique is sensitive enough to measure small values of branching content (~0.08 LCB per 1000 monomer units), but is not useful for telling use structurally about the resins other than the number of branch ends.

The number of branch points per chain can also be calculated using ^{13}C NMR in solution via the method of Randall[16]. This method is not accurate for detecting long-chain branching content lower than 1 LCB per 10^4 carbons due to limited solubility and low natural abundance of ^{13}C nuclei [17]. Another shortcoming of this method is the inability to distinguish branch lengths beyond six monomer units due to the insensitivity of the chemical shifts measured. This makes it difficult to distinguish long chain branches from short chain branches that are larger than six carbons in polyethylenes [17].

Janzen and Colby[17] attempted to quantify LCB content via η_0 and molecular weight data via a phenomenological approach originally proposed by Lusignan *et al.*[18]

$$\eta_0 = AM_b\left[1+\left(\frac{M_b}{M_c}\right)^{2.4}\right]\left(\frac{M_w}{M_b}\right)^{s/\gamma} \qquad (2.1\text{-}2)$$

where *A* is a temperature dependant material factor, M_b is the molecular weight between branches, M_c is the critical molecular weight for entanglements, M_w is the weight average molecular weight, and s/γ is

$$\frac{s}{\gamma} = \max\left[1,\frac{3}{2}+\left(\frac{9}{8}\right)B*\ln\left(\frac{M_b}{90M_{Kuhn}}\right)\right] \qquad (2.1\text{-}3)$$

where M_{Kuhn} is the molecular weight of a statistical Kuhn segment (~146 g/mol for PE)[9] and *B* is a material specific constant (~6.0 for PE) [9]. M_b can be calculated if a Cayley tree structure is assumed (see Fig. 2.3.25) and the number of branch points, α, is known

$$M_b = \left[\frac{2\alpha}{M_1} + M_w^{-1}\right] \qquad (2.1\text{-}4)$$

where M_1 is the repeat unit molecular weight[19]. Janzen and Colby[17] found that the η_0 enhancement was a function of the distance between branch points in peroxide-induced, LCB PEs. Doerpinghaus[9] illustrated the effect of LCB content on the reduced η_0 using the Janzen and Colby[17] relationship (Fig. 2.1.3), where reduced zero-shear viscosity was defined as the viscosity of the branched resin divided the zero-shear viscosity for a linear material of the same molecular weight. Notice that for a given MW, the reduced η_0 passed through a maximum before dropping to values lower than its linear counterpart. Janzen and Colby[17] claimed that their method was capable of detecting branching content as low as 1 LCB in 10^6 carbon atoms [17].

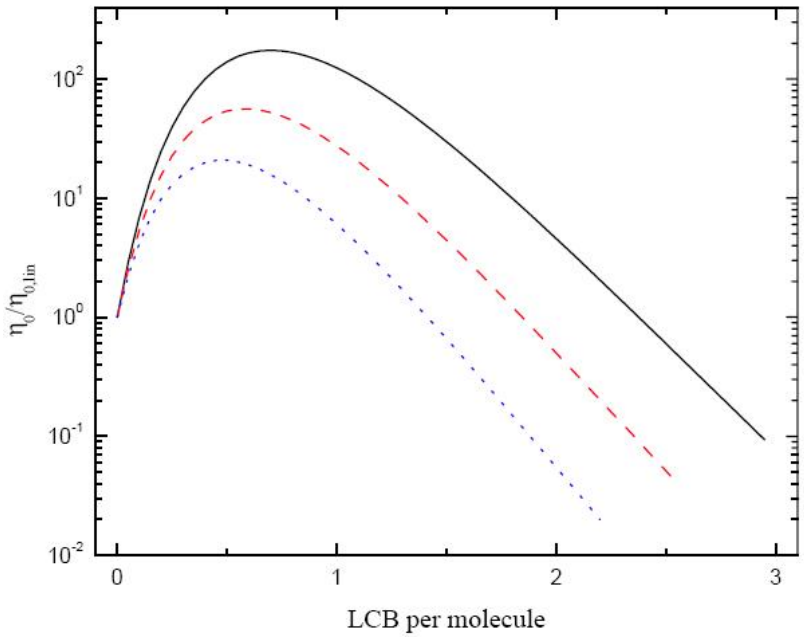

Figure 2.1.3 Predicted reduced zero-shear viscosity as a function of LCB using the Janzen and Colby[17] viscosity relationship for constant molecular weights equal to 100,000 g/mol *(line)*, 88,000 g/mol *(dots)*, and 120,000 *(dashes)* [9].

2.1.2 – The Effect of Molecular Architecture on Shear Material Functions

The rheological response of polymeric melts is more complex than that of Newtonian fluids. An incompressible Newtonian fluid at a constant temperature has it velocity and stress defined by two material constants, density and viscosity. However, an incompressible non-Newtonian fluid characterized in isothermal flows yields material functions beyond just viscosity such as those associated with fluid elasticity and memory that vary with factors such as shear rate, frequency, and time. These material parameters serve to characterize fluids in the framework of specific constitutive equations.

Fundamental to any discussion on material functions are the flow types used to characterize polymeric materials. Two flows commonly used are shear flow and shear-free flow. Relative material particle motion is noticeably different for these two types of flow as is the type of material information that can be gathered. For example, extensional viscosity measurements appear more sensitive to the certain structural components (i.e. very low levels of LCB) relative to simple steady shear flows. Understanding these flow types are important as they are dominant in many polymer processing processes (i.e. film blowing, film casting, and injection molding).

Presented in the remainder of this section is a review of relevant steady and unsteady state shear flows and their corresponding material functions, a review of the relevant effects branching and molecular topology plays on the shear response with emphasis on mPEs, and a separate review on different materials response in a special kind of shear flow called step-strain. This final section is necessary as there is much debate in the literature as to the validity of the relaxation modulus data gathered at short times in step-strain experiments. Therefore, any thorough research based on step-strain experiments requires a full understanding and, therefore, a full review, of contemporary experimental results.

2.1.2.1 – Shear Flow Definitions and Material Functions

Simple shear flow is defined by the following velocity field:

$$v_x = \dot{\gamma}_{yx} y \; ; \qquad v_y = 0 \; ; \qquad v_z = 0 \tag{2.1-5}$$

where $\dot{\gamma}_{yx}$ is the time-dependant velocity gradient. The absolute value of $\dot{\gamma}_{yx}$ is known as the shear rate $\dot{\gamma}$. In Table 2.1.1 is illustrated the simple shear flow types defined in this subsection that are experimentally relevant to this work. Several other types of simple shearing flows are commonly used but are not discussed here for brevity, and readers should refer to Bird *et al.* [20] for more information.

Table 2.1.1 - Simple Shear Flow Types

Steady shear flow - *(Section 2.1.2.1.1)*	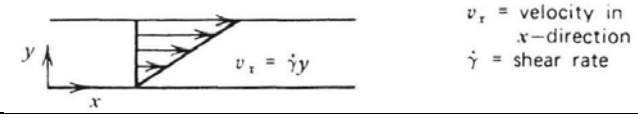
Small-amplitude oscillatory shear - *(Section 2.1.2.1.2)*	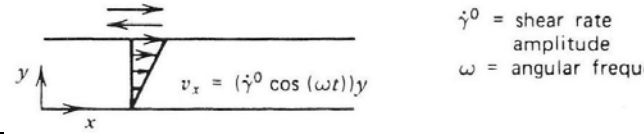
Transient stress growth *(Section 2.1.2.1.3)*	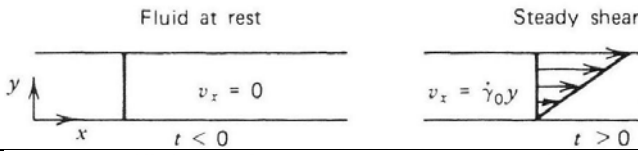
Step-strain *(Section 2.1.2.1.4)*	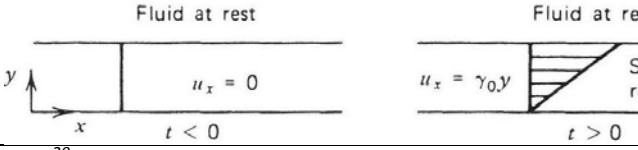

*Figures adapted from Bird *et al.*[20]

2.1.2.1.1 – Simple Steady Shear Flow Definitions and Material Functions

Steady simple shear is defined by a constant shear rate $\dot{\gamma} = \dot{\gamma}_0$. Deformation of a unit cube in steady simple shear is illustrated in Fig. 2.1.4. This type of flow provides an excellent opportunity to observe how the distance between two neighboring particles separated by an initial length l_0 on the *y*-axis evolve with time

$$l = l_0\sqrt{1 + (\dot{\gamma} t)^2} \quad \sim \quad l_0 \dot{\gamma} t \;\; \text{for large } t. \tag{2.1-6}$$

As *t* becomes sufficiently large, the length between the two particles increases linearly with time.

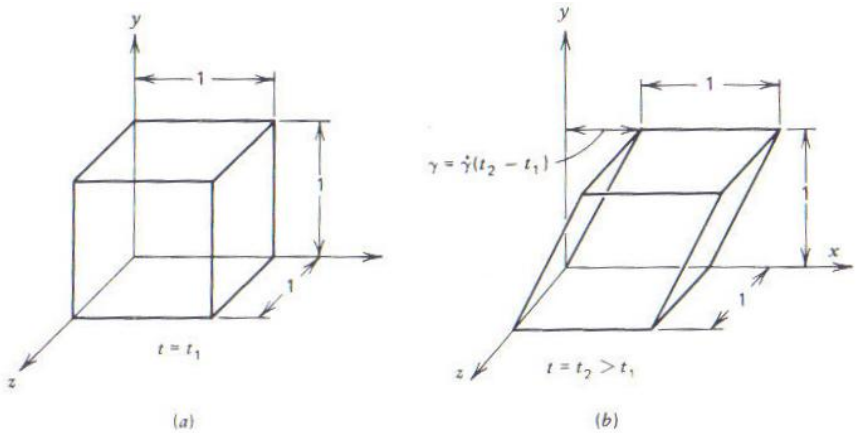

Figure 2.1.4 Steady simple shear deformation of a unit cube. Undeformed cube *(left)* and deformed cub *(right)* are shown[20].

The total stress tensor, $\boldsymbol{\pi}$, for simple shearing flow is

$$\boldsymbol{\pi} = p\boldsymbol{\delta} + \boldsymbol{\tau} = \begin{pmatrix} p + \tau_{xx} & \tau_{yx} & 0 \\ \tau_{yx} & p + \tau_{yy} & 0 \\ 0 & 0 & p + \tau_{zz} \end{pmatrix} \qquad (2.1\text{-}7)$$

where p is pressure, $\boldsymbol{\delta}$ is the identity tensor, and $\boldsymbol{\tau}$ is the molecular or "extra" stress [20]. Experimentally, the pressure and normal stresses cannot be separated in simple shear flow, thereby limiting the quantities of rheological interest to three: shear stress τ_{yx}, first normal stress difference $\tau_{xx} - \tau_{yy}$, and second normal stress difference $\tau_{yy} - \tau_{zz}$.

The stress components outlined above are linked to the resulting flow kinematics by material functions. The resulting non-Newtonian viscosity material function η in simple shear flow is defined as

$$\tau_{yx} = -\eta(\dot{\gamma})\dot{\gamma}_{yx} \, . \qquad (2.1\text{-}8)$$

Recall that for a Newtonian fluid, $\eta(\dot{\gamma})$ is a constant relative to the shear rate. In Fig. 2.1.5 is illustrated the temperature and shear rate dependence of viscosity for an LDPE[20, 21]. The shape of the viscosity curve at a given temperature has several notable features. At low shear rates, the viscosity plateaus to a value known as the zero-shear viscosity η_0. The viscosity decreases at higher shear rates, as is the case for most polymeric fluids[20]. This behavior is known as "shear-thinning" or pseudoplastic. There exists a small class of polymeric fluids that exhibit an increasing viscosity with an increasing shear rate, and are

called “shear-thickening” fluids. Information on this class of fluids can be found elsewhere[22, 23] and are not of interest to our specific research.

The material functions for first and second normal stress coefficients, $\boldsymbol{\Psi_1}$ and $\boldsymbol{\Psi_2}$, are given by

$$\tau_{xx} - \tau_{yy} = -\boldsymbol{\Psi_1}(\dot{\gamma})\dot{\gamma}_{yx}^2 \qquad (2.1\text{-}9)$$

$$\tau_{yy} - \tau_{zz} = -\boldsymbol{\Psi_2}(\dot{\gamma})\dot{\gamma}_{yx}^2. \qquad (2.1\text{-}10)$$

$\boldsymbol{\Psi_2}$ is usually 10% of $\boldsymbol{\Psi_1}$, and is negative. For Newtonian fluids, $\boldsymbol{\Psi_2}$ and $\boldsymbol{\Psi_1}$ are both equal to zero as only a shearing force is needed to maintain steady shear flow between two plates. Conversely, a normal force is required to keep the plates together in shearing flows for non-Newtonian polymeric melts, leading to non-zero values of $\boldsymbol{\Psi_1}$ and $\boldsymbol{\Psi_2}$ [20].

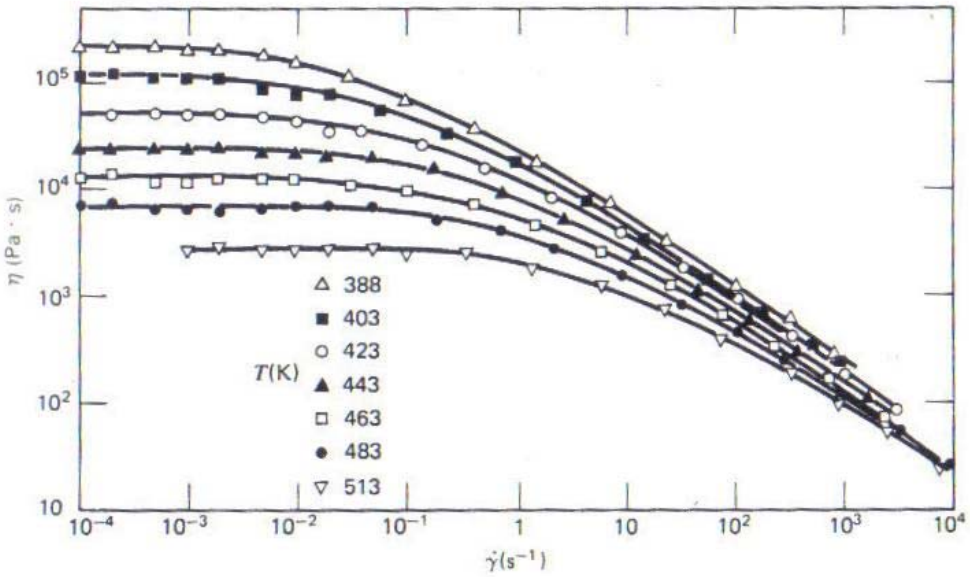

Figure 2.1.5 Shear-shear dependant viscosity of LDPE Melt 1 measured at different temperatures[20, 21].

Another interesting region of the viscosity curve for a shear-thinning material is the “power-law” region at higher shear rates where a linear relationship is seen between log η and log $\dot{\gamma}$. The region of transition from the zero-shear region to power-law region increases and shifts to lower shear rates with increasing MWD [24]. Lastly, at very high shear rates the viscosity may again become independent of shear rate, reaching a plateau at the “infinite-shear-rate viscosity” η_∞. However, it is experimentally

difficult to measure η_∞ in polymeric melts due to either the onset of degradation or melt fracture in the sample material prior to obtaining high enough shear rates[20].

In Fig. 2.1.5 it is shown that the measured viscosity decreases for all shear rates as the temperature increases, but the general shape of the curve does not change. Instead, the zero-shear viscosity decreases with increasing temperature and the onset of shear-thinning is shifted to higher shear rates. A shift factor, a_T, is used to produce a master curve at some reference temperature, T_0, from data collected at various temperatures and shear rates. a_T is defined as $\eta_0(T)/\eta_0(T_0)$ for fluids of nearly constant density. This master curve is illustrated in Fig. 2.1.6 for the LDPE data from Fig. 2.1.5. The shear rate is shifted by multiplying by a_T, and the viscosity is shifted by dividing by a_T. The first and second normal stress coefficients, $\boldsymbol{\Psi_1}$ and $\boldsymbol{\Psi_2}$, are shifted by dividing through by (a_T^2) [20].

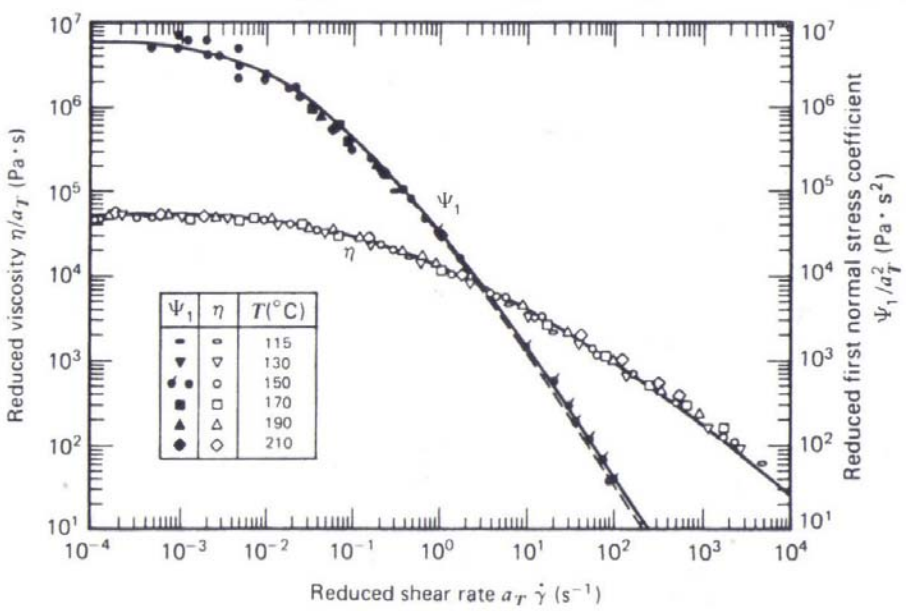

Figure 2.1.6 Master viscosity and first normal stress coefficient for LDPE Melt 1 at 150 °C. Data was shifted across a wide range of temperatures using the shift factor a_T [20].

2.1.2.1.2 – Dynamic Oscillatory Simple Shear Flow Definitions and Material Functions

Small-amplitude oscillatory shear experiments provide the ability to capture the linear viscoelastic behavior of a material over several frequency decades in one test. Similar to steady shear

flows, the only three measurable quantities of importance are the viscosity and two normal stress differences. These are represented by the time-dependant and shear rate-dependent analogs of η, $\boldsymbol{\Psi_1}$, and $\boldsymbol{\Psi_2}$. Of interest to our research are small-amplitude oscillatory shearing, transient start-up of shear flow, and step-strain experiments.

In small-amplitude oscillatory shear experiments, the unsteady material response is measured for a flow in which a sample is placed between two plates, and the top plate is oscillated sinusoidally at small amplitudes with a frequency ω. The shear strain and shear rate are given by

$$\gamma_{yx}(0,t) = \gamma^0 \sin(\omega t) \tag{2.1-11}$$

$$\dot{\gamma}_{yx}(0,t) = \gamma^0 \omega \cos(\omega t) = \dot{\gamma}^0 \cos(\omega t) \tag{2.1-12}$$

where γ^0 and $\dot{\gamma}^0$ are the positive amplitudes of the shear strain and shear rate oscillations. The resulting material input and output responses are illustrated in Fig. 2.1.7. For a polymeric fluid, the shear stress response oscillates at the same frequency of ω, but out of phase with both the shear strain and strain rate.

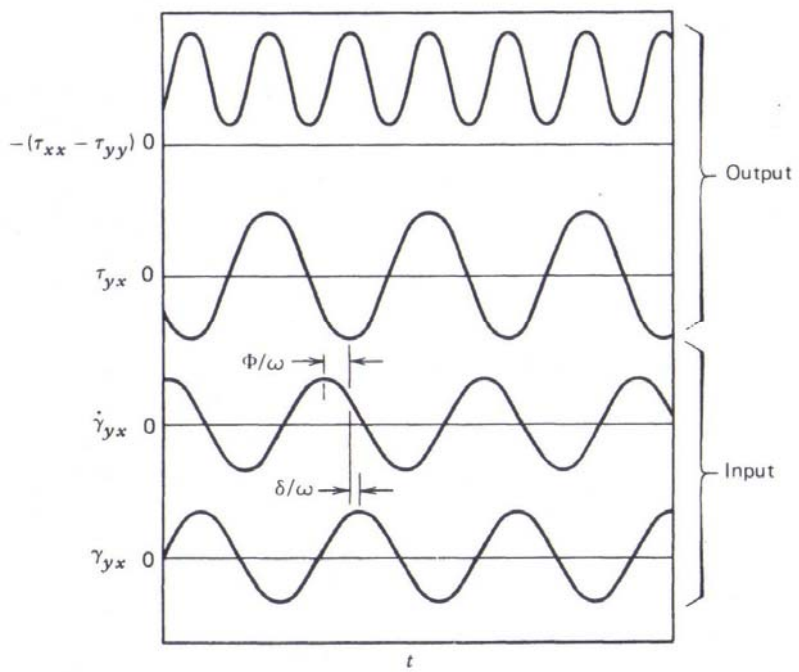

Figure 2.1.7 Oscillatory shear stress and normal stress responses stemming from the corresponding oscillatory shear strain and shear rate input [20].

Assuming the shear strain amplitude is sufficiently small so that the shear stress is linear in strain, τ_{yx} is given by two equivalent sets of viscoelastic material functions *G′*, *G″* and η', η''

$$\tau_{yx} = -G'(\omega)\gamma^0 \sin(\omega t) - G''(\omega)\gamma^0 \cos(\omega t) \quad (2.1\text{-}13)$$

$$\tau_{yx} = -\eta'(\omega)\gamma^0 \cos(\omega t) - \eta''(\omega)\gamma^0 \sin(\omega t). \quad (2.1\text{-}14)$$

The storage modulus *G′* $(= \eta''\omega)$ is thought of as the elastic component of the fluid, or the amount of energy stored during deformation. Likewise, the loss modulus *G″* $(= \eta'\omega)$ is thought of as the viscous component of the fluid, or the amount of energy dissipated during deformation. Both *G′* and *G″* can undergo time-temperature superposition by shifting the frequency by the shift factor a_T discussed above. For a Newtonian fluid, *G′* is equal to the constant shear modulus *G*, η' is equal to the Newtonian viscosity μ, and *G″* and η'' are equal to zero. Experimental results for small-amplitude oscillatory shear tests are traditionally reported as the absolute values of the complex modulus $|G^*|$ and complex viscosity $|\eta^*|$ which are calculated using their real and imaginary portions

$$G^* = G' + iG'' \quad (2.1\text{-}15)$$

$$\eta^* = \eta' - i\eta'' \quad (2.1\text{-}16)$$

$$|G^*| = \sqrt{G'^2 + G''^2} \quad (2.1\text{-}17)$$

$$|\eta^*| = \sqrt{\eta'^2 + \eta''^2}. \quad (2.1\text{-}18)$$

The Cox-Merz rule[25] is used to relate the absolute value of complex viscosity measured in oscillatory shear with the viscosity measured in steady shear through

$$\eta(\dot{\gamma}) = |\eta^*(\omega)| \text{ for } \omega = \dot{\gamma}. \quad (2.1\text{-}19)$$

This relationship has been observed to be valid for a large number of polymeric melts[2, 19, 26, 27], and provides a means for obtaining shear viscosity over a large range of shear rates (frequencies) with relatively few tests. Dynamic oscillatory shear experimental results can be used to fit the linear viscoelastic parameters in constitutive models.

2.1.2.1.3 –Transient Simple Shear Flow Definitions and Material Functions

Unsteady simple shearing flow experiments provide useful rheological information via the transient response of polymeric melts. Transient stress growth experiments analyze a material's response in the startup of steady shear flow at a constant shear rate $\dot{\gamma_0}$. Transient material functions $\eta^+(t,\dot{\gamma_0})$, $\mathbf{\Psi_1}^+(t,\dot{\gamma_0})$, and $\mathbf{\Psi_2}^+(t,\dot{\gamma_0})$ are defined analogously to Eqs. 2.1-8 through 2.1-10, with the "plus sign" indicating transient behavior.

$$\tau_{yx} = -\eta^+(\dot{\gamma})\dot{\gamma}_{yx} \tag{2.1-20}$$

$$\tau_{xx} - \tau_{yy} = -\mathbf{\Psi_1}^+(\dot{\gamma})\dot{\gamma}_{yx}^2 \tag{2.1-21}$$

$$\tau_{yy} - \tau_{zz} = -\mathbf{\Psi_2}^+(\dot{\gamma})\dot{\gamma}_{yx}^2. \tag{2.1-22}$$

In Fig. 2.1.8 is shown the transient shear stress growth curves for an LDPE. At low shear rates, a steady-state value is reached in a monotonic fashion, with no overshoot. This particular viscosity curve forms an envelope that serves as an upper bound for the transient viscosity curves measured at higher shear rates. As shear rate increases, the magnitude of the stress overshoot increases and the steady-state viscosity decreases. These experiments in tandem with transient extensional stress growth experiments provide a set of data used for testing the nonlinear robustness of constitutive rheological models described in section 2.3.

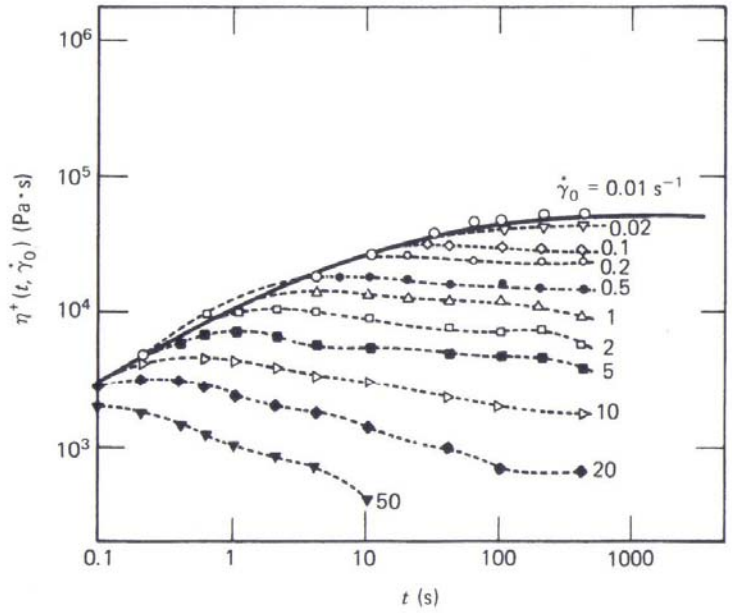

Figure 2.1.8 Transient shear stress growth for LDPE Melt 1 for various shear rates. Linear viscoelastic response given by solid line [20].

2.1.2.1.4 –Step-strain Flow Definitions and Material Functions

The final simple shearing flow experiment relevant to this research is stress relaxation following a sudden shearing displacement, commonly called step-strain experiments. An "instantaneous" shear strain γ_0 is imposed on a fluid at rest so that

$$\dot{\gamma}_{yx} = \gamma_0 \delta(t) \tag{2.1-21}$$

where $\delta(t)$ is the Dirac delta. The resulting stress relaxation $G(t, \gamma_0)$ is measured for $t > 0$. Material functions for step-strained are defined as

$$\tau_{yx} = -G(t, \gamma_0) * \gamma_0 \tag{2.1-22}$$

$$\tau_{xx} - \tau_{yy} = -G_{\Psi_1}(t, \gamma_0)\gamma_0^2. \tag{2.1-23}$$

It is found that after some characteristic time τ_k the behavior of the relaxation modulus becomes independent of strain, leading to a time-strain factorability form of the relaxation modulus

$$G(t, \gamma_0) = G^0(t) * h(\gamma_0). \tag{2.1-24}$$

$G^0(t)$ is the time-dependant modulus in the linear range and $h(\gamma_0)$ is the strain-dependant damping function that can be determined from either theoretically from constitutive relationships or experimentally by shifting the relaxation modulus curves at long times for a variety of strains. In Fig. 2.1.9 is illustrated this time-strain separability for a blend of 20% polystyrene in Aroclor[20, 28]. Time-strain separability is seen beyond timescales larger than 20 seconds. Discussion on the significance of the both short-time and long-time behavior is covered in section 2.1.2.3.

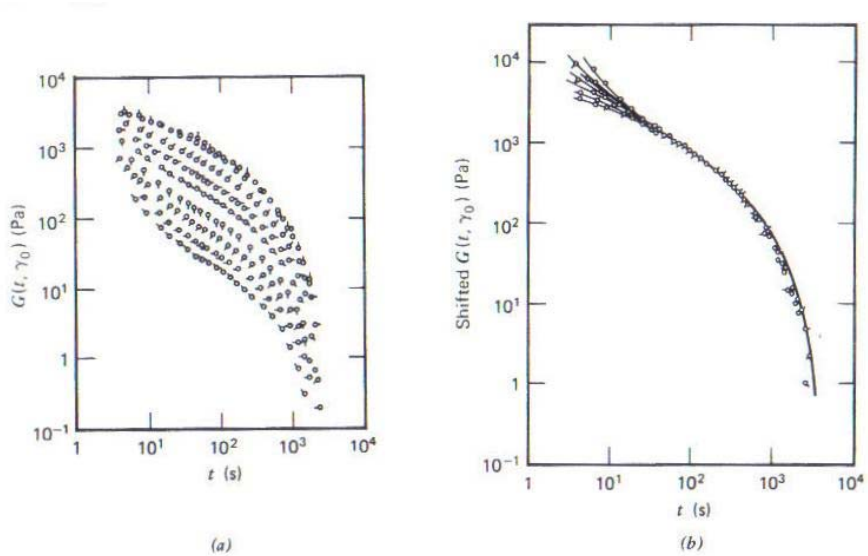

Figure 2.1.9 Shear stress relaxation modulus for 20% polystyrene in Aroclor. Initial shear strains range from 0.41 to 25.4. Strain values increase from top to bottom for the unshifted modulii *(left)*. Shifted modulii *(right)* for the same data show time-strain separability at times greater than 20 seconds [20, 28].

While it is common practice to measure step-strain in a strain controlled rheometer with a cone-and-plate fixture, Stadler *et al.*[29] measured the relaxation response using a stress-controlled rheometer with a parallel plate geometry in order to achieve higher values of strain. The parallel plate geometry was found to be able to measure higher values of strain due to a lower sensitivity to gap errors relative to the cone and plate geometry[29]. A "creep test" was imposed with the maximum stress acting until the desired deformation was achieved. The upper limit of strain was determined solely by the material instead of the rheometer rotation for stress controlled experiments. Inhomogeneous flow fields in the

form of strain amplitude variation as a function of radius required a correction[30] of the apparent relaxation modulus G_{app} measured by the rheometer

$$G(t,\gamma_0) = G_{app}(t,\gamma_0)\left(1+\frac{1}{4}\frac{d\log G_{app}}{d\log\gamma_0}\right). \quad (2.1\text{-}27)$$

2.1.2.2 – Effect of Molecular Architecture on Simple Shear Behavior

This section addresses four major molecular factors that can affect the shear rheological response. Molecular weight, molecular weight distribution, SCB content, and LCB content effects are investigated. Emphasis is placed on the behavior of sparsely-branched mPEs as they are systems of particular interest in this research. The shear response of the model polymer architectures is reserved for a later discussion (section 2.2).

Change in molecular weight directly impacts the simple shear rheological response. A well known relationship in literature[20] is the molecular weight, *M*, dependence of the zero-shear viscosity

$$\eta_0 = k * M \text{ for } M < M_C \quad (2.1\text{-}28)$$

$$\eta_0 = k * M^{\alpha} \text{ for } M > M_C \quad (2.1\text{-}29)$$

where *k* is a material constant and M_C is the critical molecular weight for the onset of entanglements, and has a value on the order of two times the entanglement molecular weight M_e for most polymeric melts[14]. Increases in molecular weight of the polymer melt results in an increase in the number of chain segments whose motion must coordinate during deformation. At the critical molecular weight, a marked increase in the molecular weight dependence of viscosity is seen due to the presence of entanglements between molecules. For a wide range of materials, $\alpha = 3.4$ [20, 31]. Münstedt and Auhl[14] found $\alpha = 3.6$ for HDPE across a wide range of molecular weights and molecular weight distributions. Münstedt and Auhl[14] also concluded that polydispersity did not affect zero-shear viscosity values in HDPE with MWD between 1.4 to 8. This finding was consistent with other works[6, 14, 32, 33] that showed that MWD did not affect the relationship given in Eq. 2.1-29 for a variety of materials.

Münstedt and Auhl[14] found that the type of long-chain branching affected the zero-shear response for a given molecular weight. Metallocene catalyzed HDPE and LLDPE resins characterized by long branches were seen to have enhanced zero-shear viscosities for given molecular weight relative to Eq. 2.1-29. Polyethylenes polymerized by high-pressure reaction characterized by many relatively short branches were seen to have reduced zero-shear viscosities relative to Eq. 2.1-26 [14]. Both sets of materials were described by the well-known relationship[14, 34, 35]

$$\eta_0 \propto exp\left(\frac{M_a}{M_e}\right) \tag{2.1-30}$$

where M_a is the molar mass of the branches.

Doerpinghaus and Baird[19] investigated the effect of sparse long-chain branching (< 1 LCB per 10^4 carbons) on the viscous response for metallocene catalyzed LLDPEs. The authors used a shift factor based on the zero-shear viscosities to isolate the effect of LCB from differences in molecular weight in three sparsely branched commercial polyethylenes with similar MWDs (Affinity PL1840, Affinity PL1880, and Exact 0201), using a linear LLDPE (Exact 3132) as the reference material. Also investigated for comparison was a highly branched LDPE (NA952) and a linear LLDPE with a high MWD (NTX 101). In Fig. 2.1.10 is illustrated the shifted shear viscosity curves for each material. η_0 enhancement was seen for the sparsely branched materials, with shifted η_0 increasing with LCB content. The highly branched NA952 showed a marked decrease in the shifted η_0. The authors attributed this behavior of the η_0 relative to LCB content within the phenomenological framework of the aforementioned work of Janzen and Colby[17] (see Fig. 2.1.3), finding the behavior to be in qualitative, but not quantitative, agreement with Eq. 2.1-2. Doerpinghaus and Baird[19] also found that varying the MWD had relatively little effect on the value of the shifted η_0 in that the broad MWD resin overlapped the narrow MWD at short frequencies which was in agreement with literature[6, 14, 32, 33]. It has also been seen elsewhere in literature that increases in LCB or MWD increases the onset and severity of shear thinning[4, 36].

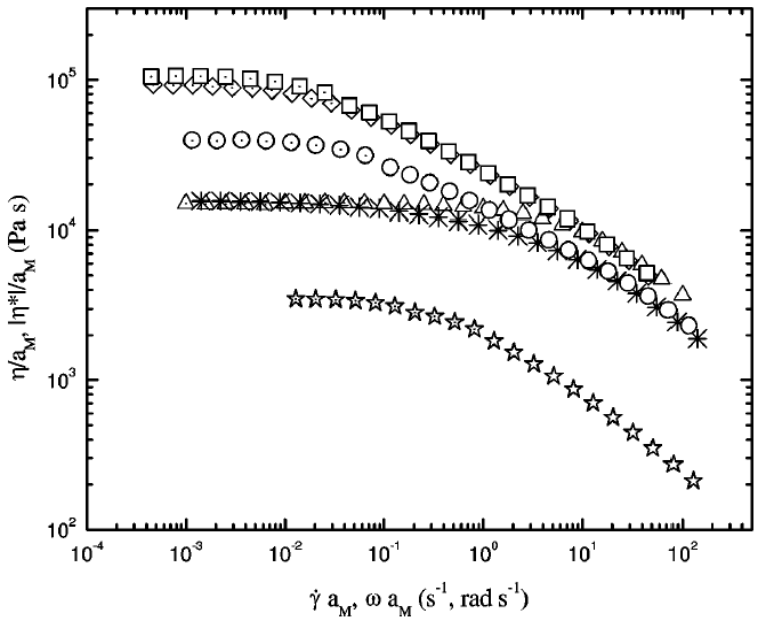

Figure 2.1.10 Shifted steady shear viscosity curves (M_{ref} = 111,000 g/mol) for the sparsely branched Exact 3132 (◊), Affinity PL1840 (□), and Affinity PL1880 (○), the highly branched LDPE NA952 (☆), the linear LLDPE with a large MWD NTX101 (✳), and the linear reference material Exact 3132 (Δ). Dotted symbols represent steady shear measurements; open symbols represent dynamic oscillatory measurements[19].

Doerpinghaus and Baird[19] also analyzed the effect of sparse LCB on two indicators of elastic properties: the storage modulus, *G'*, and the primary normal stress difference, N_1 (Figs. 2.1.11a and b). At lower frequencies, the sparsely branched resins showed a marked increase in *G'* relative to the linear resins. The broad MWD linear NTX 101 also displayed an enhanced *G'* at the same low frequencies, suggesting that while broadening MWD does not affect η_0, it can affect *G'*. It was observed that the sparsely-branched resins merged with the linear resins at higher frequencies. The authors attributed this to branching being present only on the longer backbones. Therefore, the shortest backbones were predominately linear and dominated the elastic response at higher frequencies[19, 26]. Similar findings were found for the primary normal stress difference, N_1, with the sparsely branched resins having higher values of N_1 than either linear resin. Breadth of MWD was also seen to increase N_1, but not to the degree of branching.

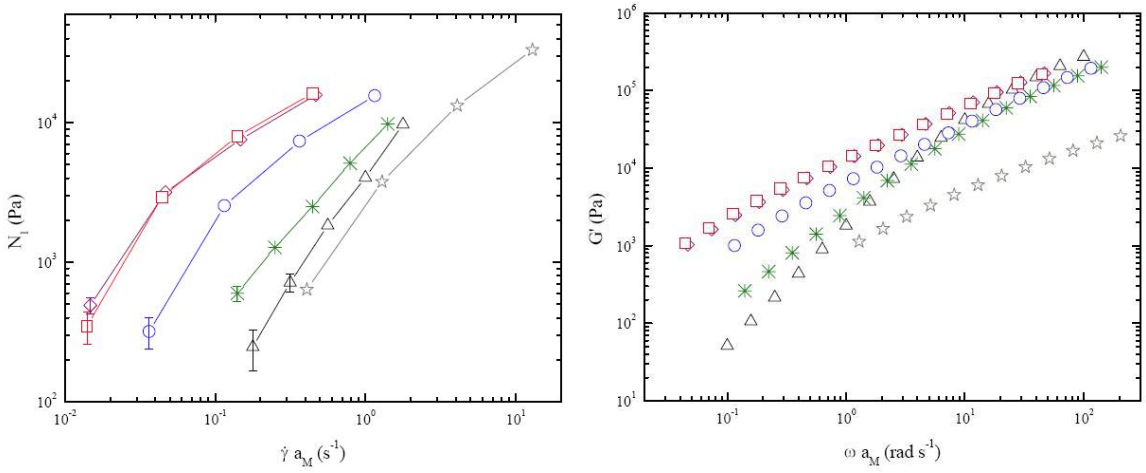

Figure 2.1.11 Shifted dynamic storage moduli *(left)* and shifted primary normal stress difference *(right)* (M_{ref} = 111,000 g/mol) for the sparsely branched Exact 3132 (◊), Affinity PL1840 (□), and Affinity PL1880 (○), the highly branched LDPE NA952 (☆), the linear LLDPE with a large MWD NTX101 (✳), and the linear reference material Exact 3132 (Δ). All measurements were taken at 150 °C [19].

Wood-Adams *et al.*[37] investigated the effect of variation in the degree of sparse LCB in mHDPE on the measured shear response. Shown in Fig. 2.1.12 is the shear viscosity of several mHDPEs with varying degrees of LCB (0 to 0.79 LCB per 10^4 C). As LCB content increased, so did η_0 which was in qualitative agreement with Janzen and Colby[17] for low levels of branching. The authors also found that the loss angle was a sensitive indicator of the amount LCB branching for the same series of sparsely branched mHDPEs (Fig. 2.1.13). This behavior was also seen by Koopmans[38] in the comparison of the response of an LDPE, an LLDPE, and two branched mPEs [37].

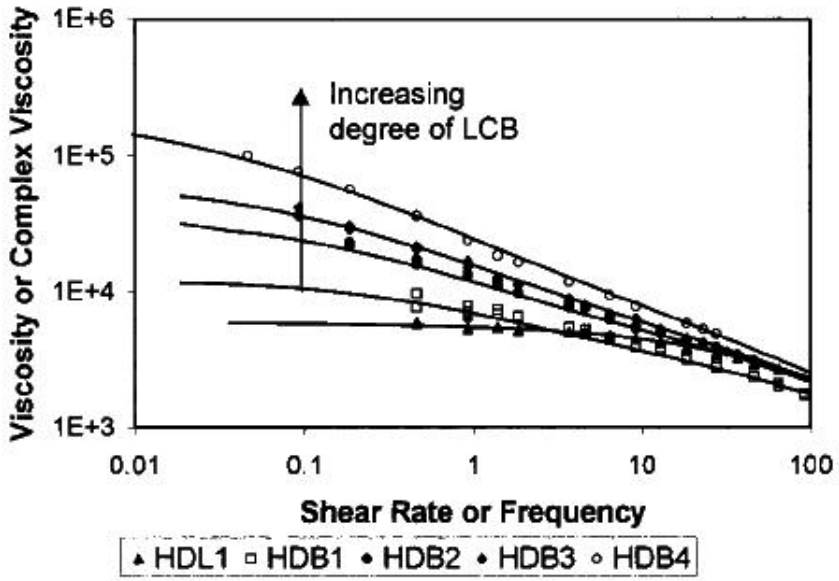

Figure 2.1.12 Shear viscosity (symbols) and complex viscosity (lines) data for metallocene catalyzed HDPE with varying degrees of long-chain branching[37].

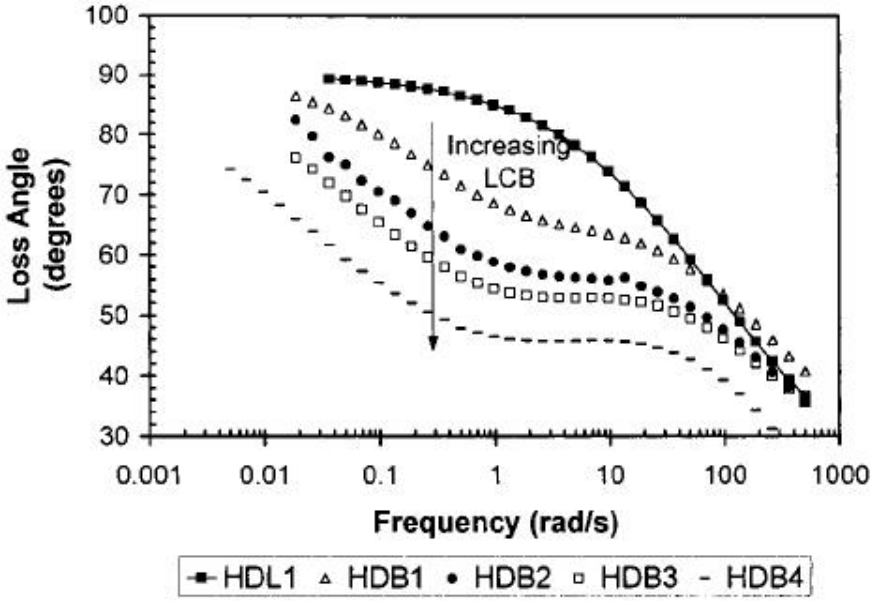

Figure 2.1.13 Effect of LCB on loss angle for sparsely-branched HDPEs at 150 ^{o}C[37].

Because sparsely-branched mLLDPEs contain both SCB and LCB (see Fig. 2.1.2), a brief discussion on their differing behaviors in shear is presented. Vega *et al.*[39] observed distinct differences in the behavior of long-chain branched polyethylenes versus purely short-chain branched polyethylenes of similar MWD and MW in small-amplitude oscillatory shear flow measurements. The dynamic viscosity

at low frequencies was significantly higher for the LCB materials relative to the SCB materials. LCB materials exhibited higher values of the elastic modulus compared to SCB of similar MWD and MW, but on the same order of magnitude as those SCB resins with a higher MWD. Finally, the LCB exhibited higher activation energies of flow than their SCB counterparts[39].

2.1.2.3 – Review of Step-strain

Step-strain tests are used to determine the strain dependence of the relaxation modulus. Recall that step-strain tests are defined by a sudden shearing displacement on a fluid at rest to some strain γ_0. Beyond some characteristic time τ_k after the imposition of a step shear strain, the relaxation modulus, *G(t,γ)*, can be factored into separate time and strain functions for most polymers[30, 40, 41]

$$G(t,\gamma) = G^0(t)h(\gamma). \qquad (2.1\text{-}31)$$

where $G^0(t)$ is the linear relaxation modulus, and $h(\gamma)$ is the strain dependant damping function. This phenomenon is known as time-strain separability[42-44] (see Fig. 2.1.9 for example of this behavior). The behavior of polymeric melts, both before and after τ_k, is not fully understood, thereby leading to much debate in the literature as to why differences in the shape of the relaxation and damping function curves are seen for different materials. Therefore a brief review of contemporary works is deemed necessary for any intelligent research pertaining to a material's step-strain response.

2.1.2.3.1 – Material Response Prior to Time-Strain Separability

Much of the disagreement in the literature stems from mechanical problems inherent in a rheometer's imposition of strain. Three major issues arise in the literature. The first is created by the fact that it is physically impossible with current rheometer technology to instantaneously shear a fluid to a desired strain. Instead, there exists some finite rise time for the imposition of strain. This finite rise time is a point of contention as it is unknown if the data preceding τ_k is truly accurate or an artifact of

the experimental apparatus. Vega and Milner[42] asserted that in the framework of the BKZ constitutive model, the finite rise time was the primary reason time-strain separability was not observed until some time τ_k. Sui and McKenna[45] attributed deviations at short times to different loading times of the normal force and torque response (i.e. reaching maximum value) in linear and dendritic PIB. Venerus[46] simulated the effect of finite rise time on the response of the relaxation modulus, finding that differences at times less than τ_k was still seen as a function of the imposed strain. This suggests that the short time response prior to τ_k was realistic, and not an artifact of the experimental apparatus. Stadler *et al.*[29] stated that the finite-rise (step) time had no relevant influence on the relaxation modulus after times longer than ten times the step time. Venerus and Kahvand[47] found for a PS solution with an average of seven entanglements per molecule that the measured shear stress was independent of the step time for times roughly three times larger than the finite rise time.

Second, transducer overloads and material ruptures can occur at higher strains for materials with a high plateau modulus, such as some entangled polyethlyenes[42]. Transducer overloads have been shown to be avoidable by utilizing plate fixtures with smaller diameters (i.e. 10mm instead of 25mm)[48-50]. This allows for relaxation measurements taken at higher values of strain due to the smaller sample size. However, this reduced sample size causes reduced accuracy and increased error at long times [42]. Stadler *et al.*[29] argued that sample rupture was not present in melts that had a measurable damping function, $h(\gamma)$. The authors argued that the sample rupture would have changed the shape of the relaxation modulus thereby making the measurement of a realistic $h(\gamma_0)$ impossible. This finding made the detection of rupture simpler in that a complicated and expensive rheo-optical measurement systems was not necessary[29].

Third, wall slip at the polymer-plate interface was found to be a major source of error in step-strain [44, 51]. Wall slip occurs when the wall stress exceeds some threshold that the surface bond between the polymeric melt and the wall. If slip occurs, the applied strain is lower than the desired

strain. Wall slip depends on the surface characteristics and the dynamic modulus at timescales on the order of the applied strain. This causes the measured damping function, $h(\gamma)$, to be too small[42], thereby causing a "kink" in the damping function curve as strain is increased[46]. Vega and Milner[42] observed the deformation of a vertical line initially drawn on the undeformed sample to confirm the presence/absence of wall slip. If the line deformed affinely with the plates, slip was not present. Likewise if the line was under-deformed, slip was present. Vega and Milner[42] also observed that slip occurred in well-entangled polyethylenes at strains as low as 2.0. Sanchez-Reyes and Archer[44] found that slip could be mitigated in well-entangled polystyrenes ($\geq$ 37 entanglements) by attaching a single layer of micron-sized glass beads to the plate surface. Vega and Milner[42] reduced wall-slip and transducer overload by blending low MW PE with entangled PE.

It has also been proposed in several theories that the relaxation modulus' behavior prior to τ_k is not a mechanical artifact. Vega and Milner[42] found disagreement in the literature as to the reason for a material's behavior at times less than τ_k. Some works claimed the value of τ_k was related to the time required for a complete relaxation of the contour length, τ_s, via $\tau_k \sim \tau_s \sim 4\tau_R$, where τ_R is the longest Rouse time of the chain[52, 53]. Other, more contemporary, results[44, 54] suggested that τ_k was not dictated by τ_R. Measurements of the dynamic moduli for well-entangled linear polystyrene solutions displayed time-strain superposition at times comparable to the terminal relaxation of the chain τ_d ($\sim\tau_k$). For weakly entangled systems, values of τ_s approach τ_k. Seay[2] attributed the differences at short times to the delayed (retarded) stretch relaxation of branched polymers versus that of linear materials. Sparsely-branched polyethylene resins were found to have a larger value of τ_k compared to a linear polyethylene of similar MWD and MW. The presence of multiple branch points was theorized to have served as "pinning-points" that increased the time required for a material relax especially at higher strains, thereby increasing the value of τ_k [2].

Regardless of the origin of such short-time behavior, the imperfect strain history caused by the finite rise time must be accounted for in any constitutive modeling. Sui and McKenna[45] cited a correction necessary for any constitutive modeling of $G(t,\gamma)$ originally put forward by Zapas and Craft[55] to correct for the imperfect strain history that arose from the finite rise time

$$t_{corrected} = t - \frac{\tau}{2} \qquad (2.1\text{-}32)$$

where t was the raw measured experimental time, $t_{corrected}$ was the corrected time, and τ was the finite time required to impose the desired strain. τ was determined to be the time at which the normal force and torque response reached their maximum value [45]. τ was found to occur on timescales less than the onset of time-strain separability, τ_k, for linear and dendritic PIB [45].

2.1.2.3.2 – Material Response after Time-Strain Separability

While the short times of the relaxation modulus are of primary interest to our work, the behavior beyond τ_k is useful in that it has been linked to the molecular structure of the melt. Stadler *et al.*[29] summarized contemporary works that highlighted the effect of molecular structure on the behavior of time-strain superposition in literature. The damping function, $h(\gamma_0)$, was found to be independent of molar mass[56, 57] and temperature[56, 58, 59] in linear polymer melts. MWD has been shown to affect the value of $h(\gamma_0)$ [60-62]. The chemical structure has been shown to affect $h(\gamma_0)$, for example, in commercial linear PE and PP [63]. The damping function of LCB polymers with multiple branch points (both commercial resins and model systems) had been shown[43, 48, 59, 63] to have a weaker dependence on strain than their linear counterparts. Hepperle and Münstedt[59] observed that increasing arm length in nearly monodisperse combs reduced the strain dependence of $h(\gamma_0)$. Polymeric melts of three- and four-armed star (only one LCB branch point) have shown only weak deviation from the non-linear behavior of linear polymer melts[34, 64, 65]. The exact reason for such a wide variety of strain dependences of $h(\gamma_0)$ is unknown. It has been theorized that the non-linear strain dependence originated from the induced

chain anisotropy and the decrease in entanglement density induced by the large shear amplitutde[29]. For branched polymers, the retarded relaxation of the backbone chain due to the pinned branch points was theorized to be the reason for the weaken strain dependence of $h(\gamma_0)$ [66].

Formulations modeling the strain dependence of $h(\gamma_0)$ have been proposed to describe the non-linear response of polymeric melts. An expression based on the Doi-Edwards (DE) tube model [52] with independent alignment

$$h(\gamma_0) = \frac{\alpha}{\alpha+\gamma_0^{\beta}} \qquad (2.1\text{-}33)$$

was found to accurately model the damping function seen in linear and some star polymer melts with narrow MWD [34, 59, 65]. No physical meaning was given for the coefficients α and β, but values of α = 5 and β = 2 were suggested[34, 59, 67, 68]. Eq. 2.1-33 was shown to be unable to describe systems with high MWD or LCB [29]. The proposed Papanastasiou-Scriven-Macosko (PSM) model was Eq. 2.1-33 with α = 7.8 and β = 2. Soskey and Winter[30] proposed a similar model, but with adjustable parameters α (= 1/*a*) and β (= *b*).

Stadler *et al.*[29] observed that the shape of $\log h(\gamma_0)$ versus log γ_0 resembled that of a simple shear viscosity curve. In Fig. 2.1.14 is shown the typical response of $\log h(\gamma_0)$ plotted as a function of log γ_0, which is similar in shape to the curve given in Fig. 2.1.14. Stadler *et al.*[29] proposed a numerical damping function based on the Carreau-Yasuda model originally developed for shear viscosity profiles[69, 70]

$$h(\gamma_0) = \left[1 + \left(\frac{\gamma_0}{\gamma_c}\right)^b\right]^{m/b} \qquad (2.1\text{-}34)$$

where γ_c was defined as the critical deformation at which the tangent of $h(\gamma_0)$ at high strains equals one, *m* was defined as the slope of $h(\gamma_0)$ for higher strains, and *b* defined by the width of the transition zone. γ_c best described the onset of nonlinear behavior corresponding as the start of the disentanglement of the chains (retraction in DE tube model)[29, 52]. *m* best described the sensitivity of the

entanglement network toward disentanglement, and was found to not be a function of MW or MWD > 2.0 [29, 62]. It was theorized that branched polymers with more than two branch points were not able to disentangle as easy as linear polymers due to the pinned inner segments. Therefore, *m* was seen as an indicator of inner segments in the sample. *b* best described the composition of the melt. A sample with a large mixture of architectures was expected to show a larger *b* relative to a homogeneous melt (i.e. a melt of all combs) [29]. Eq. 2.1-34 was able to accurately describe a series of linear and branched PEs and a set of irradiated PPs for a large range of MWD. It was found for the same series of resins, that neither the DE or the PSM model was able to accurately describe a large portion of these materials [29].

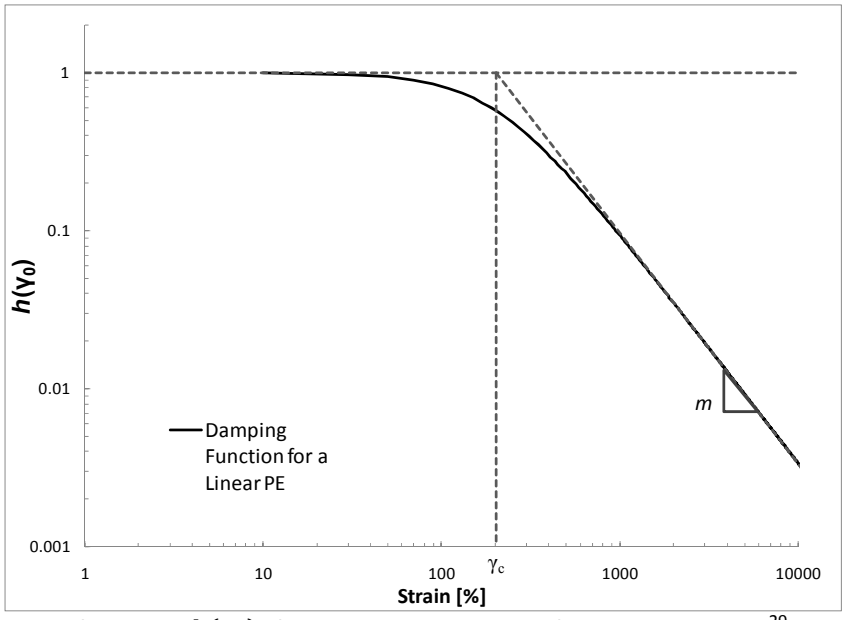

Figure 2.1.14 Damping function, $h(\gamma_0)$, for a linear PE adapted from Stadler *et al*.[29]. The general shape of the curve is preserved for a wide range of polymeric melts. Shown also are physical interpretations of the model parameters given by Eq. 2.1-34.

2.1.3 – Behavior in Extensional Flow

Shear-free flows are commonly used to access non-linear viscoelastic behavior of polymer melts. Following a brief review of the shear-free flows and material functions, the general role of molecular architecture on the rheological response is discussed, primarily in transient uniaxial extensional flow. Once again, emphasis is placed on the behavior on metallocene-catalyzed sparsely-branched PE resins

for reasons discussed in section 2.1. The third and final part of this section is a review of a phenomenon called ductile failure that can occur in uniaxial extensional flow, making it difficult to measure extensional viscosity at higher units of strain.

2.1.3.1 – Extensional Flow Definitions and Material Functions

Simple shear-free deformation is defined by the following velocity field:

$$v_x = -\frac{1}{2}\dot{\varepsilon}(1+b)x\,; \qquad v_y = -\frac{1}{2}\dot{\varepsilon}(1-b)y\,; \quad v_z = \dot{\varepsilon}z \tag{2.1-35}$$

where $0 \leq b \leq 1$ and $\dot{\varepsilon}$ is the elongational (or extension) rate. Several common shear-free flows types are defined by the choice of b: elongational flow for $b = 0$ and $\dot{\varepsilon} > 0$, biaxial stretching flow for $b = 0$ and $\dot{\varepsilon} < 0$, and planar elongational flow for b = 1 [20]. These three deformations of a unit cube are illustrated in Fig. 2.1.15. Consider the evolution of the distance between two neighboring particles separated by an initial length l_0 on the *z*-axis in shear-free deformation:

$$l = l_0 e^{\dot{\varepsilon}t} \text{ for } \dot{\varepsilon} = \text{constant.} \tag{2.1-36}$$

The exponential dependence of separation on time shows a marked increase when compared to the linear dependence seen in simple steady shear flow (Eq. 2.1-5).

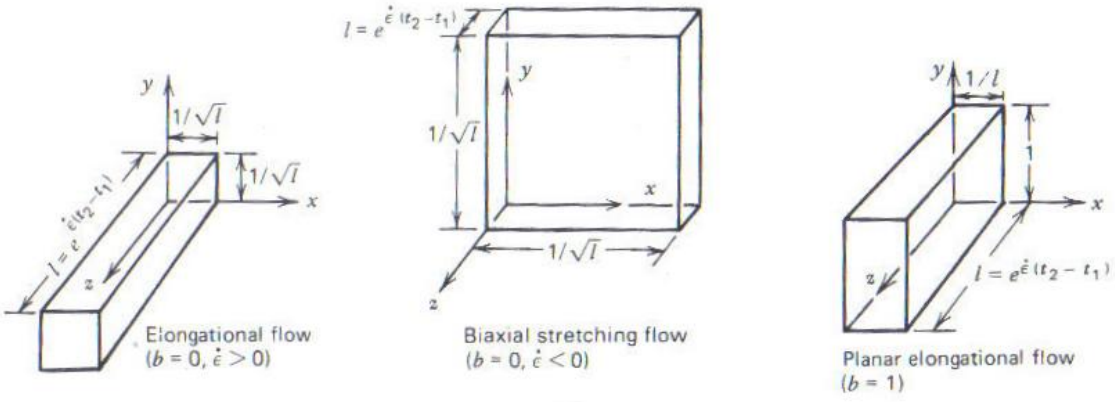

Figure 2.1.15 Three steady simple shear-free deformation of a unit cube. Undeformed cube is the same as in Fig. 2.1.4 [20].

The total stress tensor $\boldsymbol{\pi}$ for shear-free flow is

$$\boldsymbol{\pi} = p\boldsymbol{\delta} + \boldsymbol{\tau} = \begin{pmatrix} p + \tau_{xx} & 0 & 0 \\ 0 & p + \tau_{yy} & 0 \\ 0 & 0 & p + \tau_{zz} \end{pmatrix}. \qquad (2.1\text{-}37)$$

Since there are no shearing forces present in shear-free, the *xy*-component of the stress tensor is zero. Once again, limiting our analysis to incompressible fluids, the only experimental values of consequence are the two normal stress differences: $\tau_{zz} - \tau_{xx}$ and $\tau_{yy} - \tau_{xx}$. For b = 0 (elongational and biaxial stretching flows), $\tau_{yy} - \tau_{xx} = 0$ as the *x*- and *y*-directions become indistinguishable[20].

Like in shear flow, the stress field is linked to the resulting stress field by material functions. In steady simple shear-free flows, two viscosity functions, $\bar{\eta}_1$ and $\bar{\eta}_2$, relate the stress differences to the strain rate

$$\tau_{zz} - \tau_{xx} = -\bar{\eta}_1(\dot{\varepsilon}, b)\dot{\varepsilon} \qquad (2.1\text{-}38)$$

$$\tau_{yy} - \tau_{xx} = -\bar{\eta}_2(\dot{\varepsilon}, b)\dot{\varepsilon}. \qquad (2.1\text{-}39)$$

For b = 0, $\bar{\eta}_1$ equals the elongational (extensional) viscosity $\bar{\eta}$. In Fig. 2.1.16 is shown the steady elongational viscosity $\bar{\eta}(\dot{\varepsilon})$ and the viscosity $\eta(\dot{\gamma})$ for a PS melt. For low deformation rates, the uniaxial elongational viscosity is three times that of the shear viscosity. This is similar to the behavior seen in Newtonian fluids in that $\bar{\eta} = 3\mu$ [20].

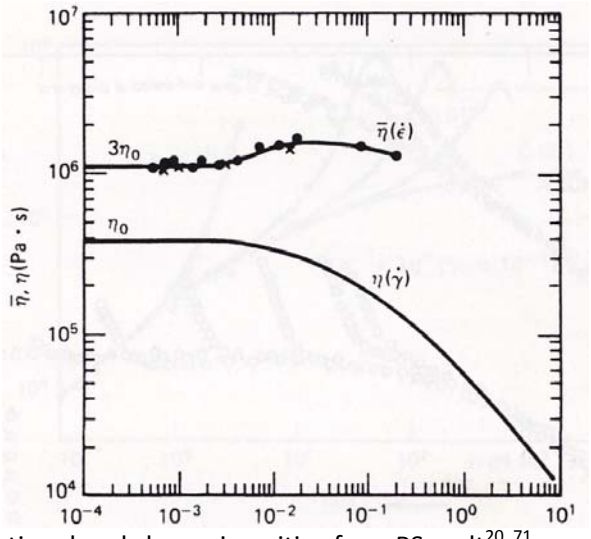

Figure 2.1.16 Steady elongational and shear viscosities for a PS melt[20, 71].

Transient elongational flows are useful in accessing the non-linear behavior of a polymeric material. Stress growth is measured using two viscosity material functions $\bar{\eta}^{+}_{1}$ and $\bar{\eta}^{+}_{2}$ where the "plus" sign signifies transient behavior. For b = 0, $\bar{\eta}^{+}_{1}$ equals the transient elongational viscosity $\bar{\eta}^{+}$, and $\bar{\eta}^{+}_{2}$ equals zero. The elongational rate is held constant rate during deformation, and is equal to $\dot{\varepsilon}_0$. Of specific interest to this work is a material's response in uniaxial elongational flow. In Fig. 2.1.17 is shown a materials response in uniaxial elongational flow for several values of $\dot{\varepsilon}_0$. At low Hencky strains, ε $(= \dot{\varepsilon}_0 t)$, $\bar{\eta}^{+}$ is equal to $3\eta_0$. The short time (strain) response of the transient stress growth in uniaxial extensional flow $\bar{\eta}^{+}$ has been shown to be a function of molecular weight distributions in linear polystyrenes[71]. At higher strains, deviation can be seen from the $3\eta_0$ (or linear viscoelastic) curve, especially for larger strain rates. This deviation is known as "strain-hardening", and its magnitude is a function of a material's topology and polydispersity[19, 20, 26, 37, 71-75].

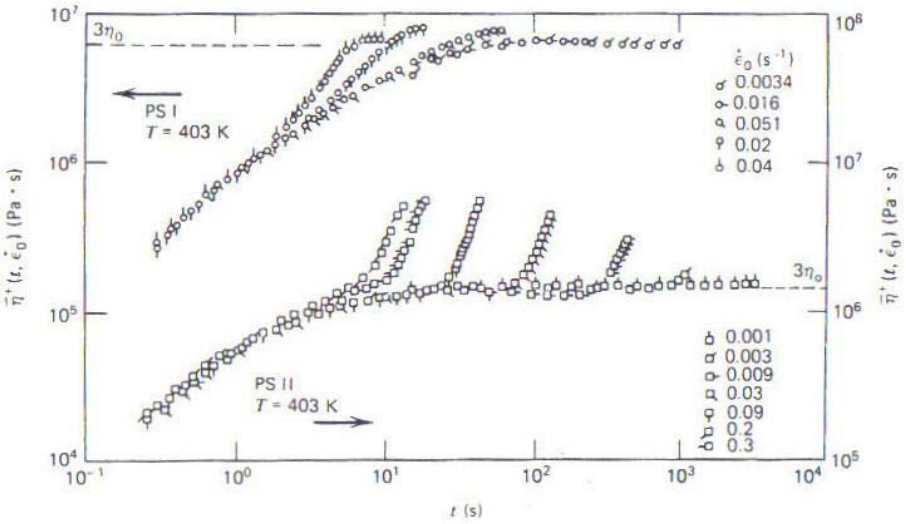

Figure 2.1.17 Transient uniaxial elongational stress growth viscosity at various strain rates $\dot{\varepsilon}_0$ for two polystyrenes. Strain hardening (rise above the $3\eta_0$ curve) is observed at higher strain rates for both materials[20, 71].

2.1.3.2 – Effect of Molecular Architecture in Shear-free Flow

The response of a polymeric melt in uniaxial extensional (elongational) flow is dependent on several properties of a material. While it has been shown that small amounts of high molecular weight material in linear polymers result in strain hardening[76-78], the presence, level, and type of long-chain branching directly impacts the magnitude of strain hardening. Although specific levels of branching cannot be determined from extensional viscosity alone, the strain hardening response can give rise to information on the branching structure and topology via constitutive models discussed in later sections. In this section, a review of the general features and causes of strain hardening is presented. Once again, an emphasis is placed on sparsely-branched mPEs for reasons outlined in section 2.1. First, though, the work of Münstedt and Auhl[14] is used to illustrate that even very small amounts of LCB in irradiated PPs result in the occurrence of strain-hardening.

Münstedt and Auhl[14] found that for irradiated polypropylenes, increases in branching content increased the magnitude of strain hardening. This is illustrated in Fig. 2.1.18. The transient extensional viscosity response underwent a sharper and more drastic upturn as the amount of LCB increased. Notice that the linear material (PP-0) exhibited no strain hardening at any extension rate. Münstedt and Auhl[14] also found that levels of branching that were not detectable using radius of gyration characterization via MALLS detection caused significant strain hardening behavior.

Gabriel and Münstedt[78] found that for metallocene catalyzed LLDPE of similar molecular weights and MWD, the presence of a small amount of long-chain branching showed a direct effect on the transient uniaxial elongational viscosity in the form of strain-hardening. In Fig. 2.1.19 is shown this effect for a variety of strain rates ($\dot{\varepsilon}_0 = 0.01 - 1.0\ s^{-1}$) at 150 ^{o}C. Only the LCB-mLLDPE showed strain hardening (rise above the $3\eta^+$ curve), while the mLLDPE resin (no LCB) did not show strain hardening at any $\dot{\varepsilon}_0$. Similar behavior was seen by Gabriel and Münstedt[78] in branched polypropylenes relative to

their linear counterparts (Fig. 2.1.20). The branched resins PP and PP 2 exhibit strain hardening while the linear PP 3 did not at any strain rates investigated.

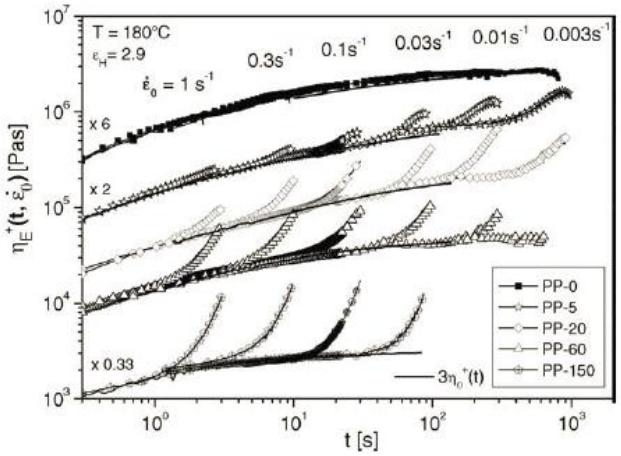

Figure 2.1.18 Transient uniaxial elongational stress growth viscosity at various strain rates $\dot{\varepsilon}_0$ for a series of irradiated polypropylenes. Strain hardening (rise above the $3\eta_0$ curve) is seen to increase with irradiation dosage (dosage given by the number in PP-#). PP-0 (top set of data) is a linear material, and shows no observed strain hardening. PP-5 (second from top) shows significant strain hardening even though its branching content is too low (< 0.08 LCB per 1000 monomers) for detection in MALLS[32].

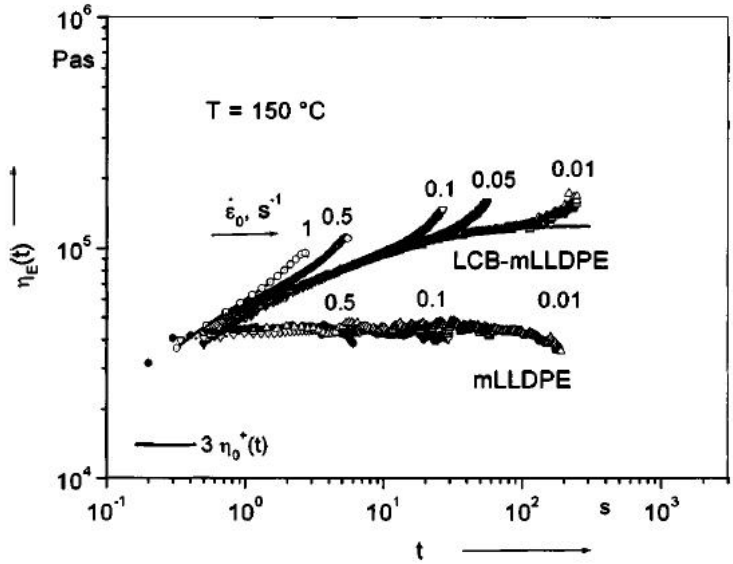

Figure 2.1.19 Transient uniaxial viscosity for a linear and q slightly long-chained branched LLDPE of similar MWD at various strain rates [78].

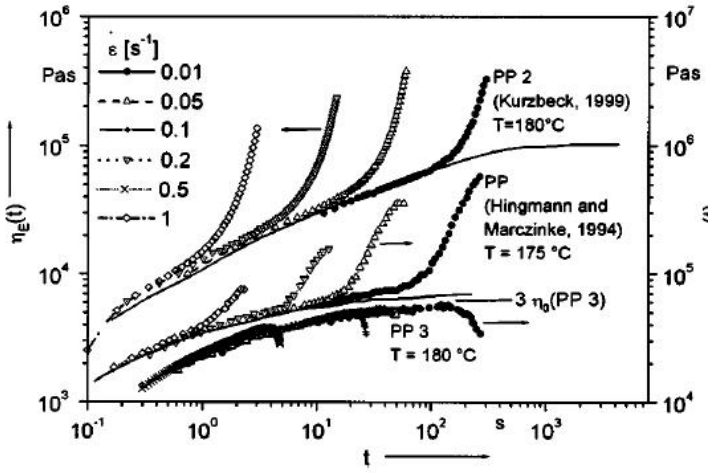

Figure 2.1.20 Transient uniaxial viscosity for branched (PP and PP 2) and unbranched (PP 3) polypropylenes at various strain rates [78].

Gabriel and Münstedt[78] correlated the strain hardening response seen in the uniaxial extensional viscosity of various branched polyethylenes to the enhancement seen in the zero-shear viscosity, η_0, relative to the linear polymer. The authors found that the polyethylenes underwent four types of strain hardening. Type I strain hardening was defined as being approximately independent of the elongational rate, $\dot{\varepsilon}_0$. Type II strain hardening decreased in magnitude with increasing $\dot{\varepsilon}_0$. Type III strain hardening increased with $\dot{\varepsilon}_0$. Materials that exhibit no strain hardening were classified as type IV. Polyethylenes of type IV obeyed Eq. 2.1-29 with $\alpha = 3.4$. Type I and II polyethylenes exhibit enhanced η_0 relative to their linear counterparts while type III polyethylenes exhibited η_0 values less than their linear counterparts[78].

Doerpinghaus and Baird[26] analyzed the extensional viscosity of several metallocene catalyzed LLDPEs with varying degrees of LCB (0 to 0.79 LCB/10^4) and an LDPE. In Fig. 2.1.21 is shown the extensional viscosity profile of a LDPE, a sparsely-branched LLDPE, and two linear LLDPEs at a strain rate of 0.1 s^{-1}. It was seen that the higher level of branching in the LDPE corresponded to a large strain hardening response. For the sparsely branched LLDPE, strain hardening was observed, but to a much low degree. Finally, the linear resins exhibited no stress growth above the linear response even when

MWD was broad. This qualitatively exhibited the evolution of strain hardening as branching content ranged from linear to sparsely-branched to hyperbranched systems.

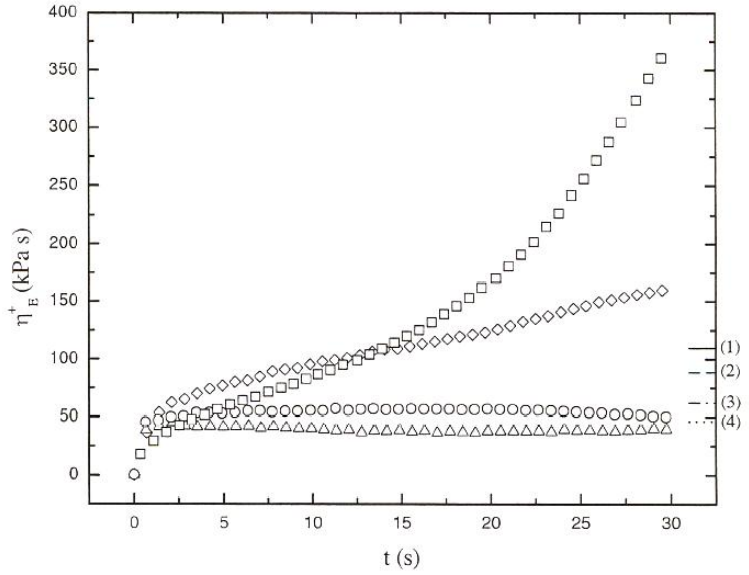

Figure 2.1.21 Transient extensional viscosities for the hyperbranched LDPE NA952 (□), the sparsely branched Exact 0201 (◇), and the linear LLDPE resins NTX101 (○) and Exact 3132 (△) measured at 150 °C and a extension rate of 0.1 s^{-1}. The linear response level ($3\eta^+(t)$) at t = 30 s is given for Exact 0201 (1), NA952 (2), NTX101 (3), and Exact 3132 (4) [9].

Bin Wadud and Baird[79] compared the strain hardening response of two sparsely-branched metallocene-catalyzed LLDPEs (Affinity series) and a linear LLDPE (Exact 3022). The branching contents of the Affinity PL1840 and PL1880 were determined by SEC-MALLS to be 0.17 and 0.57 per 10^4 carbons. The activation energy of the linear PE was found to be lower than either of the mLLDPEs. In Fig. 2.1.22 is shown the shear viscosity and extensional stress curves for the aforementioned resins. Extensional stress was related to extensional viscosity proportionally by the elongation rate (see Eq. 2.1-38). Differentiation was seen in the extensional stress curves of the sparsely-branched mLLDPEs that was not apparent in the shear viscosity curves. The higher branched resin exhibited a greater magnitude of strain hardening at higher strain rates. This suggested that transient uniaxial extension was not only sensitive to the presence of LCB, but to the quantity of LCB, especially relative to simple steady shear flow.

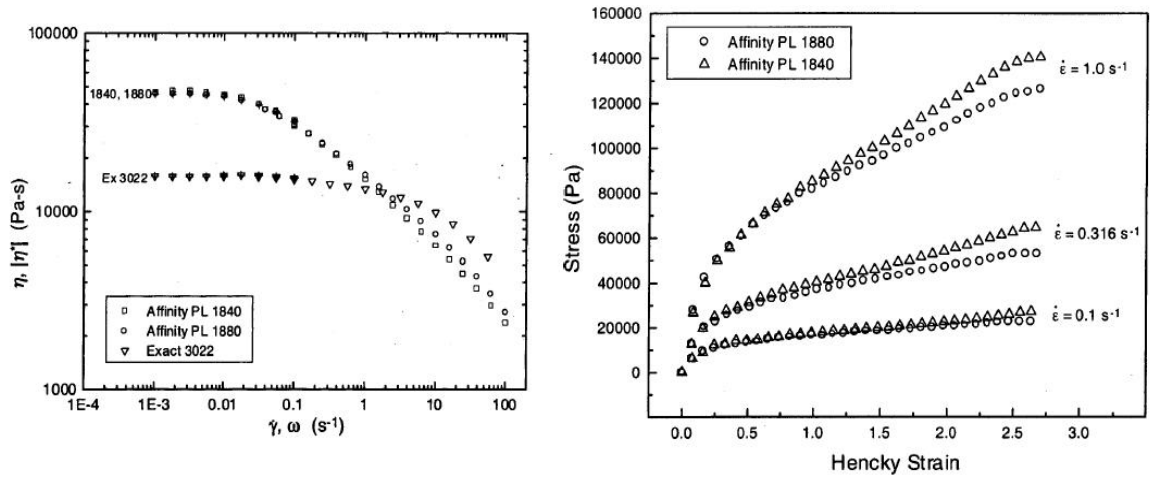

Figure 2.1.22 Shear viscosity of the linear Exact 3022 LLDPE and sparsely-branched Affinity PL1840 and PL1880 LLDPEs *(left)* and extensional stress growth for the sparsely-branched Affinity PL1840 and PL1880 LLDPEs at 135 ^{o}C *(right)*.

Shear-free flows, especially uniaxial elongation, are sensitive qualitative indicators to the presence of LCB in polymeric materials, even more so than traditional methods such as ^{13}C NMR. While the strain hardening response has been shown to be a function of LCB, no technique has been shown able to quantitatively measure LCB content from extensional viscosity. However, with the use of constitutive models discussed later, the non-linear behavior can be used to give insight as to the topology and branching structure of polymeric melts. Before leaving the general response of polymeric materials in shear-free flows, it is worthwhile to discuss a material phenomenon that makes measuring extensional viscosity at high strains difficult.

2.1.3.3 – Review of Ductile Failure

Ductile failure of materials in elongational flow prevents the measurement of the extensional viscosity growth at higher strains for certain materials that exhibit strain hardening. This material phenomenon reduces the precision of parameters in constitutive equations that are determined using transient extensional stress growth because of the inability to experimentally measure viscosity at

higher strains. This leads to less robust constitutive equation predictions of the behavior of the same material in extensional driven process such as film-casting.

In Fig. 2.1.23 is shown an example of ductile failure. Ductile failure in extension is defined as the development of a perturbation or structural defect in the sample that occurs before reaching either the maximum strain imposed by the testing device or the transient viscosity plateau. Typical examples of ductile failure are non-uniform deformation and necking[80]. Continued extension of a sample after the onset of ductile failure results in an increase in the severity of necking that ultimately leads the sample to rupture into two distinct fluid domains. Obviously, no further viscosity data can be captured following such a rupture event. More so, the forced non-homogeneity in deformation that occurs after the onset of failure, but before rupture, brings into question the quantitative validity of any data collected after the onset of ductile failure due to the reduced cross-sectional area at the point of failure [81, 82].

Figure 2.1.23 Illustration of ductile failure in a HDPE *(top sample)* compared to uniform deformation of an LLDPE *(bottom sample)*.

In Fig. 2.1.24 is illustrated the inability of measuring the transient extensional viscosity plateau when ductile failure occurs. This phenomenon has consequences in the calculation of dynamic variables in constitutive equations that are based on molecular topology. For example, transient extensional viscosity plays a prominent role in predicting the nonlinear parameters in the multimode McLeish-Larson pom-pom model proposed by Inkson *et al.*[83]. Specifically, the extensional viscosity plateau at a given extension rate, $\dot{\varepsilon}_0$ determines the theoretical number of branch point arms corresponding to backbone orientation and stretch relaxation times that are on the order of $\dot{\varepsilon}_0^{-1}$. The ability to reach the

transient extensional viscosity plateau experimentally across many strain rates largely affects the values and accuracy of these non-linear parameters.

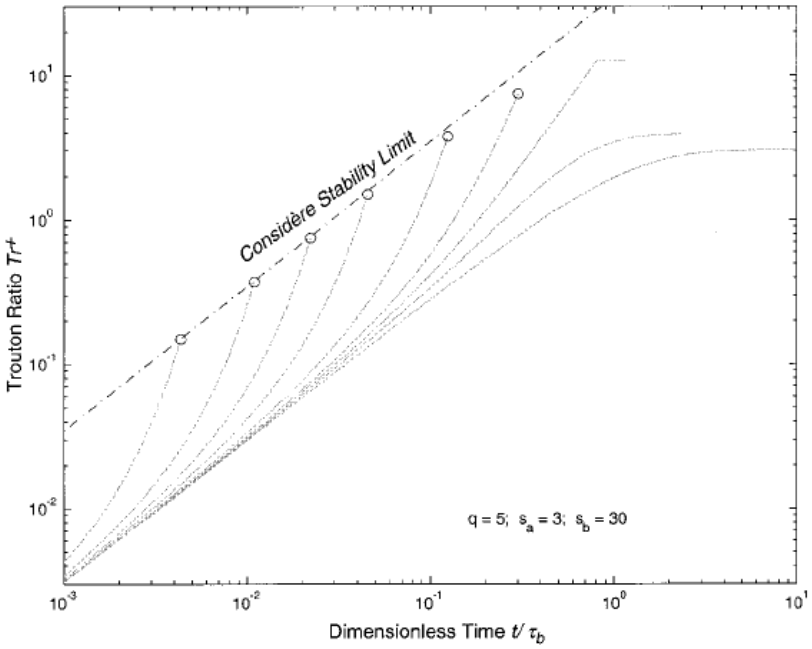

Figure 2.1.24 Stability envelope for onset of necking instabilities in transient uniaxial extensional rheometry of a branched polymeric material described by the differential pom-pom model[84].

McKinley and Hassager[84] used the Considère condition, which was originally derived in solid mechanics[85], in the limit of rapid elongation to quantitatively predict the critical Hencky strain ($\varepsilon \equiv \dot{\varepsilon_0} t$) for the onset of failure using both the Doi-Edwards[86] and the McLeish-Larson pom-pom constitutive equations[87]. The authors found that molecular topology in the form of pom-pom branch points affect the onset of material failure. Joshi and Denn[88, 89] constructed a model for viscoelastic fluids that attributed the onset of ductile failure to the frictional force on entangled chains being unable to balance tension in the chain, finding that total strain at rupture decreased as extension rate increased. Yao *et al.* [90, 91] found that the rate of necking was a function of the magnitude of strain hardening that occurred in uniaxial extension. Yao *et al.* [90] also show that numerical calculations demonstrate that concurrent measurement of the tensile force in extensional flow and the "necking" filament's profile could be used along with the appropriate force balance[92] to determine the transient extensional viscosity. While

adequate modeling exists to predict both the onset of ductile failure and the viscosity profile prior to material rupture, there lacks a technique to obtain transient viscosity data at strains higher than the rupture strain in Münstedt type elongational rheometers.

2.2 – Rheological Behavior of Model Branched Systems

In this section is presented a review of the rheological properties of model architecture systems. This review is necessary as numerical studies by Soares and Hamilec[10-12] predict that a distribution of molecules containing linear, star, and higher branched structures (comb, pom-pom) exist in sparsely long-chain branched mPEs, which are of primary interest in this research. There exists an imbalance as to the amount of information available to the behavior of certain architectures in certain flows. For example the zero-shear behavior of star polymers is well understood, but little work has been to study the elongational behavior of the same melts. This lack of information can sometimes make it difficult to draw complete quantitative conclusions as to the structure-property relationships of certain model systems in common flow types. However, enough work exists to draw qualitative conclusions as to the individual contributions of model systems in certain types, making it possible to draw educated conclusions on blend behavior. The rheological behavior of linear polymers is discussed in section 2.2.1, stars in section 2.2.2, combs in section 2.2.3, and pom-poms in section 2.2.4. Discussions on more complex branching structures that have multiple layers of branching (i.e. Cayley trees) is not discussed, as it is expected that the mPEs of interest to our work are characterized by branching only on the backbone. Work on such complex model systems can be found elsewhere[93-95]. As a final note, the use of the term monodisperse and nearly monodisperse is interchangeable in this section. PDI for most model systems is less 1.09 for results presented here.

2.2.1 – Linear Polymer Systems

The rheological behavior of nearly monodisperse linear chains in shear and shear-free flows is reviewed in this section. It is logical to start with linear resins for two reasons: 1) they are the simplest class of polymer architectures and have no branch points, and 2) they, by definition, make up a large fraction of the chains in the sparsely-branched commercial mHDPE systems of interest to this study.

Specifically in this section, the generic molecular "fingerprint" of linear chains in dynamic oscillatory shear and the response in uniaxial elongation are reviewed. Additionally, the behavior of bi-disperse blends of linear resins in the same flows is also reviewed to simulate the effect of differing chain lengths.

Auhl *et al*.[96] investigated the dynamic oscillatory response of a large number of nearly monodisperse linear polyisoprenes synthesized by anionic polymerization. These materials varied in average molecular weight from 2.4 to 1,131 kg/mol, and had PDI $\leq$ 1.09. Taking the M_e = 4.82 kg/mol for PI[96], their number of entanglements, *Z*, ranged from 0.5 to 230. In Fig 2.2.1 is shown the storage and loss moduli (*G'* and *G"*) for these materials, with *Z* decreasing from left to right. Noticeable trends appear in the data that characterize the linear material. At high frequencies corresponding to times on the order of the inverse of the Rouse time for one entanglement, both the *G'* and *G"* experimental curves begin to merge, corresponding to relaxation dominated by Rouse-like behavior. At intermediate frequencies the plateau region, which corresponds with entangled behavior, increases in frequency width with the number of entanglements before relaxing into the terminal region.

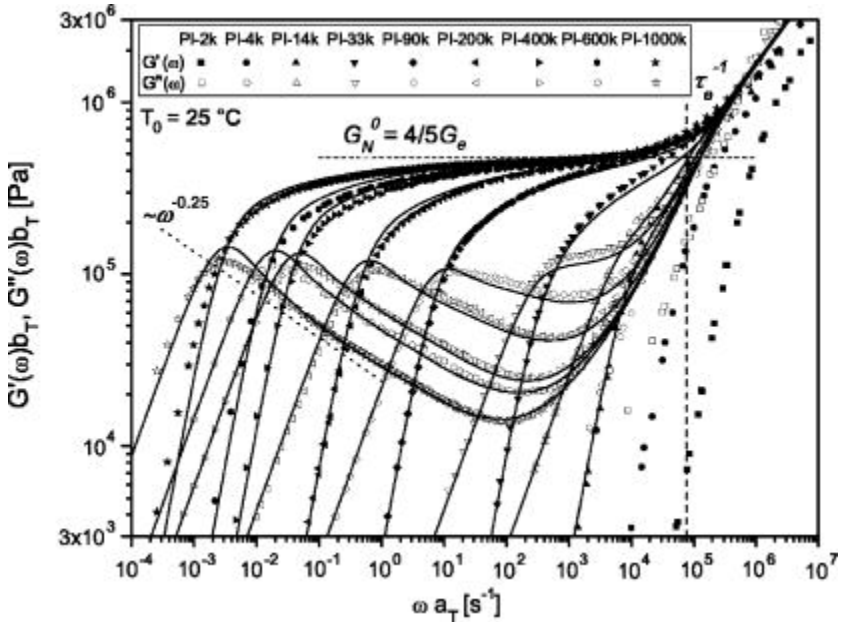

Figure 2.2.1 Storage *(filled symbols)* and loss *(empty symbols)* moduli from dynamic osicillatory shear measurements for various PI samples shifted to 25 ^{o}C [96]. Lines are predictions of the LM model not discussed in this work.

Uniaxial extensional viscosity can give topological insight as to the relaxation behavior and timescales of nearly monodisperse linear resins. The response of a nearly monodisperse linear resin can be qualitatively described in Fig 2.2.2. Prior to some critical strain rate, the extensional viscosity response mimics that of the linear viscoelastic response. Beyond this strain rate, the linear material exhibits a non-linear strain hardening response. This crossover has long thought to have been a function of the inverse Rouse relaxation time, τ_R.[97] Collis *et al.*[98] observed strain hardening only at rates longer than the longest Rouse relaxation time in highly entangled monodisperse linear polystyrene at 160 °C. Bach *et al.*[99], however, observed this crossover to occur at slightly lower elongation rates that were below the inverse Rouse time in PS melts elongated at 130 °C. Wagner and Kheirandish[100] used the concept of interchain pressure originally proposed by Marrucci and Ianniruberto[101] in the framework of the Doi-Edwards tube model to explain this deviation. Interchain pressure was defined as the lateral forces between the chain and the tube wall[100]. Nielsen *et al.*[102] observed in linear PS that increases in chain molecular weight resulted in higher steady-state extensional values. However, the ultimate rise in strain hardening relative to the linear response was found to decrease with increasing molecular weight[102].

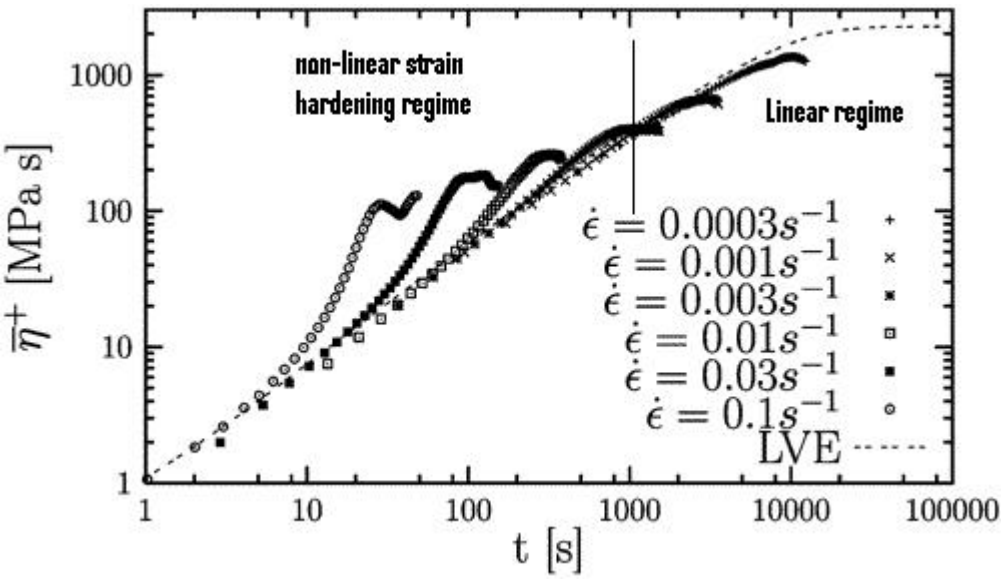

Figure 2.2.2 Transient extensional viscosity of a 390 kg/mol linear PS measured at 130 °C. Vertical serves to mark the transition from linear to non-linear behavior as a function of the strain rate $\dot{\varepsilon}_0$. Figure adapted from Auhl *et al.*[96].

While nearly monodisperse linear resins have very identifiable responses in both shear and shear-free flows, these responses become less clear when the melt in question is no longer monodisperse. Model bi-disperse systems provide the easiest way to observe the effect of deviation from monodisperse behavior. Nielsen *et al.*[102] investigated the differences in the response of monodisperse and bi-disperse blends of linear PS. Three different weight fraction blends of monodisperse resins were prepared. Blend 1 consisted of 96% PS50K (~50 kg/mol) blended with 4% PS390K (~390 kg/mol). Blend 2 was an 86/14% mixture of the same two materials. Blend 3 was a 86/14% mixture of PS100K (~100kg/mol)/PS390K. In Fig. 2.2.3 is illustrated the storage and loss moduli of the blends and the individual resins. Each blend response leaves the plateau modulus on the order of the same frequency as the weight fraction majority component (lower molecular weight resin). Deviation occurs at lower frequencies as a second plateau is briefly seen due to the higher molecular weight component. This plateau terminates at frequencies higher than its pure species counterpart. In Fig. 2.2.4 is shown the transient elongational viscosity of Blend 1 *(left)* and PS50K *(right)*. At an elongation rate of 0.1 s^{-1}, the monodisperse PS50K has a viscosity response qualitatively similar in shape to the linear response. However, the introduction of only 4% of the high molecular weight material results in a very different material response, with viscosity growth on the order of 10x the linear viscoelastic response. The change in behavior makes sense if one thinks of the increased Rouse relaxation time of the mixture. An increase in the Rouse time results in a decrease for the critical strain rate required for the onset of strain hardening.

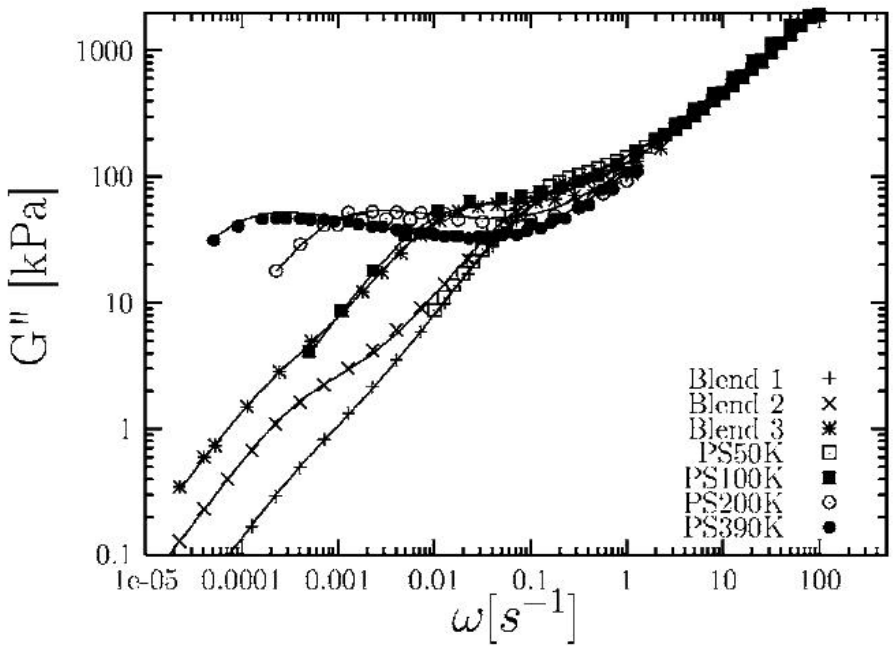

Figure 2.2.3 Results of linear viscoelastic measurements of G" as a function of the angular frequency for monodisperse and bi-disperse blends of PS. The data are all time-temperature shifted to a reference temperature of 130 °C.

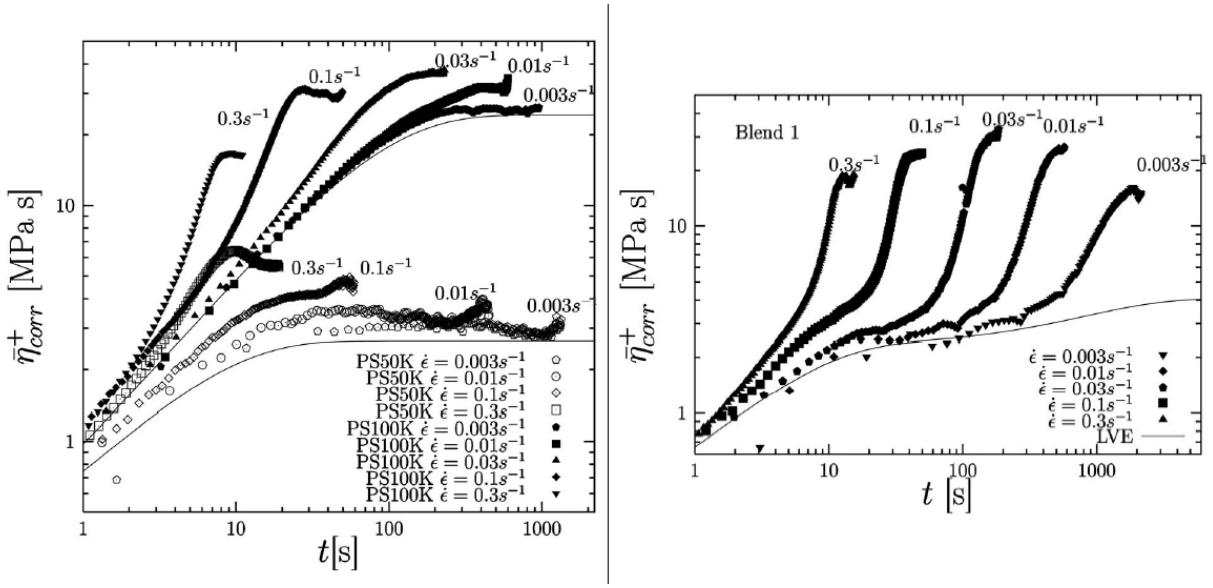

Figure 2.2.4 Transient elongational viscosity of linear monodisperse PS *(left)* and the bi-disperse Blend 1 *(right)*. The addition of a small amount of high MW linear PS results in significant strain hardening at lower extension rates relative to the pure PS50K melt[102].

2.2.2 – Star Polymer Systems

Star polymers are defined as a branched resin in which all branches emanate from a single branch point. The primary relaxation behavior of a star melt is not free reptation as is seen in linear chains, but reptation (fluctuation) of the free of the branch ends. This relaxation behavior leads to a very different response in shear flows, especially in the storage modulus and zero-shear viscosity. Reviewed in this section are the viscous and elastic responses of model star systems in oscillatory shear, the effect of the star structure on the zero-shear viscosity, the step-strain response of star materials, and a review of the limited data in the literature on the elongational response of star systems.

The characteristic response of the storage and loss modulus of a star polymer is different than that of a linear resin. In Fig. 2.2.5 is shown the data of Fetters *et al.*[34] that compared the storage and loss moduli of a linear *(left)* and star *(right)* PI resin with similar viscosities. For both polymers the frequency (ω_c) at which *G'* crosses *G"* is approximately the reciprocal of the longest relaxation time. At higher frequencies, the value of *G"* decreases for linear polymers, while *G"* increases for the star resin until reaching a maximum at some frequency, ω_{max}. It has been shown by Roovers[103] and Fetters *et al.*[34] that ${\omega_{max}}^{-1}$ is on the order of the longest arm relaxation time. The region between ω_c and ω_{max} is increased as arm molecular weight is increased.

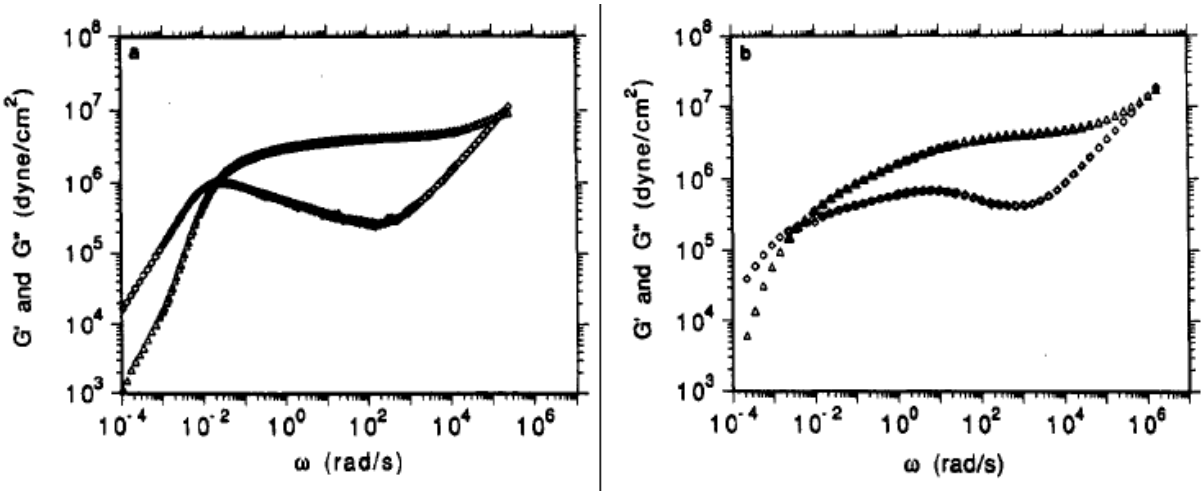

Figure 2.2.5 Comparison of the dynamic moduli of a linear *(a, left)* and a 4-arm star *(b, right)* polymer having similar viscosities [34].

The relationship between the zero-shear viscosity, η_0, of a star polymer melt and its structure is well understood. While entangled linear polymers are observed to have zero-shear viscosities scaled with their molecular weight to the 3.4 power (Eq. 2.1-29), the response of entangled stars is more complex, but equally quantifiable. Fetters *et al.*[34] along with others[104, 105] observed that the η_0 of star melts was an exponential function of only the arm molecular weight, M_a, for stars with a functionality, f, ≥ 4. The authors attributed this exponential dependence to the stress relaxation of star molecules being controlled by arm retraction rather than chain reptation. The exponential dependence has also been shown to result in an enhanced η_0 relative to a linear chain with the same molecular weight. Jordan *et al.*[106] and Gell *et al.*[107] found in asymmetric three-arm stars melts of PB and PEP that the shortest arm molecular weight had to be larger than the molecular weight for entanglement before any zero-shear enhancement was seen. Lohse *et al.*[1] found arm lengths of 5 kg/mol to be sufficient for η_0 enhancement in PE. Lohse *et al.*[1] also cited a proposed equation that relates η_0 to M_a

$$\eta_0 = A * exp\left\{\gamma \frac{M_{arm}}{M_e}\right\} \qquad (2.2\text{-}1)$$

where A and γ are adjustable parameters. It has been found[1] that $\gamma \cong 6$. For stars with functionality less than four, a small dependence of η_0 on the numbers of arms has been observed. Fetters *et al.*[34] found that the η_0 of 3-arm PI resins was approximately 20% less than 4-arm PI stars with the same arm molecular weight.

The step-strain response of star polymers has been observed to mimic that of entangled linear resins[34, 42, 108]. Archer and Juliana[108] observed that the measured damping function, $h(\gamma)$, of an entangled 6-arm PB star blended with 50% unentangled linear PB behaved like an entangled linear melt and was more strain-softening than any more complex branched structure measured. The authors attributed this behavior to the lack of multiple branch points that can serve to retard stretch in strong flows. Vega and Milner[42] observed in entangled PE stars that were blended with both an entangled linear PE and

50% by weight low molecular weight PE wax that increasing star concentration resulted in higher values of the relaxation moduli, *G(t,γ)*, and increased the strain dependence of *h(γ)*. This later finding suggests that higher star concentration results in a *h(γ)* that mimics the Doi-Edwards prediction for entangled linear melts.

The effect of the star architecture in transient uniaxial extension was investigated by Lohse *et al.*[1]. In Fig. 2.2.6 is shown the extensional viscosity of a LLDPE (Exceed 103), a blend of 3% 3-arm entangled PE star with 97% Exceed 103, and a blend of 3% 23-arm entangled PE comb with 97% Exceed 103. Both the pure linear polymer and the star blend do not exhibit strain hardening. However, the same weight amount of comb material resulted in significant strain-hardening. It has been suggested[87] that the reason for this difference in behavior is due to the lack of multiple branch points in the star melt that do not serve to retard the stretch relaxation of the molecule. However, Nielson *et al.*[109] observed strain hardening in a melt of 4-armed asymmetric PS stars where one arm was significantly larger than the other three. The authors fail to speculate on the effect of such a large arm on the extensional viscosity response. If one was to extend the logic used in linear systems, this increase in arm molecular weight might cause the resulting terminal relaxation time to become so great that the material strain hardens at any measureable extension rate! However, the general lack of published data for star systems makes it impossible to draw any definite conclusions as to the overall behavior of star melts in extensional flows.

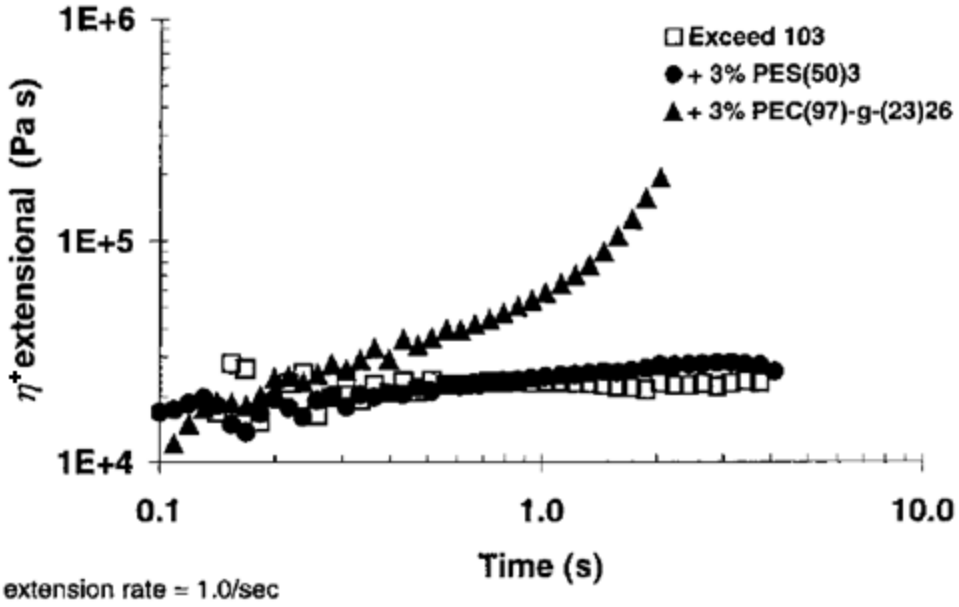

Figure 2.2.6 Extensional viscosity of a LLDPE *(squares)*, a 3% blend of stars with the same LLDPE *(circles)*, and a 3% blend of combs with the same LLDPE *(triangles)*[1].

2.2.3 – Comb Polymer Systems

Comb polymers are one of the simplest architectures with multiple branch points. A comb polymer is defined as a branched material with multiple branch points that all emanate for the backbone. The presence of multiple branch points modifies the viscous response from that observed in simpler architectures. Instead of direct relaxation by either reptation or arm retraction, a comb must undergo hierarchical relaxation in which the outer arm must retract in star-arm fashion before allowing the backbone to relax by reptation. Presented in this section is a review of the characteristic "signature" of the comb polymer in oscillatory shear, a review of the dependence of η_0 on the molecular structure of the comb, and a review of the only current work on the step-strain of entangled combs. No papers were found in the literature on the elongational behavior of comb systems other than the work of Lohse *et al.*[1] outlined in section 2.2.2.

Comb polymers have a definitive "signature" in dynamic oscillatory shear. The distribution of arms along the cross-bar introduces an additional spectrum of relaxations at lower frequencies. This

results in different rheological response at lower frequencies[110]. Daniels *et al.*[110] investigated the shear response of 10 polybutadiene (PB) combs with varying backbone lengths, branch points, and branch lengths. In Fig. 2.2.7 is illustrated the storage and loss moduli for two of these comb melts. The authors found the general trends in the loss modulus, *G"*, curves that give structural and relaxation behavior of the material. At higher frequencies, free Rouse modes within the tube yields frequency dependence of *G"* that depends on the one-half power ($\omega^{1/2}$) that progresses to lower frequencies until reaching a minimum at the inverse of the Rouse relaxation time for one entanglement, τ_e. This marks the onset of the entangled modes, and is followed by an extended "shoulder" in the data whose width scales with the arm molecular weight. This "shoulder" represents the relaxation by activated arm retraction. Finally, at low frequencies, there is a weak maximum or step that results from the relaxation of the crossbars (backbone). The more highly entangled the crossbars are with themselves, the more sharp this reptation peak is. An increase in backbone molecular weight moves this reptation peak to lower frequencies. A shorter backbone molecular weight reduces the magnitude of this peak[110]. This behavior at low frequencies can also be thought of as the arms retracting and swelling the backbone tube, thereby reducing the number of entanglements and approaching Rouse-like behavior[111]. Similar relaxation behavior was seen by Kapnistos *et al.*[112] in comb PB and PS.

The η_0 dependence of comb polymers on molecular structure is not as well understood as it is in simpler (linear and star) topologies. Like stars, dependence of the arm molecular weight is more important than the number of arms. For example, Lohse *et al.*[1] found that in PE an asymmetric 3-arm star with a 5 kg/mol arm has the same η_0 enhancement that a *30-arm* comb that has a similar arm molecular weight! The only work that systematically attempts to quantify the zero-shear viscosity as a detailed function of structural variables is that of Inkson *et al.*[113]. An analytical expression for PE combs at 190 ^{o}C was presented by the authors [Eq.25 in [113]] that depends solely on the chemical structure, with no fitting parameters. The equation is quite lengthy, and is not presented here. Instead, a qualitatively

highlight is presented that outlines their findings. η_0 was found to grow exponentially with arm length and arm volume fraction (similar to star behavior). η_0 was found to vary with square of the backbone molecular weight. Changes in the backbone length was found to horizontally and vertically shift η_0, but to a lesser extent than changes in arm molecular weight. Increased number of arms was found to increase the molecular weight, but reduce η_0. This qualitative picture gives insight as to the η_0 dependence on the comb structure, but further work is needed for quantification on a more universal level.

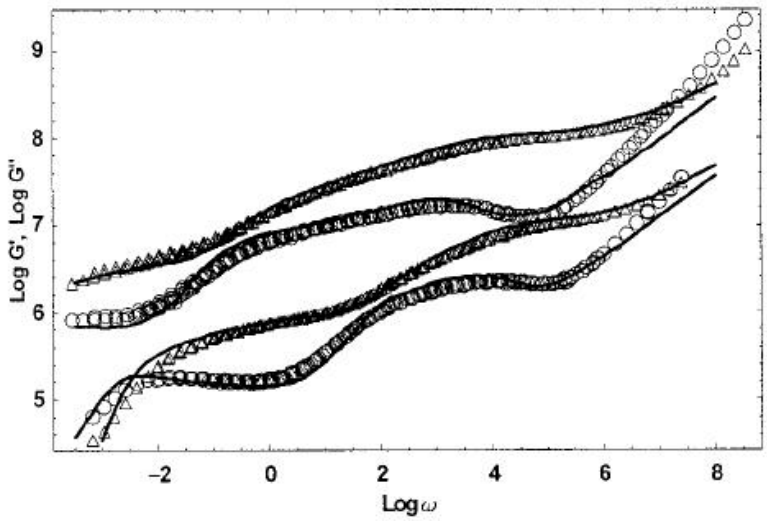

Figure 2.2.7 Storage and loss moduli for two PB combs with differing number of arms. The upper data set has been shifted by a factor of 100 for clarity [110].

The step-strain response of comb polymers is of interest due to the strong nature of the flow coupled with the multiple branch-points in the comb. The only major work in this field is that of Vega and Milner[42] who studied 5 blends of PE combs with entangled linear PE and 50% low molecular weight PE wax. Comb weight fractions varied from 1.25 to 20%. The maximum strain measured was five. The PE wax was used to reduce wall-slip and transducer overload errors common to step-strain experiments. An increase in comb content was found to both broaden the relaxation spectrum and increase the terminal time across all strains investigated. This is illustrated in Fig. 2.2.8 for both the relaxation modulus *G(t,γ)* and the shifted relaxation modulus *G(t)*h(γ)* for a variety of comb weight fractions

(ϕ_{comb}). The characteristic time for time-strain superposition, τ_k, (section 2.1.2.1.4) was found to scale with $(\phi_{comb})^{3.2}$. Note that this indicates a deviation from Rouse-like behavior ($\tau_k \sim \phi_{comb}^{0.0}$). Sanchez-Reyes and Archer[44] observed a similar non-Rouse-like dependence in blends of linear resins, leading them to suggest that τ_k is not dependant on the longest Rouse relaxation time. In Fig. 2.2.9 is shown the damping function *h(γ)* for all comb concentrations. As comb content increased, the strain dependence of the *h(γ)* increased, mimicking Doi-Edwards behavior for entangle *linear* chains. The authors attributed this unexpected trend to the comb arms relaxing on the order of the finite rise time associated with the imposition of the desired strain. Therefore, the backbones were the only species relaxing at times longer than the finite rise time. The increased comb content resulted in more of these "backbone only unrelaxed species" and thereby increased the entanglements of an essentially "linear" system.

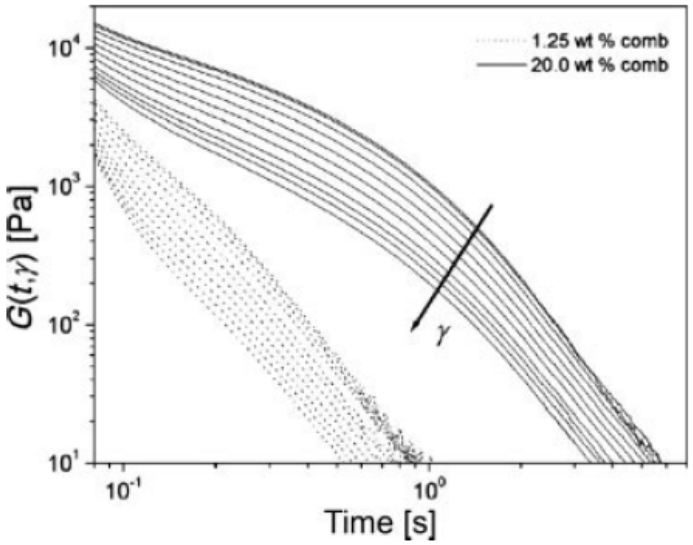

Figure 2.2.8 Nonlinear relaxation modulus for comb/linear blends. Strains of 0.2 to 5.0 were investigated. Increases in comb concentration increased both terminal relaxation time and relaxation spectrum[42].

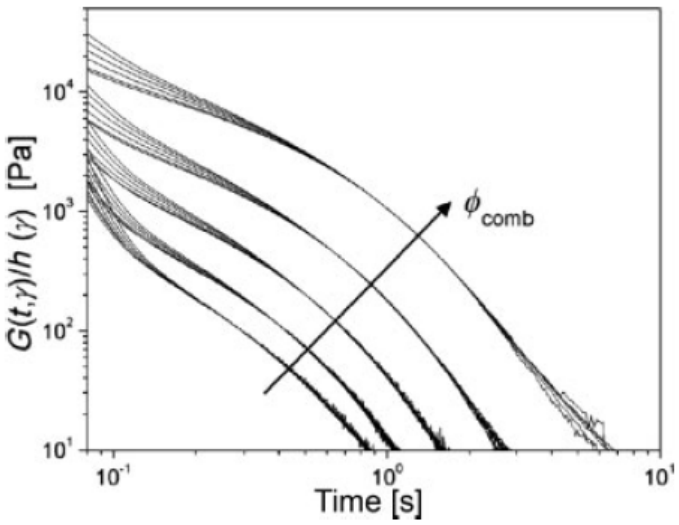

Figure 2.2.9 Reduced relaxation modulus for 5 comb/linear blends. Increases in comb concentration increased both terminal relaxation time and relaxation spectrum[42].

2.2.4 – Pom-pom Polymer Systems

The pom-pom polymer is another simple molecule with a backbone containing a branch point at either end with *q* number of arms. Its unique architecture provides a clear demonstration of a retarded stretch relaxation time that leads to observable hierarchical relaxation in its simplest form[50]. This branching structure serves as the basis for a new class of constitutive equations discussed in section 2.3. Presented in this section is a review of the molecular "fingerprint" seen in dynamic oscillatory shear, a review of step-strain response of pom-pom melts and blends, and a review of the only two found that measure the transient elongation of pom-pom melts.

Similar to the behavior seen in other model architectures, it has been claimed[50] that the pom-pom molecule exhibits its own "fingerprint" in the dynamic relaxation spectrum, especially in the loss modulus. In Fig. 2.2.10 is illustrated *G'* and *G"* for a series of pom-pom polymer melts with *q* equal to two measured by McLeish *et al.*[50]. Similar to other model architectures, free Rouse modes within the tube at high frequencies yield a G" that scales with $\omega^{1/2}$ until the onset of entanglements at ω_e. This is followed by an extended shoulder feature whose width grows with the length of the dangling arms.

Finally, there is a weak minimum or step at lower frequencies coming from the relaxation of the crossbars. The more highly entangled the crossbars are with themselves, the sharper their reptation peak. Archer and Varshney[48] found that a small increase (~30%) in arm molecular weight caused an eight-fold increase in the frequency at which *G'* crossed over *G"* in 3-armed PB melts. van Ruymbeke *et al.*[114] found that in the branch arms were unentangled, that storage and loss moduli would resemble the relaxation of an entangled linear polymer with an added shoulder in the terminal region of the tan δ versus ω plot.

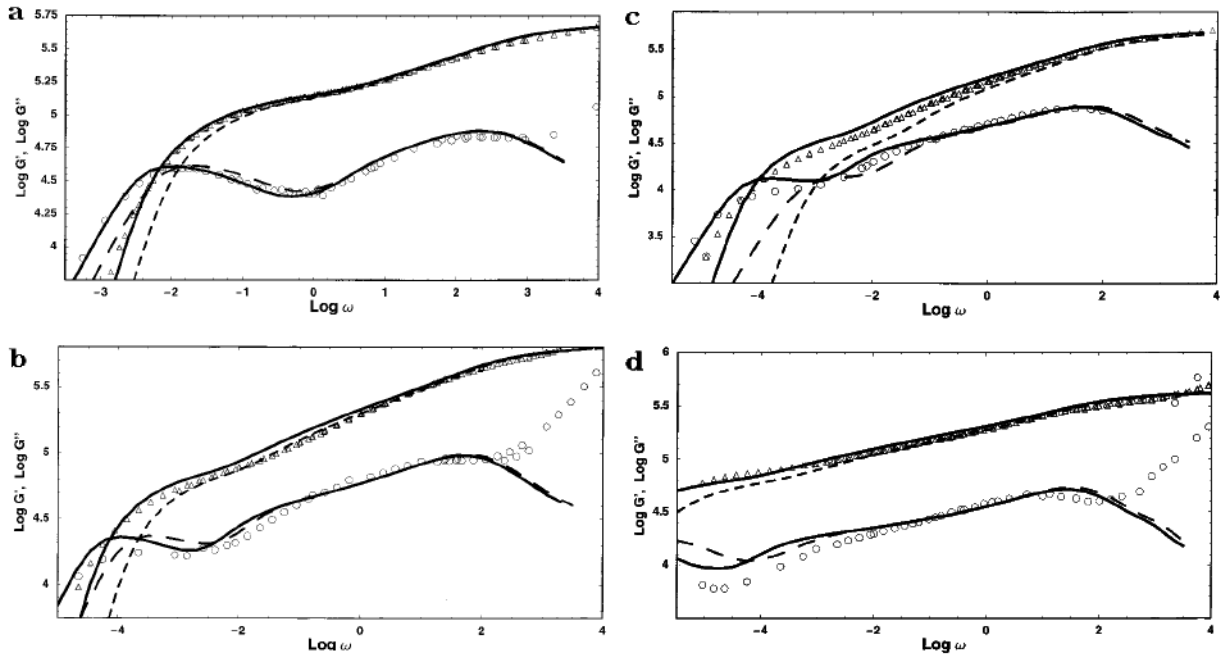

Figure 2.2.10 Storage (*triangles*) and loss (*circles*) for four PI pom-pom polymers. Each polymer has two arms of equal length at each branch point[50].

Three works exist in the literature that are connected with measurements of the step-strain response of model pom-pom systems. The step-strain response of pom-pom polymers is of interest due to the strong nature of the flow giving rise to non-linear stretch relaxation of the backbone that are not present in star or linear melts. McLeish *et al.*[50] found in monodisperse H-polymers that once the imposed strain crossed some critical value, an additional relaxation became apparent at time prior to the onset of time-strain superposition, which was found to be on the order of the backbone stretch

relaxation time τ_s. At even higher strains (γ = 500%), an increased strain softening was seen at short times, corresponding to branch-arm retraction in the backbone tube. This was in agreement with the findings of Archer and Varshney[48] who observed branch-point withdrawal at high strains (γ = 600%)in three-armed PB pom-poms.

In the most exhaustive work of the step-strain behavior of pom-pom melts, Archer and Juliani[108] investigated the response of three armed PB pom-pom melts at varying degrees of dilution (weight fractions of pom-pom in the blends are 100%, 83% and 50%) in unentangled linear PB. The authors found in 100% pom-pom melts, the onset of time-strain separation was comparable to the terminal relaxation time of the polymer. At long times, longer than τ_k, the relaxation response mimics the Doi-Edwards response associated with entangled linear polymer melts. The authors attributed this behavior to complete stretch relaxation of the backbone to its original length. Finally, the authors observed as the pom-pom concentration was decreased, *G(t,γ)* and τ_k were reduced as well. At lowest concentration (50%), the damping function, *h(γ),* mimics the Doi-Edwards damping function for virtual all strains investigated.

Finally, there are two published data sets that discussed the behavior of model pom-pom melts in extensional flow. Nielsen *et al.*[109] observed strain hardening for a wide range of extension rates (=0.0003 to 0.1 s^{-1}) in nearly monodisperse three-armed pom-pom PS melts with entangled arms. At the lowest extension rate (=0.00003 s^{-1}), a more linear behavior was observed. McLeish *et al.*[50] observed similar behavior in 2-armed PI pom-poms. Strain-hardening was observed only at extension rates that had values $\dot{\varepsilon}_0\tau_s > 1$, where τ_s was the stretch relaxation time of the backbone segment. This is illustrated in Fig. 2.2.11 for two extension rates, one of which is $\dot{\varepsilon}_0\tau_s > 1$ and one of which is $\dot{\varepsilon}_0\tau_s < 1$ for one of the PI pom-poms.

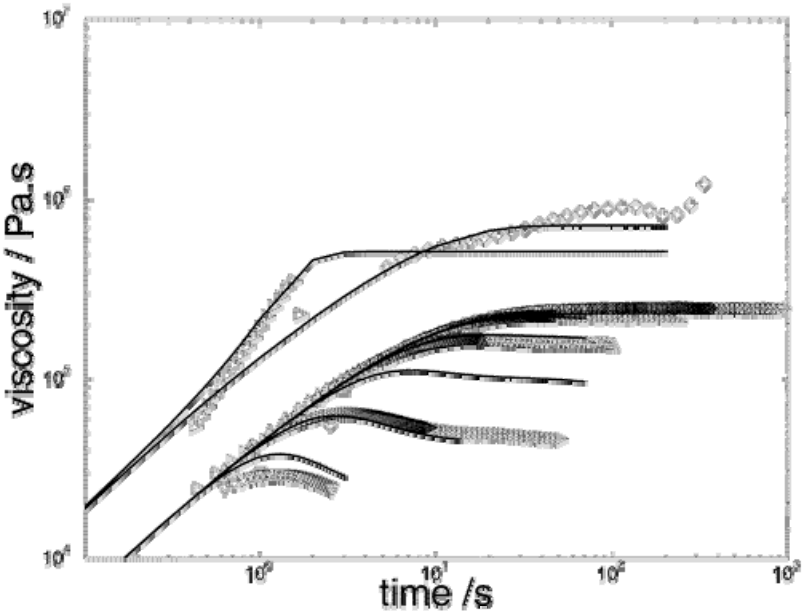

Figure 2.2.11 Transient extensional and shear response of a two-arm entangled PI pom-pom molecule. Strain hardening is not seen in extensional flow until $\dot{\varepsilon}_0\tau_s > 1$ (*triangles*). For $\dot{\varepsilon}_0\tau_s < 1$ (*diamonds*) a linear response is observed[50].

2.3 – Evolution of the Pom-Pom Constitutive Equation

Presented in this chapter is a review of the evolution of the pom-pom constitutive model originally put forth by McLeish and Larson (ML)[87]. In section 2.3.1 is briefly reviewed the Doi-Edwards tube theory for entangled polymer chains. In section 2.3.2 is provided a theoretical basis for a constitutive equation based upon an ideal pom-pom molecule. In section 2.3.3 is defined the integro-differential form of the pom-pom model and analyzes its behavior in a variety of flows and thermodynamic frameworks. In section 2.3.4 is reviewed a derivation of a K-BKZ analog capable of modeling stress relaxation following a step-strain. In section 2.3.5 is reviewed a simplified differential form of the pom-pom model designed for complex flows. In section 2.3.6 is described how a constitutive model based on an ideal architecture can be extended to "real" commercial systems via a multimode approach. In section 2.3.6 is also presented a review of all major work and critique of the multimode form. In section 2.3.7 is introduced and reviewed the eXteneded Pom-Pom (XPP) model derived to correct three shortcomings of the ML multi-mode form. The XPP model is found, however, to have major shortcomings that makes it ill-posed relative to the ML form for our current studies, most notably its inability to model sparsely branched resins[115].

2.3.1 – Doi-Edwards Tube Theory

The tube theory of de Gennes[116] developed into a full constitutive theory by Doi and Edwards[52] serves as the theoretical basis for the pom-pom model. In linear melts, Doi-Edwards (DE) tube theory assumes that the movement restricting entanglements confine the polymer to a tube as illustrated in Fig. 2.3.1. The path along the centerline of such a tube is defined as the primitive path, and corresponds spatially to the lowest values of free energy for the chain. The tube radius, a, is defined by the largest movements from the centerline of a chain segment that has a free energy equal to kT. Segmental movements are confined to the tube radius. At equilibrium, there is little change to the overall tube

length. On length scales shorter than the tube diameter, relaxation occurs in a similar fashion to unentangled melts, obeying Rouse dynamics on timescales shorter than reptation.

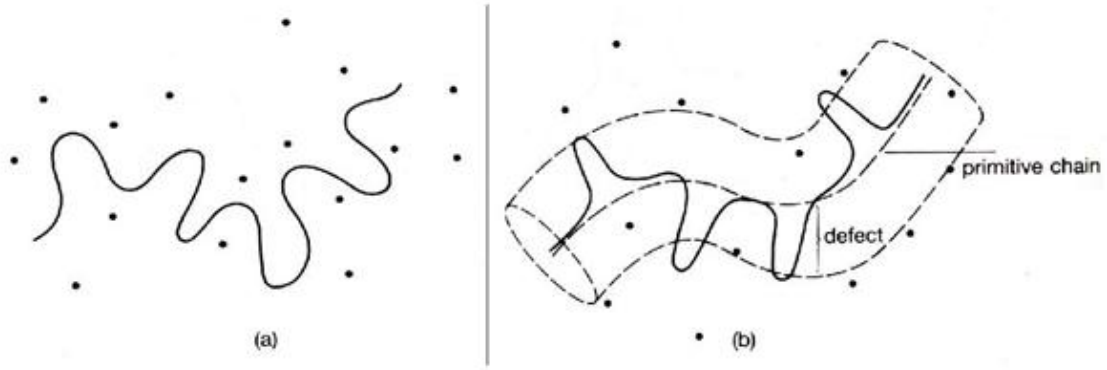

Figure 2.3.1 *(a)* Illustration of a chain trapped in a fixed network of obstacles, such as entanglements. *(b)* The tube of radius *a* centered around the primitive chain[52].

For length scales longer than the tube diameter, relaxation occurs via reptation and retraction. Reptation, illustrated in Fig. 2.3.2, is the diffusive movement of the chain through the tube, along the primitive path. The head end of the chain is allowed to move freely and create a "new" section of the tube. The tail moves in a curvilinear fashion along the primitive path, and the recently vacated section is then available to be occupied by the remainder of the network. Retraction, illustrated in Fig 2.3.3, is the retraction of the polymer chain after a large step-strain. Following deformation, the polymer chain assumes a new, stretched conformation. Prior to reptation, the chain retracts to its original tube length, but retains its new conformation prior to reptation.

The relaxation dynamics for branched polymers are more complicated. Branch points suppress reptation by restricting movement of the backbone through the tube, allowing only the free ends to move. For example, star polymers do not reptate like a linear polymer, and require arm fluctuations to relax stress[35, 83, 117, 118]. As the number of branch points increase, relaxation behavior deviates away from linear tube behavior. For a branched material that undergoes a deformation and has multiple branch points, the branch points act as a pinning point in that only the free ends can initially retract into its tube following stretch. The innermost segments can then only retract when it becomes entropically

favorable to withdrawal the branch points into their tube[83, 119]. This retardation of stretch causes stress buildup that is seen in extensional flows in the form of strain hardening[87]. The DE tube model cannot accurately model non-linear phenomenon, thereby necessitating the need for a more robust class of constitutive equation.

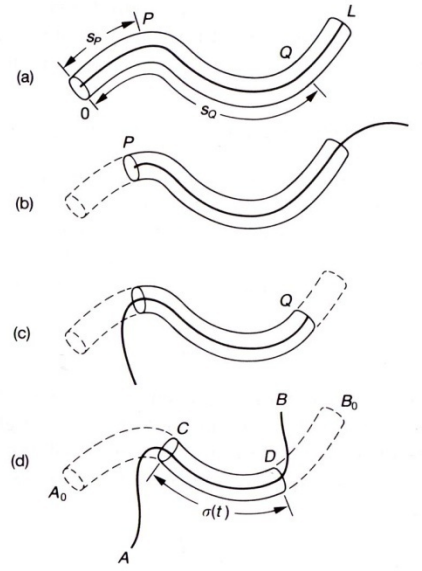

Figure 2.3.2 Illustration of a reptating chain. *(a)* Initial conformation of the primitive chain in the original tube. *(b)* and *(c)* Movement of the free ends out of the original tube, leaving vacant tube segments. *(d)* Confirmation at some later time *t* where tube segments have vanished when they are reached by either chain end [52].

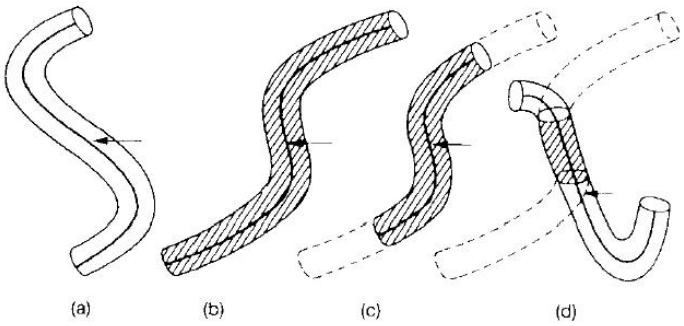

Figure 2.3.3 Stress relaxation of linear polymer after a large step-strain. *(a)* Chain conformation is in equilibrium prior to deformation. *(b)* Immediately after deformation, the primitive chain is in the affinely deformed conformation. *(c)* Contraction of the primitive chain along the tube to the original equilibrium length. *(d)* Onset of reptation following retraction [52].

2.3.2 - Theoretical Pom-Pom Model

In order to understand these non-linear behaviors, McLeish and Larson[87] introduced a constitutive model based on the pom-pom molecule. The ideal McLeish-Larson pom-pom molecule is illustrated in Fig. 2.3.4. The backbone length is measured by the dimensionless quantity s_b, which is equal to the backbone molecular mass divided by the critical molecular mass for entanglement. This backbone has a branch point at either end bonded to q arms. The characteristic arm molecular mass, s_a, is defined as arm molecular weight divided by the critical molecular weight for entanglement. λ is the ratio of backbone stretch defined by the backbone length at a given time divided by its equilibrium, undeformed value.

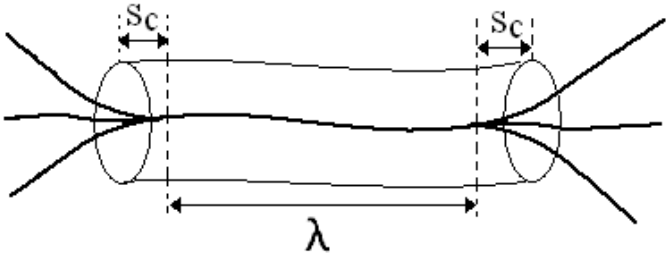

Figure 2.3.4 The ideal pom-pom molecule. The backbone length is measured by the number of entanglements, s_b. This backbone has a branch point at either end bonded to q arms. The arm length, s_a, is defined as the number of entanglements for each arm. λ is the ratio of backbone stretch defined by the backbone length at a given time divided by its equilibrium value. s_c is defined as the amount of each arm material withdrawn into the backbone tube in units of entanglements. Figure adapted from Lee *et al.*[120].

The branch point ends serve to retard the backbone stretch. These pinning points do not allow the backbone to readily retract back within its tube. However, this resistance to retraction is not infinite; otherwise the response would be comparable to that of a network. The maximum curvilinear tension at each branch point during stretch is equal to the sum of the net Brownian force of the free ends equal to qkT/a where a is the tube diameter. Therefore, because all segments of the backbone share the same equilibrium tension, the maximum backbone stretch, λ, is equal to q.

At higher stretches, the tension is sufficient enough to withdraw the arm segments into the backbone tube. This phenomenon, called "branch point withdrawal," is illustrated in Fig. 2.3.5, and is entropically more favorable than continued stretching of the arm, which would result in a reduction in its configuration space. Two dynamic variables become important in the case of branch-point withdrawal. The first is the aforementioned dimensionless stretch ratio λ. The second is the amount of branch arm that is forced into the backbone tube adopting the orientation dictated by the backbone. This retraction is defined by the variable s_c measured in units of the tube diameter (i.e. $0 < s_c < M_a/M_e$). These two variables are interrelated by the configurationally entropy balance in such a way that $s_c = 0$ for all $\lambda < q$, but s_c can take on its own dynamics with the backbone stretch λ is equal to q. Likewise, this implies that the backbone stretch is fixed at q for all positive values of s_c, thereby allowing only one of the two to change dynamically at a time. This dynamic behavior of withdrawal prevents the model from predicting infinite values of extension in elongational flows. It should also be mentioned that "branch-point withdrawal" leads to obvious change in topology which in turn leads to changes in the global morphology of the melt and can lead to modification of relaxation times[121].

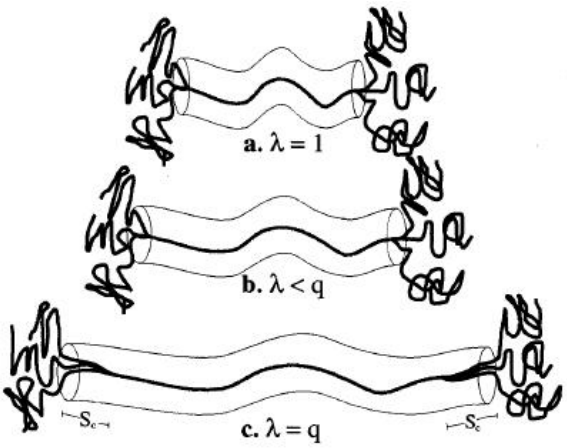

Figure 2.3.5 The ideal pom-pom molecule with *q=3* under various stages of stretch. Note that when λ equals *q*, some amount branch material, s_c, can withdrawal into the backbone tube[87].

The two branch points induce deviation from DE behavior in the linear stress relaxation regime. McLeish and Larson[87] suggest that in a melt of equivalently entangled pom-poms, the initial stress

relaxation occurs only in the branch arms, and on time scales similar to that of star arms, with segmental relaxation time increasing exponentially the closer it is to the branch point. The relaxed sections become effectively unentangled solvent that accelerate the arm relaxation time. The unrelaxed backbone segments impede relaxation time to values longer than pure star melts. This has been shown to be accurate for blends of star and linear polymers[122], and for blends of monodisperse H-polymers[50, 123]. McLeish *et al.*[50] also found that unlike star melts, an increase in polydispersity increases the terminal relaxation time of the free arms in H-polymers. Following arm relaxation, the backbones relax through reptation, with the relaxed arms acting as solvent. The effective friction to curvilinear motion is maintained at the branch point instead of being distributed across the backbone[87].

In tube theory, stress is calculated as a function of molecular orientation of the occupied tube segments. Due to the fast relaxation dynamics of the arms, the primary contribution to stress comes from the backbone segments, with the branch-arms providing a background Newtonian viscosity. This assumption holds true for time scales longer than the terminal arm relaxation time. Non-linear response is observed for flow rates between $\tau_a(0)^{-1}$ and ${\tau_b}^{-1}$, where τ_a is the terminal arm relaxation timescale and τ_b is the backbone relaxation timescale. This is due to the corresponding Weissenberg numbers being greater than one. "Weissenberg numbers" are defined by multiplying the deformation rate by the appropriate dimensionless time constant. The model assumes that the backbones are sufficiently large to self average orientation and stretch. Backbone stress increases quadratically with λ due to the linear dependence of stress on both the number of new tubes produced and the thermodynamic tension created. The only dynamic contribution from the arms comes at high values of stretch when s_c is greater than zero, resulting in some of the arm material being oriented in the backbone tube.

2.3.3 - Integro-Differential Form

The constitutive nature of the pom-pom model is not one simple equation relating stress to strain. Instead it relies on a set of equations relating three dynamic auxiliary variables: $\lambda(t)$, $s_c(t)$ and the orientation tensor, $\boldsymbol{S}(t)$, to stress, shown in Eq. 2.3-1. The expression for the orientation tensor, $\boldsymbol{S}(t)$, is given by Eq.2.3-2 where $\boldsymbol{E}(t,t')$ is the local deformation gradient and $\boldsymbol{u}(t)$ is the tube segment orientation. It is formulated with consideration of the rate of segment creation, the segments convection and extension in flow, the segments relative weight, and the survival probability of the tube itself. The dynamics of stretch, $\lambda(t)$, is formulated using a local force balance of frictional drag created by the branch point of the chain and the elastic recovery of the backbone, as given by Eq.2.3-3. The dynamics of branch-point withdrawal, $s_c(t)$, are determined by a similar force balance between an elastic restoring force and a frictional drag force as given by Eq. 2.3-4. In this case, the drag force comes only from the part of the arms that are not withdrawn into the backbone tube. $s_c(t)$ is greater than zero only for $\lambda(t)$ equal to q. An in-depth derivation of the integro-differential model can be found in McLeish and Larson (1998) [87].

McLeish-Larson Full Integro-differential Equation Set[87]

Expression for the stress:

$$\boldsymbol{\sigma} = \frac{15}{4} G_0 \phi_b \left(\phi_b \lambda^2(t) + \frac{2qs_c(t)}{2qs_a + s_b} \right) \boldsymbol{S}(t) \quad \text{with} \quad \phi_b = \frac{s_b}{2qs_a + s_b} \tag{2.3-1}$$

Evolution of orientation:

$$S(t) = \int_{-\infty}^{t} \frac{1}{\tau_b(t')} \exp\left(- \int_{t'}^{t} \frac{dt''}{\tau_b(t'')} \right) \frac{1}{\langle |\boldsymbol{E}(t,t')\cdot\boldsymbol{u}| \rangle} \left\langle \frac{\boldsymbol{E}(t,t')\cdot\boldsymbol{u}\boldsymbol{E}(t,t')\cdot\boldsymbol{u}}{|\boldsymbol{E}(t,t')\cdot\boldsymbol{u}|} \right\rangle dt' \tag{2.3-2}$$

Evolution of backbone stretch:

$$\frac{\partial}{\partial t}\lambda = \lambda(\boldsymbol{K}:\boldsymbol{S}) - \frac{1}{\tau_s}(\lambda - 1) \text{ for } \lambda > q \tag{2.3-3}$$

Evolution of arm-withdrawal measure s_c:

$$\frac{\partial s_c}{\partial t} = \left(q\frac{s_b}{2} + s_c \right) \boldsymbol{K}:\boldsymbol{S} - \frac{1}{2\tau_a(x_c)} \text{ for } \lambda = q \tag{2.3-4}$$

Timescales:

Backbone orientation: $\tau_b = \frac{4}{\pi^2} s_b^2 \phi_b \tau_a(x_c(t)) q$ with $x_c = \frac{s_c}{s_a}$ (2.3-5)

Arm spectrum: $\tau_a(x) = \tau_0 exp\left[\frac{15}{4} s_a \left(\frac{(1-x)^2}{2} - (1-\phi_b)\frac{(1-x)^3}{3} \right) \right]$ (2.3-6)

Backbone stretch: $\tau_s = s_b \tau_a(0) q$ (2.3-7)

Öttinger[124] and van Meerveld[125] investigated the thermodynamic admissibility of the pom-pom model in non-equilibrium thermodynamics using the GENERIC framework. Öttinger[124] found the integro-differential form of the pom-pom model to be admissible according to equilibrium thermodynamics. Non-equilibrium thermodynamics suggest modification of the pom-pom model is needed[124, 125]. The primary area of concern put forth is the independent formulation of the dynamics for both the configurational variables and the stress tensor[124].

The robustness of the integro-differential model is examined by McLeish and Larson[87] in a variety of flows. A representative molecular structure is selected so that neither the arm or backbone molecular weights dominate the mass fraction. This structure consisted of a pom-pom molecule with *q* equal to five, arm lengths equal to three entanglements, and a backbone 30 entanglements long. To simplify the calculation of Eq. 2.3-1, an approximation derived by Currie[126] (Eqs. 2.3-8 and 2.3-9) is inserted in place of Eq. 2.3-10, resulting in the stress tensor given in Eq. 2.3-11. Wapperom and Keunings [127] found the Currie tensor a good approximation of the Doi-Edwards tensor at moderate Weissenberg numbers in contraction/expansion flows.

$$\boldsymbol{Q} = \left(\frac{5}{J-1}\right)\boldsymbol{B} - \left(\frac{5}{(J-1)(I_2+13/4)^{1/2}}\right)\boldsymbol{C} \tag{2.3-8}$$

$$J \equiv I_1 + 2(I_2 + 13/4)^{1/2} \tag{2.3-9}$$

$$\frac{15}{4\langle|\boldsymbol{E}(t,t')\cdot\boldsymbol{u}|\rangle}\left\langle\frac{\boldsymbol{E}(t,t')\cdot\boldsymbol{u}\boldsymbol{E}(t,t')\cdot\boldsymbol{u}}{|\boldsymbol{E}(t,t')\cdot\boldsymbol{u}|}\right\rangle \tag{2.3-10}$$

$$\boldsymbol{\sigma} = G_0\phi_b\left(\phi_b\lambda^2(t) + \frac{2qs_c(t)}{2qs_a+s_b}\right)\int_{-\infty}^{t}\frac{\exp\left(-\int_{t'}^{t}\frac{dt''}{\tau_b(t'')}\right)}{\tau_b(t')}\boldsymbol{Q}dt' \tag{2.3-11}$$

Fig. 2.3.6a shows the predication of transient stress growth in uniaxial extensional flow. Simple strain hardening is observed for strain rates where the orientational Weissenberg number is greater than one. A low strain rates, simple stress growth is observed until reaching a steady-state plateau. At higher strain rates, strain hardening is observed by the increasing viscosity plateau, a feature devoid in the K-BKZ integral model. This growth corresponds to increases in the equilibrium values of λ, shown in

Fig. 2.3.6b. Beyond some critical strain rate, λ reaches its maximum value of q (in this case equal to five), marking the onset of branch point withdrawal. This is shown graphically in Fig. 2.3.6c by the rapid rise of s_c at timescales longer than the onset of the stretch plateau seen in Fig. 2.3.6b. The qualitative behavior of the model is consistent with data published for LDPE studied by Laun [128].

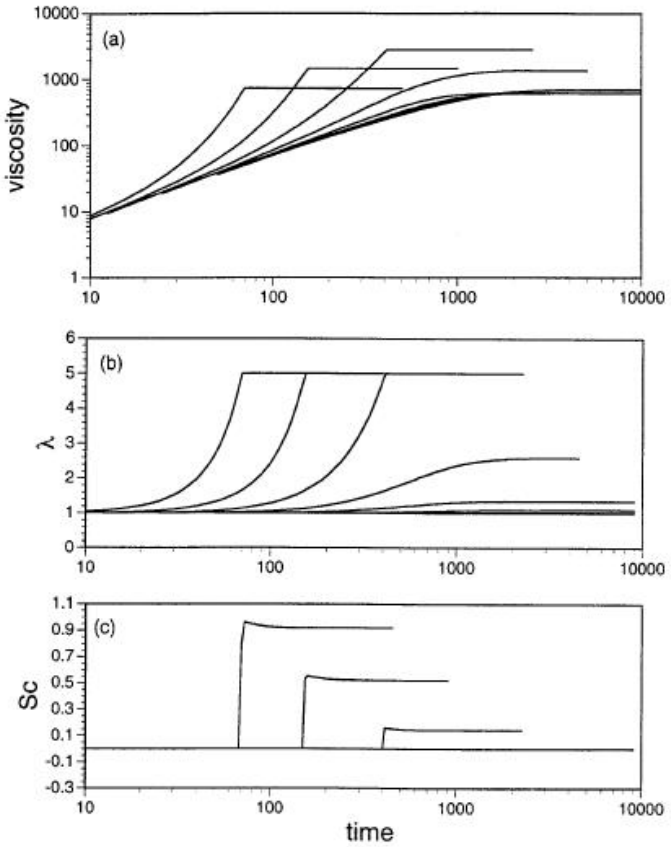

Figure 2.3.6 *(a)* Transient extensional viscosity predictions for a pom-pom model with q = 5, s_a = 3, and s_b = 30. Extension rates are 0.0003, 0.0006, 0.00125, 0.0025, 0.005, 0.01, 0.02, and 0.04 in terms of the arm relaxation time. *(b),(c)* Evolution of $\lambda(t)$ and $s_c(t)$ for the same flow rates[87].

Computations in shear flow exhibit very different behavior from those in extensional flow across the same rates examined in Fig 2.3.6. In Fig. 2.3.7a is shown the growth of shear viscosity and the first normal stress coefficient. Overshoots in both stresses are predicted, but branch point withdrawal never occurs, as evidenced in Fig. 2.3.7b. This suggests that the backbones may stretch transiently in flow, even up to their maximum value, but no hardening effects are observed. Inkson *et al.*[83] found that the maximum stretch ratio in the shear overshoot is a function of the orientation and relaxation times

$$\lambda \sim \frac{1}{1-\frac{\tau_S}{2\tau_b}}, \text{ for } \dot{\gamma} \gg \tau_S^{-1}. \qquad (2.3\text{-}12)$$

Rubio and Wagner[129] found that the full integro-differential form qualitatively calculated the values of the second normal stress difference N_2 in shear flow, leading to a ratio of second to the first normal stress difference (N_2 /N_1) equal to -2/7 for slow flows.

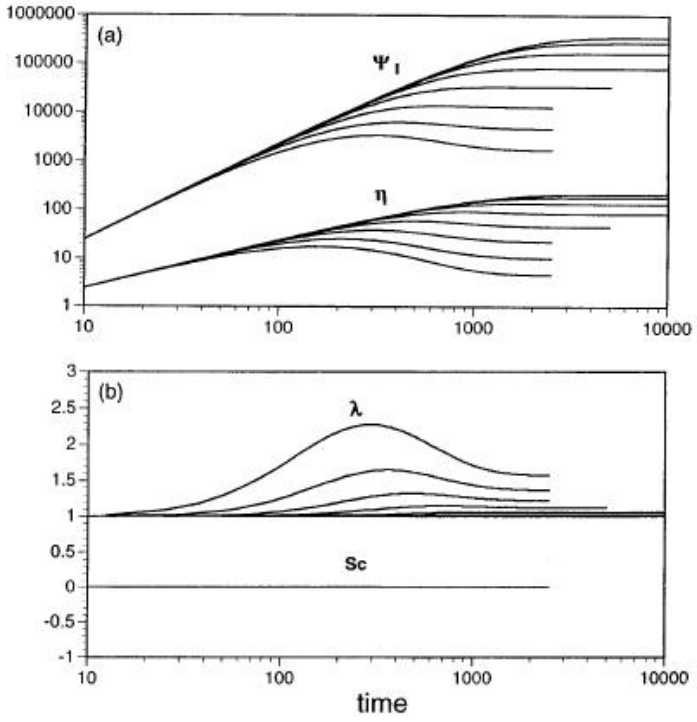

Figure 2.3.7 *(a)* Transient shear and first normal stress difference for the same flow rate and model parameters as in Fig. 2.3.6. *(b)* Dynamic evolution of $\lambda(t)$ and $s_c(t)$ for the same flow rates[87].

Steady-state flow curve predictions are shown in Fig. 2.3.8a. Concurrent observations of extensional-hardening and shear-thinning are predicted by the pom-pom model. The thinning behavior in shear suggests that the dynamics never "sample" the stretching behavior. Steady-state stretch is only observed in extensional flow, where the height of the peak corresponds to the magnitude of *q* and the strain rate at which the peak occurs is on the order of the inverse of the stretch relaxation time. In planar extension, the steady-state behavior mimics that of uniaxial extension (Fig. 2.3.8b) [87].

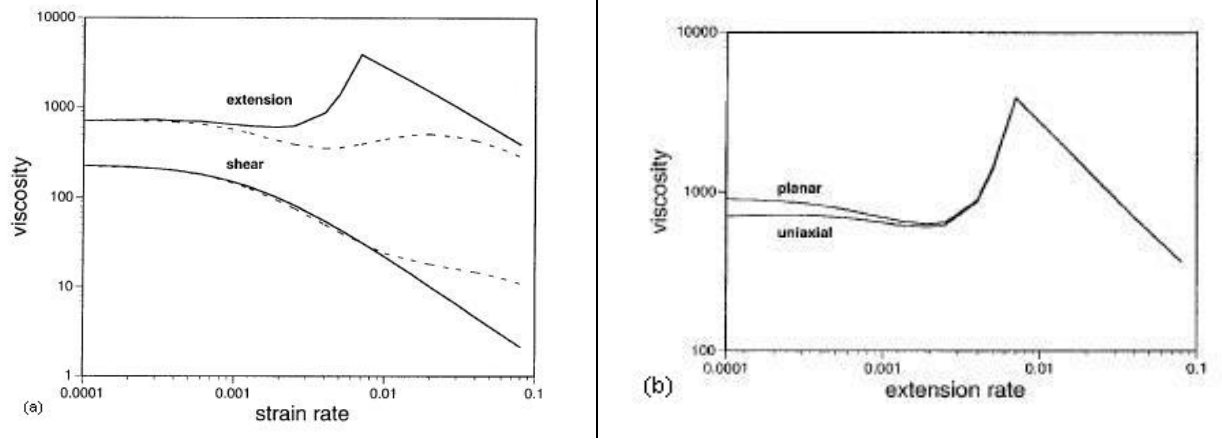

Figure 2.3.8 *(a)* Steady-state shear and extensional viscosities as a function of deformation rate. Solid line represents full integral model predictions. Dashed lines indicate K-BKZ analog predictions. *(b)* Comparison of steady-state uniaxial and planar extension as a function of deformation rates[87].

In Fig. 2.3.9a is illustrated the predicted material response of the pom-pom model for shear and extensional strain rates equal to 0.01 s^{-1}. Notice the qualitative behavior of the pom-pom model in transient flow agrees well with published data by Laun and Schuch [130] shown in Fig. 2.3.9b. The uniaxial and planar extensional viscosities have been normalized by their respective Trouton ratios of 3 and 4 so that the viscosity curves match at short times. Rubio and Wagner[131] found that the integro-differential pom-pom model predicts qualitatively accurate behavior for the primary and secondary normal stresses in planar extension. The difference in viscosity curve occurs because the uniaxial and planar extensional flows allow molecular orientation to couple strongly with stretch. This lack of coupling in shear leads to thinning below the linear viscoelastic response. Although the original pom-pom model is derived for a specific, ideal architecture, it is able to qualitatively match the behavior of LDPE in start-up flows measured previously by Meissner [132]. This comparison is shown in Fig. 2.3.10, with the most notable common features being the overshoot of viscosity in shear flow below the linear viscoelastic envelope and the presence of strain hardening above it in extension.

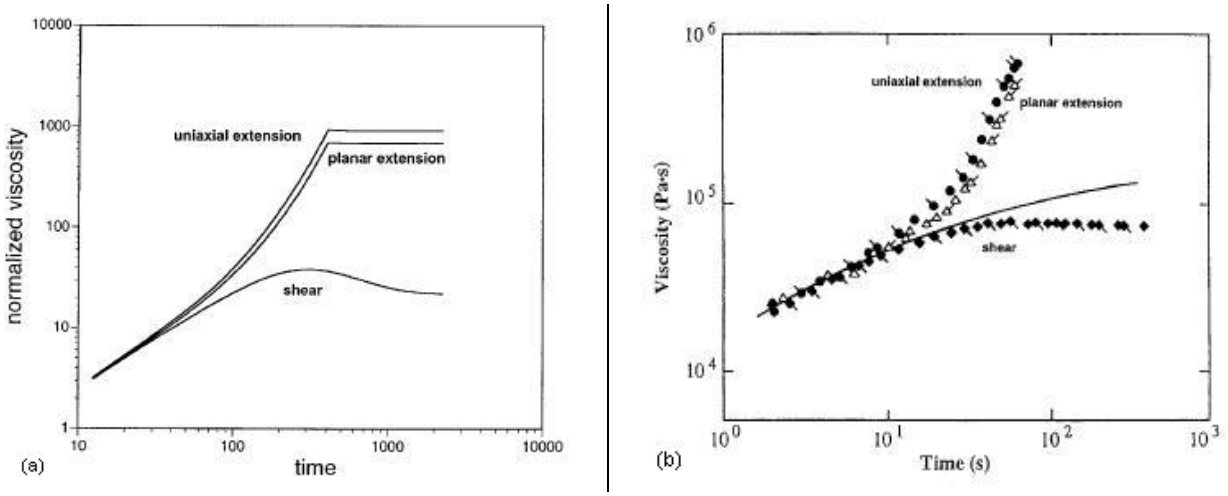

Figure 2.3.9 *(a)* Transient extensional (uniaxial and planar) and transient shear viscosities for deformation rate equal to 0.01 s^{-1}. The extensional viscosities have been normalized by their "Trouton ratios" of 3 and 4 respectively. *(b)* LDPE data from Laun and Schuch [130] at 0.05 s^{-1} plotted in the same fashion to show qualitative agreement of the model[87].

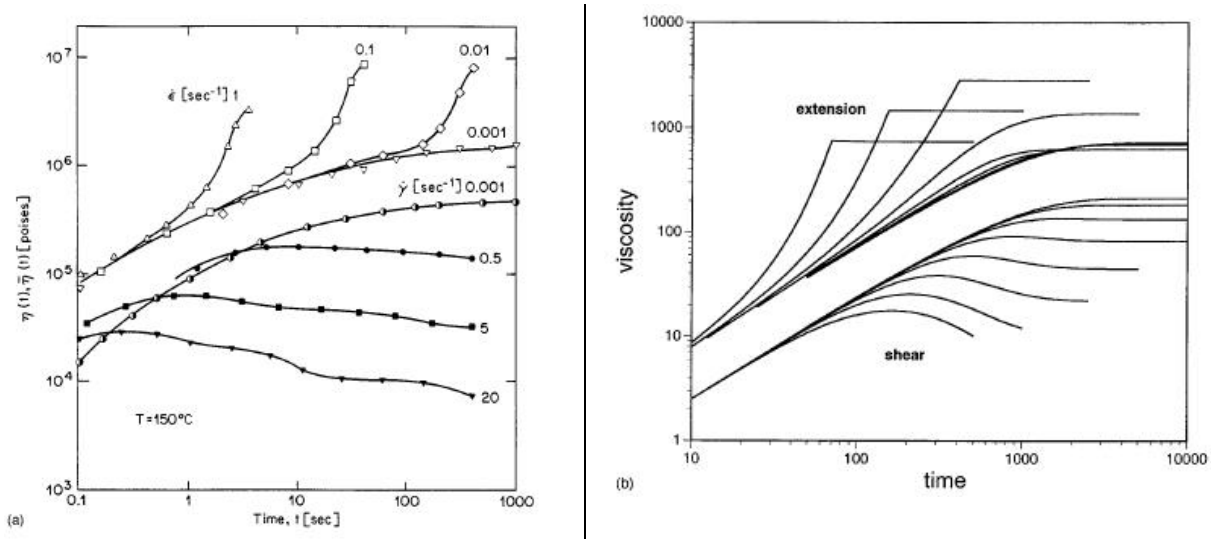

Figure 2.3.10 *(a)* Transient viscosities in uniaxial extension and shear for the LDPE melt IUPAC A from Meissner [132] at 150°C. *(b)* Transient viscosities for the pom-pom model using the same parameters and flow rates as in Fig. 2.3.6 [87].

In Fig. 2.3.11 is shown the effect of changing only the value of *q* in both transient shear and extensional flow. Other molecular parameters are held at the same values as outlined in Fig. 2.3.6. The reduction in extensional viscosity with increasing *q* at early times, as well as the behavior of shear viscosity at all times, is attributed to the diluting effects of increasing the number of arms. This effect is in competition with the increasing stress in stretch due to the increasing number of arms. At long times

in transient extensional flow, the increase in stress overcome the diluting effects and results in greater strain hardening.

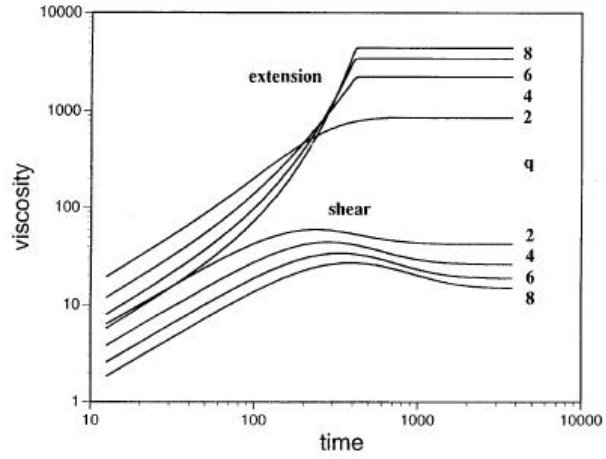

Figure 2.3.11 Transient viscosities with the same molecular parameters as Fig. 2.3.6 but varying the arm number q to 2, 4, 6, and 8 [87].

2.3.4 - K-BKZ Analog

McLeish and Larson[87] developed a K-BKZ analog relationship that predicts exactly the time-dependant stresses following any step deformation. This form produces a single equation relating stress to strain and was originally derived to point out the inability of a K-BKZ type equation to accurately predict sufficient extensional hardening and shear thinning in the steady-state viscosity of polymers with multiple branch points. This failure is illustrated in Fig. 2.3.8a by the dashed-lines. McLeish and Larson[87] concluded that the lack of vorticity terms in K-BKZ type equations was the primary reason for their inability to accurately model pom-pom molecules.

The analog model contains two major assumptions: the Currie approximation outlined in section 2.3.3 is valid and all consequences of branch-point withdrawal are neglected. The second is validated by a closer inspection of Eq. 2.3-1. Recall that branch-point withdrawal only occurs when λ equals q. Therefore, for all q > 3, the term with the factor of λ^2 in Eq. 2.3-1 becomes dominant relative to the branch-point withdrawal term that is dependent on q. This leads to the stress tensor following step-strain to be equal to Eq. 2.3-13 where $G(t, I_1, I_2)$ is equal to Eq. 2.3-14 for the pom-pom model. The K-

BKZ constitutive analog is given by Eq. 2.3-15 where *m*, the memory function, is simply the negative of the derivative of Eq. 2.3-14 with respect to time:

$$\sigma(t) = G(t, I_1, I_2)\boldsymbol{Q} \tag{2.3-13}$$

$$G(t, I_1, I_2) = G_0 e^{-t/\tau_b}\left\{[\lambda(I_1, I_2) - 1]e^{-t/\tau_s} + 1\right\}^2 \tag{2.3-14}$$

$$\sigma(t) = G_0 \int_{-\infty}^{t} m(t - t', I_1, I_2)\boldsymbol{Q}(t, t')dt' \tag{2.3-15}$$

with $\boldsymbol{Q}$ given by Eq. 2.3-8.

Another feature of this analog equation is that it fails to predict time-strain separability over the entire timescale. In fact, such behavior is not observed until after some characteristic retraction time. McLeish *et al.*[50] confirmed this experimentally in entangled H-polymers finding that time-strain separability only occurred on times scales much longer than the Rouse time. They attribute this behavior to the curvilinear stretch relaxation of the cross-bar, which is retarded by the renormalized friction of the branch points.

2.3.5 - Approximate Differential Model

A simplified form of the full integro-differential model was proposed by McLeish and Larson[87] in order to reduce calculation complexity of the orientation tensor, ***S(t)***, thereby making it possible to simulate complex flows. This differential form of orientation is given by Eq. 2.3-17. It accurately models the correct asymptotic behavior of S_{xy} in shear flow with relation to strain rate. The effect of branch-point withdrawal is also neglected, using the same argument presented in section 2.3.4. This simplified equation set is given by Eqs. 2.3-16 through 2.3-20. The response in startup is shown in Fig. 2.3.12, and appears quantitatively similar to that of the full integral form shown in Fig. 2.3.10.

McLeish-Larson Simplified Differential Equation Set

Expression for the stress:

$$\sigma = \frac{15}{4} G_0 \phi_b^2 \lambda^2(t) \boldsymbol{S}(\boldsymbol{t}) \quad \text{with} \quad \phi_b = \frac{s_b}{2qs_a + s_b} \tag{2.3-16}$$

Evolution of orientation:

$$\frac{\partial}{\partial t}\boldsymbol{A}(t) = \boldsymbol{K}\cdot\boldsymbol{S} + \boldsymbol{S}\cdot\boldsymbol{K^T} - \frac{1}{\tau_b}\left(\boldsymbol{A} - \frac{1}{3}\boldsymbol{I}\right); \qquad \boldsymbol{S}(\boldsymbol{t}) = \frac{\boldsymbol{A}(\boldsymbol{t})}{trace[\boldsymbol{A}(\boldsymbol{t})]} \tag{2.3-17}$$

Evolution of backbone stretch:

$$\frac{\partial}{\partial t}\lambda = \lambda(\boldsymbol{K}:\boldsymbol{S}) - \frac{1}{\tau_s}(\lambda - 1) \text{ for } \lambda > q \tag{2.3-18}$$

Timescales:

Backbone orientation: $\tau_b = \frac{4}{\pi^2} s_b^2 \phi_b \tau_a(0) q$ (2.3-19)

Backbone stretch: $\tau_s = s_b \tau_a(0) q$ (2.3-20)

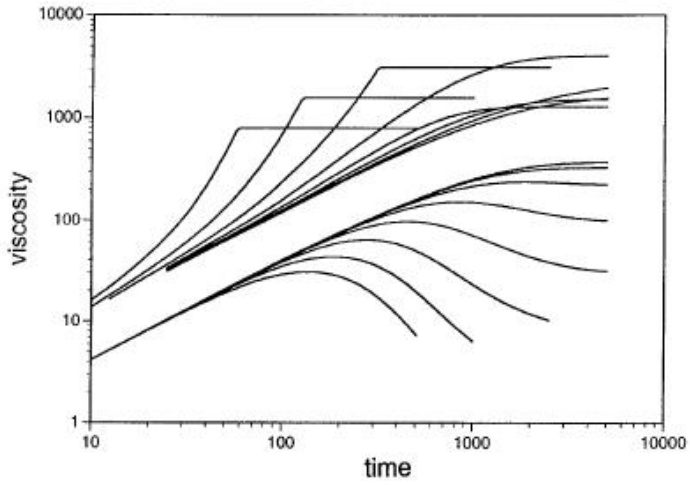

Figure 2.3.12 Transient viscosities in uniaxial extension and shear calculated using the differential form of the pom-pom model (Eqs. 2.3.6-1 through 2.3.6-6). Deformation rates are the same as in Fig. 2.3.6 [87].

Rubio and Wagner[133] compared the predictions of the differential form of the pom-pom model with that of the full integro-differential form in a variety of flows, finding several notable deviations in their behavior. The three most notable are presented here. First, the differential form does not predict a second normal stress, N_2, in shear flow. Second, in planar extension, the differential form predicts that the secondary viscosity (Eq. 2.3-21) goes to zero for all but the smallest strain rates while the full model predicts steady-state secondary viscosity values at long times for all strain rates. This behavior in planar extension is illustrated in Fig. 2.3.13. Finally, the differential form predicts both a larger stress overshoot and enhanced shear thinning in the start-up of shear flow. Rubio and Wagner[133] attributed this behavior in shear to a strong stretch relaxation process not present in the full integro-differential form.

$$\mu_{p2} = \frac{\sigma_{22} - \sigma_{33}}{\dot{\varepsilon}} \tag{2.3-21}$$

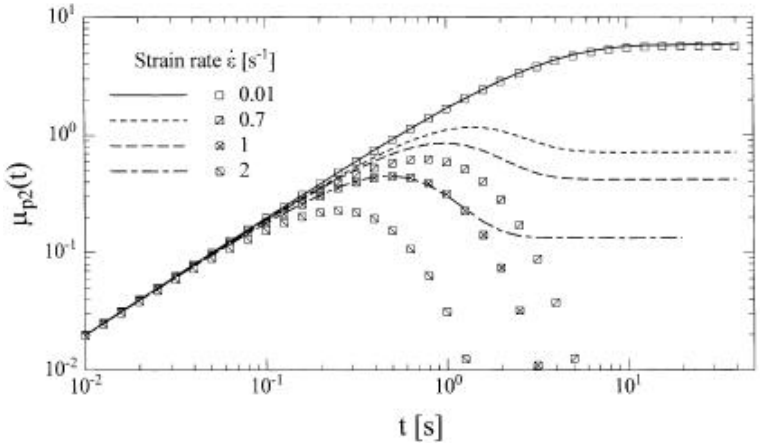

Figure 2.3.13 Planar viscosity μ_{p2} predicted by the by the full integro-differential model (lines) and the differential form (symbols) at various strain rates[133].

Lee *at al.*[120] examined the Hadamard stability of the differential form of the pom-pom model. The Hadamard stability of differential equations implies stability under extremely short and high frequency wave distributions and accounts for the elastic behavior of viscoelastic constitutive equations related to very fast responses[134]. For $\lambda < q$, the authors found the differential form to be Hadamard stable as long as the orientation tensor **S** is positive and definite. For $\lambda = q$, Hadamard stability is achieved only when branch-point withdrawal is included and the orientation tensor **S** is positive definite[120]. When branch-point withdrawal is neglected, the differential form becomes Hadamard unstable when the instantaneous dimensionless shear becomes greater than $\sqrt{3}$ [120].

Bishko *et al.*[135] examined the differential form of the pom-pom in planar 4:1 contraction flow, finding the behavior to be qualitatively similar to LDPE. Increase in branching content was found to increase corner vortex size due to the magnitude of extensional stresses increasing relative to shear stresses[135].

2.3.6 – Extension to Real Systems

The purpose of this section is to introduce and review a quantitative method for predicting the rheological response of real molecules (i.e. LDPE) using a multi-mode form of the differential pom-pom model. It has been shown that the predictions of both the full integro-differential and simplified differential forms of the pom-pom model *qualitatively* agree with published data of LDPE melts, as seen in sections 2.3.3 and 2.3.5. The hierarchical relaxation of large molecules with multiple branch points, such as LDPE, allows one to use the concepts of priority and seniority distributions to gain a *quantitative* picture of the relaxation dynamics. Rigorous calculations involving every seniority and priority distributions of a molecule are circumvented in favor of a multimode approach put forward by Inkson *et al.*[83].

In large molecules that have multiple branch points, the segmental tension is simply traced by the sum of the tensions at each branch point from the nearest free end inwards[119]. Priority is defined as the value of the summed entropic forces and can be thought of as the ratio of the maximum tension of a segment to its equilibrium tension. Priority is equal to *q* in the ideal pom-pom molecule. The short-time (immediate) response to a large strain of a branched molecule is a function of its priority distribution[83]. In Fig 2.3.14b is illustrated how priority is calculated in a complex molecule with multiple branch points simply by taking the lesser of the number of chain ends linked to either branch end[136].

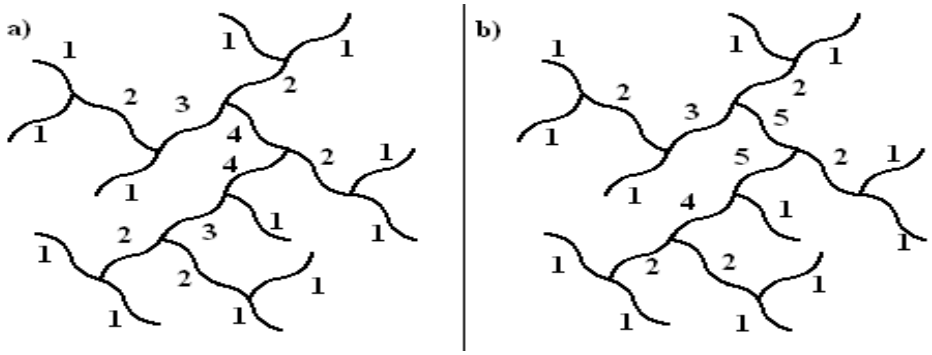

Figure 2.3.14 Illustration of calculating seniority *(a, left)* and priority *(b, right)* in branched polymer systems. Figure adapted from Read and McLeish [136].

The relaxation time of a segment is set by its path distance to the nearest free end that can release it from its tube constraint by retraction[83]. This statistic is called seniority, and it increases toward the central segment of a complex branched molecule[137]. In Fig 2.3.14a is illustrated how seniority is calculated by counting the number of strands to the furthest chain end on each side of the segments and then taking the lesser of the two values[136]. In Fig. 2.3.15 is illustrated the relaxation process of a large molecule with multiple branching levels. The free ends are the first to relax in star-arm fashion until reaching the branch point. The branch point takes a diffusive step, allowing the newly freed backbone to relax its stretch. This backbone segments relaxes in a star-arm fashion up to the next branch point, but on much longer timescales than the outer segments. This process continues on until the innermost backbone segment is relaxed.

Figure 2.3.15 Relaxation of a complex branched polymer (such as LDPE). At some flow rate $\dot{\varepsilon}$, the molecule has an unrelaxed core of relaxation times $\tau > \dot{\varepsilon}^{-1}$ connected to relaxed material of relaxation times $\tau < \dot{\varepsilon}^{-1}$ behaving as solvent[83].

The full seniority and priority distributions are required to completely calculate the full rheological response of a material. Assuming that they were even known, it would require a prohibitive amount of computational time. Instead, a multi-mode approach originally put forth by Inkson *et al.*[83] in LDPE systems can be used to model complexly branched structures as a theoretical blend of pom-pom molecules with differing number of arms that have orientational relaxation times assigned from the linear spectrum. The higher priority segments are represented by theoretical pom-pom molecules with higher number of branch arms (q) and longer orientational relaxation times (τ_b) and therefore, higher

seniority. The multi-mode model assumes that each level of branching is decoupled from the others, i.e. that segments with different priorities on the same molecule do not interact with each other.

Each *i*th mode of the multi-model is defined by four parameters: the stretch and orientation relaxation times τ_{si} and τ_{bi}, respectively, the number of arms q_i, and the contribution to the plateau modulus g_i. The two evolution equations for each mode are orientation $\boldsymbol{S}_i(t)$ and stretch $\lambda_i(t)$and are the same form as Eqs. 2.3-17 and 2.3-18. The stress contributions from each mode are additive so that

$$\boldsymbol{\sigma} = \sum_{i=1}^{n} \boldsymbol{\sigma_i} = \sum_{i=1}^{n} g_i \, \lambda_i^2(t) \boldsymbol{S_i}(t). \qquad (2.3\text{-}22)$$

Inkson *et al.*[83] presented a stability analysis to help determine the correct density of modes. Selecting too many modes can lead to ill-posed fits of the moduli[138, 139], and selecting too few can result in one mode being active over a large range of strain rates. Providing that modes are selected so that the spectra remain stable, $g\tau^2/\Delta\tau$ plotted as a function of τ should produce a smooth curve (Fig. 2.3.16)

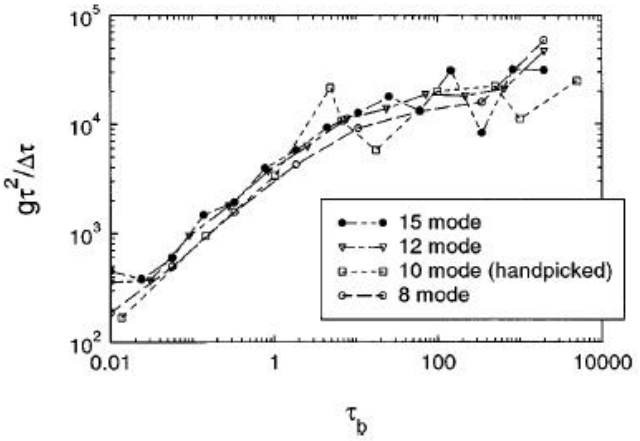

Figure 2.3.16 Stability analysis of different choices for linear relaxation spectra for LDPE B[83].

Inkson *et al.*[83] outlined a fitting procedure for the four parameters at each mode. Selection of τ_{bi}'s was arbitrary, and one to two modes per decade was sufficient. Contributions to the plateau modulus g_i's were fit using the storage and loss modulus from the linear relaxation spectrum. τ_{si}'s and q_i's were fit concurrently from transient uniaxial viscosity. Inkson *et al.*[83] verified the robustness of the model and fitting procedure on a series of four LDPEs. A 12 mode fit of LDPE B, illustrated in Fig. 2.3.17, showed good agreement with experimental data across a wide range of strain rates in the start-up of

both transient shear and uniaxial extensional flows. Similar results were found for all LDPEs studied by Inkson *et al.*[83].

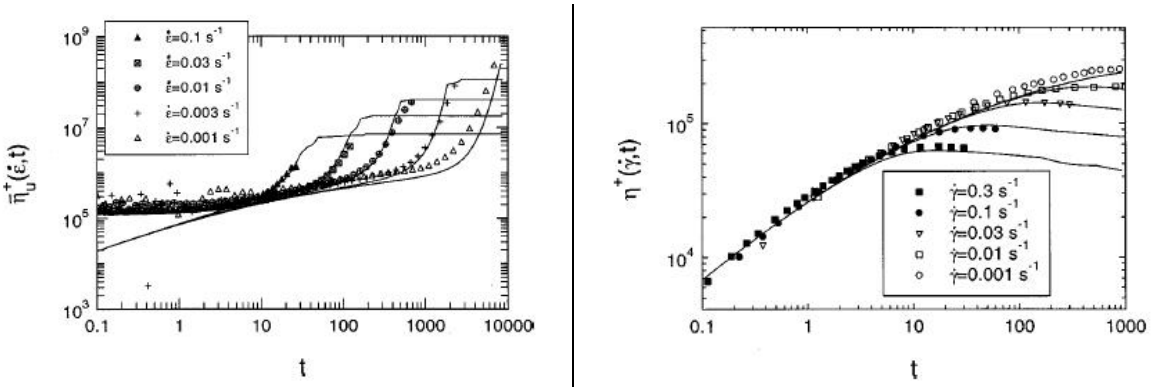

Figure 2.3.17 *(a, left)* Fits of a 12 mode pom-pom model for LDPE B in the start-up of transient uniaxial flow. *(b, right)* Fits of a 12 mode pom-pom LDPE B melt in the start-up of shear flow[83].

Rubio and Wagner[133] analyzed the full integro-differential and differential forms of the multimode pom-pom model in planar extensional flow. In Fig. 2.3.18 is shown the predictions of both the primary and secondary planar viscosities for LDPE IUPAC A using the parameters fit by Inkson *et al.*[83] using the transient uniaxial extension method outlined above. The differential form is represented by symbols and the full integro-differential form by lines. Both forms predicted strain hardening in the primary planar viscosity, which was in agreement with experimental observations. A difference appeared in the predictions of the secondary viscosity. The differential form predicted a thinning response. The full integral form predicted a strain-hardening response which the authors determined to be in disagreement with experimental data [133].

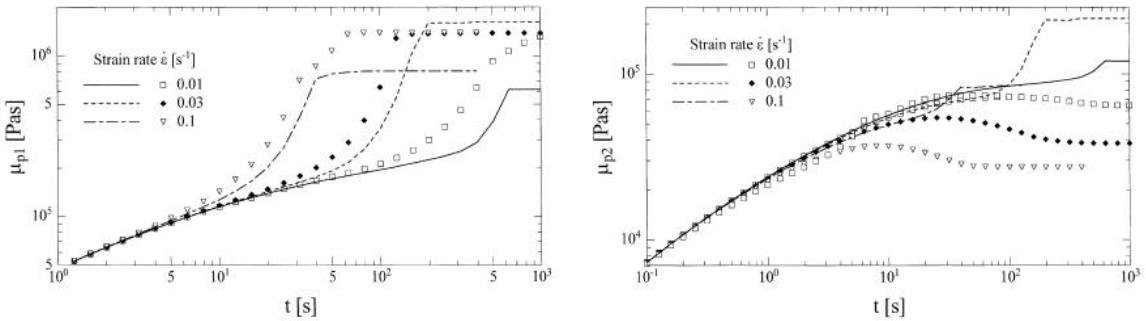

Figure 2.3.18 *(left)* Planar viscosity μ_{p1} and *(right)* planar viscosity μ_{p2} predictions using the multi-mode pom-pom model parameters determined by Inkson *et al.*[83] for LDPE IUPAC A[133].

Graham and McLeish[140] explored using exponential shear to determine the non-linear backbone stretch relaxation time τ_{si} and number of arms q_i. Exponential shear was deemed useful in that it mimics the flow direction of simple shear while stretching the backbone similar to planar extensional flow. In this work, the shear rate grew exponentially with time and was defined by

$$\dot{\gamma}(t) = \alpha(e^{\alpha t} + e^{-\alpha t}), \qquad (2.3\text{-}23)$$

where α was the characteristic strain rate of the flow. The authors found that the non-linear parameters could be fit using exponential shear, but when the same parameters were used to predict behavior in start-up of extensional flow, the predictions deviated from experimental data, especially at lower strain rates (Fig. 2.3.19). The authors attributed this deviation at low strain rates to the low moduli values g_i of the corresponding long modes being swamped by the shorter modes. Recall that lower strain rates correspond to longer relaxation times. It is these slow modes that have the greatest stretch. It is because of this that the authors concluded that while exponential shear can be used to determine non-linear pom-pom parameters, the use of start-up of uniaxial flow via the methodology of Inkson *et al*.[83] was superior.

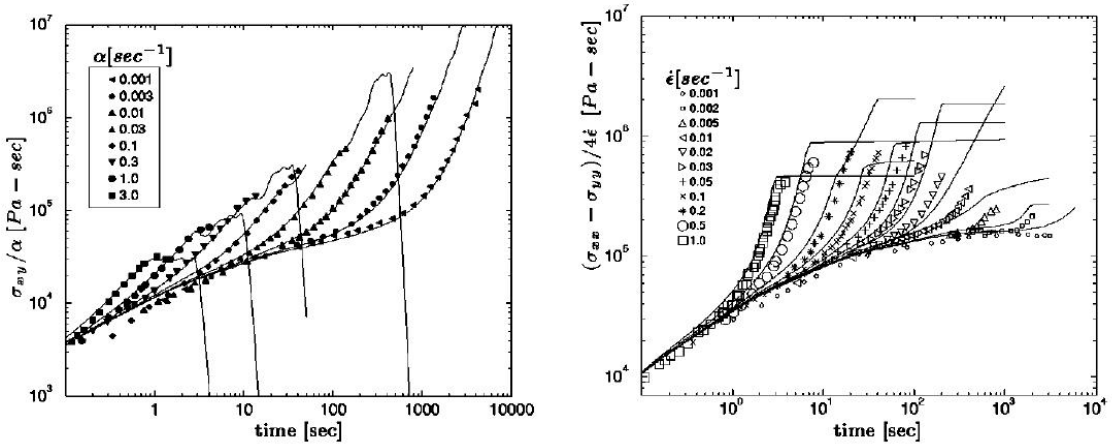

Figure 2.3.19 *(left)* Multimode pom-pom fits using exponential shear to fit non-linear parameters. *(right)* Prediction in extensional flow using parameters fit from exponential shear[140].

Seay[2] investigated using the multimode form of the K-BKZ analog (Eq. 2.3-14) to determine the non-linear stretch parameter τ_{si} at each mode from the stress relaxation modulus *G(t)* for a series of

sparsely-branched LLDPE. The K-BKZ analog form failed to quantitatively fit the relaxation modulus behavior at short times with realistic parameters. Values of τ_{bi} /τ_{si} were found to be too large, predicting on the order of 50 entanglements for sparsely-branched, relatively low MW PE resins. The author attributed the choice of a Doi-Edwards approximation for initial stretch λ as a likely source of error, as it failed to accurately dampen the modulus at longer times[2].

Rubio and Wagner[133] proposed a multi-mode form of the shear relaxation modulus

$$G(t,\gamma) = \sum_i g_i exp\left(\frac{-t}{\tau_{bi}}\right) \lambda_i^2(t,\tau_{si},q_i)\, h_{DE}(\gamma) \qquad (2.3\text{-}24)$$

where $h_{DE}(\gamma)$ is the Doi-Edwards damping function. The time-dependent stretch, λ, was calculated using Eq. 2.3-18. For step-strain

$$\lambda_i(t,\tau_{si},q_i) = 1 + (\lambda(0^+) - 1)exp\left(\frac{-t}{\tau_{si}}\right) \qquad (2.3\text{-}25)$$

strictly for $\lambda_i < q_i$, otherwise $\lambda_i = q_i$. $\lambda(0^+)$ was the instantaneous stretch. The authors did not attempt to determine parameters using Eq. 2.3-24 in tandem with the linear relaxation spectrum.

Chodankar *et al.*[141] derived expressions for the multimode forms of both the differential and integro-differential shear relaxation moduli following a step-strain. The multimode form of the shear relaxation modulus for the differential form was found to be

$$G(t,\gamma) = 3\sum_i g_i \lambda_i^2(\gamma,t) \frac{exp\left(\frac{-t}{\tau_{bi}}\right)}{3+\gamma^2 exp\left(\frac{-t}{\tau_{bi}}\right)}, \qquad (2.3\text{-}26)$$

and the integro-differential model was Eq. 2.3-25 with

$$h_{DE}(\gamma) = \frac{1}{1+a\gamma^2} \qquad (2.3\text{-}27)$$

where *a* was an adjustable parameter. The qualitative behavior of these two equations was analyzed using parameters fit to a LDPE resin by Graham *et al.*[140]. Fig. 2.3.20 shows the shear relaxation modulus for each form. Moderate deviations from time-strain factorability were seen in both forms of the shear modulus. The authors suggested that better time-strain factorability could be obtained using

parameters fit using a technique different from Graham *et al.*[140]. No mention was made by the authors about using the experimental step-strain data to determine the non-linear stretch parameter for each mode. Damping functions calculated from the shear modulus curves given in Fig. 2.3.20 were found to be in reasonable agreement with experimental data (Fig. 2.3.21), and were a better representation of the data than predicted by the Doi-Edwards damping function given by Eq. 2.3-27 [141].

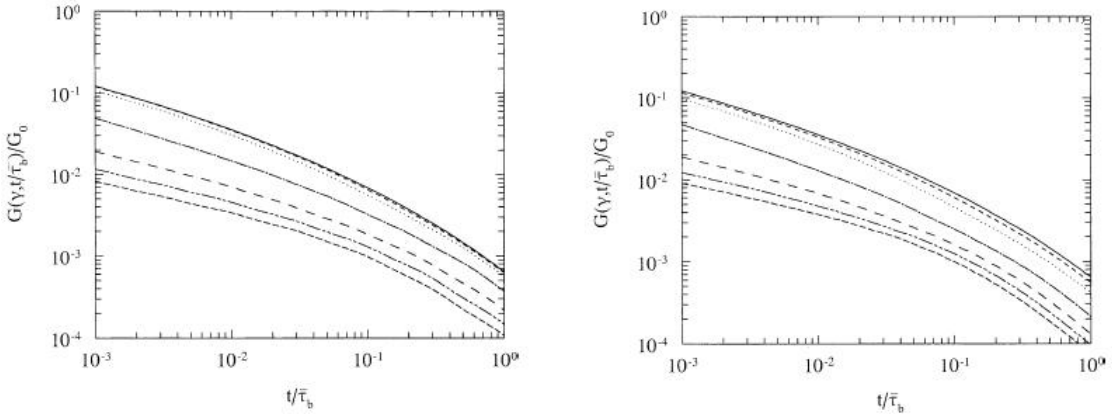

Figure 2.3.20 Shear relaxation modulus predicted by the multimode integro-differential *(left)* and differential *(right)* pom-pom models for shear strains γ= 10%, 100%, 200%, 500%, 1500% and 2000% (top to bottom)[141].

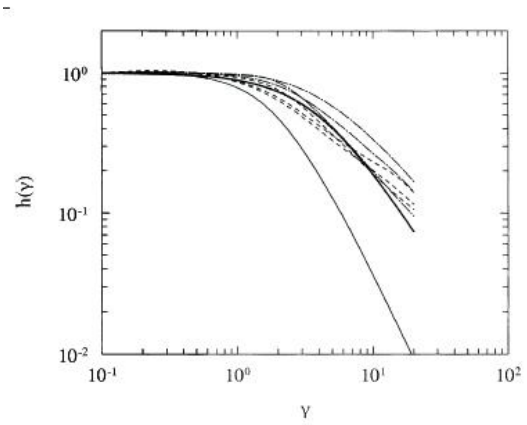

Figure 2.3.21 Comparison of various damping functions calculated from the differential form *(dashed-dot lines)* and the integral form *(dashed lines)* with the experimentally determined damping function *(dark solid line)* for 1810H LDPE at 150 °C. Shown also is predicted damping function Eq. 2.3-27 *(solid line)*[141].

Blackwell *et al.*[142] proposed a mechanism for "smoothing" the sharp slope discontinuity seen in the steady-state extensional viscosity curves (Fig 2.3.8) that coincided with the onset of branch-point withdrawal. They proposed that prior to the backbone achieving its maximum stretch, it could relax

locally (on length scales less than the tube diameter *a*) by branch-point displacement, causing some of the branch material to become aligned with in the backbone tube. This phenomenon, called "local branch-point withdrawal," was defined as the alignment resulting from the force balance between the elastic tension of the backbone segments with the Rouse drag of the arms. The oriented arm segments became essentially backbone material, thereby reducing the primitive path and relaxation time of the unoriented arms. This in turn reduced the backbone stretch relaxation time, τ_s, by the following:

$$\tau_s \rightarrow \tau_s e^{-\nu^*(\lambda-1)} \qquad (2.3\text{-}28)$$

where v* was an adjustable parameter related to magnitude of the quadratic localizing potential of the branch point. v* could also have been thought of as a measure of the influence of the surrounding polymer chains on the backbone tube stretch[143]. In Fig. 2.3.22 is shown the effect of varying v* in steady-state uniaxial extension. v* equal to zero was equivalent to the unmodified pom-pom model. Increasing values of v* served to "smooth" the viscosity curve at the point of maximum backbone stretch. Local branch-point withdrawal can be incorporated into both the full integro-differential and simplified differential forms of the pom-pom model by substituting Eq. 2.3-28 into Eqs. 2.3-3 and 2.3-18, respectively.

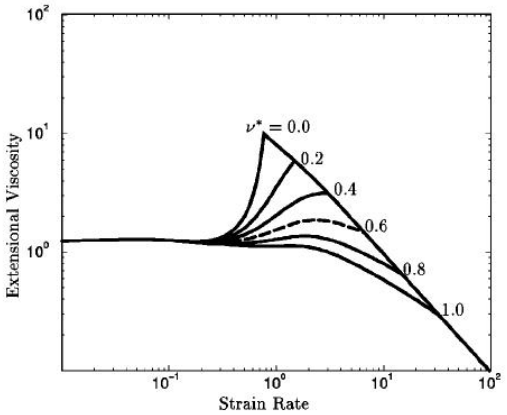

Figure 2.3.22 The steady-state viscosity in uniaxial extension for values of v* from 0.0 to 1.0. Units were chosen with $G_0 = 1$ and $\tau_s = 1$ [142].

The robustness of Eq. 2.3-28 in the differential pom-pom model was tested by Blackwell *et al.*[142] on the transient extensional viscosity of the IUPAC A LDPE across various strain rates (Fig. 2.3.23).

Calculations incorporating local branch-point withdrawal into the pom-pom model were shown to improve model fits. For these calculations, the best value of v* was found to be equal to $2.0/q_i$. For v* equal to zero (equivalent to the unmodified pom-pom equation), the model fits were less robust. In Fig. 2.3.24 is shown the calculation of steady-state viscosity of IUPAC A LDPE in both uniaxial and shear flow using the multi-mode pom-pom model with local drag-strain coupling (v* = $2.0/q_i$), and without local drag-strain coupling (dashed). Local branch-point withdrawal significantly improved the ability of the model to fit the data. Most notable was that it removes the sharp peaks predicted in steady-state extensional flows by the unmodified form.

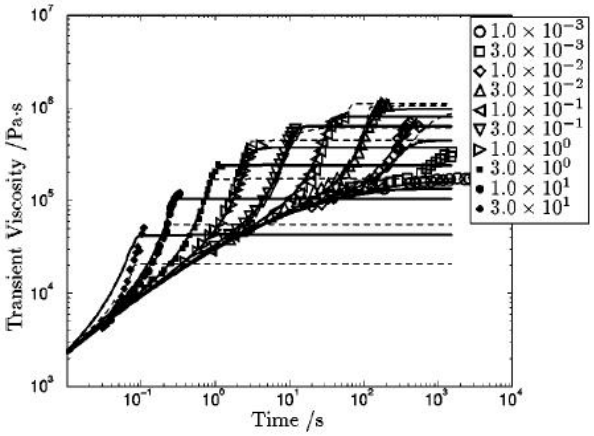

Figure 2.3.23 Fit transient viscosity of the IUPAC A LDPE in transient uniaxial extension calculated using the multimode pom-pom model with local drag–strain coupling (v*= $2.0/q_i$, solid lines) and without local drag–strain coupling (dashed lines). Data was taken at 150 °C[142].

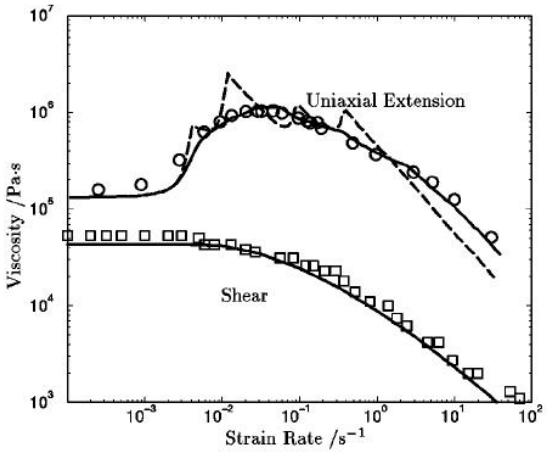

Figure 2.3.24 Steady-state viscosity of the IUPAC A LDPE in extension and shear calculated using the multimode pom-pom model with local drag–strain coupling (v*= $2.0/q_i$, solid) and without local drag–strain coupling (v*= 0, dashed)[142].

Blackwell *et al.*[144] used the Cayley tree structure, an ideal, multiple branch-level structure, to compare linear and nonlinear viscoelastic responses of molecular calculations with that of the multimode differential pom-pom model with local branch-point withdrawal. In Fig. 2.3.25a is illustrated the ideal three-level Cayley tree studied. In Fig. 2.3.25b is shown a comparison of molecular calculations (lines) and four mode pom-pom fit (symbols) in shear and extension. All analysis was purely computational, but yielded interesting observations on the behavior of the multi-mode pom-pom model. Points of departure from the shear curve and steady-state viscosities were reasonable well-predicted by the pom-pom model. However, the shape of the shear curves was very different from the full Cayley tree calculations, most notably the shape of the stress overshoot. Deviation was also seen in the transient extension curves. This behavior was attributed to fitting a single stretch relaxation time to each level (mode) in the multimode pom-pom model, and illustrated the lack of time-dependant priority in the multimode pom-pom model[144].

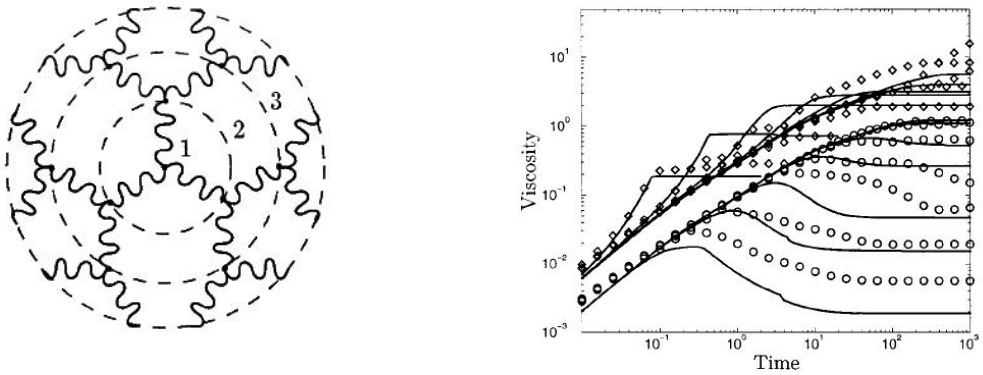

Figure 2.3.25 *(a,left)* An ideal three-level Cayley tree. *(b,right)* Comparison of full Cayley tree molecular calculations (lines) compared with four-mode pom-pom parameter fits (symbols) in startup of shear and extensional flow[144].

Doerpinghaus and Baird[26] showed that the multimode differential pom-pom model was capable of modeling the simple shear and uniaxial extensional rheological behavior of sparsely branched ($\leq$ 0.79 LCB per 10,000 carbons) and linear LLDPEs. In Fig. 2.3.26 is illustrated fits of transient shear and uniaxial extensional viscosities for a sparsely branched LLDPE (Exact 0201, 0.79 LCB per 10,000 C) and a linear

LLDPE (Affinity PL1880). Fit model parameters suggested that branching occured on the longest backbones for the sparsely branched resins. Doerpinghaus and Baird[26] found the predicted number of branch arms to be unrealistically large and in disagreement with dilute solution measurements.

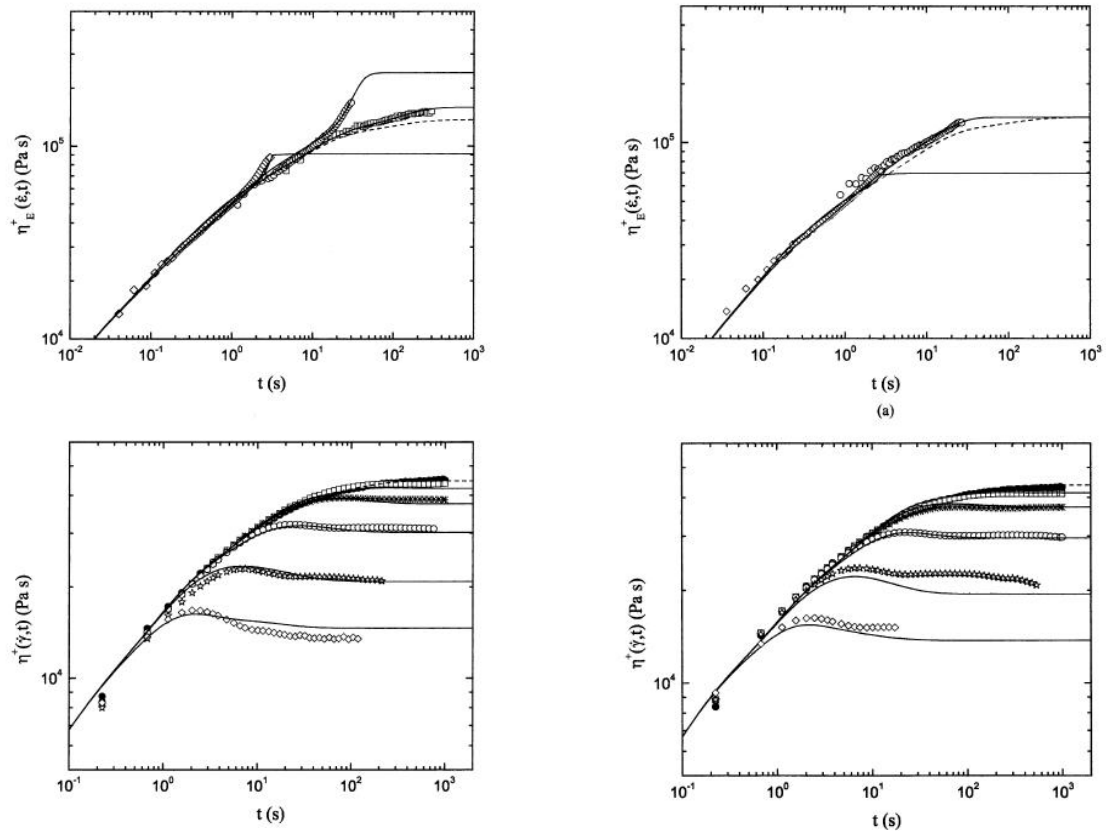

Figure 2.3.26 Transient extensional *(top left)* and shear viscosity *(bottom left)* growth curves for a sparsely branched LLDPE (Exact 0201). The same data is given for a linear LLDPE (Affinity 1840) *(top right)* and *(bottom right)* [26].

Chodankar *et al.*[145] showed that the differential and integro-differential multimode pom-pom models with local drag strain coupling (Eq. 2.3.28) could accurately model double-step-strain flows in LDPE melts. In this double-step-strain experiment, a strain of γ_1 was imposed on a fluid at $t = 0$ and second step, giving a total strain of γ_2, was imposed at $t = t_1$. In Figs. 2.3.27 and 2.3.28 are compared experimental results in double-step-strain with both multimode model fits using parameters determined in planar extension by Graham *et al.*[140] for a LDPE melt. Both forms of the multi-mode pom-pom model reasonably explained the data, with the differential model modeling the data better than the integro-

differential form. The authors attributed this to the fact the model parameters had been fit using the differential theory[145].

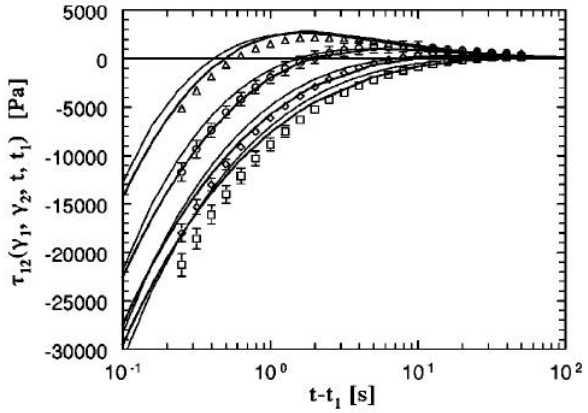

Figure 2.3.27 Double-step-strain (γ_1 = 400%, γ_1 = 200%) data at different values of t_1 (1.0, 2.0, 10.0, 30.0; *top to bottom*). Solid lines denote the multimode integral pom-pom model and the thick solid lines are the K-BKZ predictions.

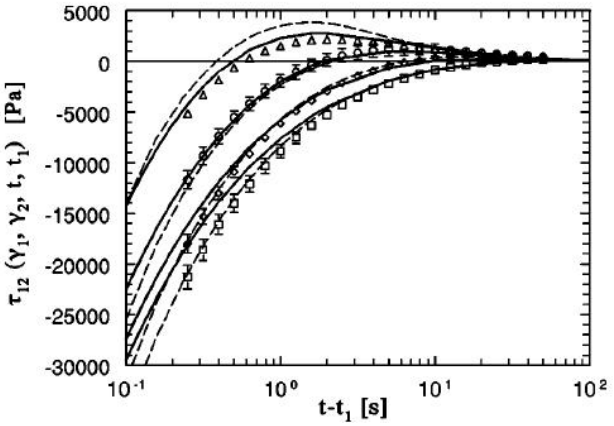

Figure 2.3.28 Double-step-strain (γ_1 = 400%, γ_1 = 200%) data at different values of t_1 (1.0, 2.0, 10.0, 30.0; *top to bottom*). Solid lines denote the multimode differential pom-pom model and the thick solid lines are the K-BKZ predictions.

2.3.7 – Extended Pom-Pom (XPP) Model

The multimode pom-pom model with local branch-point displacement[142] has three observed shortcomings. The first issue being that the orientation equation (Eq. 2.3-17) was found to be unbounded for higher strain rates ($\dot{\varepsilon}\tau_{bo} > 1$) [143]. The second issue was that discontinuities in the steady-state extension curves (Fig. 2.3.22) can still appear even with the assumption of local branch-

point withdrawal. This was due to finite extensibility ($\lambda_{max} = q$) [143]. The third issue was that it does not predict a secondary normal stress in shear even though non-zero values had been shown experimentally[143, 146]. Verbeeten *et al.*[143] proposed a modified form of the pom-pom model, the eXtended Pom-Pom model (XPP), that attempted improve three issues in the model.

2.3.7.1 – Theoretical Basis of the eXtended Pom-Pom (XPP) Model

Presented here is a brief summary of the XPP constitutive equation derivation that is meant to highlight some of the models assumptions. A full derivation of the XPP constitutive equation set can be found in Verbeeten *et al.*[143]. The XPP was formulated by representing the molecules with connector vectors $\mathbf{R}_i$, as is illustrated in Fig 2.3.29 for an ideal pom-pom molecule. A segment of the backbone tube was defined as the dimensionless connector vector $\mathbf{R}_i$, with a normalized length Λ_i (equal the dimensionless stretch length λ(t) from McLeish and Larson[87]) and direction $\mathbf{n}_i$.

$$\boldsymbol{R_i} = |\boldsymbol{R_i}|\mathbf{n_i} = \Lambda_i \mathbf{n_i} \qquad (2.3\text{-}29)$$

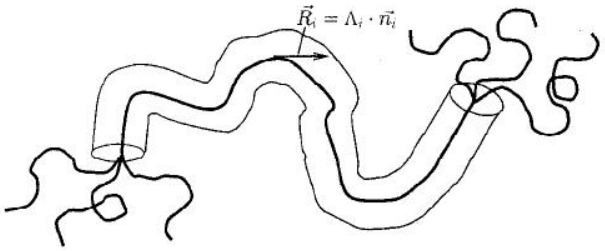

Figure 2.3.29 Illustration of the connector vector for an ideal pom-pom molecule[143].

The equation of motion for a vector **R** [Eq. (9) in Verbeeten *et al.*[143]] was coupled with the appropriate slip tensor **B** [Eq. (17) in Verbeeten *et al.*[143]] to account for slippage of the element with respect to the continuum[143]**.** This lead to the expressions for stress (Eq. 2.3-30), stretch (Eq. 2.3-31), and orientation (Eq. 2.3-32) for the "Double-equation XPP equation set," and a single expression for viscoelastic stress (Eq. 2.3-33) for the "Single-equation XPP equation set." The set of Eq. 2.3-30 through 2.3-32 or Eq. 2.3-33 was referred to as the XPP model[143]. Nomenclature in the remainder of this work

was adapted from Verbeeten *et al.*[143] to match the form used by McLeish and Larson[87]. The XPP model introduced a material parameter α (≥ 0) that defined the amount of anisotropy. α was fit using either second normal stress coefficient data or second planar viscosity data. For α greater than zero, the XPP predicted a non-zero second normal stress coefficient. For α=0, Eq. 2.3-31 mimiced the original differential form for orientation presented in Eq. 2.3-17 [143]. Soulages *et al.*[147] suggested that the value of α be constrained so that 0 ≤ α ≤ 1 based on the non-equilibrium thermodynamics analyzed using the GENERIC framework. Öttinger[124] derived a similar equation for the evolution of orientation based on non-equilibrium thermodynamics that utilized α to obtain non-zero secondary stress coefficients $\boldsymbol{\Psi}_2$.

Double-equation XPP Model[143]

Viscoelastic Stress:

$$\boldsymbol{\sigma} = G_0(3\lambda^2\,\boldsymbol{S} - \boldsymbol{I}) \tag{2.3-30}$$

Evolution of orientation:

$$\overset{\nabla}{\boldsymbol{S}} + 2[\boldsymbol{K}{:}\boldsymbol{S}]\boldsymbol{S} + \frac{1}{\tau_{0b}\lambda^2}\left[3\alpha\lambda^4\boldsymbol{S}\cdot\boldsymbol{S} + \left(1-\alpha-3\alpha\lambda^4 I_{\boldsymbol{S}\cdot\boldsymbol{S}}\right)\boldsymbol{S} - \frac{1-\alpha}{3}\boldsymbol{I}\right] = 0 \tag{2.3-31}$$

Evolution of the backbone stretch:

$$\frac{\partial}{\partial t}\lambda = \lambda(\boldsymbol{K}{:}\boldsymbol{S}) - \frac{1}{\tau_s}(\lambda-1), \quad \tau_s = \tau_{0s}e^{-\nu^*(\lambda-1)}, \;\; \nu^* = \frac{2}{q} \tag{2.3-32}$$

Single-equation XPP Model[143]

Viscoelastic Stress:

$$\overset{\nabla}{\boldsymbol{\sigma}} + \boldsymbol{\tau}(\boldsymbol{\sigma})^{-1}\boldsymbol{\sigma} = 2G_0\boldsymbol{K} \tag{2.3-33}$$

Relaxation time tensor:

$$\boldsymbol{\tau}(\boldsymbol{\sigma})^{-1} = \frac{1}{\boldsymbol{\tau_{0b}}} + \left\{\frac{\alpha}{G_0}\boldsymbol{\sigma} + f(\boldsymbol{\sigma})^{-1}\boldsymbol{I} + G_0[f(\boldsymbol{\sigma})^{-1}-1]\boldsymbol{\sigma}^{-1}\right\} \tag{2.3-34}$$

Extra function:

$$\frac{1}{\tau_{b0}}f(\boldsymbol{\sigma})^{-1} = \frac{2}{\tau_s}\left(1-\frac{1}{\lambda}\right) + \frac{1}{\lambda^2\tau_{b0}}\left(1-\frac{\alpha I_{\boldsymbol{\sigma\sigma}}}{3G_0^2}\right) \tag{2.3-35}$$

Backbone stretch and stretch relaxation time:

$$\lambda = \sqrt{1+\frac{I_{\boldsymbol{\sigma}}}{3G_0}}, \tag{2.3-36}$$

$$\tau_s = \tau_{0s}e^{-\nu^*(\lambda-1)}, \quad \nu^* = \frac{2}{q} \tag{2.3-37}$$

An important feature of the model was that it neglected finite extensibility (i.e. limiting λ to values less than or equal to *q*). Verbeeten *et al.*[143] argued that the finite extensibility condition forced a discrete value of stretch that lead to discontinuities seen in the steady-state extension viscosity predictions in both the original (Fig. 2.3.8) and local branch-point withdrawal forms (Fig. 2.3.22). Eq.

2.3-32 was derived on the basis on an *average* backbone stretch. This average implied that some molecules would reach their maximum stretch before others, thereby giving a maximum stretch distribution. Verbeeten *et al.*[143] concluded that a finite extensibility condition, which yielded only a discrete condition, was unphysical, especially if polydispersity was introduced. Instead they proposed that the exponential term in Eq. 2.3-32 kept the stretch relaxation time from becoming unbounded at higher strains.

2.3.7.2 – Roboustness of the eXtended Pom-Pom (XPP) Model

The single mode form of the XPP model was examined in several simple flows by Verbeeten *et al.* [143] to highlight the effect of the parameter related to anisotropy α. Molecular architecture was chosen to be the same studied by McLeish and Larson[87] and Blackwell *et al.*[142] with q equal to five, s_a equal to three and s_b equal to 30. Of interest was the XPP model's behavior in shear and planar flow, where secondary stress differences were present.

In Fig 2.3.30 are shown the transient and steady state viscosity, transient second over first normal stress coefficient rate $\left(-\boldsymbol{\Psi}_2/\boldsymbol{\Psi}_1\right)$, steady state shear orientation S_{12}, and transient backbone stretch Λ (λ in McLeish and Larson[87]) for simple shear. α was seen to have little effect on either the steady state or transient viscosity. α had the largest influence on $\boldsymbol{\Psi}_2$**.** It should be noted that for α equal to zero, $\boldsymbol{\Psi}_2$ equaled zero. Shear orientation S_{12} decreased with $\dot{\gamma}^{1/2}$ at higher shear rates. The XPP model showed characteristic shear thinning and backbone stretch overshoot that was seen in the original form of the pom-pom model[87, 143].

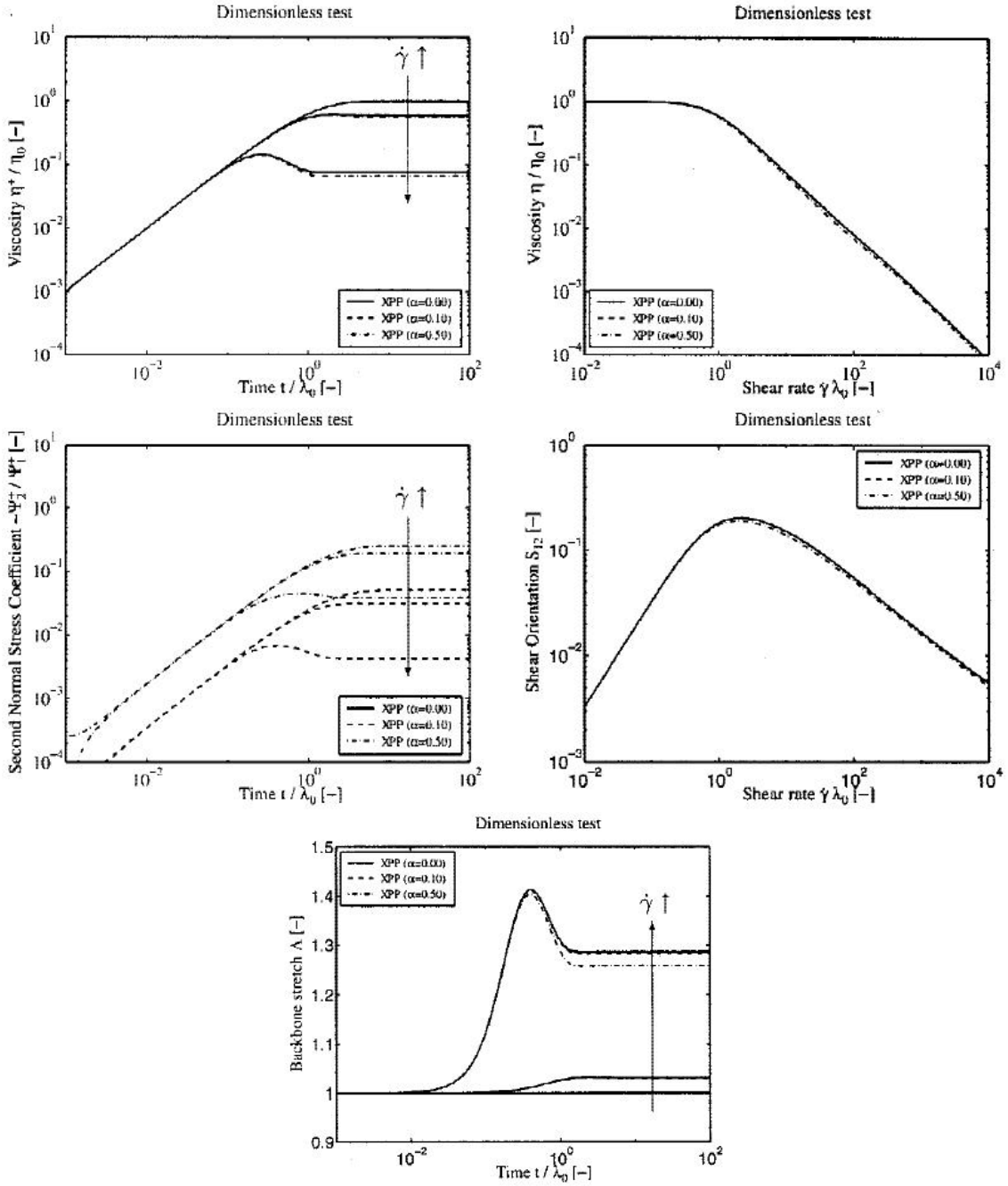

Figure 2.3.30 Behavior of an ideal pom-pom molecule (q = 5, s_a = 3 and s_b = 30) in the XPP framework in simple shear: transient viscosity *(top left)*, steady state viscosity *(top right)*, transient second over first normal stress coefficient ratio *(left middle)*, steady state orientation component S_{12} *(right middle)*, and transient backbone stretch *(bottom).* Values of α investigated are 0, 0.1 and 0.5[143].

In Fig. 2.3.31 is illustrated the effect of varying α on the transient and steady state first planar viscosities, transient second planar viscosity (Eq. 2.3-21), and backbone stretch in planar elongational

flow. α had no visible effect on either the transient or steady state first planar viscosity, but had a marked influence on the second planar viscosity. A notable feature of the XPP model seen was a smooth steady state first planar viscosity curve that was due to the relaxation of the of finite extensibility condition[143]. Even without finite extensibility, the predicted backbone stretch remained realistic and below the McLeish-Larson[87] theoretical value of $\lambda_{max} = q = 5$.

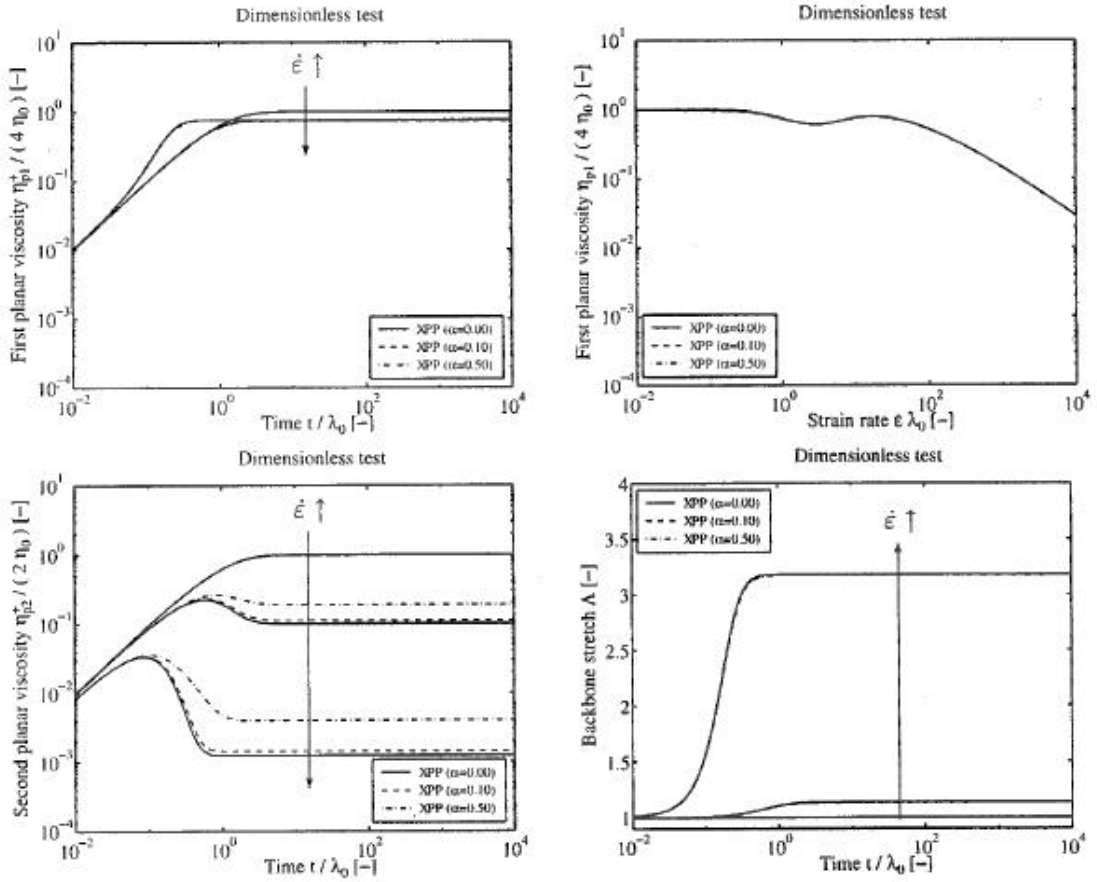

Figure 2.3.31 Dimensionless behavior of an ideal pom-pom molecule (q = 5, s_a = 3 and s_b = 30) in the XPP framework in planar elogation: transient first viscosity *(top left)*, steady state first planar viscosity *(top right)*, transient second planar viscosity *(bottom left)*, and transient backbone stretch *(bottom right).* Values of α investigated are 0 (solid line), 0.1 (dashed line) and 0.5 (dash-dot line)[143].

Bogaerds *et al.*[148] found that a XPP fluid was stable across a wide range of Weissenberg numbers in two simple shearing flows, Couette and Poiseuille flow. In this work, Couette flow was defined as being driven by the movement of the walls, while Poiseuille flow was defined as being driven by a

pressure gradient perpendicular to the walls. The addition of a small second normal stress difference ($\alpha = 0.1$ as opposed to $\alpha = 0$) was found to have a stabilizing effect on these simple shear flows[148].

Verbeeten *et al.*[143] investigated the multi-mode form of the XPP model for a couple LDPEs (BASF Lupolen 1810H and IUPAC A LDPE) and a HDPE (linear, high polydispersity) using the procedure outlined by Inkson *et al.*[83]. Fits for the anisotropy parameter α_i were done using second planar viscosity, however, second normal stress from shear could have been used if available. If neither set of secondary stress differences were available for fitting, a recommended a value of $\alpha_i = 0.1/q_i$ was suggested. The authors theorized that α_i would decrease inwards on the molecule (corresponding to increasing backbone relaxation times) [143].

Using experimental data from previous studies[149, 150], Verbeeten *et al.*[143] analyzed the XPP model in simple shear, uniaxial extension, planar extension, and reversing flows using the fitting procedure outlined above. Fits of the XPP multimode model in transient uniaxial viscosity are shown in Fig. 2.3.32, with steady state extension shown in the inset. Note that steady-state values were simply the maximum value seen in transient extension for a given rate and may not have been the terminal value (machine or material limitations), and therefore, it was called the quasisteady state value. Excellent agreement was seen between the experimental data and XPP model, although this was expected as two non-linear parameters were fit exclusively to this data set.

In Fig. 2.3.33 is illustrated the predictions of both the first and second planar viscosities, again with steady-state values in the inset. Excellent agreement was seen for the first planar viscosity. However, fits were quantitatively poor for the second planar viscosity. This poor fit was surprising considering that the predominate feature of the XPP model was the introduction of the anisotropy parameter, α, which was supposed to model such secondary stresses. The authors attributed this behavior to three possible reasons. First, it was difficult to measure second planar viscosity experimentally. Second, they argued that it was possible that not enough modes were used in their

modeling. This conclusion is questionable in that a simple stability analysis could have been performed to determine if the correct number of modes was used via the procedure outlined by Inkson *et al.*[83]. Thirdly, they argued that further modification to the orientation evolution equation could have improved predictions. The authors defended the last two points by pointing out the unphysical "bumpy" steady-state behavior predicted by the XPP model[143].

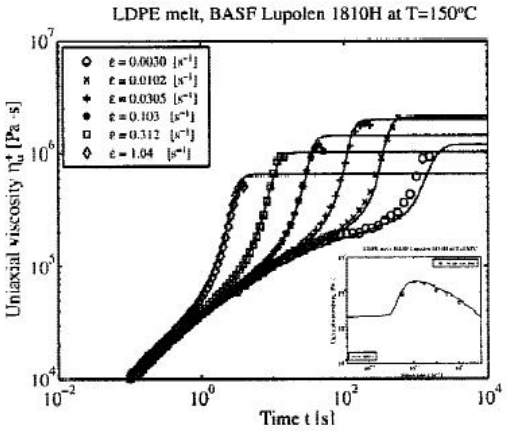

Figure 2.3.32 Transient and quasisteady state (inset) uniaxial elongational viscosity. Experimental values (symbols) and XPP model fits (lines) for Lupolen 1810H LDPE melt at 150 °C[143].

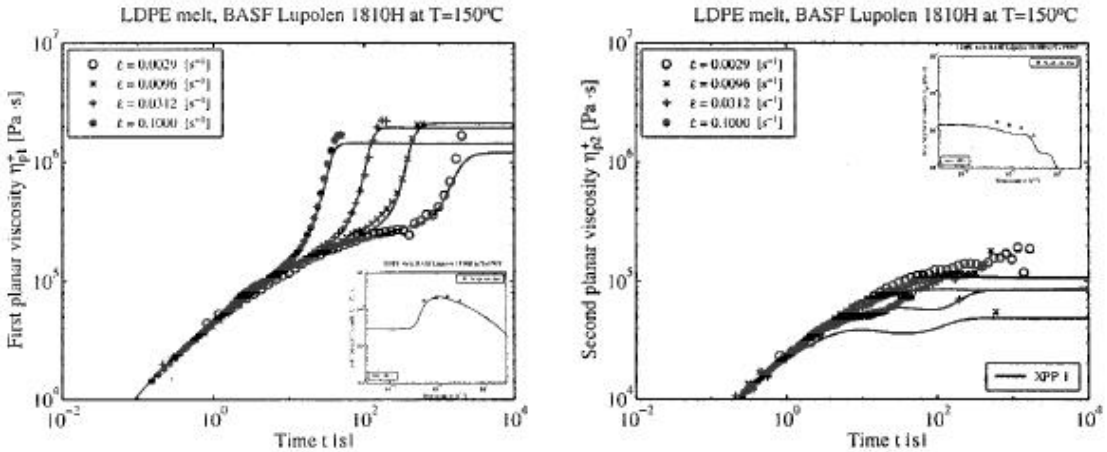

Figure 2.3.33 Transient and quasisteady state *(inset)* first planar viscosity *(left)* and second planar viscosity *(right)*. Experimental values (symbols) and XPP model fits (lines) for Lupolen 1810H LDPE melt at 150 °C[143].

Predictions of transient shear viscosity and first normal stress difference are given in Fig. 2.3.34. Excellent agreement was found between experimental and XPP model viscosity data at all strain rates studied. Values of the first normal stress coefficient Ψ_1 were not quantitatively accurate. The general qualitative shape was seen at all strain rates, but became less accurate as strain rates are decreased[143]. Surprisingly not included in this study were any predictions of the second normal stress coefficient Ψ_2. Even if experimental data was not available for direct comparison, a qualitative discussion of the form of the predictions with previously published data would have been useful in determining if the inclusion of the anisotropy term, α, was useful.

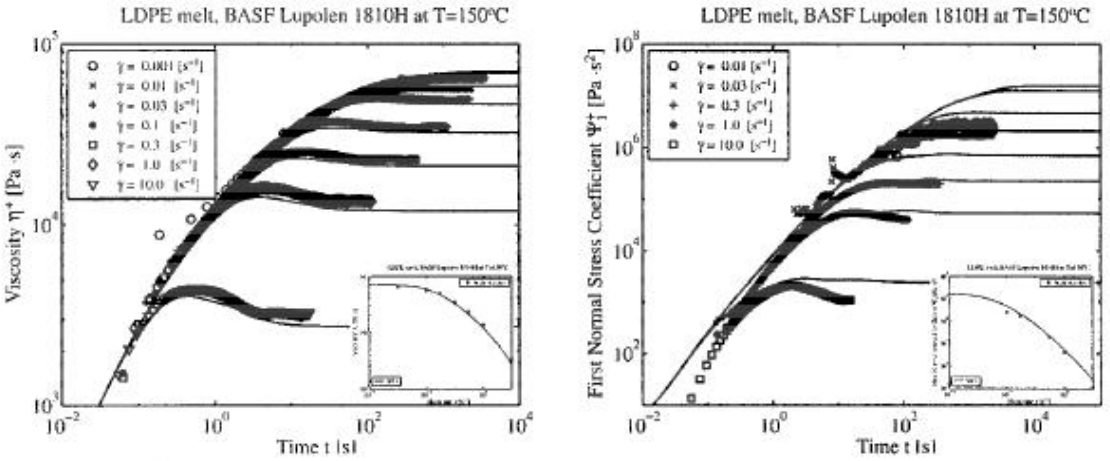

Figure 2.3.34 Transient and steady state (inset) shear viscosity *(left)* and first normal stress coefficient Ψ_1 *(right)*. Experimental values (symbols) and XPP model fits (lines) for Lupolen 1810H LDPE melt at 150 °C[143].

In Fig. 2.3.35 is investigated the XPP multimode model predictions in reversing shear flows. This reversing shear flow was defined as applying a strain rate of 1.0 s^{-1} in one direction before reversing the flow at some time *t** in the opposite direction with the same magnitude. Further detail on reversing flow was given elsewhere[150]. All features seen experimentally were predicted by the XPP multimode model; most notably were the departure behavior at the reversing time and the behavior prior to reaching steady state.

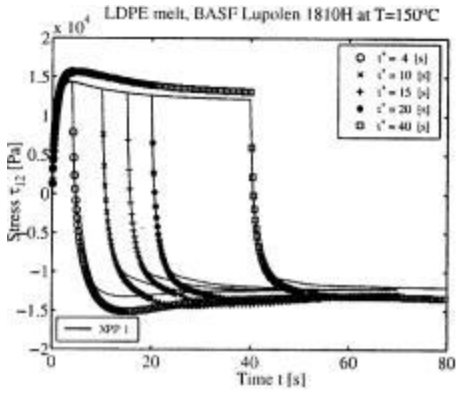

Figure 2.3.35 Shear stress measured in reversing flow for Lupolen 1810H LDPE melt at 150 ^{o}C and a strain of 1.0 s^{-1}. XPP multimode model predictions are given by the solid lines[143].

Verbeeten *et al.*[143] observed similar behavior in the fitting of rheological data for the IUPAC A LDPE melt using rheological data from previous studies[151, 152]. The authors remarked that excellent results were seen in fitting uniaxial extensional data, and good to excellent results were seen in shear flow. No remarks were made as to the predictions in planar extensional flow[143].

Verbeeten *et al.*[143] extended the XPP multimode model to a linear, polydisperse[153] HDPE melt, Statoil 870H, using the same fitting procedure outlined above. In Fig. 2.3.36 is shown experimental data and XPP multimode fits in transient and steady (inset) uniaxial viscosity and shear viscosity. Relatively good fits were found in both flows. The authors attributed deviations to the fact that the material was a *linear* HDPE resin. Theoretically, one would expect *q* to have been equal to one at all modes for a linear material. Instead values as high as *q* equal to seven were seen. This response (as well as the strain hardening seen in transient uniaxial flow) was attributed to the polydispersity (= 5.5) [153] of the material. A long linear polymer chain could have been entangled, contributing to stretch like a branched polymer[143]. It should be noted that HDPE with a high MWD have been observed experimentally to exhibit strain hardening in transient uniaxial flow[76].

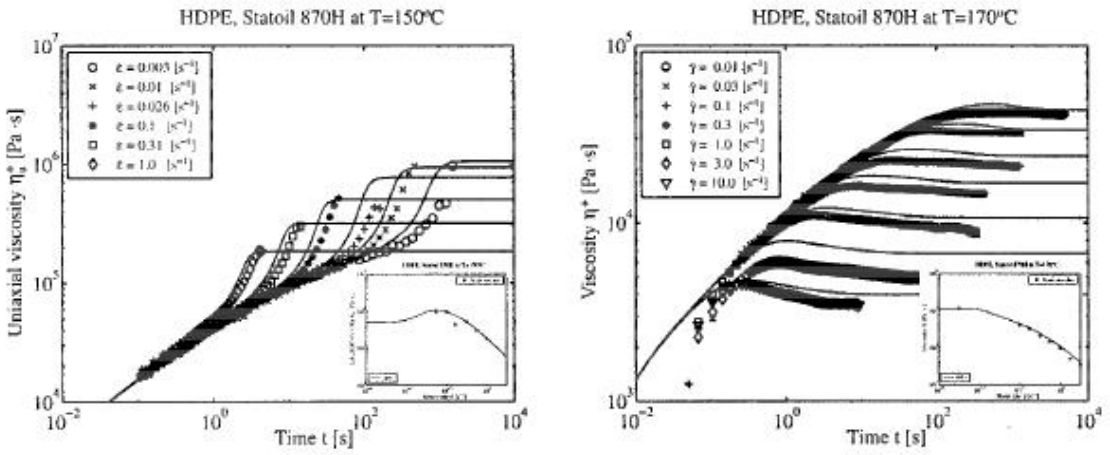

Figure 2.3.36 Transient and steady state (inset) uniaxial extensional viscosity at 150 °C *(left)* and transient and steady state (inset) shear viscosity at 170 °C *(right)* for Statoil 870H HDPE melt. Experimental values are given by symbols and XPP model fits by lines[143].

Verbeeten *et al.*[154] examined the multi-mode XPP model in two inhomogeneous flows (confined flow around a cylinder and the flow through a cross-slot device) for a commercial LDPE (Stamylan LD 2008 XC43). In both the confined flow around a cylinder and the flow through a cross-slot device, the XPP model was quantitatively able to describe key features observed from previous experimental data[155]. Most notable were the predictions of stress build-up due to planar extension and compression near the stagnation points that were followed by a slow stress relaxation[154]. It is also worth mentioning that in this study no planar viscosity or secondary normal stress data was available for the work of Verbeeten *et al.*[154]. Therefore, the authors used $\alpha_i = 0.3/q_i$. In Fig. 2.3.37 is shown quantitative agreement of the multimode XPP model and rheological data for simple shear and uniaxial viscosity. Shown for comparison are predictions of the Giesekus and exponential Phan-Thien Tanner (PTT-a)[154]. The accuracy of these fits suggested the form of $\alpha_i = constant/q_i$ proposed by originally Verbeeten *et al.*[143] could be used to quantitatively model rheological data in a variety of flows in the absence of experimental secondary stress data.

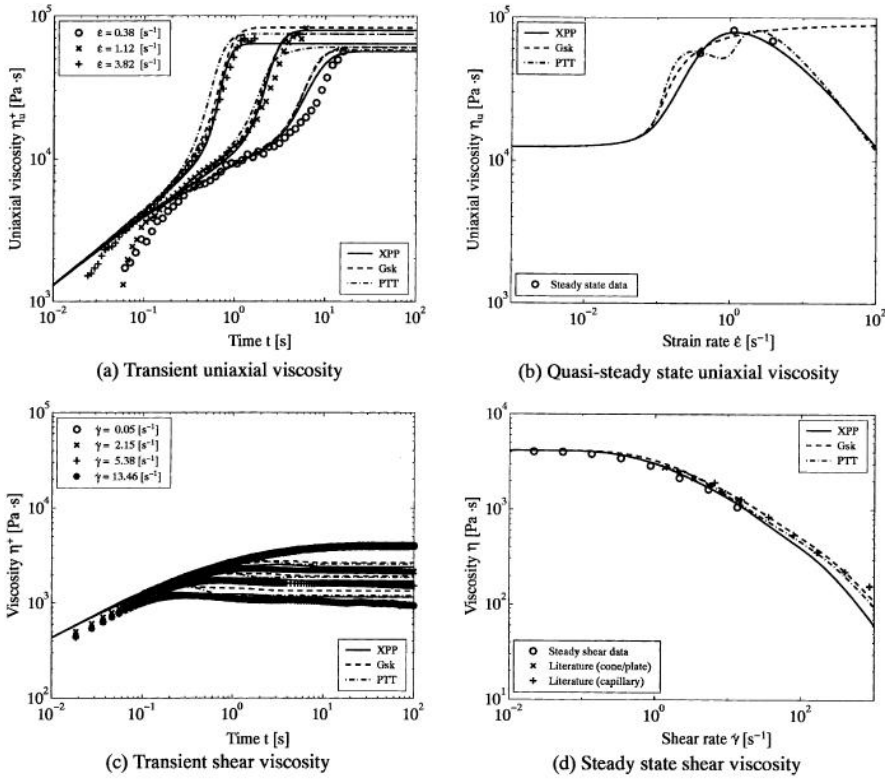

Figure 2.3.37 Transient *(a)* and steady state*(b)* uniaxial extensional viscosity, transient *(c)* and steady state *(d)* shear viscosity at 170 ^{o}C of the XPP, Giesekus, and PTT-a models for DSM Stamylan LD2008 XC43 LDPE[154].

Zatloukal[156] compared the XPP model in steady state shear and uniaxial extensional flow with modified forms of the Leonov and White-Metzner (mWM) model. The mWM model did not suffer from a predicted infinite extensional viscosity that the original WM does [157]. The Leonov model was modified by increasing the dependence of dissipation on the relaxation times[156]. In Figs. 2.3.38 and 2.3.39 are shown the predictions of the XPP, mWM, and mLeonov models in transient steady state extension and shear, and first normal stress coefficient for two LDPE resins. The non-linear parameters were *fit in steady state extension only*, unlike previous studies that used transient extensional flow [143, 158]. All three models were able to quantitatively fit each set of viscosity data to the same degree. However, while each model captured the qualitative shape of the first normal stress coefficient, deviation was seen in the quantitative predictions of the first normal stress coefficient for each material and model. These deviations could have been due to the fitting technique used, as it can be difficult to obtain true steady-

state extensional viscosities either due to material failure[84] or machine limitations. Therefore, only a quasisteady-state may have been achieved, and deficient model parameters may have been used. Presentation of the transient extensional data was not presented by the author, and therefore raises concerns as to both the steady-state values, and the quality of the model fits in transient flows.

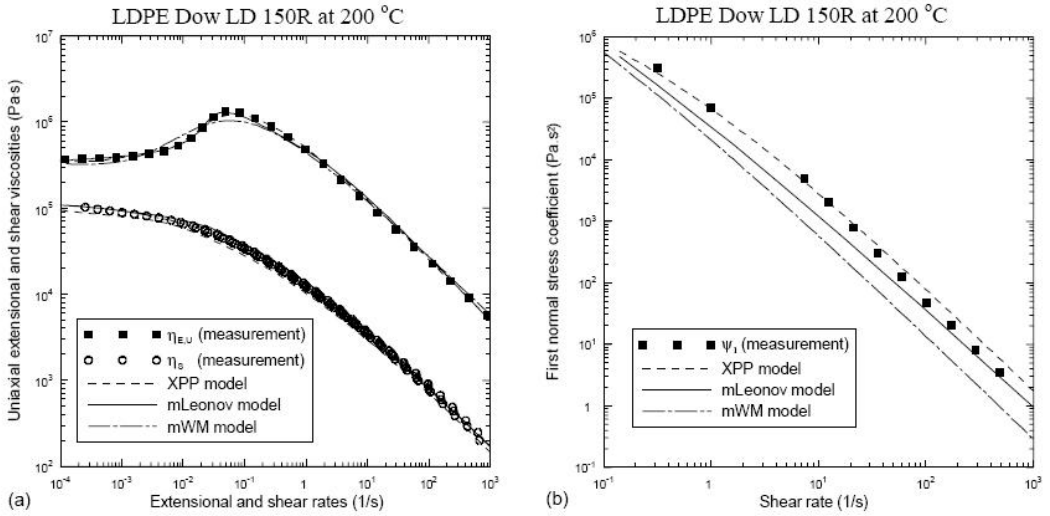

Figure 2.3.38 Model predictions vs. experimental data for a LDPE melt (DOW LD 150R) at 200 °C in steady shear and uniaxial extensional viscosities *(left)* and steady first normal stress coefficient *(right)*[156].

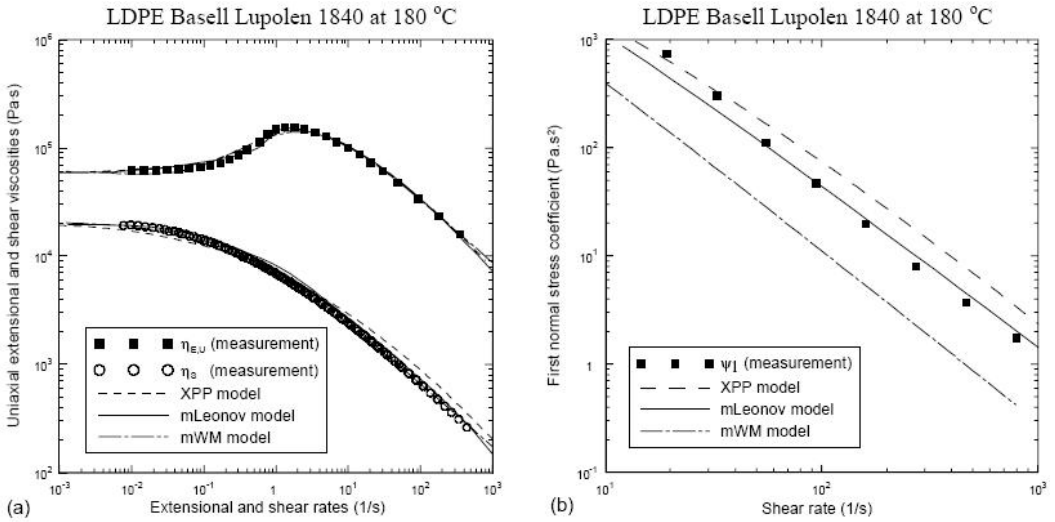

Figure 2.3.39 Model predictions vs. experimental data for a LDPE melt (Basell Lupolen 1840) at 180 °C in steady shear and uniaxial extensional viscosities *(left)* and steady first normal stress coefficient *(right)*[156].

Pivokonsky *et al.*[115, 159] followed the fitting procedure of Zatloukal[156] to compare the predictions of the multimode XPP, PTT-XPP, and mLeonov models in LDPE[159], linear HDPE[115], and a sparsely

branched mLLDPE[115] systems. All models were found to accurately describe LDPE systems, with results similar to the study by Zatloukal[156] (see Figs. 2.3.38 and 2.3.39). In Fig. 2.3.40 is illustrated the XPP model predictions of the steady shear and uniaxial extensional viscosities for a mLLDPE (Exxon Exact 0201) and a linear HDPE (Tipelin FS 450-26). The mLLDPE Exact 0201 was the same resin studied by Doerpinghaus and Baird[26] using the differential multimode pom-pom model. The XPP model showed poorer fits of the steady uniaxial extensional viscosity for the sparsely branched and linear materials[115] relative to XPP model's performance in a LDPE system[143, 156].

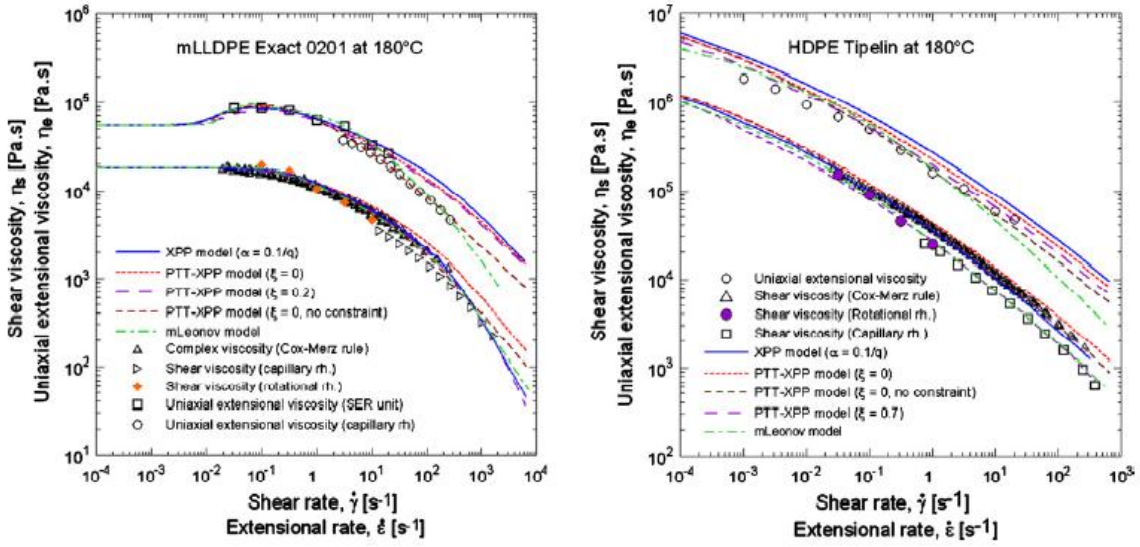

Figure 2.3.40 Steady shear and uniaxial extensional viscosity data compared with predictions of the XPP, PTT-XPP, and mLeonov models for mLLDPE (Exxon Exact 0201) and HDPE (Tipelin FS 450-26) [115].

The inability of the XPP model to fit the sparsely branched and linear resin was again seen in the prediction of the transient uniaxial extensional viscosities of either resin (Fig. 2.3.41). The XPP model qualitatively predicted the correct shape of the transient extensional curves for the mLLDPE, but failed to quantitatively predict their behavior. Furthermore, the XPP model was unable to qualitatively or quantitatively predict the transient extensional viscosity of the linear material, even when the branch arm parameter was set to q_i = 1. This failure was due to the XPP model predicting strain hardening for

material parameters that should have resulted in linear viscoelastic behavior in elongational flow. Disagreement was also seen for the transient shear viscosities as shown in Fig. 2.3.42.

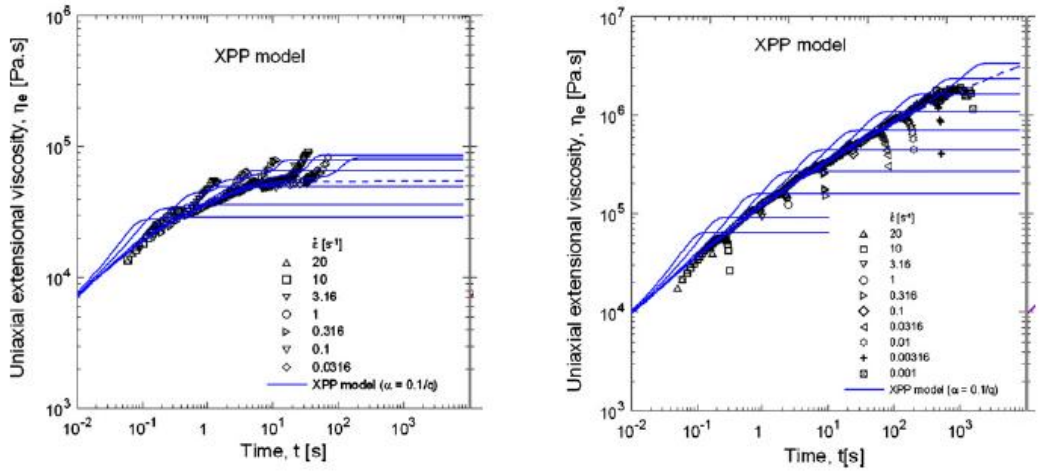

Figure 2.3.41 Transient uniaxial extensional viscosity data compared with predictions of the XPP model for mLLDPE (Exxon Exact 0201) and HDPE (Tipelin FS 450-26) [115].

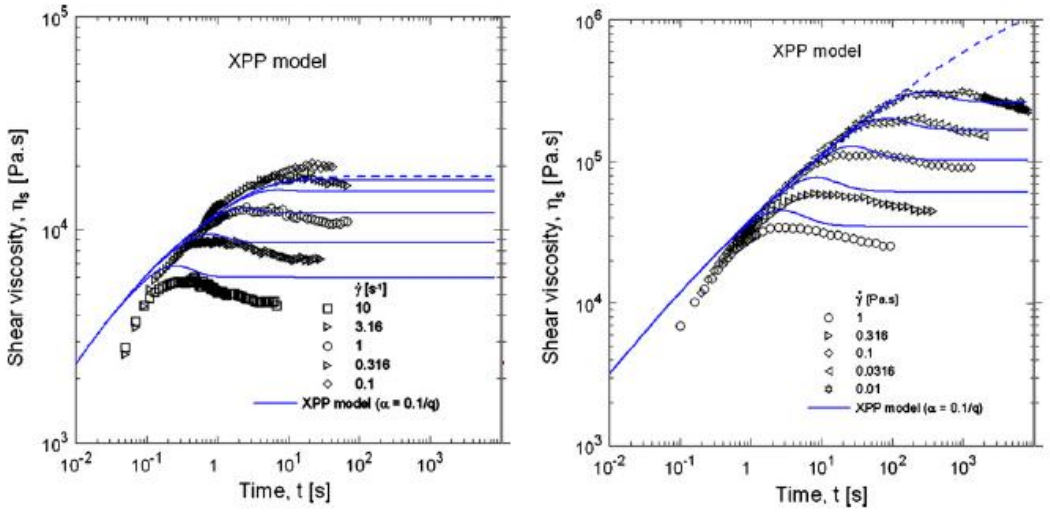

Figure 2.3.42 Transient shear viscosity data compared with predictions of the XPP model for mLLDPE (Exxon Exact 0201) and HDPE (Tipelin FS 450-26) [115].

The XPP was developed to improve shortcomings of the original pom-pom model. While the introduction of the anisotropy parameter was shown to predict non-zero secondary viscosities in planar extension, the results were quantitatively incorrect. Furthermore, the inability of the XPP to qualitatively or quantitatively model linear and sparsely-branched mPEs in transient flows makes it ill-posed to be of further use in the constitutive modeling of this work.

2.4 – References

1. D. J. Lohse, S. T. Milner, L. J. Fetters, M. Xenidou, N. Hadjichristidis, R. A. Mendelson, C. A. Garcia-Franco and M. K. Lyon. *Macromolecules* **2002,** 35, (8), 3066-3075.

2. C. W. Seay. The Role of Molecular Architecture on Rheological Properties and its Effect on Film-Casting Performance. Virginia Tech, Blacksburg, VA, 2008.

3. G. Natta. *Polym. Sci. Part A-1* **1959,** 1.

4. R. A. Bubeck. *Mater. Sci. Eng., R* **2002,** R39, (1), 1-28.

5. R. A. Bubeck and H. M. Baker. *Polymer* **1982**.

6. M. Gahleitner. *Prog. Polym. Sci.* **2001,** 26, (6), 895-944.

7. D. Yan, W.-J. Wang and S. Zhu. *Polymer* **1999,** 40, 1737-1744.

8. A. Malmberg, J. Liimatta, A. Lehtinen and B. Lofgren. *Macromolecules* **1999,** 32, 6687-6696.

9. P. J. Doerpinghaus. Flow Behavior of Sparsely Branched Metallocene-Catalyzed Polyethylenes. Virginia Tech, Blacksburg, 2002.

10. J. P. Soares and A. E. Hamielec. *Macromol. Theory Simul.* **1995,** 4, 1085.

11. J. P. Soares and A. E. Hamielec. *Macromol. Theory Simul.* **1997,** 6, 591.

12. J. P. Soares and A. E. Hamielec, *Metallocene-Catalyzed Polymers: Materials, Properties, Processing & Markets*. Plastics Design Library: New York, 1998.

13. B. H. Zimm and W. H. Stockmayer. *J. Chem. Phys.* **1948,** 17, (12), 1301-1314.

14. H. Münstedt and D. Auhl. *J. Non-Newtonian Fluid Mech.* **2005,** 128, 62-69.

15. H. G. Barth and J. W. Mays, *Modern Methods of Polymer Charaterization*. Wiley: New York, 1984.

16. J. Randall. *ACS Symp. Ser.* **1980,** 142, 93.

17. J. Janzen and R. H. Colby. *Polym. Mater. Sci. Eng.* **2000,** 82, 128-129.

18. C. P. Lusignan, T. H. Mourey, J. C. Wilson and R. H. Colby. *Phys Rev E Stat Phys Plasmas Fluids Relat Interdiscip Topics* **1999,** 60, (5 Pt B), 5657-5669.

19. P. J. Doerpinghaus and D. G. Baird. *J. Rheol.* **2003,** 47, (3), 717-736.

20. R. B. Bird, R. C. Armstrong and O. Hassager, *Dynamics of Polymeric Liquids*. 2nd ed.; John Wiley & Sons, Inc.: Hoboken, NJ, 1987; Vol. 1, p 633.

21. J. Meissner. *Kunststoffe* **1971**, (61), 576-582.

22. M. N. Layec-Raphalen and C. Wolff. *J. Non-Newtonian Fluid Mech.* **1976,** 1, 159-173.

23. S. Burrow, A. Peterlin and D. T. Turner. *Polym. Lett.* **1964,** 2, 67-70.

24. W. W. Graessley. *Adv. Polym. Sci.* **1974,** 16, 1-179.

25. W. P. Cox and E. H. Merz. *J. Polym. Sci.* **1958,** 28, 619-622.

26. P. J. Doerpinghaus and D. G. Baird. *Macromolecules* **2002,** 35, (27), 10087-10095.

27. C. Das, N. J. Inkson, D. J. Read, M. A. Kelmanson and T. C. B. McLeish. *J. Rheol.* **2006,** 50, (2), 207-234.

28. Y. Einaga, K. Osaki, M. Kurata, S. Kimura and M. Tamura. *Polym. J.* **1971,** 2, (4), 550-552.

29. F. J. Stadler, D. Auhl and H. M. Münstedt. *Macromolecules* **2008,** 41, 3720-3726.

30. P. R. Soskey and H. H. Winter. *J. Rheol.* **1984,** 28, (5), 625-645.

31. G. C. Berry and T. G. Fox. *Adv. Polym. Sci.* **1968,** 5, 261.

32. D. Auhl, J. Stange, H. Münstedt, B. Krause, D. Voigt, A. Lederer, U. Lappan and K. Lunkwitz. *Macromolecules* **2004,** 37, (25), 9465-9472.

33. R. L. Arnett and C. P. Thomas. *J. Phys. Chem.* **1980,** 84, 649.

34. L. J. Fetters, A. D. Kiss, D. S. Pearson, G. F. Quack and F. J. Vitus. *Macromolecules* **1993,** 26, (4), 647-654.

35. D. S. Pearson and E. Helfand. *Macromolecules* **1984,** 17, 888-895.

36. P. S. Chum, W. J. Kruper and M. J. Guest. *Adv. Mater.* **2000,** 12, (23), 1759-1767.

37. P. M. Wood-Adams, J. M. Dealy, A. W. deGroot and O. D. Redwine. *Macromolecules* **2000,** 33, (20), 7489-7499.

38. R. J. Koopmans. *SPE ANTEC Technol. Pap.* **1997,** 43, 1006.

39. J. F. Vega, A. Santamaria, A. Munoz-Escalona and P. Lafuente. *Macromolecules* **1998,** 31, (11), 3639-3647.

40. M. H. Wagner. *J. Non-Newtonian Fluid Mech.* **1978,** 4, (1-2), 39-55.

41. A. C. Papanastasiou, L. E. Scriven and C. W. Macosko. *J. Rheol.* **1983,** 27, (4), 387-410.

42. D. A. Vega and S. T. Milner. *J. Polym. Sci., Part B: Polym. Phys.* **2007,** 45, (23), 3117-3136.

43. K. Osaki and M. Kurata. *Macromolecules* **1980,** 13, (3), 671-676.

44. J. Sanchez-Reyes and L. A. Archer. *Macromolecules* **2002,** 35, (13), 5194-5202.

45. C. Sui, G. B. McKenna and J. E. Puskas. *J. Rheol.* **2007,** 51, (6), 1143-1169.

46. D. C. Venerus. *J. Rheol.* **2005,** 49, (1), 277-295.

47. D. C. Venerus and H. Kahvand. *Part B: Polym. Phys.* **1994,** 32, 1531-1542.

48. L. A. Archer and S. K. Varshney. *Macromolecules* **1998,** 31, (18), 6348-6355.

49. L. J. Kasehagen and C. W. Macosko. *J. Rheol.* **1998,** 42, (6), 1303-1327.

50. T. C. B. McLeish, J. Allgaier, D. K. Bick, G. Bishko, P. Biswas, R. Blackwell, B. Blottiere, N. Clarke, B. Gibbs, D. J. Groves, A. Hakiki, R. K. Heenan, J. M. Johnson, R. Kant, D. J. Read and R. N. Young. *Macromolecules* **1999,** 32, (20), 6734-6758.

51. H. Gevgilili and D. M. Kalyon. *J. Rheol.* **2001,** 45, (2), 467-475.

52. M. Doi and S. F. Edwards, *The Theory of Polymer Dynamics*. Oxford University Press: 1988.

53. K. Osaki, K. Nishizawa and M. Kurata. *Macromolecules* **1982,** 15, (4), 1068-1071.

54. T. Inoue, T. Uematsu, Y. Yamashita and K. Osaki. *Macromolecules* **2002,** 35, (12), 4718-4724.

55. L. J. Zapas and T. Craft. *J. Res. Natl. Bur. Stand.* **1965,** 69A, 541-546.

56. L. A. Archer. *J. Rheol.* **1999,** 43, (6), 1555-1571.

57. R. Fulchiron and V. Verney. *J. Non-Newtonian Fluid Mech.* **1993,** 48, (1-2), 49-61.

58. M. H. Wagner and H. M. Laun. *Rheol. Acta* **1978,** 17, (2), 138-148.

59. J. Hepperle and H. Münstedt. *Rheol. Acta* **2006,** 45, (5), 717-727.

60. O. Urakawa, M. Takahashi, T. Masuda and N. G. Ebrahimi. *Macromolecules* **1995,** 28, (21), 7196-7201.

61. K. Osaki, E. Takatori and M. Kurata. *Macromolecules* **1987,** 20, (7), 1681-1687.

62. D. C. Venerus, E. F. Brown and W. R. Burghardt. *Macromolecules* **1998,** 31, (26), 9206-9212.

63. P. J. R. Leblans, J. Sampers and H. C. Booij. *Rheol. Acta* **1985,** 24, (2), 152-158.

64. C. M. Vrentas and W. W. Graessley. *J. Rheol.* **1982,** 26, (4), 359-371.

65. K. Osaki, E. Takatori, M. Kurata, H. Watanabe, H. Yoshida and T. Kotaka. *Macromolecules* **1990,** 23, (20), 4392-4396.

66. R. G. Larson. *J. Rheol.* **1985,** 29, (6), 823-831.

67. R. G. Larson. *J. Rheol.* **1984,** 28, (5), 545-571.

68. R. G. Larson, *Constitutive Equations for Polymer Melts and Solutions*. Buttersworth: Boston, MA, 1998.

69. P. J. Carreau. *Trans. Soc. Rheol.* **1972,** 16, (1), 99-127.

70. K. Yasuda, R. C. Armstrong and R. E. Cohen. *Rheol. Acta* **1981,** 20, (2), 163-178.

71. H. Münstedt. *J. Rheol.* **1980,** 24, 847-867.

72. P. M. Wood-Adams and J. M. Dealy. *Macromolecules* **2000,** 33, (20), 7481-7488.

73. A. D. Gotsis, B. L. F. Zeevenhoven and C. Tsenoglou. *J. Rheol.* **2004,** 48, (4), 895-914.

74. H. K. Rasmussen, J. K. Nielsen, A. Bach and O. Hassager. *J. Rheol.* **2005,** 49, (2), 369-381.

75. M. H. Wagner, H. Bastian, P. Hachmann, J. Meissner, S. Kurzbeck, H. Münstedt and F. Langouche. *Rheol. Acta* **2000,** 39, (2), 97-109.

76. J. J. Linster and J. Meissner. *Polymer Bulletin* **1986,** 16, (2-3), 187-194.

77. H. Münstedt and S. Kurzbeck. *Prog. Trends Rheol. V, Proc. Eur. Rheol. Conf., 5th* **1998**, 487-488.

78. C. Gabriel and H. Münstedt. *J. Rheol.* **2003,** 47, (3), 619-630.

79. S. E. Bin Wadud and D. G. Baird. *J. Rheol.* **2000,** 44, (5), 1151-1167.

80. J. K. Lee, S. E. Solovyov, T. L. Virkler and C. E. Scott. *Rheol. Acta* **2002,** 41, (6), 567-576.

81. V. C. Barroso and J. M. Maia. *J. Non-Newtonian Fluid Mech.* **2005,** 126, (2-3), 93-103.

82. T. Schweizer. *Rheol. Acta* **2000,** 39, (5), 428-443.

83. N. J. Inkson, T. C. B. McLeish, O. G. Harlen and D. J. Groves. *J. Rheol.* **1999,** 43, (4), 873-896.

84. G. H. McKinley and O. Hassager. *J. Rheol.* **1999,** 43, (5), 1195-1212.

85. M. Considere. *Annales des Ponts et Chausees 9* **1885**, 574-605.

86. M. Doi and S. F. Edwards. *J. Chem. Soc., Faraday Trans. 2* **1978,** 74, (10), 1802-1817.

87. T. C. B. McLeish and R. G. Larson. *J. Rheol.* **1998,** 42, (1), 81-110.

88. Y. M. Joshi and M. M. Denn. *J. Rheol.* **2003,** 47, (1), 291-298.

89. Y. M. Joshi and M. M. Denn. *J. Rheol.* **2004,** 48, (3), 591-598.

90. M. Yao, G. H. McKinley and B. Debbaut. *J. Non-Newtonian Fluid Mech.* **1998,** 79, (2-3), 469-501.

91. M. Yao, S. H. Spiegelberg and G. H. McKinley. *J. Non-Newtonian Fluid Mech.* **2000,** 89, (1-2), 1-43.

92. P. Szabo. *Rheol. Acta* **1997,** 36, (3), 277-284.

93. E. van Ruymbeke, K. Orfanou, M. Kapnistos, H. Iatrou, M. Pitsikalis, N. Hadjichristidis, D. J. Lohse and D. Vlassopoulos. *Macromolecules* **2007,** 40, (16), 5941-5952.

94. J. R. Dorgan, D. M. Knauss, H. A. Al-Muallem, T. Huang and D. Vlassopoulos. *Macromolecules* **2003,** 36, (2), 380-388.

95. C. G. Robertson, C. M. Roland, C. Paulo and J. E. Puskas. *Journal of Rheology* **2001,** 45, (3), 759-772.

96. D. Auhl, J. Ramirez, A. E. Likhtman, P. Chambon and C. Fernyhough. *J. Rheol.* **2008,** 52, (3), 801-835.

97. D. W. Mead, R. G. Larson and M. Doi. *Macromolecules* **1998,** 31, (22), 7895-7914.

98. M. W. Collis, A. K. Lele, M. R. Mackley, R. S. Graham, D. J. Groves, A. E. Likhtman, T. M. Nicholson, O. G. Harlen, T. C. B. McLeish, L. R. Hutchings, C. M. Fernyhough and R. N. Young. *J. Rheol.* **2005,** 49, (2), 501-522.

99. A. Bach, K. Almdal, H. K. Rasmussen and O. Hassager. *Macromolecules* **2003,** 36, (14), 5174-5179.

100. M. H. Wagner, S. Kheirandish and O. Hassager. *J. Rheol.* **2005,** 49, (6), 1317-1327.

101. G. Marrucci and G. Ianniruberto. *Macromolecules* **2004,** 37, 3934-3942.

102. J. K. Nielsen, H. K. Rasmussen, O. Hassager and G. H. McKinley. *J. Rheol.* **2006,** 50, (4), 453.

103. J. Roovers. *Polymer* **1985,** 26, 1091.

104. V. R. Raju, H. Rachapudy and W. W. Graessley. *J. Polym. Sci., Polym. Phys. Ed.* **1979,** 17, (7), 1223-1235.

105. J. M. Carella, J. T. Gotro and W. W. Graessley. *Macromolecules* **1986,** 19, (3), 659-667.

106. E. A. Jordan, A. M. Donald, L. J. Fetters and J. Klein. *Polym. Prepr. (Am. Chem. Soc., Div. Polym. Chem.)* **1989,** 30, (1), 63-64.

107. C. B. Gell, W. W. Graessley, V. Efstratiadis, M. Pitsikalis and N. Hadjichristidis. *J. Polym. Sci., Part B: Polym. Phys.* **1997,** 35, (12), 1943-1954.

108. L. A. Archer and Juliani. *Macromolecules* **2004,** 37, (3), 1076-1088.

109. J. K. Nielsen, H. K. Rasmussen, M. Denberg, K. Almdal and O. Hassager. *Macromolecules* **2006,** 39, (25), 8844-8853.

110. D. R. Daniels, T. C. B. McLeish, B. J. Crosby, R. N. Young and C. M. Fernyhough. *Macromolecules* **2001,** 34, (20), 7025-7033.

111. M. Kapnistos, G. Koutalas, N. Hadjichristidis, J. Roovers, D. J. Lohse and D. Vlassopoulos. *Rheol. Acta* **2006,** 46, (2), 273-286.

112. M. Kapnistos, D. Vlassopoulos, J. Roovers and L. G. Leal. *Macromolecules* **2005,** 38, (18), 7852-7862.

113. N. J. Inkson, R. S. Graham, T. C. B. McLeish, D. J. Groves and C. M. Fernyhough. *Macromolecules* **2006,** 39, (12), 4217-4227.

114. E. van Ruymbeke, M. Kapnistos, D. Vlassopoulos, T. Huang and D. M. Knauss. *Macromolecules* **2007,** 40, (5), 1713-1719.

115. R. Pivokonsky, M. Zatloukal and P. Filip. *J. Non-Newtonian Fluid Mech.* **2008,** 150, (1), 56-64.

116. P. G. de Gennes. *J. Chem. Phys.* **1971,** 55, 572.

117. P. G. de Gennes. *J. of Phys.* **1975,** 36, 1199-1203.

118. R. C. Ball and T. C. B. McLeish. *Macromolecules* **1989,** 22, 1911-1913.

119. D. K. Bick and T. C. B. McLeish. *Phys. Rev. Lett.* **1996,** 76, 2587-2590.

120. J. W. Lee, D. Kim and Y. Kwon. *Rheol. Acta* **2002,** 41, (3), 223-231.

121. S. Bourrigaud, G. Marin and A. Poitou. *Macromolecules* **2003,** 36, (4), 1388-1394.

122. T. C. B. McLeish and K. P. O'Connor. *Polymer* **1993,** 34, (14), 2998-3003.

123. J. Allgaier, D. K. Bick, G. Bishko, N. Clarke, A. Hakiki, R. K. Heenan, T. C. B. McLeish, D. J. Read and R. N. Young *Neutron-scattering from labelled H-polymer melts*; Rutherford Laboratory Report: 1997.

124. H. C. Ottinger. *Rheol. Acta* **2001,** 40, (4), 317-321.

125. J. van Meerveld. *J. Non-Newtonian Fluid Mech.* **2002,** 108, (1-3), 291-299.

126. P. K. Currie In *Calculations on the Doi-Edwards Model for Concentrated Polymer Solutions*, Proceedings of the Ninth International Congress on Rheology, Acapulco, Mexico, 1984; Acapulco, Mexico, 1984.

127. P. Wapperom and R. Keunings. *J. Non-Newtonian Fluid Mech.* **2001,** 97, (2-3), 267-281.

128. H. M. Laun In Proceedings from the Ninth International Congress on Rheology, Acapulco, Mexico, 1984; Acapulco, Mexico, 1984.

129. P. Rubio and M. H. Wagner. *J. Rheol.* **1999,** 43, (6), 1709-1710.

130. H. M. Laun and H. Schuch. *J. Rheol.* **1989,** 33, (1), 119-175.

131. P. Rubio and M. H. Wagner. *Proc. Int. Congr. Rheol., 13th* **2000,** 2, 28-30.

132. J. Meissner. *J. Appl. Polym. Sci.* **1972,** 16, (11), 2877-2899.

133. P. Rubio and M. H. Wagner. *J. Non-Newtonian Fluid Mech.* **2000,** 92, (2-3), 245-259.

134. Y. Kwon and A. I. Leonov. *J. Non-Newtonian Fluid Mech.* **1995,** 58, (1), 25-46.

135. G. B. Bishko, O. G. Harlen, T. C. B. McLeish and T. M. Nicholson. *J. Non-Newtonian Fluid Mech.* **1999,** 82, (2-3), 255-273.

136. D. J. Read and T. C. B. McLeish. *Macromolecules* **2001,** 34, (6), 1928-1945.

137. M. Rubinstein, S. Zurek, T. C. B. McLeish and R. C. Ball. *Journal de Physique* **1990,** 51, (8), 757-775.

138. C. Friedrich and B. Hofmann. *Rheol. Acta* **1983,** 22, 425-434.

139. J. V. Lawler, *Techniques in Rheological Measurement*. Chapman & Hall: Cambridge, UK, 1993; p 343.

140. R. S. Graham, T. C. B. McLeish and O. G. Harlen. *J. Rheol.* **2001,** 45, (1), 275-290.

141. C. D. Chodankar, J. D. Schieber and D. C. Venerus. *Rheol. Acta* **2003,** 42, (1-2), 123-131.

142. R. J. Blackwell, T. C. B. McLeish and O. G. Harlen. *J. Rheol.* **2000,** 44, (1), 121-136.

143. W. M. H. Verbeeten, G. W. M. Peters and F. P. T. Baaijens. *J. Rheol.* **2001,** 45, (4), 823-843.

144. R. J. Blackwell, O. G. Harlen and T. C. B. McLeish. *Macromolecules* **2001,** 34, (8), 2579-2596.

145. C. D. Chodankar, J. D. Schieber and D. C. Venerus. *J. Rheol.* **2003,** 47, (2), 413-427.

146. S. G. Kalogrianitis and J. W. van Egmond. *J. Rheol.* **1997,** 41, (2), 343-364.

147. J. Soulages, M. Huetter and H. C. Oettinger. *J. Non-Newtonian Fluid Mech.* **2006,** 139, (3), 209-213.

148. A. C. B. Bogaerds, A. M. Grillet, G. W. M. Peters and F. P. T. Baaijens. *J. Non-Newtonian Fluid Mech.* **2002,** 108, (1-3), 187-208.

149. P. Hachmann. Multiaxiale Dehnung von Polymerschmelzen. Dissertation, ETH Zurich Nr. 11890, 1996.

150. M. Kraft. Untersuchungen zur scherinduzierten rheologischen Anistropie von verschiedenen Polyethylen-Schmelzen. Dissertation, ETH Zurich Nr. 11417, 1996.

151. H. Muenstedt and H. M. Laun. *Rheol. Acta* **1979,** 18, (4), 492-504.

152. J. Meissner. *Pure Appl. Chem.* **1975,** 42, (4), 551-612.

153. M. H. Wagner, P. Ehrecke, P. Hachmann and J. Meissner. *J. Rheol.* **1998,** 42, (3), 621-638.

154. W. M. H. Verbeeten, G. W. M. Peters and F. P. T. Baaijens. *J. Non-Newtonian Fluid Mech.* **2002,** 108, (1-3), 301-326.

155. J. F. M. Schoonen. Determination of Rheological Constitutive Equations using Complex Flows. Eindhoven University of Technology, Eindhoven, 1998.

156. M. Zatloukal. *J. Non-Newtonian Fluid Mech.* **2003,** 113, (2-3), 209-227.

157. H. A. Barnes and G. P. Roberts. *J. Non-Newtonian Fluid Mech.* **1992,** 44, 113-126.

158. N. Inkson, T. McLeish and O. Harlen. *Prog. Trends Rheol. V, Proc. Eur. Rheol. Conf., 5th* **1998**, 336-337.

159. R. Pivokonsky, M. Zatloukal and P. Filip. *J. Non-Newtonian Fluid Mech.* **2006,** 135, (1), 58-67.

3.0 Methodology and Experimental Methods

Preface

In this chapter is presented the materials, experimental and numerical methods, and research plans required to complete the objectives proposed in section 1.0. In section 3.1 is identified the materials that are used in the course of this research. In section 3.2 is presented the rheological methods used during this work. In sections 3.3 and 3.4 are discussed the two proposed research goals.

3.1 – Materials Selected

Two sets of materials have been carefully selected that are suitable for linking molecular structure with observed melt rheology. The first is a set of seven sparsely-branched and one linear HDPE homopolymers provided by the Dow Chemical Company. These materials are well characterized in terms of long-chain branching content. The second is a set of anionically-polymerized PS with well-defined branching structures. These materials are well classified in terms of branch location, branch length, and branch frequency.

3.1.1 – Dow Chemical Metallocene-Catalyzed HDPE

A set of well-characterized HDPE resins with varying degrees of sparse-LCB content is made available by the Dow Chemical Company in sufficient quantities for material, rheological, and processing analysis. Included are seven sparsely-branched mHDPEs that vary in branching long-chain branching content from 0.26 to 3.33 LCB per 10,000 carbons, and one linear HDPE resin (Table 3.1). Branching concentration is determined using ^{13}C NMR. The lack of short-chain branches in the material mitigate the typical pitfall of a false positive that can result in the counting of branches shorter than the entanglement molecular weight. The sparsely-branched resins are synthesized using a constrained geometry catalyst of the type described by Stevens[1, 2] in a continuous, stirred-tank reactor as described by Lai *et al.*[3]. All eight resins are linear homopolymers with narrow molecular weight distributions characteristic to metallocene type catalysts.

Table 3.1 – mHDPE Resins			
Polymer Resin ID	**M_W**	**M_W / M_N**	**LCB/10^4 C** *[as determined from ^{13}C NMR]*
HDB1	77,100	2.0	0.26
HDB2	82,000	1.9	0.37
HDB3	85,700	2.0	0.42
HDB4	96,300	2.1	0.80
HDB5	79,000	n/a	0.90
HDB6	68,000	n/a	1.88
HDB7	70,000	n/a	3.33
HDPE	113,000	2.5	Linear

3.1.2 – Anionically Polymerized PS

A set of well-defined polystyrene resins with specific branching architectures have been synthesized and characterized by Yu and Mays[4] (U. of Tennessee) for specific use in this study. The polymers are created using anionic polymerization. In Table 3.2 is shown the molecular characteristics of an entangled 4-arm star that can serve as an excellent model system for analyzing the entangled melt rheology of the star architecture. The entanglement molecular weight for polystyrene is 16,600 g/mol [5]. In Table 3.3 is shown a series of synthesized pom-pom polystyrenes. These are made by using 4-(chlorodimethylsilyl)styrene (CDMSS) to create star polymers containing a reactive anionic site by linking anionically polymerized linear chains together. The anionic site is then used to grow the "star-linear diblock," which constitutes half of the pom-pom. Coupling using dichlorodimethylsilane yields the final product. These materials have been synthesized in quantities of roughly 10 grams, and with molecular weights up to 230,000 g/mol [6]. Continued progress is being made by Yu and Mays[4] (U. of Tennessee) and Dodd and Hutchings (U. of Durham – UK) to created model comb and pom-pom systems with arms sufficiently long-enough arms for entanglement, however, no further materials were delivered to the

author for analysis. Discussion on how the existing model resins can be used in future work can be found in Section 7.0 Reccomendations.

Table 3.2 – Entangled 4-arm Star PS			
Species	**M_w**	**M_n**	**PDI**
Star Arm	54180	53680	1.009
4-Armed Star	208800	205700	1.015

Table 3.3 – Characterization of Pom-Pom PS												
ID#	**Linear**			**Star**			**Star-Linear**			**Pom-Pom**		
	M_w	**M_n**	**PDI**	**M_w**	**M_n**	**PDI**	**M_w**	**M_n**	**PDI**	**M_w**	**M_n**	**PDI**
1	5438	4970	1.09	33910	29220	1.161	47190	41310	1.142	92340	85960	1.074
2	2021	1753	1.15	18780	15770	1.191	26800	23550	1.138	54050	52200	1.035
3	2420	1882	1.286	20600	16860	1.222	49190	46860	1.05	98970	97020	1.02
4	22940	22680	1.012	92750	79490	1.167	129000	111500	1.157	229700	221000	1.039
10	1170	980	1.196	13290	10930	1.216	21370	19070	1.12	42170	40990	1.029
11	1139	977	1.165	10600	8087	1.311	23290	22030	1.057	45710	44960	1.017
6	10823	9868	1.097	55890	47990	1.165	92120	75720	1.217	180200	171300	1.051

3.2 – Rheological Characterization

Rheological characterization is utilized in the completion of each research objective. This section serves to explain the experimental procedure used for rheological measurements taken during this study. The melt rheology is important for characterizing the effects of molecular structure, especially those arising from long-chain branching. Both shear and shear-free measurements are necessary. Shear characterization is performed using a Rheometrics Mechanical Spectrometer Model 800 (RMS 800). Shear-free, or elongation/extensional, characterization is performed using either a Rheometerics Extensional Rheometer Model 9000 (RER-9000) or a Sentmanat Extension Rheometer

(SER) testing platform. The combination of these three machines provides an accurate determination of the rheological material functions that describe each material.

All shear flow testing is performed in the RMS-800 under an inert nitrogen atmosphere with cone-and-plate fixtures having a plate diameter of either 25 mm or 10 mm with a cone angle of 0.1 rad or 0.035 rad, respectively. The reduced plate diameter size allows for higher strain and strain rate measurements, but suffers from higher data scattering resulting from the smaller sample size. The cone-and-plate geometry is chosen because it provides a homogeneous deformation field.

Steady shear and small-amplitude dynamic oscillatory shear measurements are performed to obtain low and intermediate shear viscosity flow curves in the range of 0.001 to 100 s^{-1}. Relevant properties that are measured in steady shear are the shear viscosity, η, and the primary normal stress difference, N_1. Relevant properties that are measured in small-strain dynamic oscillatory shear are the complex viscosity, η^*, storage modulus, G', and the loss modulus, G''. The Cox-Merz rule (Eq. 2.1-19) is assumed to hold true. This is verified by agreement of the complex viscosity and shear viscosity at $\omega = \dot{\gamma}$.

Two transient shear flows, stress growth and step-strain, are performed to measure the non-linear viscoelastic response of the material. Transient stress growth tests are performed to measure the magnitude of the steady-state stress (viscosity) overshoot. Transient stress growth measurements at low shear rates are observed to mimic the linear viscoelastic behavior seen in steady shear. Step-strain measurements are measured at strains of 1% to 1250%. The resulting relaxation modulus, $G(t,\gamma)$, is measured.

Uniaxial extensional viscosity measurements are taken with the both the RER-9000 and the SER testing platform. The RER-9000 is based on the original Munstedt design[7]. Samples are immersed in a neutrally-buoyant silicone oil bath. After reaching thermal equilibrium, the desired extension rate deforms the sample and the resulting force is monitored using a leaf spring-LVDT assembly. The

maximum Hencky (true) strain achieved with the RER-9000 is approximately 3.0 using test specimens that are 22 mm in length prior to extension. The experimental strain rates achievable range from 0.01 to 1 s^{-1}.

The SER testing platform developed by Sentmanat[8] is used to characterize the extensional viscosity of a material at extension rates of up to 20 s^{-1}, and is designed to operate as a fixture in the RMS-800. A rectangular sample is placed on a dual counter-rotating wind-up drums where rotation is resisted by the stretching material. The elongation rate is governed by the rotation rate and radius of the drums. The resistance to rotation force is measured by the RMS-800 torque transducer. This force is converted to the resulting transient extensional viscosity, η_E^+, by dividing by both the applied strain rate and transient sample area. The maximum Hencky (true) strain achieved with the SER is approximately 4.0, a full strain higher than the RER-9000. To prevent material sagging prior to and during testing, it is recommended that the zero-shear viscosity of the melt at the testing temperature is greater than 10,000 Pa-s.

3.3 – Research Objective One

The first research objective is designed to test the robustness of the pom-pom constitutive model in connecting the melt rheology to the molecular structure for a series of sparsely-branched mHDPEs. These well-defined systems provide a basis for direct comparison with rheologically determined pom-pom parameters. The onset of ductile failure at higher strain rates in transient extension of these resins forces a change in the traditional methodology used by both Inkson *et al.*[9] and Doerpingahus and Baird[10].

A full evaluation of the pom-pom constitutive model is dependent on the ability to determine the correct material parameters from rheological data. This is problematic for the mHDPEs resins described in section 3.1.1 due to the onset of ductile failure seen at higher strain rates in uniaxial

extensional flow. This instability makes requisite a new methodology to determine a more robust set of pom-pom parameters. Four parameters are fit are each mode: τ_{si} (stretch relaxation time), q_i (theoretical number of branch arms), τ_{bi} (orientation relaxation times), and g_i (contribution to the plateau modulus). In the traditional methodology of Inkson *et al.*[9], τ_{bi} and g_i are fit from the linear viscoelastic regime of the dynamic oscillatory shear response. The choice of τ_{bi} values is arbitrary, and one to two modes per decade is sufficient. τ_{si} and q_i are fit simultaneously using transient uniaxial viscosity. Fitting two parameters per mode in a single flow type can lead to multiple "best fit" sets of parameters that increases with number as the amount and/or quality of data is decreased.

In Fig. 3.1 is shown the effect of varying q_i in the predictions of uniaxial extensional viscosity for an entangled single mode pom-pom fluid. Obviously, increasing the value of q_i results in a higher extensional viscosity plateau. However, in our mHDPE resins, it is not possible reach this viscosity plateau due to the development of an elastic instability, which is reviewed in section 2.1.3.3. Therefore, having incomplete rheological data in this flow can lead to multiple "best-fit" combinations of τ_{si} and q_i. For example, let the "X" in Fig. 3.1 be the point at which sample material fails due to this elastic instability during elongational flow. Based on the incomplete data at higher times (strains), it becomes impossible to know the exact value of q_i. Therefore, any assumptions made about the molecular structure based on these deficient parameters are also deficient in the context of the model.

A two-pronged approach is proposed to circumvent this problem. The first approach is to use shear step-strain flows to independently determine the stretch relaxation time, τ_{si}, leaving only q_i to be determined from uniaxial extension. Shear step-strain is an attractive candidate to determine the stretch relaxation time in that it is a "strong" flow that induces a non-linear stretch in the material, and can be modeled independent of q_i. The second approach is the use a novel experimental method in which the material that wants to undergo elastic failure in elongational flow is encapsulated within a stable resin of similar viscosity, and forced to deform uniformly. It is the goal that the combination of

these techniques will provide a more robust set of parameters relative to the traditional fitting method, thus yielding a more robust analysis as to the effectiveness of the pom-pom model's ability to describe the structure of our well-characterized mHDPEs.

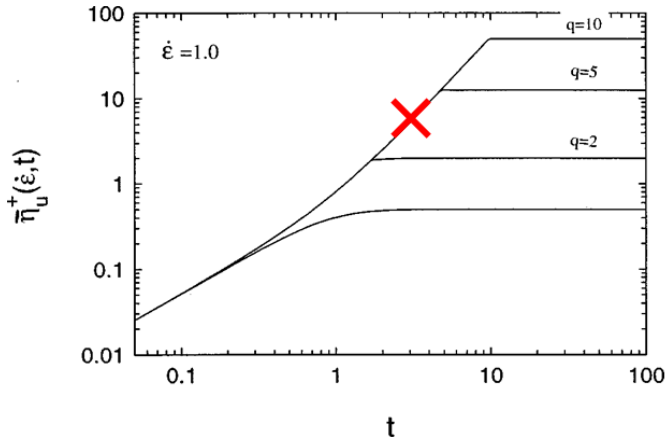

Figure 3.1 Illustration on the effect of varying q_i in extensional flow. The "X" serves to illustrate how an incomplete data set due to material or machine limitations can lead to multiple best fit values of q_i. Figure adapted from Inkson *et al.*[9].

The relevant rheological data is gathered in the following manner. The linear viscoelastic relaxation spectrum is obtained through small-strain oscillatory shear experiments. Time-temperature superposition is used to increase the range of this data to sufficient frequencies. The Cox-Merz rule (Eq. 2.1-19) is validated by comparison of the complex viscosity and shear viscosity at $\omega = \dot{\gamma}$.

Step-strain measurements are taken at strains ranging from 1% to 1250%. Care is taken to avoid mechanical errors that are outlined in section 2.1.2.3. Transducer overload is avoided by reducing the cone-and-plate diameter from 25mm to 10mm. This allows for maximum strains of 12.5 to measured, but results in a smaller sample size which can increase data scattering. Wall-slip and material rupture are avoided by inspection of the damping curve as outlined in by Stadler *et al.*[11]. Finite rise times on the order of 0.05 seconds are observed for all strains investigated. The correction of Zapas and Craft[12] is used to correct for the imperfect strain prior to any constitutive modeling. The work of Seay[13] provides data for these materials for strains up to 12.5. However, the data set is incomplete for the needs of this work. Additional measurements are taken at intermediate strains to improve the range of molecular

data modeled, most notably in the region between strains of 1.0 and 5.0. Certain data at higher strains measured by Seay[13] exhibit slip (evidenced by a "kink" in the shape of the damping function). These points are remeasured with care taken to avoid slip.

Transient elongation is measured in both the SER and RER for strains up to 4.0 and 3.0, respectively, and strains rates ranging from 0.001 to 10 s^{-1}. Preference as to which rheometer is used is dictated by each machines limitations discussed in section 3.2. When no limitation exists, preference is given to the SER due to its higher maximum strain. Materials that exhibit ductile failure are encapsulated and elongated using the novel procedure.

The rheological data is then fit using the differential form of the McLeish-Larson pom-pom model (Eq. 2.3-22). τ_{bi} and g_i are determined by simultaneously fitting the storage and loss moduli curves obtained in small-strain dynamic oscillatory shear. τ_{si} is fit to step-strain relaxation data using the multi-mode differential pom-pom form of the relaxation modulus given in Eq. 2.3-26 with the backbone stretch ratio given by Eq. 2.3-25. The quantitative validity of the τ_{si} is determined by first validating that the values are rationale in the theoretical framework of the pom-pom model. Second, τ_{si} from step-strain is compared with values of τ_{si} determined using traditional methodology of Inkson *et al.*[14]. q_i is determined by fitting the transient extensional viscosity obtain using conventional and encapsulated extensional rheology. The set of pom-pom material parameters as a whole for the mHDPE resins is then compared with the known branching-content of the materials to gauge quantitative validity.

3.4 – Research Objective Two

The second objective is to determine whether the pom-pom parameters determined from rheological measurements on a model system are consistent with those of the known chemical structure. This research serves to determine if a quantitatively accurate connection can be made between the model parameters and the molecular structure. To this end, a set of anionically-

polymerized polystyrene molecules with highly controlled model branching architectures is currently being synthesized by Yu and Mays[4] (U. of Tennessee) and Dodd and Hutchings (U. of Durham, UK). These model systems are useful for completing this research objective in that the number, location, and length of every LCB is known, thereby making it possible to use Eq. 2.3-19 and 2.3-20 to determine the relaxation times associated with the chemical structure. These parameters can then be used to compare predictions of the material's melt rheology with gathered experimental data. Obviously, the amount of progress that can be made in this objective is a function of the amount and quality of the material. Since no resins capable of adequately fulfilling the above objectives were received, further discussion for steps to achieve this goal is reserved for Section 7.0, Recommendations.

3.6 - References

1. Stevens, J., *J. of Studies in Surface Sci. and Catalysts* **1994,** 89.

2. Stevens, J., *J. of Studies in Surface Sci. and Catalysts* **1996,** 101.

3. Lai, S. Y.; Wilson, J. R.; Knight, J. R.; Stevens, G. W., **1993**.

4. Yu, X.; Mays, J., *Dept. of Chemistry - U. of Tennessee*. Knoxville, TN.

5. van Ruymbeke, E.; Kapnistos, M.; Vlassopoulos, D.; Huang, T.; Knauss, D. M., Linear Melt Rheology of Pom-Pom Polystyrenes with Unentangled Branches. *Macromolecules* **2007,** 40, (5), 1713-1719.

6. Baird, D. G.; Mays, J. W.; McGrady, C. D.; Seay, C. W.; Yu, X. *NSF - Project Activities and Results for Year 2-0602196*; NSF: Washington, D.C., 2008.

7. Münstedt, H.; Laun, H. M., Elongational behavior of a low density polyethylene melt. II. Transient behavior in constant stretching rate and tensile creep experiments. Comparison with shear data. Temperature dependence of the elongational properties. *Rheologica Acta* **1979,** 18, (4), 492-504.

8. Sentmanat, M. L., Miniature universal testing platform: from extensional melt rheology to solid-state deformation behavior. *Rheologica Acta* **2004,** 43, (6), 657-669.

9. Inkson, N. J.; McLeish, T. C. B.; Harlen, O. G.; Groves, D. J., Predicting low density polyethylene melt rheology in elongational and shear flows with "pom-pom" constitutive equations. *J. Rheol.* **1999,** 43, (4), 873-896.

10. Doerpinghaus, P. J.; Baird, D. G., Assessing the Branching Architecture of Sparsely Branched Metallocene-Catalyzed Polyethylenes Using the Pompom Constitutive Model. *Macromolecules* **2002,** 35, (27), 10087-10095.

11. Stadler, F. J.; Auhl, D.; Münstedt, H. M., Influence of the molecular structure of polyolefins on the damping function in shear. *Macromolecules* **2008,** 41, 3720-3726.

12. Zapas, L. J.; Craft, T., *J. Res. Natl. Bur. Stand.* **1965,** 69A, 541-546.

13. Seay, C. W. The Role of Molecular Architecture on Rheological Properties and its Effect on Film-Casting Performance. Virginia Tech, Blacksburg, VA, 2008.

14. Inkson, N.; McLeish, T.; Harlen, O., Modeling low density polyethylene rheology using the pom-pom model. *Progress and Trends in Rheology V, Proceedings of the European Rheology Conference, 5th, Portoroz, Slovenia, Sept. 6-11, 1998* **1998**, 336-337.

4.0 Method for overcoming ductile failure in Münstedt-type extensional rheometers

Preface

This chapter introduces a novel technique to overcome ductile failure in extensional flow called encapsulation. Development of the technique, proof of concept, and successful extension to HDPE resins that undergo ductile failure are presented. This chapter is organized as a manuscript for publication.

Method for overcoming ductile failure in Münstedt-type extensional rheometers

Christopher D. McGrady and Donald G. Baird

Department of Chemical Engineering, Virginia Tech

Blacksburg, VA 24061

4.1 – Abstract

The purpose of this work is to introduce an experimental technique to overcome ductile failure in uniaxial extensional flow and show a simple illustration of its effectiveness. Ductile failure prevents the rheological measurement of transient stress growth at higher strains for certain strain-hardening materials. This reduces the accuracy of nonlinear parameters for constitutive equations fit from transient stress growth data, as well as their effectiveness in modeling extensionally driven processes such as film casting. We propose an experimental technique to overcome ductile failure called encapsulation in which the material that undergoes ductile failure is surrounded by a resin that readily deforms homogeneously at higher strains. The materials are arranged in concentric cylinders and are deformed in parallel. A simple model is shown to calculate the viscosity of the core material and is tested for its robustness in a linear low-density polyethylene/low-density polyethylene system in which the viscosities of each resin are known at all strains, strain rates, and temperatures investigated. Agreement is found at each strain rate investigated across all strains studied. The method is then extended to measure the viscosity of a sparsely branched high-density polyethylene, HDPE, system that undergoes ductile failure at higher strain rates. The technique shows good agreement with experimental results up to the onset of ductile failure in the pure resin and predicts viscosity growth of the HDPE resin well beyond the critical strain for the onset of failure seen in experimental measurements of the pure HDPE. Repeatability of the technique is also illustrated.

4.2 – Introduction

Ductile failure, or "necking," in uniaxial extensional flow can prevent the measurement of transient stress growth at high strains for certain polymers. While techniques have been implemented using the filament stretching rheometer (FSR) to control and the Rheometric Scientific RME to delay ductile failure in the extension of melts, these methods themselves are not without flaws. Filaments stretched under controlled deformation on the FSR can still undergo ductile failure at higher extension rates [Bach *et al.* (2003)]. Excessive strain-hardening has been recorded for LLDPE melts using the RME [Schulze *et al.* 2001]. Even if these challenges can be overcome, the RME and FSR rheometers are not common to all rheological laboratories. It is, therefore, of interest to explore a technique applicable to a Münstedt-type elongational rheometer (but possibly other designs also) that can delay or control ductile failure.

Ductile failure in extension is defined as the development of a perturbation or structural defect in the sample that occurs before reaching either the maximum strain imposed by the testing device or the transient viscosity plateau. Typical examples of ductile failure are non-uniform deformation and necking [Lee *et al.* (2002)]. Continued extension of a sample after the onset of ductile failure results in an increase in the severity of necking that ultimately leads the sample to rupture into two distinct fluid domains. Obviously, no further viscosity data can be captured following such a rupture event. More so, the forced non-homogeneity in deformation that occurs after the onset of failure, but before rupture, brings into question the quantitative validity of any data collected after the onset of ductile failure due to the reduced cross-sectional area at the point of failure [Barroso and Maia (2005) and Schweizer (2000)].

This phenomenon has consequence in the calculation of dynamic variables native to constitutive equations that are based on molecular topology. For example, transient extensional viscosity plays a

prominent role in predicting the nonlinear parameters of the multimode McLeish-Larson pom-pom model proposed by Inkson *et al.* (1999). Specifically, the extensional viscosity plateau at a given extension rate, $\dot{\varepsilon}_0$ determines the theoretical number of branch point arms corresponding to backbone orientation and stretch relaxation times that are on the order of $\dot{\varepsilon}_0^{-1}$. The ability to reach the transient extensional viscosity plateau experimentally across many strain rates largely affects the values and accuracy of these non-linear parameters.

McKinley and Hassager (1999) used the Considère condition, which was originally derived in solid mechanics [Considère (1885)], in the limit of rapid elongation to quantitatively predict the critical Hencky strain ($\varepsilon \equiv \dot{\varepsilon_0} t$) for the onset of failure using both the Doi-Edwards [Doi and Edwards (1978)] and the McLeish-Larson pom-pom constitutive equations [McLeish and Larson (1998)]. The authors found that molecular topology in the form of pom-pom branch points affect the onset of material failure. Yogesh and Denn (2002 and 2004) constructed a model for viscoelastic fluids that attributed the onset of ductile failure to the frictional force on entangled chains being unable to balance tension in the chain, finding that total strain at rupture decreased as extension rate increased. Yao *et al.* (1998 and 2000) found that the rate of necking was a function of the magnitude of strain hardening that occurred in uniaxial extension. Yao *et al.* (1998) also show that numerical calculations demonstrate that concurrent measurement of the tensile force in extensional flow and the "necking" filament's profile could be used along with the appropriate force balance [Szabo (1997)] to determine the transient extensional viscosity.

In our present work we are particularly interested in the extensional behavior of polymeric resins with sparse long chain branching, LCB, in which extensional data at high strains is needed to interpret the branching architecture in the framework of certain molecular constitutive models. These materials exhibit ductile failure at Hencky strains ($\varepsilon \equiv \dot{\varepsilon_0} t$) on the order of 1.0 at extension rates on the

order of 1.0 s^{-1}. Various studies on predicting the onset of necking have been presented in the literature, most notably by McKinley and Hassager (1999), Yogesh and Denn (2002 and 2004), and Yao *et al.* (1998 and 2000). In this work we introduce an experimental technique to overcome ductile failure in Münstedt type elongational rheometers in which we encapsulate the material that undergoes ductile failure by a resin that readily deforms homogeneously at higher strains. The encapsulation technique is first shown to measure the transient extensional viscosity data of a core specimen that is in agreement with the extensional viscosity data available from the previous work of Doerpinghaus and Baird (2002 and 2003). The encapsulation technique is then applied to a resin that would traditionally undergo ductile failure at the measured strain rate. Application of the encapsulation technique allows for the measurement of transient extensional viscosity of the core material to the strain limitations of the Münstedt-type elongational rheometer used in this study. This achieved strain is higher than that of both the onset of the failure strain and the rupture strain traditionally observed.

4.3 – Procedure

In Fig. 4.1 is illustrated the approach in which the material of interest, (the material that undergoes ductile failure) is encapsulated in a sheath of material with a similar magnitude of shear viscosity. This sheath material is selected on the basis of two criteria. First, that the resin itself readily undergoes homogeneous deformation at all strain rates, strains, and temperature investigated. Second, the sheath is selected such that it does not significantly strain-harden in order to prevent its response from damping the behavior of the core. Assuming the two materials deform homogeneously in a parallel fashion, a simple parallel model outlined below could then be used to calculate viscosity of the core sample. The obvious benefit of this method would be obtaining transient viscosity data at higher

strains for the core resin that could not be obtained while running the pure resin in a traditional manner.

It is to be shown that a mathematical relationship exists that can remove the viscosity contribution of the sheath material from the total viscosity of the encapsulated sample, leaving only the viscosity profile of the core sample. In homogeneous uniaxial extension, the cross-sectional area decrease is given by:

$$A(\varepsilon) = A_0 e^{-\varepsilon} = \pi R_0^2 e^{-\varepsilon} \tag{4-1}$$

Assuming uniform deformation of the encapsulated sample, one would find that the length of the elongated core and the elongated sheath are equivalent to the length of the elongated sample. This assumption is verified both theoretically by a simple mass balance that indicates for a uniform deformation subject to Eq. 4-1, the materials must deform in tandem, and physically by visual inspection of the elongated encapsulated sample after testing. Given this condition, the tensile force measured during elongation of the encapsulated sample is simply a function of the sum of each species tensile force contribution (core and sheath) weighted by their initial cross-sectional area. Likewise, it can be said the total tensile force of the encapsulated sample, F_{encap}, that has an initial radius, R_o, elongated at an extension rate, $\dot{\varepsilon}_0$, is equivalent to the weighted sum of the forces resulting from elongating separately each of the materials at the same $\dot{\varepsilon}_0$, and R_o

$$F_{encap} = x_{core} F_{core,pure} + (1 - x_{core}) F_{sheath,pure} \tag{4-2}$$

where x_{core} is the volume fraction of the core in the encapsulated sample, $F_{core,pure}$ is the tensile force generated by elongating at the same rate as the encapsulated sample a pure filament composed of only the core resin with a radius equivalent of that of the encapsulated sample, and $F_{sheath,pure}$ is the sheath counterpart to the aforementioned $F_{core,pure}$.

Tensile force, *F(t)*, is related to transient extensional viscosity, $\eta_E^+(t)$, by

$$\eta_E^+(t) = \frac{F(t)}{\pi R_0^2 \dot{\varepsilon}_0}. \tag{4-3}$$

The transient uniaxial viscosity of the core resin can be calculated by substituting Eq. 4-3 into Eq. 4-2,

$$\eta_{E,encap}^+(t) = x_{core} * \eta_{E,core}^+(t) + [1 - x_{core}] * \eta_{E,sheath}^+(t) \tag{4-4}$$

followed by algebraic rearrangement to solve for $\eta_{E,core}^+(t)$, yielding

$$\eta_{E,core}^+(t) = \frac{\eta_{E,encap}^+(t) + [x_{core} - 1] * \eta_{E,sheath}^+(t)}{x_{core}} \tag{4-5}$$

where x_{core} is the volume fraction of the core in the encapsulated sample and $\eta_{E,i}^+(t)$, is the transient extensional viscosity of the core, sheath, or composite material. The relationship allows for calculation of the transient extensional viscosity profile of the core material provided tensile force can be measured for both the encapsulated sample and pure sheath sample over a range of Hencky strains at a given strain rate.

Three commercially available resins and one industrial model resin (HDB3) are used in this study. Relevant material properties are given in Table 4.1. The two Dow Affinity resins are metallocene-catalyzed, sparsely-branched linear low density polyethylenes, (LLDPEs). The branching content of Affinity PL 1840 and Affinity PL 1880 are 0.57 and 0.18 LCB per 10^4 carbons respectively Doerpinghaus and Baird (2002 and 2003). NA952 is a conventional low-density polyethylene (LDPE) manufactured by Equistar. The Affinity LLDPEs and NA952 LDPE resins readily deform to Hencky strains of at least 3.0 (which is the limit of the Münstedt-type extensional device used here) at all strain rates and temperatures investigated, and their transient uniaxial extensional viscosities at these conditions, as well as the linear viscoelastic response, have been measured previously by Doerpinghaus and Baird (2002 and 2003). HDB3 is a metallocene-catalyzed, sparsely-branched HDPE resin donated by the Dow

Chemical Company with LCB content of 0.42 LCB/10^4 C [Wood-Adams *et al.* (2000)]. This material undergoes ductile failure at $\dot{\varepsilon}_0$ >1.0 s^{-1} at Hencky strains lower than the experimental limit of the Münstedt-type extensional rheometer used in this study.

Transient uniaxial extensional measurements are performed using a Rheometrics Extensional Rheometer, Model 9000 (RER-9000), based upon the rod-pulling design put forth by Münstedt (1979). The maximum Hencky strain achieved is 3.0 using test specimens that were 22 mm in length prior to extension. Cylindrical samples are compression molded at 5000 psi and 175 ^oC and then are allowed to cool slowly under atmospheric pressure to eliminate any residual stresses. The samples are then bonded to test clips using Chem Grip-HT Epoxy and then mounted to the RER-9000. For encapsulated samples, the above molding process is done in the same fashion for the sheath material, but before adhesion of the samples to the clip, 50% of the sample is drilled out from the center (along the z-axis) using a drill press. The center is then filled with the desired test polymer (core specimen) and bonded to test clips. The sample is then immersed in a neutrally buoyant silicone oil bath at the test temperature. After reaching thermal equilibrium, the sample is deformed at the desired extension rate, and the resulting tensile force is monitored using a leaf spring-LVDT assembly. Linear viscoelasticity is measured using small-strain dynamic oscillatory shear measurements made on a Rheometrics RMS-800 using a 25mm cone-and-plate fixture with a 0.1 rad cone angle.

4.4 – Results and Discussion

4.4.1 – Encapsulation of a LLDPE that does not undergo ductile failure

The robustness of the encapsulation technique is tested using a system of two resins with known transient extensional viscosity profiles. Measurements are taken at 150 ^oC with $\dot{\varepsilon}_0$ = 0.1 and 1.0

s^{-1} using Affinity PL 1880 (LLDPE) as the core material and NA952 (LDPE) as the sheath material. Figs. 4.2 and 4.3 compare the viscosity of Affinity PL 1880 determined using encapsulation and Eq. 4-5 with that of the data from Doerpinghaus and Baird (2002 and 2003). Also shown for comparison in Fig. 4.2 is the linear viscoelastic envelope measured by Doerpinghaus and Baird (2002) using small-amplitude oscillatory shear. Good agreement between the two sets of viscosities is found across all strains and strain rates with the maximum deviation from experimental values being < 10%. These experimental results show that the method of encapsulation could quantitatively lead to the determination of the transient extensional viscosity of a core of LLDPE, suggesting that it is worth extending to a material that undergoes ductile failure.

4.4.2 – Encapsulation of a HDPE that undergoes ductile failure

HDB3 deformed in uniaxial extension at 170 ^{o}C undergoes homogeneous deformation at strain rates of 0.03, 0.1 and 0.3 as shown in Fig. 4.4. This is checked physically by simple inspection of the sample for homogeneous deformation after elongation. However, HDB3 that is deformed at 170 ^{o}C and $\dot{\varepsilon}_0$ = 1.0 s^{-1} undergoes ductile failure at 1.0 unit of Hencky strain before ultimately rupturing at a strain equal to 2.1. This is seen physically during testing by an onset of non-homogeneous extension, followed by the rupture of the sample into two discrete pieces. The results of this necking is shown graphically in Fig. 4.4 by the "kneecap" shape in the open circle symbol set of data that resides at strains larger than 1.0.

Application of the encapsulation technique allowed for the measurement of viscosity at strains higher than that at both the onset of the failure strain and the rupture strain. HDB3 is encapsulated in Affinity PL 1840. The extensional viscosity of pure Affinity PL 1840 deformed at $\dot{\varepsilon}_0$ = 1.0 s^{-1} and 170 ^{o}C is given in Fig. 4.5. Repeatability of the data is also given, with a maximum deviation on the order of 19%. The dark circle symbols in Fig. 4.4 show the transient extensional viscosity calculated using Eq. 4-5 in

tandem with the data obtained for the encapsulated sample. Excellent agreement is seen at strains less than the strain for the onset of ductile failure. Beyond the traditional failure strain boundary, the viscosity calculated from encapsulation shows continued stress growth. Data is obtained for an additional two units of strains before reaching the experimental limits of the apparatus. Repeatability of the method is illustrated in Fig. 4.6, with a maximum scattering of the data on the order of 23%. The agreement of the encapsulated data with pure unencapsulated experimental data at strains prior to failure coupled with continuity of the slope of the continuing predicted viscosity curve suggests merit in the predicted viscosity at higher strains.

4.5 – Conclusions

Encapsulation appears to be a viable experimental technique to gather transient extensional viscosity at strains higher than the onset of ductile failure strain in Münstedt-type extensional rheometers. The ability to increase the range of transient viscosity data available at a given strain could lead to improvements in the quality of the parameters associated with constitutive equations that attempt to model the rheology of branched polymer systems. Future publications of this technique that include more results, theory for stability, and extension to the SER testing platform are currently being investigated by the authors.

4.6 – Acknowledgements

This research is a collaborative effort for the World Wide Network of Materials – UK Leeds and is supported financially by the National Science Foundation DMR-052198. The authors greatly appreciate the contribution of samples from Dow Chemical Company, ExxonMobil Chemical Company, and Equistar

Chemical Company. The authors would also like to thank Dr. Aaron Eberle for many helpful discussions on the idea of encapsulation.

4.7 – References

Bach, A., Rasmussen, H. K., and Hassager, O.. "Extensional viscosity for polymer melts measured in the filament stretching rheometer," J. Rheol. 47, 429-441 (2003).

Barroso, V. C. and J. M. Maia, "Time dependent effects on the rupture of molten linear polymers in extension," J. Non-Newtonian Fluid Mech. 126, 93-103 (2005).

Considère, M., "Memoire sur l'emploi du fer et de l'acier dans les constructions," Annales des Ponts et Chausees 9, 574-605 (1885).

Doerpinghaus, P. J., "Flow behavior of sparsely branched metallocene catalyzed polyethylenes," Ph. D. dissertation, Virginia Tech, Blacksburg, VA (2002).

Doerpinghaus, P. J. and Baird D. G., "Assessing the branching architecture of sparsely branched metallocene-catalyzed polyethylenes using the pom-pom constitutive model," Macro. **35**, 10087-10095 (2002).

Doerpinghaus, P. J. and Baird, D. G., "Separating the effects of long-chain branching on rheology from those due to molecular weight in polyethylenes," J. Rheol. **47**, 717-736 (2003).

Doi M. and S. F. Edwards, "Dynamics of concentrated polymer systems. III. The constitutive equations," J. Chem. Soc. 74, 1818-1832 (1978).

Doi M. and S. F. Edwards, The Theory of Polymer Dynamics, Clarendon, Oxford, 1986.

Inkson, N. J., T. C. B. McLeish, and O. G. Harlen, "Predicting low density polyethylene melt rheology in elongational and shear flows with "pom-pom" constitutive equations," J. Rheol. 43, 873-896 (1999).

Lee, J. K., S. E. Solovyov, T. L. Virkler and C. E. Scott, "On modes and criteria of ABS melt failure in extension," Rheol. Acta 41, 567-576 (2002).

McKinley, G. H. and Hassager, O., "The Considère condition and rapid stretching of linear and branched polymer melts," J. Rheol. 43, 1195-1212 (1999).

Munstedt, H., "New universial extensional rheometers for polymeric melts. Measurements on a polystyrene sample," Trans. Soc. Rheol **23**, 421-436 (1979).

Schulze, J. S., Lodge, T. P., Macosko, C. W., Hepperle, J., Münstedt, H., Bastian, H., Ferri, D., Groves, D. J., Kim, Y. H., Lyon, M., Schweizer, T., Virkler, T., Wassner, E., Zoetelief, W., "A comparison of extensional viscosity measurements from various RME rheometers." Rheol. Acta **40**, 457-466 (2001).

Schweizer, T., "The uniaxial elongational rheometer RME – six years of experience," Rheol. Acta 39, 428-443 (2000).

Szabo, P., “Transient filament stretching rheometer I: Force balance analysis,” Rheol. Acta 36, 277-284 (1997).

Wood-Adams, P. M. and J. M. Dealy, “Using rheological data to determine the branching level in metallocene,” Macro. **33**, 7481-7488 (2000).

Wood-Adams, P. M., J. M. Dealy, and deGroot, W. A., “Effect of molecular structure on the linear viscoelastic behavior of polyethylene,” Macro. **33**, 7489-7499 (2000).

Yao, M., G.H. McKinley, and B. Debbaut, “Extensional deformation stress relaxation and necking failure of viscoelastic filaments,” J. Non-Newtonian Fluid Mech. 79, 469-501 (1998).

Yao, M., S.H. Spiegeelberg, and G. H. McKinley, “Dynamics of weakly strain-hardening fluids in filament stretching devices,” J. Non-Newtonian Fluid Mech. 89, 1-43 (2000).

Yogesh, M. J. and M. M. Denn, “Rupture of entangled polymeric liquids in elongational flow,” J. Rheol. 47, 291-298 (2003).

Yogesh, M. J. and M. M. Denn, “Rupture of entangled polymeric liquids in elongational flow with dissipation,” J. Rheol. 48, 591-598 (2004).

Resin	M_w	M_w/M_N	LCB/10^4 C [a as determined from GPC-LALLS b as determined from NMR]
Dow Affinity PL 1880	115.800	2.12	0.18[a]
Dow Affinity PL 1840	87,400	2.43	0.57[a]
Equistar NA952	235,500	17.1	39[b]
HDB3	85,700	2.0	0.42[a]

Table 4.1. Relevant material characteristics of the polyethylenes used. Properties for Dow Affinity and Equistar resins are from Doerpinghaus and Baird (2002 and 2003), and for the HDB3 resin is from Wood-Adams and Dealy (2000).

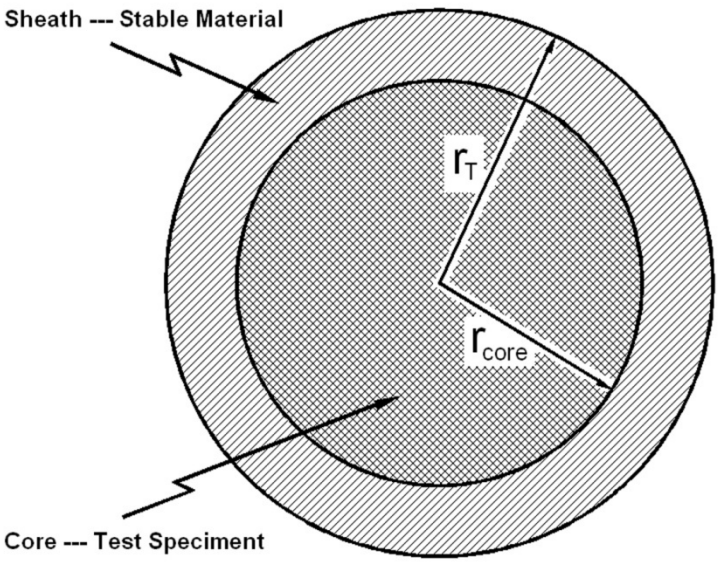

Figure 4.1. A cross-sectional diagram of the encapsulated extensional sample. Note that this point of view is on the *r,ϑ* plane of the cylindrical sample, with the *z*-axis extending into and out of the page.

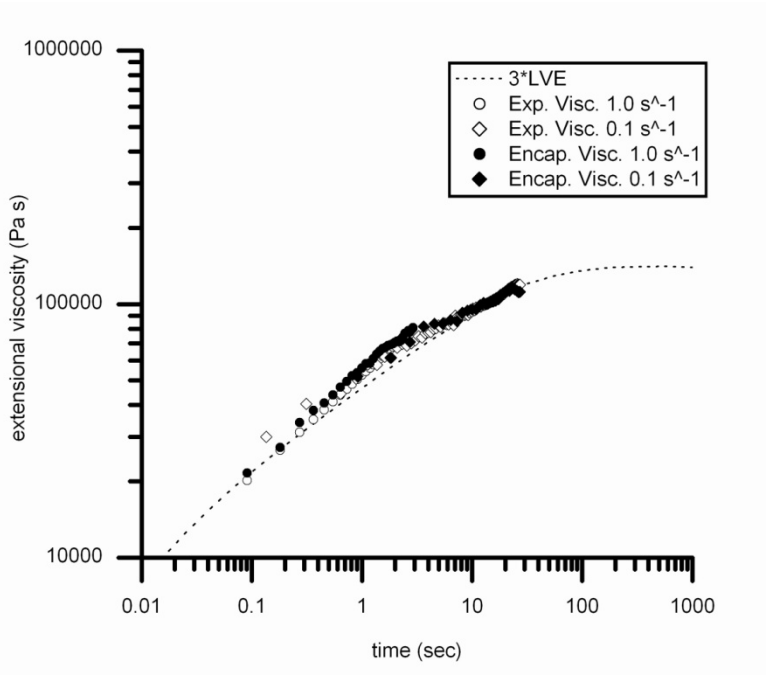

Figure 4.2. Transient uniaxial viscosity of pure, unencapsulated Affinity PL1880 at $\dot{\varepsilon}_0$= 0.1 s^{-1} (◊) and 1.0 s^{-1} (◊, filled) at 150 ^{o}C [Doerpinghaus and Baird 2002]. Transient uniaxial viscosity of Affinity PL1880 determined from encapsulation using Eq. 4-5 is shown for $\dot{\varepsilon}_0$= 0.1 s^{-1} (o) and 1.0 s^{-1} (•) at 150 ^{o}C. LVE growth curve is given by the dashed line.

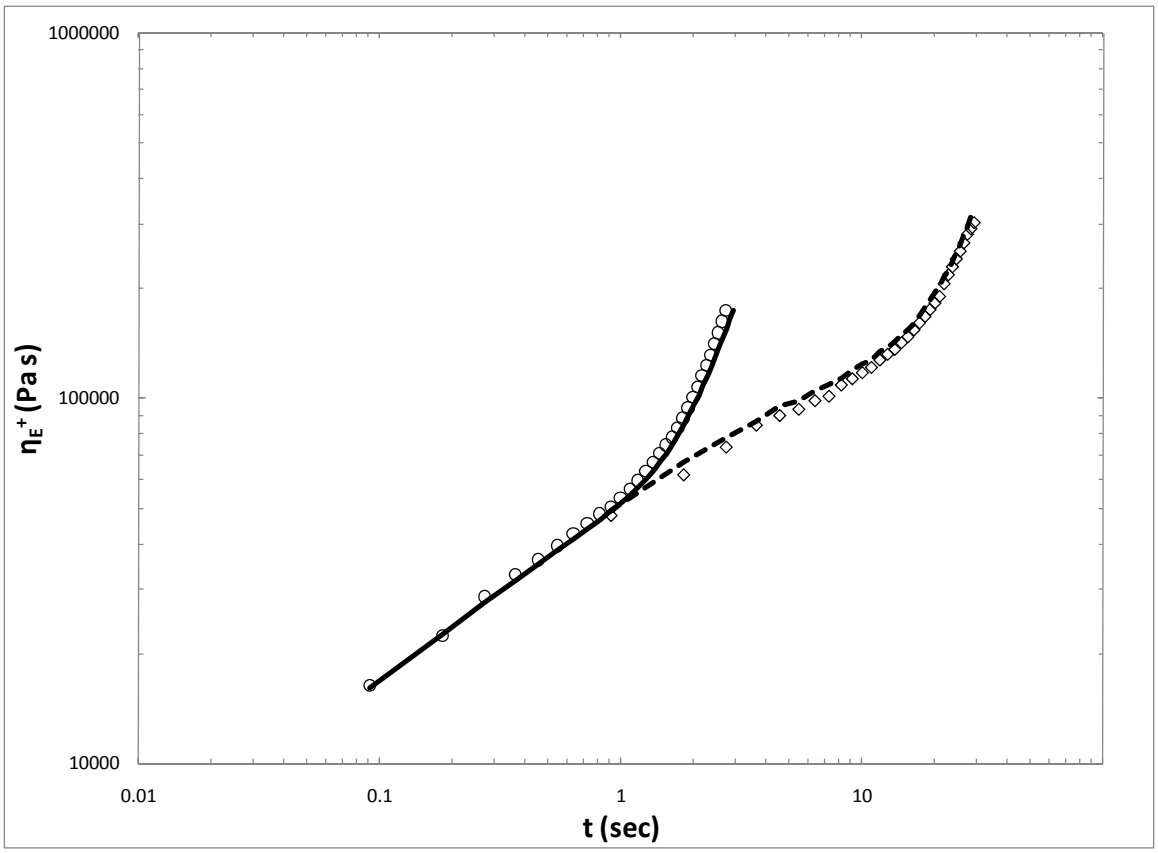

Figure 4.3. Transient uniaxial viscosity of 1880Encap at $\dot{\varepsilon}_0$ = 0.1 s^{-1} (◊) and 1.0 s^{-1} (o) at 150 ^{o}C. Transient uniaxial viscosity calculated using Eq. 4 is shown for $\dot{\varepsilon}_0$ = 0.1 s^{-1} (--) and 1.0 s^{-1} (-).

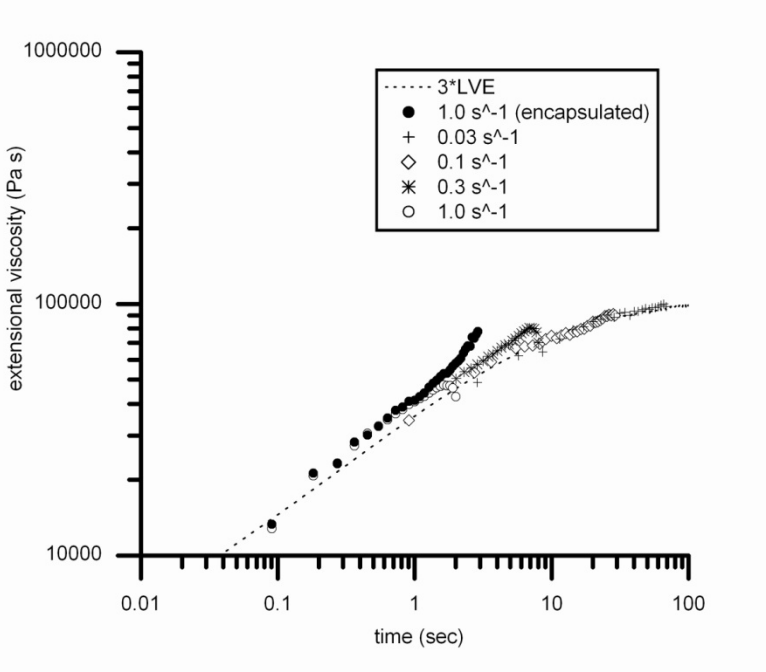

Figure 4.4. Transient uniaxial viscosity of pure, unencapsulated HDB3 at $\dot{\varepsilon}_0$= 1.0 s^{-1} (o), 0.3 s^{-1} (*), 0.1 s^{-1} (◊), and 0.03 s^{-1} (+) at 170 ^{o}C. Transient uniaxial viscosity of HDB3 determined using encapsulation and Eq. 4-5 is shown for $\dot{\varepsilon}_0$= 1.0 s^{-1} (•) at 170 ^{o}C. The LVE growth curve is given by the dashed line.

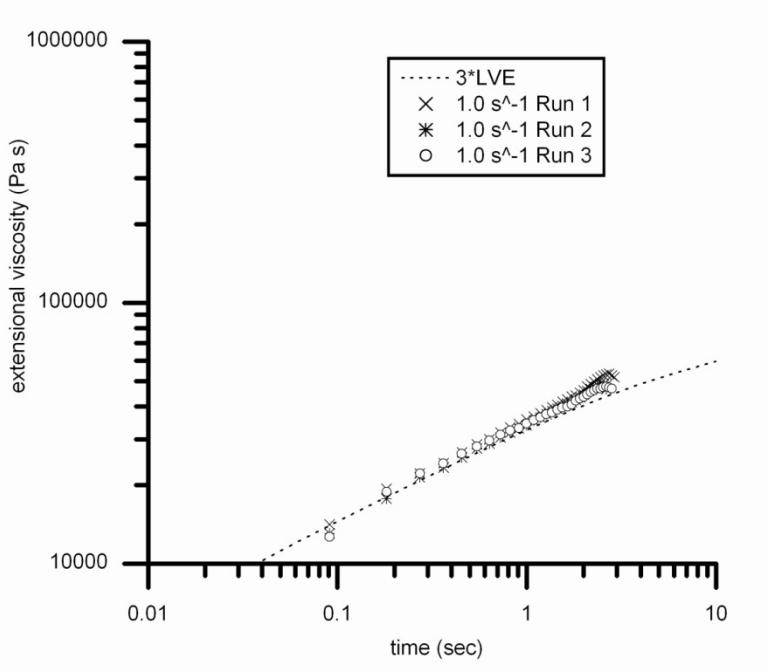

Figure 4.5. Illustration of reproducibility and scattering for the transient uniaxial viscosity of Affinity PL 1840 at $\dot{\varepsilon}_0$= 1.0 s^{-1} (o,+,◊ and,*). All measurements are taken at 170 ^{o}C. The LVE growth curve is given by the dashed line. LVE growth curve is given by the dashed line.

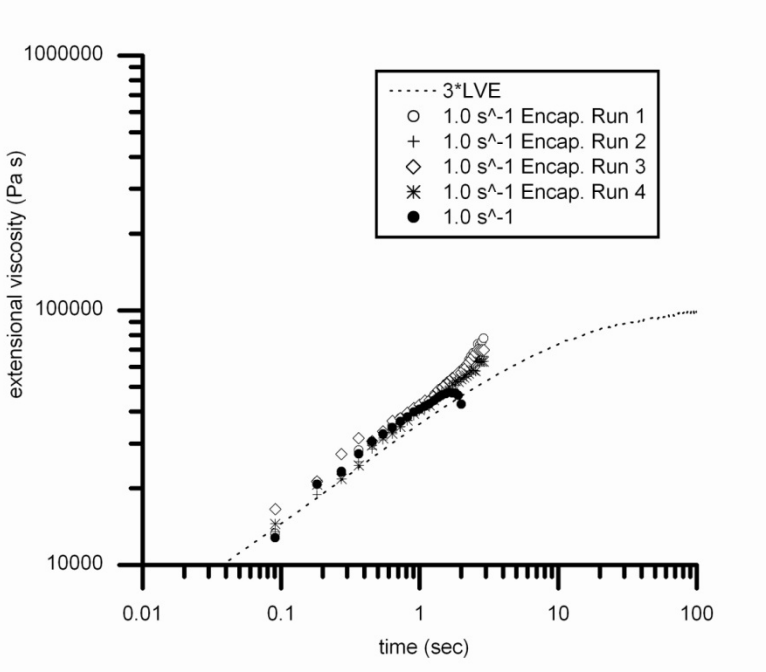

Figure 4.6. Illustration of reproducibility and scattering for the transient uniaxial viscosity of HDB3 determined using encapsulation and Eq. 4-5 elongated at $\dot{\varepsilon}_0$= 1.0 s^{-1} (o,+,◊ and,*). Transient uniaxial viscosity of pure, unencapsulated HDB3 at $\dot{\varepsilon}_0$= 1.0 s^{-1} (•) that undergoes ductile failure is shown for comparison. All measurements are taken at 170 ^{o}C. The LVE growth curve is given by the dashed line.

5.0 Effect of Sparse Long-Chain Branching on the Film-Casting Behavior for a Series of Well-Defined HDPEs

Preface

This chapter investigates the effect of sparse long chain branching, LCB, on the film-casting process is analyzed using a molecular model for the rheological behavior for a series of well-characterized, high-density polyethylene (HDPE) resins and a low-density polyethylene (LDPE) resin at various drawdown ratios. This chapter is organized as a manuscript for publication.

Effect of Sparse Long-Chain Branching on the Film-Casting Behavior for a Series of Well-Defined HDPEs

McGrady, Christopher D.; Seay, Christopher W.; Baird, Donald G.

Department of Chemical Engineering, Virginia Tech

Blacksburg, VA 24061

5.1 Abstract

The effect of sparse long chain branching, LCB, on the film-casting process is analyzed using a molecular model for the rheological behavior for a series of well-characterized, high-density polyethylene (HDPE) resins and a low-density polyethylene (LDPE) resin at various drawdown ratios. A full rheological characterization in both shear and shear-free flows is also presented. At low drawdown ratios, the LDPE exhibited the least degree of necking at distances less than the HDPE frostline. The sparsely-branched HDPE resins films had similar final film-widths that were larger than those of the linear HDPE. As the drawdown ratio was increased, film width profiles separated based on branching level. Small amounts of LCB were found to reduce the amount of necking at intermediate drawdown ratios. At higher drawdown ratios, the sparsely-branched HDPE resins of lower LCB had content film-widths that mimicked that of the linear HDPE, while the sparsely-branched HDPE resins of higher LCB content retained a larger film width. Molecular structural analysis via the Pom-pom constitutive model suggested that branching that was distributed across a larger range of backbone lengths serve to improve resistance to necking. As the drawdown ratio increased, the length of the backbones dominating the response decreased, so that the linear chains were controlling the necking behavior of the sparsely-branched resins of lower LCB content while remaining in branched regime for higher LCB content HDPEs. Other processing variables such as shear viscosity magnitude, extrudate swell, and non-

isothermal processing conditions were eliminated as contributing factors to the differences in the film width profile.

5.2 Introduction

Flow phenomena such as necking, edge-bead, and draw resonance affect the quality of drawn films in the film-casting process (Sollogoub *et al.* 2006). Necking is characterized by a reduction of the film width relative to the original die width. It is the product of drawing the film at larger velocities than it is extruded. Edge-beading is characterized by variation in the film thickness perpendicular to the direction of flow with an increased thickness usually observed at the edge. Draw resonance is a transient phenomenon characterized by periodic fluctuations in both the film width and thickness that occurs at drawdown ratios beyond the critical value.

Such phenomena are not only a function of the imposed processing conditions (i.e. drawdown ratio and extrusion rate), but also depend on the viscoelastic properties of the material. These viscoelastic properties, which are at the focus of this work, were shown in numerous studies to be a function of molecular weight (Auhl *et al.* 2008; Collis *et al.* 2005; Nielsen *et al.* 2006), molecular weight distribution (Linster and Meissner 1986; Munstedt and Kurzbeck 1998), molecular architecture (Fetters *et al.* 1993; Lohse *et al.* 2002; McLeish *et al.* 1999; Roovers 1985), and long-chain branching (LCB) content (Bin Wadud and Baird 2000; Doerpinghaus and Baird 2002; Münstedt and Auhl 2005; Wood-Adams *et al.* 2000). Seay and Baird (2009) illustrated the connection between viscoelastic properties and the film-casting process using two polyethylenes that have known differences in their branching topology and viscoelastic response, especially in their extensional rheology (Doerpinghaus and Baird 2002). The authors showed that the highly-branched low-density polyethylene (LDPE) material has drastically reduced necking when compared to the linear low-density polyethylene (LLDPE) resin at identical processing conditions [(Seay and Baird 2009) Fig. 1].

The amount of necking was shown in numerous works (Canning and Co 2000; Ito *et al.* 2003; Kajiwara *et al.* 2006; Kim *et al.* 2005; Sakaki *et al.* 1996; Satoh *et al.* 2001; Seay and Baird 2009; Silagy *et al.* 1996; 1998; Smith and Stolle 2003; Zheng *et al.* 2006) to be a function of both the processing conditions and the viscoelastic properties. It was observed that an increase in the extensional strain-hardening of a material reduces the degree of necking observed in films. Ito *et al.* (2003), Kajiwara *et al.* (2006), and Satoh *et al.* (2001) ascribed this behavior to the difference in the uniaxial and planar extensional strain-hardening based on the work of Dobroth and Erwin (1986). Canning and Co (2000) have verified the effect of strain hardening on necking experimentally. A LDPE, which extensional strain-hardens, was observed to neck less than either of two LLDPE materials that do not exhibit extensional strain-hardening. The authors also observed a correlation between the degree of necking and the drawdown ratio. The LDPE was observed to have reductions in necking with increasing drawdown ratio whereas the two LLDPE materials were observed to have increases in necking with increasing drawdown ratio. These results suggested that differences in molecular structure that are observable through viscoelastic measurements can affect the amount of necking present in the final film. Furthermore, these differences in molecular structure vary the effect that changing processing conditions has on final film shape. However, it was suggested in the simulation works of Kim *et al*. (2005), Sakaki *et al*. (1996), and Zheng *et al*. (2006) that necking is always increased by increasing drawdown ratios and air gap lengths.

Current literature correlating the viscoelastic behavior of polymer melts to edge-bead has only been investigated through simulation. It was shown through simulations (Ito *et al.* 2003; Kim *et al.* 2005; Silagy *et al.* 1996; 1998) that an increase in strain-hardening increases both the magnitude and gradient of the edge-bead. It was also shown that a higher gradient can lead to a larger area of usable film. Processing conditions have been shown to affect edge-bead as well. It was shown through simulations (Kim *et al.* 2005; Sakaki *et al.* 1996; Zheng *et al.* 2006) that an increase in both (or either) the

drawdown ratio and air gap length increased edge-beading. This was confirmed experimentally in a LDPE system by Canning and Co (2000).

Draw resonance was shown (Iyengar and Co 1996; Kim *et al.* 2005; Pis-Lopez and Co 1996a,b; Silagy *et al.* 1996; 1998; Smith and Stolle 2003) to be stabilized by the strain-hardening property of materials. Increased strain-hardening was shown to push the critical draw ratio for the onset of draw resonance to higher values. Conversely the same work showed that shear- and extensional-thinning enhanced draw resonance. Simulation work by Kim *et al. (Kim et al. 2005),* amongst others (Lee *et al.* 2001; Silagy *et al.* 1996; 1998), found that the optimal air gap for reducing draw resonance was equal to the width of the die.

Constitutive relationships, especially those with parameters directly related to structure, are useful in understanding the viscoelastic properties of polymeric resins. Successful numerical simulation of polymer melts in any industrial polymer processing operation, including film-casting, requires a solid underlying viscoelastic constitutive equation. Without such a constitutive relationship, modeling efforts would be unable to accurately describe the non-Newtonian behavior of the fluids in the complex flows of interest. Therefore, any viscoelastic model chosen should be able to accurately describe the rheological properties of the materials to be modeled. The differential form of the pom-pom model (Inkson *et al.* 1999) originally developed by McLeish and Larson (1998) is a highly successful molecular theory that was shown to model the rheology of long-chain branched polyethylenes, including sparsely-branched resins (Doerpinghaus and Baird 2002; Inkson *et al.* 1998; McLeish and Larson 1998).

The tube theory of de Gennes (1971) developed into a full constitutive theory by Doi and Edwards (1988) serves as the theoretical basis for the Pom-pom model. The governing equations are derived using a novel molecular structure, the “pom-pom” molecule. The most notable feature of this model is the ability to correctly predict strain hardening in both uniaxial and planar extensional flows. Furthermore, the model parameters determined from simple flows have the potential to describe

specific structural features of the molecule, thus shedding light on specific structural features that yield desired (or undesired) processing qualities. This model was successfully extended to sparsely branched polyethylene commercial systems in previous studies (Doerpinghaus and Baird 2002) using a procedure laid out by Inkson *et al. (1998)* via a multi-mode approach. This approach addresses large molecules with multiple branch points by modeling them as a series of theoretical pom-pom molecules with a different number of arms and assigning orientation relaxation time modes from the linear spectra. In the simplest terms, this model assumes that the free branch ends relax first. The associated branch points with these free ends take a diffusive step, and the attached backbone relaxes in a star-arm fashion on much longer timescales than the outer arms. This continues until the innermost branch points relax. The relaxation time of a segment is determined by its path distance to the nearest free end.

Linking the specific effect of LCB and molecular structure to final film dimensions is still largely not understood. The most recent work is that of Seay and Baird (2009) who analyzed the necking behavior of several commercially available LLDPEs in the framework of the differential pom-pom model. The authors concluded that necking was a function of LCB content, MWD, and branching distribution. At the lowest drawdown ratio, and, therefore, lowest extension rate, the most obvious separation in necking was seen as a function of LCB content despite only slight differences in the degree of LCB. As the drawdown ratio was increased the film profiles merged with the exception of the highly-branched LDPE. The authors used rheological behavior to attribute this response to the distribution of branching in the sparsely-branched resins, indicating that linear chains were dominating the processing behavior. The authors concluded that a sparsely LCB systems more comparable in structure to LDPE with branches present on a spectrum of backbone segments would provide stabilization across a broader range of extension rates. The authors also found that an increased MWD reduced necking as well, but not on the order of LCB content variation.

The objective of this paper is to build upon the work of Seay and Baird (2009) using a series of well-characterized, sparsely-branched HDPE resins. The effect of sparse LCB on the film-cast process is analyzed using a rheological and constitutive analysis. This paper enhances the work of Seay and Baird (2009) in both its experimental methodology and conclusions. Rheological measurements are made over a larger range of strain and extensional rates using both the Sentmanat Extensional Rheometer (SER) rheometer (Sentmanat 2004) and novel experimental techniques (McGrady and Baird 2009). This allows for a full rheological characterization that builds upon the fundamental shear rheology work of Wood-Adams *et al.* (Wood-Adams 2001; Wood-Adams and Dealy 2000; Wood-Adams et al. 2000) by providing a clearer understanding of how minute differences in LCB content affect the flow and, therefore, the processing behavior of polymeric systems. The necking behavior is shown to be tied to the extensional flow behavior through branching distribution rather than shear flow properties such as the absolute value of the shear viscosity and primary normal stress. The Pom-pom model parameters determined from the flows can be used to provide insight as to how the LCB's are distributed across the backbone length spectrum. This distribution is then used to establish a more qualitative relationship between branching structure and distribution with resin performance in film casting. Furthermore, these parameters can serve as a foundation for future simulation work on the film-casting process.

5.3 Experimental materials and methods

5.3.1 MATERIALS

A series of sparsely long-chain branched and linear metallocene-catalyzed high density polyethylene homopolymers polyethylenes with varying degrees of LCB were used. The branched resins were synthesized using a constrained geometry catalyst of the type described by Stevens (1994; 1996) in a continuous, stirred-tank reactor as described by Lai *et al.* (1993). Both the sparsely-branched resins and the linear resin are homopolymers with narrow molecular weight distributions, MWD, characteristic

to metallocene type catalysts. These materials are henceforth referred to collectively as the HDB series. The HDB resins are ideal for this study for three primary reasons. First, the HDB resins were well-characterized in previous studies (Das *et al.* 2006; McGrady and Baird 2009; Wood-Adams 2001; Wood-Adams *et al.* 2000), most notably the linear rheology of HDBL, HDB1, and HDB3 by Wood-Adams and Dealy (2000). Second, they were readily available in sufficient quantities to both run controlled film-casting experiments with and accurately measure the viscoelastic properties of. Finally, their branching content is well-known based on ^{13}C NMR, providing an excellent opportunity to measure the effect of slight variations in the long-chain branching content on the film-cast process. MW, MWD, and LCB content for these resins are given in Table 5.1. For comparison of a system with a large number of LCB's, a well-characterized LDPE (Lupolen 1840H) was used. Relevant material properties were was determined by Gabriel *et al.* (1998) under the material name LDPE 1 and are given here in Table 5.1. Branching content calculated by Gabriel *et al.* (1998) was determined to be 230 branches per 10,000 C. Note that this value includes the combined total of both long- and short-chain branches.

5.3.2 RHEOLOGY

Linear viscoelastic shear measurements were conducted using a Rheometrics RMS-800. 25- and 10-mm cone-and-plate fixtures with cone angles of 0.1 and 0.05 radians, respectively, were used. An angular frequency range of 0.01-100 s^{-1} was probed. All tests were performed under an inert N_2 atmosphere in order to prevent oxidative degradation. The test samples were prepared by compression molding preforms at 170 °C under nominal pressure and allowing them to cool slowly under no pressure. This method provided homogenous samples with minimal residual stress. Shear viscosity curves were reproduced to the film-cast temperature using the Bird-Carreau model to quantify the onset and magnitude of shear-thinning.

Transient uniaxial extensional measurements were performed using both a Rheometrics Extensional Rheometer, Model 9000 (RER-9000), and the Sentmanat Extensional Rheometer (SER) (Sentmanat *et al.* 2005) manufactured by X-Pansion Instruments at 170 ^{o}C. The RER-9000 is based upon the rod-pulling design put forth by Münstedt (1979). The maximum Hencky strain achieved was on the order of 3.0 using test specimens that were 22 mm in length prior to extension. Cylindrical samples were compression molded at 5000 psi and 175 ^{o}C and then were allowed to cool slowly under atmospheric pressure to eliminate any residual stresses. The samples were then bonded to test clips using Chem Grip-HT Epoxy and then mounted to the RER-9000. After reaching thermal equilibrium, the sample was deformed at the desired extension rate, and the resulting tensile force was monitored using a leaf spring-LVDT assembly. For materials that underwent ductile failure at a given strain rate, the method of McGrady and Baird (2009) was used to reduced this phenomenon. The SER testing platform is designed to operate as a fixture in the RMS-800. A rectangular sample (8-10 mm width, 1.2-1.4 mm thickness, and 15-20 mm length) was placed on dual counter-rotating wind-up drums where rotation was resisted by the stretching material. The resistance to rotation force was measured by the RMS-800 torque transducer. This force was converted to the resulting transient extensional viscosity by dividing by both the applied strain rate and transient sample area. A test temperature was selected to reduce material sagging so that the zero-shear viscosity was sufficiently high, as per the recommendation of Sentmanat (2005).

5.3.3 FILM-CASTING

Film-casting experiments were performed by vertically extruding each polyethylene resin directly through an adjustable thickness slit die with a coathanger manifold. The width of the slit die was 101.6 mm and its thickness was 0.57 mm. The extruded films were then drawn by a chill roll positioned 141.4 mm away from the die. This distance was selected to enhance film stability and due to

limitations of the current equipment setup. A non-isothermal process is expected because of the distance from the die exit to the chill roll. Consideration for this non-isothermal behavior is given in a later section. The polymer was extruded at a temperature of 190°C.

Processing conditions generated in the film-casting process such as shear rate, strain, and extension rate were calculated as described in the subsequent text. Every polyethylene resin was extruded at a velocity in the z-direction of 1.385 mm/s. Mass flow rate was monitored to maintain a constant throughput for the extruder. The initial velocity was calculated using the density of each polyethylene resin and the cross-sectional area at the die exit. The apparent shear rate was determined using the exit velocity from the die and parallel plate flow following Eq. 5-1,

$$\dot{\gamma} = \frac{6Q}{WH^2}. \qquad (5\text{-}1)$$

A strain rate of $\dot{\gamma}$=15.54 1/sec was used for all measurements. Applied drawdown ratios and average strains are given in Table 5.2. Drawdown ratios ranging from 1.18-20.50 were applied resulting in strains ranging from 0.17-3.24. The drawdown ratio was determined as the ratio of the velocities of take-up roll and film extrusion speed out of the die. Strains, γ, were calculated by multiplying the residence time by the average extension rate. Residence time of the polymer was determined according to Eq. 5-2 where the average velocity was calculated by taking the integral of the velocity in the z-direction over the total length of the material (Baird and Collias 1998).

$$\gamma = \frac{\dot{\varepsilon} L}{\frac{\int_0^L v_{z0} (DR)^{\frac{z}{L}} dz}{\int_0^L z dz}} = \frac{\dot{\varepsilon} L}{v_{z0}\left[\frac{DR}{\ln(DR)} - \frac{1}{\ln(DR)}\right]} \qquad (5\text{-}2)$$

Extension rates are defined by subtracting the speed at which the polymer is extruded from the speed at which the polymer is taken up and dividing over the distance in which the polymer is subjected to

stretching. Applied extension rates ranged from 0.0036-1.3214 s^{-1} and are tabulated in Table 5.2 for each polyethylene resin at all applied drawdown ratios.

Digital photographs were taken of the films after steady state conditions were reached for each extrusion speed and drawdown ratio scenario. Measurements of the evolution of film-width were then made using a pixel counting software to determine film-widths at various positions in the z-direction. Analysis of the photographs allowed for measurements to the nearest one hundredth of a millimeter. Combined error for the experimental casting and measurements falls within +/-3%. The edge-bead phenomenon, while present, was too small to be captured by the tracking software used.

5.4 Results

5.4.1 RHEOLOGY

The shear viscosity curves at 170 ^{o}C for each material are given in Fig. 5.1. The Cox-Merz relationship (Bird *et al.* 1987) was validated for the HDPE materials (Das *et al.* 2006; Wood-Adams 2001) and the LDPE (Gabriel *et al.* 1998) in previous studies, suggesting that the magnitude of complex viscosity determined from small-angle oscillatory shear is a good approximation of the steady-shear viscosity. All branched-resins were found to have an enhanced zero-shear viscosity relative to the linear HDPE. The correlation of LCB content to the level of zero-shear viscosity enhancement was found to pass through a maximum, which is in agreement with the findings of Janzen and Colby (2000), among other works(Doerpinghaus and Baird 2002; 2003). Furthermore, HDB3 and HDB6 were found to have similar shear viscosity flow curves despite differences in LCB content (0.37 versus 1.66 LCB/10^4 C). This allows for direct comparison of the effect of LCB content on the necking response for materials with relatively identical shear viscosity curves.

Transient extensional viscosity versus time curves at a range of extension rates are given in Fig. 5.2. The extensional viscosity curves for HDB6 and Lupolen 1840H are shifted in the plot by a factor of

ten and 100, respectively, for clarity. To prevent material sagging during testing, measurements were made at 170 ^{o}C in which the zero-shear viscosity was large enough as per the recommendation of Sentmanat (2005). This facilitated the need for the above shear measurements to be made at 170 ^{o}C in order to provide the linear viscoelastic baseline. Strain-hardening was seen to increase with branching content, similar to the finds of Bid Wadud and Baird (2000), among others (Auhl *et al.* 2004; Doerpinghaus and Baird 2002). The plateau extensional viscosity was not reached for Lupolen 1840H at higher extensional rates. This is consistent with the known behavior of an LDPE, which was shown by Bach *et al.* (2003) to not plateau until strains on the order of five, which were not reached with either of extensional rheometers employed in this study. Linear viscoelastic theory predictions are given by the dashed lines.

5.4.2 FILM-CASTING

Necking is evaluated by analyzing the film half-width as a function of the distance from the die. For each material and drawdown ratio, changes in film width were monitored as a function of distance away from the die until a frost line (due to cooling-induced crystallization) was observed. This point is, henceforth, referred to as the final film (half-) width. For comparison, the film-width of the highly-branched LDPE was compared at the frost-line distance calculated for the HDPE resins. Full film half-width profiles for a low (1.76), medium (5.93), and high (17.79) drawdown ratio are given in Figs. 5.3 through 5.5. In Fig. 5.6 is given the final film width as a function of drawdown ratio for all resins and drawdown ratios investigated. Previous works (Canning and Co 2000; Ito *et al.* 2003; Kajiwara *et al.* 2006; Kim *et al.* 2005; Satoh *et al.* 2001; Silagy *et al.* 1996; 1998; Smith and Stolle 2003) suggest that an increase in the strain-hardening properties of the material will lead to a resistance to necking. The most recent work on the topic by Seay and Baird (2009) found that both the strain-hardening behavior of the material and the LCB distribution contributed to a material's necking response. Specifically, the authors

observed that sparsely-branched resins final film width mimics that of a linear resin at higher drawdown ratios due to a distribution of branches occurring only on the larger backbones. Therefore, it is expected that the LDPE resin will be more resistant to necking relative to the HDPE resins. Furthermore, we expect our sparsely-branched resins (HDB1, HDB3, HDB6) to exhibit a stronger resistance to necking relative to the linear HDBL resin at low to intermediate drawdown ratios, before mimicking the linear resin at higher drawdown ratios.

The data presented in Fig. 5.3 are the film half-width profiles for all five polyethylene resins at a relatively low drawdown ratio of 1.76. The Lupolen 1840H LDPE showed the most resistance to necking over the film-length evaluated. The sparsely-branched HDB1, HDB3, and HDB6 resins exhibited a much larger degree of necking up until their frost line relative to Lupolen 1840H resin. The highest sparsely-branched resin HDB6 exhibited the largest resistance to necking. However, no correlation to branching content to final film half-width was observed, as HDB1 and HDB3 exhibit almost identical profiles. The linear HDB resin had the largest degree of necking. It should be noted that the final film widths were found to be relatively equal for all resins considering the experimental error.

Presented in Fig. 5.4 are the film half-width profiles for all five polyethylene resins at a relatively intermediate drawdown ratio of 5.93. Significant differences that were greater than the range of experimental error were observed. The Lupolen 1840H LDPE showed the most resistance to necking over the film-length evaluated. The sparsely-branched HDB1, HDB3, and HDB6 resins exhibited a much larger degree of necking relative to the LDPE as the distance from the die was increased. Once again, no significant difference that was greater than experimental error is observed in the profiles of the sparsely-branched resins (HDB1, HDB3, and HDB6). Linear HDBL was observed to neck more than the all other resins across the entire profile.

In Fig. 5.5 is shown the film half-width profiles for all five polyethylene resins at a relatively high drawdown ratio of 17.79. The highly-branched Lupolen 1840H showed a significant resistance to

necking relative to the HDB resins. The sparsely-branched HDB6 resin necked more than the Lupolen 1840H resins, but less than either the HDB1, HDB3, and HDBL resins. The sparsely-branched HDB1 and HDB3, and the linear HDBL resins final film-width were equal in light of experimental error.

Finally, in Fig. 5.6 is given the final film half-width of each resin at each measured draw-down ratio. Once again, the final film half-width for LDPE was evaluated at the frost-line distance of the HDPE resins. The trends given here mimicked the results laid out earlier. The highly-branched Lupolen 1840H was found to maintain a large film width relative to the other resins as drawdown ratio was increased. The sparsely-branched HDB6 was observed to have final film-width profiles similar HDB1, and HDB3 at low to intermediate drawdown ratios. However, at higher drawdown ratios, HDB6 was seen to be more resistant to necking than HDB1, HDB3, or HDBL. At the highest drawdown ratios, the sparsely-branched HDB1 and HDB3 resins had final film widths similar to the linear HDBL.

5.5 Discussion

5.5.1 RHEOLOGICAL ANALYSIS

5.5.1.1 Shear rheology

In order to evaluate the effect of shear viscosity at the film-casting temperature of 190 ^{o}C, the shear viscosity of all five polyethylene resins measured at 170 ^{o}C were fit to the Bird-Carreau (BC) model (Bird *et al.* 1987) using non-linear least squares regression. These parameters are tabulated in Table 5.3. The resulting viscosity flow curves are given in Fig. 5.7. All resins exhibited a higher zero-shear viscosity relative to the linear resin, with the level of enhancement passing through a maximum as a function of LCB content. The onset and severity of shear thinning can be quantified by the values of the BC model parameters. n represents the degree of shear-thinning and λ represents the onset of shear-thinning. The degree of shear-thinning increased (decreasing n) with increasing LCB content. Likewise, the onset of shear-thinning decreased (increasing λ) with increasing LCB content.

The selected apparent shear rate at the wall in the film-casting process was chosen to minimize the effect of different absolute shear viscosities of the materials ($\dot{\gamma}$=14.54 1/sec). Only the Lupolen 1840H LDPE was seen to exhibit a relatively different (lower) shear viscosity. Seay and Baird (2009) observed that a LDPE film produced at higher shear rates and, therefore, lower shear viscosities suffered more necking than a LDPE film cast a lower shear rates, and, therefore, higher viscosities. This finding suggests that Lupolen 1840H's lower viscosity at the apparent shear rate of interest to this study is not the cause for its resistance to necking relative to the HDB series. Furthermore, HDB3 and HDB6 exhibited almost identical shear viscosity curves at shear rates less than 30 1/s. Because all measurements were made at $\dot{\gamma}$=14.54 1/sec, the aforementioned differences in film-casting behavior of HDB3 and HDB6 signify that materials with very similar absolute shear viscosities produce different film width profiles.

The effect of extrudate swell on the evolution of necking was also considered. Materials that undergo a higher level of extrude swell should undergo a larger degree of necking at similar processing conditions if one considers a simple mass balance. Increases in the primary normal stress difference, N_1, were shown to have been correlated with the magnitude of extrudate swell (Tanner 1970). The magnitude of N_1 was estimated from our dynamic viscosity data using Laun's approximation (Bird *et al.* 1987) given in Eq. 5-6 where G' and G" are the storage modulus and loss modulus, respectively:

$$N_1 = 2G'\left[1+\left(\frac{G'}{G''}\right)^2\right]^{0.7}. \qquad (5\text{-}6)$$

This data is given in Fig. 5.8. At the shear rate of interest to this work, $\dot{\gamma}$=14.54 1/sec, N_1 is virtually identical for all of the tested resins, with HDB1 being somewhat lower than the other resins. All resin values fell within the same order of magnitude. These results suggest that extrudate swell should be somewhat similar for all of the tested resins.

5.5.1.2 Extensional rheology

In this section, the reliance of the film half-width profiles is correlated to the extensional flow behavior. First, Pom-pom model parameters are determined from simple shear and shear-free flow data presented earlier. Second, the general correlation between molecular structure and model parameters are investigated using known material properties (i.e. LCB content) from Table 5.1. Third, the film-width profiles from Figs. 5.3 through 5.6 are analyzed in terms of the expected response relative to extensional viscosity. Finally, the molecular structure features determined from model parameters are used to explain in deviations from predicted film half-width behavior.

The dynamic shear and transient shear-free data in Figs. 5.1 and 5.2 were fit with the differential multimode Pom-pom model. Extension rates probed ranged from 0.003 to 10 1/sec. The parameters determined from these fits are given in Fig. 5.9 for the five resins employed in this study. Both the contribution to the plateau moduli, g_i, and theoretical number of arms per mode, q_i, are plotted versus the backbone orientation time, τ_{bi}.

The Pom-pom model is a constitutive relationship that has the potential to link simple rheological behavior to branching structure. A full derivation of the model can be found elsewhere (McLeish and Larson 1998), along with subsequent improvements (Blackwell *et al.* 2000; Inkson *et al.* 1999). The Pom-pom constitutive model is highly successful in describing the melt rheology of branched and linear polymers (Blackwell *et al.* 2000; Doerpinghaus and Baird 2002; Inkson *et al.* 1998; McLeish and Larson 1998). It is an extension of the tube model of de Gennes (1971) developed into a full constitutive theory by Doi and Edwards (1988) to non-linear architectures. An ideal "pom-pom" architecture is assumed in which an equal number of *q* arms are attached to both ends of a linear chain. Molecular entanglements around the backbone are modeled as a tube that moves affinely with the applied deformation. The branch points act to retard the diffusive movement along the tube. This gives

rise to differences in flow behavior relative to linear chains primarily due to the extended stretch relaxation time.

Inkson *et al.* (1999) extended the model to explain polydisperse systems with complex branching via the superposition of Pom-pom modes in LDPE systems. Blackwell *et al.* (2000) improved the stretch dynamics of the model by introducing the concept of branch-point displacement, allowing local movement of the arms into the backbone tube on length scales on the order of the back tube diameter. This served to smooth the unrealistic cusps predicted in steady-state uniaxial extension by the original model.

The differential multimode Pom-pom model is given by Eqs. 5-4 through 5-7 in Table 5.3. The configuration of pom-pom molecules can be described by two dynamic variables, **S** and λ. The tensor **S** describes the average backbone tube orientation and the scalar λ describes the average backbone stretch. Furthermore, the timescales for backbone orientation and stretch are determined by two separate relaxation times, τ_b and τ_s, respectively. The maximum backbone stretch, and thus the maximum accumulated stress, is determined by the number of pom-pom arms, q. The differential approximation for **S** has been chosen for this study because it provides a similar asymptotic behavior to the full integral form, but also provides analytical solutions for the orientation tensor components under homogeneous flow conditions. In this case, the parameter ν* has been approximated by the suggested (Blackwell *et al.* 2000) value of $2/(q\text{-}1)$. Each mode has four unknown parameters: the backbone orientation time τ_{bi}, the individual contribution to the plateau modulus g_i, the number of pom-pom arms q_i, and the backbone stretch orientation time τ_{si}. These unknown parameters are determined from fitting the shear and extensional rheological data. Model parameters were determined in the following fashion. First, the backbone orientation times and individual plateau moduli were determined from linear viscoelastic measurements. This was accomplished by fitting a Maxwell mode spectrum to the available G' and G" data, and is shown in Fig. 5.10. In this case, the choice of τ_{bi} was arbitrary and two

constitutive modes per decade of shear rate or angular frequency were used. Second, q_i and τ_{si} were determined from transient extensional growth measurements. An increasing q_i correlates to the magnitude of strain-hardening observed in extensional flow. Strain-hardening in extensional flow is defined as deviation from the linear viscoelastic envelope. In the framework of the Pom-pom model, a q_i value greater than one indicates branching. Fitting the slowest extension rate first and proceeding to higher rates generally provided the best results.

The extensional viscosity profiles in Fig. 5.2 coupled with the values of the model parameters given in Fig. 5.9 are used to explain the film half-width profile data given in Figs. 5.3 through 5.6 in terms of not only LCB content, but structure. An analysis of the model parameters in terms of branching distribution is given to see if the determined parameters make sense in terms of what is known about the materials (i.e. material properties in Table 5.1). Recall that the backbone orientation relaxation time, τ_{bi}, is directly and positively correlated with backbone length, and q_i greater than one corresponds to the presence of LCB. First consider the q_i distribution for Lupolen 1840H, a highly-branched LDPE resin. All q_i modes in Fig. 5.9 for Lupolen 1840H are greater than one. This is consistent with the known structure of LDPE. LDPE's are characterized by levels of complex branching across all backbone lengths (Doerpinghaus 2002). Likewise for the linear HDBL, the model predicted q_i equal to one for all backbone lengths, which is consistent with known structure. The model predictions are also consistent with the known structural information of the sparsely-branched resins HDB1, HDB3, and HDB6. Consider from the molecular data given in Table 5.1 that each of the sparsely-branched resins statistically cannot have a LCB on every chain, and, therefore, the polymer system must be comprised of a mixture of linear and long-chain branched chains. The model predictions are in agreement with branching occurring on the longer backbones and no branching occurs on the shorter backbones. Furthermore, the level of branching (i.e. the magnitude of q_i) increases as a function of the known LCB content from Table 5.1.

Finally, the model predicts a distribution of branching across a larger range of backbones in the HDB6 system.

The final film dimensions with respect to the differences in planar and uniaxial extensional viscosities were investigated by Dobroth and Erwin (1986). Whether a film undergoes planar or uniaxial deformation is material dependent and is observed in the degree of necking. The resistance to necking observed in the Lupolen 1840H resembles more of a planar extension behavior, while samples that experience enhanced necking like HDBL and HDB1 more closely resemble uniaxial extension. It is a material's underlying branching structure, and therefore its strain-hardening behavior that allows it to "choose" either a planar or uniaxial stretch in the film-cast process. As one increases the drawdown ratio, and, therefore, the extension rate, one is now decreasing the backbone orientation time (and length) that is dominating the response.

Taking what is known from material properties in Table 5.1 coupled with the determined model parameters from Fig. 5.9, the necking behavior for all resins studied can be explained. First, similar to the findings of Seay and Baird (2009), the highly branched LDPE has its branching spread over most backbone lengths and, therefore, no matter what drawdown ratio is employed, branched chains are dominating the response. Second, similar to the findings of Seay and Baird (2009), the sparsely-branched resins HDB1 and HDB3 behave like a linear resins in terms of the final film half-width at higher drawdown ratios. This happens because branching was found to occur on the longest backbones only. Therefore, at higher drawdown ratios, the shorter, linear chains are dominating the response. Finally, unique to this work, is the behavior of HDB6. HDB6 proves to be more resistant to necking than HDB1, HDB3 or HDBL at higher drawdown ratios. An examination of its branching distribution determined by the Pom-pom model shows that branching occurs across a wider span of backbone lengths. Therefore, as the drawdown ratio is increased to the point it is probing the linear chains in HDB1 and HDB3, it is still probing branched chains in the HDB6 resin. This supports the hypothesis that sparsely branching resins

can reduce the effects of necking relative to their linear counterparts only when the branched chains are being probed by the process flow.

5.5.2 NON-ISOTHERMAL CONSIDERATIONS

The non-isothermal nature of the experimental setup must also be addressed. The appearance of frostlines prior to contact with the chill roll makes it readily apparent that the materials are undergoing significant temperature changes from the time they exit the die until contacting the chill roll. What must be considered in this analysis is the effect of an increasing viscosity observed during cooling, which could lead to the sample mimicking strain-hardening behavior (Minoshima and White 1986), and possibly affecting the relative final film dimensions. The activation energy can be used to gauge a material's viscosity dependence on temperature. Shear viscosity curves at 170 ^{o}C from Fig. 5.1 in tandem with the shear viscosity curves produced with the Bird-Carreau parameters in Table 5.3 were used to determine shift factors which in turn lead to the calculation of the activation energies. These activation energies for each polyethylene resin are given in Table 5.3. Higher activation energies indicate a larger dependence of viscosity on temperature. There was little relative difference in the activation energies of the resins, having values on the order of $\Delta E \sim$ 30-40 kJ/mol. Lupolen 1840H and HDB3 have the highest values, and HDBL the lowest relative to the other resins. The effects of non-isothermal behavior as the leading cause of film-width differentiation can be ruled out based on a simple comparison of the behavior of the HDB3 and Lupolen 1840H film profiles. Even though these two resins have almost identical ΔE values, their film width profile is quite different at higher drawdown ratios, as shown in Figs. 5.5 and 5.6.

5.6 Conclusions

A series of well-defined HDPE resins with known levels of LCB content were film-cast to compare the evolution of necking with the degree of LCB at varying drawdown ratios. At low drawdown ratios, Lupolen 1840H exhibited the biggest resistance to necking at distances less than the HDB frostline. HDB1, HDB3 and HDB6 films had similar final film-widths larger than HDBL, but the differences fell within the window of experimental error. This relative uniformity was attributed to the low strains probed in which the materials have yet to enter the strain-hardening regime. As drawdown ratio was increased, film width profiles separated based on branching level to distances larger than associated with experimental error. The LDPE remained the most resilient to the effect of necking, while the sparsely-branched HDPEs have reduced film widths that are still greater than the linear HDBL. Small amounts of LCB were found to reduce the amount of necking at intermediate drawdown ratios relative to linear resins. However, at higher drawdown ratios, HDB1 and HDB3 film-widths mimicked that of the linear HDBL, while the sparsely-branched HDB6 retained a larger film width. At this higher extension rate, shorter relaxation times and hence shorter chains were dominating the viscoelastic response of the resins. Molecular structural analysis via the Pom-pom constitutive model suggested that HDB6's branching was distributed across a larger range of backbone lengths relative to the sparsely-branched resins HDB1 and HDB3. As the extension rate (drawdown ratio) increased, the length of the backbones dominating the response decreased, so that the linear chains were controlling the necking behavior of sparsely-branched HDB1 and HDB3 while remaining in branched regime for HDB6.

Other processing variables that could affect the film width profile were examined. Shear thinning was investigated via an examination of the absolute shear viscosity value at the process shear rate. Furthermore, it was found that materials with virtually identical shear viscosity curves (HDB3 and HDB6) exhibited different necking responses, especially at higher drawdown ratios. Extrudate swell was studied via an investigation of N_1 determined from Laun's approximation. Values of N_1 were found to be

similar for all resins at the process conditions. Finally, the effect of non-isothermal behavior was evaluated. Lupolen 1840H and HDB3 had virtually identical activation energies, but exhibit very different film-width profiles. All resins were found to yield similar activation energies for flow, ranging on the order of 30-40 kJ/mol. The results presented in this paper, including the derived model parameters, allow for future works in which the film-casting process for branched viscoelastic fluid can be modeled.

5.7 Acknowledgements

This research is a collaborative effort for the World Network of Materials – UK Leeds and is supported financially by the National Science Foundation DMR-052198. Gratitude is given as well to Dow Chemical Company, ExxonMobil Chemical Company, and Equistar Chemical Company for supplying their respective PE materials.

Table 5.1 - Material Properties				
Material	**M_w [g/mol]**	**M_w/M_n**	**LCB/10,000 C**	**Avg. # of branches per chain**
HDBL	113,000	2.5	Linear	Linear
HDB1	77,100	2.0	0.26	0.14
HDB3	85,700	1.9	0.37	0.26
HDB6	68,000	-	1.88	0.91
Lupolen 1840H	240,000	14	230[+]	394[+]
[+] Lupolen 1840H's branching content determined by Gabriel *et al.* (1998) included both long- and short-chain branch arms.				

Table 5.2 – Film-Casting Conditions at 190 °C						
Resin	DR= 1.18 Strain= 0.17	DR= 1.76 Strain= 0.57	DR= 2.96 Strain= 1.09	DR= 5.93 Strain= 1.78	DR= 8.89 Strain= 2.18	DR= 11.86 Strain= 2.47
	$\dot{\varepsilon}$ [1/s]	$\dot{\varepsilon}$ [1/s]	$\dot{\varepsilon}$ [1/s]	$\dot{\varepsilon}$ [1/s]	$\dot{\varepsilon}$ [1/s]	$\dot{\varepsilon}$ [1/s]
HDB1	0.0086	0.0314	0.0885	0.2136	0.3141	0.3994
HDB3	0.0079	0.0341	0.0758	0.1884	0.2958	0.4107
HDB6	0.0091	0.0378	0.0867	0.1619	0.2974	0.4344
Linear HDB	0.0086	0.0324	0.0750	0.1485	0.2744	0.3459
Lupolen 1840H	0.0036	0.0144	0.0347	0.0483	0.0773	0.1064
	DR= 14.82 Strain= 2.70	DR= 17.79 Strain= 2.88	DR= 20.75 Strain= 3.03	DR= 23.72 Strain= 3.17	DR= 25.50 Strain= 3.24	
	$\dot{\varepsilon}$ [1/s]	$\dot{\varepsilon}$ [1/s]	$\dot{\varepsilon}$ [1/s]	$\dot{\varepsilon}$ 1/s]	$\dot{\varepsilon}$ [1/s]	
HDB1	0.5263	0.6508	0.7031	0.8645	0.8663	
HDB3	-	0.5399	-	0.7669	-	
HDB6	0.4964	0.6300	0.8438	0.9228	1.0263	
Linear HDB	-	0.5687	-	0.7467	0.7432	
Lupolen 1840H	-	0.1645	-	-	-	

Table 5.3 – Bird-Carreau Model Parameters at 170 °C				
Resin	**η_0**	**n**	**λ**	**ΔE [KJ/mol]**
HDB1	7998	0.754	5.6	34.9
HDB3	39970	0.637	25.2	39.1
HDB6	38080	0.641	29.0	32.5
HDBL	7021	0.788	0.727	26.5
Lupolen 1840H	24960	0.598	20.3	40.0

Table 5.4 – Differential Multimode Pom-pom Model

$$\underline{\underline{\sigma}} = 3\sum_{i}^{N} g_i \lambda_i^2(t)\underline{\underline{S}}_i(t) \tag{5-4}$$

$$\frac{D\underline{\underline{A}}}{Dt} = \underline{\underline{K}} \bullet \underline{\underline{A}} + \underline{\underline{A}} \bullet \underline{\underline{K}}^T - \frac{1}{\tau_{bi}}\left(\underline{\underline{A}} - \underline{\underline{I}}\right) \tag{5-5}$$

$$\underline{\underline{S}} = \frac{\underline{\underline{A}}}{tr\,\underline{\underline{A}}} \tag{5-6}$$

$$\frac{D\lambda_i(t)}{Dt} = \lambda_i(t)\underline{\underline{K}} : \underline{\underline{S}} - \frac{1}{\tau_{si}}\left(\lambda_i(t) - 1\right)e^{\upsilon^*(\lambda_i - 1)} \tag{5-7}$$

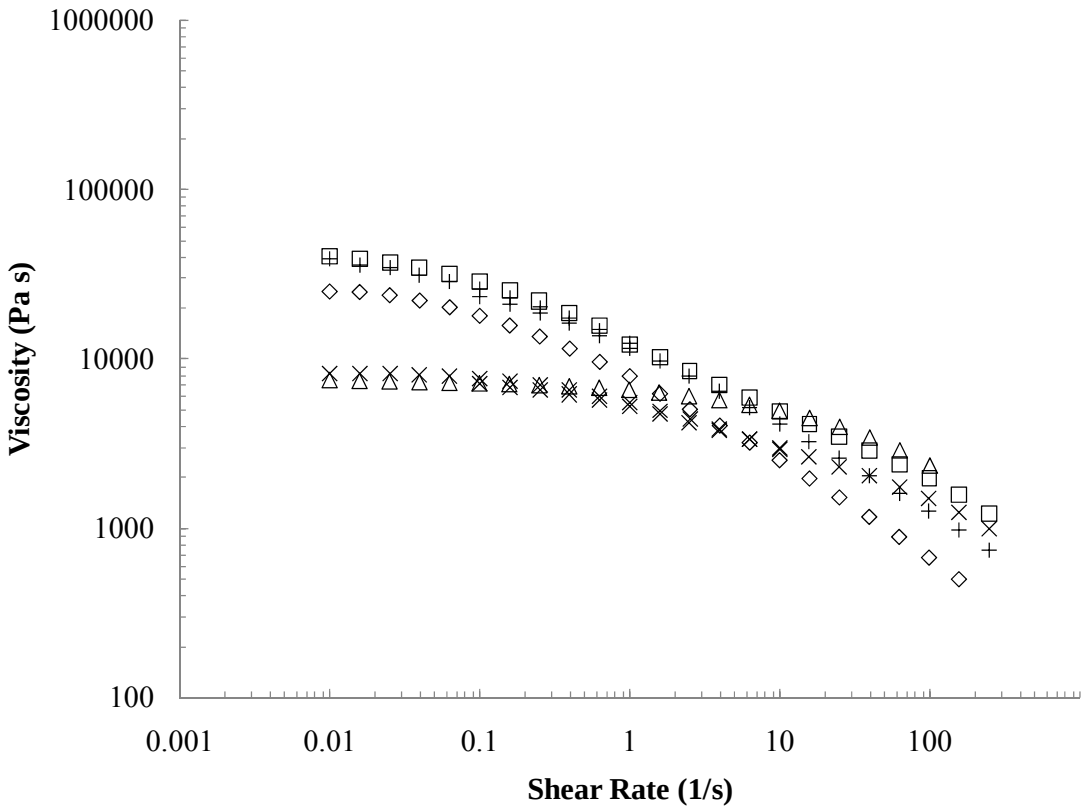

Figure 5.1: Shear viscosity of HDBL (Δ), HDB1 (x), HDB3 (□), HDB6 (+), and Lupolen 1840H (◊) various PE resins at 170 °C.

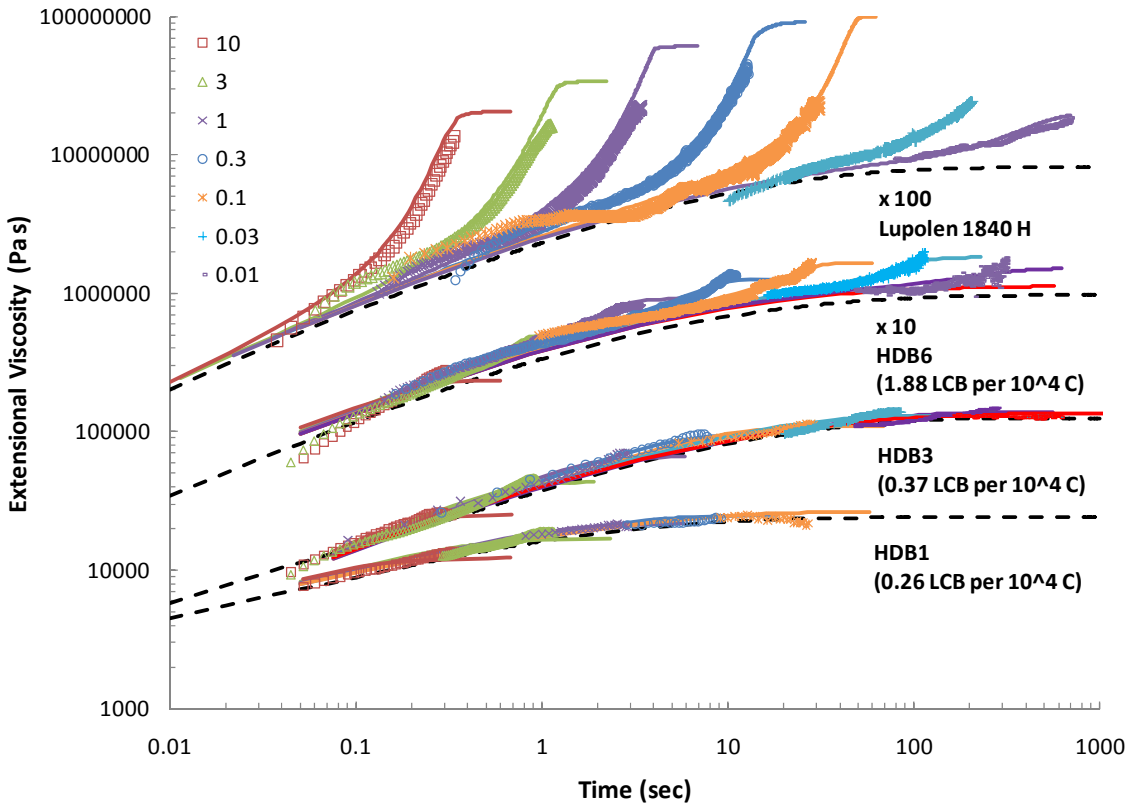

Figure 5.2: Transient extensional viscosity for the sparsely-branched HDPE resins measured at 170 °C. All extensional rates are given in inverse seconds. The viscosity profiles for HDB6 and Lupolen 1840 H are multiplied by a factor of ten and 100, respectively, in order to prevent overlap with HDB3. Extensional viscosity predictions from the differential multimode pom-pom model are given by the solid lines. Linear viscoelastic predictions are given by the dashed lines.

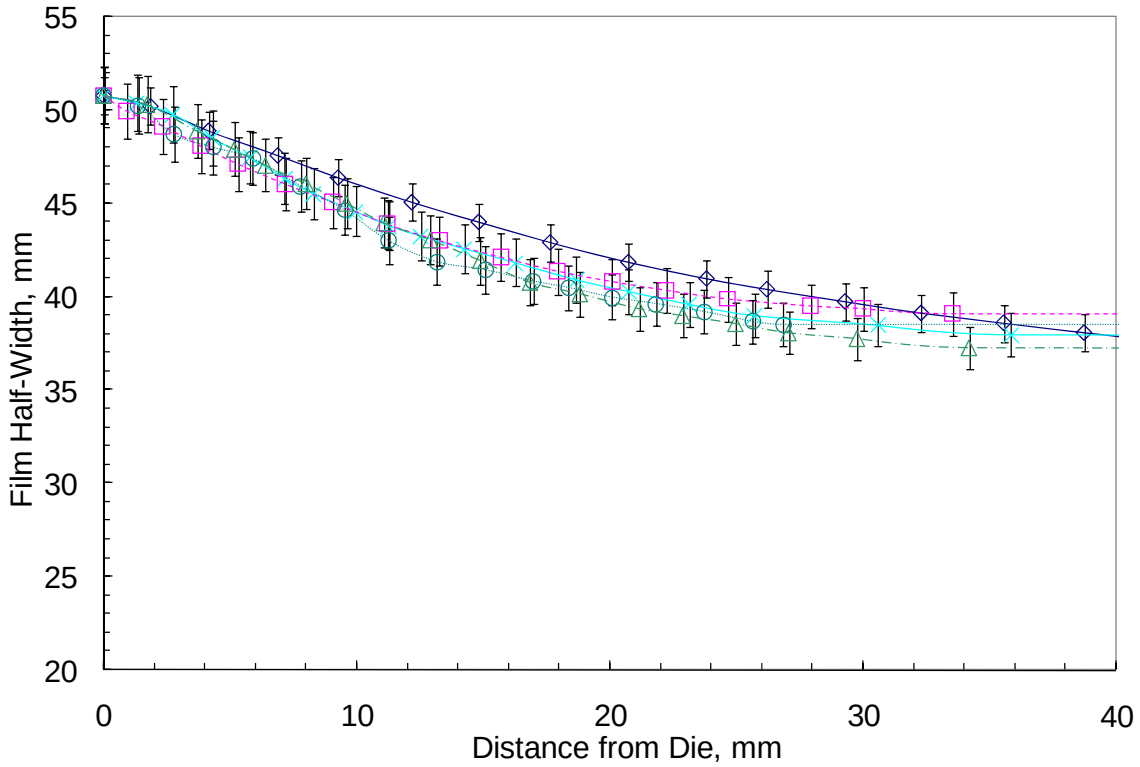

Figure 5.3: Film half-width profile of HDBL (Δ), HDB1 (x), HDB3 (□), HDB6 (o), and Lupolen 1840H (◊) evaluated to the frostline at a drawdown ratio of 1.76 corresponding to a strain of 0.57. All measurements were taken at a temperature of 190 ^{o}C.

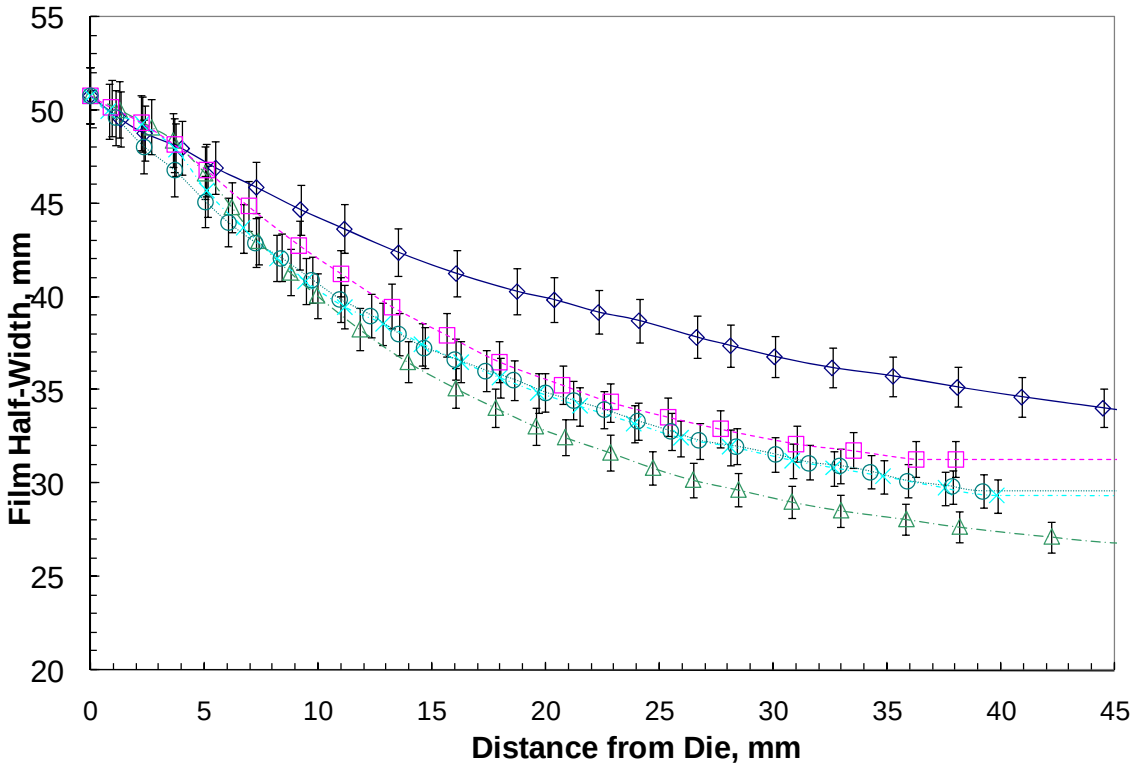

Figure 5.4: Film half-width profile of HDBL (Δ), HDB1 (x), HDB3 (□), HDB6 (o), and Lupolen 1840H (◊) evaluated to the frostline at a drawdown ratio of 5.93 corresponding to a strain of 1.78. All measurements were taken at a temperature of 190 ^{o}C.

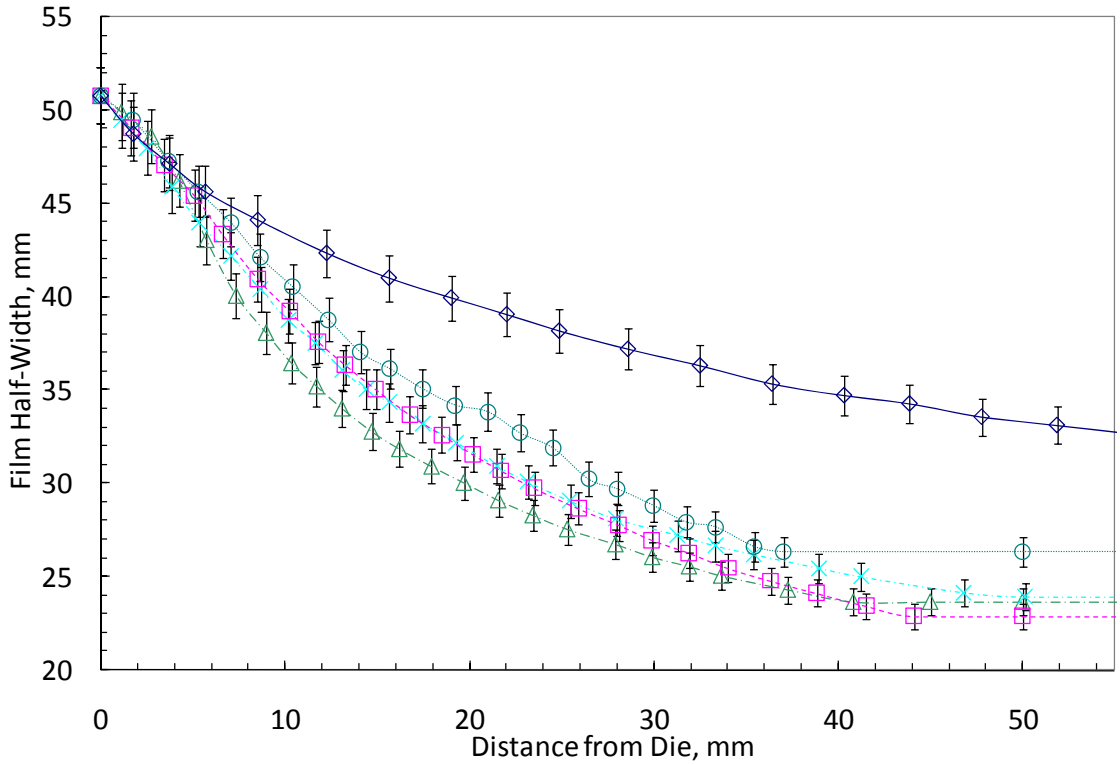

Figure 5.5: Film half-width profile of HDBL (Δ), HDB1 (x), HDB3 (□), HDB6 (o), and Lupolen 1840H (◊) evaluated to the frostline at a drawdown ratio of 17.79 corresponding to a strain of 2.88. All measurements were taken at a temperature of 190 °C. The data point and error bars at 50mm are added to aid the evaluation of the final film half-width.

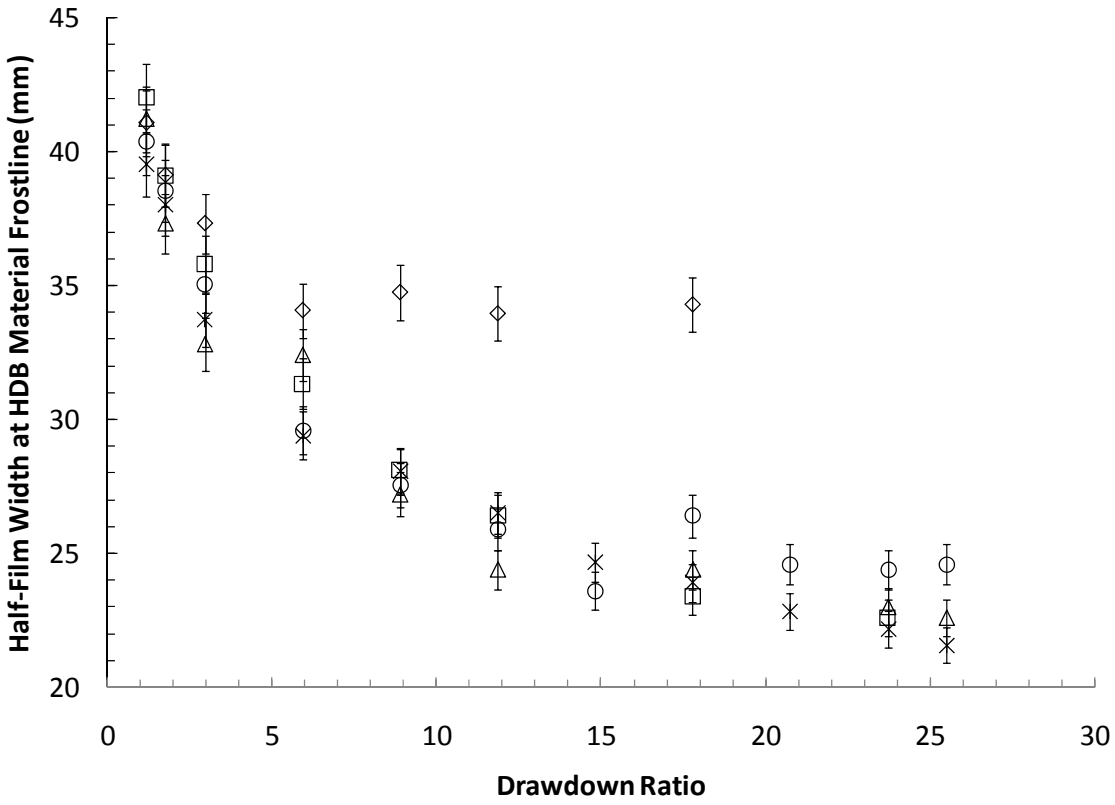

Figure 5.6: Final film half-width profile of HDBL (Δ), HDB1 (x), HDB3 (□), HDB6 (o), and Lupolen 1840H (◊) as a function of drawdown ratio for each resin and drawdown ratio investigated. All measurements were taken at a die temperature of 190 ^{o}C.

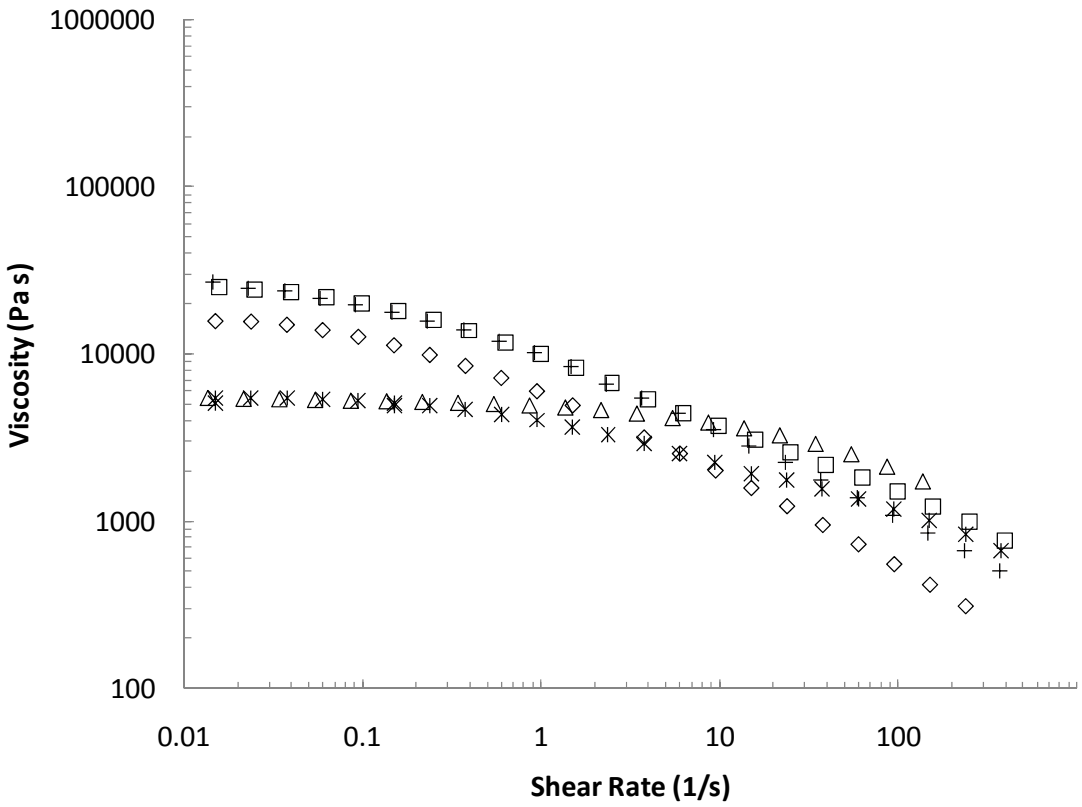

Figure 5.7: Shear viscosity of HDBL (Δ), HDB1 (x), HDB3 (□), HDB6 (+), and Lupolen 1840H (◊) resins at 190 °C.

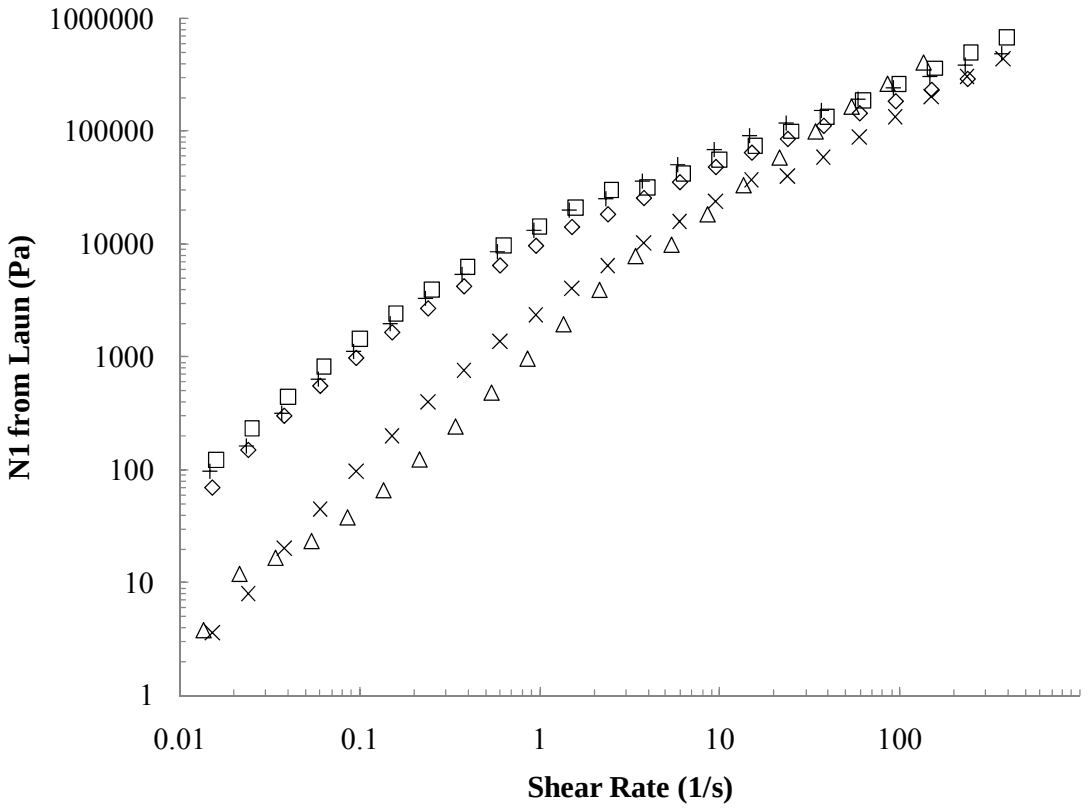

Figure 5.8: Primary normal stress difference of HDBL (Δ), HDB1 (x), HDB3 (□), HDB6 (+), and Lupolen 1840H (◊) resins at 190 °C estimated using Laun's approximation (Eq. 5-3).

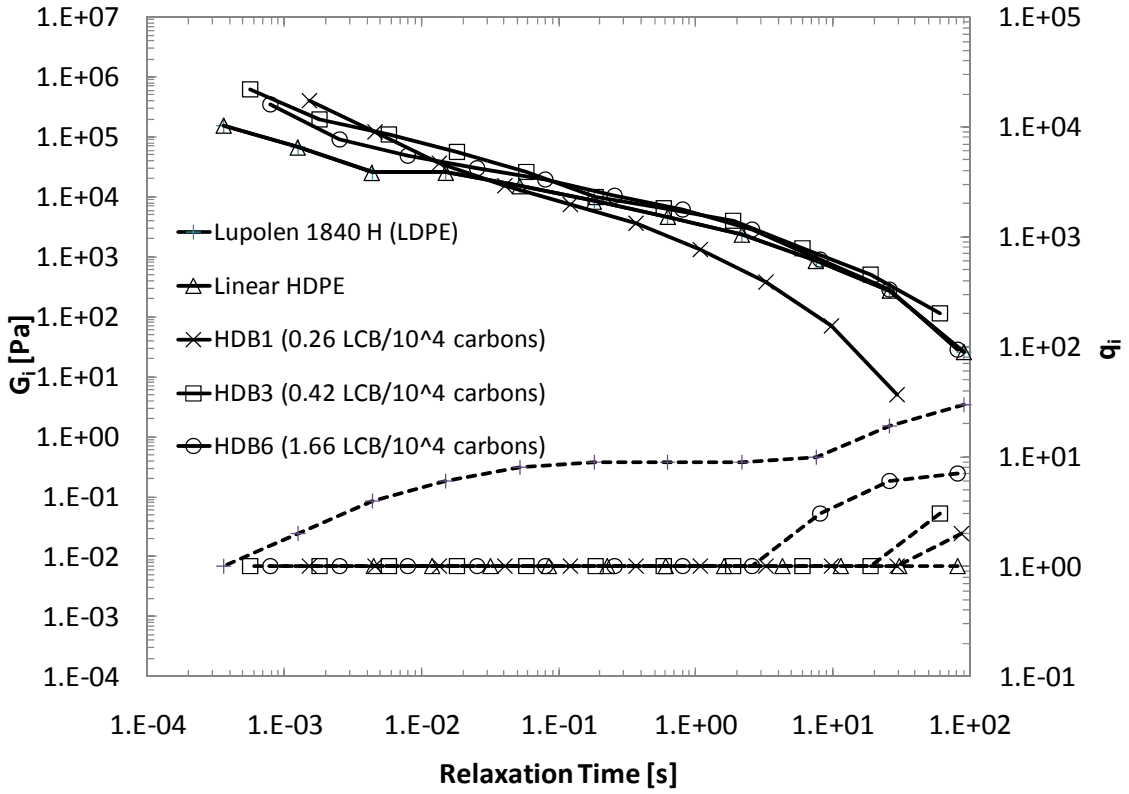

Figure 5.9: Differential Pom-pom model parameters for the five PE resins of interest to this work. Both the contribution to the plateau moduli, g_i, (solid lines) and theoretical number of arms per mode, q_i, (dashed lines) are plotted versus the backbone relaxation time, τ_{bi}.

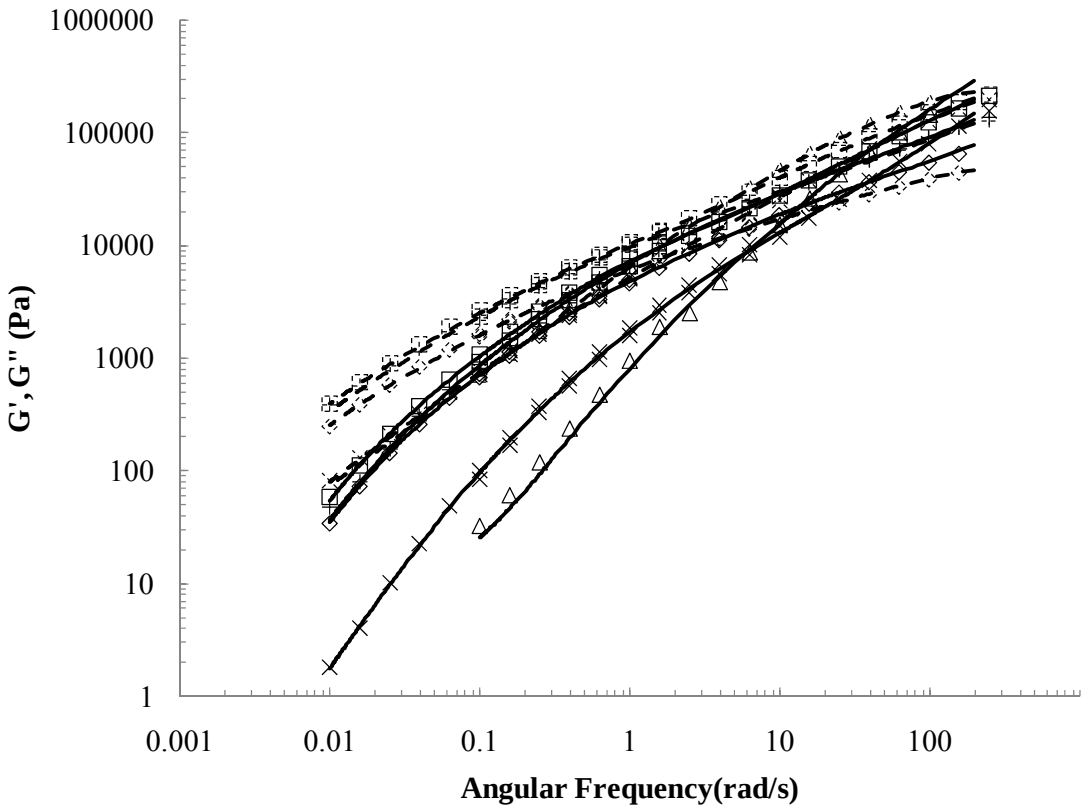

Figure 5.10: Storage (closed symbols) and loss (dashed symbols) moduli of HDBL (Δ), HDB1 (x), HDB3 (□), HDB6 (+), and Lupolen 1840H (◊) resins measured at 170 °C. Maxwell mode fits for the storage and loss moduli are given by the solid and dashed lines respectively.

5.8 **References**

Auhl, D., J. Ramirez, et al. (2008). "Linear and nonlinear shear flow behavior of monodisperse polyisoprene melts with a large range of molecular weights." J. Rheol. **52(3)**: 801-835.

Auhl, D., J. Stange, et al. (2004). "Long-Chain Branched Polypropylenes by Electron Beam Irradiation and Their Rheological Properties." Macromolecules **37(25)**: 9465-9472.

Bach, A., H. K. Rasmussen, et al. (2003). "Extensional viscosity for polymer melts measured in the filament stretching rheometer." J. Rheol. **47(2)**: 429-441.

Baird, D. G. and D. I. Collias (1998). Polymer Processing. New York, John Wiley & Sons, Inc.

Bin Wadud, S. E. and D. G. Baird (2000). "Shear and extensional rheology of sparsely branched metallocene-catalyzed polyethylenes." J. Rheol. **44(5)**: 1151-1167.

Bird, R. B., R. C. Armstrong, et al. (1987). Dynamics of Polymeric Liquids. Hoboken, NJ, John Wiley & Sons, Inc.

Blackwell, R. J., T. C. B. McLeish, et al. (2000). "Molecular drag-strain coupling in branched polymer melts." J. Rheol. **44(1)**: 121-136.

Canning, K. and A. Co (2000). "Edge effects in film casting of molten polymers." J. Plast. Film Sheeting **16(3)**: 188-203.

Collis, M. W., A. K. Lele, et al. (2005). "Constriction flows of monodisperse linear entangled polymers: Multiscale modeling and flow visualization." J. Rheol. **49(2)**: 501-522.

Das, C., N. J. Inkson, et al. (2006). "Computational linear rheology of general branch-on-branch polymers." J. Rheol. **50(2)**: 207-234.

de Gennes, P. G. (1971). “Reptation of a Polymer Chain in the Presence of Fixed Obstacles.” J. Chem. Phys. **55**: 572.

Dobroth, T. and L. Erwin (1986). "Causes of edge beads in cast films." Polym. Eng. Sci. **26(7)**: 462-7.

Doerpinghaus, P. J. (2002). Flow Behavior of Sparsely Branched Metallocene-Catalyzed Polyethylenes. Chemical Engineering. Blacksburg, Virginia Tech. Ph.D.

Doerpinghaus, P. J. and D. G. Baird (2002). "Assessing the Branching Architecture of Sparsely Branched Metallocene-Catalyzed Polyethylenes Using the Pompom Constitutive Model." Macromolecules **35(27)**: 10087-10095.

Doerpinghaus, P. J. and D. G. Baird (2003). "Separating the effects of sparse long-chain branching on rheology from those due to molecular weight in polyethylenes." J. Rheol. **47(3)**: 717-736.

Doi, M. and S. F. Edwards (1988). The Theory of Polymer Dynamics, Oxford University Press.

Fetters, L. J., A. D. Kiss, et al. (1993). "Rheological behavior of star-shaped polymers." Macromolecules **26(4)**: 647-54.

Gabriel, C., J. Kaschta, et al. (1998). "Influence of molecular structure on rheological properties of polyethylenes. Part 1. Creep recovery measurements in shear." Rheol. Acta **37(1)**: 7-20.

Inkson, N., T. McLeish, et al. (1998). "Modeling low density polyethylene rheology using the pom-pom model." Prog. Trends Rheol. V, Proc. Eur. Rheol. Conf., 5th: 336-337.

Inkson, N. J., T. C. B. McLeish, et al. (1999). "Predicting low density polyethylene melt rheology in elongational and shear flows with "pom-pom" constitutive equations." J. Rheol. **43(4)**: 873-896.

Ito, H., M. Doi, et al. (2003). "A model of neck-in phenomenon in film casting process." J. Soc. Rheol., Jpn. **31(3)**: 157-163.

Iyengar, V. R. and A. Co (1996). "Film casting of a modified Giesekus fluid: stability analysis." Chem. Eng. Sci. **51(9)**: 1417-30.

Janzen, J. and R. H. Colby (2000). "Rheological detection of long-chain branching in high-density polyethylenes." Polym. Mater. Sci. Eng. **82**: 128-129.

Kajiwara, T., M. Yamamura, et al. (2006). "Relationship between neck-in phenomena and rheological properties in film casting." Nihon Reoroji Gakkaishi **34(2)**: 97-103.

Kim, J. M., J. S. Lee, et al. (2005). "Transient solutions of the dynamics of film casting process using a 2-D viscoelastic model." J. Non-Newtonian Fluid Mech. **132**: 53-60.

Lai, S. Y., J. R. Wilson, et al. “Flexible substantially linear olefin polymers.” PCT Int. Appl. (1993).

Lee, J. S., H. W. Jung, et al. (2001). "Kinematic waves and draw resonance in film casting process." J. Non-Newtonian Fluid Mech. **101(1-3)**: 43-54.

Linster, J. J. and J. Meissner (1986). "Melt elongation and structure of linear polyethylene (HDPE)." Polymer Bulletin **16(2-3)**: 187-94.

Lohse, D. J., S. T. Milner, et al. (2002). "Well-Defined, Model Long Chain Branched Polyethylene. 2. Melt Rheological Behavior." Macromolecules **35(8)**: 3066-3075.

McGrady, C. D. and D. G. Baird (2009). ‘‘Method for overcoming ductile failure in Munstedt-type extensional rheometers.” *J. Rheol.* **53(3)**, 2009: 539-545.

McLeish, T. C. B., J. Allgaier, et al. (1999). "Dynamics of entangled H-polymers: theory, rheology, and neutron-scattering." Macromolecules **32(20)**: 6734-6758.

McLeish, T. C. B. and R. G. Larson (1998). "Molecular constitutive equations for a class of branched polymers: The pom-pom polymer." J. Rheol. **42(1)**: 81-110.

Minoshima, W. and J. L. White (1986). "Instability phenomena in tubular film, and melt spinning of rheologically characterized high-density, low-density and linear low-density polyethylenes." J. Non-Newtonian Fluid Mech. **19(3)**: 275-302.

Münstedt, H. and D. Auhl (2005). "Rheological measuring techniques and their relevance for the molecular charecterization of polymers." J. Non-Newtonian Fluid Mech. 128: 62-69.

Munstedt, H. and S. Kurzbeck (1998). "Elongational behavior and molecular structure of polymer melts." Prog. Trends Rheol. V, Proc. Eur. Rheol. Conf., 5th: 41-44.

Münstedt, H. and H. M. Laun (1979). "Elongational behavior of a low density polyethylene melt. II. Transient behavior in constant stretching rate and tensile creep experiments. Comparison with shear data. Temperature dependence of the elongational properties." Rheol. Acta 18(4): 492-504.

Nielsen, J. K., H. K. Rasmussen, et al. "Elongational viscosity of monodisperse and bidisperse polystyrene melts." (2006). J. Rheol. **50(4)**: 453.

Pis-Lopez, M. E. and A. Co (1996). "Multilayer film casting of modified Giesekus fluids. Part 1. Steady-state analysis." J. Non-Newtonian Fluid Mech**. 66(1)**: 71-93.

Pis-Lopez, M. E. and A. Co (1996). "Multilayer film casting of modified Giesekus fluids. Part 2. Linear stability analysis." J. Non-Newtonian Fluid Mech. **66(1)**: 95-114.

Roovers, J. (1985). "Properties of the plateau zone of star-branched polybutadienes and polystyrenes." Polymer **26**: 1091.

Sakaki, K., R. Katsumoto, et al. (1996). "Three-dimensional flow simulation of a film-casting process." Polym. Eng. Sci. **36(13)**: 1821-1831.

Satoh, N., H. Tomiyama, et al. (2001). "Viscoelastic simulation of film casting process for a polymer melt." Polym. Eng. Sci. **41(9)**: 1564-1579.

Seay, C. W. and D. G. Baird (2009). "Sparse long-chain branching's effect on the film-casting behavior of PE." Int. Polym. Process. **24(1)**: 41-49.

Sentmanat, M., B. N. Wang, et al. (2005). "Measuring the transient extensional rheology of polyethylene melts using the SER universal testing platform." Journal of Rheology **49(3)**: 585-606.

Sentmanat, M. L. (2004). "Miniature universal testing platform: from extensional melt rheology to solid-state deformation behavior." Rheol. Acta **43(6)**: 657-669.

Silagy, D., Y. Demay, et al. (1996). "Study of the stability of the film casting process." Polym. Eng. Sci. **36(21)**: 2614-2625.

Silagy, D., Y. Demay, et al. (1998). "Stationary and stability analysis of the film casting process." J. Non-Newtonian Fluid Mech. **79(2-3)**: 563-584.

Smith, S. and D. Stolle (2003). "Numerical simulation of film casting using an updated Lagrangian finite element algorithm." Polym. Eng. Sci. **43(5)**: 1105-1122.

Sollogoub, C., Y. Demay, et al. (2006). "Non-isothermal viscoelastic numerical model of the cast-film process." J. Non-Newtonian Fluid Mech. **138(2-3)**: 76-86.

Stevens, J. (1994). J. of Studies in Surface Sci. and Catalysts **89**.

Stevens, J. (1996). J. of Studies in Surface Sci. and Catalysts **101**.

Tanner, R. I. (1970). "Theory of die-swell." J. Polym. Sci., Polym. Phys. Ed. **8(12)**: 2067-78.

Wood-Adams, P. M. (2001). "The effect of long chain branches on the shear flow behavior of polyethylene." J. Rheol. **45(1)**: 203-210.

Wood-Adams, P. M. and J. M. Dealy (2000). "Using Rheological Data To Determine the Branching Level in Metallocene Polyethylenes." Macromolecules **33(20)**: 7481-7488.

Wood-Adams, P. M., J. M. Dealy, et al. (2000). "Effect of Molecular Structure on the Linear Viscoelastic Behavior of Polyethylene." Macromolecules **33(20)**: 7489-7499.

Zheng, H., W. Yu, et al. (2006). "Three-dimensional simulation of the non-isothermal cast film process of polymer melts." J. Polym. Res. **13(6)**: 433-440.

6.0 Effect of Sparse Long-Chain Branching on the Step-Strain Behavior in a Series of Well-Defined HDPEs

Preface

The effect of sparse long chain branching, LCB, on the shear step-strain relaxation modulus is analyzed using a series of eight well-characterized, high-density polyethylene (HDPE) resins. The motivation for this work is in assessing the ability of step-strain flows to provide specific information about a material's branching architecture. Fundamental to this goal is proving the validity of relaxation moduli data at times shorter than the onset of time-strain separability. This chapter is organized as a manuscript for publication.

Effect of Sparse Long-Chain Branching on the Step-Strain Behavior of a Series of Well-Defined Polyethylenes

McGrady, Christopher D.; Seay, Christopher W.; Baird, Donald G.

Department of Chemical Engineering, Virginia Tech

Blacksburg, VA 24061

6.1 Abstract

The effect of sparse long chain branching, LCB, on the shear step-strain relaxation modulus is analyzed using a series of eight well-characterized, high-density polyethylene (HDPE) resins. The motivation for this work is in assessing the ability of step-strain deformation to provide specific information about a material's branching architecture through the stretch relaxation time. Fundamental to this goal is proving the validity of relaxation moduli data at times shorter than the onset of time-strain separability. Strains of 1% to 1250% are imposed on materials with LCB content ranging from zero to 3.33 LCB per 10,000 carbon atoms. All materials are observed to obey time-strain separation beyond some characteristic time, τ_k. The presence of LCB is observed to increase the value of τ_k relative to the linear resin and in a manner consistent with an increase in LCB content. The behavior of the relaxation modulus at times shorter than τ_k is investigated by an analysis of the enhancement seen in the linear relaxation modulus, $G^0(t)$, as a function of strain and LCB content. This enhancement is seen to 1) increase with increasing strain in all resins, 2) be significantly larger in the sparsely-branched HDPE resins relative to the linear HDPE resin, and 3) increase in magnitude with increasing LCB content. The shape and smoothness of the damping function is investigated to rule out the presence of wall-slip and material rupture during testing. The finite rise time to impose the desired strain is carefully monitored and compared to the Rouse relaxation time of the linear HDPE resins studied. Sparse LCB is found to increase the magnitude of the relaxation modulus at short times relative to the linear resin. It is shown

that these differences are due to variations in the material architecture, specifically LCB content, and not because of mechanical anomalies.

6.2 Introduction

Step-strain tests are used to determine the strain dependence of the relaxation modulus. These tests are defined by a sudden shearing displacement of a fluid at rest to some strain, γ_0. Beyond some characteristic time, τ_k, after the imposition of a step shear strain the relaxation modulus, *G(t,γ)*, for a wide range of polymers[1-3] can be factored into separate time and strain functions:

$$G(t,\gamma) = G^0(t)h(\gamma) \tag{6-1}$$

where $G^0(t)$ is the linear relaxation modulus, and $h(\gamma)$ is the strain dependant damping function. This phenomenon is known as time-strain separability[4-6], and is illustrated in Fig. 6.1 for a sparsely-branched HDPE resin. The behavior of the relaxation moduli for polymeric melts, both before and after τ_k, is not fully understood, thereby leading to much debate in the literature as to why differences in the shape of the relaxation and damping function curves are seen for different materials.

Much of the disagreement in the literature regarding a material's behavior at times shorter than τ_k stems from the mechanical issues inherent in a rheometer's imposition of an instantaneous strain. Three main issues are the focus of much of the discussion. First is the amount of time needed to impose this "instantaneous" strain, called the finite rise time. The second issue is that of transducer overloads and material rupture. Third is wall-slip at the polymer-plate surface interface.

Finite rise times are created by the fact that it is physically impossible with current rheometer technology to instantaneously shear a fluid to a desired strain. Instead, there exists some finite rise time for the imposition of strain. This finite rise time is a point of contention as it is unknown if the data preceding τ_k is truly accurate or an artifact of the experimental apparatus. Vega and Milner[4] proposed that in the framework of the BKZ constitutive model, the finite rise time was the primary reason time-

strain separability was not observed until after some time τ_k. Sui and McKenna[7] attributed deviations at short times to different loading times of the normal force and torque response (i.e. reaching maximum value) in linear and dendritic PIB. Venerus[8] simulated the effect of finite rise time on the response of the relaxation modulus, finding that differences at times less than τ_k were still seen as a function of the imposed strain. This suggested that the short time response prior to τ_k was realistic and not an artifact of the experimental apparatus. Stadler *et al.*[9] stated that the finite rise (step) time had no relevant influence on the relaxation modulus after times longer than ten times the step time. Venerus and Kahvand[10] found for a PS solution with an average of seven entanglements per molecule that the measured shear stress was independent of the step time for times roughly three times larger than the step time.

Transducer overloads and material ruptures can occur at higher strains for materials with a high plateau modulus, such as some entangled polyethlyenes[4]. Transducer overloads have been shown to be avoidable by utilizing plate fixtures with smaller diameters[11-13]. This technique has been shown to suffer from a reduced accuracy and increased error at long times due to the smaller sample size[4]. Stadler *et al.*[9] argued that sample rupture was not present in melts that had a measureable damping function, $h(\gamma)$. The authors argued that the sample rupture would have changed the shape of the relaxation modulus thereby making the measurement of a realistic $h(\gamma_0)$ impossible. This finding made the detection of rupture simpler in that a complicated and expensive rheo-optical measurement systems was not necessary[9].

Wall slip at the polymer-plate interface was found to be a major source of error in step strain [6, 14]. Wall slip occurs when the wall stress exceeds some threshold value greater than the surface bond between the polymeric melt and the wall. If slip occurs, the applied strain is lower than the desired strain. Wall slip depends on the surface characteristics and the dynamic modulus at timescales on the order of the applied strain. This causes the measured damping function, $h(\gamma)$, to be too small[4]. Slip was

also found to cause a "kink" in the damping function curve at higher strains[8]. Vega and Milner[4] observed the deformation of a vertical line initially drawn on the undeformed sample to confirm the presence/absence of wall slip. If the line deformed affinely with the plates, slip was not present. Likewise if the line was under-deformed, slip was present. Vega and Milner[4] also observed that slip occurred in well-entangled polyethylenes at strains as low as 2.0. Sanchez-Reyes and Archer[6] found that slip could be mitigated in well-entangled polystyrenes ($\geq$ 37 entanglements) by attaching a single layer of micron-sized glass beads to the plate surface. Vega and Milner[4] reduced wall-slip and transducer overload by blending low MW PE with entangled PE.

It has also been proposed that the relaxation modulus' behavior prior to τ_k is not a mechanical artifact. Vega and Milner[4] found disagreement in the literature as to the reason for a material's behavior at times less than τ_k. In some works it has been claimed that the value of τ_k was related to the time required for a complete relaxation of the contour length, τ_s,[15, 16] via $\tau_k \sim \tau_s \sim 4\tau_R$, where τ_R is the longest Rouse time of the chain. Other, more contemporary, results[6, 17] suggested that τ_k was not dictated by τ_R. Measurements of the dynamic moduli for well-entangled linear polystyrene solutions displayed time-strain separation at times comparable to the terminal relaxation of the chain τ_d ($\sim\tau_k$). For weakly entangled systems, values of τ_s approach τ_k.

Regardless of the origin of such short-time behavior, the imperfect strain history must be accounted for in any constitutive modeling. Sui and McKenna[7] cited a correction necessary for any constitutive modeling of $G(t,\gamma)$ originally put forward by Zapas and Craft[18] to correct for the imperfect strain history that arose from the finite rise time

$$t_{corrected} = t - \frac{\tau}{2} \tag{6-2}$$

where t was the raw measured experimental time, $t_{corrected}$ was the corrected time, and τ was the finite time required to impose the desired strain. τ was determined to be the time at which the normal

force and torque response reached their maximum value [7]. τ was found to occur on timescales less than the onset of time-strain separability, τ_k, for linear and dendritic PIB [7].

While the short times of the relaxation modulus are of primary interest to this work, the behavior beyond τ_k is useful in that it has been linked to the molecular structure of the melt. Stadler *et al.*[9] summarized contemporary works that highlighted the effect of molecular structure on the behavior of time-strain separation in the literature. The damping function $h(\gamma_0)$ was found to be independent of molar mass[19, 20] and temperature[19, 21, 22] in linear polymer melts. Molecular weight distribution, MWD, has been shown to affect the value of $h(\gamma_0)$ [23-25]. The chemical structure has been shown to affect $h(\gamma_0)$, for example, in commercial linear PE and PP [26]. The damping function of LCB polymers with multiple branch points (both commercial resins and model systems) has been shown[5, 11, 22, 26] to have a weaker dependence on strain than their linear counterparts. Hepperle and Münstedt[22] observed that increasing arm length in nearly monodisperse combs reduced the strain dependence of $h(\gamma_0)$. Polymeric melts of three- and four-armed star (only one LCB branch point) have shown only weak deviation from the non-linear behavior of linear polymer melts[27-29]. The exact reason for such a wide variety of strain dependences of $h(\gamma_0)$ is unknown. It has been theorized that the non-linear strain dependence originated from the induced chain anisotropy and the decrease in entanglement density induced by the large shear amplitutde[9]. For branched polymers, the retarded relaxation of the backbone chain due to the pinned branch points was theorized to be the reason for the weaken strain dependence of $h(\gamma_0)$ [30].

The strain dependence of $h(\gamma_0)$ has been modeled to describe the non-linear response of polymeric melts. An expression based on the Doi-Edwards (DE) tube model[15] with independent alignment was found to accurately model the damping function seen in linear and some star polymer melts with narrow MWD [22, 28, 29]. Stadler *et al.*[9] observed that the shape of $\log h(\gamma_0)$ versus log γ_0

resembled that of a simple shear viscosity curve, and proposed a numerical damping function based on the Carreau-Yasuda model originally developed for shear viscosity profiles[31, 32]

The objective of this paper is to investigate the specific relationship between LCB content and the step-strain behavior using a series of well-characterized, sparsely-branched HDPE resins. Specifically, it is the goal of this work to illustrate that rheological data measured prior to the onset of time-strain separability is indeed a property of the material and not a mechanical artifact. The materials selected are well understood in terms of their branching content and rheological behavior[33-37], and make excellent candidates for such an analysis. The shape and smoothness of the damping function is investigated to rule out the presence of slip and material rupture during testing. The finite rise time to impose the desired strain is carefully monitored and compared to the Rouse relaxation time of the linear HDPE resin studied. Transducer overloads are mitigated by using smaller cone-and-plate fixtures. All materials are checked to see if time-strain separation is observed beyond some characteristic time, τ_k. The effect of LCB is then correlated to the magnitude of τ_k. The behavior of the relaxation modulus at times shorter than τ_k is investigated by an analysis of the enhancement seen to the linear relaxation modulus, $G^0(t)$, as a function of strain and LCB content. Correlation between this enhancement and LCB content is made. Discussion is also given regarding the differences seen in the short-time behavior of materials with similar shear viscosity curves, but different LCB content. Information reported in this study can possibly be extrapolated in future works using constitutive relationships to determine information regarding specific molecular structure.

6.3 Experimental materials and methods

6.3.1 Materials

A series of sparsely long-chain branched and linear metallocene-catalyzed high density polyethylene homopolymers polyethylenes with varying degrees of LCB made available by the Dow

Chemical Company were used. MW, MWD, and LCB content for these resins are given in Table 6.1. The sparsely long-chain branched metallocene-catalyzed polyethylene resins include HDB1, HDB2, HDB3, HDB4, HDB5, HDB6, and HDB7 and were synthesized using a constrained geometry catalyst of the type described by Stevens[38, 39] in a continuous, stirred-tank reactor as described by Lai *et al.*[40]. No information was provided as to the method of synthesis for the linear resin HDPE resin HDBL. Both the sparsely-branched resins and the linear resin are homopolymers with narrow molecular weight distributions, MWD, characteristic to metallocene type catalysts. These materials are henceforth referred to collectively as the HDB series.

The HDB resins are ideal for this study for three primary reasons. First, the HDB resins were well-characterized in previous studies[33-37, 41], most notably the linear rheology of HDBL, HDB1, HDB3 and HDB4 by Wood-Adams and Dealy[35, 36]. Second, they were readily available in sufficient quantities to accurately measure the viscoelastic properties. Finally, their branching content is well-known based on ^{13}C NMR, providing an excellent opportunity to measure the effect of slight variations in the long-chain branching content when subjected to step-strain deformation.

6.3.2 Rheology

Shear step-strain experiments were conducted using a Rheometrics RMS-800 fitted with 25 mm cone and plate fixtures with a cone angle of 0.1 radians and 10 mm cone and plate fixtures with a cone angle of 0.035 radians. Tests were carried out at a temperature of 170°C. Strains of 0.01, 0.1, and 1 strain units were evaluated using the 25 mm diameter plates and strains of 1, 5, 7.5, 10, and 12.5 strain units were evaluated using the 10 mm diameter plates. Finite rise time to impose the desired strain was found to range from 0.055 to 0.065 sec and increased with strain. The presence of wall-slip and rupture were investigated via inspection of the experimentally determined damping function as per the recommendations of Stadler *et al.*[9] and Vega and Milner[4]. Linear viscoelastic shear measurements were

conducted using a Rheometrics RMS-800. 25- and 10-mm cone-and-plate fixtures with cone angles of 0.1 and 0.05 radians, respectively, were used. An angular frequency range of 0.01-100 s^{-1} was probed. All tests were performed under an inert N_2 atmosphere in order to prevent oxidative degradation. The test samples were prepared by compression molding preforms at 170 °C under nominal pressure and allowing them to cool slowly under no pressure. This method provided homogenous samples with minimal residual stress.

6.4 Results

The results of both the step-strain and shear viscosity curves are presented in this section for all eight resins of interest. Several materials are found to have relative identical shear viscosity curves, allowing for comparisons of the resins' relaxation modulus behavior on the basis of not only LCB content but relative to simple shear flow behavior as well. General trends and observations are given here, while a more detailed analysis is reserved for the discussion section presented later.

Shown in Fig. 6.1a are the relaxation moduli, $G(t,\gamma)$, for HDB1. Increasing the strain decreases the overall magnitude of $G(t,\gamma)$, especially at longer times. However, the general shape of the curve appears similar at each strain as time is increased. $G(t,\gamma)$ is then divided through by an experimentally determined damping function to gauge time-strain separability and is shown in Fig. 6.1b. At long times, the shifted moduli curves overlap, obeying Eq. 6-1, while at short times, $G(t,\gamma)/h(\gamma)$ increased with the value of strain. τ_k was found to be equal to 0.135 sec. for HDB1. The remainder of the relaxation moduli results presented in this work are given as $G(t,\gamma)/h(\gamma)$ versus time to emphasize both the onset of time-strain separability and the behavior of the resins at short times.

In Figs. 6.2 through 6.7 are given the dampened step-strain behavior for the remainder of the sparsely-branched resins, HDB2, HDB3, HDB4, HDB5, HDB6, and HDB7. Each resin was observed to obey Eq. 6-1 beyond some value of τ_k that was found to range from 0.135 to 0.490 seconds. Furthermore, for

each branched resin, the magnitude of $G(t,\gamma)/h(\gamma)$ and the value for of τ_k as a function of strain was observed at short times to increase with the value of strain. Finally, in Fig. 6.8 are given the curves showing the shifted relaxation moduli for the linear HDPE resin HDBL. Similar to the branched resins, HDBL obeys Eq. 6-1 beyond some characteristic time τ_k. The value of τ_k was found to be equal to 0.11 sec. Also, the magnitude of the enhancement of $G(t,\gamma)/h(\gamma)$ as a function of strain was much lower than that for the sparsely-branched resins. Further discussion regarding the ramifications and implications of the linear resin's behavior relative to the sparsely-branched system is reserved for discussion later in this work.

The magnitude of complex viscosity versus angular frequency curves at 170 ^{o}C for each material is given in Fig. 6.9. The Cox-Merz relationship[42] was validated for the HDPE materials in previous studies [33, 34], suggesting that the magnitude of complex viscosity determined from small-angle oscillatory shear is a good approximation of the steady-shear viscosity. All branched-resins were found to have an enhanced zero-shear viscosity relative to the linear HDPE. The correlation of LCB content to the level of zero-shear viscosity enhancement was found to pass through a maximum, which is in agreement with the findings of Janzen and Colby[43], among other works[44-46]. Furthermore, HDB3, HDB5, and HDB6 were found to have similar shear viscosity flow curves despite differences in LCB content (0.37 versus 0.90 versus 1.66 LCB/10^4 C, respectively). This allows for direct comparison of the effect of LCB content on the step-strain for materials with relatively identical shear viscosity curves.

6.5 Discussion

6.5.1 Considerations for finite rise time

Finite rise times arise from the inability of a rheometer to instantly apply the desired strain to a material. Instead, a relatively small amount of time passes prior to the implementation of the desired strain. This can affect the stress relaxation modulus output by artificially damping the results due

relaxation occurring prior to complete deformation[47]. The maximum time required for implementation of the highest strain used in this work (γ=12.5) was 0.065 seconds. No experimental data was used until at least 95% of the desired strain was reached. The importance of the finite rise time for linear resins lies in its comparison to the Rouse relaxation time, τ_R. For the relaxation modulus curves to be unaffected by relaxation that takes place prior to reaching the applied strain, τ_R should be sufficiently greater than the finite rise time. τ_R for HDBL was calculated following the method of Elbirli and Shaw[48], given by Eq. 6-3:

$$\tau_R = \frac{6\eta_0 M_W}{\pi^2 \rho RT} \tag{6-3}$$

where η_0 is the zero-shear viscosity at the test temperature, M_W is the molecular weight, and ρ is the material density at the test temperature, *T*. Because Rouse dynamics were derived under the assumption of a linear architecture, it is inappropriate to calculate values of τ_R for LCB resins. However, as it has been shown[13] that the relaxation time for LCB resins was longer than linear resins of similar molecular weight, it is expected that the value of τ_R for HDBL will be the minimum value of the resins investigated in this work. Using the shear viscosity data given in Fig. 6.9, resin data from Table 6.1, and the density of HDPE at 170 ^{o}C equal to 0.7719 g/cm^3 (see Baird and Collias[49], pg. 105), τ_R for HDBL was calculated to be 0.170 sec., a value that is nearly three times that of the longest finite rise time, suggesting that the materials were not sufficiently relaxed prior to the inception of the full strain. Furthermore, from a qualitative perspective, if the finite rise time was allowing for significant relaxation of the material, one would expect to see a trend of decreasing values of $G(t,\gamma)/h(\gamma)$ at very low times (say t = 0.05 sec.) as a function of strain. This trend was not observed in any of the resins (see Figs. 6.1 through 6.8), further suggesting that the finite rise time is not significantly affecting the material data at times shorter than τ_R.

6.5.2 Behavior after time-strain separation ($t > \tau_k$)

In Fig. 6.10 is given the damping function, *h(γ)*, for each of the eight resins investigated. Also plotted are a *h(γ)* curve predicted by Doi-Edwards theory[15] and the *h(γ)* curve for a sparsely-branched HDPE resin from a previous study[9]. According to Stadler *et al.*[9] and Vega and Milner[4], the presence of an irregularly or illogically shaped *h(γ)* curve (i.e. a "kink") would correspond to material rupture or slip at the plate-polymer interface. From a physical point of view, if the material underwent slip during a test, the resulting applied strain would be less than the desired strain. Therefore, the value of *h(γ)* at the applied strain would be higher than the value of *h(γ)* at the desired strain, resulting in a "kink". One can imagine the same scenario for a material rupture, which is simply slip at some polymer-polymer interface within the homogeneous polymer matrix. An investigation of the data given in Fig. 6.10 shows that the data set is devoid of any major "kinks" for any of the resins investigated. This suggested that the results presented in Figs. 6.1 through 6.8 were devoid of any major slip or rupture. An observed trend that was consistent with previous works [4, 9] was the reduction of the strain dependence in sparsely-branched LCB resins. This is evidenced in Fig. 6.10 by *h(γ)* having a smaller slope than that of the linear HDBL at higher strains. Vega and Milner[4] attributed this behavior to the quick relaxation times of the branched arms, suggesting that a substantial portion of the branched material has relaxed prior to τ_k. Regardless of the mechanism, the data in Fig. 6.10 suggest that wall-slip and sample rupture were not responsible for the relaxation behavior of the HDPE resins.

At times longer than τ_k, values of *G(t,γ)* as a function of LCB were reminiscent of the behavior of η_0 as a function of LCB content. In Fig. 6.11 is shown *G(t,γ=1.0)* as function of time for the eight HDPE resins. It was observed that HDBL had the lowest relaxation modulus value at *t* equal to one second, suggesting that the material had relaxed its stress faster than the sparsely-branched resins. At the same time, the sparsely-branched resins exhibited an enhanced relaxation modulus. This enhancement increased up through LCB contents of 0.80 LCB per 10^4 carbons (corresponding to HDB4). At higher LCB

concentrations (HDB5, HDB6, and HDB7), this enhancement was reduced as a function of LCB content, but still remained higher than the linear HDBL resin. This dependence of *G(t,γ)* on LCB content is similar to that observed in Fig. 6.9 for η_0 as a function of LCB content. The data in Fig. 6.11 suggest that LCB has an enhancing effect on the magnitude of the relaxation modulus at times longer than τ_k, up until some critical value before this enhancement begins to decrease approaching values similar to the linear resin.

6.5.3 Behavior before time-strain separation ($t \leq \tau_k$)

Now that wall-slip, sample rupture, and transducer overload were eliminated as potential explanations for the behavior of *G(t,γ)* at times less than τ_k, the effect of sparse LCB content at these short times was investigated. This was done by investigating two characteristics of the *G(t,γ)/h(γ)* curve at short times. First, the magnitude of $G^0(t=0.05\ s, \gamma)/ G^0(t=0.05\ s,\gamma=0.01)$ enhancement as a function strain, LCB content, average number of branches per chain was studied. Second, the effect of LCB content of the value of τ_k was investigated. Both characteristics were found to correlate positively with LCB content and average number of LCB per chain.

In Fig. 6.12 is plotted $G^0(t=0.05\ s, \gamma)/ G^0(t=0.05\ s,\gamma=0.01)$ versus LCB per 10,000 carbon atoms. In an effort to eliminate the slight differences in the MW of the resins, the same enhancement values are plotted as function of the average number of LCB per backbone chain in Fig. 6.13. The two strains investigated were γ = 5.0 (x's) and γ = 12.5 (squares). These values correspond to the relative magnitude of the inflection at short times given in Figs. 6.1 through 6.8. Increasing LCB content served to enhance the initial magnitude and inflection of the shifted relaxation modulus at short times. Furthermore, materials with similar simple shear viscosity curves (HDB3, HDB5, and HDB6) were observed to exhibit different short-time behavior, suggesting that step-strain was more sensitive to LCB content, akin to the response seen in uniaxial extension[46].

Finally, in Fig. 6.14 is shown the effect of LCB content per 10^4 carbon atoms (squares) and average number of LCB per backbone (x's) on the time for the occurrence of time-strain separation ($t = \tau_k$). Solid and dashed lines are given only to aid the eye and show proof of a strong positive correlation. Both increasing LCB content per 10^4 carbons and average number of LCB per backbone were shown to increase the value of τ_k. This suggested that an increased LCB content served to increase the time required for sparsely-branched LCB systems to enter the linear relaxation region given by $G^0(t, \gamma)$ in Eq. 6-1.

6.6 Conclusions

The effect of sparse LCB on the shear step-strain relaxation modulus was analyzed using a series of eight well-characterized, HDPE resins. Strains of 1% to 1250% were imposed on materials with LCB content ranging from zero to 3.33 LCB per 10,000 carbons. The shape and smoothness of the damping function was investigated to rule out the presence of wall-slip and material rupture during testing. The finite rise time to impose the desired strain was carefully monitored and compared to the Rouse relaxation time of the linear HDPE resins studied. Transducer overloads were mitigated by using smaller cone-and-plate fixtures. All materials were observed to obey time-strain separation beyond some characteristic time, τ_k. LCB content in sparsely branched resins was observed to increase the value of τ_k relative to the linear resin. Furthermore, the amount of LCB content was seen to correlate positively with increasing τ_k. The values of $G(t,\gamma)$ at long times were seen to behave as a function of LCB content similar to that of the zero-shear viscosity. Enhancement of the magnitude of $G(t,\gamma)$ relative to that of the linear HDBL as a function of LCB passed through a maximum at a LCB content of 0.80 LCB/ 10^4 carbon atoms before decreasing in value, while remaining above the linear resin. The behavior of the relaxation modulus at times shorter than τ_k was investigated by an analysis of the enhancement seen to the linear relaxation modulus, $G^0(t)$, as a function of strain and LCB content. All eight HDPE resins were

seen to exhibit enhancement. It was observed that that this enhancement was significantly larger in the sparsely-branched HDPE resins relative to the linear HDPE resin. Furthermore, the enhancement was seen to increase in magnitude with increasing LCB content. The results presented in this work suggest that increasing sparse LCB served to enhance both the amount of time needed for and magnitude of stress relaxation relative to the linear resin.

6.7 Acknowledgements

This research is a collaborative effort for the World Network of Materials – UK Leeds and is supported financially by the National Science Foundation DMR-052198. Gratitude is given as well to the Dow Chemical Company for making their respective PE materials available.

Table 6.1 - Material Properties				
Material	**M_w [g/mol]**	**M_w/M_n**	**LCB/10,000 C**	**Avg. # of branches per chain**
HDBL	113,000	2.5	Linear	Linear
HDB1	77,100	2.0	0.26	0.14
HDB2	82,000	1.9	0.37	0.22
HDB3	85,700	2.0	0.42	0.26
HDB4	96,300	2.1	0.80	0.55
HDB5	79,000	-	0.90	0.51
HDB6	68,000	-	1.88	0.91
HDB7	70,000	-	3.33	1.66

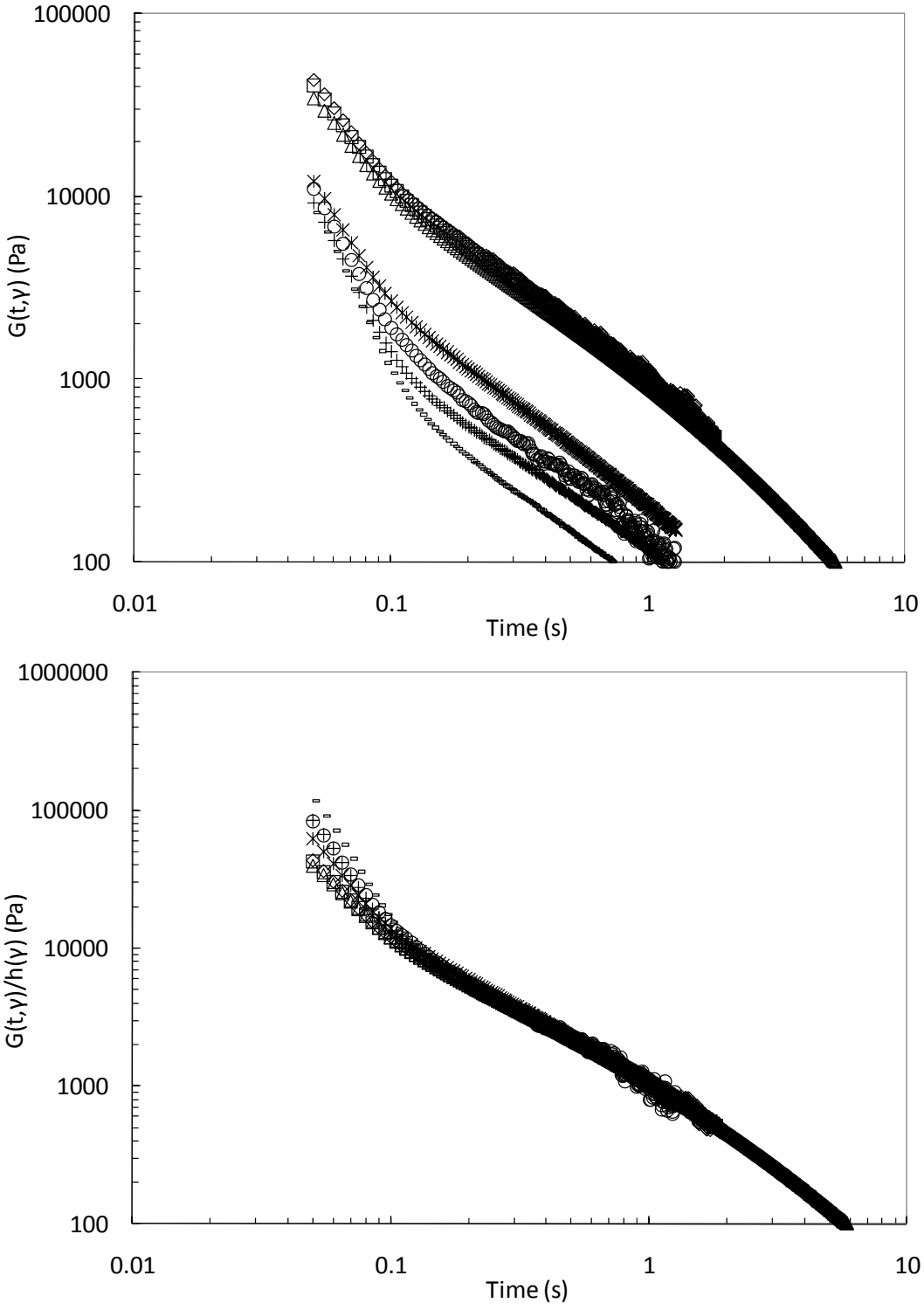

Figure 6.1: Stress relaxation moduli curves, G(t,γ), *(top)* and shifted stress relaxation moduli curves, G(t,γ)/h(γ) *(bottom)*, as a function of time for HDB1 subjected to strains, γ, equal to 0.01 (◊), 0.1 (□), 1.0 (Δ), 5.0 (*), 7.5 (o), 10.0 (+),and 12.5 (-) at 170 ^{o}C.

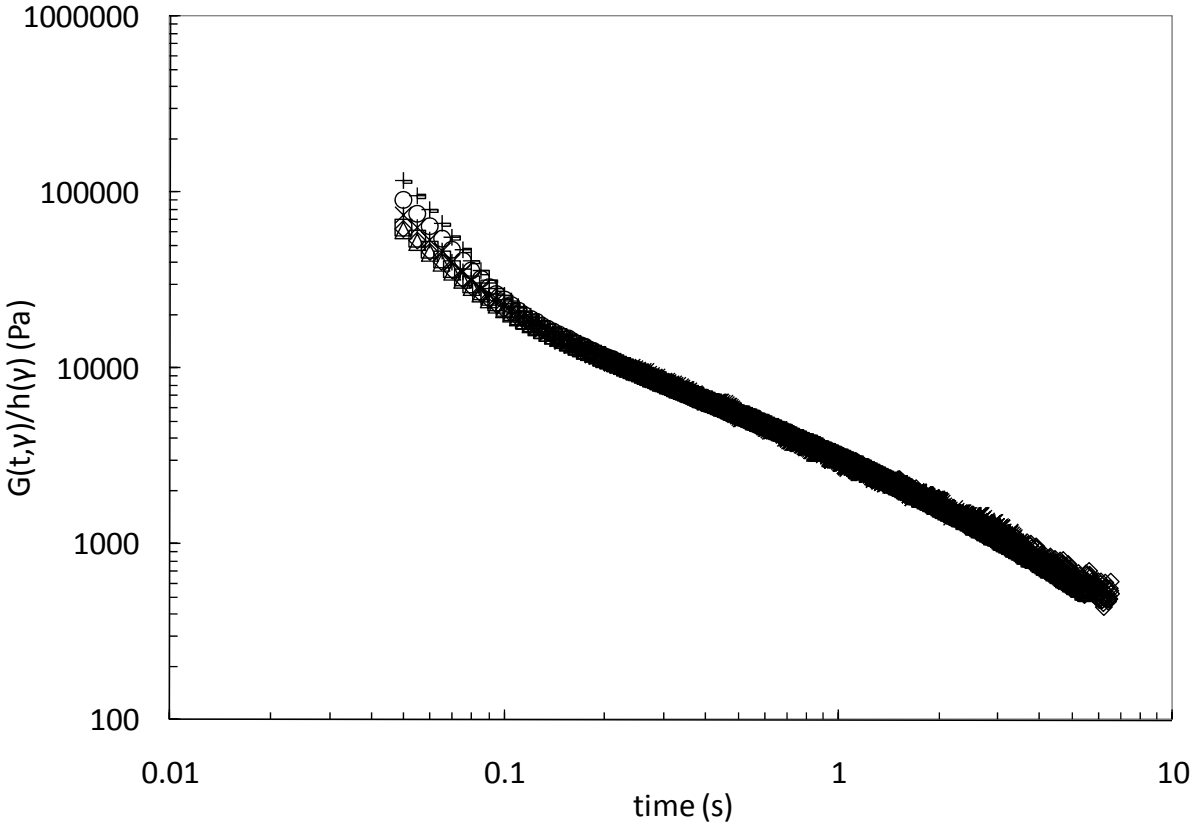

Figure 6.2: Shifted stress relaxation moduli curves, G(t,γ)/h(γ), as a function of time for HDB2 subjected to strains, γ, equal to 0.01 (◊), 0.1 (□), 1.0 (Δ), 5.0 (*), 7.5 (o), 10.0 (+), and 12.5 (-) at 170 ^{o}C.

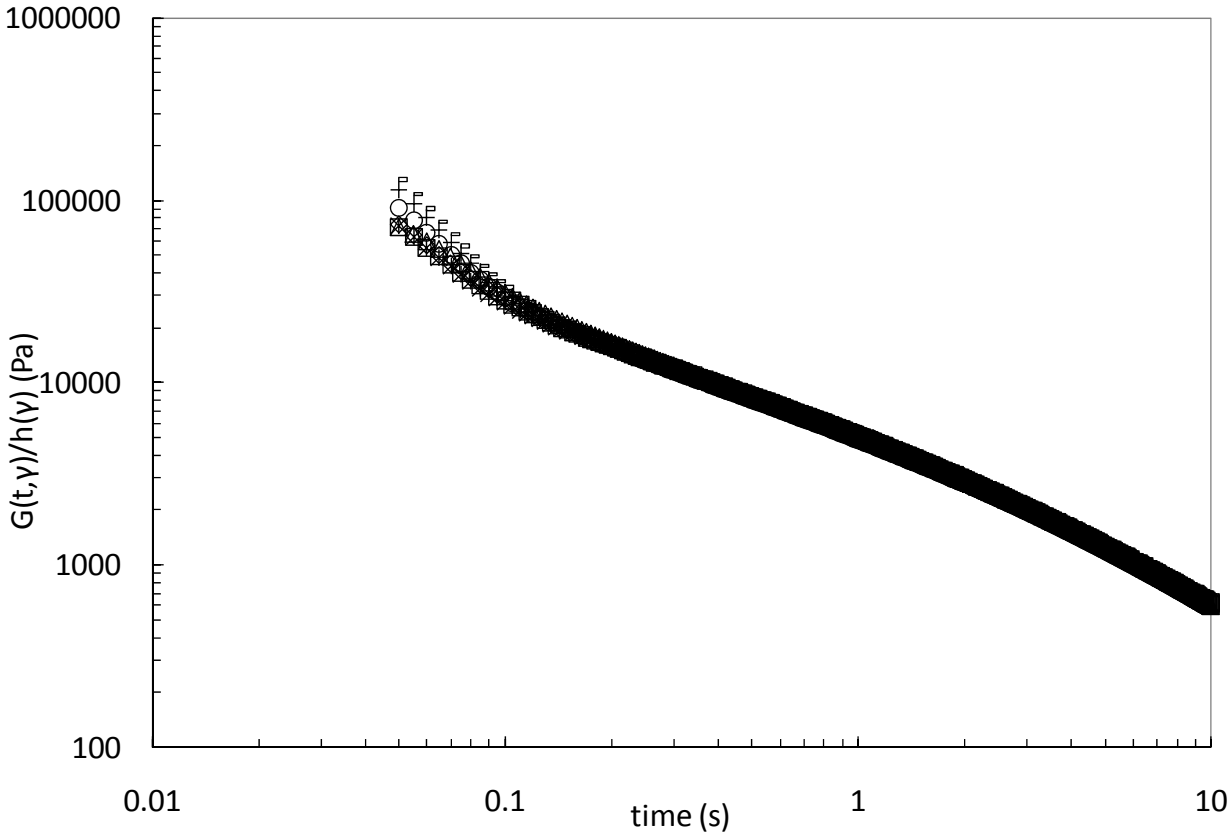

Figure 6.3: Shifted stress relaxation moduli curves, G(t,γ)/h(γ), as a function of time for HDB3 subjected to strains, γ, equal to 0.01 (◊), 0.1 (□), 1.0 (Δ), 5.0 (*), 7.5 (o), 10.0 (+), and 12.5 (-) at 170 ^{o}C.

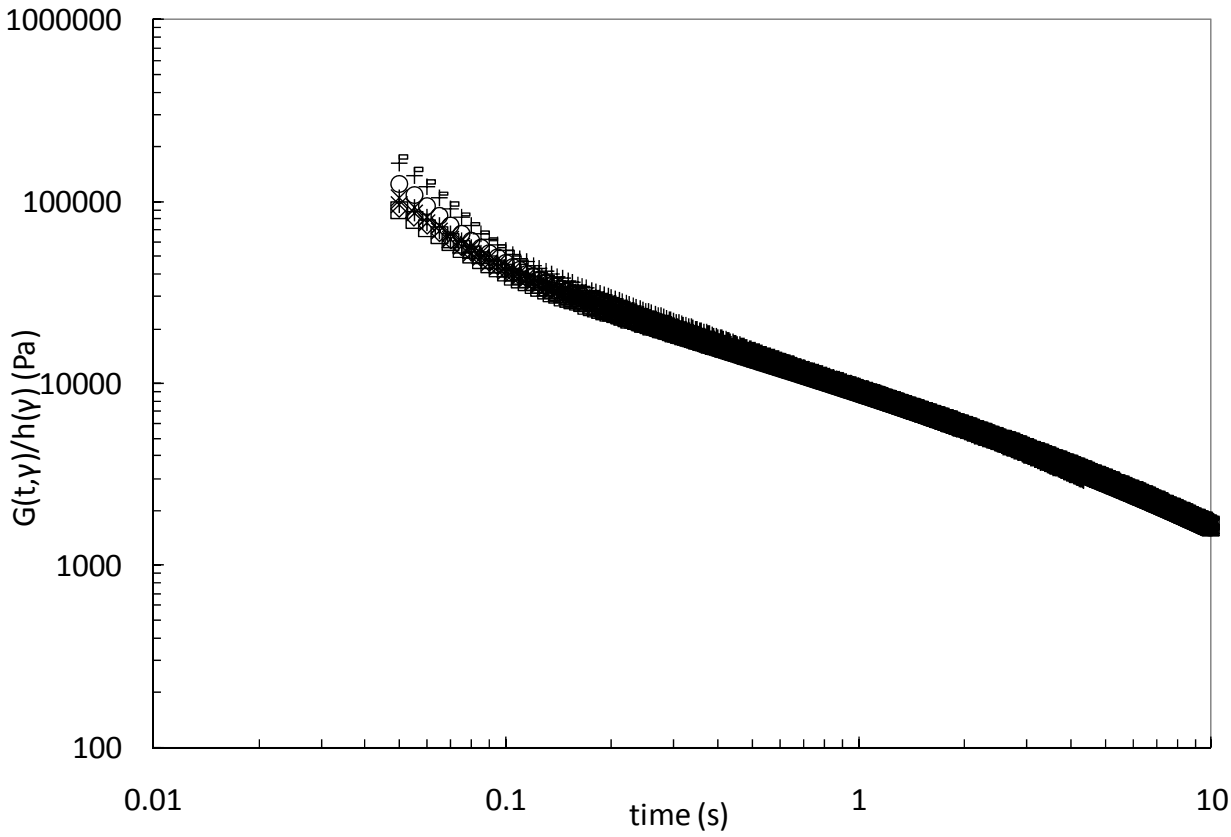

Figure 6.4: Shifted stress relaxation moduli curves, G(t,γ)/h(γ), as a function of time for HDB4 subjected to strains, γ, equal to 0.01 (◊), 0.1 (□), 1.0 (Δ), 5.0 (*), 7.5 (o), 10.0 (+), and 12.5 (-) at 170 ^{o}C.

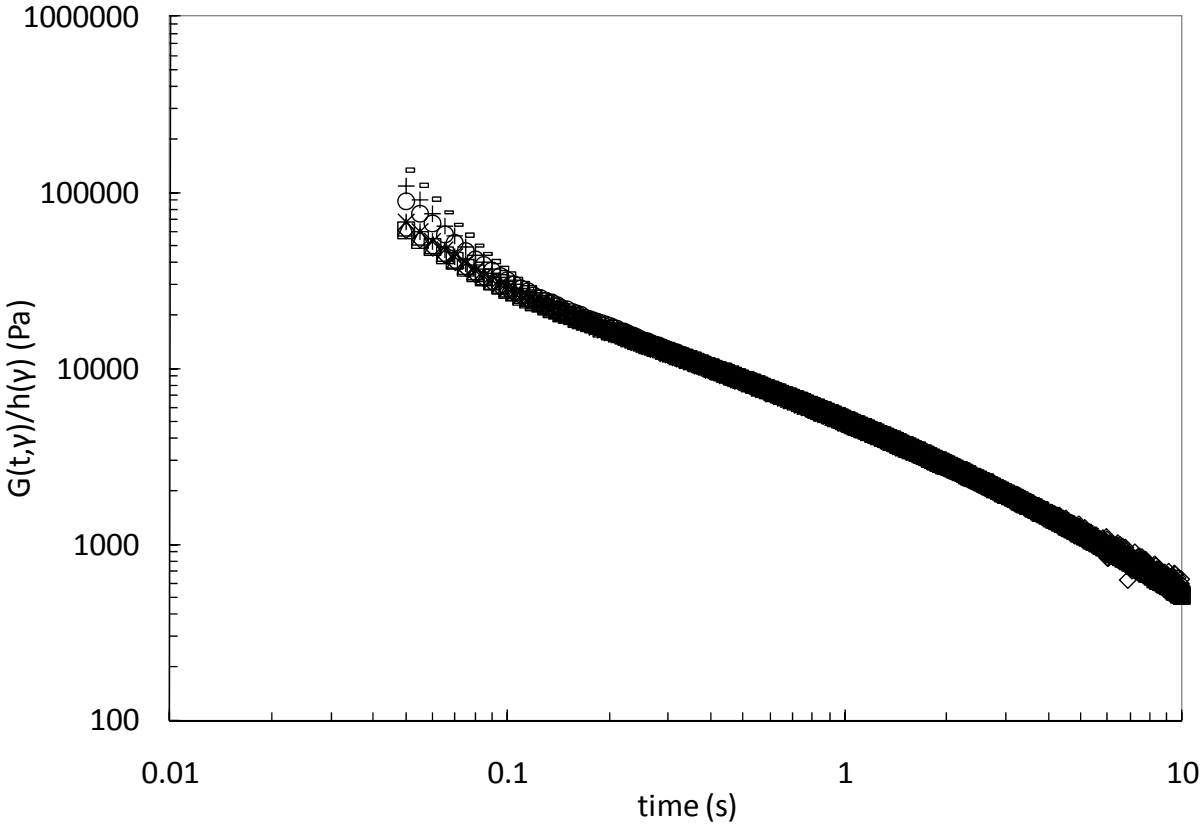

Figure 6.5: Shifted stress relaxation moduli curves, G(t,γ)/h(γ), as a function of time for HDB5 subjected to strains, γ, equal to 0.01 (◊), 0.1 (□), 1.0 (Δ), 5.0 (*), 7.5 (o), 10.0 (+), and 12.5 (-) at 170 ^{o}C.

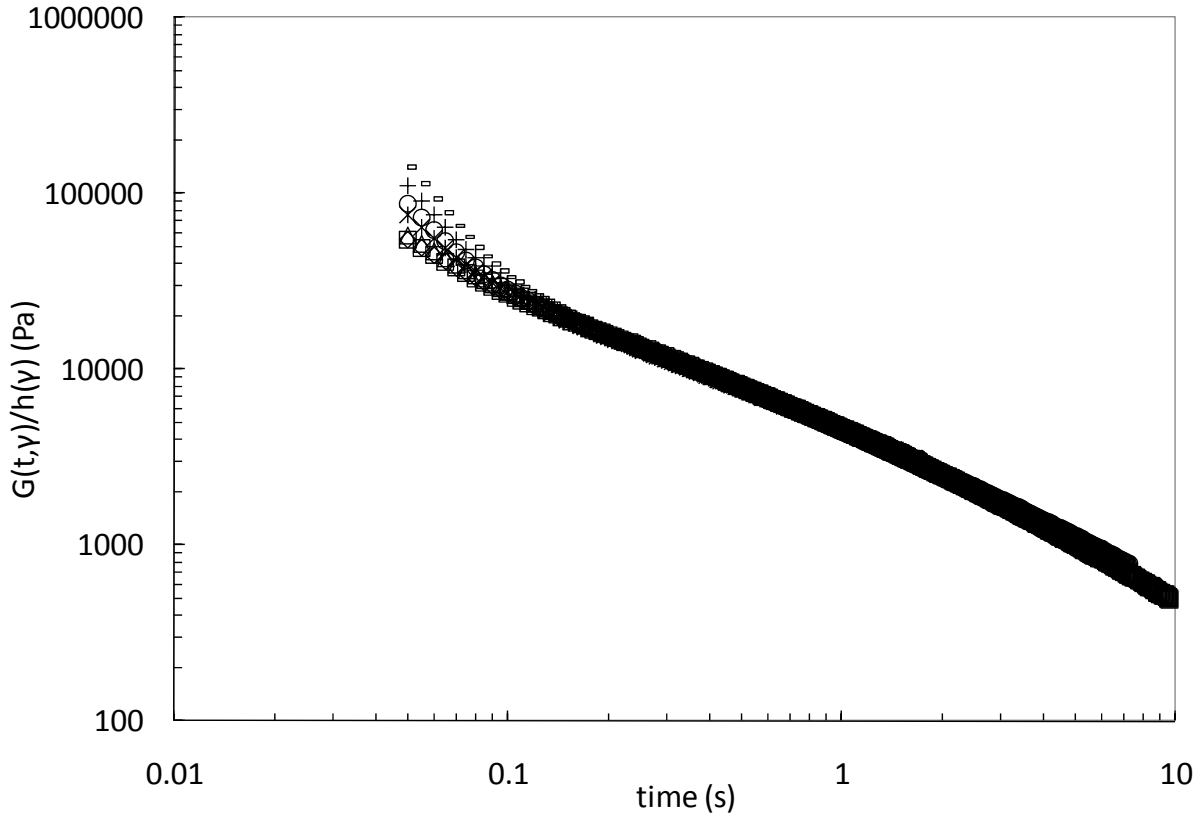

Figure 6.6: Shifted stress relaxation moduli curves, G(t,γ)/h(γ), as a function of time for HDB6 subjected to strains, γ, equal to 0.01 (◊), 0.1 (□), 1.0 (Δ), 5.0 (*), 7.5 (o), 10.0 (+), and 12.5 (-) at 170 ^{o}C.

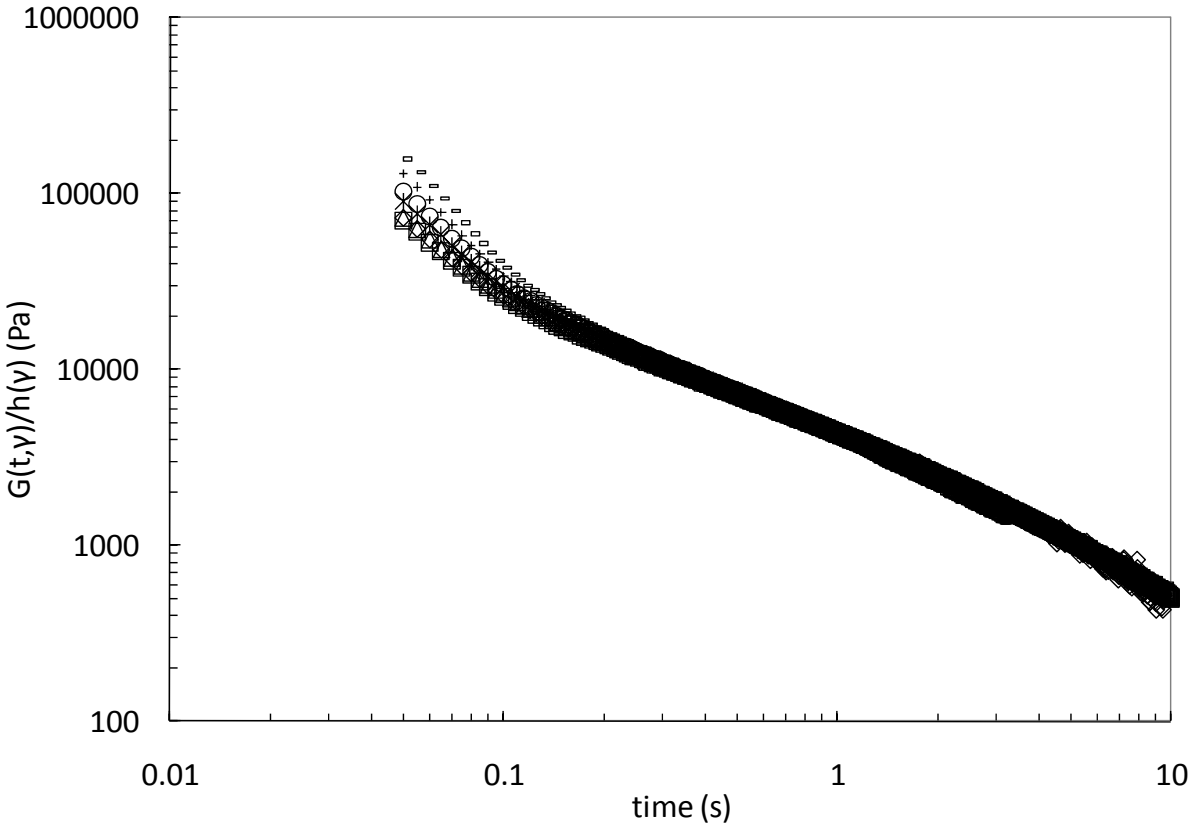

Figure 6.7: Shifted stress relaxation moduli curves, G(t,γ)/h(γ), as a function of time for HDB7 subjected to strains, γ, equal to 0.01 (◊), 0.1 (□), 1.0 (Δ), 5.0 (*), 7.5 (o), 10.0 (+), and 12.5 (-) at 170 ^{o}C.

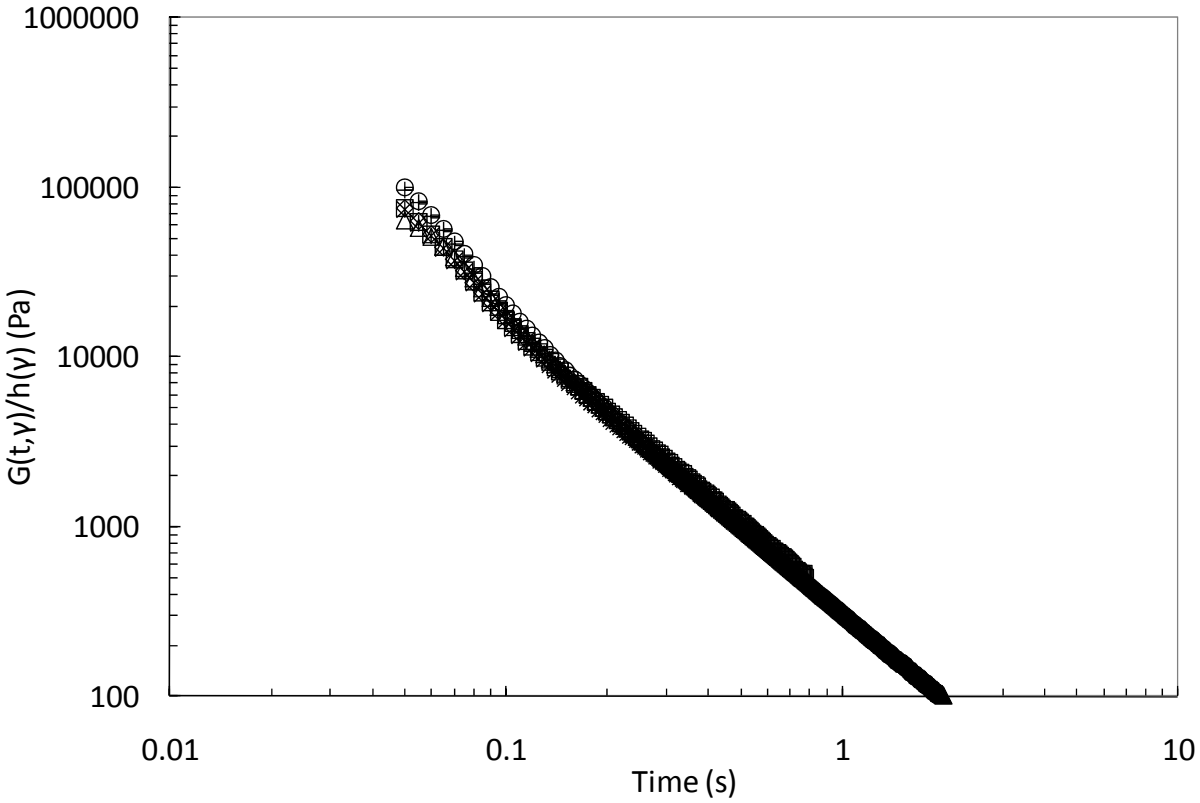

Figure 6.8: Shifted stress relaxation moduli curves, G(t,γ)/h(γ), as a function of time for HDBL subjected to strains, γ, equal to 0.01 (◊), 0.1 (□), 1.0 (Δ), 5.0 (*), 7.5 (o), 10.0 (+), and 12.5 (-) at 170 ^{o}C.

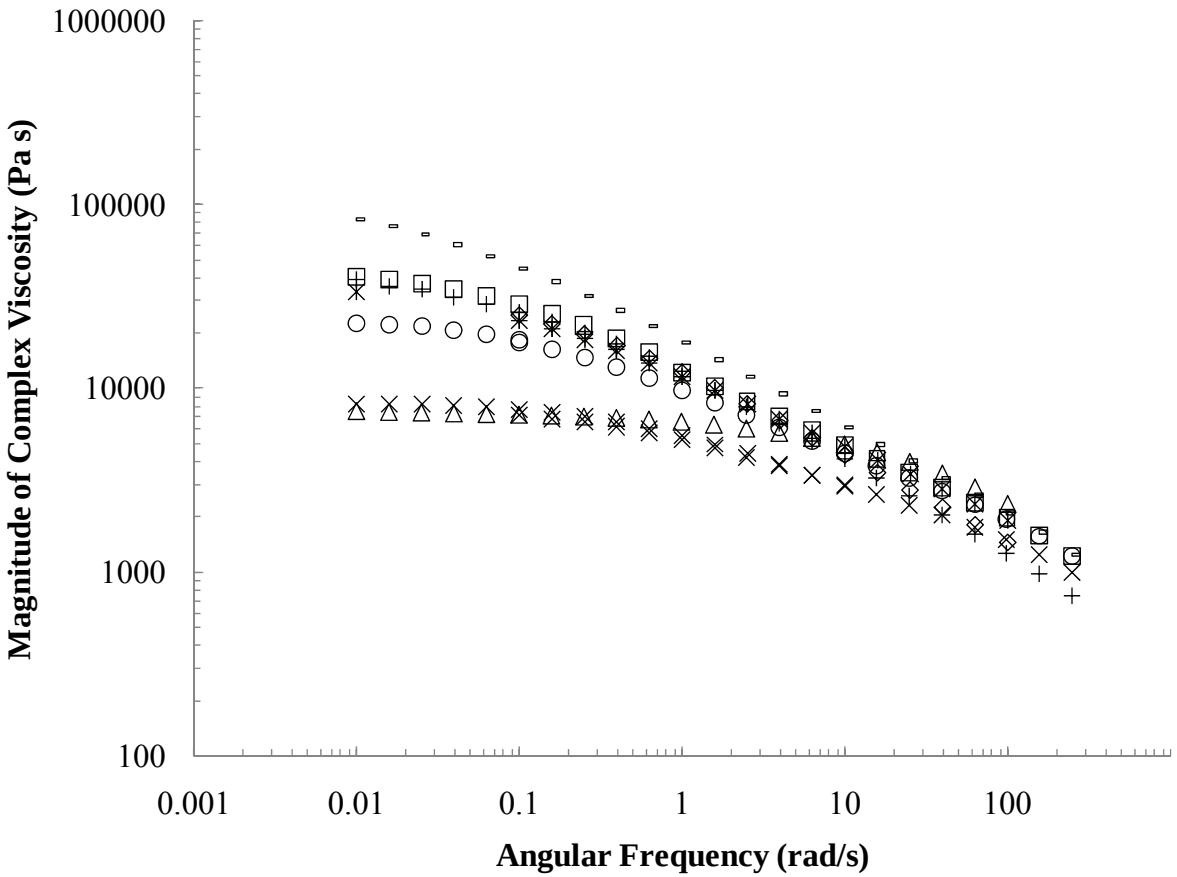

Figure 6.9: Shear viscosity of HDBL (Δ), HDB1 (x), HDB2 (O), HDB3 (□), HDB4 (-), HDB5 (◊), HDB6 (+), and HDB7 (*) PE resins at 170 ^{o}C.

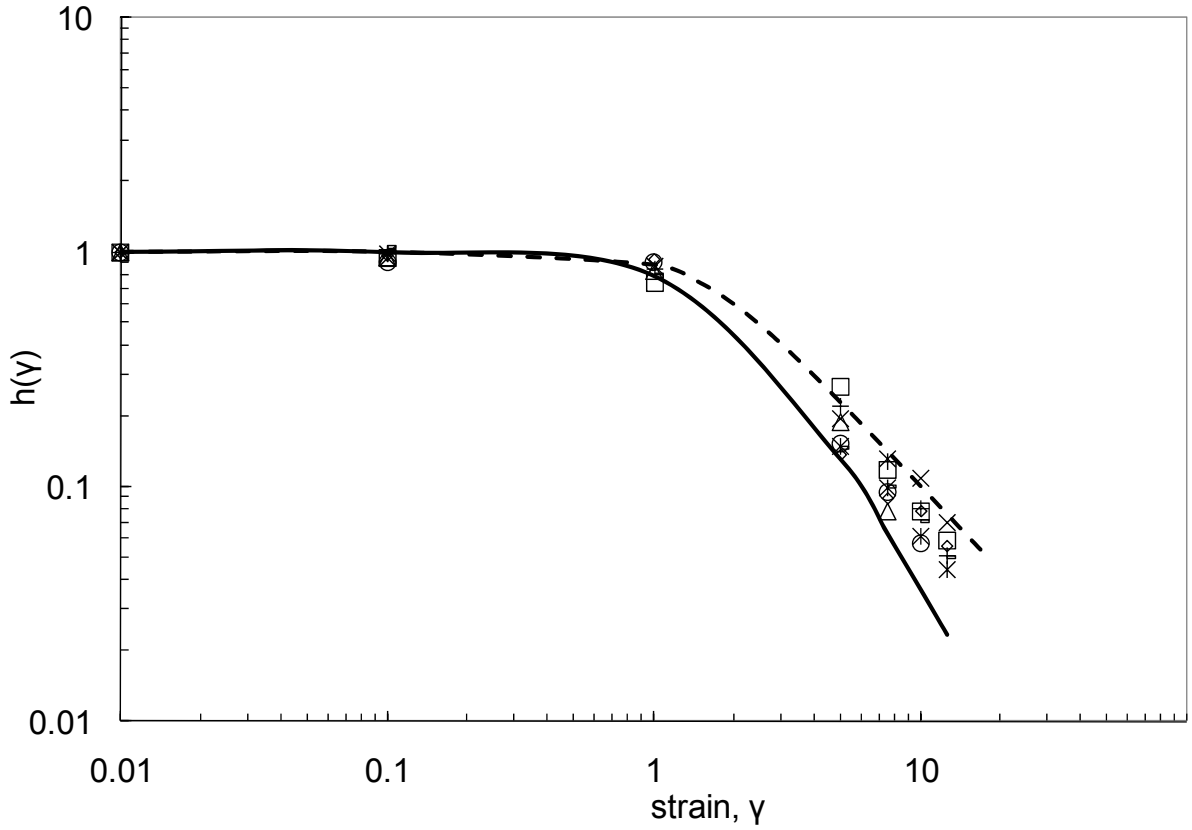

Figure 6.10: Damping function, *h(γ)*, for HDBL (Δ), HDB1 (x), HDB2 (O), HDB3 (□), HDB4 (-), HDB5 (◊), HDB6 (+), and HDB7 (*) PE resins, Doi-Edwards tube theory predictions for a linear chain (solid line), and data from the work of Stadler *et al.*[9] for sparsely-branched HDPE (dashed line) are given at a temperature at 170 ^{o}C.

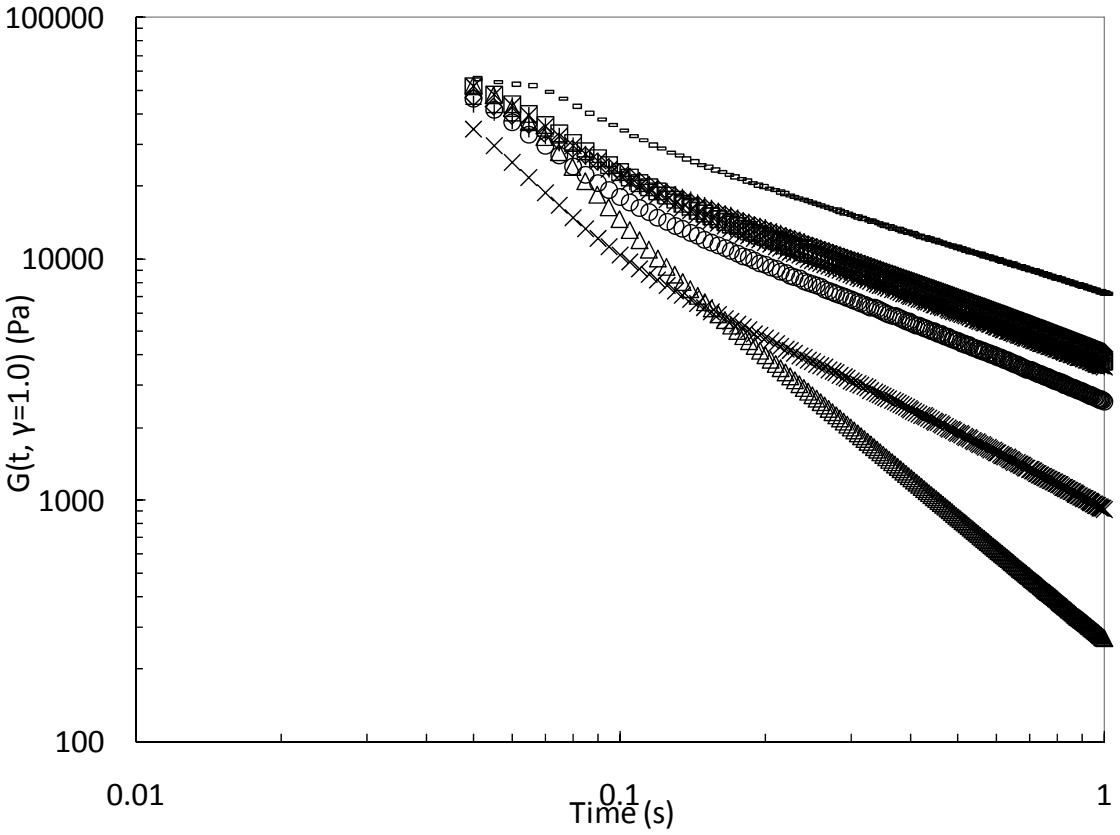

Figure 6.11: Relaxation modulus of HDBL (Δ), HDB1 (x), HDB2 (O), HDB3 (□), HDB4 (-), HDB5 (◊), HDB6 (+), and HDB7 (*) PE resins at a strain of 1.0 and a temperature at 170 ^{o}C.

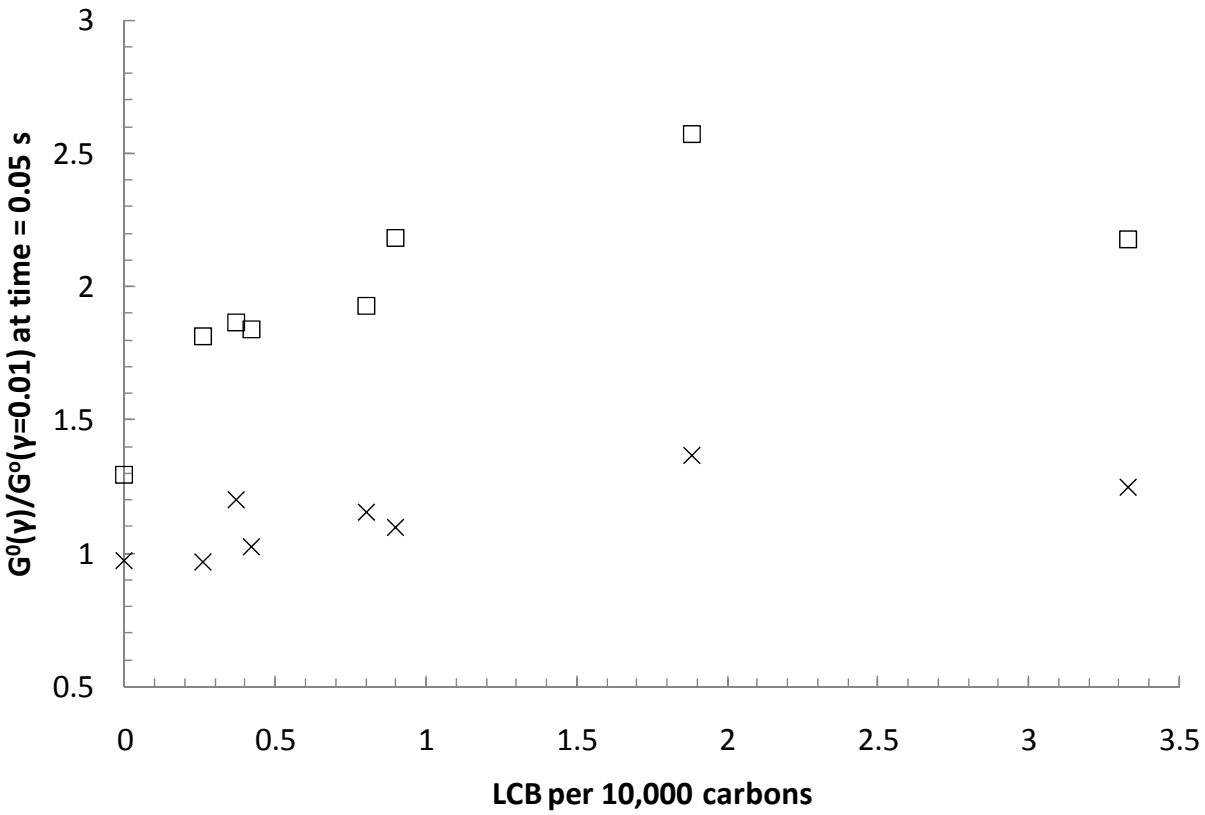

Figure 6.12: Magnitude of $G^0(\gamma)/ G^0(\gamma=0.01)$ evaluated at t = 0.05 sec. and γ = 5.0 (x) and 12.5 (□) as a function of LCB per 10,000 carbons.

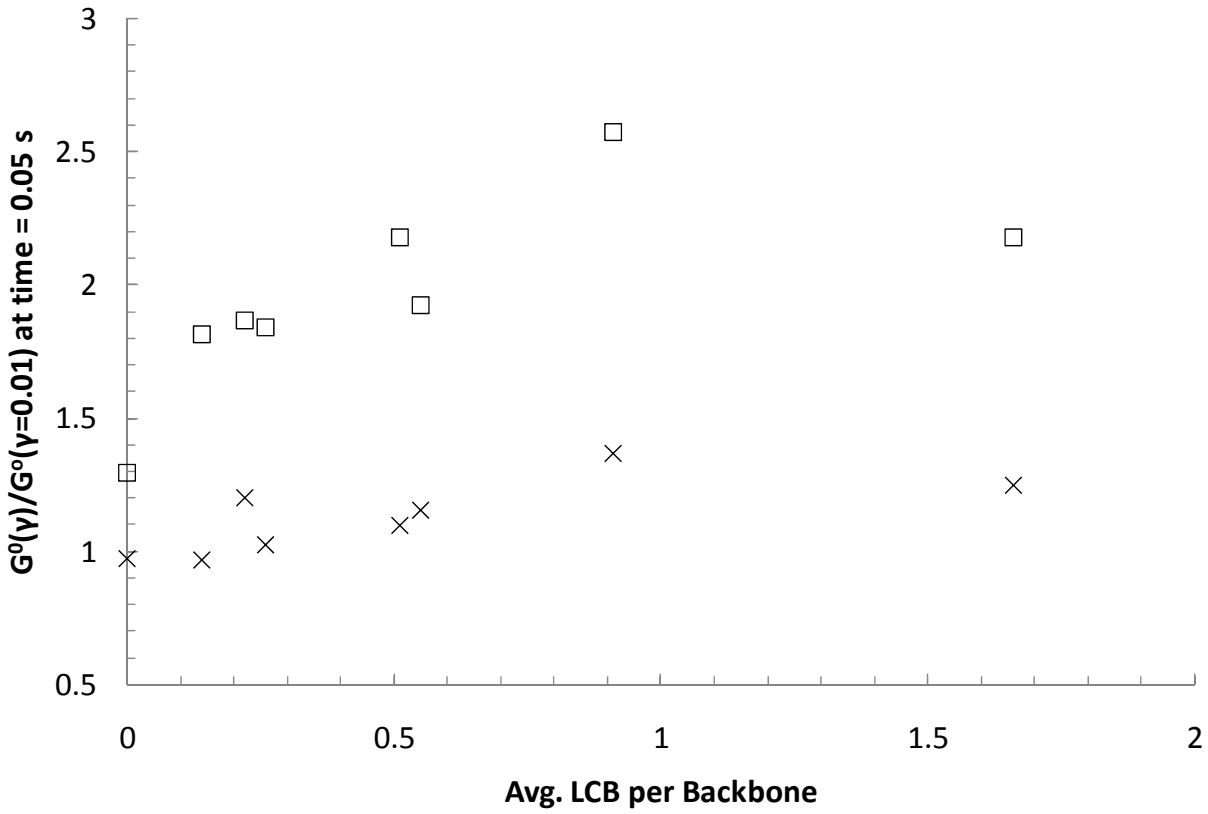

Figure 6.13: Magnitude of $G^0(\gamma)/ G^0(\gamma=0.01)$ evaluated at t = 0.05 sec. and γ = 5.0 (x) and 12.5 (□) as a function of the average number of LCB per backbone chain. All measurements were made at 170 °C.

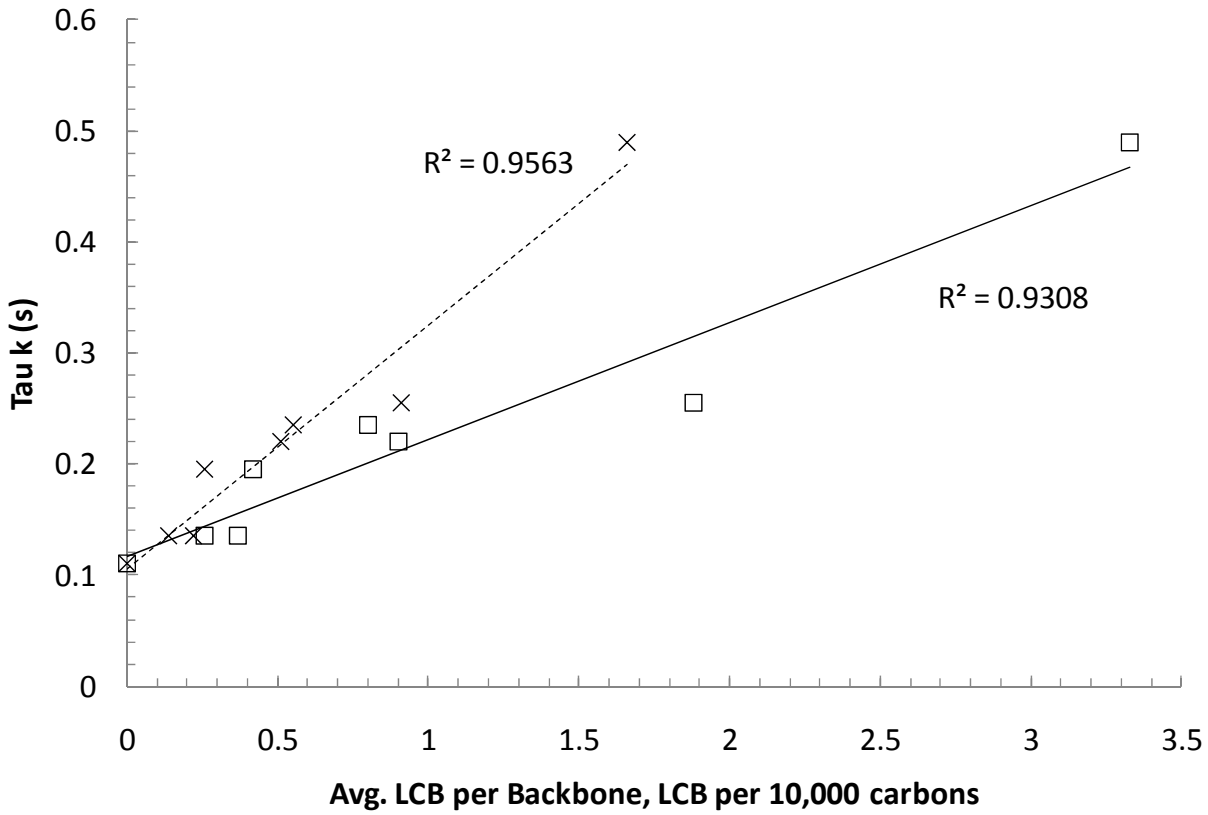

Figure 6.14: Magnitude of τ_k in sec. evaluated as a function of LCB per 10,000 carbons (□) and average number of LCB per backbone chain (x). All measurements are taken at 170 ^{o}C.

6.8 References

1. M. H. Wagner. *J. Non-Newtonian Fluid Mech.* **1978,** 4, (1-2), 39-55.

2. A. C. Papanastasiou, L. E. Scriven and C. W. Macosko. *J. Rheol.* **1983,** 27, (4), 387-410.

3. P. R. Soskey and H. H. Winter. *J. Rheol.* **1984,** 28, (5), 625-645.

4. D. A. Vega and S. T. Milner. *J. Polym. Sci., Part B: Polym. Phys.* **2007,** 45, (23), 3117-3136.

5. K. Osaki and M. Kurata. *Macromolecules* **1980,** 13, (3), 671-676.

6. J. Sanchez-Reyes and L. A. Archer. *Macromolecules* **2002,** 35, (13), 5194-5202.

7. C. Sui, G. B. McKenna and J. E. Puskas. *J. Rheol.* **2007,** 51, (6), 1143-1169.

8. D. C. Venerus. *J. Rheol.* **2005,** 49, (1), 277-295.

9. F. J. Stadler, D. Auhl and H. M. Münstedt. *Macromolecules* **2008,** 41, 3720-3726.

10. D. C. Venerus and H. Kahvand. *Part B: Polym. Phys.* **1994,** 32, 1531-1542.

11. L. A. Archer and S. K. Varshney. *Macromolecules* **1998,** 31, (18), 6348-6355.

12. L. J. Kasehagen and C. W. Macosko. *J. Rheol.* **1998,** 42, (6), 1303-1327.

13. T. C. B. McLeish, J. Allgaier, D. K. Bick, G. Bishko, P. Biswas, R. Blackwell, B. Blottiere, N. Clarke, B. Gibbs, D. J. Groves, A. Hakiki, R. K. Heenan, J. M. Johnson, R. Kant, D. J. Read and R. N. Young. *Macromolecules* **1999,** 32, (20), 6734-6758.

14. H. Gevgilili and D. M. Kalyon. *J. Rheol.* **2001,** 45, (2), 467-475.

15. M. Doi and S. F. Edwards, *The Theory of Polymer Dynamics*. Oxford University Press: 1988.

16. K. Osaki, K. Nishizawa and M. Kurata. *Macromolecules* **1982,** 15, (4), 1068-1071.

17. T. Inoue, T. Uematsu, Y. Yamashita and K. Osaki. *Macromolecules* **2002,** 35, (12), 4718-4724.

18. L. J. Zapas and T. Craft. *J. Res. Natl. Bur. Stand.* **1965,** 69A, 541-546.

19. L. A. Archer. *J. Rheol.* **1999,** 43, (6), 1555-1571.

20. R. Fulchiron and V. Verney. *J. Non-Newtonian Fluid Mech.* **1993,** 48, (1-2), 49-61.

21. M. H. Wagner and H. M. Laun. *Rheol. Acta* **1978,** 17, (2), 138-148.

22. J. Hepperle and H. Münstedt. *Rheol. Acta* **2006,** 45, (5), 717-727.

23. O. Urakawa, M. Takahashi, T. Masuda and N. G. Ebrahimi. *Macromolecules* **1995,** 28, (21), 7196-7201.

24. K. Osaki, E. Takatori and M. Kurata. *Macromolecules* **1987,** 20, (7), 1681-1687.

25. D. C. Venerus, E. F. Brown and W. R. Burghardt. *Macromolecules* **1998,** 31, (26), 9206-9212.

26. P. J. R. Leblans, J. Sampers and H. C. Booij. *Rheol. Acta* **1985,** 24, (2), 152-158.

27. C. M. Vrentas and W. W. Graessley. *J. Rheol.* **1982,** 26, (4), 359-371.

28. K. Osaki, E. Takatori, M. Kurata, H. Watanabe, H. Yoshida and T. Kotaka. *Macromolecules* **1990,** 23, (20), 4392-4396.

29. L. J. Fetters, A. D. Kiss, D. S. Pearson, G. F. Quack and F. J. Vitus. *Macromolecules* **1993,** 26, (4), 647-654.

30. R. G. Larson. *J. Rheol.* **1985,** 29, (6), 823-831.

31. P. J. Carreau. *Trans. Soc. Rheol.* **1972,** 16, (1), 99-127.

32. K. Yasuda, R. C. Armstrong and R. E. Cohen. *Rheol. Acta* **1981,** 20, (2), 163-178.

33. C. Das, N. J. Inkson, D. J. Read, M. A. Kelmanson and T. C. B. McLeish. *J. Rheol.* **2006,** 50, (2), 207-234.

34. P. M. Wood-Adams. *J. Rheol.* **2001,** 45, (1), 203-210.

35. P. M. Wood-Adams and J. M. Dealy. *Macromolecules* **2000,** 33, (20), 7481-7488.

36. P. M. Wood-Adams, J. M. Dealy, A. W. deGroot and O. D. Redwine. *Macromolecules* **2000,** 33, (20), 7489-7499.

37. C. D. McGrady and D. G. Baird. *Journal of Rheology* **2009,** 53, (3), 539-545.

38. J. Stevens. *J. of Studies in Surface Sci. and Catalysts* **1994,** 89.

39. J. Stevens. *J. of Studies in Surface Sci. and Catalysts* **1996,** 101.

40. S. Y. Lai, J. R. Wilson, J. R. Knight and G. W. Stevens. *PCT Int. Appl.* **1993**.

41. P. Wood-Adams and J. M. Dealy. *Annu. Tech. Conf. - Soc. Plast. Eng.* **1999,** 57th, (Vol. 1), 1205-1209.

42. R. B. Bird, R. C. Armstrong and O. Hassager, *Dynamics of Polymeric Liquids*. 2nd ed.; John Wiley & Sons, Inc.: Hoboken, NJ, 1987; Vol. 1, p 633.

43. J. Janzen and R. H. Colby. *Polym. Mater. Sci. Eng.* **2000,** 82, 128-129.

44. P. J. Doerpinghaus and D. G. Baird. *Macromolecules* **2002,** 35, (27), 10087-10095.

45. P. J. Doerpinghaus and D. G. Baird. *J. Rheol.* **2003,** 47, (3), 717-736.

46. S. E. Bin Wadud and D. G. Baird. *J. Rheol.* **2000,** 44, (5), 1151-1167.

47. H. M. Laun. *Rheol. Acta* **1978,** 17, (1), 1-15.

48. B. Elbirli and M. T. Shaw. *J. Rheol. (N. Y., NY, U. S.)* **1978,** 22, (5), 561-570.

49. D. G. Baird and D. I. Collias, *Polymer Processing*. John Wiley & Sons, Inc.: New York, 1998.

7.0 – Recommendations

7.0 – Recommendations

7.1 – Rheological Considerations

1) The encapsulation technique presented in this work should be extended to more contemporary extensional rheometers such as the SER[1], which have higher achievable Hencky strains relative to the RER used in our study. The technique can be replicated to the SER by taking a "sandwich" approach in which the rectangular core sample has a stable resin placed on both the top and bottom (perpendicular to the direction of flow). Unlike the RER approach, this technique will introduce more free surface area, so care will have to be taken to ensure uniform sample deformation.
2) Further validation of the behavior seen at short times in the relaxation modulus curves following the step-strain of LCB polymers should be investigated. This can be done by both varying the cone-and-plate geometry and the rheometer used. This variation can serve to eliminate the presence of mechanical artifacts.

7.2 – Processing Considerations

1) The exact effect of LCB distribution on the film-casting process should be investigated using a series of blended model and linear resins. LCB concentration and distribution can be controlled by carefully selecting model branching systems with known branching structure and blending them with monodisperse linear systems to concentrations reminiscent of sparsely-branched systems. The length of the linear systems should be selected so that they are different in length than the branched backbones in order to gain an understanding of the presence (or absence) of LCB across different backbone molecular weights. Furthermore, since material quantity will be an issue when dealing with model systems, a microtruder, which requires less material, should be employed.

2) The air-gap length in the film-casting experiments should be reduced to mimic the response of industrial process. This will allow for analysis that is based more on the LCB content of the material rather than the non-isothermal nature native to larger air-gap lengths.

3) Why a material chooses to neck or thin during the film-casting process is not well-understood. The evolution of film thickness as function of distance from the die should be investigated for a series of PE resins with varying LCB contents. This can either be done with either an online video capture sensitive enough to measure variation in film-thickness, or by inducing a rapid temperature drop of the film prior to contacting the chill roll. This allows for the study of the evolution of thinning in a similar fashion to that used to study film-thickness in this work.

7.3 – Modeling Considerations

1) The quantitative validity of the Pom-pom model to predict specific molecular features needs to be validated. For this, as series of well-defined comb resins with known branching content and structure should be utilized to formulate Pom-pom parameters based solely on structure. These parameters can then be tested by comparing their predictions for simple rheological flows with measured experimental values.

2) Full three-dimensional film-casting flow simulations that improve upon the approach of Ito and Doi[2] should be employed using Polyflow® software. This can allow for a fundamental understanding of how the viscoelastic properties of the material affect both the necking and thinning behavior of drawn films.

7.4 – References

1. M. Sentmanat, B. N. Wang and G. H. McKinley. *Journal of Rheology* **2005,** 49, (3), 585-606.

2. H. Ito, M. Doi, T. Isaki and M. Takeo. *J. Soc. Rheol., Jpn.* **2003,** 31, (3), 157-163.

8.0 – Appendix

8.1 – Dynamic Oscillatory Data

Table of Contents

8.1.1 – HDBL

Dynamic Oscillatory Test – 25mm C & P – 170 °C

ω (rad/sec)	G' (Pa)	G" (Pa)	|η*| (Pa s)
0.1	17.29573	678.6417	6788.595
0.158489	35.3711	1067.009	6736.074
0.25119	76.31869	1679.662	6693.713
0.398109	167.0283	2629.784	6618.991
0.630966	333.1372	4094.155	6510.152
1.000031	664.2717	6338.923	6373.439
1.584961	1310.588	9728.758	6193.614
2.512024	2530.946	14781.3	5969.854
3.981323	4770.518	22101.88	5679.231
6.310059	8724.801	32501.04	5333.032
10.00073	15422.27	46795.87	4926.809
15.8501	26276.64	65761.4	4467.911
25.12061	43036.77	89871.05	3966.633
39.81348	67655.23	118897.5	3435.987
63.10059	101500.6	151653.3	2891.984
100	145218.7	185807.1	2358.235

Dynamic Oscillatory Test – 50mm C & P – 170 °C

ω (rad/sec)	G' (Pa)	G" (Pa)	|η*| (Pa s)
0.01	1.886286	75.00178	7502.556
0.015849	5.936389	117.4058	7417.185
0.025119	8.255402	184.9251	7369.204
0.039811	11.61819	290.0486	7291.456
0.063097	18.83766	455.3016	7222.073
0.100002	32.7529	716.7026	7174.341
0.158493	61.42284	1123.703	7100.505
0.251198	120.0741	1755.463	7004.697
0.398125	239.3176	2735.117	6896.25
0.630981	477.4682	4238.372	6759.599
1.000031	956.3394	6505.419	6575.136
1.584961	1907.095	9870.889	6343.014
2.512024	3739.36	14710.17	6042.141

8.1.2 – HDB1

Dynamic Oscillatory Test – 25mm C & P –170 °C

ω (rad/sec)	G' (Pa)	G" (Pa)	|η*| (Pa s)
0.1	84.03716	711.6143	7165.565
0.158489	170.2768	1070.714	6840.647
0.25119	326.6381	1627.719	6609.212
0.398109	571.4735	2399.493	6195.8
0.630966	976.8436	3487.127	5739.395
1.000031	1596.223	4992.652	5241.453
1.584961	2500.584	7075.413	4734.685
2.512024	3824.815	9938.286	4239.166
3.981323	5652.62	13939.45	3778.129
6.310059	8281.193	19512.69	3359.278
10.00073	12035.93	27257.58	2979.445
15.8501	17548.26	37949.01	2637.833
25.12061	25727.68	52508.21	2327.668
39.81348	37904.79	71914.88	2041.842
63.10059	55659.99	96838.35	1770.105
100.0078	80971.96	127299.4	1508.576
158.5039	115101.8	162338.7	1255.51
251.2109	156811.5	195990.6	999.1694

Dynamic Oscillatory Test – 50mm C & P – 170 °C

ω (rad/sec)	G' (Pa)	G" (Pa)	|η*| (Pa s)
0.01	1.803822	82.09737	8211.726
0.015849	4.050373	130.2778	8223.854
0.025119	10.24243	205.5003	8191.126
0.039811	22.57066	321.6166	8098.429
0.063097	48.7828	497.3441	7920.04
0.100002	100.1858	764.5712	7710.896
0.158493	197.839	1157.016	7406.057
0.251198	371.0659	1726.818	7031.257
0.398125	661.923	2534.958	6580.734
0.630981	1128.739	3652.841	6059.224
1.000031	1857.428	5181.995	5504.658
1.584961	2935.726	7243.354	4931.142
2.512024	4501.724	10018.72	4372.424
3.981323	6789.42	13716.83	3844.236
6.310059	10111.44	18593.15	3354.128
10	15010.72	24864.59	2904.427

8.1.3 – HDB2

Dynamic Oscillatory Test – 25mm C & P – 170 °C

ω (rad/sec)	G' (Pa)	G" (Pa)	|η*| (Pa s)
0.1	474.2427	1719.466	17836.61
0.158489	821.4525	2444.617	16272.03
0.25119	1330.473	3435.332	14666.07
0.398109	2082.257	4728.763	12978.63
0.630966	3137.52	6425.795	11333.2
1.000031	4573.263	8675.983	9807.22
1.584961	6473.731	11638.28	8402.485
2.512024	9002.111	15571.73	7160.191
3.981323	12359.77	20881.76	6094.818
6.310059	16861.74	28087.41	5191.719
10.00073	23008.1	37890.71	4432.596
15.8501	31610.7	51065.56	3789.106
25.12061	43672.01	68420.87	3231.234
39.81348	60861.47	90845.91	2746.52
63.10059	84802.9	118712.4	2312.038
100.0078	116998.5	151714.3	1915.728
158.5039	158598.8	188619	1554.763
251.2109	206480.8	223100.1	1210.086

Dynamic Oscillatory Test – 50mm C & P – 170 °C

ω (rad/sec)	G' (Pa)	G" (Pa)	|η*| (Pa s)
0.01	16.62026	224.6431	22525.73
0.015849	35.99997	351.1323	22270.83
0.025119	74.44399	538.6902	21649.08
0.039811	144.6391	814.9421	20790.12
0.063097	275.5056	1209.44	19658.98
0.100002	494.3516	1766.807	18346.22
0.158493	851.1954	2528.169	16831.12
0.251198	1405.63	3539.42	15160.64
0.398125	2214.999	4865.918	13428.81
0.630981	3377.375	6575.157	11714.84
1.000031	4969.348	8774.216	10083.41
1.584961	7168.514	11505.72	8552.985
2.512024	10058.6	15127.11	7231.634

8.1.4 – HDB3

Dynamic Oscillatory Test – 25mm C & P – 170 °C

ω (rad/sec)	G' (Pa)	G" (Pa)	|η*| (Pa s)
0.1	943.5531	2340.753	25237.61
0.158489	1459.982	3272.713	22611.01
0.25119	2252.222	4445.596	19839.77
0.398109	3314.405	5932.69	17070.03
0.630966	4756.877	7826.825	14515.82
1.000031	6627.979	10228.15	12187.54
1.584961	9044.971	13389.5	10194.75
2.512024	12149.45	17488.27	8476.964
3.981323	16128.03	22918.36	7038.956
6.310059	21348.5	30238.49	5866.062
10.00073	28243.62	40031.03	4898.81
15.8501	37673.97	53011.54	4103.129
25.12061	50667.18	70010.59	3440.256
39.81348	68657.24	91661.76	2876.508
63.10059	93116.62	118382.8	2386.92
100.0078	125504.5	149668.1	1953.099
158.5039	166717.8	184386.6	1568.305
251.2109	213260.4	216593.4	1209.986

Dynamic Oscillatory Test – 50mm C & P – 170 °C

ω (rad/sec)	G' (Pa)	G" (Pa)	|η*| (Pa s)
0.01	59.7066	396.7965	40126.38
0.015849	112.3976	607.5931	38986.52
0.025119	214.4091	908.8155	37173.2
0.039811	384.4393	1326.736	34696.62
0.063097	659.2424	1896.217	31816.82
0.100002	1088.047	2649.282	28639.42
0.158493	1728.414	3621.089	25316.21
0.251198	2634.491	4855.508	21991.33
0.398125	3890.277	6391.438	18793.85
0.630981	5566.488	8279.738	15811.82
1.000031	7765.227	10561.93	13108.87
1.584961	10627.33	13252.67	10717.9

8.1.5 – HDB4

Dynamic Oscillatory Test – 25mm C & P – 170 °C

ω (rad/sec)	G' (Pa)	G" (Pa)	|η*| (Pa s)
0.1	2184.16	3876.385	44493.56
0.158489	3172.278	5129.587	38054.66
0.25119	4512.124	6603.544	31839.93
0.398109	6235.011	8448.135	26374.22
0.630966	8431.546	10743.62	21644.74
1.000031	11183.92	13584.55	17595.48
1.584961	14635.01	17208.08	14252.63
2.512024	18875.01	21875.08	11501.74
3.981323	24271.23	27856.3	9280.029
6.310059	31120.04	35650.79	7499.562
10.00073	39972.74	45803.62	6078.857
15.8501	51570.4	58759.22	4932.478
25.12061	66811.48	75277.41	4006.679
39.81348	86947.58	95764.81	3248.837
63.10059	113132.4	120433.6	2618.625
100.0078	146475.2	149000.8	2089.244
158.5039	187337	180467.6	1641.111
251.2109	232097.1	209081.3	1243.515

Dynamic Oscillatory Test – 50mm C & P – 170 °C

ω (rad/sec)	G' (Pa)	G" (Pa)	|η*| (Pa s)
0.01	2350.308	7909.081	82509.17
0.015849	4015.191	11375.36	76112.74
0.025119	6609.147	15824.75	68271.99
0.039811	10458.94	21594.69	60269.99
0.063097	16007.66	28820.13	52248.65
0.100002	23756.46	37767.11	44616.51
0.158493	34125.73	48525.06	37429.55
0.251198	47812	61338.08	30960.11
0.398125	65059.02	76054.31	25139.02

8.1.6 – HDB6

Dynamic Oscillatory Test – 25mm C & P – 170 ^{o}C

ω (rad/sec)	G' (Pa)	G" (Pa)	|η*| (Pa s)
0.1	816.8775	2192.935	23401.31
0.158489	1301.826	3069.791	21038.79
0.25119	2034.127	4206.289	18600.71
0.398109	3099.197	5657.499	16203.49
0.630966	4558.752	7426.633	13810.87
1.000031	6547.683	9639.337	11652.5
1.584961	9160.002	12319.38	9685.813
2.512024	12510.95	15549.45	7944.862
3.981323	16732.85	19386.36	6432.275
6.310059	22004.75	24077.65	5169.227
10.00073	28477.09	29767.89	4119.252
15.8501	36415.26	36703.09	3261.992
25.12061	46036.34	45400.31	2573.865
39.81348	57914.77	56290.78	2028.551
63.10059	72602.91	69832.53	1596.437
100.0078	90730.02	86447.23	1253.101
158.5039	112850.4	105931.5	976.503
251.2109	137657.5	124769.8	739.5687

Dynamic Oscillatory Test – 50mm C & P – 170 ^{o}C

ω (rad/sec)	G' (Pa)	G" (Pa)	|η*| (Pa s)
0.01	47.61739	390.4155	39330.9
0.015849	79.74508	566.1417	36073.34
0.025119	155.2733	853.9415	34552.84
0.039811	301.4295	1213.84	31416
0.063097	522.4232	1747.338	28904.13
0.100002	888.8649	2425.159	25828.61
0.158493	1456.747	3347.5	23034.04
0.251198	2283.74	4524.92	20177.59
0.398125	3470.074	6014.517	17441.17
0.630981	5124.288	7794.622	14783.56
1	7339.98	9878.273	12306.73

8.1.7 – Lupolen 1840H

Dynamic Oscillatory Test – 25mm C & P – 170 °C

ω (rad/sec)	G' (Pa)	G" (Pa)	|η*| (Pa s)
0.1	679.7955	1558.275	17000.94
0.158489	1054.281	2115.962	14916.25
0.25119	1585.763	2822.384	12888.08
0.398109	2328.123	3700.41	10981.56
0.630966	3331.74	4773.387	9225.761
1.000031	4629.793	6065.094	7629.993
1.584961	6333.395	7611.519	6247.393
2.512024	8451.589	9447.004	5046.04
3.981323	11151.58	11612.98	4043.952
6.310059	14493.61	14110.44	3205.665
10.00073	18573.96	17020.17	2519.098
15.8501	23506.46	20368.09	1962.339
25.12061	29418.73	24171.99	1515.71
39.81348	36433.88	28525.04	1162.221
63.10059	44690.48	33396.04	884.1454
100.0078	54197.37	38800.73	666.4951
158.5039	64914.55	44425.56	496.2707

Dynamic Oscillatory Test – 50mm C & P – 170 °C

ω (rad/sec)	G' (Pa)	G" (Pa)	|η*| (Pa s)
0.01	34.42231	247.5815	24996.32
0.015849	73.30758	386.6484	24830.19
0.025119	144.4982	579.2402	23766.25
0.039811	260.0977	839.9666	22087.16
0.063097	446.9359	1189.658	20141.07
0.100002	727.5877	1638.22	17924.85
0.158493	1140.611	2211.761	15701.32
0.251198	1716.276	2925.77	13503.34
0.398125	2507.518	3802.873	11441.54
0.630981	3563.502	4849.712	9537.776
1	4952.611	6085.76	7846.326

Appendix 8.2 – Transient Extensional Data

Table of Contents

8.2.1 – HDB1

8.2.1.1 – HDB1 – Elongational Viscosity – 170 °C – Strain Rate = 10 s^{-1}

Time (sec)	Stress (Pa)	Viscosity (Pa s)
0.053	76015.721	7601.572
0.060	80411.850	8041.185
0.068	83938.173	8393.817
0.075	86999.940	8699.994
0.082	89815.194	8981.519
0.090	92391.949	9239.195
0.098	94659.311	9465.931
0.105	96808.846	9680.885
0.113	98529.119	9852.912
0.120	100237.159	10023.716
0.128	101890.199	10189.020
0.135	103613.463	10361.346
0.143	105306.505	10530.651
0.150	106845.188	10684.519
0.158	108355.878	10835.588
0.165	109858.754	10985.875
0.173	111374.940	11137.494
0.180	112739.195	11273.920
0.188	114348.546	11434.855
0.195	115634.674	11563.467
0.203	117128.149	11712.815
0.210	118530.383	11853.038
0.218	119970.719	11997.072
0.225	121211.098	12121.110
0.233	122709.917	12270.992
0.240	124138.212	12413.821
0.247	125317.909	12531.791
0.255	126924.457	12692.446
0.263	128129.064	12812.906
0.270	129672.271	12967.227
0.277	130309.731	13030.973
0.285	131329.841	13132.984
0.293	132153.578	13215.358
0.300	132932.912	13293.291
0.307	133789.196	13378.920
0.315	134514.796	13451.480
0.323	135227.746	13522.775
0.330	135126.482	13512.648
0.337	135554.292	13555.429

8.2.1.2 – HDB1 – Elongational Viscosity – 170 °C – Strain Rate = 3 s^{-1}

Time (sec)	Stress (Pa)	Viscosity (Pa s)
0.293	38006.098	12668.699
0.300	38116.313	12705.438
0.307	38244.349	12748.116
0.315	38489.364	12829.788
0.323	38692.774	12897.591
0.330	39057.178	13019.059
0.337	39418.130	13139.377
0.345	39811.642	13270.547
0.353	40128.289	13376.096
0.360	40439.884	13479.961
0.367	40782.593	13594.198
0.375	41001.837	13667.279
0.383	41330.759	13776.920
0.390	41611.806	13870.602
0.397	41969.351	13989.784
0.405	42299.867	14099.956
0.413	42577.830	14192.610
0.420	42801.010	14267.003
0.428	43013.006	14337.669
0.435	43141.051	14380.350
0.443	43180.339	14393.446
0.450	43420.970	14473.657
0.458	43474.197	14491.399
0.465	43532.621	14510.874
0.473	43597.851	14532.617
0.480	43832.619	14610.873
0.488	43972.723	14657.574
0.495	44067.997	14689.332
0.502	44260.580	14753.527
0.510	44380.377	14793.459
0.518	44603.782	14867.927
0.525	44658.408	14886.136
0.533	44946.667	14982.222
0.540	45192.300	15064.100
0.548	45360.106	15120.035
0.555	45512.149	15170.716
0.562	45751.285	15250.428
0.570	45942.035	15314.012
0.577	46009.351	15336.450
0.585	46240.403	15413.468
0.593	46307.679	15435.893
0.600	46586.080	15528.693
0.608	46575.933	15525.311
0.615	46743.034	15581.011
0.622	47018.991	15672.997
0.630	47240.561	15746.854
0.637	47447.872	15815.957
0.645	47684.870	15894.957
0.653	47999.532	15999.844
0.660	48023.223	16007.741
0.668	48168.083	16056.028
0.675	48147.170	16049.057
0.682	48423.297	16141.099
0.690	48611.080	16203.693
0.697	48860.841	16286.947
0.705	49255.759	16418.586
0.713	49588.595	16529.532
0.720	49883.934	16627.978
0.728	49938.850	16646.283
0.735	50233.088	16744.363
0.742	50187.244	16729.081
0.750	50478.081	16826.027
0.757	50570.098	16856.699
0.765	50798.433	16932.811
0.773	51011.977	17003.992
0.780	51307.442	17102.481
0.788	51590.976	17196.992
0.795	51755.672	17251.891
0.803	52079.348	17359.783
0.810	52099.797	17366.599
0.817	52429.499	17476.500
0.825	52594.950	17531.650
0.833	53091.513	17697.171
0.840	53384.020	17794.673
0.848	53539.228	17846.409
0.855	53757.807	17919.269
0.863	53916.983	17972.328
0.870	54184.620	18061.540
0.877	54259.631	18086.544
0.885	54674.616	18224.872
0.893	54519.602	18173.201
0.900	54760.108	18253.369
0.908	54688.540	18229.513
0.915	54687.384	18229.128
0.923	54707.695	18235.898
0.930	54909.271	18303.090
0.937	55199.214	18399.738
0.945	55199.007	18399.669
0.952	55674.605	18558.202
0.960	55685.790	18561.930
0.968	56311.229	18770.410
0.975	56428.577	18809.526
0.983	56369.218	18789.739
0.990	56215.968	18738.656
0.998	55994.373	18664.791
1.005	56190.378	18730.126
1.013	56233.705	18744.568
1.020	56624.434	18874.811
1.028	56096.882	18698.961
1.035	56229.695	18743.232
1.043	55937.707	18645.902
1.050	56126.141	18708.714
1.058	56103.858	18701.286
1.065	56168.533	18722.844
1.073	56246.179	18748.726
1.080	56217.090	18739.030
1.088	56576.555	18858.852
1.095	55896.353	18632.118
1.102	56337.119	18779.040
1.110	55962.718	18654.239
1.118	56320.645	18773.548
1.125	56291.308	18763.769
1.133	56519.521	18839.840
1.140	56287.846	18762.615
1.148	55915.424	18638.475
1.155	55908.285	18636.095
1.163	55764.686	18588.229

8.2.1.3 – HDB1 – Elongational Viscosity – 170 °C – Strain Rate = 1 s^{-1}

Time (sec)	Stress (Pa)	Viscosity (Pa s)
0.724	15738.182	15738.182
0.731	15751.072	15751.072
0.739	15734.677	15734.677
0.746	15756.040	15756.040
0.754	15717.899	15717.899
0.761	15776.850	15776.850
0.769	15756.541	15756.541
0.776	15804.788	15804.788
0.784	15792.759	15792.759
0.791	15850.466	15850.466
0.799	15887.805	15887.805
0.806	15986.919	15986.919
0.814	16086.306	16086.306
0.821	16081.633	16081.633
0.829	16118.218	16118.218
0.836	16080.045	16080.045
0.844	16072.460	16072.460
0.851	15988.329	15988.329
0.859	16000.041	16000.041
0.866	15977.880	15977.880
0.874	16042.848	16042.848
0.881	16097.016	16097.016
0.889	16105.894	16105.894
0.896	16193.335	16193.335
0.904	16156.059	16156.059
0.911	16208.698	16208.698
0.919	16145.846	16145.846
0.926	16209.453	16209.453
0.934	16190.729	16190.729
0.941	16194.258	16194.258
0.949	16220.920	16220.920
0.956	16283.327	16283.327
0.964	16381.554	16381.554
0.971	16419.727	16419.727
0.979	16530.975	16530.975
0.986	16482.551	16482.551
0.994	16506.997	16506.997
1.001	16518.233	16518.233
1.009	16604.754	16604.754
1.016	16602.183	16602.183
1.024	16637.428	16637.428
1.031	16620.540	16620.540
1.039	16589.330	16589.330
1.046	16661.712	16661.712
1.054	16641.773	16641.773
1.061	16740.203	16740.203
1.069	16718.658	16718.658
1.076	16817.675	16817.675
1.084	16807.798	16807.798
1.091	16783.402	16783.402
1.099	16743.751	16743.751
1.106	16688.506	16688.506
1.114	16715.949	16715.949
1.121	16686.265	16686.265
1.129	16754.864	16754.864
1.136	16780.573	16780.573
1.144	16935.621	16935.621
1.151	16902.855	16902.855
1.159	16942.193	16942.193
1.166	16936.430	16936.430
1.174	16944.643	16944.643
1.181	16936.882	16936.882
1.189	16867.499	16867.499
1.196	16918.579	16918.579
1.204	16830.601	16830.601
1.211	16942.180	16942.180
1.219	16960.185	16960.185
1.226	17056.678	17056.678
1.234	17105.797	17105.797
1.241	17154.689	17154.689
1.249	17219.545	17219.545
1.256	17171.175	17171.175
1.264	17137.540	17137.540
1.271	17036.172	17036.172
1.279	17148.241	17148.241
1.286	17093.405	17093.405
1.294	17188.722	17188.722
1.301	17182.612	17182.612
1.309	17226.504	17226.504
1.316	17270.611	17270.611
1.324	17278.962	17278.962
1.331	17286.993	17286.993
1.339	17206.103	17206.103
1.346	17300.197	17300.197
1.354	17189.509	17189.509
1.361	17265.095	17265.095
1.369	17231.838	17231.838
1.376	17297.730	17297.730
1.384	17336.115	17336.115
1.391	17373.815	17373.815
1.399	17429.915	17429.915
1.406	17476.685	17476.685
1.414	17560.792	17560.792
1.421	17463.813	17463.813
1.429	17518.317	17518.317
1.436	17388.549	17388.549
1.444	17470.548	17470.548
1.451	17493.907	17493.907
1.459	17585.948	17585.948
1.466	17618.298	17618.298
1.474	17650.448	17650.448
1.481	17803.760	17803.760
1.489	17784.317	17784.317
1.496	17877.028	17877.028
1.504	17731.692	17731.692
1.511	17760.856	17760.856
1.519	17599.806	17599.806
1.526	17573.286	17573.286
1.534	17588.115	17588.115
1.541	17591.325	17591.325
1.549	17658.504	17658.504
1.556	17649.277	17649.277
1.564	17815.431	17815.431
1.571	17716.480	17716.480
1.579	17894.566	17894.566
1.586	17894.134	17894.134
1.594	18017.410	18017.410
1.601	17970.133	17970.133
1.609	17967.193	17967.193
1.616	17893.740	17893.740
1.624	17782.816	17782.816
1.631	17881.437	17881.437
1.639	17802.587	17802.587
1.646	18032.276	18032.276
1.654	17950.968	17950.968
1.661	18049.782	18049.782

8.2.1.3 Continued

Time (sec)	Stress (Pa)	Viscosity (Pa s)
1.669	18075.497	18075.497
1.676	18125.406	18125.406
1.684	18137.892	18137.892
1.691	18111.726	18111.726
1.699	18210.362	18210.362
1.706	18131.489	18131.489
1.714	18280.878	18280.878
1.721	18160.699	18160.699
1.729	18323.194	18323.194
1.736	18304.118	18304.118
1.744	18415.750	18415.750
1.751	18528.025	18528.025
1.759	18654.022	18654.022
1.766	18659.416	18659.416
1.774	18541.882	18541.882
1.781	18654.303	18654.303
1.789	18422.513	18422.513
1.796	18491.624	18491.624
1.804	18476.957	18476.957
1.811	18545.427	18545.427
1.819	18514.521	18514.521
1.826	18467.672	18467.672
1.834	18534.907	18534.907
1.841	18543.529	18543.529
1.849	18697.884	18697.884
1.856	18631.880	18631.880
1.864	18816.622	18816.622
1.871	18658.758	18658.758
1.879	18724.127	18724.127
1.886	18652.022	18652.022
1.894	18685.337	18685.337
1.901	18995.638	18995.638
1.909	19169.974	19169.974
1.916	19376.952	19376.952
1.924	19207.162	19207.162
1.931	19335.734	19335.734
1.939	19208.805	19208.805
1.946	19273.070	19273.070
1.954	19239.384	19239.384
1.961	19253.131	19253.131
1.969	19315.398	19315.398
1.976	19344.499	19344.499

Time (sec)	Stress (Pa)	Viscosity (Pa s)
1.984	19406.203	19406.203
1.991	19265.114	19265.114
1.999	19410.149	19410.149
2.006	19110.879	19110.879
2.014	19341.230	19341.230
2.021	19364.636	19364.636
2.029	19440.299	19440.299
2.036	19304.046	19304.046
2.044	19289.617	19289.617
2.051	19309.467	19309.467
2.059	19219.855	19219.855
2.066	19419.009	19419.009
2.074	19271.797	19271.797
2.081	19416.883	19416.883
2.089	19339.680	19339.680
2.096	19504.170	19504.170
2.104	19405.214	19405.214
2.111	19494.328	19494.328
2.119	19487.632	19487.632
2.126	19421.900	19421.900
2.134	19509.851	19509.851
2.141	19342.835	19342.835
2.149	19468.535	19468.535
2.156	19356.056	19356.056
2.164	19662.292	19662.292
2.171	19810.311	19810.311
2.179	20040.915	20040.915
2.186	19966.217	19966.217
2.194	19816.336	19816.336
2.201	19882.194	19882.194
2.209	19716.250	19716.250
2.216	19917.627	19917.627
2.224	19800.523	19800.523
2.231	19971.213	19971.213
2.239	19894.067	19894.067
2.246	20021.876	20021.876
2.254	20040.544	20040.544
2.261	20113.741	20113.741
2.269	20298.850	20298.850
2.276	20260.377	20260.377
2.284	20582.829	20582.829
2.291	20406.504	20406.504

Time (sec)	Stress (Pa)	Viscosity (Pa s)
2.299	20502.629	20502.629
2.306	20286.073	20286.073
2.314	20427.043	20427.043
2.321	20522.019	20522.019
2.329	20640.745	20640.745
2.336	20664.728	20664.728
2.344	20435.218	20435.218
2.351	20625.273	20625.273
2.359	20462.987	20462.987
2.366	20752.437	20752.437
2.374	20499.020	20499.020
2.381	20740.911	20740.911
2.389	20783.885	20783.885
2.396	20724.675	20724.675
2.404	20829.298	20829.298
2.411	20806.013	20806.013
2.419	21014.427	21014.427
2.426	20976.681	20976.681
2.434	21305.538	21305.538
2.441	21041.418	21041.418
2.449	21133.016	21133.016
2.456	20847.231	20847.231
2.464	21045.108	21045.108
2.471	20971.069	20971.069
2.479	21073.961	21073.961
2.486	21301.965	21301.965
2.494	21364.329	21364.329
2.501	21651.803	21651.803
2.509	21431.587	21431.587
2.516	21664.395	21664.395
2.524	21481.503	21481.503
2.531	21483.521	21483.521
2.299	20502.629	20502.629
2.306	20286.073	20286.073
2.314	20427.043	20427.043
2.321	20522.019	20522.019
2.329	20640.745	20640.745
2.336	20664.728	20664.728
2.344	20435.218	20435.218
2.351	20625.273	20625.273
2.359	20462.987	20462.987
2.366	20752.437	20752.437

8.2.1.3 Continued

Time (sec)	Stress (Pa)	Viscosity (Pa s)
2.374	20499.020	20499.020
2.381	20740.911	20740.911
2.389	20783.885	20783.885
2.396	20724.675	20724.675
2.404	20829.298	20829.298
2.411	20806.013	20806.013
2.419	21014.427	21014.427
2.426	20976.681	20976.681
2.434	21305.538	21305.538
2.441	21041.418	21041.418
2.449	21133.016	21133.016
2.456	20847.231	20847.231
2.464	21045.108	21045.108
2.471	20971.069	20971.069
2.479	21073.961	21073.961
2.486	21301.965	21301.965
2.494	21364.329	21364.329
2.501	21651.803	21651.803
2.509	21431.587	21431.587
2.516	21664.395	21664.395
2.524	21481.503	21481.503
2.531	21483.521	21483.521
2.539	21308.752	21308.752
2.546	21528.442	21528.442
2.554	21630.789	21630.789
2.561	21404.799	21404.799
2.569	21550.781	21550.781
2.576	21409.003	21409.003
2.584	21769.246	21769.246
2.591	21578.491	21578.491
2.599	21927.401	21927.401
2.606	21936.074	21936.074
2.614	22101.217	22101.217
2.621	22156.270	22156.270
2.629	22226.994	22226.994
2.636	22426.750	22426.750
2.644	22221.828	22221.828
2.651	22667.431	22667.431
2.659	22408.916	22408.916
2.666	22959.883	22959.883
2.674	22814.411	22814.411
2.681	22901.873	22901.873

Time (sec)	Stress (Pa)	Viscosity (Pa s)
2.689	22904.431	22904.431
2.696	22854.086	22854.086
2.704	23060.826	23060.826
2.711	22973.861	22973.861
2.719	23199.105	23199.105
2.726	22597.434	22597.434
2.734	22660.841	22660.841
2.741	22293.876	22293.876
2.749	22479.858	22479.858
2.756	22594.243	22594.243
2.764	22782.756	22782.756
2.771	22899.156	22899.156
2.779	22587.675	22587.675
2.786	23001.475	23001.475
2.794	23004.385	23004.385
2.801	23310.854	23310.854
2.809	22834.759	22834.759
2.816	23045.488	23045.488
2.824	22946.346	22946.346
2.831	23314.955	23314.955
2.839	23510.327	23510.327
2.846	23508.498	23508.498
2.854	23965.803	23965.803
2.861	23903.781	23903.781
2.869	24165.568	24165.568
2.876	23629.794	23629.794
2.884	23828.457	23828.457
2.891	23549.410	23549.410
2.899	23747.776	23747.776
2.906	23651.715	23651.715
2.914	23617.069	23617.069
2.921	23773.299	23773.299
2.929	23671.834	23671.834
2.936	24415.795	24415.795
2.944	23963.434	23963.434
2.951	24298.688	24298.688
2.959	23880.599	23880.599
2.966	24037.828	24037.828
2.974	24127.894	24127.894
2.981	24332.426	24332.426
2.989	24377.906	24377.906
2.996	24422.686	24422.686

Time (sec)	Stress (Pa)	Viscosity (Pa s)
3.004	24839.991	24839.991
3.011	24440.052	24440.052
3.019	25025.967	25025.967
3.026	24380.524	24380.524
3.034	24468.279	24468.279
3.041	24047.671	24047.671
3.049	24082.486	24082.486
3.056	24018.502	24018.502
3.064	23803.759	23803.759
3.071	24156.800	24156.800
3.079	24213.223	24213.223
3.086	25103.673	25103.673
3.094	24732.105	24732.105
3.101	25458.039	25458.039
3.109	24795.365	24795.365
3.116	24904.210	24904.210
3.124	24671.683	24671.683
3.131	24592.222	24592.222
3.139	24644.168	24644.168
3.146	24789.598	24789.598
3.154	25476.632	25476.632
3.161	25259.767	25259.767
3.169	25944.506	25944.506
3.176	25240.181	25240.181
3.184	25444.208	25444.208
3.191	25242.045	25242.045
3.199	25191.475	25191.475
3.206	25096.149	25096.149
3.214	25327.970	25327.970
3.221	25793.813	25793.813
3.229	25185.591	25185.591
3.236	25111.079	25111.079
3.244	24366.967	24366.967

8.2.1.4 – HDB1 – Elongational Viscosity – 170 °C – Strain Rate = 0.3 s^{-1}

Time (sec)	Stress (Pa)	Viscosity (Pa s)
2.873	6394.080	21313.600
3.160	6412.560	21375.200
3.448	6352.500	21175.000
3.735	6546.540	21821.800
4.022	6569.640	21898.800
4.310	6518.820	21729.400
4.597	6715.170	22383.900
4.884	6585.810	21952.700

Time (sec)	Stress (Pa)	Viscosity (Pa s)
5.171	6553.470	21844.900
5.459	6583.500	21945.000
5.746	6574.260	21914.200
6.033	6703.620	22345.400
6.320	6715.170	22383.900
6.608	6715.170	22383.900
6.895	6782.160	22607.200
7.182	6856.080	22853.600

Time (sec)	Stress (Pa)	Viscosity (Pa s)
7.470	6860.700	22869.000
7.757	6978.510	23261.700
8.044	6957.720	23192.400
8.332	7003.920	23346.400
8.619	7135.590	23785.300
8.906	7121.730	23739.100
9.193	7082.460	23608.200

8.2.1.5 – HDB1 – Elongational Viscosity – 170 °C – Strain Rate = 0.1 s^{-1}

Time (sec)	Stress (Pa)	Viscosity (Pa s)
9.082	2407.860	24078.600
9.990	2396.520	23965.200
10.900	2446.500	24465.000
11.810	2443.560	24435.600
12.720	2510.760	25107.600
13.620	2443.980	24439.800
14.530	2354.520	23545.200
15.440	2443.140	24431.400

Time (sec)	Stress (Pa)	Viscosity (Pa s)
16.350	2295.720	22957.200
17.260	2429.700	24297.000
18.160	2405.340	24053.400
19.070	2360.400	23604.000
19.980	2378.460	23784.600
20.890	2312.940	23129.400
21.800	2338.560	23385.600
22.710	2199.120	21991.200

Time (sec)	Stress (Pa)	Viscosity (Pa s)
23.610	2260.440	22604.400
24.520	2201.220	22012.200
25.430	2188.200	21882.000
26.340	2116.380	21163.800
27.250	2173.080	21730.800
28.160	2068.920	20689.200
29.060	1970.640	19706.400

8.2.2 – HDB2

8.2.2.1 – HDB2 – Elongational Viscosity – 170 °C – Strain Rate = 10 s^{-1}

Time (sec)	Stress (Pa)	Viscosity (Pa s)
0.049	96235.233	9623.523
0.056	104008.271	10400.827
0.064	110389.775	11038.977
0.071	116170.956	11617.096
0.079	121750.131	12175.013
0.086	127024.165	12702.416
0.094	132180.632	13218.063
0.101	137150.249	13715.025
0.109	141862.738	14186.274
0.116	146597.129	14659.713
0.124	150804.433	15080.443
0.131	154925.985	15492.598
0.139	159089.349	15908.935
0.146	162958.854	16295.885

Time (sec)	Stress (Pa)	Viscosity (Pa s)
0.154	166837.193	16683.719
0.161	170725.069	17072.507
0.169	174634.439	17463.444
0.176	178458.649	17845.865
0.184	182441.583	18244.158
0.191	186363.328	18636.333
0.199	190366.820	19036.682
0.206	194329.236	19432.924
0.214	198420.031	19842.003
0.221	202692.619	20269.262
0.229	207010.343	20701.034
0.236	211293.992	21129.399
0.244	215217.369	21521.737
0.251	219562.056	21956.206

Time (sec)	Stress (Pa)	Viscosity (Pa s)
0.259	223149.568	22314.957
0.266	227094.018	22709.402
0.274	230602.683	23060.268
0.281	233944.344	23394.434
0.289	236575.867	23657.587
0.296	238776.756	23877.676
0.304	240704.395	24070.439
0.311	241932.052	24193.205
0.319	242575.281	24257.528
0.326	241961.552	24196.155
0.334	241872.700	24187.270
0.341	240448.930	24044.893
0.349	238309.465	23830.947

8.2.2.2 – HDB2 – Elongational Viscosity – 170 °C – Strain Rate = 3 s^{-1}

Time (sec)	Stress (Pa)	Viscosity (Pa s)
0.191	46310.390	15436.797
0.199	47227.836	15742.612
0.206	48161.987	16053.996
0.214	48935.365	16311.788
0.221	49681.979	16560.660
0.229	50476.247	16825.416
0.236	51202.303	17067.434
0.244	51858.439	17286.146
0.251	52516.691	17505.564
0.259	53260.928	17753.643
0.266	53843.603	17947.868
0.274	54425.219	18141.740
0.281	55005.424	18335.141
0.289	55673.161	18557.720
0.296	56297.836	18765.945
0.304	56827.262	18942.421
0.311	57497.146	19165.715
0.319	58068.879	19356.293
0.326	58586.114	19528.705
0.334	59148.717	19716.239
0.341	59759.662	19919.887
0.349	60422.070	20140.690
0.356	61137.510	20379.170
0.364	61685.606	20561.869
0.371	62283.298	20761.099
0.379	62878.055	20959.352
0.386	63347.984	21115.995
0.394	63804.854	21268.285
0.401	64501.955	21500.652
0.409	65069.734	21689.911
0.416	65366.121	21788.707
0.424	65810.176	21936.725
0.431	66206.887	22068.962
0.439	66587.576	22195.859
0.446	66986.580	22328.860
0.454	67516.883	22505.628
0.461	67961.717	22653.906
0.469	68391.835	22797.278
0.476	68884.720	22961.573
0.484	69364.608	23121.536
0.491	69954.263	23318.088
0.506	70934.113	23644.704
0.514	71402.736	23800.912
0.521	72170.599	24056.866
0.529	72614.632	24204.877
0.536	73135.337	24378.446
0.544	73882.766	24627.589
0.551	74331.919	24777.306
0.559	74761.710	24920.570
0.566	75174.157	25058.052
0.574	75618.352	25206.117
0.581	75936.453	25312.151
0.589	76393.786	25464.595
0.596	77003.683	25667.894
0.604	77486.892	25828.964
0.611	77950.415	25983.472
0.619	78455.923	26151.974
0.626	79066.980	26355.660
0.634	79603.337	26534.446
0.641	80123.162	26707.721
0.649	80625.444	26875.148
0.656	81378.033	27126.011
0.664	81710.518	27236.839
0.671	82225.909	27408.636
0.679	82795.500	27598.500
0.686	83423.131	27807.710
0.694	83883.654	27961.218
0.701	84400.077	28133.359
0.709	85293.766	28431.255
0.716	85857.452	28619.151
0.724	86488.757	28829.586
0.731	87018.839	29006.280
0.739	87872.751	29290.917
0.746	88456.219	29485.406
0.754	88883.531	29627.844
0.761	89607.680	29869.227
0.769	90317.304	30105.768
0.776	91012.843	30337.614
0.784	91494.610	30498.203
0.791	92306.329	30768.776
0.799	92952.166	30984.055
0.806	93581.226	31193.742
0.821	94942.543	31647.514
0.829	95568.653	31856.218
0.836	95883.012	31961.004
0.844	96637.831	32212.610
0.851	97134.106	32378.035
0.859	97853.610	32617.870
0.866	98299.180	32766.393
0.874	99040.139	33013.380
0.881	99562.794	33187.598
0.889	100128.598	33376.199
0.896	100596.364	33532.121
0.904	101035.721	33678.574
0.911	101587.485	33862.495
0.919	102037.020	34012.340
0.926	102835.762	34278.587
0.934	103541.918	34513.973
0.941	104144.263	34714.754
0.949	104397.002	34799.001
0.956	105022.053	35007.351
0.964	105538.231	35179.410
0.971	106023.512	35341.171
0.979	106296.565	35432.188
0.986	106435.287	35478.429
0.994	106807.168	35602.389
1.001	106756.462	35585.487
1.009	107234.879	35744.960
1.016	107381.279	35793.760
1.024	107886.936	35962.312
1.031	107942.582	35980.861
1.039	108264.289	36088.096
1.046	108654.713	36218.238
1.054	108894.399	36298.133
1.061	109317.011	36439.004
1.069	109353.082	36451.027
1.076	109751.747	36583.916
1.084	109867.625	36622.542
1.091	110242.859	36747.620
1.099	109877.955	36625.985
1.106	110091.738	36697.246
1.114	110056.413	36685.471

8.2.2.3 – HDB2 – Elongational Viscosity – 170 °C – Strain Rate = 1 s^{-1}

Time (sec)	Stress (Pa)	Viscosity (Pa s)
0.694	26961.211	26961.211
0.701	27009.071	27009.071
0.709	27078.644	27078.644
0.716	27080.354	27080.354
0.724	27126.274	27126.274
0.731	27170.656	27170.656
0.739	27329.492	27329.492
0.746	27442.420	27442.420
0.754	27556.214	27556.214
0.761	27645.710	27645.710
0.769	27688.619	27688.619
0.776	27753.967	27753.967
0.784	27770.183	27770.183
0.791	27833.985	27833.985
0.799	27848.636	27848.636
0.806	27935.658	27935.658
0.814	27972.388	27972.388
0.821	28108.128	28108.128
0.829	28244.328	28244.328
0.836	28380.984	28380.984
0.844	28518.097	28518.097
0.851	28553.363	28553.363
0.859	28638.289	28638.289
0.866	28671.749	28671.749
0.874	28755.601	28755.601
0.881	28787.191	28787.191
0.889	28789.849	28789.849
0.896	28818.903	28818.903
0.904	28954.579	28954.579
0.911	29090.667	29090.667
0.919	29199.379	29199.379
0.926	29336.069	29336.069
0.934	29333.862	29333.862
0.941	29357.513	29357.513
0.949	29295.705	29295.705
0.956	29344.931	29344.931
0.964	29421.421	29421.421
0.971	29469.004	29469.004
0.979	29545.138	29545.138
0.986	29620.747	29620.747
0.994	29724.861	29724.861
1.001	29769.433	29769.433
1.009	29904.189	29904.189
1.106	30672.154	30672.154
1.114	30752.654	30752.654
1.121	30882.625	30882.625
1.129	30979.056	30979.056
1.136	30904.093	30904.093
1.144	30860.514	30860.514
1.151	30796.993	30796.993
1.159	30958.742	30958.742
1.166	31050.544	31050.544
1.174	31231.064	31231.064
1.181	31358.358	31358.358
1.189	31468.152	31468.152
1.196	31486.708	31486.708
1.204	31448.905	31448.905
1.211	31464.017	31464.017
1.219	31403.139	31403.139
1.226	31377.342	31377.342
1.234	31348.802	31348.802
1.241	31394.766	31394.766
1.249	31458.381	31458.381
1.256	31540.645	31540.645
1.264	31603.342	31603.342
1.271	31625.070	31625.070
1.279	31665.856	31665.856
1.286	31605.769	31605.769
1.294	31642.810	31642.810
1.301	31658.871	31658.871
1.309	31734.313	31734.313
1.316	31788.422	31788.422
1.324	31842.179	31842.179
1.331	31935.641	31935.641
1.339	32008.843	32008.843
1.346	32101.352	32101.352
1.354	32172.624	32172.624
1.361	32286.400	32286.400
1.369	32248.223	32248.223
1.376	32273.489	32273.489
1.384	32253.080	32253.080
1.391	32341.266	32341.266
1.399	32384.057	32384.057
1.406	32425.658	32425.658
1.414	32511.622	32511.622
1.421	32574.086	32574.086
1.429	32727.480	32727.480
1.436	32719.599	32719.599
1.444	32872.697	32872.697
1.451	32885.009	32885.009
1.459	32943.317	32943.317
1.466	32953.337	32953.337
1.474	33033.503	33033.503
1.481	33039.860	33039.860
1.489	33093.569	33093.569
1.496	33195.714	33195.714
1.504	33222.716	33222.716
1.511	33373.095	33373.095
1.519	33322.898	33322.898
1.526	33371.285	33371.285
1.534	33469.905	33469.905
1.541	33670.098	33670.098
1.549	33768.660	33768.660
1.556	33814.241	33814.241
1.564	33805.640	33805.640
1.571	33742.449	33742.449
1.579	33863.713	33863.713
1.586	33930.733	33930.733
1.594	34131.609	34131.609
1.601	34225.290	34225.290
1.609	34373.004	34373.004
1.616	34410.232	34410.232
1.624	34417.957	34417.957
1.631	34368.058	34368.058
1.639	34315.457	34315.457
1.646	34345.501	34345.501
1.654	34287.148	34287.148
1.661	34401.105	34401.105
1.669	34455.113	34455.113
1.676	34656.139	34656.139
1.684	34709.879	34709.879
1.691	34821.708	34821.708
1.699	34843.262	34843.262
1.706	34863.167	34863.167
1.714	34912.154	34912.154
1.721	34866.934	34866.934
1.729	34943.954	34943.954
1.736	34895.262	34895.262
1.744	35000.430	35000.430

8.2.2.3 Continued

Time (sec)	Stress (Pa)	Viscosity (Pa s)
1.751	35073.270	35073.270
1.759	35209.570	35209.570
1.766	35345.941	35345.941
1.774	35418.031	35418.031
1.781	35521.118	35521.118
1.789	35525.276	35525.276
1.796	35594.301	35594.301
1.804	35561.375	35561.375
1.811	35694.470	35694.470
1.819	35657.751	35657.751
1.826	35756.155	35756.155
1.834	35783.600	35783.600
1.841	35914.272	35914.272
1.849	36010.741	36010.741
1.856	35964.728	35964.728
1.864	36057.864	36057.864
1.871	36043.425	36043.425
1.879	36207.025	36207.025
1.886	36262.500	36262.500
1.894	36425.007	36425.007
1.901	36386.634	36386.634
1.909	36345.057	36345.057
1.916	36394.383	36394.383
1.924	36499.321	36499.321
1.931	36679.086	36679.086
1.939	36725.823	36725.823
1.946	36964.081	36964.081
1.954	36970.392	36970.392
1.961	37033.805	37033.805
1.969	36879.555	36879.555
1.976	36958.420	36958.420
1.984	36976.554	36976.554
1.991	36952.893	36952.893
1.999	36987.503	36987.503
2.006	37082.368	37082.368
2.014	37320.002	37320.002
2.021	37393.682	37393.682
2.029	37675.185	37675.185
2.036	37621.634	37621.634
2.044	37671.475	37671.475
2.051	37612.801	37612.801
2.059	37637.320	37637.320

Time (sec)	Stress (Pa)	Viscosity (Pa s)
2.066	37811.916	37811.916
2.074	37856.085	37856.085
2.081	38008.470	38008.470
2.089	38050.470	38050.470
2.096	38359.479	38359.479
2.104	38467.888	38467.888
2.111	38689.513	38689.513
2.119	38751.569	38751.569
2.126	38858.845	38858.845
2.134	38756.968	38756.968
2.141	38650.652	38650.652
2.149	38588.062	38588.062
2.156	38450.521	38450.521
2.164	38644.223	38644.223
2.171	38718.623	38718.623
2.179	39204.516	39204.516
2.186	39377.046	39377.046
2.194	39525.099	39525.099
2.201	39500.120	39500.120
2.209	39521.470	39521.470
2.216	39541.661	39541.661
2.224	39432.626	39432.626
2.231	39524.603	39524.603
2.239	39358.080	39358.080
2.246	39472.590	39472.590
2.254	39377.043	39377.043
2.261	39673.489	39673.489
2.269	39998.134	39998.134
2.276	40111.922	40111.922
2.284	40009.238	40009.238
2.291	39956.697	39956.697
2.299	39956.319	39956.319
2.306	39815.428	39815.428
2.314	40115.174	40115.174
2.321	40052.659	40052.659
2.329	40298.148	40298.148
2.336	40430.406	40430.406
2.344	40677.898	40677.898
2.351	40811.310	40811.310
2.359	40943.539	40943.539
2.366	41134.526	41134.526
2.374	41149.313	41149.313

Time (sec)	Stress (Pa)	Viscosity (Pa s)
2.381	41280.107	41280.107
2.389	41021.489	41021.489
2.396	41149.545	41149.545
2.404	41123.868	41123.868
2.411	41127.306	41127.306
2.419	41127.533	41127.533
2.426	41312.646	41312.646
2.434	41498.220	41498.220
2.441	41716.076	41716.076
2.449	42125.390	42125.390
2.456	42154.590	42154.590
2.464	42406.812	42406.812
2.471	42303.567	42303.567
2.479	42293.504	42293.504
2.486	42116.405	42116.405
2.494	42200.630	42200.630
2.501	42149.546	42149.546
2.509	42196.442	42196.442
2.516	42343.562	42343.562
2.524	42318.682	42318.682
2.531	42603.494	42603.494
2.539	42540.277	42540.277
2.546	42650.500	42650.500
2.554	42547.301	42547.301
2.561	42689.211	42689.211
2.569	42723.449	42723.449
2.576	42755.779	42755.779
2.584	42859.615	42859.615
2.591	42851.609	42851.609
2.599	43136.932	43136.932
2.606	43089.621	43089.621
2.614	43376.173	43376.173
2.621	43514.451	43514.451
2.629	43651.183	43651.183
2.636	43557.720	43557.720
2.644	43537.145	43537.145
2.651	43513.797	43513.797
2.659	43449.263	43449.263
2.666	43538.346	43538.346
2.674	43468.066	43468.066
2.681	43754.825	43754.825
2.689	43719.709	43719.709

8.2.2.3 Continued

Time (sec)	Stress (Pa)	Viscosity (Pa s)
2.696	43967.914	43967.914
2.704	44093.199	44093.199
2.711	44135.731	44135.731
2.719	44134.403	44134.403
2.726	44172.871	44172.871
2.734	44420.101	44420.101
2.741	44371.648	44371.648
2.749	44619.085	44619.085
2.756	44305.909	44305.909
2.764	44508.923	44508.923
2.771	44799.720	44799.720
2.779	45136.976	45136.976
2.786	45343.273	45343.273
2.794	45504.845	45504.845
2.801	45620.629	45620.629
2.809	45325.985	45325.985
2.816	45620.881	45620.881
2.824	45292.561	45292.561
2.831	45213.892	45213.892
2.839	45178.129	45178.129
2.846	45352.630	45352.630
2.854	45431.000	45431.000
2.861	45629.122	45629.122
2.869	45633.110	45633.110
2.876	45489.265	45489.265
2.884	45708.573	45708.573
2.891	45458.057	45458.057
2.899	45600.573	45600.573
2.906	45314.927	45314.927
2.914	45580.238	45580.238
2.921	45642.735	45642.735
2.929	45754.654	45754.654
2.936	45684.441	45684.441
2.944	45689.518	45689.518
2.951	45769.991	45769.991
2.959	45531.845	45531.845
2.966	45820.794	45820.794
2.974	45708.946	45708.946
2.981	45944.625	45944.625
2.989	45907.702	45907.702
2.996	45895.355	45895.355
3.004	45798.092	45798.092

Time (sec)	Stress (Pa)	Viscosity (Pa s)
3.011	45863.108	45863.108
3.019	46067.432	46067.432
3.026	46187.376	46187.376
3.034	46649.375	46649.375
3.041	46338.714	46338.714
3.049	46659.224	46659.224
3.056	46484.068	46484.068
3.064	46716.256	46716.256
3.071	46682.113	46682.113
3.079	46585.497	46585.497
3.086	46574.871	46574.871
3.094	46440.120	46440.120
3.101	46789.726	46789.726
3.109	46464.933	46464.933
3.116	46938.849	46938.849
3.124	46823.539	46823.539
3.131	47018.316	47018.316
3.139	46959.499	46959.499
3.146	47089.468	47089.468
3.154	47122.327	47122.327
3.161	47054.903	47054.903
3.169	47114.605	47114.605
3.176	47008.553	47008.553
3.184	47362.442	47362.442
3.191	47083.817	47083.817
3.199	47438.283	47438.283
3.206	47116.421	47116.421
3.214	47299.831	47299.831
3.221	47242.378	47242.378
3.229	47320.250	47320.250
3.236	47396.625	47396.625
3.244	47189.488	47189.488
3.251	47474.266	47474.266
3.259	47116.080	47116.080
3.266	47362.907	47362.907
3.274	47065.150	47065.150
3.281	46980.355	46980.355
3.289	47113.382	47113.382
3.296	47244.609	47244.609
3.304	47338.589	47338.589
3.311	47469.291	47469.291
3.319	47674.682	47674.682

Time (sec)	Stress (Pa)	Viscosity (Pa s)
3.326	47344.003	47344.003
3.334	47546.164	47546.164
3.341	47360.707	47360.707
3.349	47756.690	47756.690
3.356	47405.640	47405.640
3.364	47643.598	47643.598
3.371	47882.455	47882.455
3.379	47838.897	47838.897
3.386	48280.955	48280.955
3.394	47989.213	47989.213
3.401	48392.054	48392.054
3.409	48049.372	48049.372
3.416	48453.294	48453.294
3.424	48057.862	48057.862
3.431	47697.861	47697.861
3.439	47714.267	47714.267
3.446	47857.347	47857.347
3.454	48303.927	48303.927
3.461	48099.035	48099.035
3.469	48461.143	48461.143
3.476	48024.790	48024.790
3.484	48565.550	48565.550
3.491	48119.264	48119.264
3.499	48253.746	48253.746
3.506	47839.009	47839.009
3.514	47829.773	47829.773
3.521	47817.701	47817.701
3.529	47661.041	47661.041
3.536	48351.477	48351.477
3.544	48000.733	48000.733
3.551	48170.341	48170.341
3.559	47857.565	47857.565
3.566	48072.228	48072.228
3.574	47796.416	47796.416
3.581	47661.521	47661.521
3.589	47396.519	47396.519
3.596	47225.890	47225.890

8.2.2.4 – HDB2 – Elongational Viscosity – 170 °C – Strain Rate = 0.3 s^{-1}

Time (sec)	Stress (Pa)	Viscosity (Pa s)
0.287	5727.078	19090.260
0.575	7348.453	24494.843
0.862	8864.534	29548.447
1.149	10065.496	33551.653
1.437	10623.249	35410.830
1.724	11123.014	37076.713
2.011	12272.855	40909.517
2.298	12032.510	40108.367
2.586	12480.391	41601.303
2.873	12774.909	42583.030
3.160	13233.472	44111.573

Time (sec)	Stress (Pa)	Viscosity (Pa s)
3.448	13227.368	44091.227
3.735	13518.071	45060.237
4.022	13779.017	45930.057
4.310	13806.485	46021.617
4.597	14042.252	46807.507
4.884	14204.771	47349.237
5.171	14512.260	48374.200
5.459	14751.079	49170.263
5.746	14925.806	49752.687
6.033	15185.989	50619.963
6.320	15301.965	51006.550

Time (sec)	Stress (Pa)	Viscosity (Pa s)
6.608	15446.172	51487.240
6.895	15644.552	52148.507
7.182	15798.678	52662.260
7.470	16081.751	53605.837
7.757	16241.218	54137.393
8.044	16370.928	54569.760
8.332	16567.019	55223.397
8.619	16638.741	55462.470
8.906	16586.857	55289.523
9.193	16485.378	54951.260

8.2.2.5 – HDB2 – Elongational Viscosity – 170 °C – Strain Rate = 0.1 s^{-1}

Time (sec)	Stress (Pa)	Viscosity (Pa s)
0.908	2754.743	27547.427
1.816	3538.836	35388.360
2.725	4176.816	41768.160
3.633	4452.840	44528.400
4.541	4930.529	49305.293
5.449	5078.089	50780.893
6.357	5216.391	52163.907
7.266	5307.531	53075.307
8.174	5512.089	55120.893
9.082	5710.861	57108.613
9.990	5526.556	55265.560

Time (sec)	Stress (Pa)	Viscosity (Pa s)
10.900	5743.267	57432.667
11.810	5959.399	59593.987
12.720	5897.771	58977.707
13.620	6036.940	60369.400
14.530	6108.116	61081.160
15.440	6216.037	62160.373
16.350	6249.889	62498.893
17.260	6350.577	63505.773
18.160	6328.299	63282.987
19.070	6437.956	64379.560
19.980	6500.163	65001.627

Time (sec)	Stress (Pa)	Viscosity (Pa s)
20.890	6535.172	65351.720
21.800	6491.193	64911.933
22.710	6621.104	66211.040
23.610	6641.936	66419.360
24.520	6673.473	66734.733
25.430	6680.707	66807.067
26.340	6686.493	66864.933
27.250	6633.835	66338.347
28.160	6644.540	66445.400
29.060	6732.642	67326.420

8.2.2.6 – HDB2 – Elongational Viscosity – 170 °C – Strain Rate = 0.03 s^{-1}

Time (sec)	Stress (Pa)	Viscosity (Pa s)
5.746	1408.670	46955.650
8.619	1619.499	53983.300
11.490	1724.793	57493.100
14.370	1747.253	58241.750
17.240	1818.495	60616.500
20.110	1896.500	63216.650
22.980	1908.575	63619.150
25.860	1916.786	63892.850
28.730	1923.065	64102.150
31.600	2012.178	67072.600
34.480	1893.843	63128.100

Time (sec)	Stress (Pa)	Viscosity (Pa s)
37.350	1923.548	64118.250
40.220	1970.640	65688.000
43.100	1996.481	66549.350
45.970	2007.831	66927.700
48.840	2016.042	67201.400
51.710	2056.856	68561.850
54.590	1987.062	66235.400
57.460	2010.246	67008.200
60.330	2113.125	70437.500
63.210	2034.879	67829.300
66.080	2050.094	68336.450

Time (sec)	Stress (Pa)	Viscosity (Pa s)
68.950	2108.537	70284.550
71.820	2047.679	68255.950
74.700	2131.238	71041.250
77.570	2065.791	68859.700
80.440	2076.659	69221.950
83.320	2081.247	69374.900
86.190	1987.545	66251.500
89.060	1996.722	66557.400
91.940	1960.497	65349.900

8.2.2.7 – HDB2 – Elongational Viscosity – 170 °C – Strain Rate = 0.003 s^{-1}

Time (sec)	Stress (Pa)	Viscosity (Pa s)
115.625	194.480	64826.533
117.875	196.449	65482.862
120.125	198.600	66200.148
122.375	200.829	66942.852
124.625	202.755	67585.102
126.875	204.131	68043.705
129.125	205.148	68382.736
131.375	206.234	68744.630
133.625	207.529	69176.372
135.875	208.692	69563.857
138.125	209.295	69764.840
140.375	209.358	69786.137
142.625	209.354	69784.634
144.875	209.681	69893.606
147.125	210.272	70090.802
149.375	210.777	70259.074
151.625	211.056	70352.013
153.875	211.352	70450.602
156.125	211.981	70660.484
158.375	212.981	70993.619
160.625	214.150	71383.335
162.875	215.364	71787.874
165.125	216.702	72234.071
167.375	218.270	72756.581
169.625	219.993	73330.901
171.875	221.694	73897.923
174.125	223.304	74434.749
176.375	224.910	74969.951
178.625	226.574	75524.811
180.875	228.217	76072.171
183.125	229.701	76566.979
185.375	231.002	77000.640
187.625	232.209	77402.863
189.875	233.400	77800.099
192.125	234.589	78196.365
194.375	235.786	78595.461
196.625	237.057	79018.898
198.875	238.444	79481.482
201.125	239.911	79970.238
203.375	241.405	80468.441
205.625	243.000	80999.863
207.875	244.859	81619.593
210.125	247.047	82348.974
212.375	249.417	83138.839
214.625	251.757	83919.060
216.875	254.051	84683.750
219.125	256.486	85495.458
221.375	259.199	86399.800
223.625	262.067	87355.596
225.875	264.827	88275.795
228.125	267.384	89128.102
230.375	269.889	89963.107
232.625	272.500	90833.316
234.875	275.138	91712.591
237.125	277.589	92529.807
239.375	279.775	93258.370
241.625	281.814	93937.837
243.875	283.862	94620.601
246.125	285.848	95282.520
248.375	287.589	95862.906
250.625	289.106	96368.578
252.875	290.542	96847.360
255.125	291.849	97283.027

8.2.3 – HDB3

8.2.3.1 – HDB3 – Elongational Viscosity – 170 °C – Strain Rate = 10 s^{-1}

Time (sec)	Stress (Pa)	Viscosity (Pa s)
0.045	97174.213	9717.421
0.053	109460.422	10946.042
0.060	119901.907	11990.191
0.068	128970.820	12897.082
0.075	137174.643	13717.464
0.082	144624.598	14462.460
0.090	151724.424	15172.442
0.098	158328.938	15832.894
0.105	164777.774	16477.777
0.113	170848.003	17084.800
0.120	176715.470	17671.547
0.128	182295.165	18229.517
0.135	187315.559	18731.556
0.143	192204.281	19220.428
0.150	196825.020	19682.502
0.158	201327.645	20132.765
0.165	205695.054	20569.505
0.173	210291.698	21029.170
0.180	214356.621	21435.662
0.188	218674.024	21867.402
0.195	222526.038	22252.604
0.203	226341.254	22634.125
0.210	230527.264	23052.726
0.218	234990.825	23499.082
0.225	240279.144	24027.914
0.233	244958.653	24495.865
0.240	249920.622	24992.062
0.247	253217.001	25321.700
0.255	256098.312	25609.831
0.263	258520.605	25852.060
0.270	259428.160	25942.816
0.277	259829.760	25982.976
0.285	259706.795	25970.680
0.293	259260.605	25926.060
0.300	258097.746	25809.775
0.307	256909.128	25690.913
0.315	254223.127	25422.313
0.323	251387.473	25138.747
0.330	246876.508	24687.651

8.2.3.2 – HDB3 – Elongational Viscosity – 170 °C – Strain Rate = 3 s^{-1}

Time (sec)	Stress (Pa)	Viscosity (Pa s)
0.045	27612.195	9204.065
0.053	31714.562	10571.521
0.060	35068.215	11689.405
0.068	37912.715	12637.572
0.075	40372.000	13457.333
0.082	42332.142	14110.714
0.090	44015.816	14671.939
0.097	45577.437	15192.479
0.105	46976.111	15658.704
0.113	48167.692	16055.897
0.120	49295.584	16431.861
0.128	50449.875	16816.625
0.135	51400.052	17133.351
0.143	52266.207	17422.069
0.150	53145.156	17715.052
0.158	54142.861	18047.620
0.165	55013.791	18337.930
0.172	55896.318	18632.106
0.180	56904.885	18968.295
0.187	58006.009	19335.336
0.195	59010.587	19670.196
0.202	60030.846	20010.282
0.210	61149.134	20383.045
0.217	62160.549	20720.183
0.225	63056.781	21018.927
0.232	64049.498	21349.833
0.240	65056.122	21685.374
0.248	65935.379	21978.460
0.255	66822.407	22274.136
0.262	67810.351	22603.450
0.270	68810.165	22936.722
0.278	69718.237	23239.412
0.285	70529.121	23509.707
0.292	71499.450	23833.150
0.300	72479.077	24159.692
0.308	73298.634	24432.878
0.315	74173.371	24724.457
0.322	75166.863	25055.621
0.330	76167.168	25389.056
0.338	77114.787	25704.929
0.345	77878.499	25959.500
0.352	78828.899	26276.300
0.360	79780.243	26593.414
0.367	80535.401	26845.134
0.375	81488.886	27162.962
0.382	82581.890	27527.297
0.390	83398.331	27799.444
0.397	84209.170	28069.723
0.405	85236.055	28412.018
0.412	86266.072	28755.357
0.420	86987.950	28995.983
0.427	87858.205	29286.068
0.435	88966.290	29655.430
0.442	89911.754	29970.585
0.450	90685.404	30228.468
0.457	91535.332	30511.777
0.465	92553.547	30851.182
0.472	93479.019	31159.673
0.480	94307.779	31435.926
0.487	95314.718	31771.573
0.495	96416.720	32138.907
0.502	97169.991	32389.997
0.510	98011.780	32670.593
0.518	98890.817	32963.606
0.525	99814.390	33271.463
0.533	100564.175	33521.392
0.540	101298.087	33766.029
0.547	102295.121	34098.374
0.555	103229.924	34409.975
0.562	104152.491	34717.497
0.570	104881.223	34960.408
0.578	106025.039	35341.680
0.585	107038.117	35679.372
0.593	107717.904	35905.968
0.600	108373.202	36124.401
0.607	109206.623	36402.208
0.615	110092.148	36697.383
0.622	110889.537	36963.179
0.630	112031.584	37343.861
0.638	113090.724	37696.908
0.645	114065.480	38021.827
0.653	114716.190	38238.730
0.660	115734.786	38578.262
0.667	116658.069	38886.023
0.675	117563.442	39187.814
0.682	118280.098	39426.699
0.690	119227.226	39742.409
0.698	120158.957	40052.986
0.705	120979.267	40326.422
0.713	121963.014	40654.338
0.720	122736.286	40912.095
0.727	123580.079	41193.360
0.735	124096.524	41365.508
0.742	125084.508	41694.836
0.750	126158.575	42052.858
0.757	127216.760	42405.587
0.765	128037.344	42679.115
0.773	128720.066	42906.689
0.780	129709.958	43236.653
0.787	130560.339	43520.113
0.795	131502.856	43834.285
0.802	132416.926	44138.975
0.810	133809.141	44603.047
0.817	134554.908	44851.636
0.825	135133.408	45044.469
0.833	135402.681	45134.227
0.840	135616.330	45205.443
0.847	135904.351	45301.450
0.855	136058.698	45352.899
0.862	136664.333	45554.778
0.870	136851.761	45617.254
0.877	136976.972	45658.991
0.885	137192.632	45730.877
0.893	137748.666	45916.222
0.900	137768.190	45922.730
0.908	137128.268	45709.423
0.915	136733.625	45577.875
0.922	136073.213	45357.738
0.930	135490.032	45163.344
0.937	133986.033	44662.011
0.945	132999.708	44333.236

8.2.3.3 – HDB3 – Elongational Viscosity – 170 °C – Strain Rate = 1 s^{-1}

Time (sec)	Stress (Pa)	Viscosity (Pa s)
0.091	16560.444	16560.444
0.182	21300.481	21300.481
0.273	27227.407	27227.407
0.363	31428.704	31428.704
0.454	30583.519	30583.519
0.545	33416.963	33416.963
0.636	36762.185	36762.185
0.727	37705.889	37705.889
0.817	39528.481	39528.481
0.908	41292.222	41292.222
0.999	42529.148	42529.148

Time (sec)	Stress (Pa)	Viscosity (Pa s)
1.090	44126.185	44126.185
1.181	44437.037	44437.037
1.272	46078.667	46078.667
1.362	48547.333	48547.333
1.453	49651.778	49651.778
1.544	51150.037	51150.037
1.635	52572.593	52572.593
1.726	54133.852	54133.852
1.816	55407.593	55407.593
1.907	56836.630	56836.630
1.998	56994.519	56994.519

Time (sec)	Stress (Pa)	Viscosity (Pa s)
2.089	58457.000	58457.000
2.180	59911.185	59911.185
2.271	62524.519	62524.519
2.361	64162.000	64162.000
2.452	66062.111	66062.111
2.543	68032.741	68032.741
2.634	70064.556	70064.556
2.725	69753.833	69753.833
2.816	69808.278	69808.278
2.906	69889.556	69889.556

8.2.3.4 – HDB3 – Elongational Viscosity – 170 °C – Strain Rate = 0.3 s^{-1}

Time (sec)	Stress (Pa)	Viscosity (Pa s)
0.287	7809.480	26031.600
0.575	10926.720	36422.400
0.862	13643.280	45477.600
1.149	14787.360	49291.200
1.437	16296.840	54322.800
1.724	17503.920	58346.400
2.011	18179.280	60597.600
2.298	19315.800	64386.000
2.586	19983.600	66612.000
2.873	20699.280	68997.600

Time (sec)	Stress (Pa)	Viscosity (Pa s)
3.160	21351.960	71173.200
3.448	22233.960	74113.200
3.735	22717.800	75726.000
4.022	23420.880	78069.600
4.310	24129.000	80430.000
4.597	24617.880	82059.600
4.884	24877.440	82924.800
5.171	25704.000	85680.000
5.459	26208.000	87360.000
3.160	21351.960	71173.200

Time (sec)	Stress (Pa)	Viscosity (Pa s)
5.746	26838.000	89460.000
6.033	27493.200	91644.000
6.320	28022.400	93408.000
6.608	28425.600	94752.000
6.895	28929.600	96432.000
7.182	28803.600	96012.000
7.470	28652.400	95508.000
7.757	27770.400	92568.000
8.044	25250.400	84168.000

8.2.3.5 – HDB3 – Elongational Viscosity – 170 °C – Strain Rate = 0.1 s^{-1}

Time (sec)	Stress (Pa)	Viscosity (Pa s)
5.449	8302.410	83024.100
6.357	8430.300	84303.000
7.266	8485.110	84851.100
8.174	8620.830	86208.300
9.082	9004.500	90045.000
9.990	9282.900	92829.000
10.900	9091.500	90915.000
11.810	9317.700	93177.000
12.720	9500.400	95004.000

Time (sec)	Stress (Pa)	Viscosity (Pa s)
13.620	9378.600	93786.000
14.530	9639.600	96396.000
15.440	9665.700	96657.000
16.350	9874.500	98745.000
17.260	9900.600	99006.000
18.160	10135.500	101355.000
19.070	10170.300	101703.000
19.980	10561.800	105618.000
20.890	10535.700	105357.000

Time (sec)	Stress (Pa)	Viscosity (Pa s)
21.800	10596.600	105966.000
22.710	10727.100	107271.000
23.610	10866.300	108663.000
24.520	11101.200	111012.000
25.430	11127.300	111273.000
26.340	11266.500	112665.000
27.250	11188.200	111882.000
28.160	11336.100	113361.000
29.060	11170.800	111708.000

8.2.3.6 – HDB3 – Elongational Viscosity – 170 °C – Strain Rate = 0.044 s^{-1}

Time (sec)	Stress (Pa)	Viscosity (Pa s)
20.090	4179.606	96047.464
20.285	4192.691	96348.159
20.485	4200.568	96529.172
20.690	4204.817	96626.814
20.900	4209.981	96745.469
21.110	4218.590	96943.310
21.325	4230.583	97218.913
21.550	4245.368	97558.661
21.780	4255.827	97799.012
22.010	4268.123	98081.583
22.245	4282.156	98404.069
22.490	4299.358	98799.364
22.745	4316.440	99191.908
23.005	4331.149	99529.925
23.265	4341.848	99775.780
23.530	4356.678	100116.588
23.805	4373.124	100494.502
24.090	4389.574	100872.535
24.380	4400.350	101120.162
24.675	4408.607	101309.912
24.980	4423.083	101642.556
25.290	4435.688	101932.232
25.605	4449.041	102239.078
25.930	4468.850	102694.297
26.265	4486.447	103098.672
26.605	4501.960	103455.173
26.950	4521.381	103901.446
27.310	4543.415	104407.790
27.680	4568.495	104984.143
28.050	4588.704	105448.540
28.430	4610.435	105947.911
28.825	4629.971	106396.855
29.230	4651.320	106887.462
29.640	4673.010	107385.895
30.060	4690.432	107786.244
30.495	4710.967	108258.144
30.935	4732.841	108760.810
31.385	4760.751	109402.181
31.850	4788.721	110044.935
32.325	4810.917	110554.997
32.810	4832.059	111040.855
33.305	4855.002	111568.068
33.815	4877.965	112095.763
34.340	4900.366	112610.552
34.875	4929.050	113269.709
37.140	4950.182	113755.321
37.740	4972.377	114265.354
38.355	4988.593	114637.997
38.985	5005.801	115033.445
39.630	5027.490	115531.857
40.290	5044.314	115918.471
40.965	5061.533	116314.159
41.655	5082.224	116789.644
42.010	5103.826	117286.067
43.000	5121.513	117692.509
43.980	5140.132	118120.363
44.390	5158.083	118532.893
44.455	5177.153	118971.114
44.520	5196.275	119410.537
44.740	5216.153	119867.330
44.815	5230.887	120205.935
45.055	5239.860	120412.124
45.135	5250.207	120649.899
45.310	5259.432	120861.900
45.400	5274.980	121219.181
45.590	5288.322	121525.785
45.685	5302.565	121853.090
45.790	5307.947	121976.775
46.000	5321.734	122293.588
46.225	5334.913	122596.442
46.345	5352.714	123005.510
46.465	5368.490	123368.039
46.585	5375.819	123536.461
46.710	5379.511	123621.312
46.975	5386.539	123782.810
47.110	5395.255	123983.105
47.250	5392.928	123929.641
47.395	5406.871	124250.037
47.540	5409.848	124318.451
47.695	5421.530	124586.896
47.855	5430.829	124800.590
48.015	5437.275	124948.716
48.180	5434.825	124892.436
48.350	5441.313	125041.517
48.525	5452.344	125295.004
48.705	5463.525	125551.954
48.890	5482.246	125982.169
49.275	5491.552	126196.012
49.475	5502.705	126452.311
49.680	5507.515	126562.834
49.890	5513.749	126706.106
50.105	5518.085	126805.742
50.330	5530.837	127098.781
50.560	5530.803	127098.009
50.795	5536.712	127233.781
51.035	5542.424	127365.063
51.285	5562.946	127836.660
51.545	5571.574	128034.929
51.805	5576.115	128139.283
52.075	5591.913	128502.314
52.355	5596.996	128619.115
52.640	5605.634	128817.618
52.930	5609.460	128905.546
53.230	5612.172	128967.863
53.540	5619.193	129129.207
53.855	5635.984	129515.054
54.180	5647.448	129778.508
54.515	5653.266	129912.204
54.860	5657.298	130004.870
55.215	5660.841	130086.270
55.580	5664.475	130169.793
55.955	5671.407	130329.080
56.340	5684.424	130628.213
56.735	5694.661	130863.473
57.140	5706.571	131137.157
57.555	5708.592	131183.588
57.985	5723.252	131520.488
58.425	5728.912	131650.555
58.875	5751.289	132164.768
59.340	5758.362	132327.308
59.820	5775.611	132723.685
60.310	5793.059	133124.646
60.815	5807.672	133460.462
61.335	5814.235	133611.265
61.865	5836.255	134117.300
62.410	5861.173	134689.924
62.970	5881.948	135167.330
63.550	5896.588	135503.751
64.145	5913.845	135900.323

8.2.3.6 Continued

Time (sec)	Stress (Pa)	Viscosity (Pa s)
64.755	5930.588	136285.074
65.380	5950.445	136741.393
66.025	5967.588	137135.344
66.690	5973.770	137277.390
67.370	5985.172	137539.404
68.065	5993.769	137736.974
68.780	6001.005	137903.249
69.520	6012.536	138168.228
70.280	6020.910	138360.674

Time (sec)	Stress (Pa)	Viscosity (Pa s)
71.060	6030.074	138571.274
71.860	6039.945	138798.095
72.680	6055.154	139147.611
73.525	6056.026	139167.647
74.395	6065.359	139382.103
75.285	6066.873	139416.914
76.200	6071.281	139518.198
77.140	6075.382	139612.448
78.110	6089.594	139939.035

Time (sec)	Stress (Pa)	Viscosity (Pa s)
79.105	6090.446	139958.617
80.125	6076.346	139634.592
81.175	6074.830	139599.760
82.255	6076.391	139635.638
83.365	6072.769	139552.389
84.500	6061.008	139282.116
85.670	6051.569	139065.220

8.2.3.7 – HDB3 – Elongational Viscosity – 170 ^{o}C – Strain Rate = 0.015 s^{-1}

Time (sec)	Stress (Pa)	Viscosity (Pa s)
50.075	1588.969	109543.665
50.355	1594.129	109899.375
50.640	1597.929	110161.358
50.930	1615.790	111392.680
51.230	1625.740	112078.670
51.540	1629.583	112343.562
51.855	1624.135	111967.990
52.180	1620.702	111731.299
52.515	1631.915	112504.332
52.860	1637.549	112892.781
53.215	1637.561	112893.584
53.580	1631.860	112500.541
53.955	1626.741	112147.689
54.340	1620.696	111730.880
54.735	1616.055	111410.950
55.140	1610.379	111019.686
55.555	1606.940	110782.592
55.985	1600.629	110347.509
56.425	1598.515	110201.781
56.875	1612.490	111165.171
57.340	1616.909	111469.858
57.820	1624.061	111962.872
58.310	1620.822	111739.600
58.815	1622.948	111886.146
59.335	1622.643	111865.155
59.865	1613.556	111238.695
60.410	1615.134	111347.474
60.970	1615.385	111364.767
61.550	1621.451	111782.956

Time (sec)	Stress (Pa)	Viscosity (Pa s)
62.145	1629.823	112360.142
62.755	1633.743	112630.359
63.380	1632.810	112566.087
64.025	1622.597	111861.979
64.690	1619.090	111620.222
65.370	1614.299	111289.894
66.065	1614.834	111326.795
66.780	1615.785	111392.326
67.520	1632.298	112530.759
68.280	1645.946	113471.679
69.060	1657.138	114243.260
69.860	1660.763	114493.163
70.680	1658.829	114359.817
71.525	1652.402	113916.753
72.395	1646.029	113477.380
73.285	1637.212	112869.523
74.200	1638.367	112949.162
75.140	1643.010	113269.242
76.110	1668.265	115010.295
77.105	1680.550	115857.279
78.125	1683.521	116062.087
79.175	1680.610	115861.402
80.255	1682.080	115962.729
81.365	1683.119	116034.326
82.500	1674.447	115436.537
83.670	1678.359	115706.206
84.875	1692.968	116713.359
86.110	1707.074	117685.790
87.380	1710.884	117948.456

Time (sec)	Stress (Pa)	Viscosity (Pa s)
88.685	1705.851	117601.496
90.025	1699.791	117183.758
91.405	1705.026	117544.622
92.820	1715.328	118254.830
94.275	1731.604	119376.952
95.770	1735.102	119618.073
97.305	1750.081	120650.699
98.885	1741.163	120035.935
100.500	1743.375	120188.391
102.170	1742.918	120156.908
103.880	1753.212	120866.550
111.210	1767.644	121861.533
113.180	1767.020	121818.517
115.190	1786.359	123151.699
117.260	1790.167	123414.250
119.390	1805.967	124503.537
121.580	1816.032	125197.369
123.820	1828.019	126023.756
126.130	1839.390	126807.726
128.500	1855.512	127919.135
130.940	1877.816	129456.810
133.440	1890.989	130364.921
136.020	1898.936	130912.799
138.660	1902.259	131141.889
140.010	1914.013	131952.241
142.020	1917.995	132226.754
143.490	1919.652	132340.966
143.940	1922.713	132551.962
144.190	1919.217	132310.979

8.2.3.7 Continued

Time (sec)	Stress (Pa)	Viscosity (Pa s)
145.180	1925.518	132745.385
145.350	1921.509	132469.012
146.040	1925.260	132727.596
147.240	1914.152	131961.802
147.930	1899.331	130940.030
148.170	1895.406	130669.469
148.430	1901.387	131081.770
149.800	1909.497	131640.860
151.070	1905.648	131375.538
151.420	1904.224	131277.327
151.770	1895.896	130703.239
152.890	1897.713	130828.504
153.710	1906.092	131406.119
154.130	1920.121	132373.298
154.570	1922.047	132506.096
156.440	1919.800	132351.184
156.960	1914.511	131986.534
158.010	1927.713	132896.678
158.570	1920.843	132423.089
159.140	1919.571	132335.368
160.350	1914.617	131993.871
162.970	1922.660	132548.306
163.680	1938.363	133630.922
166.750	1927.109	132855.066

Time (sec)	Stress (Pa)	Viscosity (Pa s)
168.430	1913.011	131883.165
171.140	1897.720	130828.969
172.100	1902.374	131149.849
175.170	1890.370	130322.256
176.250	1893.421	130532.583
177.380	1894.316	130594.325
178.530	1922.378	132528.921
179.720	1922.257	132520.533
180.940	1933.054	133264.872
182.210	1929.357	133010.054
183.510	1928.730	132966.803
184.850	1925.572	132749.096
186.240	1915.118	132028.395
187.660	1931.872	133183.378
189.130	1923.156	132582.529
190.650	1955.967	134844.555
192.220	1954.841	134766.876
193.830	1978.360	136388.317
195.490	1954.076	134714.127
197.210	1955.511	134813.113
198.970	1937.035	133539.348
200.790	1959.982	135121.338
202.670	1955.750	134829.531
204.600	1981.868	136630.107

Time (sec)	Stress (Pa)	Viscosity (Pa s)
206.600	1985.245	136862.978
208.650	2015.469	138946.586
210.770	2003.500	138121.421
212.960	2001.794	138003.848
215.210	1979.501	136466.990
217.530	1984.202	136791.062
219.930	1999.406	137839.225
222.390	2023.764	139518.444
224.940	2034.019	140225.402
227.570	2052.079	141470.519
230.260	2079.266	143344.754
233.050	2090.199	144098.487
235.920	2082.327	143555.821
238.890	2049.688	141305.680
241.940	2050.284	141346.744
245.090	2051.525	141432.283
248.330	2060.164	142027.869
251.680	2089.527	144052.181
255.130	2051.608	141438.007
258.680	2081.805	143519.791
266.130	2055.264	141690.095
270.020	2130.476	146875.160
274.030	2122.232	146306.877
278.170	2164.443	149216.858

8.2.3.8 – HDB3 – Elongational Viscosity – 170 °C – Strain Rate = 0.004 s^{-1}

Time (sec)	Stress (Pa)	Viscosity (Pa s)
162.100	573.248	131732.644
164.110	574.111	131930.784
165.170	573.530	131797.366
166.250	572.327	131520.891
167.380	571.251	131273.709
168.530	571.946	131433.303
169.720	574.314	131977.477
170.940	575.796	132318.148
172.210	572.804	131630.622
173.510	573.585	131810.102
174.850	569.840	130949.393
176.240	569.360	130839.078
177.660	560.853	128884.098
179.130	559.437	128558.868

Time (sec)	Stress (Pa)	Viscosity (Pa s)
180.650	557.977	128223.278
182.220	561.393	129008.307
183.830	563.546	129503.048
185.490	564.767	129783.678
187.210	565.952	130055.858
188.970	565.494	129950.610
190.790	563.921	129589.181
192.670	564.891	129812.033
194.600	560.930	128901.838
196.600	561.926	129130.745
198.650	559.664	128610.964
200.770	561.156	128953.878
202.960	562.336	129225.072
205.210	559.488	128570.392

Time (sec)	Stress (Pa)	Viscosity (Pa s)
207.530	554.593	127445.595
209.930	553.678	127235.245
212.390	553.908	127288.167
214.940	563.701	129538.580
217.570	563.849	129572.645
220.260	568.316	130599.179
223.050	565.694	129996.574
225.920	562.585	129282.110
228.890	560.989	128915.392
231.940	559.964	128679.917
235.090	568.709	130689.556
238.330	568.421	130623.225
241.680	569.444	130858.394
245.130	564.360	129690.150

8.2.3.8 Continued

Time (sec)	Stress (Pa)	Viscosity (Pa s)
248.680	564.542	129731.892
252.350	562.559	129276.143
256.130	560.513	128806.055
260.020	556.917	127979.731
264.030	553.945	127296.775
268.170	552.575	126981.953
272.440	553.598	127216.946
276.830	555.860	127736.741
281.360	559.964	128679.838
286.040	558.691	128387.304
290.860	557.437	128099.180
295.820	556.975	127993.086
300.950	558.783	128408.598
306.230	558.640	128375.542
311.660	558.747	128400.172
329.020	560.696	128848.091
335.160	557.247	128055.521
341.500	556.137	127800.476
348.030	550.341	126468.406
354.760	554.012	127312.007
361.700	548.521	126050.361
368.850	550.547	126515.897
376.230	551.880	126822.172
383.830	553.380	127166.832
391.660	557.437	128099.197
399.740	552.806	127035.065
416.660	553.398	127170.988
430.340	555.702	127700.530
436.040	564.854	129803.517

Time (sec)	Stress (Pa)	Viscosity (Pa s)
440.040	571.089	131236.342
440.390	577.455	132699.257
440.740	576.259	132424.366
441.500	572.752	131618.471
442.300	562.979	129372.612
443.170	552.449	126952.970
443.630	546.785	125651.404
444.580	543.978	125006.284
445.090	556.121	127796.799
445.610	559.790	128639.932
446.150	561.094	128939.642
446.710	553.781	127258.961
447.290	549.195	126205.266
448.500	541.681	124478.545
449.140	539.751	124034.968
449.800	545.752	125413.963
451.180	559.703	128619.878
451.920	565.723	130003.193
452.680	576.189	132408.288
453.460	573.371	131760.696
454.270	580.593	133420.440
455.110	578.884	133027.720
455.970	573.735	131844.482
456.880	565.118	129864.291
460.790	553.312	127151.297
462.940	566.214	130116.062
466.480	570.302	131055.586
467.740	586.009	134664.978
469.040	578.025	132830.293

Time (sec)	Stress (Pa)	Viscosity (Pa s)
471.790	569.960	130976.946
473.230	553.471	127187.886
474.720	543.427	124879.559
483.000	537.832	123594.001
486.720	537.806	123587.898
488.680	544.009	125013.386
494.980	553.292	127146.705
497.220	561.495	129031.620
507.000	568.204	130573.454
509.660	575.913	132344.964
512.410	570.339	131064.088
515.270	561.561	129046.775
521.260	556.200	127814.989
524.410	564.455	129711.811
527.670	577.688	132752.817
531.040	584.291	134270.288
538.140	579.637	133200.797
541.890	576.094	132386.584
545.750	564.255	129666.046
549.740	558.984	128454.703
553.880	555.043	127549.129
562.580	557.522	128118.639
571.900	562.318	129220.816
576.800	561.110	128943.273
587.130	561.775	129096.071
592.550	561.481	129028.462
598.170	558.397	128319.859
603.970	557.520	128118.145
609.980	552.850	127045.071

8.2.4 – HDB4

8.2.4.1 – HDB4 – Elongational Viscosity – 170 ^{o}C – Strain Rate = 10 s^{-1}

Time (sec)	Stress (Pa)	Viscosity (Pa s)
0.049	130025.586	13002.559
0.056	143994.108	14399.411
0.064	156954.028	15695.403
0.071	169178.259	16917.826
0.079	180582.954	18058.295
0.086	191643.098	19164.310

Time (sec)	Stress (Pa)	Viscosity (Pa s)
0.094	202006.498	20200.650
0.101	212035.235	21203.524
0.109	221710.006	22171.001
0.116	230872.368	23087.237
0.124	239320.619	23932.062
0.131	247042.077	24704.208

Time (sec)	Stress (Pa)	Viscosity (Pa s)
0.139	254521.746	25452.175
0.146	261409.045	26140.904
0.154	267295.969	26729.597
0.161	269908.965	26990.897
0.169	262902.561	26290.256
0.176	241420.191	24142.019

8.2.4.2 – HDB4 – Elongational Viscosity – 170 °C – Strain Rate = 3 s^{-1}

Time (sec)	Stress (Pa)	Viscosity (Pa s)
0.060	35827.646	11942.549
0.068	40870.372	13623.457
0.075	45218.915	15072.972
0.082	48963.320	16321.107
0.090	52181.020	17393.673
0.098	54917.727	18305.909
0.105	57530.986	19176.995
0.113	59920.534	19973.511
0.120	62067.685	20689.228
0.128	64043.671	21347.890
0.135	66031.745	22010.582
0.143	68025.867	22675.289
0.150	69826.716	23275.572
0.158	71620.671	23873.557
0.165	73461.732	24487.244
0.173	75240.595	25080.198
0.180	76898.699	25632.900
0.188	78648.533	26216.178
0.195	80379.934	26793.311
0.203	82032.065	27344.022
0.210	83597.752	27865.917
0.218	85252.654	28417.551
0.225	86814.040	28938.013
0.233	88337.162	29445.721
0.240	89820.005	29940.002
0.247	91390.702	30463.567
0.255	93058.236	31019.412
0.263	94469.031	31489.677
0.270	95895.858	31965.286
0.277	97340.959	32446.986
0.285	98876.175	32958.725
0.293	100199.092	33399.697
0.300	101531.027	33843.676
0.307	103195.735	34398.578
0.315	104716.670	34905.557
0.323	106085.188	35361.729
0.330	107289.752	35763.251
0.337	108670.131	36223.377
0.345	109875.094	36625.031
0.353	110990.845	36996.948
0.360	112285.798	37428.599
0.367	113679.953	37893.318
0.375	114882.526	38294.175
0.383	115978.753	38659.584
0.390	117375.867	39125.289
0.397	118669.583	39556.528
0.405	119745.981	39915.327
0.413	120701.457	40233.819
0.420	121974.668	40658.223
0.428	123129.878	41043.293
0.435	124035.165	41345.055
0.443	125162.689	41720.896
0.450	126398.667	42132.889
0.458	127501.952	42500.651
0.465	128330.102	42776.701
0.473	129460.665	43153.555
0.480	130576.221	43525.407
0.488	131537.557	43845.852
0.495	132475.039	44158.346
0.502	133531.375	44510.458
0.510	134642.119	44880.706
0.518	135506.724	45168.908
0.525	136495.311	45498.437
0.533	137458.721	45819.574
0.540	138638.781	46212.927
0.548	139552.350	46517.450
0.555	140521.477	46840.492
0.562	141722.917	47240.972
0.570	142993.273	47664.424
0.577	143794.869	47931.623
0.585	144467.944	48155.981
0.593	145475.253	48491.751
0.600	146257.267	48752.422
0.608	147102.981	49034.327
0.615	148113.689	49371.230
0.622	149301.066	49767.022
0.630	150254.249	50084.750
0.637	151063.648	50354.549
0.645	151941.063	50647.021
0.653	152898.539	50966.180
0.660	153703.396	51234.465
0.668	154225.343	51408.448
0.675	155179.427	51726.476
0.682	155849.430	51949.810
0.690	156722.854	52240.951
0.697	157296.303	52432.101
0.705	158079.645	52693.215
0.713	158546.206	52848.735
0.720	158947.901	52982.634
0.728	159434.019	53144.673
0.735	159855.500	53285.167
0.742	160218.165	53406.055
0.750	159446.332	53148.777
0.757	156216.226	52072.075
0.765	148991.990	49663.997
0.773	137348.167	45782.722

8.2.4.3 – HDB4 – Elongational Viscosity – 170 °C – Strain Rate = 1 s^{-1}

Time (sec)	Stress (Pa)	Viscosity (Pa s)
0.285	31600.962	31600.962
0.293	31785.737	31785.737
0.300	32078.549	32078.549
0.307	32320.042	32320.042
0.315	32635.430	32635.430
0.323	32954.288	32954.288
0.330	33276.101	33276.101
0.337	33600.325	33600.325
0.345	33946.968	33946.968
0.353	34239.939	34239.939
0.360	34440.871	34440.871
0.367	34662.168	34662.168
0.375	34807.729	34807.729
0.383	35011.643	35011.643
0.390	35196.931	35196.931
0.397	35442.033	35442.033
0.405	35708.848	35708.848
0.413	36037.568	36037.568
0.420	36389.535	36389.535
0.428	36703.807	36703.807
0.435	37041.383	37041.383
0.443	37279.301	37279.301
0.450	37539.004	37539.004
0.458	37696.299	37696.299
0.465	37916.960	37916.960
0.473	38118.036	38118.036
0.480	38340.918	38340.918
0.488	38586.733	38586.733
0.495	38898.460	38898.460
0.502	39235.432	39235.432
0.510	39574.602	39574.602
0.518	39939.056	39939.056
0.525	40217.156	40217.156
0.533	40497.175	40497.175
0.540	40688.874	40688.874
0.548	40858.081	40858.081
0.555	40981.717	40981.717
0.562	41127.621	41127.621
0.570	41344.227	41344.227
0.577	41655.474	41655.474
0.585	42016.275	42016.275
0.593	42332.581	42332.581
0.600	42651.269	42651.269
0.608	42851.281	42851.281
0.615	43051.140	43051.140
0.622	43227.453	43227.453
0.630	43379.667	43379.667
0.637	43530.958	43530.958
0.645	43682.072	43682.072
0.653	43909.914	43909.914
0.660	44137.924	44137.924
0.668	44470.202	44470.202
0.675	44804.983	44804.983
0.682	45063.821	45063.821
0.690	45244.961	45244.961
0.697	45426.279	45426.279
0.705	45581.559	45581.559
0.713	45763.003	45763.003
0.720	45998.623	45998.623
0.728	46126.324	46126.324
0.735	46252.500	46252.500
0.742	46434.066	46434.066
0.750	46783.630	46783.630
0.757	47108.211	47108.211
0.765	47377.642	47377.642
0.773	47590.637	47590.637
0.780	47747.672	47747.672
0.788	47932.824	47932.824
0.795	48088.493	48088.493
0.803	48362.048	48362.048
0.810	48518.761	48518.761
0.817	48763.975	48763.975
0.825	48980.588	48980.588
0.833	49258.166	49258.166
0.840	49506.214	49506.214
0.848	49724.990	49724.990
0.855	50006.096	50006.096
0.863	50288.615	50288.615
0.870	50603.458	50603.458
0.877	50953.268	50953.268
0.885	51304.506	51304.506
0.893	51432.943	51432.943
0.900	51461.877	51461.877
0.908	51555.516	51555.516
0.915	51811.296	51811.296
0.923	52167.757	52167.757
0.930	52493.828	52493.828
0.937	52821.852	52821.852
0.945	53015.478	53015.478
0.952	53242.578	53242.578
0.960	53402.477	53402.477
0.968	53665.029	53665.029
0.975	53789.063	53789.063
0.983	53804.925	53804.925
0.990	53819.071	53819.071
0.998	53973.000	53973.000
1.005	54343.946	54343.946
1.013	54716.310	54716.310
1.020	55055.291	55055.291
1.028	55321.663	55321.663
1.035	55664.100	55664.100
1.043	55858.224	55858.224
1.050	55863.661	55863.661
1.058	55864.833	55864.833
1.065	55902.773	55902.773
1.073	55936.931	55936.931
1.080	56047.074	56047.074
1.088	56311.757	56311.757
1.095	56538.544	56538.544
1.102	56844.752	56844.752
1.110	57032.063	57032.063
1.118	57259.793	57259.793
1.125	57324.448	57324.448
1.133	57345.401	57345.401
1.140	57529.147	57529.147
1.148	57670.349	57670.349
1.155	57852.794	57852.794
1.163	57950.615	57950.615
1.170	58216.099	58216.099
1.178	58396.931	58396.931
1.185	58664.521	58664.521
1.193	58888.831	58888.831
1.200	59111.852	59111.852
1.208	59248.271	59248.271
1.215	59248.395	59248.395
1.223	59335.841	59335.841
1.230	59511.220	59511.220
1.238	59685.884	59685.884
1.245	59767.051	59767.051

8.2.4.3 Continued

Time (sec)	Stress (Pa)	Viscosity (Pa s)
1.253	60032.942	60032.942
1.260	60250.954	60250.954
1.268	60517.707	60517.707
1.275	60689.495	60689.495
1.283	60860.440	60860.440
1.290	61079.019	61079.019
1.298	61199.711	61199.711
1.305	61318.764	61318.764
1.313	61388.016	61388.016
1.320	61603.276	61603.276
1.328	61618.393	61618.393
1.335	61830.121	61830.121
1.343	62043.091	62043.091
1.350	62305.706	62305.706
1.357	62518.438	62518.438
1.365	62678.568	62678.568
1.373	62993.991	62993.991
1.380	63363.686	63363.686
1.388	63628.430	63628.430
1.395	63735.212	63735.212
1.403	63784.071	63784.071
1.410	63669.299	63669.299
1.418	63712.820	63712.820
1.425	63972.089	63972.089
1.433	64231.636	64231.636
1.440	64604.186	64604.186
1.448	64865.141	64865.141
1.455	65240.783	65240.783
1.463	65218.438	65218.438
1.470	65250.124	65250.124
1.477	65161.574	65161.574
1.485	65185.904	65185.904
1.493	65147.508	65147.508
1.500	65222.702	65222.702
1.508	65355.625	65355.625
1.515	65608.342	65608.342
1.523	65920.502	65920.502
1.530	66050.538	66050.538
1.538	66301.154	66301.154
1.545	66365.915	66365.915
1.553	66554.033	66554.033
1.560	66552.527	66552.527

Time (sec)	Stress (Pa)	Viscosity (Pa s)
1.568	66547.227	66547.227
1.575	66665.117	66665.117
1.583	66781.010	66781.010
1.590	66958.364	66958.364
1.598	67136.600	67136.600
1.605	67511.099	67511.099
1.613	67753.517	67753.517
1.620	68063.214	68063.214
1.628	68239.844	68239.844
1.635	68278.298	68278.298
1.643	68247.601	68247.601
1.650	68416.925	68416.925
1.658	68514.879	68514.879
1.665	68470.356	68470.356
1.673	68773.580	68773.580
1.680	68936.384	68936.384
1.688	69204.900	69204.900
1.695	69292.853	69292.853
1.703	69450.371	69450.371
1.710	69607.448	69607.448
1.718	69688.577	69688.577
1.725	69840.789	69840.789
1.732	70066.839	70066.839
1.740	70292.343	70292.343
1.748	70251.340	70251.340
1.755	70512.274	70512.274
1.763	70695.353	70695.353
1.770	70916.390	70916.390
1.778	71136.743	71136.743
1.785	71356.398	71356.398
1.793	71655.497	71655.497
1.800	71594.029	71594.029
1.808	71527.561	71527.561
1.815	71454.792	71454.792
1.823	71583.413	71583.413
1.830	71503.095	71503.095
1.838	71750.410	71750.410
1.845	71996.117	71996.117
1.852	72327.868	72327.868
1.860	72616.363	72616.363
1.868	72991.525	72991.525
1.875	73282.451	73282.451

Time (sec)	Stress (Pa)	Viscosity (Pa s)
1.883	73267.939	73267.939
1.890	73381.617	73381.617
1.898	73227.078	73227.078
1.905	73332.474	73332.474
1.913	73391.489	73391.489
1.920	73582.452	73582.452
1.928	73772.152	73772.152
1.935	74190.250	74190.250
1.943	74563.887	74563.887
1.950	74752.680	74752.680
1.958	75175.029	75175.029
1.965	75126.073	75126.073
1.973	75120.109	75120.109
1.980	74869.489	74869.489
1.988	74999.119	74999.119
1.995	74979.183	74979.183
2.002	75151.006	75151.006
2.010	75419.338	75419.338
2.018	75638.739	75638.739
2.025	76157.590	76157.590
2.032	76377.288	76377.288
2.040	76647.341	76647.341
2.048	76658.469	76658.469
2.055	76771.237	76771.237
2.063	76618.828	76618.828
2.070	76618.467	76618.467
2.078	76613.762	76613.762
2.085	76550.933	76550.933
2.093	76805.860	76805.860
2.100	77004.093	77004.093
2.107	77638.717	77638.717
2.115	77839.177	77839.177
2.123	78092.303	78092.303
2.130	78234.183	78234.183
2.137	78262.278	78262.278
2.145	78172.337	78172.337
2.153	78134.033	78134.033
2.160	78204.757	78204.757
2.167	78098.901	78098.901
2.175	78394.825	78394.825
2.183	78516.732	78516.732
2.190	79048.159	79048.159

8.2.4.3 Continued

Time (sec)	Stress (Pa)	Viscosity (Pa s)
2.198	79284.486	79284.486
2.205	79701.524	79701.524
2.213	79696.992	79696.992
2.220	79686.004	79686.004
2.228	79548.377	79548.377
2.235	79404.133	79404.133
2.242	79441.808	79441.808
2.250	79222.217	79222.217
2.258	79375.758	79375.758
2.265	79462.840	79462.840
2.272	79739.100	79739.100
2.280	80015.041	80015.041
2.288	80356.356	80356.356
2.295	80435.260	80435.260
2.303	80446.093	80446.093
2.310	80650.194	80650.194
2.318	80382.586	80382.586
2.325	80379.466	80379.466
2.333	80234.191	80234.191
2.340	80355.161	80355.161
2.348	80475.534	80475.534
2.355	80802.088	80802.088
2.363	80847.639	80847.639
2.370	80960.685	80960.685
2.377	81140.628	81140.628
2.385	81105.627	81105.627
2.393	81280.169	81280.169
2.400	81089.253	81089.253
2.407	81185.181	81185.181
2.415	80906.739	80906.739
2.423	80842.997	80842.997
2.430	81001.193	81001.193
2.438	81154.899	81154.899
2.445	81231.666	81231.666
2.453	81382.553	81382.553
2.460	81760.787	81760.787
2.468	81596.178	81596.178
2.475	81501.348	81501.348
2.482	81085.636	81085.636
2.490	81056.796	81056.796
2.498	80941.776	80941.776
2.505	81023.539	81023.539
2.512	81184.294	81184.294
2.520	81053.756	81053.756
2.528	81249.748	81249.748
2.535	81317.762	81317.762
2.542	81677.925	81677.925
2.550	81996.166	81996.166
2.558	82527.300	82527.300
2.565	82245.147	82245.147
2.573	82038.887	82038.887
2.580	81695.346	81695.346
2.588	81429.425	81429.425
2.595	81554.606	81554.606
2.603	81498.227	81498.227
2.610	81931.554	81931.554
2.617	81822.131	81822.131
2.625	82209.112	82209.112
2.633	81999.352	81999.352
2.640	81966.047	81966.047
2.647	81741.927	81741.927
2.655	81555.870	81555.870
2.663	81268.111	81268.111
2.670	81114.541	81114.541
2.678	81243.985	81243.985
2.685	81272.901	81272.901
2.693	82031.132	82031.132
2.700	82352.174	82352.174
2.708	82724.975	82724.975
2.715	82597.555	82597.555
2.723	82462.012	82462.012
2.730	82118.107	82118.107
2.738	81559.671	81559.671
2.745	81296.742	81296.742
2.752	80403.417	80403.417
2.760	80275.165	80275.165
2.768	79824.797	79824.797
2.775	80000.689	80000.689
2.782	79854.321	79854.321
2.790	80078.369	80078.369
2.798	80246.484	80246.484
2.805	80631.592	80631.592
2.813	80852.909	80852.909
2.820	80350.044	80350.044
2.828	80059.017	80059.017
2.835	79250.861	79250.861
2.843	79165.398	79165.398
2.850	79074.134	79074.134
2.857	79151.431	79151.431
2.865	79339.037	79339.037
2.873	79644.787	79644.787
2.880	79712.802	79712.802
2.887	79481.387	79481.387
2.895	79659.049	79659.049
2.903	79293.029	79293.029
2.910	79160.236	79160.236
2.917	78409.197	78409.197
2.925	78320.934	78320.934
2.933	77915.436	77915.436
2.940	77562.530	77562.530
2.948	77072.690	77072.690
2.955	76763.337	76763.337
2.963	77084.875	77084.875
2.970	76760.200	76760.200
2.978	76428.276	76428.276
2.985	75626.654	75626.654
2.992	75667.655	75667.655
3.000	75239.763	75239.763
3.008	74934.162	74934.162
3.015	74823.884	74823.884
3.022	74774.181	74774.181
3.030	74652.523	74652.523
3.038	74522.659	74522.659
3.045	74875.407	74875.407
3.053	74387.773	74387.773
3.060	74522.785	74522.785
3.068	74229.604	74229.604
3.075	74072.314	74072.314
3.083	73546.617	73546.617
3.090	73189.959	73189.959
3.098	73154.141	73154.141
3.105	73077.518	73077.518
3.113	73552.646	73552.646
3.120	73243.904	73243.904

8.2.4.4 – HDB4 – Elongational Viscosity – 170 °C – Strain Rate = 0.3 s^{-1}

Time (sec)	Stress (Pa)	Viscosity (Pa s)
1.198	60525.993	60525.993
1.221	60842.225	60842.225
1.243	61114.224	61114.224
1.266	61387.117	61387.117
1.288	61756.521	61756.521
1.311	62078.522	62078.522
1.333	62236.117	62236.117
1.356	62342.738	62342.738
1.378	62498.550	62498.550
1.401	63019.241	63019.241
1.423	63200.152	63200.152
1.446	63702.620	63702.620
1.468	64183.002	64183.002
1.491	64543.803	64543.803
1.513	64777.911	64777.911
1.536	65191.671	65191.671
1.558	65606.497	65606.497
1.581	65895.838	65895.838
1.603	66082.587	66082.587
1.626	66190.291	66190.291
1.648	66189.900	66189.900
1.671	66266.088	66266.088
1.693	66448.239	66448.239
1.716	66791.230	66791.230
1.738	67377.909	67377.909
1.761	67725.733	67725.733
1.783	68019.725	68019.725
1.806	68590.393	68590.393
1.828	68971.471	68971.471
1.851	69129.890	69129.890
1.873	69119.803	69119.803
1.896	69162.038	69162.038
1.918	69287.431	69287.431
1.941	69726.743	69726.743
1.963	70113.839	70113.839
1.986	70238.668	70238.668
2.008	70683.815	70683.815
2.031	71222.283	71222.283
2.053	71646.339	71646.339
2.076	72010.483	72010.483
2.098	72407.682	72407.682
2.121	72777.205	72777.205
2.143	73178.369	73178.369
2.166	73581.622	73581.622
2.188	73708.009	73708.009
2.211	73395.187	73395.187
2.233	73609.503	73609.503
2.256	73982.169	73982.169
2.278	74387.698	74387.698
2.301	74763.922	74763.922
2.323	75139.853	75139.853
2.346	75421.942	75421.942
2.368	75540.153	75540.153
2.391	76051.774	76051.774
2.413	76367.884	76367.884
2.436	76502.863	76502.863
2.458	76700.998	76700.998
2.481	76846.507	76846.507
2.503	76872.614	76872.614
2.526	77151.749	77151.749
2.548	77363.494	77363.494
2.571	77956.638	77956.638
2.593	78327.117	78327.117
2.616	78539.384	78539.384
2.638	78822.604	78822.604
2.661	79123.560	79123.560
2.683	79263.151	79263.151
2.706	79490.781	79490.781
2.728	79628.595	79628.595
2.751	79872.466	79872.466
2.773	80136.349	80136.349
2.796	80361.416	80361.416
2.818	80624.847	80624.847
2.841	80793.521	80793.521
2.863	81093.233	81093.233
2.886	81316.098	81316.098
2.908	81615.996	81615.996
2.931	82110.663	82110.663
2.953	82354.033	82354.033
2.976	82538.052	82538.052
2.998	82720.780	82720.780
3.021	83101.972	83101.972
3.043	83262.564	83262.564
3.066	82998.014	82998.014
3.088	82786.976	82786.976
3.111	83122.419	83122.419
3.133	83643.810	83643.810
3.156	84023.853	84023.853
3.178	84341.353	84341.353
3.201	84533.298	84533.298
3.223	85021.691	85021.691
3.246	85278.245	85278.245
3.268	85404.492	85404.492
3.291	85679.119	85679.119
3.313	85715.503	85715.503
3.336	85550.307	85550.307
3.358	85821.046	85821.046
3.381	85892.050	85892.050
3.403	86003.800	86003.800
3.426	86428.110	86428.110
3.448	86855.603	86855.603
3.471	87351.847	87351.847
3.493	87644.490	87644.490
3.516	87937.100	87937.100
3.538	88347.729	88347.729
3.561	88500.638	88500.638
3.583	88863.540	88863.540
3.606	89488.632	89488.632
3.628	89736.612	89736.612
3.651	89331.972	89331.972
3.673	88966.614	88966.614
3.696	88909.914	88909.914
3.718	89265.812	89265.812
3.741	89970.182	89970.182
3.763	90504.943	90504.943
3.786	91041.298	91041.298
3.808	91431.126	91431.126
3.831	91643.442	91643.442
3.853	91854.437	91854.437
3.876	91832.670	91832.670
3.898	91546.454	91546.454
3.921	91382.995	91382.995
3.943	91500.694	91500.694
3.966	91724.154	91724.154
3.988	92052.271	92052.271
4.011	92675.725	92675.725
4.033	93087.193	93087.193
4.056	93607.990	93607.990
4.078	94104.808	94104.808

8.2.4.4 Continued

Time (sec)	Stress (Pa)	Viscosity (Pa s)
4.101	94356.477	94356.477
4.123	94634.364	94634.364
4.146	94633.431	94633.431
4.168	94344.563	94344.563
4.191	94191.051	94191.051
4.213	94315.093	94315.093
4.236	94466.302	94466.302
4.258	94961.311	94961.311
4.281	95371.594	95371.594
4.303	95929.827	95929.827
4.326	96460.624	96460.624
4.348	97144.778	97144.778
4.371	97473.984	97473.984
4.393	97652.423	97652.423
4.416	97615.924	97615.924
4.438	97729.140	97729.140
4.461	97561.708	97561.708
4.483	97480.090	97480.090
4.506	97735.220	97735.220
4.528	98209.529	98209.529
4.551	98084.331	98084.331
4.573	98399.306	98399.306
4.596	99001.272	99001.272
4.618	99640.322	99640.322
4.641	100380.526	100380.526
4.663	100569.906	100569.906
4.686	100528.403	100528.403
4.708	100514.065	100514.065
4.731	100995.446	100995.446
4.753	101142.785	101142.785
4.776	101118.390	101118.390
4.798	101089.021	101089.021
4.821	101328.436	101328.436
4.843	101671.689	101671.689
4.866	102220.463	102220.463
4.888	102494.704	102494.704
4.911	103012.788	103012.788
4.933	103321.307	103321.307
4.956	103664.109	103664.109
4.978	103936.688	103936.688
5.001	104278.806	104278.806
5.023	104403.108	104403.108

Time (sec)	Stress (Pa)	Viscosity (Pa s)
5.046	104376.715	104376.715
5.068	104237.115	104237.115
5.091	104274.426	104274.426
5.113	104681.706	104681.706
5.136	105052.968	105052.968
5.158	105801.481	105801.481
5.181	106518.060	106518.060
5.203	106894.856	106894.856
5.226	107078.319	107078.319
5.248	107725.126	107725.126
5.271	107318.324	107318.324
5.293	107414.121	107414.121
5.316	107627.527	107627.527
5.338	107594.764	107594.764
5.361	107802.413	107802.413
5.383	108126.701	108126.701
5.406	109020.955	109020.955
5.428	109513.541	109513.541
5.451	109593.660	109593.660
5.473	109921.528	109921.528
5.496	110161.797	110161.797
5.518	110485.301	110485.301
5.541	111147.984	111147.984
5.563	111903.392	111903.392
5.586	111626.569	111626.569
5.608	111125.109	111125.109
5.631	111288.715	111288.715
5.653	111800.955	111800.955
5.676	111827.395	111827.395
5.698	112407.994	112407.994
5.721	112854.422	112854.422
5.743	113483.691	113483.691
5.766	114206.497	114206.497
5.788	114271.663	114271.663
5.811	114608.165	114608.165
5.833	115129.488	115129.488
5.856	115115.132	115115.132
5.878	115260.350	115260.350
5.901	115449.967	115449.967
5.923	115421.526	115421.526
5.946	115579.277	115579.277
5.968	115831.200	115831.200

Time (sec)	Stress (Pa)	Viscosity (Pa s)
5.991	116202.984	116202.984
6.013	116891.358	116891.358
6.036	117461.844	117461.844
6.058	118083.166	118083.166
6.081	118483.307	118483.307
6.103	119110.723	119110.723
6.126	119486.111	119486.111
6.148	119607.413	119607.413
6.171	119083.978	119083.978
6.193	118702.587	118702.587
6.216	118985.570	118985.570
6.238	119006.297	119006.297
6.261	119364.756	119364.756
6.283	119960.869	119960.869
6.306	120533.477	120533.477
6.328	121106.692	121106.692
6.351	121520.073	121520.073
6.373	121608.776	121608.776
6.396	121662.923	121662.923
6.418	122100.440	122100.440
6.441	122370.056	122370.056
6.463	122863.562	122863.562
6.486	122681.255	122681.255
6.508	122516.846	122516.846
6.531	123004.473	123004.473
6.553	123521.203	123521.203
6.576	124212.697	124212.697
6.598	125636.493	125636.493
6.621	126781.545	126781.545
6.643	127197.837	127197.837
6.666	127017.690	127017.690
6.688	126558.412	126558.412
6.711	126601.151	126601.151
6.733	126516.237	126516.237
6.756	126762.405	126762.405
6.778	126605.603	126605.603
6.801	126904.630	126904.630
6.823	126921.765	126921.765
6.846	127372.693	127372.693
6.868	127729.259	127729.259
6.891	128563.232	128563.232
6.913	129273.421	129273.421

8.2.4.4 Continued

Time (sec)	Stress (Pa)	Viscosity (Pa s)
6.936	129697.553	129697.553
6.958	129925.027	129925.027
6.981	130675.121	130675.121
7.003	130900.368	130900.368
7.026	130428.039	130428.039
7.048	130210.399	130210.399
7.071	130150.082	130150.082
7.093	130490.112	130490.112
7.116	131068.055	131068.055
7.138	131783.990	131783.990
7.161	132193.610	132193.610
7.183	132984.895	132984.895
7.206	133116.066	133116.066
7.228	133488.242	133488.242
7.251	133861.516	133861.516
7.273	133945.801	133945.801
7.296	134277.626	134277.626
7.318	134318.177	134318.177
7.341	134170.585	134170.585
7.363	134823.816	134823.816
7.386	135071.389	135071.389
7.408	135538.727	135538.727
7.431	136008.502	136008.502
7.453	136515.247	136515.247
7.476	136679.573	136679.573
7.498	136536.497	136536.497
7.521	136883.279	136883.279
7.543	137656.629	137656.629
7.566	138238.895	138238.895
7.588	137878.142	137878.142
7.611	138338.880	138338.880
7.633	138838.399	138838.399
7.656	139377.503	139377.503
7.678	139636.748	139636.748
7.701	139932.791	139932.791
7.723	141165.141	141165.141
7.746	141588.376	141588.376
7.768	142005.810	142005.810
7.791	142093.753	142093.753
7.813	142132.779	142132.779
7.836	142586.720	142586.720
7.858	143383.449	143383.449

Time (sec)	Stress (Pa)	Viscosity (Pa s)
7.881	143367.824	143367.824
7.903	143087.173	143087.173
7.926	143101.210	143101.210
7.948	143063.485	143063.485
7.971	143768.906	143768.906
7.993	144344.681	144344.681
8.016	144294.779	144294.779
8.038	144824.798	144824.798
8.061	144718.596	144718.596
8.083	145722.392	145722.392
8.106	146318.735	146318.735
8.128	146848.809	146848.809
8.151	147796.562	147796.562
8.173	147440.301	147440.301
8.196	146978.939	146978.939
8.218	146954.930	146954.930
8.241	147234.391	147234.391
8.263	147631.254	147631.254
8.286	148509.970	148509.970
8.308	148785.311	148785.311
8.331	149743.590	149743.590
8.353	150536.065	150536.065
8.376	151232.244	151232.244
8.398	151405.163	151405.163
8.421	151976.658	151976.658
8.443	151661.227	151661.227
8.466	150774.612	150774.612
8.488	151049.905	151049.905
8.511	151813.659	151813.659
8.533	152112.906	152112.906
8.556	152433.267	152433.267
8.578	152833.268	152833.268
8.601	153363.267	153363.267
8.623	153677.572	153677.572
8.646	154125.752	154125.752
8.668	154112.184	154112.184
8.691	154473.480	154473.480
8.713	154721.738	154721.738
8.736	154633.063	154633.063
8.758	154817.055	154817.055
8.781	155164.461	155164.461
8.803	155480.114	155480.114

Time (sec)	Stress (Pa)	Viscosity (Pa s)
8.826	156077.904	156077.904
8.848	156933.819	156933.819
8.871	157535.256	157535.256
8.893	157703.233	157703.233
8.916	158858.753	158858.753
8.938	159228.359	159228.359
8.961	159507.014	159507.014
8.983	160139.199	160139.199
9.006	159422.783	159422.783
9.028	159171.235	159171.235
9.051	159946.270	159946.270
9.073	160048.868	160048.868
9.096	160023.046	160023.046
9.118	161074.615	161074.615
9.141	162291.591	162291.591
9.163	163831.084	163831.084
9.186	164812.922	164812.922
9.208	163855.546	163855.546
9.231	164290.355	164290.355
9.253	165371.461	165371.461
9.276	165546.833	165546.833
9.298	164177.272	164177.272
9.321	164099.900	164099.900
9.343	164249.366	164249.366
9.366	163755.851	163755.851
9.388	164797.059	164797.059
9.411	165710.250	165710.250
9.433	166559.446	166559.446
9.456	166312.612	166312.612
9.478	166955.016	166955.016
9.501	167700.676	167700.676
9.523	168206.723	168206.723
9.546	168356.104	168356.104
9.568	168964.416	168964.416
9.591	168425.657	168425.657
9.613	168846.761	168846.761
9.636	169084.164	169084.164
9.658	169388.411	169388.411
9.681	169873.173	169873.173
9.703	171245.269	171245.269
9.726	170727.512	170727.512
9.748	171022.170	171022.170

8.2.4.4 Continued

Time (sec)	Stress (Pa)	Viscosity (Pa s)
9.771	171802.105	171802.105
9.793	172206.142	172206.142
9.816	172416.019	172416.019
9.838	172851.566	172851.566
9.861	172702.002	172702.002
9.883	172972.030	172972.030
9.906	173437.194	173437.194
9.928	173320.226	173320.226
9.951	174054.547	174054.547
9.973	175435.654	175435.654
9.996	175711.825	175711.825
10.018	176901.892	176901.892
10.041	177709.735	177709.735

Time (sec)	Stress (Pa)	Viscosity (Pa s)
10.063	178500.260	178500.260
10.086	178730.389	178730.389
10.108	178621.007	178621.007
10.131	177995.595	177995.595
10.153	177948.686	177948.686
10.176	178020.637	178020.637
10.198	178107.694	178107.694
10.221	178771.341	178771.341
10.243	178737.942	178737.942
10.266	178939.467	178939.467
10.288	180194.505	180194.505
10.311	180792.324	180792.324
10.333	181814.684	181814.684

Time (sec)	Stress (Pa)	Viscosity (Pa s)
10.36	182865.97	182865.97
10.38	182741.07	182741.07
10.40	183888.16	183888.16
10.42	182991.21	182991.21
10.45	183558.22	183558.22
10.47	183470.37	183470.37
10.49	183961.34	183961.34
10.51	184402.98	184402.98
10.54	184675.27	184675.27
10.56	185518.43	185518.43
10.58	186292.47	186292.47
10.60	188721.10	188721.10
10.63	189461.07	189461.07

8.2.4.5 – HDB4 – Elongational Viscosity – 170 °C – Strain Rate = 0.03 s^{-1}

Time (sec)	Stress (Pa)	Viscosity (Pa s)
10.491	4465.075	148835.841
10.603	4450.170	148339.002
10.716	4467.180	148906.016
10.828	4485.364	149512.149
10.941	4471.088	149036.274
11.053	4478.136	149271.211
11.166	4494.770	149825.665
11.278	4508.466	150282.204
11.391	4512.424	150414.123
11.503	4497.235	149907.821
11.616	4480.377	149345.891
11.728	4458.794	148626.473
11.841	4452.518	148417.278
11.953	4473.309	149110.290
12.066	4510.438	150347.927
12.178	4520.936	150697.875
12.291	4511.876	150395.853
12.403	4539.795	151326.493
12.516	4535.561	151185.352
12.628	4536.581	151219.353
12.741	4607.014	153567.125
12.853	4613.419	153780.619
12.966	4613.373	153779.109
13.078	4649.544	154984.812
13.191	4631.782	154392.741

Time (sec)	Stress (Pa)	Viscosity (Pa s)
13.303	4688.072	156269.080
13.416	4729.502	157650.062
13.528	4732.524	157750.792
13.641	4703.991	156799.694
13.753	4678.979	155965.971
13.866	4713.163	157105.426
13.978	4689.260	156308.678
14.091	4669.901	155663.359
14.203	4677.367	155912.223
14.316	4658.413	155280.423
14.428	4644.359	154811.960
14.541	4637.047	154568.222
14.653	4624.378	154145.925
14.766	4612.403	153746.752
14.878	4648.877	154962.556
14.991	4665.152	155505.052
15.103	4686.109	156203.626
15.216	4677.201	155906.712
15.328	4692.308	156410.268
15.441	4693.731	156457.691
15.553	4725.367	157512.223
15.666	4755.880	158529.345
15.778	4747.646	158254.859
15.891	4789.813	159660.441
16.003	4784.264	159475.478

Time (sec)	Stress (Pa)	Viscosity (Pa s)
16.116	4765.187	158839.582
16.228	4778.688	159289.598
16.341	4789.825	159660.840
16.453	4779.019	159300.625
16.566	4831.125	161037.502
16.678	4839.450	161315.003
16.791	4878.662	162622.063
16.903	4883.617	162787.245
17.016	4859.162	161972.061
17.128	4789.286	159642.859
17.241	4776.487	159216.238
17.353	4811.302	160376.729
17.466	4797.404	159913.458
17.578	4791.357	159711.906
17.691	4822.171	160739.040
17.803	4837.562	161252.062
17.916	4827.688	160922.944
18.028	4821.977	160732.556
18.141	4795.983	159866.107
18.253	4840.233	161341.087
18.366	4864.092	162136.399
18.478	4835.174	161172.471
18.591	4847.397	161579.900
18.703	4839.506	161316.866
18.816	4838.008	161266.917

8.2.4.5 Continued

Time (sec)	Stress (Pa)	Viscosity (Pa s)
18.928	4861.673	162055.751
19.041	4896.562	163218.730
19.153	4916.281	163876.032
19.266	4945.922	164864.065
19.378	4909.507	163650.243
19.491	4956.479	165215.971
19.603	4971.632	165721.058
19.716	4949.972	164999.082
19.828	4946.197	164873.247
19.941	4956.357	165211.894
20.053	4998.069	166602.313
20.166	4975.406	165846.861
20.278	4920.941	164031.356
20.391	4931.910	164397.009
20.503	4974.539	165817.979
20.616	4967.876	165595.873
20.728	4919.965	163998.842
20.841	4954.244	165141.480
20.953	4964.897	165496.551
21.066	4988.888	166296.271
21.178	5025.009	167500.304
21.291	5040.225	168007.511
21.403	5014.261	167142.041
21.516	5023.993	167466.439
21.628	5054.273	168475.769
21.741	5073.669	169122.308
21.853	5069.542	168984.736
21.966	5084.442	169481.413
22.078	5096.362	169878.738
22.191	5105.877	170195.895
22.303	5080.001	169333.379
22.416	5079.199	169306.627
22.528	5080.785	169359.497
22.641	5117.992	170599.747
22.753	5150.457	171681.904
22.866	5116.568	170552.262
22.978	5118.157	170605.232
23.091	5134.125	171137.486
23.203	5098.318	169943.933
23.316	5069.024	168967.480
23.428	5084.182	169472.735
23.541	5137.203	171240.105
23.653	5138.450	171281.679
23.766	5137.011	171233.716
23.878	5143.984	171466.133
23.991	5123.499	170783.292
24.103	5142.380	171412.679
24.216	5153.041	171768.049
24.328	5182.107	172736.900
24.441	5246.362	174878.728
24.553	5271.728	175724.262
24.666	5251.367	175045.551
24.778	5220.785	174026.154
24.891	5276.783	175892.752
25.003	5317.161	177238.713
25.116	5316.306	177210.212
25.228	5285.856	176195.212
25.341	5296.295	176543.180
25.453	5328.348	177611.594
25.566	5363.338	178777.935
25.678	5332.967	177765.551
25.791	5314.688	177156.280
25.903	5316.960	177231.995
26.016	5288.465	176282.167
26.128	5305.661	176855.383
26.241	5299.912	176663.748
26.353	5225.320	174177.334
26.466	5274.025	175800.834
26.578	5299.567	176652.228
26.691	5306.670	176888.995
26.803	5312.665	177088.839
26.916	5340.114	178003.791
27.028	5397.451	179915.044
27.141	5437.921	181264.019
27.253	5443.996	181466.537
27.366	5433.346	181111.522
27.478	5438.307	181276.889
27.591	5454.653	181821.783
27.703	5444.255	181475.174
27.816	5422.335	180744.501
27.928	5447.050	181568.317
28.041	5417.221	180574.024
28.153	5413.457	180448.557
28.266	5449.751	181658.352
28.378	5439.790	181326.318
28.491	5409.909	180330.299
28.603	5373.460	179115.348
28.716	5432.634	181087.810
28.828	5496.483	183216.105
28.941	5447.247	181574.906
29.053	5410.819	180360.649
29.166	5423.876	180795.872
29.278	5394.825	179827.490
29.391	5455.340	181844.668
29.503	5526.349	184211.631
29.616	5493.479	183115.974
29.728	5458.694	181956.480
29.841	5511.168	183705.607
29.953	5535.270	184509.000
30.066	5553.435	185114.484
30.178	5550.069	185002.305
30.291	5607.293	186909.762
30.403	5635.343	187844.770
30.516	5545.463	184848.780
30.628	5589.889	186329.636
30.741	5593.328	186444.255
30.853	5603.807	186793.569
30.966	5663.353	188778.423
31.078	5696.757	189891.907
31.191	5712.837	190427.902
31.303	5721.099	190703.310
31.416	5740.783	191359.448
31.528	5715.688	190522.942
31.641	5657.673	188589.097
31.753	5633.843	187794.760
31.866	5599.706	186656.868
31.978	5559.230	185307.658
32.091	5620.485	187349.487
32.203	5716.736	190557.861
32.316	5703.766	190125.531
32.428	5669.078	188969.280
32.541	5652.419	188413.970
32.653	5679.714	189323.795
32.766	5742.245	191408.154
32.878	5736.694	191223.141
32.991	5755.609	191853.637

8.2.4.5 Continued

Time (sec)	Stress (Pa)	Viscosity (Pa s)
33.103	5754.385	191812.834
33.216	5763.462	192115.410
33.328	5765.635	192187.818
33.441	5819.017	193967.231
33.553	5780.673	192689.091
33.666	5755.701	191856.690
33.778	5806.941	193564.684
33.891	5836.175	194539.183
34.003	5809.331	193644.374
34.116	5816.203	193873.443
34.228	5836.986	194566.207
34.341	5808.173	193605.765
34.453	5794.000	193133.317
34.566	5827.910	194263.680
34.678	5757.853	191928.434
34.791	5722.927	190764.241
34.903	5768.293	192276.444
35.016	5787.157	192905.234
35.128	5800.460	193348.678
35.241	5857.508	195250.270
35.353	5887.731	196257.709
35.466	5927.772	197592.414
35.578	5873.081	195769.372
35.691	5879.161	195972.018
35.803	5888.214	196273.788
35.916	5802.144	193404.811
36.028	5861.536	195384.547
36.141	5924.425	197480.832
36.253	5914.187	197139.577
36.366	5884.717	196157.220
36.478	5969.945	198998.171
36.591	5956.883	198562.775
36.703	6013.191	200439.707
36.816	5951.527	198384.217
36.928	5901.649	196721.641
37.041	5949.208	198306.935
37.153	5868.161	195605.380
37.266	5865.248	195508.254
37.378	5954.384	198479.474
37.491	5934.050	197801.683
37.603	5920.806	197360.203
37.716	5944.827	198160.905
37.828	6038.224	201274.121
37.941	6018.179	200605.972
38.053	5977.982	199266.058
38.166	5984.895	199496.498
38.278	6052.458	201748.595
38.391	6061.928	202064.252
38.503	6101.368	203378.923
38.616	6141.857	204728.567
38.728	6148.671	204955.687
38.841	6140.748	204691.587
38.953	6114.643	203821.424
39.066	6177.017	205900.556
39.178	6250.997	208366.574
39.291	6225.948	207531.585
39.403	6103.183	203439.422
39.516	6043.066	201435.548
39.628	6049.895	201663.167
39.741	6030.727	201024.220
39.853	6039.631	201321.030
39.966	6086.789	202892.979
40.078	6158.212	205273.731
40.191	6076.104	202536.812
40.303	6031.427	201047.568
40.416	6140.617	204687.242
40.528	6184.666	206155.536
40.641	6180.397	206013.245
40.753	6123.236	204107.875
40.866	6147.580	204919.323
40.978	6255.628	208520.934
41.091	6189.369	206312.314
41.203	6231.606	207720.196
41.316	6337.595	211253.164
41.428	6446.853	214895.106
41.541	6502.879	216762.617
41.653	6460.678	215355.941
41.766	6373.833	212461.108
41.878	6342.967	211432.226
41.991	6331.599	211053.302
42.103	6341.506	211383.533
42.216	6317.583	210586.103
42.328	6315.628	210520.938
42.441	6231.321	207710.685
42.553	6206.084	206869.474
42.666	6239.722	207990.733
42.778	6360.639	212021.285
42.891	6337.949	211264.974
43.003	6300.307	210010.220
43.116	6277.276	209242.535
43.228	6338.416	211280.530
43.341	6380.606	212686.871
43.453	6282.761	209425.383
43.566	6280.301	209343.372
43.678	6350.250	211674.986
43.791	6484.893	216163.096
43.903	6452.449	215081.624
44.016	6572.688	219089.603
44.128	6588.046	219601.517
44.241	6586.804	219560.129
44.353	6461.448	215381.603
44.466	6594.723	219824.103
44.578	6603.106	220103.519
44.691	6677.691	222589.696
44.803	6742.798	224759.935
44.972	6721.740	224057.992
45.197	6696.401	223213.352
45.422	6627.080	220902.654
45.647	6594.530	219817.667
45.872	6549.065	218302.156
46.097	6592.532	219751.073
46.322	6570.679	219022.626
46.547	6624.720	220823.987
46.772	6526.618	217553.926
46.997	6701.442	223381.415
47.222	6518.348	217278.266
47.447	6511.646	217054.851
47.672	6615.134	220504.462
47.897	6673.057	222435.238
48.122	6535.031	217834.352
48.347	6467.398	215579.919
48.572	6417.676	213922.529
48.797	6403.953	213465.088
49.022	6308.524	210284.117
49.247	6340.418	211347.271
49.472	6432.484	214416.128

8.2.4.5 Continued

Time (sec)	Stress (Pa)	Viscosity (Pa s)
49.697	6503.251	216775.033
49.922	6506.468	216882.252
50.147	6508.227	216940.897
50.372	6618.520	220617.319
50.597	6546.281	218209.350
50.822	6560.540	218684.652
51.047	6614.449	220481.624
51.272	6689.424	222980.790
51.497	6785.259	226175.311
51.722	6732.834	224427.815
51.947	6687.325	222910.835
52.172	6702.361	223412.032
52.397	6799.346	226644.861
52.622	6867.857	228928.567
52.847	6788.262	226275.410
53.072	6805.454	226848.452
53.297	6820.361	227345.360
53.522	6863.781	228792.696
53.747	6793.775	226459.156
53.972	6731.389	224379.646
54.197	6771.433	225714.447
54.422	6630.262	221008.740
54.647	6706.723	223557.442
54.872	6767.396	225579.858
55.097	6750.773	225025.770
55.322	6699.893	223329.769
55.547	6723.932	224131.080
55.772	6758.198	225273.273
55.997	6846.747	228224.901
56.222	6812.037	227067.905
56.447	6710.053	223668.429
56.672	6808.905	226963.514
56.897	6757.919	225263.961
57.122	6731.635	224387.844
57.347	6888.217	229607.233
57.572	6791.811	226393.700
57.797	6632.362	221078.741
58.022	6693.408	223113.593
58.247	6785.400	226180.005
58.472	6633.417	221113.897
58.697	6667.720	222257.326
58.922	6706.878	223562.600
59.147	6698.982	223299.416
59.372	6770.401	225680.029
59.597	6900.385	230012.827
59.822	6926.348	230878.264
60.047	6762.909	225430.298
60.272	6838.734	227957.795
60.497	6865.494	228849.815
60.722	6888.586	229619.544
60.947	6940.926	231364.194
61.172	6943.277	231442.553
61.397	6957.003	231900.106
61.622	7048.821	234960.711
61.847	7097.701	236590.021
62.072	6874.073	229135.779
62.297	6824.638	227487.950
62.522	6940.036	231334.537
62.747	7002.548	233418.277
62.972	7331.909	244396.966
63.197	7834.027	261134.225
63.422	7860.210	262007.006
63.647	7935.692	264523.080
63.872	8027.272	267575.726
64.097	8037.305	267910.153
64.322	8154.016	271800.522
64.547	8055.431	268514.351
64.772	8224.106	274136.879
64.997	8006.197	266873.250
65.222	8144.890	271496.343
65.447	8186.568	272885.611
65.672	8237.382	274579.397
65.897	8075.917	269197.234
66.122	8197.802	273260.061
66.347	8123.580	270786.015
66.572	8301.183	276706.099
66.797	8302.390	276746.320
67.022	8189.627	272987.582
67.247	8186.484	272882.808
67.472	8142.968	271432.276
67.697	8120.212	270673.718
67.922	8100.362	270012.057
68.147	7737.166	257905.532
68.372	8208.725	273624.166
68.597	8256.650	275221.667
68.822	8486.199	282873.312
69.047	8463.077	282102.567
69.272	8681.792	289393.062
69.497	8839.124	294637.482
69.722	8823.420	294113.988
69.947	8982.143	299404.765
70.172	9126.341	304211.366
70.397	9085.450	302848.323
70.622	8932.776	297759.216
70.847	8751.130	291704.328
71.072	8954.644	298488.143
71.297	9031.554	301051.792
71.522	9383.230	312774.323
71.747	9446.013	314867.115
71.972	9595.473	319849.089
72.197	9690.183	323006.110
72.422	9345.678	311522.591
72.647	9160.085	305336.152
72.872	9033.202	301106.720
73.097	9185.593	306186.424
73.322	8832.072	294402.394
73.547	8956.624	298554.134
73.772	8830.932	294364.395
73.997	8824.102	294136.740
74.222	9101.656	303388.522
74.447	9130.046	304334.868
74.672	8982.433	299414.448
74.897	9059.701	301990.033
75.122	9313.419	310447.316
75.347	9184.545	306151.509
75.572	8795.968	293198.922
75.797	9008.551	300285.027
76.022	8693.055	289768.502
76.247	8781.545	292718.173
76.472	8933.559	297785.283
76.697	8637.422	287914.083
76.922	8811.205	293706.839
77.147	8844.288	294809.603
77.372	8781.213	292707.108
77.597	8688.782	289626.083
77.822	9360.058	312001.934

8.2.4.5 Continued

Time (sec)	Stress (Pa)	Viscosity (Pa s)
78.047	9521.622	317387.400
78.272	9563.965	318798.833
78.497	9620.057	320668.555
78.722	10089.708	336323.608
78.947	10396.152	346538.416
79.172	10586.305	352876.818
79.397	10954.802	365160.059
79.622	11142.597	371419.912
79.847	11508.880	383629.328
80.072	11637.264	387908.795
80.297	11895.913	396530.433
80.522	11812.887	393762.910
80.747	12072.910	402430.338
80.972	11961.059	398701.960
81.197	9549.170	318305.660
81.422	9081.450	302715.014
81.647	9028.174	300939.121
81.872	8950.906	298363.535
82.097	9188.529	306284.313
82.322	8933.586	297786.197
82.547	8813.229	293774.283
82.772	8888.259	296275.295
82.997	8582.354	286078.469
83.222	8744.325	291477.490
83.447	8590.783	286359.431
83.672	8750.108	291670.277
83.897	8313.485	277116.152
84.122	8740.264	291342.133
84.347	8690.378	289679.273
84.572	8897.779	296592.642
84.797	8585.800	286193.327
85.022	8573.022	285767.400
85.247	8928.069	297602.301
85.472	8373.624	279120.797
85.697	8602.036	286734.544
85.922	8763.662	292122.067
86.147	9136.099	304536.647
86.372	9085.180	302839.327
86.597	8942.936	298097.866
86.822	8664.887	288829.558
87.047	8662.609	288753.622
87.272	8920.371	297345.694
87.497	8582.365	286078.843
87.722	8770.950	292365.001
87.947	8922.588	297419.601
88.172	8900.512	296683.748
88.397	9217.570	307252.328
88.622	9031.977	301065.884
88.847	8703.232	290107.737
89.072	8916.397	297213.234
89.297	9075.753	302525.085
89.522	9384.353	312811.765
89.747	9235.611	307853.711
89.972	8651.324	288377.472
90.197	8669.081	288969.370
90.422	8492.693	283089.769
90.647	8422.151	280738.364
90.872	8540.425	284680.844
91.097	8597.585	286586.159
91.322	8607.887	286929.568
91.547	8480.813	282693.783
91.772	8815.049	293834.951
91.997	8361.039	278701.289
92.222	8631.807	287726.894
92.447	8650.681	288356.045
92.672	8479.475	282649.167
92.897	8413.999	280466.625
93.122	8251.350	275045.007
93.347	8265.284	275509.459
93.572	8336.202	277873.401
93.797	8601.377	286712.568
94.022	8513.252	283775.076
94.247	8292.166	276405.531
94.472	8370.878	279029.269
94.697	8517.426	283914.194
94.922	8291.433	276381.107
95.147	8634.930	287830.999
95.372	8589.456	286315.213
95.597	8570.411	285680.378
95.822	8854.390	295146.318
96.047	8421.887	280729.582
96.272	9003.333	300111.098
96.497	8529.104	284303.459
96.722	8772.361	292412.043
96.947	8660.948	288698.283
97.172	9129.327	304310.889
97.397	9749.701	324990.032
97.622	10546.341	351544.696
97.847	12380.967	412698.887
98.072	15055.647	501854.914
98.297	14422.263	480742.112
98.522	13675.193	455839.762
98.747	13212.896	440429.869
98.972	13121.728	437390.934
99.197	11312.082	377069.405
99.422	12368.015	412267.175
99.647	12556.463	418548.753
99.872	12935.841	431194.688
100.097	12669.923	422330.754
100.322	12566.705	418890.180
100.547	11939.238	397974.603
100.772	11983.475	399449.168
100.997	13073.595	435786.493
101.222	13519.221	450640.711
101.447	13032.642	434421.392
101.672	12102.836	403427.876
101.897	12107.147	403571.575
102.122	11665.683	388856.102
102.347	11128.408	370946.950
102.572	11842.117	394737.227
102.797	11726.750	390891.671
103.022	11423.647	380788.233
103.247	11502.744	383424.784
103.472	10971.757	365725.235
103.697	10947.355	364911.821
103.922	10705.492	356849.748
104.147	11347.674	378255.807
104.372	11411.014	380367.141
104.597	11198.435	373281.157
104.822	10402.675	346755.824
105.047	10825.487	360849.564
105.272	11144.821	371494.027
105.497	11062.568	368752.268
105.722	11261.508	375383.612
105.947	11072.296	369076.526
106.172	11275.410	375847.001

8.2.4.5 Continued

Time (sec)	Stress (Pa)	Viscosity (Pa s)
106.397	11300.559	376685.305
106.622	11156.381	371879.375
106.847	10942.436	364747.877
107.072	11084.851	369495.044
107.297	10653.785	355126.177
107.522	10604.014	353467.137
107.747	11513.938	383797.928
107.972	11698.173	389939.106
108.197	10867.843	362261.435
108.422	10087.496	336249.863
108.647	10264.245	342141.485
108.872	10479.847	349328.225
109.097	10546.123	351537.421
109.322	11940.266	398008.855
109.547	12326.429	410880.955
109.772	11206.558	373551.936
109.997	11427.367	380912.246
110.222	10871.656	362388.547
110.447	11195.289	373176.289
110.672	11633.405	387780.162
110.897	12246.597	408219.908

Time (sec)	Stress (Pa)	Viscosity (Pa s)
111.12	11709.40	390313.20
111.35	10911.60	363720.03
111.57	10367.85	345595.00
111.80	11246.15	374871.83
112.02	11653.23	388441.09
112.25	11350.08	378335.90
112.47	13088.86	436295.45
112.70	12231.10	407703.17
112.92	12057.52	401917.27
113.15	12519.11	417303.72
113.37	12439.21	414640.26
113.60	12314.93	410497.82
113.82	12236.83	407894.26
114.05	12075.62	402520.78
114.27	12117.25	403908.48
114.50	11965.23	398840.86
114.72	11677.35	389244.92
114.95	11380.82	379360.62
115.17	11438.68	381289.40
115.40	11506.92	383564.14
115.62	11644.90	388163.38

Time (sec)	Stress (Pa)	Viscosity (Pa s)
115.847	11808.685	393622.826
116.072	11607.921	386930.695
116.297	12439.832	414661.061
116.522	11369.512	378983.734
116.747	10966.884	365562.794
116.972	10854.149	361804.962
117.197	10932.346	364411.539
117.422	10951.314	365043.797
117.647	10385.754	346191.794
117.872	10859.472	361982.392
118.097	11293.900	376463.324
118.322	10716.798	357226.602
118.547	11283.920	376130.676
118.772	10756.789	358559.643
118.997	10740.267	358008.886
119.222	10627.670	354255.653
119.447	10868.205	362273.500
119.672	10566.905	352230.155
119.897	10761.783	358726.101
120.122	11444.764	381492.142

8.2.4.6 – HDB4 – Elongational Viscosity – 170 ^{o}C – Strain Rate = 0.1 s^{-1}

Time (sec)	Stress (Pa)	Viscosity (Pa s)
10.509	14415.271	144152.714
10.547	14399.773	143997.733
10.584	14323.415	143234.149
10.622	14325.876	143258.755
10.659	14267.157	142671.573
10.697	14184.511	141845.106
10.734	14209.530	142095.301
10.772	14333.869	143338.688
10.809	14335.397	143353.968
10.847	14389.255	143892.554
10.884	14385.618	143856.177
10.922	14449.368	144493.681
10.959	14445.818	144458.179
10.997	14475.804	144758.038
11.034	14530.190	145301.900
11.072	14580.003	145800.035
11.109	14615.013	146150.126

Time (sec)	Stress (Pa)	Viscosity (Pa s)
11.147	14635.345	146353.448
11.184	14650.795	146507.949
11.222	14676.151	146761.505
11.259	14681.420	146814.203
11.297	14676.758	146767.583
11.334	14671.547	146715.467
11.372	14681.464	146814.636
11.409	14711.312	147113.118
11.447	14553.730	145537.305
11.484	14363.971	143639.712
11.522	14443.534	144435.342
11.559	14595.246	145952.455
11.597	14634.670	146346.696
11.634	14611.992	146119.916
11.672	14599.396	145993.956
11.709	14555.327	145553.270
11.747	14552.545	145525.452

Time (sec)	Stress (Pa)	Viscosity (Pa s)
11.784	14523.258	145232.584
11.822	14641.189	146411.893
11.859	14695.876	146958.759
11.897	14793.868	147938.678
11.934	14977.295	149772.947
11.972	14980.014	149800.139
12.009	14901.913	149019.135
12.047	14877.301	148773.006
12.084	14787.238	147872.375
12.122	14842.794	148427.938
12.159	14925.508	149255.083
12.197	14894.419	148944.189
12.234	14846.128	148461.282
12.272	14857.828	148578.283
12.309	14924.795	149247.951
12.347	14902.897	149028.972
12.384	14736.004	147360.039

8.2.4.6 Continued

Time (sec)	Stress (Pa)	Viscosity (Pa s)
12.422	14735.353	147353.532
12.459	14818.827	148188.271
12.497	14801.547	148015.470
12.534	14789.109	147891.093
12.572	14787.810	147878.096
12.609	14854.854	148548.542
12.647	14973.543	149735.432
12.684	15001.047	150010.469
12.722	14942.316	149423.159
12.759	15073.702	150737.017
12.797	15165.088	151650.879
12.834	15157.994	151579.941
12.872	15132.770	151327.695
12.909	15101.762	151017.620
12.947	15123.221	151232.209
12.984	15168.117	151681.174
13.022	15171.792	151717.916
13.059	15127.225	151272.248
13.097	15148.249	151482.489
13.134	15169.215	151692.148
13.172	15021.144	150211.437
13.209	14968.563	149685.635
13.247	15043.348	150433.479
13.284	15118.110	151181.101
13.322	15021.681	150216.813
13.359	14986.214	149862.139
13.397	15097.869	150978.689
13.434	15161.017	151610.166
13.472	15130.722	151307.220
13.509	15194.041	151940.411
13.547	15350.888	153508.881
13.584	15352.164	153521.643
13.622	15321.654	153216.539
13.659	15271.757	152717.566
13.697	15436.997	154369.967
13.734	15431.123	154311.233
13.772	15278.000	152780.002
13.809	15316.172	153161.721
13.847	15360.718	153607.180
13.884	15334.219	153342.189
13.922	15300.957	153009.569
13.959	15345.298	153452.983
13.997	15448.930	154489.304
14.034	15382.161	153821.614
14.072	15367.443	153674.425
14.109	15404.963	154049.628
14.147	15410.078	154100.776
14.184	15321.315	153213.145
14.222	15338.394	153383.944
14.259	15389.453	153894.527
14.297	15399.893	153998.925
14.334	15437.487	154374.870
14.372	15380.089	153800.890
14.409	15485.788	154857.881
14.447	15571.153	155711.525
14.484	15636.372	156363.718
14.522	15605.366	156053.656
14.559	15567.140	155671.401
14.597	15653.646	156536.464
14.634	15635.751	156357.507
14.672	15673.538	156735.375
14.728	15691.402	156914.022
14.803	15852.003	158520.032
14.878	15621.145	156211.451
14.953	15598.404	155984.039
15.028	15606.791	156067.909
15.103	15596.555	155965.552
15.178	15706.321	157063.211
15.253	15776.509	157765.090
15.328	15951.457	159514.569
15.403	16067.401	160674.010
15.478	15960.705	159607.046
15.553	16042.554	160425.542
15.628	15993.888	159938.878
15.703	15846.366	158463.658
15.778	15852.430	158524.297
15.853	16034.829	160348.292
15.928	15790.340	157903.396
16.003	15965.408	159654.082
16.078	15968.424	159684.238
16.153	16259.274	162592.738
16.228	16156.282	161562.816
16.303	16319.701	163197.010
16.378	16371.536	163715.365
16.453	16344.252	163442.523
16.528	16351.168	163511.675
16.603	16121.954	161219.542
16.678	16102.175	161021.745
16.753	16221.289	162212.895
16.828	16276.009	162760.091
16.903	16251.775	162517.750
16.978	16404.827	164048.271
17.053	16448.540	164485.402
17.128	16413.515	164135.147
17.203	16543.689	165436.895
17.278	16509.200	165092.003
17.353	16425.155	164251.550
17.428	16435.545	164355.450
17.503	16424.724	164247.245
17.578	16445.412	164454.123
17.653	16465.482	164654.822
17.728	16560.697	165606.965
17.803	16652.021	166520.209
17.878	17112.763	171127.625
17.953	17231.789	172317.894
18.028	17106.927	171069.266
18.103	16956.599	169565.989
18.178	17012.581	170125.809
18.253	16909.954	169099.539
18.328	16852.904	168529.043
18.403	16855.541	168555.410
18.478	16861.639	168616.390
18.553	16764.089	167640.894
18.628	16973.839	169738.388
18.703	16996.642	169966.423
18.778	17005.608	170056.079
18.853	17152.475	171524.749
18.928	17206.311	172063.109
19.003	17214.479	172144.789
19.078	17216.142	172161.418
19.153	17244.643	172446.434
19.228	17043.230	170432.304
19.303	17093.369	170933.694
19.378	17092.966	170929.658
19.453	17252.693	172526.929
19.528	17414.205	174142.047

8.2.4.6 Continued

Time (sec)	Stress (Pa)	Viscosity (Pa s)
19.603	17605.186	176051.861
19.678	17532.723	175327.233
19.753	17606.415	176064.154
19.828	17663.027	176630.273
19.903	17565.409	175654.091
19.978	17319.888	173198.882
20.053	17504.122	175041.225
20.128	17605.635	176056.349
20.203	17595.381	175953.812
20.278	17651.041	176510.411
20.353	17694.084	176940.835
20.428	17899.164	178991.643
20.503	18039.662	180396.624
20.578	17963.907	179639.066
20.653	17768.134	177681.337
20.728	17866.625	178666.246
20.803	17962.432	179624.322
20.878	18022.471	180224.706
20.953	18013.854	180138.537
21.028	18030.337	180303.371
21.103	18129.455	181294.545
21.178	18041.293	180412.925
21.253	18079.226	180792.264
21.328	18218.658	182186.579
21.403	18461.887	184618.870
21.478	18483.861	184838.614
21.553	18507.673	185076.728
21.628	18481.917	184819.166
21.703	18437.005	184370.047
21.778	18533.147	185331.468
21.853	18489.789	184897.891
21.928	18564.028	185640.283
22.003	18244.352	182443.515
22.078	18591.164	185911.640
22.153	18749.200	187492.003
22.228	18633.094	186330.943
22.303	18683.452	186834.520
22.378	18578.218	185782.176
22.453	18874.543	188745.434
22.528	18824.741	188247.411
22.603	18733.882	187338.818
22.678	18726.791	187267.911
22.753	18754.045	187540.447
22.828	18911.182	189111.815
22.903	18873.807	188738.068
22.978	18879.456	188794.561
23.053	19138.773	191387.731
23.128	19213.606	192136.063
23.203	19239.286	192392.863
23.278	19396.263	193962.629
23.353	19701.255	197012.553
23.428	18874.170	188741.698
23.503	18986.261	189862.610
23.578	19142.219	191422.192
23.653	19200.220	192002.197
23.728	19180.243	191802.430
23.803	19337.958	193379.579
23.878	19255.316	192553.156
23.953	19311.541	193115.414
24.028	19470.007	194700.073
24.103	19535.846	195358.460
24.178	19547.343	195473.428
24.253	19561.812	195618.119
24.328	19295.092	192950.921
24.403	19259.815	192598.146
24.478	19498.321	194983.209
24.553	19593.401	195934.012
24.628	19518.059	195180.591
24.703	19908.180	199081.799
24.778	20183.206	201832.059
24.853	19593.974	195939.743
24.928	19892.382	198923.821
25.003	20032.523	200325.231
25.078	19826.712	198267.124
25.153	19641.072	196410.724
25.228	19683.221	196832.208
25.303	19872.268	198722.678
25.378	19753.594	197535.941
25.453	19968.932	199689.324
25.528	20458.730	204587.300
25.603	20649.756	206497.560
25.678	20420.754	204207.540
25.753	20404.455	204044.552
25.828	20549.905	205499.054
25.903	20405.105	204051.046
25.978	20341.424	203414.240
26.053	20012.644	200126.443
26.128	20041.584	200415.842
26.203	19986.820	199868.196
26.278	20420.248	204202.481
26.353	20040.245	200402.454
26.428	19978.022	199780.217
26.503	20475.422	204754.221
26.578	20782.213	207822.130
26.653	20182.438	201824.382
26.728	20258.327	202583.267
26.803	20301.476	203014.758
26.878	19990.757	199907.568
26.953	20039.003	200390.026
27.028	20078.386	200783.860
27.103	20046.793	200467.926
27.178	20672.764	206727.640
27.253	20433.296	204332.961
27.328	20384.671	203846.710
27.403	19879.997	198799.974
27.478	20812.821	208128.206
27.553	20215.726	202157.264
27.628	20476.521	204765.207
27.703	20304.372	203043.725
27.778	19992.056	199920.560
27.853	19791.354	197913.536
27.928	20102.174	201021.742
28.003	20510.250	205102.496
28.078	20439.897	204398.974
28.153	20394.501	203945.013
28.228	20803.151	208031.510
28.303	20884.529	208845.289
28.378	20778.993	207789.931
28.453	20611.286	206112.860
28.528	20587.778	205877.783
28.603	20106.664	201066.644
28.678	20749.654	207496.544
28.753	20069.538	200695.383
28.828	20249.695	202496.948
28.903	20620.484	206204.838
28.978	20746.208	207462.083

8.2.4.6 Continued

Time (sec)	Stress (Pa)	Viscosity (Pa s)
29.053	20692.006	206920.062
29.128	20486.489	204864.892
29.203	20809.915	208099.151
29.278	20462.983	204629.829
29.353	20427.170	204271.701
29.428	20047.292	200472.923
29.503	20449.378	204493.785
29.578	20475.134	204751.344
29.653	20334.134	203341.339
29.728	20412.511	204125.113
29.803	20486.058	204860.577
29.878	20339.402	203394.020
29.953	20532.938	205329.381
30.028	20638.351	206383.507
30.103	20769.201	207692.013
30.178	20400.245	204002.446
30.253	20070.273	200702.731
30.328	20431.696	204316.958
30.403	20458.157	204581.567
30.478	19879.171	198791.707
30.553	20316.170	203161.701
30.628	20975.890	209758.895
30.703	20619.490	206194.900
30.778	20550.426	205504.255
30.853	20558.971	205589.714
30.928	20450.735	204507.347
31.003	20303.575	203035.750
31.078	20021.752	200217.522
31.153	20811.056	208110.558
31.228	19970.456	199704.556
31.303	20088.637	200886.370
31.378	20416.646	204166.461
31.453	20302.900	203028.996
31.528	20526.716	205267.156
31.603	21038.773	210387.730
31.678	20245.943	202459.428
31.753	21337.850	213378.497
31.828	20829.591	208295.910
31.903	20499.974	204999.743
31.978	20614.459	206144.589
32.053	20500.261	205002.606
32.128	20453.631	204536.314
32.203	20252.668	202526.681
32.278	20349.163	203491.631
32.353	20512.373	205123.730
32.428	20781.069	207810.687
32.503	21334.437	213344.371
32.578	20995.160	209951.600
32.653	20755.464	207554.635
32.728	20276.751	202767.511
32.803	20485.770	204857.702
32.878	20550.180	205501.801
32.953	20150.965	201509.651
33.028	19389.610	193896.100

8.2.4.7 – HDB4 – Elongational Viscosity – 170 ^{o}C – Strain Rate = 0.03 s^{-1}

Time (sec)	Stress (Pa)	Viscosity (Pa s)
10.491	4465.075	148835.841
10.603	4450.170	148339.002
10.716	4467.180	148906.016
10.828	4485.364	149512.149
10.941	4471.088	149036.274
11.053	4478.136	149271.211
11.166	4494.770	149825.665
11.278	4508.466	150282.204
11.391	4512.424	150414.123
11.503	4497.235	149907.821
11.616	4480.377	149345.891
11.728	4458.794	148626.473
11.841	4452.518	148417.278
11.953	4473.309	149110.290
12.066	4510.438	150347.927
12.178	4520.936	150697.875
12.291	4511.876	150395.853
12.403	4539.795	151326.493
12.516	4535.561	151185.352
12.628	4536.581	151219.353
12.741	4607.014	153567.125
12.853	4613.419	153780.619
12.966	4613.373	153779.109
13.078	4649.544	154984.812
13.191	4631.782	154392.741
13.303	4688.072	156269.080
13.416	4729.502	157650.062
13.528	4732.524	157750.792
13.641	4703.991	156799.694
13.753	4678.979	155965.971
13.866	4713.163	157105.426
13.978	4689.260	156308.678
14.091	4669.901	155663.359
14.203	4677.367	155912.223
14.316	4658.413	155280.423
14.428	4644.359	154811.960
14.541	4637.047	154568.222
14.653	4624.378	154145.925
14.766	4612.403	153746.752
14.878	4648.877	154962.556
14.991	4665.152	155505.052
15.103	4686.109	156203.626
15.216	4677.201	155906.712
15.328	4692.308	156410.268
15.441	4693.731	156457.691
15.553	4725.367	157512.223
15.666	4755.880	158529.345
15.778	4747.646	158254.859
15.891	4789.813	159660.441
16.003	4784.264	159475.478
16.116	4765.187	158839.582
16.228	4778.688	159289.598
16.341	4789.825	159660.840
16.453	4779.019	159300.625
16.566	4831.125	161037.502
16.678	4839.450	161315.003
16.791	4878.662	162622.063
16.903	4883.617	162787.245
17.016	4859.162	161972.061
17.128	4789.286	159642.859

8.2.4.7 Continued

Time (sec)	Stress (Pa)	Viscosity (Pa s)
17.241	4776.487	159216.238
17.353	4811.302	160376.729
17.466	4797.404	159913.458
17.578	4791.357	159711.906
17.691	4822.171	160739.040
17.803	4837.562	161252.062
17.916	4827.688	160922.944
18.028	4821.977	160732.556
18.141	4795.983	159866.107
18.253	4840.233	161341.087
18.366	4864.092	162136.399
18.478	4835.174	161172.471
18.591	4847.397	161579.900
18.703	4839.506	161316.866
18.816	4838.008	161266.917
18.928	4861.673	162055.751
19.041	4896.562	163218.730
19.153	4916.281	163876.032
19.266	4945.922	164864.065
19.378	4909.507	163650.243
19.491	4956.479	165215.971
19.603	4971.632	165721.058
19.716	4949.972	164999.082
19.828	4946.197	164873.247
19.941	4956.357	165211.894
20.053	4998.069	166602.313
20.166	4975.406	165846.861
20.278	4920.941	164031.356
20.391	4931.910	164397.009
20.503	4974.539	165817.979
20.616	4967.876	165595.873
20.728	4919.965	163998.842
20.841	4954.244	165141.480
20.953	4964.897	165496.551
21.066	4988.888	166296.271
21.178	5025.009	167500.304
21.291	5040.225	168007.511
21.403	5014.261	167142.041
21.516	5023.993	167466.439
21.628	5054.273	168475.769
21.741	5073.669	169122.308
21.853	5069.542	168984.736
21.966	5084.442	169481.413
22.078	5096.362	169878.738
22.191	5105.877	170195.895
22.303	5080.001	169333.379
22.416	5079.199	169306.627
22.528	5080.785	169359.497
22.641	5117.992	170599.747
22.753	5150.457	171681.904
22.866	5116.568	170552.262
22.978	5118.157	170605.232
23.091	5134.125	171137.486
23.203	5098.318	169943.933
23.316	5069.024	168967.480
23.428	5084.182	169472.735
23.541	5137.203	171240.105
23.653	5138.450	171281.679
23.766	5137.011	171233.716
23.878	5143.984	171466.133
23.991	5123.499	170783.292
24.103	5142.380	171412.679
24.216	5153.041	171768.049
24.328	5182.107	172736.900
24.441	5246.362	174878.728
24.553	5271.728	175724.262
24.666	5251.367	175045.551
24.778	5220.785	174026.154
24.891	5276.783	175892.752
25.003	5317.161	177238.713
25.116	5316.306	177210.212
25.228	5285.856	176195.212
25.341	5296.295	176543.180
25.453	5328.348	177611.594
25.566	5363.338	178777.935
25.678	5332.967	177765.551
25.791	5314.688	177156.280
25.903	5316.960	177231.995
26.016	5288.465	176282.167
26.128	5305.661	176855.383
26.241	5299.912	176663.748
26.353	5225.320	174177.334
26.466	5274.025	175800.834
26.578	5299.567	176652.228
26.691	5306.670	176888.995
26.803	5312.665	177088.839
26.916	5340.114	178003.791
27.028	5397.451	179915.044
27.141	5437.921	181264.019
27.253	5443.996	181466.537
27.366	5433.346	181111.522
27.478	5438.307	181276.889
27.591	5454.653	181821.783
27.703	5444.255	181475.174
27.816	5422.335	180744.501
27.928	5447.050	181568.317
28.041	5417.221	180574.024
28.153	5413.457	180448.557
28.266	5449.751	181658.352
28.378	5439.790	181326.318
28.491	5409.909	180330.299
28.603	5373.460	179115.348
28.716	5432.634	181087.810
28.828	5496.483	183216.105
28.941	5447.247	181574.906
29.053	5410.819	180360.649
29.166	5423.876	180795.872
29.278	5394.825	179827.490
29.391	5455.340	181844.668
29.503	5526.349	184211.631
29.616	5493.479	183115.974
29.728	5458.694	181956.480
29.841	5511.168	183705.607
29.953	5535.270	184509.000
30.066	5553.435	185114.484
30.178	5550.069	185002.305
30.291	5607.293	186909.762
30.403	5635.343	187844.770
30.516	5545.463	184848.780
30.628	5589.889	186329.636
30.741	5593.328	186444.255
30.853	5603.807	186793.569
30.966	5663.353	188778.423
31.078	5696.757	189891.907
31.191	5712.837	190427.902
31.303	5721.099	190703.310

8.2.4.7 Continued

Time (sec)	Stress (Pa)	Viscosity (Pa s)
31.416	5740.783	191359.448
31.528	5715.688	190522.942
31.641	5657.673	188589.097
31.753	5633.843	187794.760
31.866	5599.706	186656.868
31.978	5559.230	185307.658
32.091	5620.485	187349.487
32.203	5716.736	190557.861
32.316	5703.766	190125.531
32.428	5669.078	188969.280
32.541	5652.419	188413.970
32.653	5679.714	189323.795
32.766	5742.245	191408.154
32.878	5736.694	191223.141
32.991	5755.609	191853.637
33.103	5754.385	191812.834
33.216	5763.462	192115.410
33.328	5765.635	192187.818
33.441	5819.017	193967.231
33.553	5780.673	192689.091
33.666	5755.701	191856.690
33.778	5806.941	193564.684
33.891	5836.175	194539.183
34.003	5809.331	193644.374
34.116	5816.203	193873.443
34.228	5836.986	194566.207
34.341	5808.173	193605.765
34.453	5794.000	193133.317
34.566	5827.910	194263.680
34.678	5757.853	191928.434
34.791	5722.927	190764.241
34.903	5768.293	192276.444
35.016	5787.157	192905.234
35.128	5800.460	193348.678
35.241	5857.508	195250.270
35.353	5887.731	196257.709
35.466	5927.772	197592.414
35.578	5873.081	195769.372
35.691	5879.161	195972.018
35.803	5888.214	196273.788
35.916	5802.144	193404.811
36.028	5861.536	195384.547
36.141	5924.425	197480.832
36.253	5914.187	197139.577
36.366	5884.717	196157.220
36.478	5969.945	198998.171
36.591	5956.883	198562.775
36.703	6013.191	200439.707
36.816	5951.527	198384.217
36.928	5901.649	196721.641
37.041	5949.208	198306.935
37.153	5868.161	195605.380
37.266	5865.248	195508.254
37.378	5954.384	198479.474
37.491	5934.050	197801.683
37.603	5920.806	197360.203
37.716	5944.827	198160.905
37.828	6038.224	201274.121
37.941	6018.179	200605.972
38.053	5977.982	199266.058
38.166	5984.895	199496.498
38.278	6052.458	201748.595
38.391	6061.928	202064.252
38.503	6101.368	203378.923
38.616	6141.857	204728.567
38.728	6148.671	204955.687
38.841	6140.748	204691.587
38.953	6114.643	203821.424
39.066	6177.017	205900.556
39.178	6250.997	208366.574
39.291	6225.948	207531.585
39.403	6103.183	203439.422
39.516	6043.066	201435.548
39.628	6049.895	201663.167
39.741	6030.727	201024.220
39.853	6039.631	201321.030
39.966	6086.789	202892.979
40.078	6158.212	205273.731
40.191	6076.104	202536.812
40.303	6031.427	201047.568
40.416	6140.617	204687.242
40.528	6184.666	206155.536
40.641	6180.397	206013.245
40.753	6123.236	204107.875
40.866	6147.580	204919.323
40.978	6255.628	208520.934
41.091	6189.369	206312.314
41.203	6231.606	207720.196
41.316	6337.595	211253.164
41.428	6446.853	214895.106
41.541	6502.879	216762.617
41.653	6460.678	215355.941
41.766	6373.833	212461.108
41.878	6342.967	211432.226
41.991	6331.599	211053.302
42.103	6341.506	211383.533
42.216	6317.583	210586.103
42.328	6315.628	210520.938
42.441	6231.321	207710.685
42.553	6206.084	206869.474
42.666	6239.722	207990.733
42.778	6360.639	212021.285
42.891	6337.949	211264.974
43.003	6300.307	210010.220
43.116	6277.276	209242.535
43.228	6338.416	211280.530
43.341	6380.606	212686.871
43.453	6282.761	209425.383
43.566	6280.301	209343.372
43.678	6350.250	211674.986
43.791	6484.893	216163.096
43.903	6452.449	215081.624
44.016	6572.688	219089.603
44.128	6588.046	219601.517
44.241	6586.804	219560.129
44.353	6461.448	215381.603
44.466	6594.723	219824.103
44.578	6603.106	220103.519
44.691	6677.691	222589.696
44.803	6742.798	224759.935
44.972	6721.740	224057.992
45.197	6696.401	223213.352
45.422	6627.080	220902.654
45.647	6594.530	219817.667
45.872	6549.065	218302.156
46.097	6592.532	219751.073

8.2.4.7 Continued

Time (sec)	Stress (Pa)	Viscosity (Pa s)
46.322	6570.679	219022.626
46.547	6624.720	220823.987
46.772	6526.618	217553.926
46.997	6701.442	223381.415
47.222	6518.348	217278.266
47.447	6511.646	217054.851
47.672	6615.134	220504.462
47.897	6673.057	222435.238
48.122	6535.031	217834.352
48.347	6467.398	215579.919
48.572	6417.676	213922.529
48.797	6403.953	213465.088
49.022	6308.524	210284.117
49.247	6340.418	211347.271
49.472	6432.484	214416.128
49.697	6503.251	216775.033
49.922	6506.468	216882.252
50.147	6508.227	216940.897
50.372	6618.520	220617.319
50.597	6546.281	218209.350
50.822	6560.540	218684.652
51.047	6614.449	220481.624
51.272	6689.424	222980.790
51.497	6785.259	226175.311
51.722	6732.834	224427.815
51.947	6687.325	222910.835
52.172	6702.361	223412.032
52.397	6799.346	226644.861
52.622	6867.857	228928.567
52.847	6788.262	226275.410
53.072	6805.454	226848.452
53.297	6820.361	227345.360
53.522	6863.781	228792.696
53.747	6793.775	226459.156
53.972	6731.389	224379.646
54.197	6771.433	225714.447
54.422	6630.262	221008.740
54.647	6706.723	223557.442
54.872	6767.396	225579.858
55.097	6750.773	225025.770
55.322	6699.893	223329.769
55.547	6723.932	224131.080
55.772	6758.198	225273.273
55.997	6846.747	228224.901
56.222	6812.037	227067.905
56.447	6710.053	223668.429
56.672	6808.905	226963.514
56.897	6757.919	225263.961
57.122	6731.635	224387.844
57.347	6888.217	229607.233
57.572	6791.811	226393.700
57.797	6632.362	221078.741
58.022	6693.408	223113.593
58.247	6785.400	226180.005
58.472	6633.417	221113.897
58.697	6667.720	222257.326
58.922	6706.878	223562.600
59.147	6698.982	223299.416
59.372	6770.401	225680.029
59.597	6900.385	230012.827
59.822	6926.348	230878.264
60.047	6762.909	225430.298
60.272	6838.734	227957.795
60.497	6865.494	228849.815
60.722	6888.586	229619.544
60.947	6940.926	231364.194
61.172	6943.277	231442.553
61.397	6957.003	231900.106
61.622	7048.821	234960.711
61.847	7097.701	236590.021
62.072	6874.073	229135.779
62.297	6824.638	227487.950
62.522	6940.036	231334.537
62.747	7002.548	233418.277
62.972	7331.909	244396.966
63.197	7834.027	261134.225
63.422	7860.210	262007.006
63.647	7935.692	264523.080
63.872	8027.272	267575.726
64.097	8037.305	267910.153
64.322	8154.016	271800.522
64.547	8055.431	268514.351
64.772	8224.106	274136.879
64.997	8006.197	266873.250
65.222	8144.890	271496.343
65.447	8186.568	272885.611
65.672	8237.382	274579.397
65.897	8075.917	269197.234
66.122	8197.802	273260.061
66.347	8123.580	270786.015
66.572	8301.183	276706.099
66.797	8302.390	276746.320
67.022	8189.627	272987.582
67.247	8186.484	272882.808
67.472	8142.968	271432.276
67.697	8120.212	270673.718
67.922	8100.362	270012.057
68.147	7737.166	257905.532
68.372	8208.725	273624.166
68.597	8256.650	275221.667
68.822	8486.199	282873.312
69.047	8463.077	282102.567
69.272	8681.792	289393.062
69.497	8839.124	294637.482
69.722	8823.420	294113.988
69.947	8982.143	299404.765
70.172	9126.341	304211.366
70.397	9085.450	302848.323
70.622	8932.776	297759.216
70.847	8751.130	291704.328
71.072	8954.644	298488.143
71.297	9031.554	301051.792
71.522	9383.230	312774.323
71.747	9446.013	314867.115
71.972	9595.473	319849.089
72.197	9690.183	323006.110
72.422	9345.678	311522.591
72.647	9160.085	305336.152
72.872	9033.202	301106.720
73.097	9185.593	306186.424
73.322	8832.072	294402.394
73.547	8956.624	298554.134
73.772	8830.932	294364.395
73.997	8824.102	294136.740
74.222	9101.656	303388.522
74.447	9130.046	304334.868

8.2.4.7 Continued

Time (sec)	Stress (Pa)	Viscosity (Pa s)
74.672	8982.433	299414.448
74.897	9059.701	301990.033
75.122	9313.419	310447.316
75.347	9184.545	306151.509
75.572	8795.968	293198.922
75.797	9008.551	300285.027
76.022	8693.055	289768.502
76.247	8781.545	292718.173
76.472	8933.559	297785.283
76.697	8637.422	287914.083
76.922	8811.205	293706.839
77.147	8844.288	294809.603
77.372	8781.213	292707.108
77.597	8688.782	289626.083
77.822	9360.058	312001.934
78.047	9521.622	317387.400
78.272	9563.965	318798.833
78.497	9620.057	320668.555
78.722	10089.708	336323.608
78.947	10396.152	346538.416
79.172	10586.305	352876.818
79.397	10954.802	365160.059
79.622	11142.597	371419.912
79.847	11508.880	383629.328
80.072	11637.264	387908.795
80.297	11895.913	396530.433
80.522	11812.887	393762.910
80.747	12072.910	402430.338
80.972	11961.059	398701.960
81.197	9549.170	318305.660
81.422	9081.450	302715.014
81.647	9028.174	300939.121
81.872	8950.906	298363.535
82.097	9188.529	306284.313
82.322	8933.586	297786.197
82.547	8813.229	293774.283
82.772	8888.259	296275.295
82.997	8582.354	286078.469
83.222	8744.325	291477.490
83.447	8590.783	286359.431
83.672	8750.108	291670.277
83.897	8313.485	277116.152
84.122	8740.264	291342.133
84.347	8690.378	289679.273
84.572	8897.779	296592.642
84.797	8585.800	286193.327
85.022	8573.022	285767.400
85.247	8928.069	297602.301
85.472	8373.624	279120.797
85.697	8602.036	286734.544
85.922	8763.662	292122.067
86.147	9136.099	304536.647
86.372	9085.180	302839.327
86.597	8942.936	298097.866
86.822	8664.887	288829.558
87.047	8662.609	288753.622
87.272	8920.371	297345.694
87.497	8582.365	286078.843
87.722	8770.950	292365.001
87.947	8922.588	297419.601
88.172	8900.512	296683.748
88.397	9217.570	307252.328
88.622	9031.977	301065.884
88.847	8703.232	290107.737
89.072	8916.397	297213.234
89.297	9075.753	302525.085
89.522	9384.353	312811.765
89.747	9235.611	307853.711
89.972	8651.324	288377.472
90.197	8669.081	288969.370
90.422	8492.693	283089.769
90.647	8422.151	280738.364
90.872	8540.425	284680.844
91.097	8597.585	286586.159
91.322	8607.887	286929.568
91.547	8480.813	282693.783
91.772	8815.049	293834.951
91.997	8361.039	278701.289
92.222	8631.807	287726.894
92.447	8650.681	288356.045
92.672	8479.475	282649.167
92.897	8413.999	280466.625
93.122	8251.350	275045.007
93.347	8265.284	275509.459
93.572	8336.202	277873.401
93.797	8601.377	286712.568
94.022	8513.252	283775.076
94.247	8292.166	276405.531
94.472	8370.878	279029.269
94.697	8517.426	283914.194
94.922	8291.433	276381.107
95.147	8634.930	287830.999
95.372	8589.456	286315.213
95.597	8570.411	285680.378
95.822	8854.390	295146.318
96.047	8421.887	280729.582
96.272	9003.333	300111.098
96.497	8529.104	284303.459
96.722	8772.361	292412.043
96.947	8660.948	288698.283
97.172	9129.327	304310.889
97.397	9749.701	324990.032
97.622	10546.341	351544.696
97.847	12380.967	412698.887
98.072	15055.647	501854.914
98.297	14422.263	480742.112
98.522	13675.193	455839.762
98.747	13212.896	440429.869
98.972	13121.728	437390.934
99.197	11312.082	377069.405
99.422	12368.015	412267.175
99.647	12556.463	418548.753
99.872	12935.841	431194.688
100.097	12669.923	422330.754
100.322	12566.705	418890.180
100.547	11939.238	397974.603
100.772	11983.475	399449.168
100.997	13073.595	435786.493
101.222	13519.221	450640.711
101.447	13032.642	434421.392
101.672	12102.836	403427.876
101.897	12107.147	403571.575
102.122	11665.683	388856.102
102.347	11128.408	370946.950
102.572	11842.117	394737.227
102.797	11726.750	390891.671

8.2.4.7 Continued

Time (sec)	Stress (Pa)	Viscosity (Pa s)
103.022	11423.647	380788.233
103.247	11502.744	383424.784
103.472	10971.757	365725.235
103.697	10947.355	364911.821
103.922	10705.492	356849.748
104.147	11347.674	378255.807
104.372	11411.014	380367.141
104.597	11198.435	373281.157
104.822	10402.675	346755.824
105.047	10825.487	360849.564
105.272	11144.821	371494.027
105.497	11062.568	368752.268
105.722	11261.508	375383.612
105.947	11072.296	369076.526
106.172	11275.410	375847.001
106.397	11300.559	376685.305
106.622	11156.381	371879.375
106.847	10942.436	364747.877
107.072	11084.851	369495.044
107.297	10653.785	355126.177
107.522	10604.014	353467.137
107.747	11513.938	383797.928
107.972	11698.173	389939.106
108.197	10867.843	362261.435
108.422	10087.496	336249.863
108.647	10264.245	342141.485

Time (sec)	Stress (Pa)	Viscosity (Pa s)
108.87	10479.85	349328.22
109.10	10546.12	351537.42
109.32	11940.27	398008.86
109.55	12326.43	410880.95
109.77	11206.56	373551.94
110.00	11427.37	380912.25
110.22	10871.66	362388.55
110.45	11195.29	373176.29
110.67	11633.40	387780.16
110.90	12246.60	408219.91
111.12	11709.40	390313.20
111.35	10911.60	363720.03
111.57	10367.85	345595.00
111.80	11246.15	374871.83
112.02	11653.23	388441.09
112.25	11350.08	378335.90
112.47	13088.86	436295.45
112.70	12231.10	407703.17
112.92	12057.52	401917.27
113.15	12519.11	417303.72
113.37	12439.21	414640.26
113.60	12314.93	410497.82
113.82	12236.83	407894.26
114.05	12075.62	402520.78
114.27	12117.25	403908.48
114.50	11965.23	398840.86

Time (sec)	Stress (Pa)	Viscosity (Pa s)
114.72	11677.35	389244.92
114.95	11380.82	379360.62
115.17	11438.68	381289.40
115.40	11506.92	383564.14
115.62	11644.90	388163.38
115.85	11808.68	393622.83
116.07	11607.92	386930.69
116.30	12439.83	414661.06
116.52	11369.51	378983.73
116.75	10966.88	365562.79
116.97	10854.15	361804.96
117.20	10932.35	364411.54
117.42	10951.31	365043.80
117.65	10385.75	346191.79
117.872	10859.472	361982.392
118.097	11293.900	376463.324
118.322	10716.798	357226.602
118.547	11283.920	376130.676
118.772	10756.789	358559.643
118.997	10740.267	358008.886
119.222	10627.670	354255.653
119.447	10868.205	362273.500
119.672	10566.905	352230.155
119.897	10761.783	358726.101
120.122	11444.764	381492.142

8.2.4.8 – HDB4 – Elongational Viscosity – 170 °C – Strain Rate = 0.01 s^{-1}

Time (sec)	Stress (Pa)	Viscosity (Pa s)
37.781	2285.365	228536.472
38.156	2303.784	230378.412
38.531	2267.994	226799.365
38.906	2246.913	224691.263
39.281	2281.572	228157.174
39.656	2319.727	231972.653
40.031	2312.229	231222.863
40.406	2265.632	226563.247
40.781	2316.298	231629.800
41.156	2303.814	230381.390
41.531	2323.380	232337.983
41.906	2301.420	230141.984

Time (sec)	Stress (Pa)	Viscosity (Pa s)
42.281	2336.834	233683.375
42.656	2333.083	233308.327
43.031	2275.584	227558.385
43.406	2237.279	223727.852
43.781	2233.706	223370.565
44.156	2220.835	222083.521
44.531	2230.005	223000.476
44.906	2285.181	228518.095
45.281	2260.104	226010.416
45.656	2228.832	222883.246
46.031	2268.607	226860.746
46.406	2288.392	228839.222

Time (sec)	Stress (Pa)	Viscosity (Pa s)
46.781	2312.711	231271.092
47.156	2285.796	228579.632
47.531	2280.704	228070.437
47.906	2212.931	221293.070
48.281	2327.879	232787.934
48.656	2331.396	233139.606
49.031	2309.658	230965.804
49.406	2299.795	229979.515
49.781	2338.627	233862.680
50.156	2326.785	232678.453
50.531	2316.102	231610.164
50.906	2315.393	231539.310

8.2.4.8 Continued

Time (sec)	Stress (Pa)	Viscosity (Pa s)
51.281	2367.515	236751.494
51.656	2373.068	237306.755
52.031	2448.327	244832.660
52.406	2491.955	249195.536
52.781	2464.758	246475.761
53.156	2376.250	237625.036
53.531	2334.999	233499.854
53.906	2364.700	236469.968
54.281	2418.959	241895.946
54.656	2438.731	243873.116
55.031	2358.999	235899.941
55.406	2322.894	232289.406
55.781	2423.744	242374.352
56.156	2429.068	242906.815
56.531	2409.333	240933.273
56.906	2418.744	241874.403
57.281	2446.736	244673.634
57.656	2430.941	243094.129
58.031	2465.156	246515.585
58.406	2470.915	247091.481
58.781	2480.418	248041.779
59.156	2486.134	248613.427
59.531	2500.936	250093.599
59.906	2474.405	247440.541
60.281	2450.168	245016.813
60.656	2449.597	244959.677
61.031	2522.102	252210.186
61.406	2412.168	241216.780
61.781	2417.532	241753.204
62.156	2521.695	252169.505
62.531	2506.530	250653.029
62.906	2482.438	248243.789
63.281	2531.989	253198.907
63.656	2493.820	249382.023
64.031	2468.066	246806.588
64.406	2456.030	245603.003
64.781	2502.279	250227.891
65.156	2405.663	240566.316
65.531	2427.239	242723.915
65.906	2456.101	245610.105
66.281	2484.672	248467.185
66.656	2494.720	249472.000
67.031	2533.764	253376.375
67.406	2489.547	248954.734
67.781	2461.153	246115.268
68.156	2482.949	248294.885
68.531	2454.083	245408.341
68.906	2501.560	250155.985
69.281	2497.616	249761.598
69.656	2463.719	246371.903
70.031	2456.909	245690.947
70.406	2466.140	246614.018
70.781	2454.016	245401.577
71.156	2460.168	246016.830
71.531	2485.138	248513.756
71.906	2459.981	245998.068
72.281	2461.594	246159.403
72.656	2497.265	249726.492
73.031	2473.115	247311.476
73.406	2463.627	246362.726
73.781	2524.922	252492.217
74.156	2475.511	247551.099
74.531	2444.942	244494.172
74.906	2487.262	248726.207
75.281	2536.042	253604.242
75.656	2651.705	265170.521
76.031	2597.434	259743.412
76.406	2533.458	253345.765
76.781	2550.737	255073.681
77.156	2532.109	253210.883
77.531	2583.501	258350.120
77.906	2557.556	255755.631
78.281	2528.621	252862.064
78.656	2525.835	252583.462
79.031	2491.377	249137.726
79.406	2492.770	249277.037
79.781	2496.940	249693.985
80.156	2568.996	256899.649
80.531	2546.965	254696.544
80.906	2585.001	258500.097
81.281	2605.262	260526.169
81.656	2597.326	259732.566
82.031	2625.614	262561.395
82.406	2647.120	264712.038
82.781	2633.368	263336.813
83.156	2727.427	272742.681
83.531	2732.327	273232.661
83.906	2655.674	265567.438
84.281	2710.597	271059.725
84.656	2660.819	266081.861
85.031	2680.006	268000.554
85.406	2655.374	265537.443
85.781	2780.924	278092.353
86.156	2730.214	273021.387
86.531	2618.228	261822.837
86.906	2666.055	266605.499
87.281	2708.360	270835.974
87.656	2711.740	271174.032
88.031	2661.380	266137.977
88.406	2564.011	256401.077
88.781	2681.168	268116.803
89.156	2754.162	275416.217
89.531	2708.724	270872.385
89.906	2700.852	270085.214
90.281	2793.150	279314.985
90.656	2844.143	284414.325
91.031	2844.464	284446.368
91.406	2889.763	288976.297
91.781	2787.681	278768.134
92.156	2773.406	277340.610
92.531	2778.539	277853.948
92.906	2776.769	277676.871
93.281	2796.768	279676.772
93.656	2810.909	281090.872
94.031	2853.720	285372.043
94.406	2819.780	281978.010
94.781	2843.393	284339.254
95.156	2881.000	288100.032
95.531	2816.722	281672.238
95.906	2863.298	286329.824
96.281	2774.143	277414.316
96.656	2759.320	275931.975
97.031	2765.499	276549.898
97.406	2680.343	268034.279
97.781	2711.293	271129.265
98.156	2742.871	274287.114

8.2.4.8 Continued

Time (sec)	Stress (Pa)	Viscosity (Pa s)
98.531	2773.722	277372.246
98.906	2763.739	276373.904
99.281	2758.967	275896.725
99.656	2730.090	273009.033
100.031	2712.631	271263.056
100.406	2745.534	274553.430
100.781	2710.645	271064.461
101.156	2743.712	274371.165
101.531	2799.396	279939.643
101.906	2791.481	279148.090
102.281	2806.834	280683.438
102.656	2790.346	279034.596
103.031	2749.123	274912.318
103.406	2598.086	259808.589
103.781	2675.565	267556.511
104.156	2870.106	287010.607
104.531	2840.786	284078.577
104.906	2799.239	279923.854
105.281	2724.572	272457.197
105.656	2720.470	272046.991
106.031	2661.490	266149.048
106.406	2735.820	273582.031
106.781	2825.526	282552.644
107.156	2802.398	280239.804
107.531	2767.488	276748.762
107.906	2740.595	274059.486
108.281	2750.651	275065.131
108.656	2895.107	289510.698
109.031	2869.180	286917.983
109.406	2801.457	280145.713
109.781	2811.189	281118.931
110.156	2797.631	279763.133
110.531	2800.338	280033.819
110.906	2746.837	274683.699
111.281	2665.901	266590.110
111.656	2752.477	275247.692
112.031	2804.797	280479.741
112.406	2809.450	280944.978
112.781	2699.215	269921.501
113.156	2633.847	263384.671
113.531	2679.327	267932.740
113.906	2774.179	277417.906

Time (sec)	Stress (Pa)	Viscosity (Pa s)
114.281	2733.054	273305.443
114.656	2758.755	275875.518
115.031	2721.684	272168.439
115.406	2704.877	270487.694
115.781	2680.458	268045.754
116.156	2662.252	266225.167
116.531	2662.401	266240.144
116.906	2761.147	276114.684
117.281	2711.369	271136.950
117.656	2639.470	263947.002
118.031	2725.754	272575.380
118.406	2848.815	284881.540
118.781	2823.483	282348.309
119.156	2691.150	269114.970
119.531	2690.772	269077.162
119.906	2678.205	267820.510
120.281	2719.428	271942.816
120.656	2671.849	267184.937
121.031	2529.825	252982.506
121.406	2587.079	258707.910
121.781	2953.480	295348.035
122.156	2856.418	285641.788
122.531	2536.812	253681.192
122.906	2702.674	270267.426
123.281	2796.733	279673.267
123.656	2758.684	275868.415
124.031	2650.755	265075.473
124.406	2652.031	265203.090
124.781	2633.793	263379.303
125.156	2671.640	267164.037
125.531	2612.285	261228.467
125.906	2602.966	260296.571
126.281	2698.701	269870.092
126.656	2766.889	276688.878
127.031	2714.524	271452.404
127.406	2754.766	275476.586
127.781	2772.125	277212.502
128.156	2754.909	275490.929
128.531	2643.507	264350.748
128.906	2782.221	278222.112
129.281	2753.094	275309.367
129.656	2846.838	284683.824

Time (sec)	Stress (Pa)	Viscosity (Pa s)
130.031	2786.440	278643.996
130.406	2627.427	262742.719
130.781	2704.864	270486.439
131.156	2789.115	278911.468
131.531	2824.837	282483.727
131.906	2764.533	276453.284
132.281	2640.800	264080.035
132.656	2856.413	285641.288
133.031	2872.839	287283.901
133.406	2914.374	291437.441
133.781	2892.605	289260.528
134.156	2883.628	288362.822
134.531	2812.519	281251.897
134.906	2847.785	284778.452
135.281	2872.965	287296.510
135.656	2908.091	290809.095
136.031	2867.633	286763.285
136.406	2872.517	287251.672
136.781	2848.236	284823.584
137.156	2790.853	279085.293
137.531	2789.425	278942.513
137.906	2900.416	290041.638
138.281	2837.674	283767.406
138.656	2779.874	277987.374

8.2.4.9 – HDB4 – Elongational Viscosity – 170 °C – Strain Rate = 0.03 s^{-1}

Time (sec)	Stress (Pa)	Viscosity (Pa s)
59.063	749.317	249772.235
61.313	732.006	244002.050
63.563	678.008	226002.711
65.813	701.230	233743.432
68.063	819.046	273015.315
70.313	793.046	264348.700
72.563	757.097	252365.763
74.813	744.607	248202.365
77.063	727.967	242655.777
79.313	728.804	242934.631
81.563	733.544	244514.762
83.813	749.126	249708.749
86.063	749.477	249825.643
88.313	770.990	256996.531
90.563	760.845	253614.860
92.813	754.208	251402.629
95.063	737.016	245671.975
97.313	778.512	259503.839
99.563	751.319	250439.606
101.813	766.739	255579.766
104.063	740.857	246952.461
106.313	760.365	253455.053
108.563	744.561	248187.010
110.813	762.856	254285.170
113.063	763.748	254582.511
115.313	759.345	253115.162
117.563	777.507	259169.015
119.813	764.454	254817.859
122.063	784.905	261635.045
124.313	790.680	263559.996
126.563	803.272	267757.333
128.813	785.086	261695.369
131.063	809.997	269999.040
133.313	818.833	272944.255
135.563	816.232	272077.258
137.813	819.386	273128.501
140.063	833.411	277803.749
142.313	836.510	278836.552
144.563	833.340	277780.016
146.813	823.433	274477.586
149.063	847.137	282379.119
151.313	840.663	280220.909
153.563	870.923	290307.792
155.813	887.672	295890.643
158.063	873.722	291240.585
160.313	881.297	293765.570
162.563	915.172	305057.169
164.813	895.339	298446.462
167.063	881.353	293784.398
169.313	885.047	295015.616
171.563	887.460	295820.146
173.813	885.358	295119.298
176.063	894.683	298227.744
178.313	915.637	305212.168
180.563	915.427	305142.320
182.813	911.320	303773.281
185.063	907.399	302466.243
187.313	926.780	308926.596
189.563	912.790	304263.379
191.813	903.216	301072.040
194.063	930.398	310132.768
196.313	882.611	294203.709
198.563	901.028	300342.604
200.813	876.478	292159.465
203.063	870.819	290273.056
205.313	911.774	303924.833
207.563	879.148	293049.256
209.813	923.331	307777.102
212.063	907.541	302513.753
214.313	885.539	295179.737
216.563	889.813	296604.386
218.813	887.662	295887.187
221.063	935.036	311678.821
223.313	925.427	308475.631
225.563	883.930	294643.195
227.813	902.149	300716.478
230.063	898.846	299615.309
232.313	886.392	295464.071
234.563	893.402	297800.669
236.813	896.481	298827.130
239.063	870.881	290293.751
241.313	905.259	301753.030
243.563	882.549	294182.957
245.813	893.491	297830.258
248.063	896.368	298789.335
250.313	900.106	300035.174
252.563	889.778	296592.577
254.813	885.675	295225.055
257.063	878.298	292765.963
259.313	901.819	300606.488
261.563	868.808	289602.525
263.813	903.068	301022.768
266.063	910.972	303657.167
268.313	917.409	305803.018
270.563	921.617	307205.771
272.813	950.815	316938.282
275.063	967.384	322461.359
277.313	953.848	317949.260
279.563	918.630	306210.023
281.813	960.088	320029.381
284.063	967.590	322529.931
286.313	955.596	318532.015
288.563	961.408	320469.390
290.813	960.783	320260.871
293.063	935.250	311749.916
295.313	967.884	322628.115
297.563	926.112	308704.047
299.813	977.709	325902.880
302.063	932.621	310873.602
304.313	953.432	317810.504
306.563	925.882	308627.355
308.813	980.102	326700.638

8.2.5 – HDB6

8.2.5.1 – HDB6 – Elongational Viscosity – 170 °C – Strain Rate = 10 s^{-1}

Time (sec)	Stress (Pa)	Viscosity (Pa s)
0.052	74063.089	7406.309
0.060	85343.805	8534.380
0.068	95922.685	9592.269
0.075	105900.472	10590.047
0.083	115083.073	11508.307
0.090	123933.141	12393.314
0.098	132621.563	13262.156
0.105	141390.048	14139.005
0.113	149179.381	14917.938
0.120	156413.138	15641.314
0.128	163385.179	16338.518
0.135	170231.096	17023.110

Time (sec)	Stress (Pa)	Viscosity (Pa s)
0.143	177436.187	17743.619
0.150	184318.847	18431.885
0.158	190981.980	19098.198
0.165	197564.889	19756.489
0.173	204652.048	20465.205
0.180	211779.545	21177.954
0.187	219225.562	21922.556
0.195	226703.519	22670.352
0.202	234364.740	23436.474
0.210	242395.994	24239.599
0.217	250661.240	25066.124
0.225	259179.860	25917.986

Time (sec)	Stress (Pa)	Viscosity (Pa s)
0.232	267497.705	26749.770
0.240	275792.508	27579.251
0.248	283483.592	28348.359
0.255	290699.710	29069.971
0.263	297325.194	29732.519
0.270	303385.089	30338.509
0.278	308222.328	30822.233
0.285	311382.597	31138.260
0.293	314645.331	31464.533
0.300	322473.655	32247.365

8.2.5.2 – HDB6 – Elongational Viscosity – 170 °C – Strain Rate = 3 s^{-1}

Time (sec)	Stress (Pa)	Viscosity (Pa s)
0.045	18208.004	6069.335
0.053	22279.155	7426.385
0.060	25861.883	8620.628
0.068	29052.896	9684.299
0.075	32028.494	10676.165
0.082	34580.151	11526.717
0.090	36747.292	12249.097
0.098	38796.520	12932.173
0.105	40667.200	13555.733
0.113	42343.597	14114.532
0.120	43916.257	14638.752
0.128	45430.723	15143.574
0.135	46880.230	15626.743
0.143	48145.701	16048.567
0.150	49269.663	16423.221
0.158	50420.745	16806.915
0.165	51446.459	17148.820
0.173	52276.274	17425.425
0.180	53338.611	17779.537
0.188	54520.555	18173.518
0.195	55694.131	18564.710
0.203	56826.405	18942.135
0.210	58049.365	19349.788
0.218	59263.782	19754.594
0.225	60394.497	20131.499

Time (sec)	Stress (Pa)	Viscosity (Pa s)
0.233	61583.495	20527.832
0.240	62832.532	20944.177
0.247	63991.195	21330.398
0.255	65010.746	21670.249
0.263	66083.362	22027.787
0.270	67130.429	22376.810
0.277	68062.126	22687.375
0.285	69002.801	23000.934
0.293	69951.046	23317.015
0.300	70906.710	23635.570
0.307	71868.222	23956.074
0.315	72838.247	24279.416
0.323	73961.116	24653.705
0.330	75196.365	25065.455
0.337	76346.734	25448.911
0.345	77043.774	25681.258
0.353	78212.001	26070.667
0.360	79665.113	26555.038
0.367	80753.589	26917.863
0.375	81623.754	27207.918
0.383	82725.248	27575.083
0.390	83593.928	27864.643
0.397	84522.707	28174.236
0.405	85324.598	28441.533
0.413	86181.645	28727.215

Time (sec)	Stress (Pa)	Viscosity (Pa s)
0.420	86839.996	28946.665
0.428	87616.315	29205.438
0.435	88382.988	29460.996
0.443	89070.902	29690.301
0.450	89742.170	29914.057
0.458	90326.419	30108.806
0.465	91262.976	30420.992
0.473	92118.328	30706.109
0.480	93046.547	31015.516
0.488	93886.265	31295.422
0.495	94880.905	31626.968
0.502	95703.557	31901.186
0.510	96174.788	32058.263
0.518	96965.389	32321.796
0.525	97832.363	32610.788
0.533	98780.849	32926.950
0.540	99441.615	33147.205
0.548	100461.490	33487.163
0.555	101479.284	33826.428
0.562	102289.482	34096.494
0.570	103184.120	34394.707
0.577	104279.309	34759.770
0.585	105315.282	35105.094
0.593	106290.849	35430.283
0.600	107256.279	35752.093

8.2.5.2 Continued

Time (sec)	Stress (Pa)	Viscosity (Pa s)
0.608	108266.616	36088.872
0.615	109269.200	36423.067
0.622	110021.469	36673.823
0.630	110933.051	36977.684
0.637	111957.490	37319.163
0.645	112777.201	37592.400
0.653	113640.324	37880.108
0.660	114621.630	38207.210
0.668	115792.071	38597.357
0.675	116465.535	38821.845
0.682	117254.397	39084.799
0.690	118164.594	39388.198
0.697	119055.517	39685.172
0.705	119695.954	39898.651
0.713	120303.871	40101.290
0.720	121358.335	40452.778
0.728	122235.414	40745.138
0.735	123089.556	41029.852
0.742	123832.671	41277.557
0.750	124983.435	41661.145
0.757	125946.738	41982.246

Time (sec)	Stress (Pa)	Viscosity (Pa s)
0.765	126793.692	42264.564
0.773	127803.544	42601.181
0.780	128984.599	42994.866
0.788	129759.691	43253.230
0.795	130303.566	43434.522
0.803	131320.355	43773.452
0.810	131788.862	43929.621
0.817	132424.353	44141.451
0.825	132912.955	44304.318
0.833	133578.737	44526.246
0.840	134205.969	44735.323
0.848	134792.580	44930.860
0.855	135340.071	45113.357
0.863	135838.932	45279.644
0.870	136290.413	45430.138
0.877	136692.110	45564.037
0.885	137568.763	45856.254
0.893	138007.044	46002.348
0.900	138537.151	46179.050
0.908	138524.737	46174.912
0.915	138865.016	46288.339

Time (sec)	Stress (Pa)	Viscosity (Pa s)
0.923	139223.365	46407.788
0.930	139222.084	46407.361
0.937	139151.010	46383.670
0.945	138845.613	46281.871
0.952	138858.363	46286.121
0.960	138716.668	46238.889
0.968	139004.376	46334.792
0.975	138972.365	46324.122
0.983	138958.589	46319.530
0.990	138596.481	46198.827
0.998	138334.908	46111.636
1.005	137894.469	45964.823
1.013	137359.407	45786.469
1.020	137126.876	45708.959
1.028	136306.549	45435.516
1.035	136204.787	45401.596
1.043	135708.247	45236.082
1.050	135339.808	45113.269
1.058	134549.989	44849.996

8.2.5.3 – HDB6 – Elongational Viscosity – 170 °C – Strain Rate = 1 s^{-1}

Time (sec)	Stress (Pa)	Viscosity (Pa s)
0.143	16966.781	16966.781
0.150	17737.640	17737.640
0.158	18504.715	18504.715
0.165	19178.295	19178.295
0.172	19845.863	19845.863
0.180	20416.786	20416.786
0.187	20889.238	20889.238
0.195	21291.339	21291.339
0.202	21636.520	21636.520
0.210	22016.583	22016.583
0.217	22432.742	22432.742
0.225	22947.987	22947.987
0.232	23390.982	23390.982
0.240	23838.857	23838.857
0.248	24275.868	24275.868
0.255	24686.293	24686.293
0.262	25019.382	25019.382

Time (sec)	Stress (Pa)	Viscosity (Pa s)
0.270	25322.785	25322.785
0.278	25596.799	25596.799
0.285	25789.496	25789.496
0.292	26118.344	26118.344
0.300	26434.044	26434.044
0.308	26821.125	26821.125
0.315	27143.384	27143.384
0.322	27521.627	27521.627
0.330	27886.346	27886.346
0.338	28219.905	28219.905
0.345	28538.956	28538.956
0.352	28807.510	28807.510
0.360	29060.264	29060.264
0.367	29242.879	29242.879
0.375	29463.026	29463.026
0.382	29684.829	29684.829
0.390	29945.281	29945.281

Time (sec)	Stress (Pa)	Viscosity (Pa s)
0.397	30226.894	30226.894
0.405	30530.105	30530.105
0.412	30797.765	30797.765
0.420	31067.726	31067.726
0.427	31359.496	31359.496
0.435	31556.893	31556.893
0.442	31715.911	31715.911
0.450	31836.264	31836.264
0.457	32036.368	32036.368
0.465	32257.308	32257.308
0.472	32500.147	32500.147
0.480	32785.902	32785.902
0.487	33052.791	33052.791
0.495	33322.474	33322.474
0.502	33552.319	33552.319
0.510	33826.080	33826.080
0.518	33996.060	33996.060

8.2.5.3 Continued

Time (sec)	Stress (Pa)	Viscosity (Pa s)
0.638	37497.525	37497.525
0.645	37755.583	37755.583
0.653	37943.650	37943.650
0.660	38229.297	38229.297
0.667	38418.724	38418.724
0.675	38609.596	38609.596
0.682	38750.851	38750.851
0.690	38941.970	38941.970
0.698	39083.471	39083.471
0.705	39174.222	39174.222
0.713	39238.201	39238.201
0.720	39300.929	39300.929
0.727	39466.028	39466.028
0.735	39684.405	39684.405
0.742	39930.548	39930.548
0.750	40018.311	40018.311
0.757	40105.129	40105.129
0.765	40190.165	40190.165
0.773	40220.825	40220.825
0.780	40303.448	40303.448
0.787	40468.856	40468.856
0.795	40606.320	40606.320
0.802	40715.199	40715.199
0.810	40936.851	40936.851
0.817	41131.614	41131.614
0.825	41326.115	41326.115
0.833	41463.644	41463.644
0.840	41658.899	41658.899
0.847	41855.644	41855.644
0.855	41963.321	41963.321
0.862	42219.909	42219.909
0.870	42417.300	42417.300
0.877	42555.054	42555.054
0.885	42540.343	42540.343
0.893	42768.438	42768.438
0.900	43214.523	43214.523
0.908	43726.952	43726.952
0.915	44181.168	44181.168
0.922	44577.728	44577.728
0.930	44944.559	44944.559
0.937	45218.973	45218.973
0.945	45623.809	45623.809

Time (sec)	Stress (Pa)	Viscosity (Pa s)
0.953	45902.372	45902.372
0.960	45985.353	45985.353
0.968	45867.301	45867.301
0.975	45845.966	45845.966
0.982	46023.385	46023.385
0.990	46268.263	46268.263
0.997	46582.112	46582.112
1.005	46898.064	46898.064
1.012	47217.191	47217.191
1.020	47397.457	47397.457
1.027	47648.798	47648.798
1.035	47653.990	47653.990
1.043	47762.544	47762.544
1.050	47906.348	47906.348
1.057	48049.615	48049.615
1.065	48266.076	48266.076
1.072	48629.433	48629.433
1.080	49031.825	49031.825
1.087	49252.374	49252.374
1.095	49472.306	49472.306
1.102	49617.366	49617.366
1.110	49647.251	49647.251
1.117	49598.217	49598.217
1.125	49699.890	49699.890
1.132	49684.319	49684.319
1.140	49586.201	49586.201
1.147	49443.745	49443.745
1.155	49336.684	49336.684
1.162	49466.648	49466.648
1.170	49554.826	49554.826
1.177	49805.337	49805.337
1.185	50016.495	50016.495
1.192	50184.847	50184.847
1.200	50396.386	50396.386
1.207	50606.979	50606.979
1.215	50819.183	50819.183
1.222	50945.382	50945.382
1.230	51156.272	51156.272
1.237	51151.000	51151.000
1.245	51229.720	51229.720
1.252	51175.978	51175.978
1.260	51250.251	51250.251

Time (sec)	Stress (Pa)	Viscosity (Pa s)
1.267	51278.961	51278.961
1.275	51484.405	51484.405
1.282	51645.589	51645.589
1.290	51804.894	51804.894
1.298	52011.607	52011.607
1.305	51985.520	51985.520
1.312	52236.613	52236.613
1.320	52347.233	52347.233
1.327	52550.985	52550.985
1.335	52659.695	52659.695
1.342	52622.532	52622.532
1.350	52581.820	52581.820
1.357	52684.238	52684.238
1.365	53130.632	53130.632
1.372	53381.675	53381.675
1.380	53733.014	53733.014
1.387	53683.974	53683.974
1.395	53581.411	53581.411
1.402	53524.376	53524.376
1.410	53670.135	53670.135
1.418	53969.260	53969.260
1.425	54324.294	54324.294
1.432	54784.895	54784.895
1.440	55197.327	55197.327
1.447	55612.863	55612.863
1.455	55708.043	55708.043
1.462	55856.379	55856.379
1.470	55784.314	55784.314
1.477	55817.726	55817.726
1.485	55794.060	55794.060
1.492	55766.864	55766.864
1.500	55849.175	55849.175
1.507	55927.830	55927.830
1.515	56004.502	56004.502
1.522	56050.026	56050.026
1.530	56209.582	56209.582
1.537	56134.455	56134.455
1.545	56083.923	56083.923
1.552	56118.589	56118.589
1.560	56121.271	56121.271
1.567	56240.866	56240.866
1.575	56420.482	56420.482

8.2.5.3 Continued

Time (sec)	Stress (Pa)	Viscosity (Pa s)
1.582	56753.358	56753.358
1.590	56964.323	56964.323
1.597	57268.506	57268.506
1.605	57354.484	57354.484
1.612	57659.707	57659.707
1.620	57774.557	57774.557
1.627	57856.485	57856.485
1.635	58000.593	58000.593
1.642	58209.291	58209.291
1.650	58384.742	58384.742
1.657	58493.853	58493.853
1.665	58833.429	58833.429
1.673	59007.605	59007.605
1.680	59316.436	59316.436
1.687	59388.151	59388.151
1.695	59629.618	59629.618
1.702	59870.306	59870.306
1.710	60147.441	60147.441
1.717	60494.021	60494.021
1.725	60701.876	60701.876
1.732	60837.569	60837.569
1.740	60792.984	60792.984
1.747	60960.973	60960.973
1.755	61018.894	61018.894
1.762	61257.159	61257.159
1.770	61459.371	61459.371
1.777	61698.753	61698.753
1.785	61712.132	61712.132
1.793	61532.552	61532.552
1.800	61499.405	61499.405
1.807	61424.710	61424.710
1.815	61499.170	61499.170
1.822	61494.998	61494.998
1.830	61643.361	61643.361
1.837	61869.117	61869.117
1.845	62215.429	62215.429
1.852	62441.887	62441.887
1.860	62749.887	62749.887
1.867	62855.791	62855.791
1.875	62712.306	62712.306
1.882	62727.609	62727.609
1.890	62657.995	62657.995

Time (sec)	Stress (Pa)	Viscosity (Pa s)
1.897	62708.373	62708.373
1.905	62798.668	62798.668
1.912	63143.634	63143.634
1.920	63446.899	63446.899
1.927	63665.107	63665.107
1.935	63838.993	63838.993
1.942	63878.869	63878.869
1.950	64137.745	64137.745
1.957	64129.564	64129.564
1.965	64162.976	64162.976
1.972	64056.179	64056.179
1.980	64126.893	64126.893
1.987	64057.290	64057.290
1.995	64215.238	64215.238
2.003	64279.215	64279.215
2.010	64527.369	64527.369
2.017	64965.351	64965.351
2.025	65023.951	65023.951
2.033	65225.322	65225.322
2.040	65183.095	65183.095
2.047	65184.295	65184.295
2.055	65084.094	65084.094
2.062	65177.139	65177.139
2.070	65168.684	65168.684
2.077	65154.868	65154.868
2.085	65442.399	65442.399
2.092	65782.073	65782.073
2.100	66329.189	66329.189
2.108	66465.647	66465.647
2.115	66756.852	66756.852
2.122	66784.864	66784.864
2.130	66809.505	66809.505
2.138	66832.388	66832.388
2.145	67011.394	67011.394
2.152	67081.575	67081.575
2.160	67204.116	67204.116
2.168	67598.997	67598.997
2.175	67775.598	67775.598
2.182	68229.454	68229.454
2.190	68517.667	68517.667
2.197	68977.987	68977.987
2.205	69095.465	69095.465

Time (sec)	Stress (Pa)	Viscosity (Pa s)
2.212	69098.146	69098.146
2.220	69153.715	69153.715
2.227	69206.188	69206.188
2.235	69431.953	69431.953
2.243	69539.319	69539.319
2.250	70002.511	70002.511
2.257	70227.560	70227.560
2.265	70574.445	70574.445
2.273	70799.251	70799.251
2.280	71209.831	71209.831
2.287	71311.442	71311.442
2.295	71347.496	71347.496
2.302	71252.915	71252.915
2.310	71026.752	71026.752
2.317	71305.337	71305.337
2.325	71584.122	71584.122
2.332	71994.023	71994.023
2.340	72142.107	72142.107
2.347	72290.353	72290.353
2.355	72369.786	72369.786
2.362	72511.729	72511.729
2.370	72719.702	72719.702
2.378	72588.356	72588.356
2.385	72791.794	72791.794
2.392	72720.254	72720.254
2.400	72989.573	72989.573
2.408	73047.072	73047.072
2.415	73245.678	73245.678
2.422	73297.648	73297.648
2.430	73562.866	73562.866
2.437	73757.361	73757.361
2.445	73875.111	73875.111
2.452	74138.132	74138.132
2.460	74254.411	74254.411
2.467	74515.858	74515.858
2.475	74251.820	74251.820
2.483	74395.791	74395.791
2.490	74347.207	74347.207
2.497	74561.674	74561.674
2.505	74737.420	74737.420
2.513	74988.830	74988.830
2.520	75396.557	75396.557

8.2.5.3 Continued

Time (sec)	Stress (Pa)	Viscosity (Pa s)
2.527	75490.234	75490.234
2.535	75820.387	75820.387
2.543	75788.921	75788.921
2.550	75875.993	75875.993
2.557	75755.045	75755.045
2.565	76120.032	76120.032
2.572	76115.337	76115.337
2.580	76188.879	76188.879
2.587	76469.207	76469.207
2.595	76664.309	76664.309
2.602	77155.652	77155.652
2.610	77265.023	77265.023
2.618	77933.788	77933.788
2.625	77910.284	77910.284
2.632	78103.022	78103.022
2.640	77983.841	77983.841
2.648	78036.587	78036.587
2.655	77771.979	77771.979
2.662	77543.123	77543.123
2.670	77808.445	77808.445
2.677	77706.273	77706.273
2.685	78244.672	78244.672
2.692	78508.013	78508.013
2.700	78864.047	78864.047
2.707	78890.354	78890.354
2.715	79199.153	79199.153
2.722	79219.408	79219.408
2.730	78993.333	78993.333
2.737	78711.743	78711.743
2.745	78616.290	78616.290
2.753	78912.147	78912.147
2.760	78759.116	78759.116
2.767	79451.681	79451.681
2.775	79544.729	79544.729
2.783	79581.790	79581.790
2.790	79309.137	79309.137
2.797	79181.095	79181.095
2.805	79309.269	79309.269
2.812	79013.119	79013.119
2.820	79184.649	79184.649
2.827	79246.833	79246.833
2.835	79736.827	79736.827

Time (sec)	Stress (Pa)	Viscosity (Pa s)
2.842	79796.755	79796.755
2.850	79961.279	79961.279
2.858	79793.337	79793.337
2.865	79895.477	79895.477
2.872	80386.266	80386.266
2.880	80260.593	80260.593
2.888	80130.223	80130.223
2.895	79820.915	79820.915
2.902	80018.262	80018.262
2.910	79289.491	79289.491
2.918	79245.214	79245.214
2.925	79195.752	79195.752
2.932	79198.908	79198.908
2.940	79317.878	79317.878
2.947	79674.561	79674.561
2.955	79791.728	79791.728
2.962	79293.184	79293.184
2.970	79398.328	79398.328
2.977	79190.373	79190.373
2.985	79536.909	79536.909
2.993	79256.408	79256.408
3.000	79473.936	79473.936
3.007	79943.607	79943.607
3.015	79903.360	79903.360
3.023	79790.735	79790.735
3.030	79869.189	79869.189
3.037	79880.043	79880.043
3.045	79619.478	79619.478
3.052	80418.637	80418.637
3.060	80485.927	80485.927
3.067	80820.743	80820.743
3.075	80882.939	80882.939
3.082	81149.435	81149.435
3.090	81828.067	81828.067
3.097	81885.392	81885.392
3.105	81870.220	81870.220
3.112	81492.992	81492.992
3.120	82036.687	82036.687
3.128	81573.210	81573.210
3.135	81463.368	81463.368
3.142	81055.056	81055.056
3.150	81076.452	81076.452

Time (sec)	Stress (Pa)	Viscosity (Pa s)
3.158	80944.155	80944.155
3.165	80955.812	80955.812
3.172	80887.208	80887.208
3.180	80662.486	80662.486
3.187	80735.417	80735.417
3.195	80033.839	80033.839
3.202	80250.282	80250.282
3.210	79759.132	79759.132
3.217	79729.651	79729.651
3.225	79537.755	79537.755
3.233	79497.112	79497.112
3.240	79209.114	79209.114
3.247	79034.921	79034.921
3.255	79385.287	79385.287
3.263	79117.798	79117.798
3.270	79713.405	79713.405
3.277	79394.453	79394.453
3.285	79738.783	79738.783
3.293	79745.632	79745.632
3.300	79661.884	79661.884
3.307	79271.137	79271.137
3.315	78912.421	78912.421
3.322	78631.918	78631.918
3.330	77770.986	77770.986
3.337	77734.328	77734.328
3.345	77112.358	77112.358
3.352	77242.956	77242.956
3.360	76916.459	76916.459
3.368	76900.539	76900.539
3.375	76788.520	76788.520
3.382	76948.352	76948.352
3.390	76966.246	76966.246
3.398	76697.989	76697.989
3.405	77181.124	77181.124
3.412	76422.453	76422.453
3.420	76707.813	76707.813

8.2.5.4 – HDB6 – Elongational Viscosity – 170 °C – Strain Rate = 0.3 s^{-1}

Time (sec)	Stress (Pa)	Viscosity (Pa s)
0.163	5612.124	18707.080
0.186	6112.376	20374.586
0.208	6506.372	21687.906
0.231	6909.529	23031.764
0.253	7341.228	24470.761
0.276	7723.061	25743.538
0.298	8056.186	26853.953
0.321	8438.808	28129.361
0.343	8743.707	29145.691
0.366	9034.581	30115.270
0.388	9324.959	31083.198
0.411	9481.278	31604.261
0.433	9598.933	31996.444
0.456	9807.785	32692.615
0.478	9955.738	33185.794
0.501	10205.131	34017.104
0.523	10462.488	34874.961
0.546	10662.512	35541.708
0.568	10841.767	36139.222
0.591	11022.676	36742.252
0.613	11177.622	37258.740
0.636	11343.434	37811.445
0.658	11424.928	38083.094
0.681	11550.469	38501.563
0.703	11647.916	38826.386
0.726	11673.227	38910.755
0.748	11767.272	39224.239
0.771	11930.844	39769.481
0.793	12066.324	40221.081
0.816	12218.078	40726.927
0.838	12326.075	41086.917
0.861	12434.975	41449.916
0.883	12570.374	41901.246
0.906	12696.354	42321.181
0.928	12798.159	42660.530
0.951	12895.348	42984.493
0.973	12940.366	43134.554
0.996	12969.909	43233.030
1.018	13020.382	43401.274
1.041	13092.863	43642.876
1.063	13154.200	43847.332
1.086	13259.872	44199.573
1.108	13409.773	44699.243
1.131	13517.065	45056.883
1.153	13614.027	45380.091
1.176	13689.540	45631.799
1.198	13788.088	45960.293
1.221	13903.918	46346.392
1.243	13924.036	46413.452
1.266	13892.337	46307.790
1.288	13928.638	46428.794
1.311	13947.763	46492.545
1.333	14054.016	46846.722
1.356	14131.222	47104.074
1.378	14298.249	47660.830
1.401	14454.863	48182.876
1.423	14576.614	48588.713
1.446	14693.441	48978.138
1.468	14792.958	49309.859
1.491	14887.156	49623.855
1.513	14889.214	49630.715
1.536	14927.812	49759.373
1.558	14928.802	49762.673
1.581	15080.309	50267.696
1.603	15201.422	50671.408
1.626	15202.218	50674.059
1.648	15305.180	51017.268
1.671	15512.389	51707.964
1.693	15617.452	52058.172
1.716	15644.709	52149.031
1.738	15717.597	52391.989
1.761	15777.354	52591.180
1.783	15817.169	52723.895
1.806	15809.881	52699.605
1.828	15876.354	52921.179
1.851	16004.322	53347.740
1.873	16098.857	53662.855
1.896	16138.549	53795.163
1.918	16206.134	54020.448
1.941	16302.181	54340.603
1.963	16419.496	54731.655
1.986	16537.654	55125.512
2.008	16635.666	55452.219
2.031	16654.551	55515.171
2.053	16680.024	55600.079
2.076	16727.389	55757.964
2.098	16744.980	55816.600
2.121	16858.391	56194.636
2.143	16957.541	56525.137
2.166	16974.730	56582.435
2.188	16953.986	56513.288
2.211	16969.824	56566.081
2.233	17115.170	57050.565
2.256	17277.250	57590.834
2.278	17371.503	57905.009
2.301	17340.193	57800.644
2.323	17316.315	57721.049
2.346	17330.516	57768.386
2.368	17415.735	58052.449
2.391	17501.806	58339.353
2.413	17515.155	58383.849
2.436	17674.551	58915.170
2.458	17654.604	58848.680
2.481	17716.727	59055.758
2.503	17836.719	59455.729
2.526	17982.552	59941.840
2.548	18045.207	60150.689
2.571	18099.602	60332.005
2.593	18247.727	60825.757
2.616	18371.843	61239.475
2.638	18513.175	61710.585
2.661	18560.372	61867.906
2.683	18808.709	62695.698
2.706	18918.307	63061.025
2.728	18789.158	62630.526
2.751	18674.333	62247.775
2.773	18711.136	62370.452
2.796	18910.420	63034.735
2.818	19047.419	63491.398
2.841	19093.898	63646.326
2.863	19185.913	63953.043
2.886	19260.088	64200.294
2.908	19249.602	64165.340
2.931	19502.829	65009.429
2.953	19787.640	65958.800
2.976	19815.842	66052.805
2.998	19757.585	65858.617
3.021	19871.846	66239.487
3.043	20035.667	66785.556

8.2.5.4 Continued

Time (sec)	Stress (Pa)	Viscosity (Pa s)
3.066	20328.726	67762.420
3.088	20585.533	68618.445
3.111	20754.787	69182.625
3.133	20794.838	69316.126
3.156	20703.048	69010.160
3.178	20691.064	68970.213
3.201	20718.620	69062.067
3.223	20838.165	69460.550
3.246	20782.141	69273.803
3.268	20588.459	68628.197
3.291	20538.347	68461.155
3.313	20433.888	68112.960
3.336	20524.411	68414.704
3.358	20630.962	68769.873
3.381	20662.758	68875.860
3.403	20704.672	69015.575
3.426	20768.288	69227.628
3.448	20798.806	69329.355
3.471	20917.293	69724.312
3.493	20824.416	69414.720
3.516	20948.271	69827.570
3.538	21062.122	70207.073
3.561	20982.154	69940.514
3.583	20934.858	69782.860
3.606	21024.386	70081.288
3.628	21161.090	70536.967
3.651	21339.486	71131.619
3.673	21543.114	71810.379
3.696	21653.468	72178.226
3.718	21626.634	72088.780
3.741	21634.845	72116.150
3.763	21441.893	71472.977
3.786	21354.913	71183.044
3.808	21413.615	71378.718
3.831	21305.158	71017.193
3.853	21349.806	71166.021
3.876	21325.156	71083.853
3.898	21469.588	71565.292
3.921	21570.365	71901.217
3.943	21678.162	72260.540
3.966	21702.640	72342.135
3.988	21810.814	72702.712
4.011	21951.754	73172.514
4.033	22061.089	73536.965
4.056	22243.646	74145.488
4.078	22174.574	73915.247
4.101	22076.508	73588.359
4.123	22111.372	73704.574
4.146	22301.824	74339.412
4.168	22295.270	74317.567
4.191	22363.783	74545.943
4.213	22362.288	74540.961
4.236	22492.842	74976.141
4.258	22518.913	75063.045
4.281	22586.253	75287.510
4.303	22696.562	75655.207
4.326	22936.622	76455.407
4.348	23337.291	77790.970
4.371	23648.161	78827.204
4.393	23815.930	79386.432
4.416	23689.517	78965.058
4.438	23478.706	78262.354
4.461	23443.309	78144.364
4.483	23624.600	78748.666
4.506	23868.332	79561.108
4.528	24083.546	80278.487
4.551	24100.371	80334.569
4.573	24224.892	80749.642
4.596	24101.444	80338.147
4.618	24146.981	80489.935
4.641	24089.906	80299.688
4.663	23848.125	79493.749
4.686	23761.614	79205.379
4.708	23817.848	79392.826
4.731	23695.598	78985.328
4.753	23603.481	78678.271
4.776	23730.238	79100.794
4.798	23733.903	79113.011
4.821	23770.083	79233.609
4.843	23964.344	79881.147
4.866	24033.892	80112.972
4.888	23975.650	79918.832
4.911	23924.397	79747.991
4.933	23982.836	79942.788
4.956	24223.625	80745.418
4.978	24396.216	81320.720
5.001	24368.261	81227.535
5.023	24303.149	81010.497
5.046	24111.478	80371.595
5.068	24364.590	81215.299
5.091	24647.039	82156.795
5.113	24686.858	82289.528
5.136	24798.736	82662.453
5.158	24837.858	82792.861
5.181	24867.312	82891.041
5.203	24961.033	83203.443
5.226	25026.178	83420.592
5.248	24911.880	83039.599
5.271	24947.346	83157.821
5.293	25068.272	83560.906
5.316	25344.223	84480.744
5.338	25370.390	84567.967
5.361	25375.425	84584.749
5.383	25626.131	85420.437
5.406	25760.306	85867.687
5.428	25544.945	85149.817
5.451	25335.928	84453.092
5.473	25416.626	84722.088
5.496	25517.175	85057.249
5.518	25526.415	85088.051
5.541	25771.237	85904.122
5.563	25976.910	86589.700
5.586	25933.470	86444.899
5.608	26066.616	86888.722
5.631	26051.921	86839.735
5.653	26217.924	87393.079
5.676	26363.291	87877.638
5.698	26443.938	88146.461
5.721	26481.844	88272.813
5.743	26639.074	88796.914
5.766	26730.387	89101.289
5.788	26533.548	88445.160
5.811	26444.348	88147.827
5.833	26522.185	88407.285
5.856	26678.930	88929.765
5.878	26642.469	88808.229

8.2.5.4 Continued

Time (sec)	Stress (Pa)	Viscosity (Pa s)
5.901	26615.540	88718.466
5.923	26761.122	89203.740
5.946	26977.283	89924.275
5.968	27124.844	90416.145
5.991	27213.947	90713.156
6.013	27338.642	91128.806
6.036	27296.142	90987.140
6.058	27155.267	90517.556
6.081	26986.749	89955.829
6.103	26973.811	89912.705
6.126	26910.579	89701.929
6.148	27030.754	90102.512
6.171	26951.604	89838.679
6.193	27134.143	90447.144
6.216	27331.054	91103.513
6.238	27554.275	91847.582
6.261	27496.553	91655.178
6.283	27167.140	90557.135
6.306	27467.827	91559.424
6.328	27497.226	91657.421
6.351	27208.761	90695.870
6.373	27009.090	90030.299
6.396	26857.658	89525.527
6.418	27066.655	90222.185
6.441	26965.625	89885.416
6.463	26861.985	89539.950
6.486	26948.406	89828.019
6.508	27324.083	91080.275
6.531	27453.095	91510.318
6.553	27443.243	91477.475
6.576	27487.946	91626.486
6.598	27489.968	91633.227
6.621	27447.568	91491.895
6.643	27395.871	91319.569
6.666	27436.833	91456.110
6.688	27425.900	91419.665
6.711	27465.100	91550.333
6.733	27421.906	91406.353
6.756	27377.321	91257.738
6.778	27584.696	91948.986
6.801	27817.101	92723.670
6.823	28339.260	94464.201

Time (sec)	Stress (Pa)	Viscosity (Pa s)
6.846	28195.178	93983.927
6.868	28240.018	94133.393
6.891	28314.915	94383.052
6.913	28015.687	93385.624
6.936	28008.855	93362.851
6.958	28119.873	93732.908
6.981	28238.884	94129.612
7.003	28221.713	94072.377
7.026	28291.679	94305.595
7.048	28702.490	95674.965
7.071	28946.314	96487.712
7.093	28779.942	95933.139
7.116	28916.666	96388.887
7.138	29154.294	97180.981
7.161	29452.287	98174.291
7.183	29415.243	98050.809
7.206	29350.871	97836.236
7.228	29266.482	97554.939
7.251	29413.053	98043.509
7.273	29377.760	97925.865
7.296	29384.440	97948.133
7.318	29433.959	98113.196
7.341	29748.628	99162.094
7.363	30056.940	100189.800
7.386	29892.291	99640.970
7.408	30311.871	101039.569
7.431	30863.139	102877.129
7.453	30705.379	102351.262
7.476	30867.110	102890.368
7.498	30518.217	101727.388
7.521	30172.896	100576.321
7.543	30358.844	101196.147
7.566	30402.860	101342.868
7.588	30456.578	101521.926
7.611	30883.597	102945.324
7.633	30763.543	102545.145
7.656	30796.950	102656.502
7.678	31054.660	103515.534
7.701	31027.951	103426.504
7.723	30740.771	102469.237
7.746	31169.060	103896.867
7.768	31017.639	103392.131

Time (sec)	Stress (Pa)	Viscosity (Pa s)
7.791	31035.005	103450.016
7.813	31102.338	103674.460
7.836	31106.976	103689.920
7.858	31493.447	104978.156
7.881	31738.581	105795.271
7.903	31586.289	105287.630
7.926	32011.216	106704.054
7.948	32153.315	107177.716
7.971	32093.115	106977.049
7.993	32364.473	107881.577
8.016	32398.716	107995.720
8.038	32465.309	108217.697
8.061	32421.120	108070.399
8.083	31920.917	106403.057
8.106	32426.569	108088.562
8.128	32568.020	108560.067
8.151	32629.824	108766.079
8.173	32976.616	109922.052
8.196	32901.884	109672.947
8.218	32802.086	109340.286
8.241	33000.844	110002.815
8.263	33119.393	110397.976
8.286	33202.089	110673.630
8.308	33213.461	110711.536
8.331	33164.447	110548.158
8.353	33389.054	111296.848
8.376	33796.874	112656.246
8.398	33623.520	112078.400
8.421	33495.677	111652.258
8.443	34055.646	113518.820
8.466	34174.765	113915.885
8.488	34056.367	113521.222
8.511	34740.000	115800.000
8.533	35051.165	116837.216
8.556	34611.948	115373.160
8.578	34782.799	115942.665
8.601	35147.166	117157.220
8.623	35151.349	117171.163
8.646	35048.264	116827.545
8.668	34836.548	116121.825
8.691	34727.504	115758.347
8.713	35069.767	116899.224

8.2.5.4 Continued

Time (sec)	Stress (Pa)	Viscosity (Pa s)
8.736	35374.755	117915.851
8.758	35383.238	117944.127
8.781	35554.498	118514.994
8.803	35809.576	119365.255
8.826	35733.438	119111.461
8.848	35571.231	118570.769
8.871	35630.514	118768.380
8.893	36435.954	121453.180
8.916	36014.911	120049.702
8.938	35514.810	118382.701
8.961	35711.334	119037.780
8.983	35967.380	119891.268
9.006	35816.639	119388.797
9.028	35148.422	117161.406
9.051	35682.185	118940.616
9.073	36087.732	120292.441
9.096	36256.988	120856.626
9.118	35823.367	119411.224
9.141	35533.645	118445.482
9.163	35681.713	118939.042
9.186	35661.589	118871.962
9.208	35810.210	119367.365
9.231	35927.712	119759.040
9.253	35824.142	119413.807
9.276	36066.774	120222.580
9.298	36662.666	122208.886
9.321	36814.875	122716.249
9.343	37402.842	124676.141
9.366	37786.370	125954.565
9.388	37370.847	124569.489
9.411	37525.224	125084.080
9.433	38160.740	127202.466
9.456	38051.590	126838.635
9.478	38056.395	126854.651
9.501	38093.690	126978.967
9.523	38232.901	127443.004
9.546	37804.702	126015.672
9.568	37905.487	126351.623
9.591	38336.603	127788.676
9.613	38157.331	127191.102
9.636	38434.085	128113.615
9.658	38888.625	129628.750

Time (sec)	Stress (Pa)	Viscosity (Pa s)
9.681	38741.255	129137.515
9.703	38409.731	128032.435
9.726	38724.133	129080.444
9.748	39479.139	131597.131
9.771	39029.352	130097.841
9.793	38738.895	129129.651
9.816	38907.982	129693.273
9.838	38440.804	128136.014
9.861	37889.410	126298.033
9.883	38868.084	129560.279
9.906	38843.820	129479.401
9.928	38952.766	129842.552
9.951	39159.724	130532.414
9.973	39170.918	130569.726
9.996	39436.216	131454.053
10.018	39444.619	131482.064
10.041	39373.437	131244.791
10.063	39380.350	131267.833
10.086	38938.995	129796.650
10.108	39365.417	131218.056
10.131	40247.197	134157.323
10.153	40251.658	134172.194
10.176	39860.197	132867.324
10.198	40422.344	134741.147
10.221	40296.622	134322.072
10.243	40506.176	135020.587
10.266	41099.510	136998.365
10.288	40649.048	135496.825
10.311	40989.022	136630.073
10.333	40830.841	136102.802
10.356	41217.068	137390.226
10.378	40910.408	136368.026
10.401	40508.894	135029.648
10.423	40357.370	134524.567
10.446	40608.030	135360.100
10.468	40735.714	135785.714
10.491	40885.549	136285.162
10.513	40932.470	136441.566
10.536	40526.357	135087.858
10.558	39949.400	133164.666
10.581	40924.049	136413.495
10.603	40503.900	135013.002

Time (sec)	Stress (Pa)	Viscosity (Pa s)
10.626	39623.624	132078.745
10.648	40167.258	133890.861
10.671	39872.539	132908.463
10.693	40616.245	135387.484
10.716	40818.308	136061.028
10.738	40429.384	134764.613
10.761	40864.825	136216.085
10.783	40692.233	135640.778
10.806	40238.321	134127.737
10.828	40107.013	133690.043
10.851	40212.611	134042.036
10.873	40497.461	134991.536
10.896	39959.349	133197.830
10.918	39865.774	132885.914
10.941	40162.081	133873.602
10.963	39893.992	132979.975
10.986	39819.184	132730.614
11.008	40182.418	133941.393
11.031	40131.904	133773.015
11.053	40390.516	134635.054
11.076	39709.484	132364.948
11.098	39800.427	132668.090
11.121	39572.745	131909.150
11.143	39424.014	131413.379

8.2.5.5 – HDB6 – Elongational Viscosity – 170 °C – Strain Rate = 0.1 s^{-1}

Time (sec)	Stress (Pa)	Viscosity (Pa s)
0.966	3740.776	37407.757
1.003	3840.122	38401.217
1.041	3935.037	39350.375
1.078	4028.684	40286.838
1.116	4128.355	41283.555
1.153	4191.582	41915.824
1.191	4241.031	42410.309
1.228	4340.717	43407.169
1.266	4455.285	44552.849
1.303	4502.489	45024.890
1.341	4562.635	45626.347
1.378	4606.938	46069.381
1.416	4627.904	46279.039
1.453	4712.705	47127.050
1.491	4733.984	47339.841
1.528	4792.119	47921.192
1.566	4856.249	48562.494
1.603	4894.821	48948.208
1.641	4926.246	49262.460
1.678	5002.438	50024.382
1.716	5053.095	50530.954
1.753	5117.015	51170.155
1.791	5166.387	51663.867
1.828	5240.657	52406.574
1.866	5273.678	52736.784
1.903	5291.513	52915.135
1.941	5343.982	53439.818
1.978	5375.549	53755.487
2.016	5453.526	54535.263
2.053	5487.599	54875.994
2.091	5500.391	55003.911
2.128	5534.743	55347.427
2.166	5616.103	56161.028
2.203	5656.868	56568.676
2.241	5680.046	56800.462
2.278	5679.761	56797.613
2.316	5712.863	57128.632
2.353	5728.362	57283.623
2.391	5755.993	57559.931
2.428	5759.468	57594.683
2.466	5767.074	57670.737
2.503	5823.090	58230.905
2.541	5830.705	58307.053
2.578	5860.828	58608.279
2.616	5901.216	59012.158
2.653	5960.388	59603.879
2.691	5974.472	59744.721
2.728	5967.979	59679.793
2.766	6046.468	60464.675
2.803	6052.632	60526.323
2.841	6052.240	60522.403
2.878	6137.965	61379.648
2.916	6156.776	61567.760
2.953	6167.241	61672.413
2.991	6203.255	62032.554
3.028	6213.669	62136.694
3.066	6220.022	62200.223
3.103	6211.116	62111.160
3.141	6210.747	62107.466
3.178	6244.788	62447.879
3.216	6235.742	62357.420
3.253	6265.696	62656.960
3.291	6326.534	63265.339
3.328	6334.872	63348.717
3.366	6288.095	62880.947
3.403	6316.181	63161.807
3.441	6319.826	63198.265
3.478	6350.245	63502.451
3.516	6412.249	64122.494
3.553	6476.689	64766.886
3.591	6487.522	64875.220
3.628	6523.234	65232.343
3.666	6520.400	65204.004
3.703	6535.842	65358.423
3.741	6551.308	65513.085
3.778	6559.780	65597.803
3.816	6535.960	65359.599
3.853	6551.323	65513.233
3.891	6631.724	66317.235
3.928	6633.272	66332.716
3.966	6637.026	66370.263
4.003	6664.402	66644.024
4.041	6649.383	66493.826
4.078	6650.644	66506.438
4.116	6654.144	66541.439
4.153	6698.379	66983.795
4.191	6704.384	67043.839
4.228	6674.221	66742.206
4.266	6696.938	66969.380
4.303	6784.968	67849.677
4.341	6800.808	68008.078
4.378	6762.867	67628.670
4.416	6790.669	67906.691
4.453	6811.376	68113.764
4.491	6812.248	68122.478
4.528	6778.383	67783.831
4.566	6816.302	68163.023
4.603	6914.317	69143.172
4.641	6942.743	69427.430
4.678	6873.300	68733.000
4.716	6848.559	68485.593
4.753	6854.174	68541.737
4.791	6925.589	69255.888
4.828	6918.402	69184.017
4.866	6947.054	69470.543
4.903	6962.788	69627.876
4.941	6970.973	69709.734
4.978	7004.918	70049.185
5.016	6979.132	69791.324
5.053	6906.176	69061.758
5.091	6890.190	68901.903
5.128	6955.596	69555.965
5.166	7126.857	71268.570
5.203	7169.495	71694.953
5.241	7140.705	71407.049
5.278	7135.407	71354.066
5.316	7143.554	71435.537
5.353	7146.075	71460.755
5.391	7159.565	71595.647
5.428	7191.761	71917.609
5.466	7191.529	71915.294
5.503	7158.504	71585.044
5.541	7212.855	72128.554
5.578	7217.941	72179.408
5.616	7187.034	71870.345
5.653	7175.265	71752.645
5.691	7252.356	72523.562
5.728	7296.321	72963.208
5.766	7281.612	72816.124

8.2.5.5 Continued

Time (sec)	Stress (Pa)	Viscosity (Pa s)
5.803	7314.641	73146.413
5.841	7381.628	73816.283
5.878	7383.906	73839.064
5.916	7366.109	73661.093
5.953	7376.687	73766.867
5.991	7415.784	74157.837
6.028	7478.274	74782.737
6.066	7442.851	74428.514
6.103	7482.327	74823.267
6.141	7504.572	75045.717
6.178	7553.287	75532.866
6.216	7581.665	75816.645
6.253	7571.857	75718.566
6.291	7567.823	75678.227
6.328	7682.293	76822.926
6.366	7678.247	76782.473
6.403	7662.383	76623.833
6.441	7646.109	76461.088
6.478	7665.826	76658.259
6.516	7564.696	75646.964
6.553	7574.963	75749.626
6.591	7615.695	76156.946
6.628	7616.683	76166.831
6.666	7571.671	75716.709
6.703	7581.689	75816.888
6.741	7644.150	76441.505
6.778	7651.270	76512.702
6.816	7633.231	76332.315
6.853	7658.665	76586.653
6.891	7709.475	77094.745
6.928	7785.753	77857.527
6.966	7751.682	77516.824
7.003	7698.449	76984.489
7.041	7717.647	77176.470
7.078	7743.519	77435.187
7.116	7788.681	77886.810
7.153	7837.221	78372.211
7.191	7870.022	78700.220
7.228	7854.007	78540.068
7.266	7847.706	78477.060
7.303	7798.915	77989.153
7.341	7769.088	77690.884
7.378	7873.922	78739.224
7.416	7910.170	79101.695
7.453	7866.916	78669.165
7.491	7796.574	77965.736
7.528	7872.633	78726.328
7.566	7949.154	79491.540
7.603	7931.900	79318.998
7.641	7897.467	78974.674
7.678	7940.614	79406.140
7.716	8048.898	80488.975
7.753	8072.245	80722.446
7.791	8040.724	80407.235
7.828	8098.500	80985.004
7.866	8160.191	81601.906
7.903	8103.917	81039.170
7.941	8127.340	81273.400
7.978	8143.989	81439.890
8.016	8178.231	81782.312
8.053	8117.268	81172.679
8.091	8168.937	81689.371
8.128	8284.851	82848.512
8.166	8283.981	82839.812
8.203	8282.768	82827.680
8.241	8306.650	83066.498
8.278	8330.814	83308.140
8.316	8380.011	83800.105
8.353	8288.180	82881.804
8.391	8308.411	83084.106
8.428	8270.130	82701.304
8.466	8249.613	82496.129
8.503	8188.524	81885.243
8.541	8193.301	81933.009
8.578	8272.399	82723.985
8.616	8281.166	82811.655
8.653	8297.423	82974.228
8.691	8309.785	83097.852
8.728	8333.407	83334.070
8.766	8364.715	83647.155
8.803	8392.431	83924.306
8.841	8362.950	83629.498
8.878	8352.296	83522.959
8.916	8429.662	84296.621
8.953	8469.104	84691.038
8.991	8442.771	84427.711
9.028	8396.902	83969.020
9.066	8381.530	83815.295
9.103	8377.878	83778.778
9.141	8311.209	83112.090
9.178	8354.238	83542.378
9.216	8456.946	84569.460
9.253	8472.702	84727.020
9.291	8480.663	84806.634
9.328	8456.534	84565.339
9.366	8472.108	84721.079
9.403	8532.268	85322.676
9.441	8600.672	86006.720
9.478	8620.824	86208.238
9.516	8612.354	86123.543
9.553	8652.964	86529.638
9.591	8578.545	85785.454
9.628	8668.471	86684.711
9.666	8709.385	87093.850
9.703	8621.530	86215.296
9.741	8633.282	86332.825
9.778	8669.810	86698.102
9.816	8672.860	86728.602
9.853	8735.078	87350.781
9.891	8657.711	86577.105
9.928	8694.523	86945.229
9.966	8748.427	87484.266
10.003	8687.258	86872.582
10.041	8592.949	85929.494
10.078	8646.843	86468.433
10.116	8687.928	86879.282
10.153	8662.020	86620.199
10.191	8670.443	86704.428
10.228	8661.418	86614.177
10.266	8744.576	87445.763
10.303	8839.156	88391.562
10.341	8850.315	88503.150
10.378	8832.375	88323.751
10.416	8874.554	88745.543
10.453	8889.837	88898.368
10.491	8880.530	88805.296

8.2.5.5 Continued

Time (sec)	Stress (Pa)	Viscosity (Pa s)
10.528	8839.462	88394.620
10.566	8897.576	88975.755
10.603	9044.743	90447.435
10.641	9014.741	90147.407
10.678	8966.197	89661.973
10.716	9027.551	90275.511
10.753	9075.283	90752.834
10.791	9074.570	90745.702
10.828	8950.577	89505.766
10.866	8935.161	89351.613
10.903	8907.769	89077.688
10.941	8927.159	89271.588
10.978	8915.857	89158.574
11.016	8932.711	89327.105
11.053	8916.445	89164.450
11.091	8921.220	89212.197
11.128	8916.390	89163.900
11.166	9019.672	90196.722
11.203	9068.010	90680.098
11.241	9063.299	90632.995
11.278	9087.693	90876.931
11.316	9109.607	91096.067
11.353	9146.227	91462.273
11.391	9178.185	91781.847
11.428	9111.469	91114.693
11.466	9078.638	90786.381
11.503	9105.301	91053.012
11.541	9052.113	90521.133
11.578	9036.059	90360.588
11.616	8992.096	89920.960
11.653	9028.347	90283.471
11.691	9112.897	91128.973
11.728	9053.110	90531.098
11.766	9005.224	90052.241
11.803	9026.375	90263.753
11.841	9019.110	90191.096
11.878	9052.995	90529.948
11.916	9149.240	91492.398
11.953	9240.834	92408.338
11.991	9257.205	92572.052
12.028	9247.465	92474.647
12.066	9303.266	93032.659
12.103	9235.116	92351.157
12.141	9216.852	92168.517
12.178	9224.820	92248.202
12.216	9208.730	92087.300
12.253	9305.077	93050.765
12.291	9345.297	93452.969
12.328	9250.864	92508.643
12.366	9220.524	92205.239
12.403	9263.313	92633.127
12.441	9360.865	93608.652
12.478	9401.563	94015.629
12.516	9312.961	93129.610
12.553	9215.293	92152.927
12.591	9227.722	92277.217
12.628	9234.673	92346.729
12.666	9316.819	93168.187
12.703	9320.982	93209.823
12.741	9254.712	92547.119
12.778	9176.417	91764.173
12.816	9273.269	92732.695
12.853	9387.764	93877.638
12.891	9388.817	93888.167
12.928	9415.331	94153.307
12.966	9430.654	94306.536
13.003	9399.527	93995.267
13.041	9379.907	93799.066
13.078	9546.062	95460.622
13.116	9526.402	95264.019
13.153	9509.504	95095.037
13.191	9462.663	94626.633
13.228	9548.411	95484.113
13.266	9510.156	95101.561
13.303	9405.989	94059.895
13.341	9480.041	94800.405
13.378	9572.661	95726.605
13.416	9602.738	96027.382
13.453	9554.051	95540.510
13.491	9565.664	95656.638
13.528	9592.485	95924.855
13.566	9533.838	95338.377
13.603	9584.841	95848.407
13.641	9608.620	96086.199
13.678	9653.975	96539.753
13.716	9649.865	96498.649
13.753	9726.652	97266.523
13.791	9725.758	97257.577
13.828	9784.154	97841.541
13.866	9723.343	97233.429
13.903	9744.034	97440.341
13.941	9685.439	96854.389
13.978	9858.650	98586.495
14.016	9819.108	98191.078
14.053	9833.449	98334.492
14.091	9873.543	98735.430
14.128	9907.477	99074.774
14.166	9879.853	98798.533
14.203	9890.895	98908.953
14.241	9754.628	97546.281
14.278	9709.251	97092.508
14.316	9640.244	96402.439
14.353	9861.552	98615.521
14.391	9858.848	98588.482
14.428	9722.640	97226.399
14.466	9765.707	97657.070
14.503	10024.128	100241.281
14.541	10388.738	103887.379
14.578	10580.077	105800.772
14.616	10616.302	106163.015
14.653	10632.451	106324.506
14.691	10685.982	106859.816
14.728	10726.129	107261.293
14.766	10800.961	108009.610
14.803	10851.898	108518.984
14.859	10953.284	109532.844
14.934	10848.143	108481.426
15.009	10783.304	107833.041
15.084	10620.569	106205.686
15.159	10700.522	107005.223
15.234	10829.847	108298.465
15.309	10898.480	108984.802
15.384	10782.500	107824.998
15.459	10941.539	109415.385
15.534	11044.148	110441.476
15.609	10977.222	109772.216

8.2.5.5 Continued

Time (sec)	Stress (Pa)	Viscosity (Pa s)
15.684	11122.185	111221.855
15.759	10939.621	109396.208
15.834	11027.599	110275.992
15.909	11058.443	110584.429
15.984	11307.009	113070.092
16.059	11168.531	111685.307
16.134	11294.142	112941.418
16.209	11054.633	110546.328
16.284	11113.589	111135.895
16.359	11140.702	111407.022
16.434	11228.800	112288.004
16.509	11145.124	111451.236
16.584	11379.812	113798.121
16.659	11475.916	114759.156
16.734	11474.367	114743.669
16.809	11355.381	113553.813
16.884	11696.709	116967.094
16.959	11767.456	117674.564
17.034	11704.659	117046.591
17.109	11398.550	113985.497
17.184	11293.138	112931.378
17.259	11393.558	113935.580
17.334	11686.781	116867.809
17.409	11559.166	115591.665
17.484	11634.856	116348.557
17.559	11740.821	117408.211
17.634	11544.465	115444.652
17.709	11408.929	114089.288
17.784	11511.335	115113.355
17.859	11363.008	113630.078
17.934	11489.020	114890.205
18.009	11506.194	115061.942
18.084	11539.994	115399.935
18.159	11358.117	113581.171
18.234	11367.960	113679.599
18.309	11768.072	117680.721
18.384	11643.785	116437.853
18.459	11531.887	115318.872
18.534	11576.036	115760.358
18.609	11455.665	114556.649
18.684	11426.926	114269.263
18.759	11500.394	115003.940
18.834	11664.464	116644.645
18.909	11742.079	117420.794
18.984	11604.433	116044.333
19.059	11810.841	118108.412
19.134	11942.454	119424.538
19.209	11981.458	119814.577
19.284	11941.297	119412.973
19.359	12047.529	120475.289
19.434	11929.317	119293.171
19.509	12077.328	120773.278
19.584	12146.085	121460.854
19.659	11981.613	119816.129
19.734	12048.971	120489.708
19.809	12171.059	121710.594
19.884	12124.617	121246.174
19.959	12296.951	122969.512
20.034	12221.732	122217.315
20.109	12359.551	123595.511
20.184	12179.088	121790.884
20.259	12169.012	121690.115
20.334	12141.554	121415.543
20.409	12135.767	121357.665
20.484	12150.652	121506.524
20.559	12214.310	122143.097
20.634	12368.367	123683.666
20.709	12256.402	122564.024
20.784	12283.899	122838.990
20.859	12538.654	125386.538
20.934	12466.424	124664.238
21.009	12344.039	123440.393
21.084	12383.491	123834.909
21.159	12366.767	123667.666
21.234	12338.030	123380.297
21.309	12319.299	123192.986
21.384	12380.408	123804.085
21.459	12321.651	123216.515
21.534	12543.481	125434.813
21.609	12321.054	123210.543
21.684	12467.436	124674.364
21.759	12229.056	122290.559
21.834	12428.071	124280.715
21.909	12574.761	125747.608
21.984	12674.628	126746.278
22.059	12497.555	124975.547
22.134	12488.907	124889.070
22.209	12308.091	123080.907
22.284	12459.479	124594.792
22.359	12547.653	125476.527
22.434	12526.957	125269.575
22.509	12486.056	124860.559
22.584	12438.535	124385.354
22.659	12475.143	124751.426
22.734	12682.115	126821.146
22.809	12563.186	125631.861
22.884	12626.704	126267.043
22.959	12507.941	125079.412
23.034	12366.940	123669.395
23.109	12412.508	124125.076
23.184	12596.111	125961.112
23.259	12361.798	123617.981
23.334	12594.997	125949.968
23.409	12688.066	126880.662
23.484	12777.038	127770.378
23.559	12394.539	123945.394
23.634	12706.119	127061.192
23.709	12721.428	127214.284
23.784	12789.439	127894.387
23.859	12759.203	127592.025
23.934	12716.985	127169.853
24.009	12867.120	128671.199
24.084	13042.853	130428.530
24.159	13019.561	130195.612
24.234	13422.617	134226.169
24.309	13202.927	132029.267
24.384	13306.731	133067.305
24.459	12999.162	129991.620
24.534	13071.854	130718.542
24.609	13313.396	133133.956
24.684	13048.265	130482.651
24.759	13216.571	132165.708
24.834	13346.901	133469.007
24.909	13680.814	136808.145
24.984	13803.113	138031.131
25.059	13868.414	138684.144

8.2.5.5 Continued

Time (sec)	Stress (Pa)	Viscosity (Pa s)
25.134	13977.572	139775.715
25.209	14146.821	141468.212
25.284	14018.203	140182.025
25.359	13879.555	138795.554
25.434	13740.167	137401.672
25.509	13666.646	136666.463
25.584	13652.428	136524.280
25.659	13786.191	137861.907
25.734	13799.166	137991.660
25.809	13869.055	138690.554
25.884	13818.549	138185.493
25.959	13774.234	137742.341
26.034	13920.494	139204.939
26.109	14028.236	140282.359
26.184	13962.993	139629.932
26.259	14068.444	140684.440
26.334	14009.292	140092.916
26.409	13962.623	139626.234
26.484	13875.032	138750.317
26.559	14193.159	141931.588
26.634	14328.299	143282.986

Time (sec)	Stress (Pa)	Viscosity (Pa s)
26.709	14584.589	145845.886
26.784	14237.352	142373.521
26.859	14283.842	142838.423
26.934	14376.797	143767.966
27.009	14358.589	143585.890
27.084	14419.406	144194.063
27.159	14486.146	144861.459
27.234	14457.091	144570.911
27.309	14508.347	145083.467
27.384	14540.964	145409.637
27.459	14994.754	149947.541
27.534	14773.180	147731.795
27.609	15181.057	151810.571
27.684	15301.472	153014.717
27.759	15223.625	152236.245
27.834	15047.653	150476.527
27.909	15546.584	155465.843
27.984	14808.334	148083.344
28.059	15314.871	153148.705
28.134	15065.002	150650.022
28.209	15307.647	153076.469

Time (sec)	Stress (Pa)	Viscosity (Pa s)
28.284	15065.633	150656.330
28.359	15586.140	155861.398
28.434	15323.885	153238.855
28.509	15476.702	154767.019
28.584	15682.520	156825.196
28.659	15887.184	158871.836
28.734	15563.285	155632.855
28.809	15246.045	152460.448
28.884	15406.836	154068.357
28.959	15949.639	159496.389
29.034	15348.020	153480.197
29.109	15813.537	158135.373
29.184	15656.774	156567.744
29.259	15852.020	158520.202
29.334	16077.110	160771.100
29.409	16216.585	162165.848
29.484	16075.102	160751.018
29.559	16814.344	168143.441
29.634	16608.647	166086.468
29.709	16248.278	162482.780
29.784	16283.614	162836.135

8.2.5.6 – HDB6 – Elongational Viscosity – 170 °C – Strain Rate = 0.03 s^{-1}

Time (sec)	Stress (Pa)	Viscosity (Pa s)
10.659	2882.751	96091.686
10.772	2879.606	95986.877
10.884	2901.860	96728.679
10.997	2891.955	96398.509
11.109	2877.109	95903.636
11.222	2896.551	96551.692
11.334	2906.679	96889.311
11.447	2912.627	97087.573
11.559	2895.401	96513.368
11.672	2914.612	97153.745
11.784	2899.339	96644.632
11.897	2873.502	95783.413
12.009	2914.774	97159.126
12.122	2909.914	96997.146
12.234	2949.710	98323.652
12.347	2900.863	96695.446
12.459	2879.032	95967.727

Time (sec)	Stress (Pa)	Viscosity (Pa s)
12.572	2890.509	96350.314
12.684	2887.768	96258.927
12.797	2865.702	95523.394
12.909	2888.209	96273.617
13.022	2909.022	96967.413
13.134	2872.824	95760.786
13.247	2875.594	95853.130
13.359	2880.360	96011.985
13.472	2888.216	96273.858
13.584	2878.291	95943.044
13.697	2880.670	96022.337
13.809	2894.799	96493.285
13.922	2891.417	96380.560
14.034	2908.664	96955.467
14.147	2903.228	96774.271
14.259	2870.383	95679.449
14.372	2881.560	96052.015

Time (sec)	Stress (Pa)	Viscosity (Pa s)
14.484	2936.790	97893.014
14.597	2929.759	97658.648
14.709	2925.204	97506.814
14.822	2939.666	97988.854
14.934	2905.276	96842.523
15.047	2906.972	96899.079
15.159	2893.048	96434.947
15.272	2913.657	97121.912
15.384	2915.157	97171.904
15.497	2916.967	97232.239
15.609	2878.059	95935.311
15.722	2889.754	96325.140
15.834	2889.281	96309.351
15.947	2912.076	97069.210
16.059	2883.189	96106.300
16.172	2872.193	95739.759
16.284	2885.558	96185.283

8.2.5.6 Continued

Time (sec)	Stress (Pa)	Viscosity (Pa s)
16.397	2931.604	97720.120
16.509	2902.010	96733.670
16.622	2904.189	96806.296
16.734	2926.754	97558.465
16.847	2934.864	97828.795
16.959	2951.451	98381.696
17.072	2972.159	99071.976
17.184	2942.746	98091.540
17.297	2942.746	98091.526
17.409	2930.814	97693.789
17.522	2975.779	99192.624
17.634	2966.652	98888.408
17.747	2954.528	98484.250
17.859	2980.919	99363.975
17.972	3002.380	100079.333
18.084	2967.308	98910.251
18.197	2958.704	98623.450
18.309	2985.695	99523.174
18.422	2982.744	99424.798
18.534	2960.757	98691.912
18.647	2997.347	99911.572
18.759	2971.990	99066.335
18.872	2969.764	98992.120
18.984	2972.192	99073.068
19.097	2956.306	98543.539
19.209	2968.695	98956.516
19.322	2983.751	99458.351
19.434	2992.981	99766.017
19.547	3056.048	101868.261
19.659	3054.945	101831.491
19.772	3057.209	101906.972
19.884	3042.348	101411.600
19.997	3038.413	101280.417
20.109	3028.402	100946.724
20.222	3006.001	100200.036
20.334	3044.400	101479.986
20.447	3071.922	102397.404
20.559	3049.780	101659.328
20.672	3022.671	100755.705
20.784	3022.402	100746.717
20.897	3053.947	101798.221
21.009	3054.554	101818.478
21.122	3017.147	100571.571
21.234	3050.701	101690.034
21.347	3079.681	102656.040
21.459	3084.514	102817.123
21.572	3061.182	102039.405
21.684	3041.040	101367.985
21.797	3070.758	102358.607
21.909	3076.639	102554.630
22.022	3103.599	103453.299
22.134	3076.678	102555.944
22.247	3043.362	101445.390
22.359	3017.680	100589.343
22.472	3074.127	102470.888
22.584	3106.424	103547.471
22.697	3127.856	104261.880
22.809	3127.523	104250.755
22.922	3089.557	102985.247
23.034	3119.340	103978.010
23.147	3098.625	103287.503
23.259	3089.151	102971.707
23.372	3140.714	104690.463
23.484	3119.027	103967.565
23.597	3090.177	103005.908
23.709	3060.731	102024.369
23.822	3054.456	101815.201
23.934	3101.021	103367.375
24.047	3129.901	104330.027
24.159	3100.541	103351.354
24.272	3101.360	103378.665
24.384	3120.173	104005.759
24.497	3149.430	104980.987
24.609	3129.855	104328.488
24.722	3094.290	103142.992
24.834	3109.916	103663.879
24.947	3156.206	105206.873
25.059	3133.072	104435.742
25.172	3097.909	103263.638
25.284	3138.520	104617.349
25.397	3178.090	105936.325
25.509	3167.234	105574.469
25.622	3125.502	104183.391
25.734	3164.480	105482.667
25.847	3179.140	105971.317
25.959	3201.941	106731.382
26.072	3155.364	105178.795
26.184	3180.857	106028.564
26.297	3178.907	105963.557
26.409	3137.611	104587.037
26.522	3145.237	104841.217
26.634	3177.147	105904.892
26.747	3225.916	107530.527
26.859	3171.219	105707.296
26.972	3136.064	104535.474
27.084	3118.226	103940.858
27.197	3144.388	104812.945
27.309	3113.493	103783.115
27.422	3153.022	105100.718
27.534	3129.252	104308.415
27.647	3129.139	104304.632
27.759	3136.073	104535.753
27.872	3206.365	106878.836
27.984	3177.808	105926.917
28.097	3199.944	106664.815
28.209	3159.527	105317.562
28.322	3163.074	105435.799
28.434	3168.223	105607.439
28.547	3165.695	105523.182
28.659	3184.453	106148.418
28.772	3234.565	107818.821
28.884	3241.018	108033.946
28.997	3209.579	106985.952
29.109	3161.060	105368.651
29.222	3154.572	105152.396
29.334	3161.199	105373.303
29.447	3186.717	106223.890
29.559	3231.390	107712.985
29.672	3185.575	106185.842
29.784	3178.659	105955.311
29.897	3140.935	104697.848
30.009	3192.315	106410.502
30.122	3198.309	106610.296
30.234	3177.418	105913.917
30.347	3130.781	104359.356
30.459	3161.948	105398.262

8.2.5.6 Continued

Time (sec)	Stress (Pa)	Viscosity (Pa s)
30.572	3201.521	106717.370
30.684	3186.442	106214.717
30.797	3211.151	107038.359
30.909	3190.713	106357.086
31.022	3193.384	106446.136
31.134	3252.200	108406.669
31.247	3290.455	109681.836
31.359	3220.518	107350.602
31.472	3193.813	106460.445
31.584	3189.415	106313.829
31.697	3150.354	105011.793
31.809	3263.591	108786.365
31.922	3231.144	107704.800
32.034	3178.269	105942.315
32.147	3181.248	106041.590
32.259	3201.055	106701.817
32.372	3334.137	111137.913
32.484	3311.571	110385.688
32.597	3306.068	110202.278
32.709	3279.986	109332.870
32.822	3229.033	107634.434
32.934	3263.886	108796.206
33.047	3282.254	109408.479
33.159	3205.366	106845.545
33.272	3190.643	106354.774
33.384	3200.697	106689.903
33.497	3257.183	108572.761
33.609	3182.047	106068.227
33.722	3140.086	104669.536
33.834	3316.324	110544.136
33.947	3339.128	111304.255
34.059	3297.576	109919.216
34.172	3283.049	109434.962
34.284	3254.752	108491.732
34.397	3214.056	107135.215
34.509	3230.817	107693.890
34.622	3313.813	110460.449
34.734	3349.349	111644.952
34.847	3317.458	110581.929
34.959	3306.566	110218.867
35.072	3310.722	110357.390
35.184	3317.274	110575.797
35.297	3278.996	109299.861
35.409	3223.725	107457.488
35.522	3255.196	108506.542
35.634	3222.302	107410.070
35.747	3249.364	108312.132
35.859	3243.424	108114.150
35.972	3276.387	109212.890
36.084	3297.969	109932.299
36.197	3260.132	108671.065
36.309	3298.351	109945.043
36.422	3348.029	111600.971
36.534	3309.326	110310.875
36.647	3317.641	110588.023
36.759	3299.217	109973.889
36.872	3319.319	110643.980
36.984	3326.460	110881.987
37.097	3386.668	112888.921
37.209	3354.925	111830.829
37.322	3351.699	111723.283
37.434	3411.938	113731.273
37.547	3360.747	112024.887
37.659	3339.807	111326.885
37.772	3424.557	114151.897
37.884	3365.128	112170.948
37.997	3328.914	110963.803
38.109	3302.455	110081.826
38.222	3275.779	109192.620
38.334	3267.869	108928.953
38.447	3238.829	107960.963
38.559	3301.697	110056.569
38.672	3352.359	111745.314
38.784	3307.976	110265.868
38.897	3274.589	109152.959
39.009	3361.608	112053.602
39.122	3282.454	109415.123
39.234	3339.351	111311.702
39.347	3333.116	111103.854
39.459	3339.108	111303.612
39.572	3273.645	109121.510
39.684	3266.517	108883.908
39.797	3435.063	114502.106
39.909	3401.128	113370.924
40.022	3357.981	111932.687
40.134	3408.212	113607.073
40.247	3427.936	114264.548
40.359	3325.409	110846.981
40.472	3340.882	111362.725
40.584	3320.852	110695.066
40.697	3355.195	111839.836
40.809	3353.110	111770.318
40.922	3344.132	111471.077
41.034	3238.835	107961.153
41.147	3257.594	108586.479
41.259	3365.017	112167.245
41.372	3424.658	114155.257
41.484	3310.676	110355.875
41.597	3407.855	113595.155
41.709	3387.185	112906.170
41.822	3483.369	116112.295
41.934	3520.503	117350.114
42.047	3470.959	115698.629
42.159	3342.172	111405.723
42.272	3369.627	112320.903
42.384	3408.161	113605.380
42.497	3435.521	114517.370
42.609	3300.301	110010.045
42.722	3433.094	114436.481
42.834	3404.703	113490.098
42.947	3343.920	111463.997
43.059	3361.918	112063.932
43.172	3426.902	114230.051
43.284	3398.001	113266.690
43.397	3375.846	112528.211
43.509	3528.294	117609.797
43.622	3512.716	117090.549
43.734	3420.917	114030.582
43.847	3342.165	111405.486
43.959	3414.960	113832.000
44.072	3490.734	116357.794
44.184	3413.436	113781.207
44.297	3363.361	112112.047
44.409	3433.495	114449.831
44.522	3406.098	113536.611
44.634	3324.223	110807.430

8.2.5.6 Continued

Time (sec)	Stress (Pa)	Viscosity (Pa s)
44.747	3396.367	113212.231
44.859	3412.731	113757.701
45.028	3466.305	115543.497
45.253	3396.560	113218.655
45.478	3498.731	116624.359
45.703	3510.174	117005.815
45.928	3505.184	116839.466
46.153	3437.091	114569.701
46.378	3489.465	116315.509
46.603	3447.494	114916.472
46.828	3492.840	116427.988
47.053	3451.840	115061.340
47.278	3492.388	116412.917
47.503	3480.352	116011.725
47.728	3519.072	117302.402
47.953	3554.566	118485.519
48.178	3517.983	117266.091
48.403	3589.526	119650.876
48.628	3518.271	117275.711
48.853	3498.720	116623.992
49.078	3591.773	119725.776
49.303	3508.931	116964.366
49.528	3565.269	118842.304
49.753	3520.104	117336.793
49.978	3573.009	119100.306
50.203	3646.765	121558.830
50.428	3589.329	119644.316
50.653	3514.889	117162.960
50.878	3701.274	123375.815
51.103	3567.510	118917.014
51.328	3664.618	122153.933
51.553	3664.092	122136.400
51.778	3726.583	124219.441
52.003	3630.062	121002.057
52.228	3650.563	121685.446
52.453	3606.547	120218.246
52.678	3581.883	119396.097
52.903	3547.580	118252.663
53.128	3588.905	119630.171
53.353	3628.626	120954.199
53.578	3598.142	119938.063
53.803	3674.640	122487.985
54.028	3651.962	121732.054
54.253	3627.057	120901.893
54.478	3681.515	122717.176
54.703	3703.594	123453.148
54.928	3504.152	116805.074
55.153	3549.551	118318.378
55.378	3744.787	124826.231
55.603	3810.503	127016.768
55.828	3686.335	122877.844
56.053	3737.016	124567.214
56.278	3707.799	123593.292
56.503	3733.970	124465.671
56.728	3725.311	124177.036
56.953	3637.027	121234.221
57.178	3667.478	122249.254
57.403	3730.056	124335.191
57.628	3946.809	131560.309
57.853	3872.354	129078.482
58.078	3807.384	126912.810
58.303	3686.852	122895.063
58.528	3708.533	123617.781
58.753	3596.061	119868.697
58.978	3615.416	120513.866
59.203	3830.059	127668.646
59.428	3884.543	129484.756
59.653	3841.741	128058.033
59.878	3784.122	126137.384
60.103	3830.620	127687.347
60.328	3697.336	123244.525
60.553	3761.649	125388.315
60.778	3724.810	124160.322
61.003	3876.913	129230.433
61.228	3823.113	127437.106
61.453	3873.196	129106.533
61.678	3860.616	128687.187
61.903	3849.411	128313.700
62.128	3876.736	129224.543
62.353	3863.968	128798.947
62.578	3865.217	128840.557
62.803	3969.816	132327.190
63.028	3950.243	131674.756
63.253	3991.459	133048.619
63.478	3948.407	131613.577
63.703	3795.922	126530.725
63.928	4058.047	135268.223
64.153	3848.334	128277.792
64.378	3846.133	128204.444
64.603	3907.908	130263.602
64.828	4038.201	134606.692
65.053	3954.075	131802.488
65.278	4049.106	134970.192
65.503	3975.488	132516.278
65.728	3933.128	131104.271
65.953	4148.482	138282.721
66.178	3909.826	130327.523
66.403	3874.703	129156.754
66.628	4050.812	135027.066
66.853	4147.911	138263.698
67.078	3968.170	132272.347
67.303	4039.417	134647.230
67.528	4161.674	138722.465
67.753	3891.480	129716.015
67.978	4011.267	133708.885
68.203	4152.281	138409.365
68.428	4082.559	136085.291
68.653	4247.300	141576.650
68.878	3762.188	125406.259
69.103	4109.375	136979.178
69.328	4067.081	135569.355
69.553	3939.086	131302.880
69.778	4152.198	138406.607
70.003	4178.733	139291.087
70.228	4169.659	138988.632
70.453	4193.814	139793.815
70.678	4155.300	138509.994
70.903	4181.938	139397.933
71.128	4272.911	142430.367
71.353	4152.431	138414.383
71.578	4197.839	139927.960
71.803	4220.727	140690.911
72.028	4271.634	142387.807
72.253	4240.272	141342.415
72.478	3817.251	127241.699
72.703	4371.728	145724.283

8.2.5.6 Continued

Time (sec)	Stress (Pa)	Viscosity (Pa s)
72.928	4218.492	140616.401
73.153	4179.282	139309.414
73.378	4331.299	144376.639
73.603	4287.714	142923.799
73.828	4154.859	138495.314
74.053	4290.281	143009.370
74.278	4180.858	139361.933
74.503	4223.291	140776.361
74.728	4160.641	138688.023
74.953	4291.671	143055.684
75.178	4168.911	138963.687
75.403	4287.539	142917.953
75.628	4195.648	139854.932
75.853	4459.920	148663.996
76.078	4108.926	136964.199
76.303	4101.939	136731.315
76.528	4537.713	151257.103
76.753	4389.610	146320.333
76.978	4399.845	146661.503
77.203	4283.540	142784.662
77.428	4305.380	143512.650
77.653	4066.626	135554.202
77.878	4348.895	144963.160
78.103	4373.289	145776.290
78.328	4403.065	146768.818
78.553	4099.796	136659.881
78.778	4031.831	134394.367
79.003	4188.713	139623.776
79.228	4279.169	142638.954
79.453	4121.604	137386.785
79.678	4327.697	144256.578
79.903	4664.339	155477.982
80.128	4495.722	149857.406
80.353	4514.343	150478.114
80.578	4480.853	149361.767
80.803	4513.565	150452.154
81.028	4345.333	144844.423
81.253	4542.652	151421.727
81.478	4648.368	154945.612
81.703	4159.191	138639.695
81.928	4297.734	143257.786
82.153	4533.172	151105.735
82.378	4600.517	153350.551
82.603	4559.676	151989.213
82.828	4583.471	152782.362
83.053	4306.258	143541.931
83.278	4399.984	146666.148
83.503	4215.568	140518.925
83.728	4497.298	149909.931
83.953	4235.283	141176.109
84.178	4258.550	141951.660
84.403	4437.122	147904.082
84.628	4529.668	150988.943
84.853	4519.355	150645.169
85.078	4712.545	157084.842
85.303	4570.054	152335.144
85.528	4572.407	152413.576
85.753	4493.097	149769.885
85.978	4715.702	157190.067
86.203	4553.767	151792.232
86.428	4475.872	149195.738
86.653	4796.875	159895.825
86.878	4465.797	148859.893
87.103	4401.399	146713.308
87.328	4577.421	152580.692
87.553	4523.140	150771.350
87.778	4554.296	151809.882
88.003	4693.062	156435.416
88.228	4760.291	158676.368
88.453	4527.877	150929.242
88.678	4655.628	155187.597
88.903	4685.438	156181.276
89.128	4653.014	155100.473
89.353	4427.142	147571.415
89.578	4449.877	148329.219
89.803	4327.067	144235.581
90.028	4289.793	142993.115
90.253	4678.445	155948.165
90.478	4763.849	158794.973
90.703	4725.330	157510.992
90.928	4818.759	160625.316
91.153	4494.511	149817.018
91.378	4622.574	154085.801
91.603	4696.020	156533.997
91.828	4935.714	164523.786
92.053	4725.772	157525.719
92.278	4276.436	142547.873
92.503	4491.518	149717.255
92.728	4473.282	149109.410
92.953	4606.776	153559.188
93.178	4250.905	141696.838
93.403	4920.232	164007.745
93.628	4984.194	166139.784
93.853	4806.656	160221.877
94.078	4673.632	155787.745
94.303	4955.019	165167.313
94.528	4566.650	152221.672
94.753	4466.076	148869.199
94.978	4976.041	165868.046
95.203	4832.369	161078.962
95.428	4719.907	157330.243
95.653	4273.416	142447.204
95.878	4593.237	153107.893
96.103	4743.782	158126.083
96.328	4613.162	153772.070
96.553	4635.469	154515.622
96.778	5036.459	167881.982
97.003	4865.649	162188.303
97.228	4535.178	151172.604
97.453	4793.773	159792.427
97.678	5328.504	177616.798
97.903	4929.575	164319.159
98.128	4809.922	160330.740
98.353	4910.104	163670.125
98.578	4784.930	159497.658
98.803	4653.271	155109.049
99.028	4762.308	158743.603
99.253	4810.715	160357.154
99.478	4857.636	161921.214
99.703	5033.120	167770.661
99.928	4969.212	165640.385
100.153	4986.423	166214.115
100.378	4999.084	166636.146
100.603	4990.128	166337.597
100.828	5124.451	170815.019
101.053	4542.466	151415.542

8.2.5.6 Continued

Time (sec)	Stress (Pa)	Viscosity (Pa s)
101.278	5038.532	167951.056
101.503	4974.395	165813.182
101.728	5054.743	168491.419
101.953	4710.970	157032.318
102.178	5115.589	170519.630
102.403	4850.208	161673.600
102.628	4399.989	146666.286
102.853	5112.106	170403.519
103.078	5166.657	172221.900
103.303	5199.660	173321.999
103.528	5250.735	175024.498
103.753	4547.157	151571.892
103.978	4845.715	161523.830
104.203	5125.622	170854.079
104.428	5336.297	177876.570
104.653	4697.156	156571.881
104.878	5288.969	176298.961
105.103	4816.389	160546.289
105.328	5374.245	179141.485
105.553	4970.899	165696.636

Time (sec)	Stress (Pa)	Viscosity (Pa s)
105.778	5092.611	169753.696
106.003	5038.552	167951.720
106.228	5493.811	183127.041
106.453	5078.877	169295.892
106.678	4567.523	152250.777
106.903	5581.627	186054.248
107.128	5099.364	169978.811
107.353	5222.555	174085.168
107.578	5125.978	170865.935
107.803	5365.177	178839.250
108.028	4756.783	158559.421
108.253	5560.051	185335.047
108.478	4985.559	166185.290
108.703	4905.171	163505.705
108.928	5113.189	170439.622
109.153	5471.123	182370.756
109.378	4908.820	163627.346
109.603	5227.701	174256.700
109.828	5522.443	184081.447
110.053	5424.123	180804.084

Time (sec)	Stress (Pa)	Viscosity (Pa s)
110.278	5262.078	175402.611
110.503	5483.028	182767.595
110.728	5626.344	187544.790
110.953	5495.914	183197.143
111.178	5617.976	187265.871
111.403	5423.148	180771.607
111.628	5948.688	198289.613
111.853	5748.007	191600.248
112.078	5191.055	173035.172
112.303	5393.243	179774.778
112.528	5241.820	174727.318
112.753	5641.460	188048.663
112.978	5158.465	171948.822
113.203	5451.585	181719.501
113.428	5299.569	176652.292
113.653	5371.651	179055.032
113.878	5418.279	180609.312
114.103	5916.468	197215.601
114.328	5933.343	197778.097
114.553	5037.187	167906.232

8.2.5.7 – HDB6 – Elongational Viscosity – 170 °C – Strain Rate = 0.01 s^{-1}

Time (sec)	Stress (Pa)	Viscosity (Pa s)
47.531	1057.401	105740.088
47.906	1049.171	104917.125
48.281	1035.934	103593.374
48.656	1053.657	105365.677
49.031	1056.273	105627.320
49.406	1051.012	105101.190
49.781	1053.144	105314.397
50.156	1059.248	105924.819
50.531	1041.143	104114.306
50.906	1042.605	104260.527
51.281	1036.606	103660.566
51.656	1033.158	103315.816
52.031	1032.891	103289.055
52.406	1047.505	104750.451
52.781	1034.780	103478.023
53.156	1021.967	102196.657
53.531	1017.717	101771.745
53.906	1082.918	108291.809

Time (sec)	Stress (Pa)	Viscosity (Pa s)
54.281	1058.400	105839.970
54.656	1020.988	102098.752
55.031	1032.758	103275.785
55.406	1083.057	108305.694
55.781	1097.456	109745.620
56.156	1065.546	106554.579
56.531	1014.076	101407.569
56.906	1042.248	104224.778
57.281	1027.149	102714.882
57.656	1038.018	103801.771
58.031	1015.987	101598.663
58.406	1019.628	101962.763
58.781	1041.767	104176.675
59.156	1063.703	106370.308
59.531	1062.760	106275.964
59.906	1043.100	104310.014
60.281	1053.745	105374.475
60.656	1065.197	106519.707

Time (sec)	Stress (Pa)	Viscosity (Pa s)
61.031	1021.834	102183.351
61.406	988.830	98883.021
61.781	1025.293	102529.310
62.156	1051.851	105185.099
62.531	1038.744	103874.394
62.906	1020.644	102064.437
63.281	1044.231	104423.057
63.656	1055.852	105585.229
64.031	1037.475	103747.488
64.406	1038.663	103866.273
64.781	1070.190	107018.961
65.156	1028.710	102871.033
65.531	1032.859	103285.884
65.906	1041.625	104162.468
66.281	1054.155	105415.544
66.656	1045.452	104545.202
67.031	1054.225	105422.460
67.406	1024.265	102426.495

8.2.5.7 Continued

Time (sec)	Stress (Pa)	Viscosity (Pa s)
67.781	1041.234	104123.445
68.156	1021.958	102195.837
68.531	1050.169	105016.870
68.906	1060.297	106029.703
69.281	1077.502	107750.220
69.656	1059.932	105993.233
70.031	1042.512	104251.180
70.406	1025.739	102573.932
70.781	1044.334	104433.414
71.156	1111.418	111141.773
71.531	1087.169	108716.865
71.906	1009.310	100931.035
72.281	967.275	96727.543
72.656	1029.518	102951.833
73.031	1104.261	110426.128
73.406	1099.156	109915.631
73.781	1067.312	106731.215
74.156	1043.378	104337.766
74.531	1006.477	100647.737
74.906	1034.002	103400.216
75.281	1092.142	109214.220
75.656	1085.108	108510.772
76.031	1053.783	105378.320
76.406	1025.738	102573.758
76.781	1082.869	108286.853
77.156	1047.181	104718.051
77.531	1028.818	102881.773
77.906	1053.299	105329.908
78.281	1070.811	107081.051
78.656	1052.042	105204.182
79.031	1057.238	105723.833
79.406	1077.361	107736.070
79.781	1054.108	105410.837
80.156	1038.652	103865.176
80.531	1066.793	106679.291
80.906	1061.956	106195.610
81.281	1074.796	107479.631
81.656	1045.493	104549.322
82.031	1024.036	102403.573
82.406	1060.356	106035.640
82.781	1024.698	102469.797
83.156	1083.838	108383.829
83.531	1049.950	104994.978
83.906	1022.918	102291.782
84.281	1041.837	104183.724
84.656	1018.404	101840.357
85.031	1013.156	101315.604
85.406	1087.317	108731.698
85.781	1065.394	106539.382
86.156	1038.325	103832.479
86.531	1010.017	101001.721
86.906	1051.174	105117.381
87.281	1057.531	105753.131
87.656	1038.158	103815.799
88.031	1030.667	103066.683
88.406	1017.937	101793.688
88.781	1017.111	101711.081
89.156	1045.230	104522.986
89.531	1020.232	102023.238
89.906	1014.267	101426.716
90.281	1047.886	104788.578
90.656	1065.674	106567.392
91.031	1020.986	102098.568
91.406	989.902	98990.217
91.781	1007.875	100787.495
92.156	1020.264	102026.448
92.531	984.233	98423.345
92.906	1043.385	104338.537
93.281	1062.398	106239.828
93.656	1053.650	105365.034
94.031	1040.486	104048.603
94.406	1044.647	104464.750
94.781	1054.175	105417.515
95.156	1080.536	108053.612
95.531	1056.976	105697.640
95.906	998.586	99858.644
96.281	997.165	99716.472
96.656	1066.838	106683.797
97.031	1062.591	106259.055
97.406	1092.450	109245.011
97.781	1056.923	105692.266
98.156	1006.641	100664.120
98.531	993.235	99323.505
98.906	1049.945	104994.520
99.281	1045.082	104508.212
99.656	1033.986	103398.578
100.031	1013.917	101391.725
100.406	1017.392	101739.176
100.781	1097.010	109700.955
101.156	1089.356	108935.636
101.531	1028.834	102883.430
101.906	993.710	99371.035
102.281	1058.485	105848.470
102.656	1078.010	107801.023
103.031	1055.109	105510.873
103.406	1034.763	103476.325
103.781	1031.499	103149.856
104.156	1044.743	104474.346
104.531	1060.376	106037.638
104.906	1081.559	108155.877
105.281	1066.988	106698.786
105.656	1056.651	105665.067
106.031	1060.762	106076.226
106.406	997.705	99770.477
106.781	1040.427	104042.734
107.156	1010.589	101058.940
107.531	1041.410	104140.957
107.906	1000.150	100015.006
108.281	1001.136	100113.603
108.656	1068.465	106846.541
109.031	1048.078	104807.759
109.406	1088.325	108832.538
109.781	1042.746	104274.618
110.156	1037.380	103737.952
110.531	1075.867	107586.728
110.906	1041.340	104133.956
111.281	1067.167	106716.660
111.656	1053.563	105356.337
112.031	1088.403	108840.310
112.406	1043.429	104342.867
112.781	1148.725	114872.502
113.156	1109.827	110982.739
113.531	1030.816	103081.554
113.906	1071.884	107188.409
114.281	1081.201	108120.084
114.656	1125.905	112590.524

8.2.5.7 Continued

Time (sec)	Stress (Pa)	Viscosity (Pa s)
115.031	1085.988	108598.762
115.406	1067.094	106709.393
115.781	1071.259	107125.927
116.156	1048.433	104843.314
116.531	1070.530	107053.018
116.906	1030.161	103016.137
117.281	1049.710	104971.020
117.656	1047.526	104752.619
118.031	1069.495	106949.479
118.406	1038.895	103889.489
118.781	1062.838	106283.813
119.156	1102.154	110215.423
119.531	1132.568	113256.762
119.906	1060.497	106049.677
120.281	1056.536	105653.595
120.656	1042.075	104207.465
121.031	1091.921	109192.071
121.406	1095.940	109594.047
121.781	1094.128	109412.822
122.156	1100.091	110009.107
122.531	1115.484	111548.351
122.906	1046.434	104643.377
123.281	1026.183	102618.260
123.656	1108.140	110813.978
124.031	1033.844	103384.425
124.406	1087.833	108783.282
124.781	1036.713	103671.336
125.156	1062.118	106211.775
125.531	1078.593	107859.294
125.906	1115.833	111583.271
126.281	1131.107	113110.732
126.656	1086.224	108622.406
127.031	1151.488	115148.753
127.406	1138.794	113879.372
127.781	1087.417	108741.735
128.156	1087.150	108714.960
128.531	1043.101	104310.103
128.906	1160.925	116092.482
129.281	1191.322	119132.211
129.656	1195.641	119564.087
130.031	1126.279	112627.930
130.406	1092.790	109278.988
130.781	1106.106	110610.596
131.156	1118.846	111884.642
131.531	1099.348	109934.753
131.906	1165.698	116569.792
132.281	1075.107	107510.712
132.656	1166.776	116677.621
133.031	1132.320	113231.952
133.406	1116.708	111670.801
133.781	1153.678	115367.774
134.156	1123.566	112356.615
134.531	1130.402	113040.177
134.906	1100.794	110079.447
135.281	1064.803	106480.279
135.656	1139.665	113966.542
136.031	1120.588	112058.835
136.406	1123.646	112364.649
136.781	1104.743	110474.306
137.156	1075.841	107584.062
137.531	1129.879	112987.889
137.906	1098.727	109872.698
138.281	1075.468	107546.798
138.656	1094.113	109411.260
139.031	1135.622	113562.179
139.406	1150.547	115054.675
139.781	1179.518	117951.790
140.156	1131.104	113110.353
140.531	1092.538	109253.760
140.906	1170.721	117072.146
141.281	1148.839	114883.909
141.656	1124.752	112475.225
142.031	1134.259	113425.856
142.406	1094.002	109400.212
142.781	1077.010	107701.031
143.156	1184.499	118449.853
143.531	1156.065	115606.519
143.906	1110.820	111082.041
144.281	1124.912	112491.232
144.656	1047.955	104795.453
145.031	1110.621	111062.142
145.406	1187.977	118797.664
145.781	1149.926	114992.580
146.156	1180.835	118083.456
146.719	1150.168	115016.804
147.469	1153.090	115309.030
148.219	1155.370	115537.025
148.969	1170.898	117089.803
149.719	1104.511	110451.147
150.469	1114.898	111489.810
151.219	1139.266	113926.571
151.969	1146.468	114646.838
152.719	1117.300	111729.984
153.469	1205.722	120572.153
154.219	1130.544	113054.367
154.969	1216.951	121695.142
155.719	1136.043	113604.342
156.469	1244.142	124414.233
157.219	1118.165	111816.515
157.969	1115.358	111535.833
158.719	1136.804	113680.387
159.469	1174.376	117437.638
160.219	1146.585	114658.490
160.969	1148.283	114828.287
161.719	1147.685	114768.498
162.469	1289.621	128962.053
163.219	1310.908	131090.769
163.969	1160.997	116099.669
164.719	1137.024	113702.442
165.469	1188.524	118852.361
166.219	1285.969	128596.893
166.969	1307.117	130711.721
167.719	1137.188	113718.819
168.469	1252.663	125266.338
169.219	1154.208	115420.804
169.969	1144.333	114433.322
170.719	1221.911	122191.140
171.469	1309.419	130941.862
172.219	1313.645	131364.546
172.969	1198.347	119834.727
173.719	1286.135	128613.457
174.469	1283.281	128328.091
175.219	1292.199	129219.880
175.969	1297.400	129739.973
176.719	1291.006	129100.569
177.469	1239.682	123968.228

8.2.5.7 Continued

Time (sec)	Stress (Pa)	Viscosity (Pa s)
178.219	1259.040	125904.039
178.969	1212.431	121243.076
179.719	1414.588	141458.843
180.469	1281.090	128109.030
181.219	1274.093	127409.258
181.969	1216.123	121612.298
182.719	1310.585	131058.475
183.469	1196.350	119634.983
184.219	1178.994	117899.416
184.969	1267.863	126786.324
185.719	1258.389	125838.875
186.469	1147.345	114734.543
187.219	1240.748	124074.840
187.969	1324.159	132415.893
188.719	1301.895	130189.544
189.469	1276.203	127620.274
190.219	1208.698	120869.829
190.969	1351.026	135102.609
191.719	1263.976	126397.604
192.469	1193.784	119378.419
193.219	1228.312	122831.200
193.969	1308.826	130882.639
194.719	1159.378	115937.800
195.469	1184.069	118406.943
196.219	1232.069	123206.851
196.969	1282.196	128219.629
197.719	1169.676	116967.564
198.469	1310.457	131045.744
199.219	1139.904	113990.389
199.969	1261.476	126147.583
200.719	1254.948	125494.754
201.469	1181.252	118125.205
202.219	1188.152	118815.199
202.969	1114.495	111449.489
203.719	1208.908	120890.780
204.469	1247.965	124796.524
205.219	1362.186	136218.577
205.969	1268.775	126877.463
206.719	1218.359	121835.853
207.469	1175.024	117502.400
208.219	1210.813	121081.291
208.969	1285.772	128577.226

Time (sec)	Stress (Pa)	Viscosity (Pa s)
209.719	1233.833	123383.262
210.469	945.012	94501.222
211.219	1339.066	133906.644
211.969	1221.546	122154.632
212.719	1225.466	122546.615
213.469	1202.251	120225.099
214.219	1173.653	117365.289
214.969	1259.511	125951.139
215.719	1296.045	129604.548
216.469	1264.838	126483.837
217.219	1135.385	113538.537
217.969	1191.673	119167.341
218.719	1163.750	116374.966
219.469	1278.879	127887.950
220.219	1172.377	117237.666
220.969	1263.324	126332.386
221.719	1382.694	138269.383
222.469	1142.335	114233.478
223.219	1248.303	124830.344
223.969	1346.672	134667.235
224.719	1194.997	119499.749
225.469	1572.071	157207.077
226.219	1292.359	129235.890
226.969	1293.956	129395.561
227.719	1285.635	128563.534
228.469	1150.697	115069.739
229.219	1151.225	115122.478
229.969	1231.824	123182.448
230.719	1352.737	135273.694
231.469	1243.300	124330.049
232.219	1400.864	140086.356
232.969	1450.772	145077.191
233.719	1465.726	146572.623
234.469	1391.599	139159.914
235.219	1524.655	152465.475
235.969	1496.286	149628.595
236.719	1475.714	147571.437
237.469	1444.100	144410.021
238.219	1554.148	155414.841
238.969	1461.642	146164.157
239.719	1411.822	141182.165
240.469	1390.349	139034.880

Time (sec)	Stress (Pa)	Viscosity (Pa s)
241.219	1505.751	150575.079
241.969	1353.878	135387.782
242.719	1476.602	147660.167
243.469	1459.855	145985.450
244.219	1305.086	130508.608
244.969	1506.968	150696.818
245.719	1427.666	142766.551
246.469	1424.238	142423.768
247.219	1563.319	156331.887
247.969	1491.129	149112.865
248.719	1412.266	141226.625
249.469	1416.988	141698.825
250.219	1564.268	156426.792
250.969	1349.661	134966.117
251.719	1429.426	142942.629
252.469	1435.323	143532.308
253.219	1411.128	141112.821
253.969	1486.797	148679.704
254.719	1436.724	143672.438
255.469	1330.520	133052.026
256.219	1518.681	151868.061
256.969	1348.986	134898.597
257.719	1258.753	125875.303
258.469	1384.380	138438.017
259.219	1208.487	120848.735
259.969	1499.801	149980.089
260.719	1565.539	156553.888
261.469	1355.675	135567.485
262.219	1150.669	115066.918
262.969	1274.703	127470.296
263.719	1518.407	151840.745
264.469	1506.433	150643.273
265.219	1640.817	164081.698
265.969	1372.527	137252.745
266.719	1419.872	141987.173
267.469	1372.312	137231.154
268.219	1511.720	151171.989
268.969	1337.400	133739.989
269.719	1498.795	149879.454
270.469	1152.919	115291.852
271.219	1242.170	124216.986
271.969	1381.388	138138.817

8.2.5.7 Continued

Time (sec)	Stress (Pa)	Viscosity (Pa s)
272.719	1324.817	132481.747
273.469	1593.064	159306.379
274.219	1251.769	125176.895
274.969	1349.928	134992.755
275.719	1329.451	132945.131
276.469	1252.208	125220.773
277.219	1328.253	132825.304
277.969	1402.110	140211.021
278.719	1517.141	151714.130
279.469	1144.215	114421.534
280.219	1367.845	136784.501
280.969	1389.856	138985.643
281.719	1209.431	120943.057
282.469	1237.406	123740.605
283.219	1225.938	122593.762
283.969	1306.227	130622.727
284.719	1405.370	140537.016
285.469	1457.292	145729.153
286.219	1581.948	158194.840

Time (sec)	Stress (Pa)	Viscosity (Pa s)
286.969	1101.971	110197.068
287.719	1307.538	130753.815
288.469	1286.419	128641.930
289.219	1578.853	157885.277
289.969	1521.024	152102.378
290.719	1602.040	160204.019
291.469	1615.458	161545.838
292.219	1413.147	141314.654
292.969	1317.320	131732.012
293.719	1515.040	151503.999
294.469	1638.600	163859.973
295.219	1725.406	172540.648
295.969	1713.129	171312.878
296.719	1619.845	161984.462
297.469	1314.252	131425.212
298.219	1546.526	154652.554
298.969	1712.009	171200.881
299.719	1754.939	175493.859

Time (sec)	Stress (Pa)	Viscosity (Pa s)
300.469	1625.849	162584.936
301.219	1483.616	148361.642
301.969	1651.803	165180.322
302.719	1653.476	165347.645
303.469	1528.921	152892.064
304.219	1575.710	157571.050
304.969	1501.785	150178.458
305.719	1484.029	148402.891
306.469	1500.755	150075.458
307.219	1720.643	172064.273
307.969	1528.206	152820.606
308.719	1790.273	179027.268
309.469	1535.894	153589.427
310.219	1747.661	174766.054
310.969	1811.554	181155.419
311.719	1700.858	170085.778
312.469	1635.569	163556.871
313.219	1428.186	142818.604

8.2.5.8 – HDB6 – Elongational Viscosity – 170 °C – Strain Rate = 0.003 s^{-1}

Time (sec)	Stress (Pa)	Viscosity (Pa s)
39.938	276.040	92013.265
42.188	283.083	94360.936
44.438	282.710	94236.597
46.688	283.210	94403.273
48.938	285.789	95263.099
51.188	282.252	94083.872
53.438	282.788	94262.539
55.688	282.363	94121.108
57.938	282.984	94327.929
60.188	290.311	96770.438
62.438	283.462	94487.473
64.688	290.300	96766.665
66.938	290.146	96715.240
69.188	288.275	96091.711
71.438	298.501	99500.176
73.688	291.811	97270.422
75.938	295.203	98401.080
78.188	298.079	99359.823
80.438	299.580	99860.000

Time (sec)	Stress (Pa)	Viscosity (Pa s)
82.688	298.728	99576.138
84.938	291.445	97148.277
87.188	306.087	102028.915
89.438	311.091	103696.895
91.688	306.052	102017.287
93.938	307.344	102447.877
96.188	303.479	101159.640
98.438	312.177	104058.979
100.688	309.010	103003.232
102.938	310.278	103425.860
105.188	313.005	104335.123
107.438	306.446	102148.578
109.688	310.633	103544.266
111.938	307.728	102575.897
114.188	317.860	105953.331
116.438	305.304	101767.972
118.688	315.247	105082.266
120.938	307.214	102404.507
123.188	308.620	102873.322

Time (sec)	Stress (Pa)	Viscosity (Pa s)
125.438	313.659	104553.138
127.688	316.292	105430.800
129.938	316.509	105502.845
132.188	321.824	107274.721
134.438	317.467	105822.346
136.688	315.429	105143.121
138.938	305.355	101785.108
141.188	314.229	104743.067
143.438	335.274	111757.940
145.688	327.623	109207.522
147.938	323.801	107933.587
150.188	321.023	107007.508
152.438	322.483	107494.294
154.688	332.238	110746.151
156.938	322.254	107418.038
159.188	329.189	109729.709
161.438	329.710	109903.356
163.688	330.124	110041.413
165.938	336.409	112136.405

8.2.5.8 Continued

Time (sec)	Stress (Pa)	Viscosity (Pa s)
168.188	337.754	112584.734
170.438	338.620	112873.451
172.688	343.804	114601.206
174.938	342.522	114173.980
177.188	343.051	114350.171
179.438	350.319	116773.040
181.688	348.879	116293.086
183.938	347.556	115852.048
186.188	355.764	118587.914
188.438	349.614	116538.146
190.688	353.380	117793.279
192.938	362.133	120711.140
195.188	364.158	121386.006
197.438	368.300	122766.803
199.688	362.845	120948.221
201.938	358.774	119591.316
204.188	368.862	122954.004
206.438	365.941	121980.316

Time (sec)	Stress (Pa)	Viscosity (Pa s)
208.688	375.710	125236.519
210.938	379.534	126511.176
213.188	380.258	126752.509
215.438	378.677	126225.789
217.688	379.049	126349.750
219.938	382.734	127577.980
222.188	377.654	125884.691
224.438	389.062	129687.343
226.688	392.125	130708.369
228.938	404.710	134903.416
231.188	395.527	131842.412
233.438	385.508	128502.586
235.688	406.913	135637.794
237.938	418.745	139581.683
240.188	411.803	137267.537
242.438	400.325	133441.554
244.688	416.636	138878.589
246.938	406.806	135601.853

Time (sec)	Stress (Pa)	Viscosity (Pa s)
249.188	413.083	137694.175
251.438	413.721	137907.079
253.688	411.267	137089.069
255.938	424.401	141466.869
258.188	425.742	141913.856
260.438	433.106	144368.824
262.688	442.090	147363.172
264.938	431.235	143744.995
267.188	432.064	144021.243
269.438	434.451	144817.144
271.688	444.460	148153.302
273.938	449.307	149769.153
276.188	450.904	150301.495
278.438	453.002	151000.816
280.688	460.550	153516.763
282.938	448.329	149443.029

8.2.6 Lupolen 1840 H

8.2.6.1 –Lupolen 1840 H – Elongational Viscosity – 170 ^{o}C – Strain Rate = 10 s^{-1}

Time (sec)	Stress (Pa)	Viscosity (Pa s)
0.038	45737.588	4573.759
0.045	56684.897	5668.490
0.052	67001.917	6700.192
0.060	76770.308	7677.031
0.068	87295.018	8729.502
0.075	95896.378	9589.638
0.083	105498.061	10549.806
0.090	114112.114	11411.211
0.098	124937.273	12493.727
0.105	134088.937	13408.894
0.113	145657.935	14565.794
0.120	153903.197	15390.320
0.128	166032.170	16603.217
0.135	175204.456	17520.446
0.143	188514.209	18851.421
0.150	201196.630	20119.663
0.158	216668.547	21666.855

Time (sec)	Stress (Pa)	Viscosity (Pa s)
0.165	235446.343	23544.634
0.173	252870.035	25287.004
0.180	275023.429	27502.343
0.187	292471.888	29247.189
0.195	318675.481	31867.548
0.202	335189.631	33518.963
0.210	373232.229	37323.223
0.217	403734.299	40373.430
0.225	443268.730	44326.873
0.232	472389.993	47238.999
0.240	516785.936	51678.594
0.248	553668.193	55366.819
0.255	609270.291	60927.029
0.263	655590.496	65559.050
0.270	715102.680	71510.268
0.278	770159.889	77015.989
0.285	832936.502	83293.650

Time (sec)	Stress (Pa)	Viscosity (Pa s)
0.293	897809.234	89780.923
0.300	960394.379	96039.438
0.308	1034332.797	103433.280
0.315	1095950.118	109595.012
0.323	1176180.057	117618.006
0.330	1234760.088	123476.009
0.338	1358244.233	135824.423

8.2.6.2 –Lupolen 1840 H – Elongational Viscosity – 170 °C – Strain Rate = 3 s^{-1}

Time (sec)	Stress (Pa)	Viscosity (Pa s)
0.060	22245.361	7415.120
0.068	25977.906	8659.302
0.075	29258.914	9752.971
0.082	32186.828	10728.943
0.090	33963.176	11321.059
0.097	36197.240	12065.747
0.105	37305.714	12435.238
0.113	39003.934	13001.311
0.120	39867.149	13289.050
0.128	41713.270	13904.423
0.135	42325.393	14108.464
0.143	43899.109	14633.036
0.150	44681.000	14893.667
0.158	46586.460	15528.820
0.165	47418.642	15806.214
0.172	48875.737	16291.912
0.180	49898.744	16632.915
0.187	51003.479	17001.160
0.195	51760.534	17253.511
0.202	52810.831	17603.610
0.210	54338.087	18112.696
0.217	54710.100	18236.700
0.225	56090.407	18696.802
0.232	56566.886	18855.629
0.240	58317.018	19439.006
0.248	58515.459	19505.153
0.255	60516.966	20172.322
0.262	60599.315	20199.772
0.270	62718.412	20906.137
0.278	63030.185	21010.062
0.285	65441.885	21813.962
0.292	65806.369	21935.456
0.300	67858.044	22619.348
0.308	68792.614	22930.871
0.315	70669.022	23556.341
0.322	71868.302	23956.101
0.330	73037.056	24345.685
0.338	75414.136	25138.045
0.345	76056.987	25352.329
0.352	78386.092	26128.697
0.360	78385.171	26128.390
0.367	81368.061	27122.687
0.375	81833.029	27277.676
0.382	85004.690	28334.897
0.390	84762.525	28254.175
0.397	87776.332	29258.777
0.405	87262.972	29087.657
0.412	90442.095	30147.365
0.420	90670.119	30223.373
0.427	93731.269	31243.756
0.435	94587.330	31529.110
0.442	97653.568	32551.189
0.450	99875.678	33291.893
0.457	102148.350	34049.450
0.465	105172.334	35057.445
0.472	105707.828	35235.943
0.480	108916.618	36305.539
0.487	108778.908	36259.636
0.495	112782.771	37594.257
0.502	112689.238	37563.079
0.510	116693.302	38897.767
0.518	116814.249	38938.083
0.525	121813.432	40604.477
0.533	121763.951	40587.984
0.540	126546.799	42182.266
0.547	126650.542	42216.847
0.555	131272.873	43757.624
0.562	132107.372	44035.791
0.570	136931.038	45643.679
0.578	139657.162	46552.387
0.585	143034.386	47678.129
0.593	146699.983	48899.994
0.600	148989.247	49663.082
0.607	154734.980	51578.327
0.615	156064.989	52021.663
0.622	162756.176	54252.059
0.630	163364.131	54454.710
0.638	169307.051	56435.684
0.645	169323.185	56441.062
0.653	176363.946	58787.982
0.660	176490.797	58830.266
0.667	183971.009	61323.670
0.675	184481.732	61493.911
0.682	192705.833	64235.278
0.690	192699.905	64233.302
0.698	200312.250	66770.750
0.705	201855.185	67285.062
0.713	208799.438	69599.813
0.720	213100.106	71033.369
0.727	219026.016	73008.672
0.735	225736.466	75245.489
0.742	228944.977	76314.992
0.750	237439.596	79146.532
0.757	239482.810	79827.603
0.765	248542.102	82847.367
0.773	249800.702	83266.901
0.780	260521.386	86840.462
0.787	261298.478	87099.493
0.795	270439.849	90146.616
0.802	270440.049	90146.683
0.810	280924.217	93641.406
0.817	280676.459	93558.820
0.825	291592.932	97197.644
0.833	292119.922	97373.307
0.840	303505.243	101168.414
0.847	305349.909	101783.303
0.855	316123.874	105374.625
0.862	321011.913	107003.971
0.870	329261.116	109753.705
0.877	335787.394	111929.131
0.885	340720.590	113573.530
0.893	351243.012	117081.004
0.900	350730.644	116910.215
0.908	360825.629	120275.210
0.915	359603.455	119867.818
0.922	369989.172	123329.724
0.930	367695.382	122565.127
0.937	380388.458	126796.153
0.945	378425.124	126141.708
0.953	390952.030	130317.343
0.960	388749.758	129583.253
0.968	404531.898	134843.966
0.975	401149.654	133716.551
0.982	416219.579	138739.860
0.990	415903.463	138634.488
0.997	428823.793	142941.264
1.005	430808.837	143602.946
1.012	440611.907	146870.636
1.020	446578.370	148859.457

8.2.6.2 Continued

Time (sec)	Stress (Pa)	Viscosity (Pa s)
1.027	450691.495	150230.498
1.035	460946.995	153648.998

Time (sec)	Stress (Pa)	Viscosity (Pa s)
1.043	461564.104	153854.701
1.050	476917.155	158972.385

Time (sec)	Stress (Pa)	Viscosity (Pa s)
1.057	474127.594	158042.531

8.2.6.3 –Lupolen 1840 H – Elongational Viscosity – 170 °C – Strain Rate = 1 s^{-1}

Time (sec)	Stress (Pa)	Viscosity (Pa s)
0.131	10043.143	10043.143
0.139	10429.057	10429.057
0.146	11171.294	11171.294
0.154	11447.631	11447.631
0.161	12238.311	12238.311
0.169	12369.520	12369.520
0.176	13123.053	13123.053
0.184	13340.605	13340.605
0.191	14015.659	14015.659
0.199	14354.174	14354.174
0.206	14769.969	14769.969
0.214	15126.159	15126.159
0.221	15371.615	15371.615
0.229	15768.928	15768.928
0.236	15854.247	15854.247
0.244	16301.568	16301.568
0.251	16314.058	16314.058
0.259	16821.158	16821.158
0.266	16758.667	16758.667
0.274	17439.267	17439.267
0.281	17404.703	17404.703
0.289	17958.044	17958.044
0.296	18057.778	18057.778
0.304	18354.346	18354.346
0.311	18644.463	18644.463
0.319	18730.841	18730.841
0.326	19053.981	19053.981
0.334	18977.108	18977.108
0.341	19360.631	19360.631
0.349	19319.821	19319.821
0.356	19878.556	19878.556
0.364	19706.203	19706.203
0.371	20426.388	20426.388
0.379	20273.280	20273.280
0.386	20870.734	20870.734
0.394	20715.737	20715.737

Time (sec)	Stress (Pa)	Viscosity (Pa s)
0.401	20930.615	20930.615
0.409	21028.815	21028.815
0.416	21067.496	21067.496
0.424	21487.450	21487.450
0.431	21366.062	21366.062
0.439	21791.590	21791.590
0.446	21606.578	21606.578
0.454	22141.840	22141.840
0.461	21870.549	21870.549
0.469	22581.322	22581.322
0.476	22222.467	22222.467
0.484	22666.626	22666.626
0.491	22278.712	22278.712
0.499	22489.516	22489.516
0.506	22702.899	22702.899
0.514	22697.855	22697.855
0.521	23200.576	23200.576
0.529	23040.889	23040.889
0.536	23483.768	23483.768
0.544	23162.725	23162.725
0.551	23610.942	23610.942
0.559	23236.178	23236.178
0.566	23874.881	23874.881
0.574	23458.741	23458.741
0.581	24213.026	24213.026
0.589	23979.362	23979.362
0.596	24542.788	24542.788
0.604	24438.211	24438.211
0.611	24561.732	24561.732
0.619	24746.639	24746.639
0.626	24489.048	24489.048
0.634	24971.560	24971.560
0.641	24671.501	24671.501
0.649	25222.655	25222.655
0.656	24967.936	24967.936
0.664	25757.462	25757.462

Time (sec)	Stress (Pa)	Viscosity (Pa s)
0.671	25371.268	25371.268
0.679	26107.853	26107.853
0.686	25636.775	25636.775
0.694	26199.124	26199.124
0.701	26037.616	26037.616
0.709	26327.264	26327.264
0.716	26593.019	26593.019
0.724	26589.427	26589.427
0.731	27296.007	27296.007
0.739	27115.145	27115.145
0.746	27652.927	27652.927
0.754	27188.772	27188.772
0.761	27802.821	27802.821
0.769	27287.086	27287.086
0.776	28036.663	28036.663
0.784	27511.734	27511.734
0.791	28329.836	28329.836
0.799	28118.101	28118.101
0.806	28684.065	28684.065
0.814	29093.468	29093.468
0.821	29267.190	29267.190
0.829	29789.477	29789.477
0.836	29435.934	29435.934
0.844	29810.559	29810.559
0.851	29263.147	29263.147
0.859	29919.059	29919.059
0.866	29360.800	29360.800
0.874	30339.402	30339.402
0.881	29756.431	29756.431
0.889	30749.952	30749.952
0.896	30513.403	30513.403
0.904	31117.282	31117.282
0.911	31318.496	31318.496
0.919	31323.244	31323.244
0.926	31825.356	31825.356
0.934	31343.994	31343.994

8.2.6.3 Continued

Time (sec)	Stress (Pa)	Viscosity (Pa s)
0.941	31900.844	31900.844
0.949	31238.664	31238.664
0.956	32057.227	32057.227
0.964	31486.533	31486.533
0.971	32663.448	32663.448
0.979	32049.695	32049.695
0.986	33209.978	33209.978
0.994	33210.972	33210.972
1.001	34196.134	34196.134
1.009	34706.900	34706.900
1.016	34695.146	34695.146
1.024	35267.845	35267.845
1.031	34812.509	34812.509
1.039	35447.099	35447.099
1.046	34437.860	34437.860
1.054	35037.736	35037.736
1.061	34006.130	34006.130
1.069	35049.199	35049.199
1.076	34268.531	34268.531
1.084	35227.906	35227.906
1.091	35120.294	35120.294
1.099	35542.904	35542.904
1.106	36229.086	36229.086
1.114	36080.066	36080.066
1.121	37160.788	37160.788
1.129	36401.325	36401.325
1.136	37373.179	37373.179
1.144	36537.697	36537.697
1.151	37584.139	37584.139
1.159	36712.209	36712.209
1.166	37918.919	37918.919
1.174	37117.330	37117.330
1.181	38363.450	38363.450
1.189	38435.527	38435.527
1.196	39357.330	39357.330
1.204	39895.089	39895.089
1.211	39752.781	39752.781
1.219	40453.771	40453.771
1.226	39792.404	39792.404
1.234	40884.058	40884.058
1.241	40553.257	40553.257
1.249	42122.183	42122.183

Time (sec)	Stress (Pa)	Viscosity (Pa s)
1.256	41328.024	41328.024
1.264	42665.471	42665.471
1.271	41435.951	41435.951
1.279	42457.876	42457.876
1.286	42062.175	42062.175
1.294	42450.751	42450.751
1.301	42867.197	42867.197
1.309	42458.306	42458.306
1.316	43441.493	43441.493
1.324	42579.670	42579.670
1.331	43798.570	43798.570
1.339	43223.179	43223.179
1.346	44916.084	44916.084
1.354	43902.130	43902.130
1.361	45466.135	45466.135
1.369	44565.626	44565.626
1.376	45710.116	45710.116
1.384	45712.139	45712.139
1.391	45976.977	45976.977
1.399	46830.143	46830.143
1.406	46376.160	46376.160
1.414	47618.983	47618.983
1.421	46885.289	46885.289
1.429	48448.689	48448.689
1.436	47649.728	47649.728
1.444	49432.441	49432.441
1.451	48228.957	48228.957
1.459	49839.344	49839.344
1.466	48929.078	48929.078
1.474	49988.049	49988.049
1.481	50190.858	50190.858
1.489	50305.580	50305.580
1.496	51449.944	51449.944
1.504	50651.167	50651.167
1.511	52137.197	52137.197
1.519	51025.114	51025.114
1.526	52410.281	52410.281
1.534	51093.723	51093.723
1.541	52863.016	52863.016
1.549	51649.020	51649.020
1.556	53349.903	53349.903
1.564	53121.809	53121.809

Time (sec)	Stress (Pa)	Viscosity (Pa s)
1.571	54251.116	54251.116
1.579	54947.430	54947.430
1.586	54845.848	54845.848
1.594	56199.886	56199.886
1.601	55315.396	55315.396
1.609	56620.829	56620.829
1.616	55222.246	55222.246
1.624	56941.612	56941.612
1.631	55483.925	55483.925
1.639	57463.302	57463.302
1.646	56117.819	56117.819
1.654	58159.234	58159.234
1.661	57764.008	57764.008
1.669	58618.530	58618.530
1.676	59377.210	59377.210
1.684	59220.434	59220.434
1.691	60774.784	60774.784
1.699	59538.840	59538.840
1.706	61112.337	61112.337
1.714	59488.087	59488.087
1.721	61520.499	61520.499
1.729	60163.767	60163.767
1.736	62786.135	62786.135
1.744	61336.606	61336.606
1.751	63242.163	63242.163
1.759	62149.081	62149.081
1.766	62925.386	62925.386
1.774	63438.243	63438.243
1.781	63054.221	63054.221
1.789	64870.151	64870.151
1.796	63650.522	63650.522
1.804	65489.993	65489.993
1.811	63765.278	63765.278
1.819	65911.528	65911.528
1.826	64156.460	64156.460
1.834	66494.561	66494.561
1.841	64876.100	64876.100
1.849	67289.836	67289.836
1.856	66868.997	66868.997
1.864	68349.620	68349.620
1.871	69334.879	69334.879
1.879	69382.592	69382.592

8.2.6.3 Continued

Time (sec)	Stress (Pa)	Viscosity (Pa s)
1.886	71078.246	71078.246
1.894	69774.554	69774.554
1.901	71358.861	71358.861
1.909	69717.277	69717.277
1.916	71765.763	71765.763
1.924	69552.748	69552.748
1.931	71623.023	71623.023
1.939	69870.913	69870.913
1.946	72196.687	72196.687
1.954	71856.964	71856.964
1.961	73335.018	73335.018
1.969	74453.577	74453.577
1.976	74062.819	74062.819
1.984	76202.142	76202.142
1.991	74795.890	74795.890
1.999	76770.044	76770.044
2.006	75044.824	75044.824
2.014	77930.283	77930.283
2.021	76078.724	76078.724
2.029	79207.517	79207.517
2.036	77583.196	77583.196
2.044	80608.128	80608.128
2.051	80394.692	80394.692
2.059	81671.795	81671.795
2.066	82755.425	82755.425
2.074	82067.176	82067.176
2.081	84164.178	84164.178
2.089	82668.756	82668.756
2.096	85490.204	85490.204
2.104	83756.447	83756.447
2.111	86782.214	86782.214
2.119	84255.247	84255.247
2.126	87319.282	87319.282
2.134	85193.689	85193.689
2.141	88359.744	88359.744
2.149	87837.653	87837.653
2.156	89865.537	89865.537
2.164	91114.889	91114.889
2.171	90703.014	90703.014
2.179	93190.789	93190.789
2.186	91722.640	91722.640
2.194	94777.892	94777.892

Time (sec)	Stress (Pa)	Viscosity (Pa s)
2.201	92632.345	92632.345
2.209	95788.815	95788.815
2.216	93729.507	93729.507
2.224	97420.649	97420.649
2.231	94409.525	94409.525
2.239	97593.854	97593.854
2.246	95961.891	95961.891
2.254	97937.901	97937.901
2.261	98422.201	98422.201
2.269	99227.345	99227.345
2.276	101579.934	101579.934
2.284	99563.618	99563.618
2.291	102398.696	102398.696
2.299	99821.209	99821.209
2.306	103350.332	103350.332
2.314	100395.620	100395.620
2.321	104174.037	104174.037
2.329	101305.463	101305.463
2.336	105338.359	105338.359
2.344	103383.908	103383.908
2.351	107276.868	107276.868
2.359	107247.803	107247.803
2.366	109179.156	109179.156
2.374	110779.100	110779.100
2.381	109901.590	109901.590
2.389	113172.893	113172.893
2.396	110912.714	110912.714
2.404	114662.789	114662.789
2.411	111927.048	111927.048
2.419	115581.879	115581.879
2.426	112648.322	112648.322
2.434	116878.879	116878.879
2.441	114124.212	114124.212
2.449	118034.971	118034.971
2.456	117386.255	117386.255
2.464	119431.043	119431.043
2.471	121187.827	121187.827
2.479	120451.060	120451.060
2.486	123573.165	123573.165
2.494	121871.843	121871.843
2.501	125683.802	125683.802
2.509	122902.369	122902.369

Time (sec)	Stress (Pa)	Viscosity (Pa s)
2.516	126439.362	126439.362
2.524	122869.094	122869.094
2.531	126693.230	126693.230
2.539	122974.932	122974.932
2.546	127095.384	127095.384
2.554	125764.928	125764.928
2.561	128760.701	128760.701
2.569	130675.557	130675.557
2.576	130966.015	130966.015
2.584	133959.567	133959.567
2.591	130833.895	130833.895
2.599	134565.936	134565.936
2.606	131382.343	131382.343
2.614	135789.146	135789.146
2.621	131737.532	131737.532
2.629	136656.069	136656.069
2.636	133267.687	133267.687
2.644	138814.754	138814.754
2.651	136776.412	136776.412
2.659	139970.074	139970.074
2.666	140928.249	140928.249
2.674	140367.175	140367.175
2.681	143252.111	143252.111
2.689	140353.428	140353.428
2.696	145026.214	145026.214
2.704	141196.988	141196.988
2.711	146424.483	146424.483
2.719	142629.073	142629.073
2.726	149040.148	149040.148
2.734	144784.650	144784.650
2.741	150474.913	150474.913
2.749	146560.837	146560.837
2.756	149533.375	149533.375
2.764	149928.152	149928.152
2.771	150844.566	150844.566
2.779	154844.504	154844.504
2.786	152912.110	152912.110
2.794	157401.784	157401.784
2.801	152833.690	152833.690
2.809	157703.788	157703.788
2.816	153380.729	153380.729
2.824	159531.342	159531.342

8.2.6.3 Continued

Time (sec)	Stress (Pa)	Viscosity (Pa s)
2.831	154694.776	154694.776
2.839	160253.028	160253.028
2.846	156010.080	156010.080
2.854	161644.604	161644.604
2.861	159979.513	159979.513
2.869	163389.128	163389.128
2.876	165322.833	165322.833
2.884	164915.494	164915.494
2.891	169246.386	169246.386
2.899	166092.683	166092.683
2.906	171322.047	171322.047
2.914	166296.082	166296.082
2.921	171706.737	171706.737
2.929	166836.684	166836.684
2.936	172814.900	172814.900
2.944	169358.081	169358.081
2.951	177317.162	177317.162
2.959	173190.019	173190.019
2.966	178077.880	178077.880
2.974	177740.977	177740.977
2.981	179598.771	179598.771
2.989	183697.044	183697.044
2.996	183102.438	183102.438
3.004	187406.590	187406.590
3.011	182390.492	182390.492
3.019	186461.580	186461.580
3.026	182021.920	182021.920

Time (sec)	Stress (Pa)	Viscosity (Pa s)
3.034	189141.622	189141.622
3.041	181735.329	181735.329
3.049	187691.849	187691.849
3.056	181680.782	181680.782
3.064	187426.166	187426.166
3.071	185993.681	185993.681
3.079	189541.427	189541.427
3.086	191691.074	191691.074
3.094	189351.304	189351.304
3.101	193416.059	193416.059
3.109	189409.599	189409.599
3.116	197079.371	197079.371
3.124	190776.064	190776.064
3.131	196434.651	196434.651
3.139	188638.786	188638.786
3.146	196343.153	196343.153
3.154	189792.435	189792.435
3.161	196664.760	196664.760
3.169	194383.673	194383.673
3.176	196792.099	196792.099
3.184	200343.117	200343.117
3.191	198488.731	198488.731
3.199	205309.013	205309.013
3.206	198720.938	198720.938
3.214	205463.320	205463.320
3.221	198420.605	198420.605
3.229	206571.379	206571.379

Time (sec)	Stress (Pa)	Viscosity (Pa s)
3.236	199745.100	199745.100
3.244	210704.389	210704.389
3.251	205144.256	205144.256
3.259	214401.928	214401.928
3.266	211009.154	211009.154
3.274	213639.583	213639.583
3.281	217004.513	217004.513
3.289	211920.211	211920.211
3.296	215652.190	215652.190
3.304	207591.441	207591.441
3.311	215478.692	215478.692
3.319	209271.987	209271.987
3.326	219284.264	219284.264
3.334	210955.944	210955.944
3.341	220369.063	220369.063
3.349	211892.416	211892.416
3.356	217268.710	217268.710
3.364	217380.509	217380.509
3.371	217675.030	217675.030
3.379	222986.117	222986.117
3.386	216289.238	216289.238
3.394	224396.272	224396.272
3.401	215011.102	215011.102
3.409	223601.886	223601.886
3.416	212841.921	212841.921
3.424	221114.104	221114.104
3.431	210965.627	210965.627

8.2.6.4 –Lupolen 1840 H – Elongational Viscosity – 170 °C – Strain Rate = 0.3 s^{-1}

Time (sec)	Stress (Pa)	Viscosity (Pa s)
0.343	3702.238	12340.794
0.366	4306.584	14355.281
0.388	4690.345	15634.482
0.411	5066.842	16889.474
0.433	5521.803	18406.009
0.456	5709.238	19030.793
0.478	6192.848	20642.827
0.501	6188.977	20629.924
0.523	6616.798	22055.994
0.546	6670.126	22233.753
0.568	7115.022	23716.739
0.591	7293.822	24312.741
0.613	7470.375	24901.251
0.636	7787.733	25959.112
0.658	7772.837	25909.457
0.681	8137.778	27125.925
0.703	8088.765	26962.551
0.726	8442.255	28140.849
0.748	8384.981	27949.936
0.771	8685.888	28952.960
0.793	8774.308	29247.694
0.816	8959.621	29865.402
0.838	9269.273	30897.578
0.861	9106.915	30356.383
0.883	9507.589	31691.963
0.906	9393.074	31310.247
0.928	9693.523	32311.744
0.951	9620.950	32069.834
0.973	9892.729	32975.762
0.996	9848.414	32828.047
1.018	9915.116	33050.385
1.041	10080.134	33600.447
1.063	9817.871	32726.236
1.086	10142.818	33809.393
1.108	9993.762	33312.540
1.131	10330.793	34435.975
1.153	10284.214	34280.712
1.176	10461.231	34870.769
1.198	10588.560	35295.199
1.221	10551.609	35172.031
1.243	10888.626	36295.420
1.266	10595.287	35317.622
1.288	10931.210	36437.368
1.311	10691.424	35638.081
1.333	10967.388	36557.959
1.356	10879.828	36266.094
1.378	11094.594	36981.980
1.401	11246.087	37486.958
1.423	11124.377	37081.257
1.446	11388.125	37960.416
1.468	11047.279	36824.263
1.491	11486.731	38289.104
1.513	11304.678	37682.260
1.536	11619.939	38733.131
1.558	11481.221	38270.736
1.581	11610.713	38702.377
1.603	11750.466	39168.220
1.626	11500.108	38333.692
1.648	11889.524	39631.748
1.671	11499.502	38331.674
1.693	11929.002	39763.341
1.716	11874.756	39582.519
1.738	12214.915	40716.383
1.761	12206.456	40688.188
1.783	12270.618	40902.060
1.806	12452.364	41507.879
1.828	12288.624	40962.080
1.851	12784.173	42613.911
1.873	12320.411	41068.035
1.896	12615.814	42052.714
1.918	12213.719	40712.397
1.941	12431.109	41437.030
1.963	12418.403	41394.678
1.986	12642.387	42141.290
2.008	13078.471	43594.902
2.031	12771.522	42571.741
2.053	13282.787	44275.957
2.076	12734.449	42448.165
2.098	13049.428	43498.093
2.121	12860.151	42867.170
2.143	13120.973	43736.577
2.166	13151.540	43838.467
2.188	13244.202	44147.338
2.211	13396.395	44654.649
2.233	13000.060	43333.534
2.256	13539.908	45133.027
2.278	13109.507	43698.358
2.301	13738.131	45793.770
2.323	13409.926	44699.755
2.346	13743.569	45811.895
2.368	13847.571	46158.570
2.391	14106.709	47022.365
2.413	14120.937	47069.789
2.436	13624.639	45415.463
2.458	14234.104	47447.014
2.481	13896.485	46321.618
2.503	14564.481	48548.271
2.526	14024.149	46747.163
2.548	14176.995	47256.649
2.571	14024.842	46749.472
2.593	14326.767	47755.890
2.616	14745.911	49153.035
2.638	14497.809	48326.029
2.661	15221.243	50737.478
2.683	14602.517	48675.058
2.706	15080.922	50269.739
2.728	14687.284	48957.613
2.751	15048.448	50161.494

8.2.6.4 Continued

Time (sec)	Stress (Pa)	Viscosity (Pa s)
2.773	15051.728	50172.426
2.796	15348.491	51161.635
2.818	15999.538	53331.794
2.841	15611.795	52039.316
2.863	15878.332	52927.772
2.886	14967.422	49891.406
2.908	15480.453	51601.509
2.931	15140.514	50468.379
2.953	15799.751	52665.837
2.976	15924.409	53081.364
2.998	15745.556	52485.185
3.021	15936.488	53121.625
3.043	15351.888	51172.959
3.066	16103.641	53678.802
3.088	15411.192	51370.639
3.111	15953.292	53177.640
3.133	15845.483	52818.276
3.156	16308.697	54362.322
3.178	16419.153	54730.509
3.201	16118.131	53727.105
3.223	16618.697	55395.658
3.246	15957.647	53192.158
3.268	17011.843	56706.144
3.291	16564.246	55214.155
3.313	16763.720	55879.066
3.336	16433.397	54777.990
3.358	16456.224	54854.080
3.381	16864.186	56213.955
3.403	16401.134	54670.447
3.426	17303.957	57679.855
3.448	16507.890	55026.299
3.471	17325.722	57752.406
3.493	16977.730	56592.432
3.516	17370.665	57902.218
3.538	17395.249	57984.163
3.561	17445.183	58150.610
3.583	18114.881	60382.935
3.606	17327.928	57759.760
3.628	17950.996	59836.652
3.651	17199.027	57330.091
3.673	17952.367	59841.223
3.696	17655.472	58851.573
3.718	18092.122	60307.075
3.741	18374.435	61248.118
3.763	18437.926	61459.754
3.786	19199.356	63997.855
3.808	18497.675	61658.917
3.831	19669.383	65564.609
3.853	18509.716	61699.052
3.876	18789.902	62633.006
3.898	18391.710	61305.700
3.921	18789.657	62632.189
3.943	18471.892	61572.973
3.966	18007.899	60026.330
3.988	18895.048	62983.494
4.011	18031.611	60105.370
4.033	19356.042	64520.140
4.056	19003.179	63343.930
4.078	19588.972	65296.574
4.101	19372.011	64573.370
4.123	19571.125	65237.083
4.146	19709.754	65699.180
4.168	18809.983	62699.943
4.191	19971.096	66570.319
4.213	19110.213	63700.709
4.236	20210.924	67369.745
4.258	19518.061	65060.204
4.281	19909.329	66364.429
4.303	19985.236	66617.454
4.326	19838.353	66127.844
4.348	20501.463	68338.210
4.371	19669.121	65563.735
4.393	20820.202	69400.674
4.416	19686.856	65622.853
4.438	20627.969	68759.898
4.461	20234.559	67448.531
4.483	20688.095	68960.315
4.506	20772.777	69242.589
4.528	20655.726	68852.420
4.551	21504.602	71682.007
4.573	20512.001	68373.336
4.596	21868.179	72893.931
4.618	20898.461	69661.535
4.641	21789.975	72633.250
4.663	21335.109	71117.030
4.686	22510.435	75034.784
4.708	23097.263	76990.877
4.731	23112.906	77043.020
4.753	23247.113	77490.378
4.776	21676.513	72255.042
4.798	22950.512	76501.708
4.821	21902.762	73009.208
4.843	22702.430	75674.765
4.866	21768.169	72560.564
4.888	22319.965	74399.883
4.911	22877.760	76259.200
4.933	22772.937	75909.789
4.956	23997.026	79990.085
4.978	22268.174	74227.247
5.001	23535.782	78452.608
5.023	23330.946	77769.819
5.046	25273.245	84244.149
5.068	25042.660	83475.532
5.091	24336.750	81122.500
5.113	23936.457	79788.189
5.136	22474.536	74915.119
5.158	23629.802	78766.008
5.181	22534.404	75114.681
5.203	24189.881	80632.938
5.226	24027.056	80090.186
5.248	24475.832	81586.107
5.271	24170.505	80568.350
5.293	24246.853	80822.845
5.316	25161.585	83871.951
5.338	23357.997	77859.990
5.361	24886.138	82953.792
5.383	24081.250	80270.834
5.406	25659.516	85531.719
5.428	25395.220	84650.733
5.451	25879.606	86265.352
5.473	26064.500	86881.665
5.496	25420.401	84734.672
5.518	26399.837	87999.456
5.541	24792.124	82640.414
5.563	26730.176	89100.585
5.586	25972.177	86573.923

8.2.6.4 Continued

Time (sec)	Stress (Pa)	Viscosity (Pa s)
5.608	27276.670	90922.234
5.631	26296.116	87653.721
5.653	26533.322	88444.408
5.676	26811.005	89370.016
5.698	25863.374	86211.246
5.721	27494.658	91648.860
5.743	26465.771	88219.236
5.766	28464.891	94882.971
5.788	27772.355	92574.515
5.811	29887.058	99623.525
5.833	28118.947	93729.822
5.856	27353.300	91177.667
5.878	27622.870	92076.234
5.901	28609.915	95366.385
5.923	31792.143	105973.810
5.946	30940.474	103134.912
5.968	32417.831	108059.436
5.991	29608.943	98696.476
6.013	29276.043	97586.811
6.036	26525.249	88417.498
6.058	27201.766	90672.554
6.081	28919.267	96397.557
6.103	28432.482	94774.939
6.126	30618.765	102062.549
6.148	28988.616	96628.718
6.171	30486.833	101622.776
6.193	28705.147	95683.823
6.216	29860.090	99533.632
6.238	29503.028	98343.427
6.261	29972.214	99907.381
6.283	30612.286	102040.954
6.306	29107.396	97024.653
6.328	31255.712	104185.707
6.351	29334.465	97781.551
6.373	31716.836	105722.787
6.396	30746.991	102489.970
6.418	31680.759	105602.530
6.441	30916.874	103056.248
6.463	31139.208	103797.359
6.486	32429.231	108097.435
6.508	31120.302	103734.340
6.531	32640.827	108802.755

Time (sec)	Stress (Pa)	Viscosity (Pa s)
6.553	30377.944	101259.814
6.576	32826.987	109423.289
6.598	31945.838	106486.127
6.621	34056.891	113522.969
6.643	33590.112	111967.040
6.666	33274.806	110916.021
6.688	33154.042	110513.473
6.711	31820.698	106068.992
6.733	34104.905	113683.018
6.756	31940.699	106468.995
6.778	34704.824	115682.747
6.801	33753.801	112512.670
6.823	35440.272	118134.241
6.846	34631.800	115439.335
6.868	34697.872	115659.574
6.891	35343.956	117813.188
6.913	33871.234	112904.114
6.936	36053.284	120177.614
6.958	33926.236	113087.454
6.981	36151.205	120504.015
7.003	34094.636	113648.786
7.026	35018.578	116728.592
7.048	34870.145	116233.816
7.071	35958.568	119861.892
7.093	37346.144	124487.147
7.116	35310.332	117701.107
7.138	38037.367	126791.222
7.161	35775.240	119250.800
7.183	38059.275	126864.251
7.206	36464.088	121546.958
7.228	38027.825	126759.417
7.251	38000.960	126669.868
7.273	39689.099	132296.996
7.296	40293.101	134310.338
7.318	36652.198	122173.992
7.341	37987.043	126623.477
7.363	35828.027	119426.758
7.386	39243.284	130810.947
7.408	38614.527	128715.090
7.431	40493.075	134976.916
7.453	39407.782	131359.274
7.476	38897.994	129659.980

Time (sec)	Stress (Pa)	Viscosity (Pa s)
7.498	40708.733	135695.776
7.521	38279.785	127599.283
7.543	41452.545	138175.150
7.566	38158.951	127196.504
7.588	40268.411	134228.035
7.611	39837.609	132792.031
7.633	42444.264	141480.878
7.656	42090.492	140301.640
7.678	42645.195	142150.651
7.701	44595.882	148652.939
7.723	41187.302	137291.008
7.746	43443.744	144812.479
7.768	40161.602	133872.006
7.791	42753.143	142510.476
7.813	41622.839	138742.798
7.836	42976.855	143256.184
7.858	42681.390	142271.302
7.881	41406.243	138020.809
7.903	44009.612	146698.708
7.926	42568.738	141895.792
7.948	47098.962	156996.540
7.971	44420.488	148068.293
7.993	46950.033	156500.110
8.016	44110.952	147036.506
8.038	44870.049	149566.829
8.061	45012.905	150043.017
8.083	45742.291	152474.305
8.106	49092.459	163641.531
8.128	47082.821	156942.736
8.151	49076.427	163588.092
8.173	43246.929	144156.428
8.196	44651.006	148836.688
8.218	44066.710	146889.035
8.241	47402.734	158009.115
8.263	46527.179	155090.597
8.286	45204.896	150682.986
8.308	48242.652	160808.839
8.331	45688.645	152295.483
8.353	49910.282	166367.607
8.376	46066.415	153554.717
8.398	49229.670	164098.899
8.421	47386.884	157956.280

8.2.6.4 Continued

Time (sec)	Stress (Pa)	Viscosity (Pa s)
8.443	48815.026	162716.753
8.466	49122.042	163740.141
8.488	49066.216	163554.053
8.511	51748.268	172494.228
8.533	48503.530	161678.433
8.556	52451.608	174838.695
8.578	48434.813	161449.375
8.601	53353.869	177846.232
8.623	52977.378	176591.260
8.646	55470.955	184903.185
8.668	52368.356	174561.188
8.691	50728.556	169095.186
8.713	51831.668	172772.228
8.736	49989.527	166631.755
8.758	54397.146	181323.819
8.781	49594.076	165313.585
8.803	53601.952	178673.172
8.826	51230.822	170769.406
8.848	54229.287	180764.289
8.871	53826.914	179423.048
8.893	54191.477	180638.255
8.916	56509.553	188365.178
8.938	54115.448	180384.828
8.961	59069.976	196899.920
8.983	54239.730	180799.100
9.006	58429.892	194766.307
9.028	54897.231	182990.770
9.051	56758.887	189196.290
9.073	56106.427	187021.424
9.096	55882.725	186275.750
9.118	58527.765	195092.551
9.141	55306.255	184354.182
9.163	60360.271	201200.902
9.186	55282.672	184275.573
9.208	60554.499	201848.330
9.231	58305.941	194353.137
9.253	60688.362	202294.540
9.276	60301.122	201003.740
9.298	59645.691	198818.969
9.321	63074.436	210248.121
9.343	60071.643	200238.809
9.366	65271.906	217573.020

Time (sec)	Stress (Pa)	Viscosity (Pa s)
9.388	60288.541	200961.803
9.411	65405.206	218017.352
9.433	61685.042	205616.805
9.456	63387.214	211290.713
9.478	62462.308	208207.694
9.501	62823.814	209412.712
9.523	65246.287	217487.623
9.546	61916.696	206388.988
9.568	66861.577	222871.925
9.591	61182.451	203941.503
9.613	66679.387	222264.625
9.636	63821.225	212737.418
9.658	66902.749	223009.163
9.681	67895.514	226318.382
9.703	65835.078	219450.261
9.726	68338.194	227793.980
9.748	63474.757	211582.525
9.771	69199.256	230664.187
9.793	63914.726	213049.088
9.816	69798.457	232661.523
9.838	68488.032	228293.440
9.861	70471.824	234906.080
9.883	69366.852	231222.839
9.906	67263.299	224210.995
9.928	71771.346	239237.821
9.951	67556.587	225188.624
9.973	74033.100	246776.999
9.996	68114.513	227048.377
10.018	75329.050	251096.835
10.041	75476.304	251587.680
10.063	77711.345	259037.818
10.086	76371.239	254570.797
10.108	72852.009	242840.030
10.131	73964.207	246547.356
10.153	67225.552	224085.172
10.176	74760.815	249202.716
10.198	69571.372	231904.574
10.221	76507.825	255026.084
10.243	76889.952	256299.839
10.266	78171.794	260572.647
10.288	77974.572	259915.242
10.311	76664.066	255546.886

Time (sec)	Stress (Pa)	Viscosity (Pa s)
10.333	82119.082	273730.272
10.356	76624.351	255414.503
10.378	85736.022	285786.739
10.401	80935.150	269783.834
10.423	86574.149	288580.497
10.446	80141.947	267139.824
10.468	74613.434	248711.448
10.491	71884.819	239616.064
10.513	72287.015	240956.717
10.536	80812.539	269375.130
10.558	74525.580	248418.599
10.581	83539.412	278464.708
10.603	79422.510	264741.701
10.626	84219.718	280732.394
10.648	80962.858	269876.192
10.671	81246.262	270820.873
10.693	81330.745	271102.483
10.716	79783.626	265945.420
10.738	86188.367	287294.557
10.761	79736.374	265787.912
10.783	87427.970	291426.568
10.806	79949.000	266496.668
10.828	86677.514	288925.045
10.851	83988.273	279960.911
10.873	87528.318	291761.059
10.896	86660.719	288869.062
10.918	85113.903	283713.011
10.941	88674.228	295580.759
10.963	81125.933	270419.778
10.986	89008.777	296695.923
11.008	80570.677	268568.924
11.031	89873.936	299579.788
11.053	86779.400	289264.668
11.076	89628.430	298761.432
11.098	90186.545	300621.815
11.121	90267.842	300892.806
11.143	96740.292	322467.639
11.166	89067.004	296890.012
11.188	93733.890	312446.299
11.211	83417.308	278057.695
11.233	91697.804	305659.346
11.256	89694.867	298982.889

8.2.6.4 Continued

Time (sec)	Stress (Pa)	Viscosity (Pa s)
11.278	91280.313	304267.711
11.301	93812.452	312708.173
11.323	90967.016	303223.386
11.346	97514.883	325049.611
11.368	89651.813	298839.375
11.391	103540.664	345135.546
11.413	97308.256	324360.852
11.436	99572.887	331909.624
11.458	93304.530	311015.100
11.481	93543.761	311812.536
11.503	96041.912	320139.708
11.526	92053.219	306844.065
11.548	100728.154	335760.512
11.571	90998.175	303327.249
11.593	100907.036	336356.786
11.616	95245.731	317485.772
11.638	100629.905	335433.016
11.661	97932.171	326440.569
11.683	100326.598	334421.993
11.706	106322.793	354409.309
11.728	101629.233	338764.109
11.751	111968.593	373228.642
11.773	96727.643	322425.475
11.796	103493.344	344977.814
11.818	94810.729	316035.764
11.841	100051.284	333504.281
11.863	102775.383	342584.608
11.886	104327.363	347757.876
11.908	111098.899	370329.662
11.931	101794.368	339314.561
11.953	112512.080	375040.265
11.976	99495.538	331651.793
11.998	106858.995	356196.650
12.021	102729.170	342430.566
12.043	107647.536	358825.119
12.066	110150.671	367168.904
12.088	105810.099	352700.331
12.111	113953.500	379845.000
12.133	102396.998	341323.326
12.156	112545.818	375152.726
12.178	98806.033	329353.442
12.201	102680.475	342268.252

Time (sec)	Stress (Pa)	Viscosity (Pa s)
12.223	103446.623	344822.078
12.246	106513.745	355045.817
12.268	113885.362	379617.874
12.291	105669.912	352233.040
12.313	116260.952	387536.505
12.336	102897.407	342991.356
12.358	113786.862	379289.540

Time (sec)	Stress (Pa)	Viscosity (Pa s)

8.2.6.5 –Lupolen 1840 H – Elongational Viscosity – 170 °C – Strain Rate = 0.1 s^{-1}

Time (sec)	Stress (Pa)	Viscosity (Pa s)
0.159	1288.194	12881.938
0.197	1796.030	17960.298
0.234	1932.159	19321.591
0.272	2027.794	20277.941
0.309	2116.922	21169.217
0.347	2234.238	22342.376
0.384	2376.071	23760.706
0.422	2505.450	25054.497
0.459	2603.712	26037.118
0.497	2685.052	26850.521
0.534	2772.463	27724.628
0.572	2868.088	28680.880
0.609	2957.170	29571.697
0.647	3035.701	30357.014
0.684	3114.501	31145.006
0.722	3195.549	31955.491
0.759	3261.722	32617.222
0.797	3296.620	32966.198
0.834	3306.693	33066.933
0.872	3314.571	33145.712
0.909	3332.826	33328.264
0.947	3354.044	33540.436
0.984	3367.608	33676.083
1.022	3375.477	33754.773
1.059	3386.348	33863.483
1.097	3402.571	34025.710
1.134	3420.149	34201.486
1.172	3439.408	34394.083
1.209	3468.578	34685.783
1.247	3512.993	35129.935
1.284	3565.011	35650.109
1.322	3609.917	36099.174
1.359	3639.313	36393.131
1.397	3653.655	36536.551
1.434	3655.043	36550.434
1.472	3638.674	36386.737
1.509	3635.549	36355.495
1.547	3626.352	36263.519
1.584	3614.944	36149.436
1.622	3606.066	36060.658
1.659	3601.837	36018.374
1.697	3600.239	36002.394
1.734	3597.354	35973.544
1.772	3591.469	35914.687
1.809	3584.944	35849.438
1.847	3581.831	35818.307
1.884	3583.654	35836.538
1.922	3587.719	35877.191
1.959	3589.513	35895.130
1.997	3586.571	35865.712
2.034	3580.219	35802.185
2.072	3574.209	35742.089
2.109	3571.986	35719.857
2.147	3574.528	35745.282
2.184	3579.679	35796.788
2.222	3583.280	35832.801
2.259	3581.971	35819.711
2.297	3576.081	35760.810
2.334	3569.926	35699.263
2.372	3568.446	35684.464
2.409	3572.838	35728.383
2.447	3579.483	35794.825
2.484	3583.416	35834.165
2.522	3582.880	35828.803
2.559	3580.488	35804.876
2.597	3580.376	35803.759
2.634	3584.659	35846.590
2.672	3592.342	35923.424
2.709	3600.673	36006.728
2.747	3606.958	36069.577
2.784	3609.706	36097.056
2.822	3609.170	36091.697
2.859	3607.237	36072.370
2.897	3606.276	36062.760
2.934	3607.547	36075.467
2.972	3610.815	36108.148
3.009	3615.132	36151.316
3.047	3625.469	36254.687
3.084	3638.775	36387.754
3.122	3655.823	36558.232
3.159	3675.433	36754.332
3.197	3695.359	36953.594
3.234	3714.229	37142.294
3.272	3732.446	37324.461
3.309	3751.083	37510.829
3.347	3770.155	37701.555
3.384	3788.464	37884.637
3.422	3805.423	38054.235
3.459	3822.937	38229.370
3.497	3845.029	38450.291
3.534	3875.114	38751.144
3.572	3913.198	39131.984
3.609	3955.618	39556.181
3.647	3997.675	39976.748
3.684	4036.786	40367.859
3.722	4073.148	40731.476
3.759	4107.197	41071.973
3.797	4136.473	41364.727
3.834	4155.547	41555.473
3.872	4160.083	41600.830
3.909	4151.701	41517.012
3.947	4138.662	41386.617
3.984	4130.690	41306.902
4.022	4132.157	41321.572
4.059	4140.191	41401.909
4.097	4149.920	41499.201
4.134	4161.643	41616.429
4.172	4182.147	41821.469
4.209	4218.179	42181.786
4.247	4268.546	42685.456
4.284	4323.301	43233.010
4.322	4371.364	43713.645
4.359	4409.178	44091.775
4.397	4442.050	44420.496
4.434	4477.498	44774.983
4.472	4517.716	45177.159
4.509	4558.280	45582.804
4.547	4593.290	45932.898
4.584	4621.135	46211.352
4.622	4645.689	46456.889
4.659	4672.809	46728.092
4.697	4705.967	47059.672
4.734	4744.474	47444.741
4.772	4784.971	47849.715
4.809	4824.440	48244.399
4.847	4862.338	48623.382
4.884	4900.340	49003.400
4.922	4940.052	49400.521
4.959	4980.902	49809.021

8.2.6.5 Continued

Time (sec)	Stress (Pa)	Viscosity (Pa s)
4.997	5020.367	50203.667
5.034	5056.341	50563.413
5.072	5088.994	50889.939
5.109	5119.908	51199.077
5.147	5149.447	51494.475
5.184	5175.499	51754.995
5.222	5195.206	51952.063
5.259	5207.949	52079.491
5.297	5216.543	52165.429
5.334	5225.722	52257.221
5.372	5239.570	52395.700
5.409	5259.857	52598.567
5.447	5285.865	52858.654
5.484	5315.365	53153.649
5.522	5346.366	53463.659
5.559	5378.867	53788.675
5.597	5415.045	54150.450
5.634	5457.089	54570.894
5.672	5504.328	55043.280
5.709	5552.607	55526.071
5.747	5596.855	55968.547
5.784	5634.331	56343.313
5.822	5665.511	56655.105
5.859	5692.384	56923.845
5.897	5716.503	57165.032
5.934	5738.292	57382.924
5.972	5757.071	57570.714
6.009	5771.117	57711.172
6.047	5778.501	57785.011
6.084	5779.132	57791.316
6.122	5776.071	57760.714
6.159	5773.726	57737.256
6.197	5773.886	57738.861
6.234	5773.964	57739.643
6.272	5770.050	57700.500
6.309	5761.898	57618.978
6.347	5754.227	57542.274
6.384	5752.641	57526.414
6.422	5758.573	57585.733
6.459	5768.890	57688.905
6.497	5780.503	57805.028
6.534	5794.549	57945.494
6.572	5814.978	58149.778
6.609	5842.654	58426.539
6.647	5871.746	58717.455
6.684	5893.463	58934.633
6.722	5904.128	59041.276
6.759	5908.564	59085.637
6.797	5913.675	59136.746
6.834	5918.112	59181.119
6.872	5910.045	59100.447
6.909	5877.638	58776.379
6.947	5822.528	58225.283
6.984	5761.526	57615.261
7.022	5713.296	57132.961
7.059	5683.096	56830.963
7.097	5661.279	56612.792
7.134	5636.557	56365.568
7.172	5609.276	56092.757
7.209	5590.853	55908.528
7.247	5591.503	55915.030
7.284	5610.773	56107.728
7.322	5640.537	56405.369
7.359	5674.889	56748.889
7.397	5714.283	57142.827
7.434	5759.908	57599.081
7.472	5807.053	58070.529
7.509	5847.214	58472.136
7.547	5877.148	58771.482
7.584	5903.613	59036.130
7.622	5936.881	59368.810
7.659	5979.215	59792.149
7.697	6020.868	60208.676
7.734	6048.571	60485.711
7.772	6058.379	60583.786
7.809	6060.120	60601.201
7.847	6069.055	60690.554
7.884	6092.721	60927.210
7.922	6125.292	61252.924
7.959	6154.214	61542.143
7.997	6172.073	61720.725
8.034	6182.226	61822.258
8.072	6193.803	61938.032
8.109	6212.546	62125.457
8.147	6237.062	62370.621
8.184	6262.550	62625.496
8.222	6285.631	62856.312
8.259	6304.716	63047.159
8.297	6317.904	63179.040
8.334	6323.787	63237.874
8.372	6324.888	63248.880
8.409	6327.758	63277.579
8.447	6337.268	63372.685
8.484	6351.180	63511.802
8.522	6362.326	63623.259
8.559	6366.689	63666.889
8.597	6367.973	63679.734
8.634	6373.461	63734.606
8.672	6386.627	63866.272
8.709	6405.306	64053.058
8.747	6426.299	64262.988
8.784	6449.306	64493.065
8.822	6475.116	64751.158
8.859	6501.396	65013.963
8.897	6522.677	65226.775
8.934	6535.234	65352.336
8.972	6540.889	65408.887
9.009	6544.817	65448.170
9.047	6549.615	65496.149
9.084	6552.580	65525.802
9.122	6549.806	65498.057
9.159	6543.109	65431.087
9.197	6542.147	65421.472
9.234	6558.358	65583.581
9.272	6595.832	65958.320
9.309	6648.206	66482.060
9.347	6705.274	67052.735
9.384	6762.906	67629.055
9.422	6825.545	68255.452
9.459	6897.820	68978.200
9.497	6973.781	69737.811
9.534	7036.007	70360.071
9.572	7067.209	70672.087
9.609	7063.594	70635.940

8.2.6.5 Continued

Time (sec)	Stress (Pa)	Viscosity (Pa s)
9.722	6967.462	69674.616
9.759	6929.328	69293.281
9.797	6884.543	68845.426
9.834	6837.310	68373.099
9.872	6796.895	67968.955
9.909	6768.642	67686.416
9.947	6750.369	67503.688
9.984	6738.285	67382.848
10.022	6733.810	67338.103
10.059	6741.733	67417.325
10.097	6762.344	67623.445
10.134	6788.916	67889.161
10.172	6814.881	68148.813
10.209	6841.748	68417.484
10.247	6877.154	68771.543
10.284	6925.107	69251.071
10.322	6980.276	69802.762
10.359	7032.471	70324.712
10.397	7074.660	70746.599
10.434	7104.872	71048.717
10.472	7121.658	71216.578
10.509	7120.779	71207.794
10.547	7097.734	70977.340
10.584	7052.759	70527.591
10.622	6992.640	69926.398
10.659	6928.160	69281.600
10.697	6869.910	68699.103
10.734	6824.908	68249.079
10.772	6795.171	67951.706
10.809	6779.139	67791.388
10.847	6775.733	67757.334
10.884	6787.833	67878.326
10.922	6820.912	68209.120
10.959	6876.756	68767.561
10.997	6947.828	69478.283
11.034	7018.535	70185.353
11.072	7073.594	70735.940
11.109	7106.996	71069.959
11.147	7124.286	71242.860
11.184	7136.515	71365.148
11.222	7151.188	71511.882
11.259	7167.797	71677.974
11.297	7181.323	71813.230
11.334	7190.073	71900.734
11.372	7200.328	72003.277
11.409	7223.264	72232.637
11.447	7266.822	72668.222
11.484	7329.823	73298.227
11.522	7403.459	74034.586
11.559	7478.321	74783.209
11.597	7550.144	75501.442
11.634	7619.046	76190.457
11.672	7683.682	76836.823
11.709	7737.267	77372.670
11.747	7770.979	77709.792
11.784	7782.654	77826.544
11.822	7781.768	77817.685
11.859	7783.629	77836.286
11.897	7796.272	77962.722
11.934	7812.630	78126.304
11.972	7817.402	78174.024
12.009	7803.690	78036.900
12.047	7783.009	77830.093
12.084	7777.030	77770.302
12.122	7797.256	77972.557
12.159	7832.128	78321.278
12.197	7855.141	78551.413
12.234	7847.422	78474.223
12.272	7813.937	78139.371
12.309	7778.373	77783.728
12.347	7762.059	77620.591
12.384	7766.886	77668.864
12.422	7777.475	77774.751
12.459	7779.338	77793.376
12.497	7775.188	77751.877
12.534	7783.932	77839.319
12.572	7823.168	78231.682
12.609	7891.533	78915.330
12.647	7968.161	79681.608
12.684	8031.059	80310.587
12.722	8077.498	80774.980
12.759	8125.690	81256.897
12.797	8194.485	81944.851
12.834	8281.351	82813.510
12.872	8362.933	83629.333
12.909	8419.690	84196.904
12.947	8458.958	84589.580
12.984	8510.450	85104.504
13.022	8597.130	85971.303
13.059	8710.619	87106.192
13.097	8814.509	88145.087
13.134	8869.236	88692.355
13.172	8853.536	88535.362
13.209	8767.867	87678.675
13.247	8626.149	86261.489
13.284	8447.620	84476.205
13.322	8250.781	82507.807
13.359	8046.635	80466.346
13.397	7835.856	78358.562
13.434	7617.794	76177.945
13.472	7406.973	74069.733
13.509	7238.682	72386.822
13.547	7151.330	71513.301
13.584	7157.385	71573.854
13.622	7230.191	72301.910
13.659	7321.991	73219.912
13.697	7399.858	73998.580
13.734	7468.756	74687.561
13.772	7560.746	75607.458
13.809	7698.017	76980.174
13.847	7861.774	78617.739
13.884	7997.556	79975.564
13.922	8057.412	80574.120
13.959	8043.304	80433.037
13.997	8009.375	80093.745
14.034	8016.505	80165.051
14.072	8080.150	80801.500
14.109	8161.902	81619.021
14.147	8212.458	82124.582
14.184	8221.619	82216.186
14.222	8225.576	82255.762
14.259	8268.006	82680.060
14.297	8357.936	83579.361
14.334	8465.326	84653.263
14.372	8552.341	85523.413
14.409	8604.598	86045.982

8.2.6.5 Continued

Time (sec)	Stress (Pa)	Viscosity (Pa s)
14.447	8634.598	86345.978
14.484	8662.212	86622.119
14.522	8696.220	86962.197
14.559	8731.745	87317.447
14.597	8759.434	87594.343
14.634	8774.824	87748.235
14.672	8781.691	87816.914
14.709	8789.518	87895.184
14.747	8806.791	88067.913
14.784	8833.640	88336.402
14.822	8860.185	88601.852
14.878	8891.319	88913.186
14.953	8925.518	89255.178
15.028	8957.490	89574.903
15.103	8999.771	89997.707
15.178	9050.491	90504.908
15.253	9092.012	90920.116
15.328	9107.810	91078.103
15.403	9100.791	91007.908
15.478	9093.011	90930.112
15.553	9106.066	91060.662
15.628	9141.766	91417.664
15.703	9182.090	91820.904
15.778	9207.387	92073.866
15.853	9214.541	92145.408
15.928	9218.670	92186.696
16.003	9238.387	92383.867
16.078	9279.143	92791.428
16.153	9329.506	93295.060
16.228	9373.121	93731.210
16.303	9405.005	94050.053
16.378	9436.664	94366.638
16.453	9484.810	94848.096
16.528	9554.361	95543.614
16.603	9632.447	96324.469
16.678	9699.202	96992.024
16.753	9744.190	97441.897
16.828	9772.703	97727.027
16.903	9797.933	97979.325
16.978	9829.032	98290.323
17.053	9866.243	98662.427
17.128	9904.238	99042.379
17.203	9937.545	99375.450
17.278	9963.829	99638.291
17.353	9985.764	99857.635
17.428	10012.007	100120.067
17.503	10054.589	100545.895
17.578	10121.507	101215.066
17.653	10209.369	102093.687
17.728	10303.631	103036.305
17.803	10387.966	103879.662
17.878	10455.313	104553.134
17.953	10511.327	105113.272
18.028	10567.971	105679.713
18.103	10633.297	106332.973
18.178	10705.280	107052.797
18.253	10773.305	107733.046
18.328	10826.162	108261.622
18.403	10861.944	108619.441
18.478	10892.752	108927.524
18.553	10937.956	109379.564
18.628	11008.145	110081.448
18.703	11093.794	110937.936
18.778	11173.054	111730.545
18.853	11235.096	112350.961
18.928	11295.386	112953.858
19.003	11382.803	113828.030
19.078	11507.599	115075.987
19.153	11642.623	116426.230
19.228	11739.551	117395.506
19.303	11766.733	117667.329
19.378	11733.767	117337.667
19.453	11681.667	116816.670
19.528	11649.024	116490.242
19.603	11642.860	116428.599
19.678	11636.446	116364.456
19.753	11595.349	115953.485
19.828	11512.566	115125.657
19.903	11424.384	114243.843
19.978	11390.233	113902.331
20.053	11449.650	114496.501
20.128	11593.396	115933.956
20.203	11775.990	117759.903
20.278	11957.351	119573.511
20.353	12132.759	121327.593
20.428	12324.919	123249.186
20.503	12552.138	125521.381
20.578	12807.073	128070.734
20.653	13061.926	130619.260
20.728	13286.787	132867.869
20.803	13461.892	134618.922
20.878	13580.328	135803.285
20.953	13648.454	136484.539
21.028	13684.873	136848.726
21.103	13711.676	137116.763
21.178	13739.387	137393.870
21.253	13759.820	137598.198
21.328	13758.167	137581.670
21.403	13735.014	137350.137
21.478	13714.628	137146.285
21.553	13727.664	137276.635
21.628	13784.036	137840.361
21.703	13864.693	138646.935
21.778	13942.338	139423.380
21.853	14010.116	140101.161
21.928	14087.925	140879.250
22.003	14199.330	141993.296
22.078	14343.426	143434.261
22.153	14491.321	144913.212
22.228	14611.440	146114.395
22.303	14698.706	146987.063
22.378	14778.875	147788.753
22.453	14883.459	148834.590
22.528	15018.537	150185.370
22.603	15157.141	151571.407
22.678	15263.858	152638.578
22.753	15329.608	153296.082
22.828	15382.479	153824.790
22.903	15460.985	154609.846
22.978	15573.379	155733.786
23.053	15683.940	156839.396
23.128	15743.033	157430.330
23.203	15733.816	157338.161
23.278	15689.650	156896.503
23.353	15664.423	156644.225
23.428	15684.918	156849.184

8.2.6.5 Continued

Time (sec)	Stress (Pa)	Viscosity (Pa s)
23.503	15731.634	157316.338
23.578	15765.150	157651.501
23.653	15769.637	157696.371
23.728	15769.436	157694.362
23.803	15803.319	158033.189
23.878	15884.110	158841.103
23.953	15985.791	159857.910
24.028	16070.852	160708.520
24.103	16128.228	161282.281
24.178	16181.373	161813.731
24.253	16258.725	162587.249
24.328	16359.824	163598.239
24.403	16453.968	164539.678
24.478	16511.863	165118.629
24.553	16535.957	165359.569
24.628	16559.366	165593.661
24.703	16617.828	166178.283
24.778	16722.561	167225.610
24.853	16853.344	168533.444
24.928	16968.819	169688.193
25.003	17023.027	170230.273
25.078	16985.089	169850.894
25.153	16860.326	168603.263
25.228	16698.593	166985.934
25.303	16570.557	165705.568
25.378	16516.694	165166.937
25.453	16511.012	165110.117
25.528	16484.038	164840.375
25.603	16397.144	163971.436
25.678	16299.244	162992.439
25.753	16301.140	163011.404
25.828	16483.848	164838.477
25.903	16830.940	168309.399
25.978	17252.598	172525.976
26.053	17669.735	176697.355
26.128	18065.708	180657.079
26.203	18462.314	184623.136
26.278	18868.488	188684.885
26.353	19267.049	192670.487
26.428	19635.832	196358.324
26.503	19951.323	199513.232
26.653	20208.193	202081.934
26.728	20050.142	200501.418
26.803	19762.192	197621.920
26.878	19491.084	194910.836
26.953	19351.595	193515.950
27.028	19342.220	193422.202
27.103	19372.036	193720.360
27.178	19364.919	193649.189
27.253	19327.962	193279.620
27.328	19323.245	193232.446
27.403	19392.317	193923.171
27.478	19520.639	195206.393
27.553	19666.608	196666.079
27.628	19806.124	198061.243
27.703	19941.877	199418.766
27.778	20079.707	200797.068
27.853	20210.449	202104.487
27.928	20319.711	203197.113
28.003	20410.493	204104.927
28.078	20509.402	205094.018
28.153	20645.682	206456.819
28.228	20821.539	208215.386
28.303	21004.833	210048.335
28.378	21157.808	211578.080
28.453	21279.273	212792.729
28.528	21415.626	214156.258
28.603	21620.135	216201.346
28.678	21895.962	218959.621
28.753	22185.431	221854.306
28.828	22424.485	224244.851
28.903	22606.352	226063.516
28.978	22781.423	227814.230
29.053	22990.588	229905.882
29.128	23208.718	232087.180
29.203	23366.492	233664.919
29.278	23426.403	234264.028
29.353	23422.582	234225.823
29.428	23416.848	234168.481
29.503	23425.483	234254.827
29.578	23407.822	234078.216
29.653	23330.814	233308.144
29.728	23228.500	232284.998
29.803	23181.294	231812.939
29.878	23238.172	232381.718
29.953	23370.769	233707.694
30.028	23504.493	235044.929
30.103	23586.095	235860.945
30.178	23624.627	236246.269
30.253	23682.362	236823.624
30.328	23820.918	238209.178
30.403	24015.960	240159.602
30.478	24096.090	240960.901
30.553	23807.583	238075.832
30.628	23034.565	230345.654
30.703	22012.618	220126.184
30.778	21282.745	212827.445
30.853	21330.209	213302.087
30.928	22185.239	221852.387
31.003	23355.675	233556.750

9.0 – Acknowledgements

The author would like to thank Dr. Donald G. Baird for his guidance and support resulting in the completion of this work. The author would also like to thank all members of his research committee: Dr. Richey M. Davis, Dr. Robert B. Moore, and Dr. John Y. Walz.

The author would also like to acknowledge the following people:

- His wife, Jessica, for her unflinching love and support throughout their time at Virginia Tech
- His parents, Susan and Dewayne, and his family who encouraged him to fulfill his full potential
- John Lilly, his high-school football coach, who taught him the discipline necessary to achieve it
- Barbra McElwain, his high school chemistry and physics teacher, who encouraged him to study in the field of Chemical Engineering
- Those members of the departmental staff who have helped make his time at Virginia Tech enjoyable and have helped out in more ways than though possible: Tina, Nora, Jane, Amanda, Chris, Mike, and especially Diane and Riley.
- All members, past and present, of the Polymer Processing Lab, most notably: Aaron "Worms?" Eberle, Chris "Lettuce" Seay, David "IVPAG/DIVPAG" Litchfield, Mike "Modest" Heinzer, Myoungbae "Cake" Lee, Kevin "Wade Jr." Ortman, Desmond "Purdue What?" VanHouten, Brent "N!" Cunningham, Chen "Heinzer!" Chen, Gregorio "G-money" Velez-Garcia, Syed "Wall Street" Mazahir, Neeraj "Snacks" Agarwal, Joe "Eskimo" Samaniuk, and Wade "Eeahh" Depolo
- All friends who provided a steady supply of much needed distractions: Will "Where's Wildo?" Miles, Phil "You Need 5!" Huffstetler, Adam "Benedict" Larkin, Dean "DJ" Mastropietro, Jose "Jose! Jose!" Herrera-Alonso, John "Lockjaw" Brooks and, Aliah "Hammer" Rosenthal
- Finally, his constant hiking companion, Bristo, his 9-lb miniature dachshund.